

Copper(I) Phenanthrolines in Photocatalysis

Dissertation

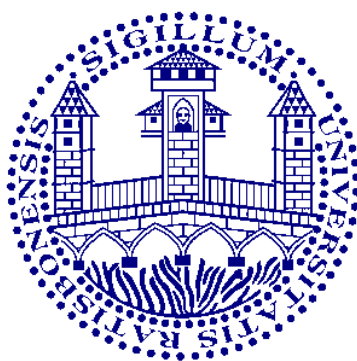
zur Erlangung des Doktorgrades der Naturwissenschaften

Dr. rer. nat.

an der

Fakultät für Chemie und Pharmazie

der Universität Regensburg



vorgelegt von

Thomas Rawner

aus Regensburg

im Jahre 2016

Die Arbeit wurde angeleitet von : Prof. Dr. Oliver Reiser

Promotionsgesuch eingereicht am : 04.05.2016

Promotionskolloquium am : 24.06.2016

Prüfungsausschuss : Vorsitz : PD Dr. Sabine Amslinger

1. Gutachter : Prof. Dr. Oliver Reiser

2. Gutachter : Prof. Dr. Kirsten Zeitler

3. Prüfer : Prof. Dr. Robert Wolf

Der experimentelle Teil der vorliegenden Arbeit wurde in der Zeit von Oktober 2012 bis Dezember 2015 unter der Leitung von Herrn Prof. Dr. Oliver Reiser am Institut für Organische Chemie der Universität Regensburg angefertigt.

Herrn Prof. Dr. Oliver Reiser möchte ich herzlich für die Aufnahme in seinen Arbeitskreis, die Überlassung des interessanten Themas, die anregenden Diskussionen und seine stete Unterstützung während der Durchführung dieser Arbeit danken.

Für meine Familie

Sic Parvis Magna

(Thus great things from small things come)

Sir Francis Drake

Table of Contents

A.	Copper(I) Phenanthrolines in Photochemistry	1
1.	Introduction.....	1
2.	Aim of this Work.....	10
3.	References	11
B.	Synthesis of new Copper(I) Phenanthroline Complexes and Their Catalytic Activity	13
1.	Introduction.....	13
2.	Synthesis of Copper(I) Phenanthroline Complexes.....	16
3.	Characterization of Copper(I) Phenanthroline Complexes	20
3.1.	X-ray Structures.....	20
3.2.	Electronic Properties.....	26
3.3.	Electrochemistry	28
3.4.	Summary of the Photophysical and Electrochemical Properties of New Copper(I) Phenanthroline Complexes	30
4.	Catalysis	32
4.1.	Atom Transfer Radical Addition	34
4.2.	Allyltrimethylsilane as Alkylating Agent	38
5.	Summary	42
6.	References	43
C.	Photochemical Iodoperfluoroalkylation	46
1.	Introduction.....	46
2.	Preliminary Studies with Styrene and Perfluorooctyl Iodide	51
3.	Variation of Perfluoroalkyl Iodide as Radical Source and Comparison of Various Photoredox Catalysts.....	53
4.	Substrate Scope	55
5.	Application	62
6.	Mechanistic Studies.....	66

Table of Contents

7.	Proposed Mechanism	70
8.	Summary	71
9.	References	72
D.	Synthesis of Trifluoromethylated Sultones From Alkenols Using a Copper Photoredox Catalyst.....	76
1.	Introduction.....	76
2.	Trifluoromethylchlorosulfonylation.....	78
3.	Preliminary Studies with Alkenols	80
4.	Optimization and Control Experiments.....	82
5.	Substrate Scope	83
6.	Variation of Sulfonyl Chlorides as Radical Source	86
7.	Application of Methodology in Pharmaceutical Chemistry	87
8.	Mechanistic Studies.....	89
9.	Proposed Mechanism	91
10.	Summary	92
11.	References	93
E.	Summary	97
1.	Summary in English.....	97
2.	Summary in German (Zusammenfassung)	98
F.	Experimental Part	100
1.	General Comments.....	100
2.	Chapter B: Synthesis of New Copper(I) Phenanthroline Complexes and Their Catalytic Activity	103
2.1.	Synthesis of Literature Known Compounds and Reagents	103
2.2.	Compound Characterization	104
2.3.	NMR Spectra	128
2.4.	X-ray.....	154
3.	Chapter C: Photochemical Iodoperfluoroalkylation.....	159

Table of Contents

3.1.	Synthesis of Literature Known Compounds and Reagents	159
3.2.	Preparation of Trifluoromethyl Iodide Stock Solution.....	160
3.3.	Compound Characterization	161
3.4.	NMR Spectra	186
4.	Chapter D: Synthesis of Trifluoromethylated Sultones From Alkenols	
	Using a Copper Photoredox Catalyst	255
4.1.	Synthesis of Literature Known Compounds and Reagents	255
4.2.	Quantum Yield Determination	256
4.3.	Karl Fischer Titration.....	258
4.5.	Compound Characterization	259
4.6.	NMR Spectra	276
4.7.	GC-MS Spectra	315
4.8.	X-ray.....	322
5.	References	323
G.	Appendix	325
1.	Curriculum Vitae	325
2.	Congresses and Scientific Meetings	327
3.	List of Publications.....	328
H.	Acknowledgement.....	329
I.	Declaration	331

Abbreviations

A	acceptor	DCE	dichloroethane
Å	Ångström (10^{-10} m)	deg	degree
Ac	acetyl	dF(CF ₃)ppy	2-(2,4-difluorophenyl)-5-(trifluoromethyl) pyridine
AIBN	2,2'-azobis(2-methylpropionitrile)	DIPEA	<i>N,N</i> -diisopropylethylamine
anh.	anhydrous	DMF	<i>N,N</i> -dimethylformamide
APCI	Atmospheric pressure chemical ionization	dmp	2,9-dimethyl-1,10-phenanthroline
Ar	aryl	DPEphos	bis(2-(diphenylphosphanyl)phenyl)ether
atm	atmosphere	dpp	2,9-diphenyl-1,10-phenanthroline
ATRA	atom transfer radical addition	dtbbpy	4,4'-di- <i>tert</i> -butyl-2,2'-bipyridine
binc	bis(2-isocyanophenyl)phenyl phosphonate	ε	molar extinction coefficient
Boc	<i>tert</i> -butoxycarbonyl	e.g.	exempli gratia (<i>Latin</i> : for example)
bpy	2,2'-bipyridine	<i>E/Z</i>	ntgegen / zusammen
BS	1,4-butane sultone	E _{1/2}	standard reduction potential
Bu	butyl	ed.	Edition
^t Bu	<i>tert</i> -butyl	Ed.	Editor
°C	degree celsius	EI	electron ionization
c	centi (10^{-2}); concentration	eq	equation
calc.	calculated	equiv	equivalent
CI	chemical ionization	ESI	electrospray ionization
CN-Xylyl	2,6-dimethylphenyl isocyanide	Et	ethyl
CT	charge-transfer	et al.	et alia (<i>Latin</i> : and others)
CV	cyclic voltammetry	eV	electronvolt
D	donor	FC	ferrocene
d	deci (10^{-1})	FD	field desorption
δ	chemical shift	FEC	fluoroethylene carbonate
d.r.	diastereomeric ratio	F-HPLC	fluorine high pressure liquid chromatography
dap	2,9-bis(<i>para</i> -anisyl)-1,10-phenanthroline	FI	field ionization
dba	dibenzalacetone		

Abbreviations

FID	flame ionization detector	LC	ligand-centered
FLLE	fluorine liquid-liquid extraction	LED	light emitting diode
FMS	fluorine mixture synthesis	LIB	lithium-ion battery
FPS	fluorine containing 1,3-propane sultone	LRMS	low resolution mass spectroscopy
FSPE	fluorine solid phase extraction	M	molar (mol L^{-1}); mega (10^6)
FTIR	Fourier transform infrared spectroscopy	m	milli (10^{-3}); multiplet (spectroscopy)
g	gram	μ	micro (10^{-6})
GC	gas chromatography	<i>m</i>	meta
Gly	glycine	<i>m/z</i>	mass to charge ratio
glyme	1,2-dimethoxyethane	Me	methyl
h	hour	MeCN	acetonitrile
<i>h</i>	Planck constant	min	minute
HCMV	human cytomegalovirus	mol	mole
Hex	hexyl	mol%	mole percent
HIV-1	human immunodeficiency virus type 1	MLCT	metal-to-ligand charge-transfer
HPLC	high pressure liquid chromatography	mp	melting point
HRMS	high resolution mass spectroscopy	MS	mass spectroscopy
HSV	herpes virus	nd	not determined
Hz	Hertz	n	nano (10^{-9})
i.e.	it est (<i>Latin</i> : that is)	ν	frequency
IR	infrared spectroscopy	NMR	nuclear magnetic resonance
ISC	intersystem crossing	NOESY	nuclear Overhauser effect spectroscopy
<i>J</i>	coupling constant (spectroscopy)	nr	no reaction
k	kilo (10^3)	<i>o</i>	ortho
L	ligand; liter	<i>o,o</i>	ortho, ortho
λ	wavelength	<i>o,p</i>	ortho, para
λ_{max}	wavelength of maximum	<i>p</i>	para
λ_{Abs}	wavelength of maximum absorption	%Ar	percent of area
		PCat	photocatalyst
		phen	1,10-phenanthroline
		PMMA	poly(methyl methacrylate)
		ppm	parts per million

Abbreviations

Ph	phenyl	UV	ultra violet
Pr	propyl	V	Volt
ⁱ Pr	<i>iso</i> -propyl	VC	vinylene carbonate
Pro	proline	VEC	vinyl ethylene carbonate
ppy	2-phenylpyridine	Vis	visible light
Pra	propargylglycine	vs	versus (Latin: against)
PS	1,3-propane sultone	VZV	varicellazoster virus
Q	quencher	W	Watt
Q-TOF	quadrupole time-of-flight	wt%	weight percent
Φ	quantum yield	X	arbitrary halogen
quant.	quantitative		
R	arbitrary rest		
RCM	ring closure metathesis		
redox	reduction-oxidation		
R _f	retardation factor;		
R _f	perfluorinated carbon chain		
rt	room temperature		
t _R	retention time		
SCE	standard calomel electrode		
SEI	solid electrolyte interphase		
SET	single electron transfer		
t	time		
τ	lifetime		
TEMPO	(2,2,6,6-tetramethyl- piperidin-1-yl)oxyl		
Tf	triflyl (= trifluoro methanesulfonyl)		
Ts	also abbreviated as "Tos" tosyl (= 4-toluenesulfonyl)		
TFA	trifluoroacetic acid		
THF	tetrahydrofuran		
TLC	thin layer chromatography		
TMEDA	<i>N,N,N',N'</i> -tetramethyl ethane-1,2-diamine		
TMS	trimethylsilyl		

A. Copper(I) Phenanthrolines in Photochemistry

1. Introduction

Currently, the major source for chemical products and energy is provided from coal, oil, and natural gas. To overcome this global dependency on non-renewable fossil fuels by most industrialized and developing countries, alternative renewable energy sources have to be found and emphasized in daily life.^[1] Moreover, the emission of carbon dioxide, which is mainly responsible for the climate change, has to be minimized in order to reduce the global surface warming and their resulting problems for the mankind.^[2] In this context, one approach is the use of sunlight as sustainable energy source. Hence, the photosynthesis in nature served as a prototype for the development of photovoltaic systems which convert sunlight into electric energy.^[3] In the last decades, also chemical transformations are more and more described in terms of atom economy, efficiency, green chemistry, or hazardous potential beyond yield and purity of the desired product.^[4] Therefore, synthetic chemists' are in pursuit towards mild and green reaction conditions. In recent years, photochemistry has been established as an efficient and green alternative to conventional thermal reactions. Photochemistry is defined as the chemical reaction of atoms or molecules initiated by absorption of light with wavelengths in the range of ca. 100 nm to 800 nm.^[5] In contrast to classic thermal reactions, photochemistry offers numerous advantages. For instance, light is considered as an ecologically clean, so-called "green" reagent. Moreover, photochemical reactions are generally performed at room temperature and therefore denoted as mild. Many conventional syntheses can be shortened by inserting photochemical reaction as keystone, too. However, the lack of visible light absorption by organic molecules has limited the wide synthetic application of photochemistry. As a result, visible light absorbing photocatalysts were developed which are able to transfer electron or energy to organic compounds making visible light as reagent accessible.^[6]

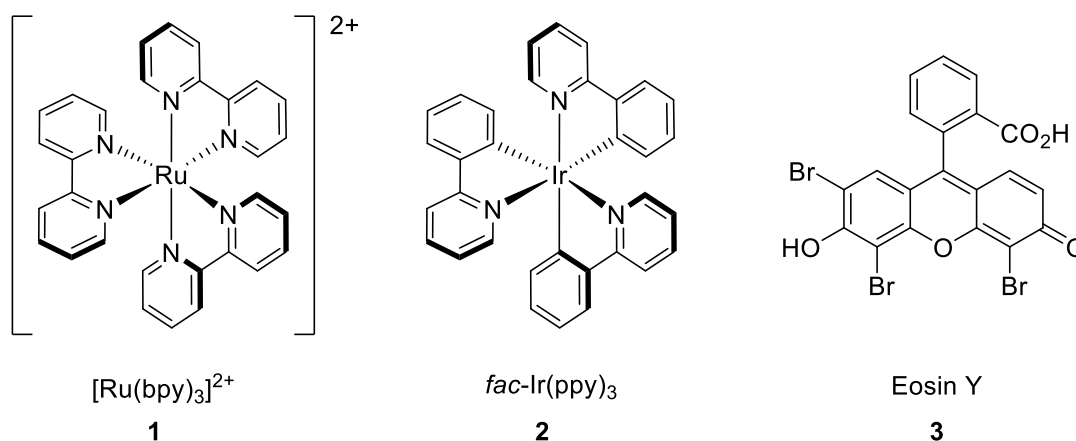


Figure 1. Examples of widely established photoredox catalysts.

The most commonly employed photocatalysts are transition metal complexes of ruthenium and iridium like $[\text{Ru}(\text{bpy})_3]^{2+}$ (**1**) and *fac*- $\text{Ir}(\text{ppy})_3$ (**2**), or organic dyes such as Eosin Y (**3**) (Figure 1). These catalysts have excellent photophysical and electrochemical properties. For example, they show sufficiently long lifetime of the excited species, absorption of visible light, and potent reduction potentials.^[7] The commonly accepted mechanism^[7] of a metal based photoredox catalyzed reaction is depicted in a Latimer-diagram (Figure 2).

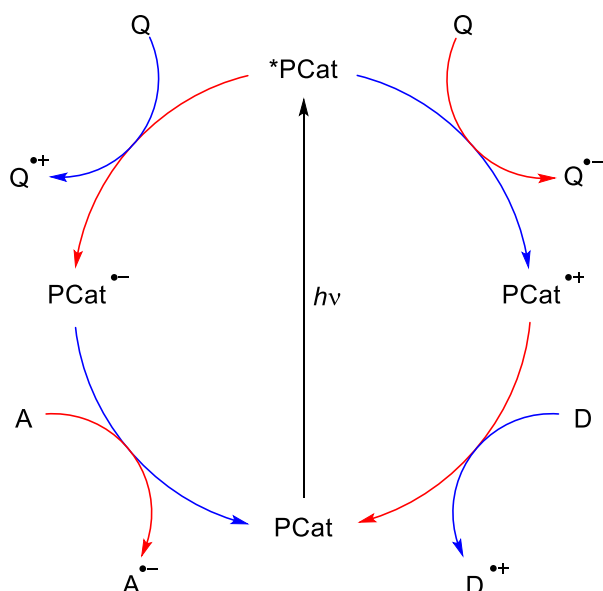


Figure 2. General scheme for photoredox catalysis (PCat = photoredox catalyst, Q = quencher, A = acceptor, D = donor, blue: oxidative quenching cycle, red: reductive quenching cycle).

First, a photon is absorbed by the photocatalyst (PCat) to generate a high energy excited singlet state (*PCat) through a metal to ligand transfer (MLCT) mechanism. Then, this singlet state undergoes rapid intersystem crossing (ISC) to give the lowest-energy triplet MLCT state^[7], which has a longer lifetime and is capable to perform a single electron transfer (SET) compared to the ground state. The photoexcited state *PCat can act as both, oxidant or reductant depending on the reaction conditions. A catalyst that accepts an electron from a non-productive quencher Q, often known as “sacrificial electron donor”, is said to undergo the reductive quenching cycle. Widely used non-productive quenchers are NEt_3 , NPh_3 , Hunig’s base, oxalate, or ascorbate.^[8] The strong reductant $\text{PCat}^{\bullet-}$ acts now as an electron donor transferring an electron to an acceptor thus closing the catalytic cycle. In contrast, in the oxidative quenching cycle the oxidized photocatalyst $\text{PCat}^{\bullet+}$ serves as an electron acceptor. Common productive quenchers Q are aryldiazonium salts, haloalkanes, viologens, or metal salts based on cobalt or iron.^[7-8] In literature, both cycles are almost equally used in chemical transformations.

However, examples of feasible photocatalysts in organic synthesis utilizing cheap, abundant and environmental friendly metals, such as copper, are scarce in literature. Considering the economic advantage of copper over expensive and rare ruthenium or iridium, photoactive homoleptic copper(I) phenanthrolines $[\text{Cu}(\text{NN})_2]^+$ (**4**) and heteroleptic versions such as **5** and **6** have emerged as a promising competitor in the last years (Figure 3).^[9]

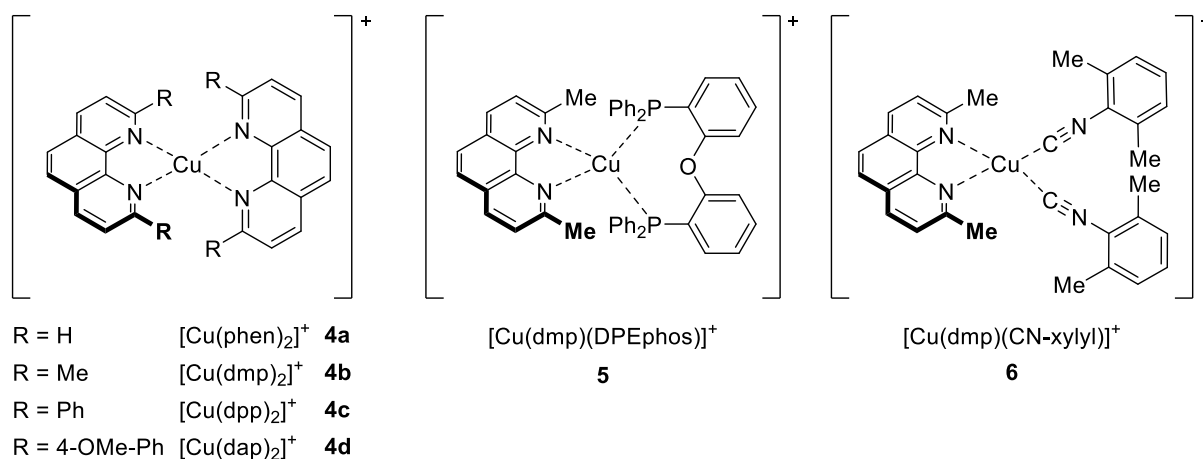
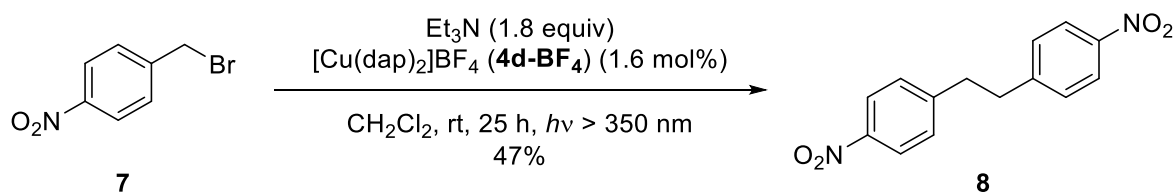


Figure 3. Examples of homoleptic and heteroleptic copper(I) phenanthroline complexes.

In 1987, three years after the first synthesis of $[\text{Cu}(\text{dap})_2]^+$ (**4d**) as disclosed by Sauvage et al.^[10], the first synthetic application of such complexes in photochemistry was published by the same group.^[11] The authors reported the photochemical conversion of *para*-nitrobenzylbromide (**7**) into their dibenzylic coupling product **8** establishing $[\text{Cu}(\text{dap})_2]\text{BF}_4$ (**4d-BF₄**) as visible light driven photocatalyst in the presence of triethylamine (Scheme 1). Furthermore, under aerobic conditions the oxidation of compound **7** to the corresponding aldehyde was observed in 95% yield.

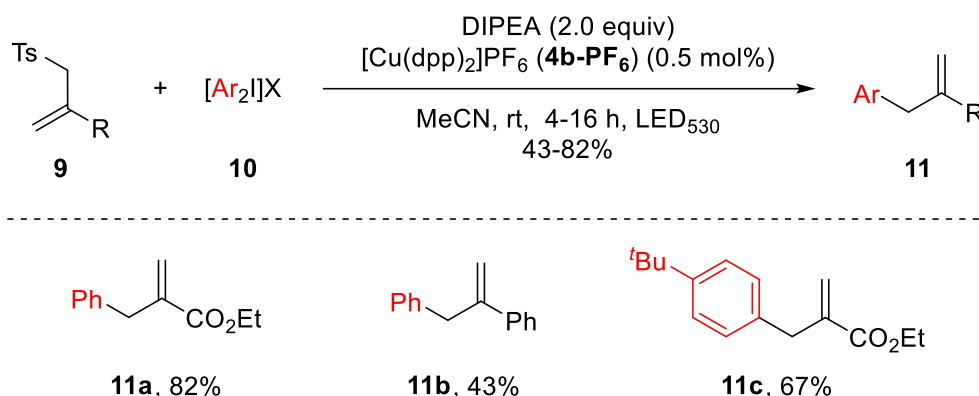
Scheme 1. First synthetic application of $[\text{Cu}(\text{dap})_2]\text{Cl}$ (**4d-BF₄**) in photoredox catalysis.^[11]



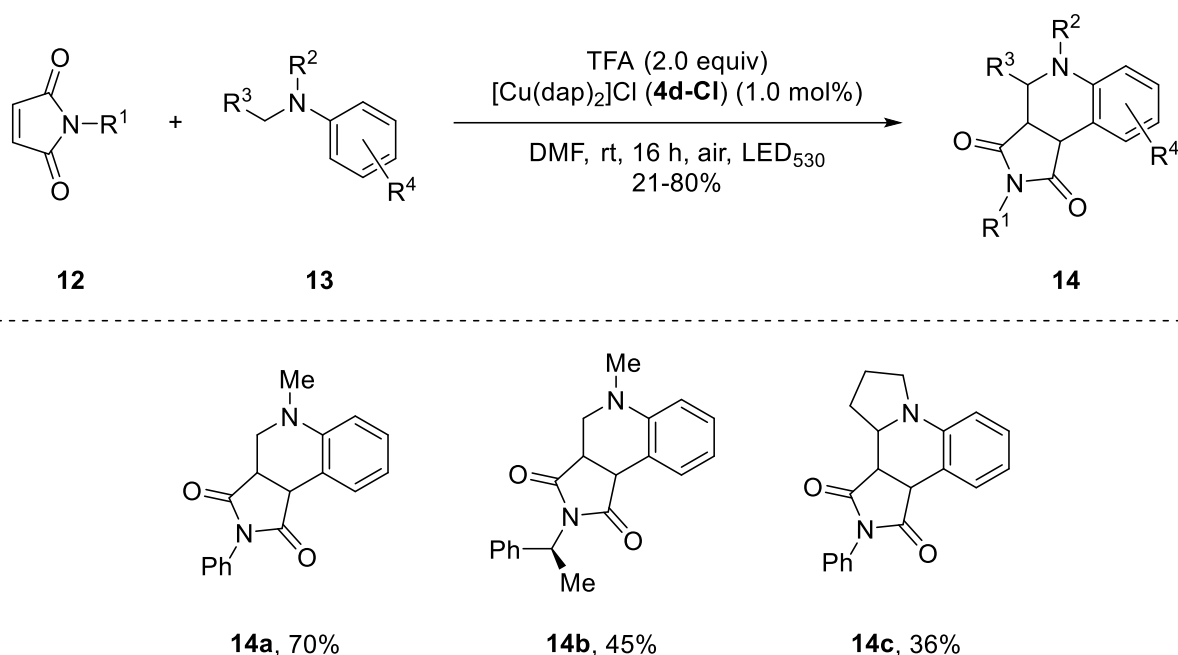
From that point on, copper(I) phenanthroline complexes entered the area of visible light mediated photoredox catalysis and proved to be an environmentally benign alternative to $[\text{Ru}(\text{bpy})_3]\text{Cl}_2$ (**1-Cl**) or *fac*- $\text{Ir}(\text{ppy})_3$ (**2**). Its synthetic application was mainly demonstrated by the groups of Bissember^[12], Collins^[13], Ollivier^[14], Dolbier^[15], Greaney^[16], and Reiser^[17] which will be highlighted in this introduction. Remarkably, great difference between copper and noble-metal photocatalysts such as $[\text{Ru}(\text{bpy})_3]\text{Cl}_2$ (**1-Cl**) or *fac*- $\text{Ir}(\text{ppy})_3$ (**2**) was also reported in literature.

Ollivier et al. identified the homoleptic complex $[\text{Cu}(\text{dpp})_2]\text{PF}_6$ (**4c-PF₆**) as an efficient catalyst for the photocatalytic reduction of diaryliodonium salts **10** to the corresponding aryl radicals.^[14] Further addition to allyl sulfone acceptor **9** gave an α -carbonyl radical, which after extrusion of the tosyl group afforded the allylated product **11** in good yields (Scheme 2). In the context of their study, it was observed that this process could be accomplished by various known photocatalysts such as $[\text{Ru}(\text{bpy})_3]\text{Cl}_2$ (**1-Cl**) or *fac*- $\text{Ir}(\text{ppy})_3$ (**2**). Since no significant improvement in yield was observed, $[\text{Cu}(\text{dpp})_2]\text{PF}_6$ (**4c-PF₆**) as environmental friendly alternative to ruthenium and iridium based catalysts was chosen. It is noteworthy that for the first time Michael systems were successfully introduced in copper photoredox catalysis although being incompatible in atom transfer radical addition (ATRA) reactions as demonstrated by M. Pirtsch.^[18] Furthermore, different commercially available iodonium salts including asymmetric versions were investigated to test the influence of aromatic substitution, steric, and electronic effects on the formation of aryl radicals. The authors have come to the conclusion that a broad range of iodonium salts are tolerated and no selectivity was obtained when either electron poor, electron rich, or bulky substituents in the aryl ring were present.

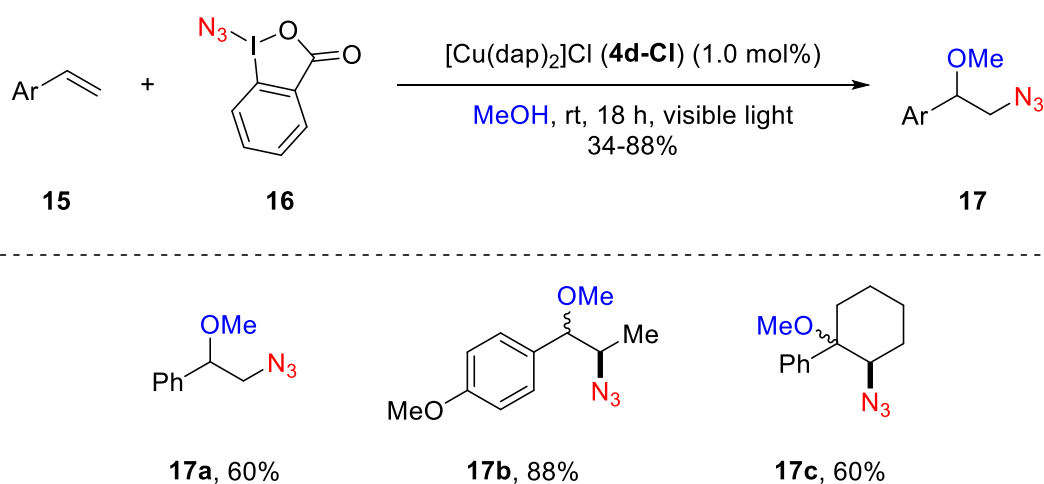
Scheme 2. Visible light mediated $[\text{Cu}(\text{dpp})_2]\text{PF}_6$ (**4b-PF₆**) catalyzed arylation reaction.^[14]



Recently, an α -amino C-H bond functionalization exploiting the oxidative quenching cycle of $[\text{Cu}(\text{dap})_2]\text{Cl}$ (**4d-Cl**) was presented by Bissember and co-workers (Scheme 3).^[12] Tetrahydroquinolines **14** were obtained in low to good yields when maleimides **12** were reacted with *N,N*-dimethylaniline derivatives **13** in the presence of stoichiometric trifluoroacetic acid (TFA). Interestingly, in the absence of acid no product formation was found indicating that the presence of TFA is crucial. To gain deeper mechanistic insight, the role of the Brønsted acid was further investigated. It is assumed that trifluoroacetic acid mediates the oxidation of photoexcited copper(I) phenanthroline complex **4d-Cl** thus facilitating the catalyst turnover. In addition, this methodology was successfully used as keystone in the synthesis of an aglycone analogue.

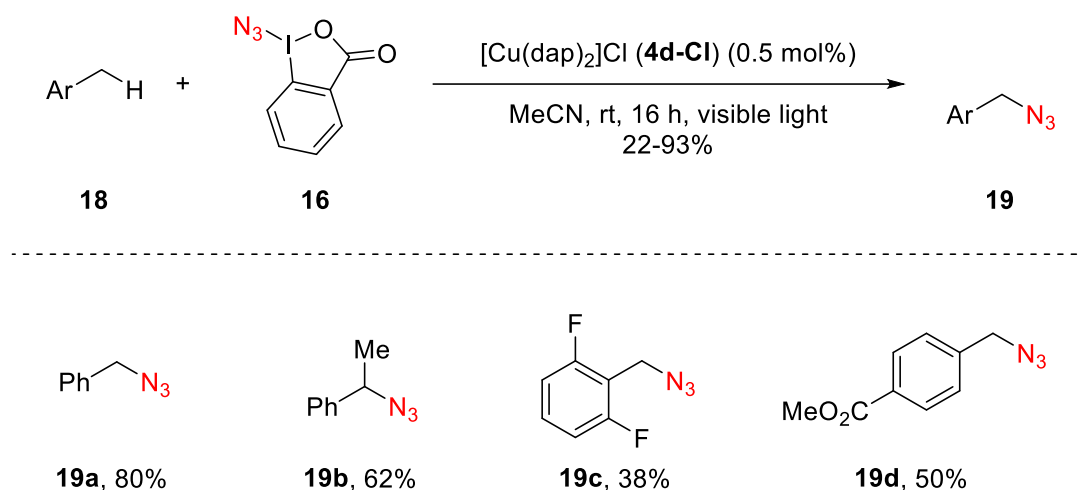
Scheme 3. [Cu(dap)₂]Cl (**4d-Cl**) photocatalyzed α -amino C-H bond functionalization.^[12]

In 2015, several reports establishing [Cu(dap)₂]Cl (**4d-Cl**) as the photocatalyst for azidation^[16a], intramolecular aminodifluoromethylation^[15b] and trifluoromethylchlorosulfonylation^[17c] of alkenes have been published demonstrating its superiority compared to widely used [Ru(bpy)₃]Cl₂ (**1-Cl**) or *fac*-Ir(ppy)₃ (**2**). In all examples, ruthenium or iridium-based catalysts failed to deliver any product in appreciable yields or even more, gave rise to different compounds. For example, in the three-component azidation reaction of styrenes **15** as described by Greaney and co-workers (Scheme 4), no reaction or even worse, decomposition of the starting material was observed when [Ru(bpy)₃]Cl₂ (**1-Cl**) or *fac*-Ir(ppy)₃ (**2**) were utilized.^[16a] Switching the catalyst to [Cu(dap)₂]Cl (**4d-Cl**) resulted in the azidomethoxylation products **17** in good yields.

Scheme 4. Visible light mediated [Cu(dap)₂]Cl (**4d-Cl**) catalyzed three-component azidation reaction.^[16a]

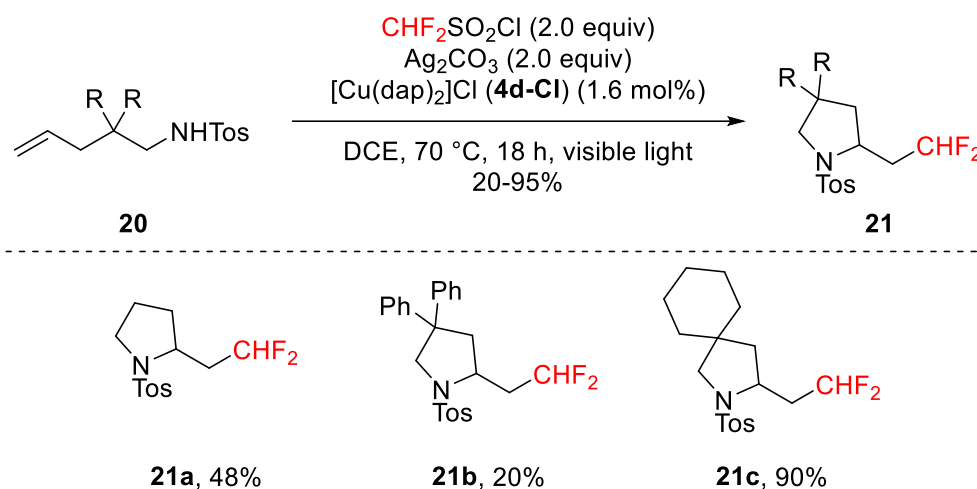
Very recently, Greaney et al. expanded their azidation protocol to the carbon-nitrogen bond formation at benzylic C-H positions establishing 0.5 mol% $[\text{Cu}(\text{dap})_2]\text{Cl}$ (**4d-Cl**) and Zhdankin reagent (**16**) (Scheme 5).^[16b] Over 30 examples were evaluated demonstrating the wide range of substrate and functional group tolerance. Moreover, the presented methodology was successfully employed in the synthesis of the antiepileptic drug rufinamide. Further screening revealed that common photocatalysts like $[\text{Ru}(\text{bpy})_3]\text{Cl}_2$ (**1-Cl**) or *fac*-Ir(ppy)₃ (**2**) were completely ineffective resulting in no product formation. Remarkably, the simple copper salt CuBr yielded the azidation product **19a** in 55% yield compared to copper photocatalyst **4d-Cl** with 80%. The authors propose a radical chain process initiated by $[\text{Cu}(\text{dap})_2]\text{Cl}$ (**4d-Cl**) being implicated by their mechanistic studies.

Scheme 5. Photoredox catalyzed benzylic azidation establishing $[\text{Cu}(\text{dap})_2]\text{Cl}$ (**4d-Cl**) as photoredox catalyst.^[16b]



Furthermore, Dolbier et al. presented the unique outcome in the photoredox catalyzed intramolecular aminodifluoromethylation reaction when copper(I) phenanthroline complex **4d-Cl** was used (Scheme 6).^[15b] Initially, the proposed transformation was tested for *fac*-Ir(ppy)₃ (**2**) with $\text{CHF}_2\text{SO}_2\text{Cl}$ as radical source but only net addition of CHF_2Cl onto unactivated alkenes **20** have been observed. Whereas, cyclization product **21** was formed in excellent yield when again, copper catalyst **4d-Cl** was established as photocatalyst. The authors suggest that excited Cu(II) oxidize the formed carbon radical intermediate less efficiently than the iridium catalyst thus suppressing the chlorine atom abstraction from $\text{CHF}_2\text{SO}_2\text{Cl}$, which would lead to simple addition reaction.

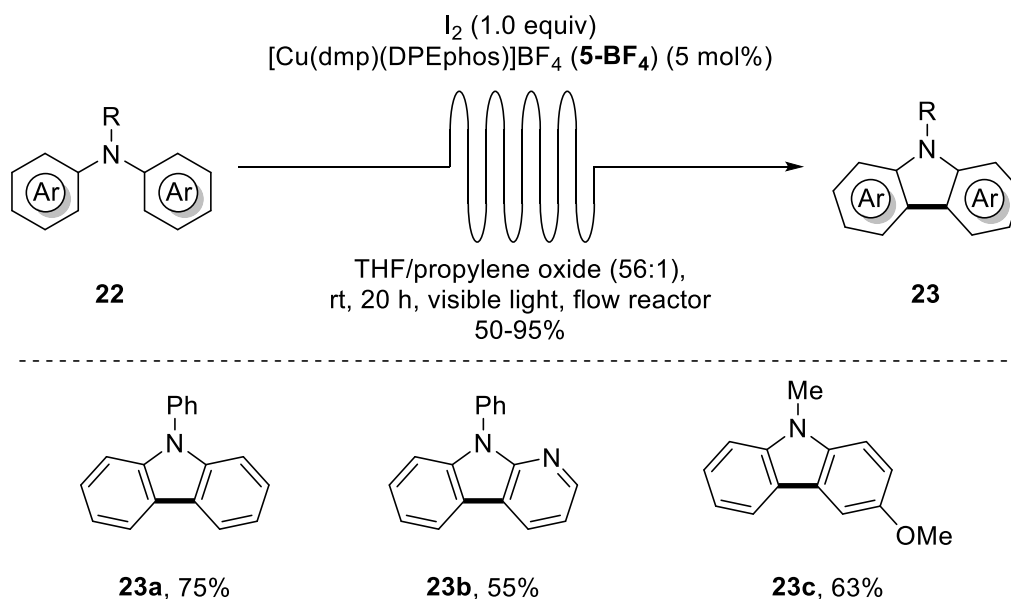
Scheme 6. Photoredox catalyzed intramolecular aminodifluoromethylation of unactivated alkenes **20** utilizing $[\text{Cu}(\text{dap})_2]\text{Cl}$ (**4d-Cl**) as photocatalyst.^[15b]



Also, copper complex $[\text{Cu}(\text{dap})_2]\text{Cl}$ (**4d-Cl**) was identified as an unique catalyst for an unprecedented visible light mediated trifluoromethylchlorosulfonylation of unactivated alkenes with triflyl chloride as demonstrated by Reiser and co-workers.^[17c] In contrast to ruthenium and iridium based photocatalysts, no SO_2 extrusion was observed in the absence of strong donor atoms leading to trifluoromethylsulfonylated products (for more details see Chapter D: Synthesis of Trifluoromethylated Sultones From Alkenols Using a Copper Photoredox Catalyst).

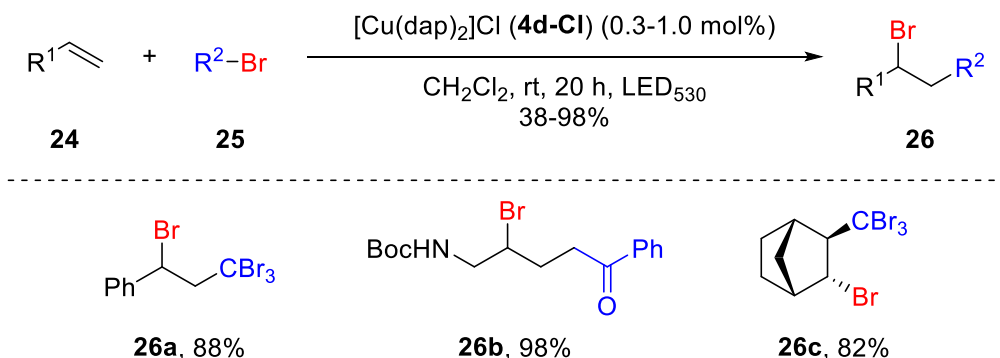
Moreover, examples of synthetic applications utilizing heteroleptic copper(I) phenanthroline complexes, where one phenanthroline ligand is exchanged by a bidentate phosphine ligand like xanthphos or DPEphos, are even less common.^[19] For instance, Collins and co-workers could demonstrate a visible light mediated photocyclization yielding [5]helicenes.^[13a] Upon investigating the reaction conditions, it was found that best results were obtained with heteroleptic copper complex $[\text{Cu}(\text{dmp})(\text{DPEphos})]\text{BF}_4$ (**5-BF₄**) whereas low yields (<10%) were achieved by popular $[\text{Ru}(\text{bpy})_3]\text{Cl}_2$ (**1-Cl**) or *fac*- $\text{Ir}(\text{ppy})_3$ (**2**). One year later, the novel photochemical route through C-C-bond formation to carbazoles was achieved by the same heteroleptic copper complex.^[13b] A variety of tertiary arylamines **22** were converted to *N*-alkyl bearing carbazoles **23** through continuous-flow conditions in moderate to good yields (Scheme 7). In contrast to ruthenium-based catalysts, heteroleptic copper catalyst **5-BF₄** were formed in situ thus providing faster screening results and therefore the ability to tune rapidly the catalyst. In addition, catalyst **5-BF₄** showed better photocatalytic performance than $[\text{Ru}(\text{bpy})_3](\text{PF}_6)_2$ (**1-PF₆**) given again the vast difference in activity between copper and typical noble-metal photocatalysts.

Scheme 7. Visible light mediated synthesis of carbazoles utilizing heteroleptic copper(I) phenanthroline complex $[\text{Cu}(\text{dmp})(\text{DPEphos})]\text{BF}_4$ (**5-BF₄**) as photoredox catalyst.^[13b]

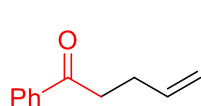
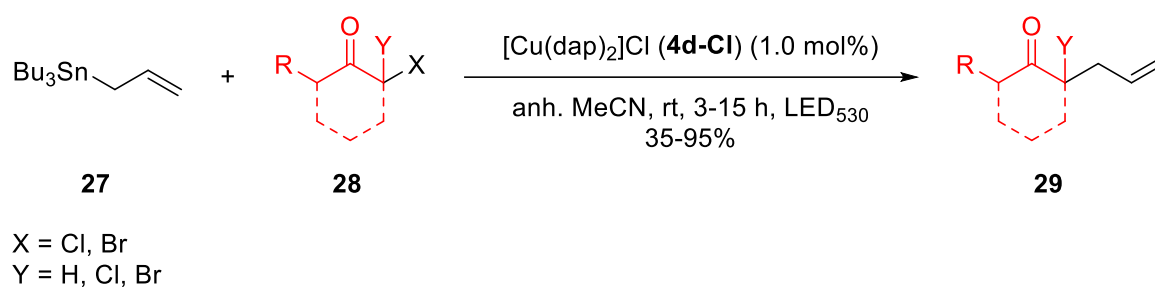
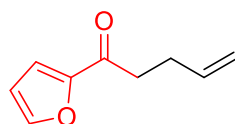
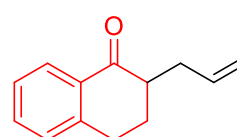


In the Reiser group, $[\text{Cu}(\text{dap})_2]\text{Cl}$ (**4d-Cl**) as photocatalyst was examined since 2012.^[17,20] The first synthetic application establishing photocatalyst **4d-Cl** under visible light conditions was demonstrated by M. Pirtsch and S. Paria.^[17a,18] The authors reported the addition of various alkyl halides **25**, e.g. CBr_4 , diethyl bromomalonate, or α -bromo acetophenone to different olefins **24** showing that copper(I) phenanthroline complex **4d-Cl** is a highly efficient photocatalyst for atom transfer radical addition (ATRA) reactions plus a viable alternative to widely used ruthenium and iridium catalysts (Scheme 8).

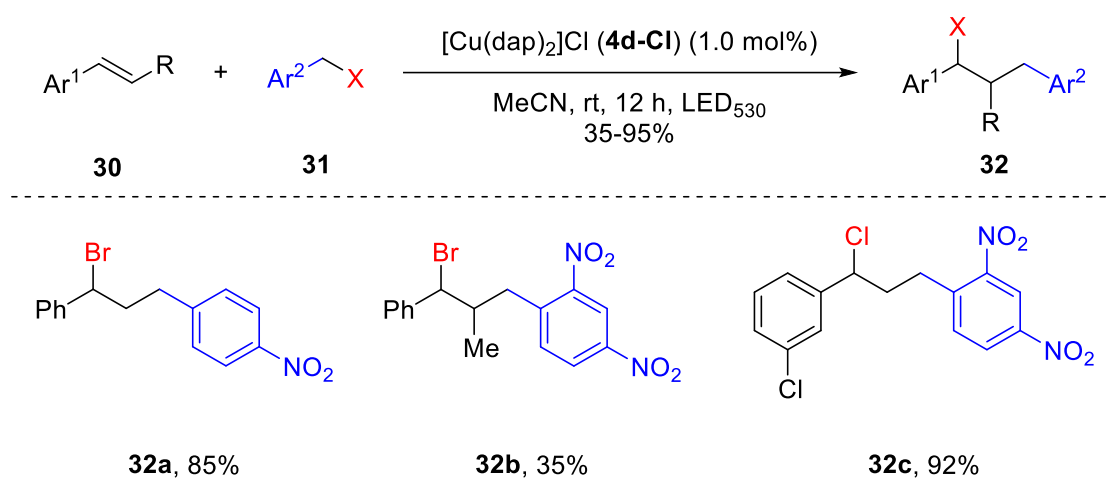
Scheme 8. Visible light mediated $[\text{Cu}(\text{dap})_2]\text{Cl}$ (**4d-Cl**) catalyzed ATRA reaction.^[17a]



As a second process, the visible light mediated allylation of α -haloketones catalyzed by the same copper complex **4d-Cl** was also investigated (Scheme 9). It was found that 1.0 mol% $[\text{Cu}(\text{dap})_2]\text{Cl}$ (**4d-Cl**), one equivalent of allyltributyltin (**27**), one equivalent of organohalide **28** in anhydrous MeCN and irradiation with green light (LED₅₃₀) for 3-15 hours furnished the allylated product **29** in good to excellent yields. It is noteworthy that this transformation under visible light has not been demonstrated in literature by then. Attempts to establish ecological more benign allyltrimethylsilane was only successful in one example.

Scheme 9. Visible light mediated $[\text{Cu}(\text{dap})_2]\text{Cl}$ (**4d-Cl**) catalyzed allylation reaction.^[17a]**29a**, 85%**29b**, 68%**29c**, 70%

2013, it was demonstrated that $[\text{Cu}(\text{dap})_2]\text{Cl}$ (**4d-Cl**) has the potential to substitute well established photocatalysts $[\text{Ru}(\text{bpy})_3]\text{Cl}_2$ (**1-Cl**) or *fac*- $\text{Ir}(\text{ppy})_3$ (**2**) in the visible light mediated ATRA reaction between electron deficient benzyl halides **31** and styrenes **30** as radical trapping reagent (Scheme 10).^[17b]

Scheme 10. Visible light mediated $[\text{Cu}(\text{dap})_2]\text{Cl}$ (**4d-Cl**) catalyzed allylation reaction.^[17b]

Moreover, better yields were obtained than employing ruthenium catalyst **1-Cl**, whereas same results were achieved as provided by the iridium catalyst **2**. Therefore, economic copper(I) phenanthroline complex **4d-Cl** was applied in this transformation. It was necessary to use electron poor benzyl bromides or chlorides as ATRA reagent, calling heteroarenes or nitro substitution in the phenyl ring of the benzyl moiety. The obtained photoproducts **32** were further converted into 2-substituted tetrahydroquinolines by either catalytic hydrogenation with palladium over charcoal or by reduction of the nitro group to the amino functionality using FeCl_3/Zn with concurrent cyclization.

2. Aim of this Work

Intrigued by these promising results *vide supra*, it was therefore decided to explore $[\text{Cu}(\text{dap})_2]\text{Cl}$ (**4d-Cl**) as alternative photoredox catalyst to broaden the range of organic transformations and compare the obtained results with widely established ruthenium and iridium catalysts. Consequently, new synthetically useful processes and practical, atom economical, and easy protocols are desirable to be developed. The photochemical addition of small molecules would be an attractive process whereas no by-products would be formed, ideally.

The aim of the present work was the development of environmental friendly, efficient, and mild visible light mediated methodology of copper based photoredox catalyst for ATRA reactions. Moreover, as part of an effort to tune the photophysical and electrochemical properties of $[\text{Cu}(\text{dap})_2]\text{Cl}$ (**4d-Cl**), various homoleptic complexes were designed, synthesized and evaluated.

3. References

- [1] a) York, R. *Nature Climate Change* **2012**, 2, 441-443; b) Trancik, J. E. *Nature* **2014**, 507, 300-302.
- [2] Clark, P. U.; Shakun, J. D.; Marcott, S. A.; Mix, A. C.; Eby, M.; Kulp, S.; Levermann, A.; Milne, G. A.; Pfister, P. L.; Santer, B. D.; Schrag, D. P.; Solomon, S.; Stocker, T. F.; Strauss, B. H.; Weaver, A. J.; Winkelmann, R.; Archer, D.; Bard, E.; Goldner, A.; Lambeck, K.; Pierrehumbert, R. T.; Plattner, G.-K. *Nature Climate Change* **2016**, 6, 360-369.
- [3] Protti, S.; Fagnoni, M. *Photochem. Photobiol. Sci.* **2009**, 8, 1499-1516.
- [4] a) Trost, B. M. *Angew. Chem. Int. Ed.* **1995**, 34, 259-281; b) Dunn, P. J. *Chem. Soc. Rev.* **2012**, 41, 1452-1461; c) Li, C. J.; Trost, B. M. *Proceed. Natl. Acad. Sci. USA* **2008**, 105, 13197-13202; d) Anastas, P. T.; Warner, J. C. *Green Chemistry: Theory and Practice*; Oxford University Press New York, 1998; e) Alfonsi, K.; Colberg, J.; Dunn, P. J.; Fevig, T.; Jennings, S.; Johnson, T. A.; Kleine, H. P.; Knight, C.; Nagy, M. A.; Perry, D. A.; Stefaniak, M. *Green Chem.* **2008**, 10, 31-36.
- [5] Pfoertner, K.-H.; Oppenländer, T. Photochemistry In *Ullmann's Encyclopedia of Industrial Chemistry*; Wiley-VCH Verlag GmbH & Co. KGaA: 2012.
- [6] Narayanam, J. M.; Stephenson, C. R. *Chem. Soc. Rev.* **2011**, 40, 102-113.
- [7] Prier, C. K.; Rankic, D. A.; MacMillan, D. W. *Chem. Rev.* **2013**, 113, 5322-5363.
- [8] Teplý, F. *Collect. Czech. Chem. Commun.* **2011**, 76, 859-917.
- [9] a) Smith, C. S.; Mann, K. R. *J. Am. Chem. Soc.* **2012**, 134, 8786-8789; b) Gushurst, A. K. I.; McMillin, D. R.; Dietrich-Buchecker, C. O.; Sauvage, J. P. *Inorg. Chem.* **1989**, 28, 4070-4072; c) Armaroli, N.; Accorsi, G.; Cardinali, F.; Listorti, A. *Top. Curr. Chem.* **2007**, 280, 69-115; d) Paria, S.; Reiser, O. *ChemCatChem* **2014**, 6, 2477-2483.
- [10] Dietrich-Buchecker, C. O.; Marnot, P. A.; Sauvage, J. P.; Kintzinger, J. P.; Maltese, P. *Nouv. J. Chim.* **1984**, 8, 573-582.
- [11] Kern, J.-M.; Sauvage, J.-P. *J. Chem. Soc., Chem. Commun.* **1987**, 546-548.
- [12] Nicholls, T. P.; Constable, G. E.; Robertson, J. C.; Gardiner, M. G.; Bissember, A. C. *ACS Catalysis* **2016**, 6, 451-457.
- [13] a) Hernandez-Perez, A. C.; Vlassova, A.; Collins, S. K. *Org. Lett.* **2012**, 14, 2988-2991; b) Hernandez-Perez, A. C.; Collins, S. K. *Angew. Chem. Int. Ed.* **2013**, 52, 12696-12700.
- [14] Baralle, A.; Fensterbank, L.; Goddard, J. P.; Ollivier, C. *Chem. Eur. J.* **2013**, 19, 10809-10813.
- [15] a) Tang, X.-J.; Dolbier, W. R. *Angew. Chem. Int. Ed.* **2015**, 54, 4246-4249; b) Zhang, Z.; Tang, X.; Thomason, C. S.; Dolbier, W. R., Jr. *Org. Lett.* **2015**, 17, 3528-3531.

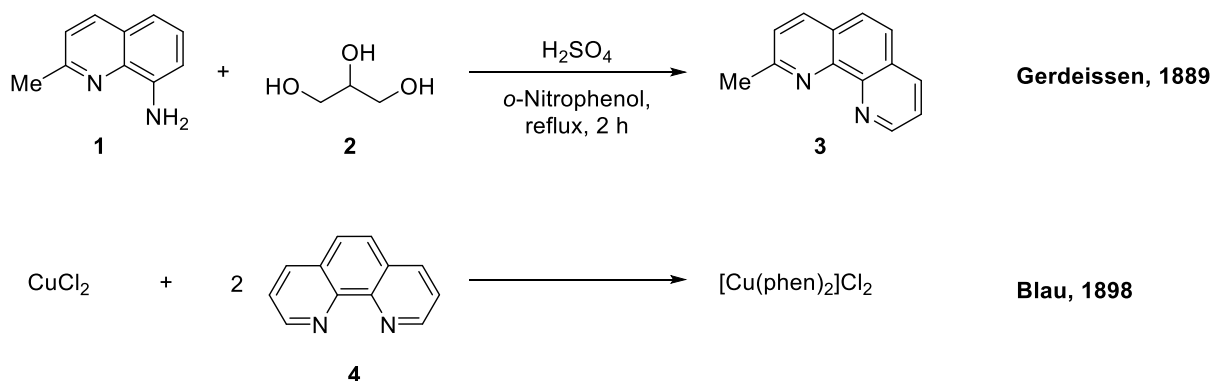
- [16] a) Fumagalli, G.; Rabet, P. T.; Boyd, S.; Greaney, M. F. *Angew. Chem. Int. Ed.* **2015**, *54*, 11481-11484; b) Rabet, P. T.; Fumagalli, G.; Boyd, S.; Greaney, M. F. *Org. Lett.* **2016**, *18*, 1646-1649.
- [17] a) Pirtsch, M.; Paria, S.; Matsuno, T.; Isobe, H.; Reiser, O. *Chem. Eur. J.* **2012**, *18*, 7336-7340; b) Reiser, O.; Paria, S.; Pirtsch, M.; Kais, V. *Synthesis* **2013**, *45*, 2689-2698; c) Bagal, D. B.; Kachkovskiy, G.; Knorn, M.; Rawner, T.; Bhanage, B. M.; Reiser, O. *Angew. Chem. Int. Ed.* **2015**, *54*, 6999-7002.
- [18] Pirtsch, M. *Photokatalyse mit [Cu(dap)₂Cl] und sichtbarem Licht*, Dissertation, Universität Regensburg, **2013**.
- [19] a) Armaroli, N. *Chem. Soc. Rev.* **2001**, *30*, 113-124; b) Wallesch, M.; Volz, D.; Zink, D. M.; Schepers, U.; Nieger, M.; Baumann, T.; Bräse, S. *Chem. Eur. J.* **2014**, *20*, 6578-6590.
- [20] Knorn, M.; Rawner, T.; Czerwieniec, R.; Reiser, O. *ACS Catalysis* **2015**, *5*, 5186-5193.

B. Synthesis of New Copper(I) Phenanthroline Complexes and Their Catalytic Activity

1. Introduction

1,10-phenanthroline (**4**) is characterized by a rigid structure with its three aromatic rings, low fluorescence quantum yield ($\Phi = 0.0087$), short singlet lifetime ($\tau < 1$ ns) and the ability to act as a triplet-state photosensitizer.^[1] In 1889, the first 1,10-phenanthroline compound was reported by Gerdeissen who described the synthesis of 2-methyl-1,10-phenanthroline (**3**).^[2] Since the first reported synthesis of a copper phenanthroline complex $[\text{Cu}(\text{phen})_2]\text{Cl}_2$ in 1898 by Blau^[3] (Scheme 1), this bidentate ligand **4** has been investigated in the early 1930s for its ability to coordinate various metals (e.g. copper, iron, nickel, platinum, or silver) and enhanced the development of analytical reagents.^[3-4]

Scheme 1. First synthetic approach towards substituted 1,10-phenanthroline and first copper phenanthroline complex.^[2-3]



In the last years, rapid progress was made in the field of visible light mediated photoredox catalysis and has established itself as a powerful technique for conducting free radical transformations. So far, the most commonly employed visible light photoredox catalysts are organic dyes or metal complexes based on ruthenium or iridium. Despite several advantages such as greater abundance, lower toxicity, and economic reasons of copper with respect to ruthenium or iridium, copper(I) phenanthrolines $[\text{Cu}(\text{NN})_2]^+$ have been much less studied than more popular ruthenium(II) polypyridine complexes. This is mainly attributed to the drawback that upon light excitation of copper(I) phenanthrolines, the metal center changes its formal oxidation state from Cu(I) to Cu(II), leading to different preferential coordination geometries in the ground (tetrahedral) and excited states (square planar), resulting in exciplex quenching.^[5] Thus, subtle structural modification of the ligands are necessary to circumvent the problem as mentioned before. Therefore, in order to tune and increase the photophysical properties, symmetric substitutions of the aromatic system, particularly at the 2,9- and 4,7-position, have

been investigated by several groups, whereas 3,8- and 5,6-substitutions are less common (Figure 1). To affect the electronic distribution of the electronic transition various functional groups were attached. For example, changing phenyl to anisyl in 2,9-position doubled the fluorescence quantum yield.^[1a,6]

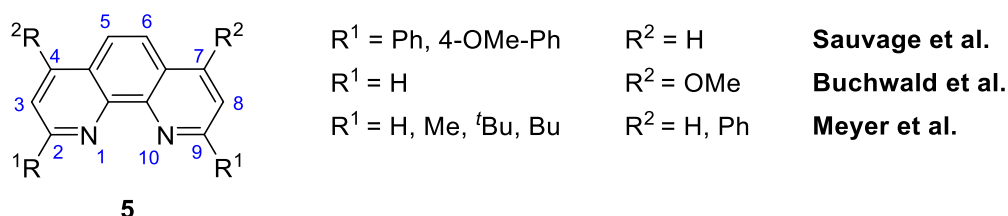


Figure 1. Substitution pattern of 1,10-phenanthroline.

The pioneering work of McMillin and co-workers reveal that the excited state of $[\text{Cu}(\text{NN})_2]^+$ tends to undergo a distinct flattening distortion (vide supra).^[7] To inhibit this distortion, bulky substituents at the 2,9-positions of 1,2-phenanthroline (**4**) have to be introduced. In 1991, Zacharias and Masood showed that *ortho* substituents of the phenyl group at the 2,9-position of 1,2-phenanthroline (**4**) improved the stability of copper(I) phenanthroline complexes compared to *para* substituents. Thus, longer excited state lifetime are expected caused by reorganization from an ideal tetrahedral to square-planar complex geometry.^[8]

Mainly three key properties have to be considered in designing new copper based photocatalysts. First, the compound has to absorb in the visible range of the light spectrum to form an excited species. Here, an elongated lifetime is efficient for transferring one electron to the copper(II) species. In addition, non-radiative quenching to the ground state should be prevented at this stage. Third, the redox potentials of possible candidates have to be considered. In photochemistry, the reduction potentials are equal to the “strength” of a given photocatalyst, resulting in the success of a reaction. Information on these key properties can be obtained by measuring UV/VIS, luminescence spectroscopy and cyclic voltammetry of the chosen compounds (Figure 2).

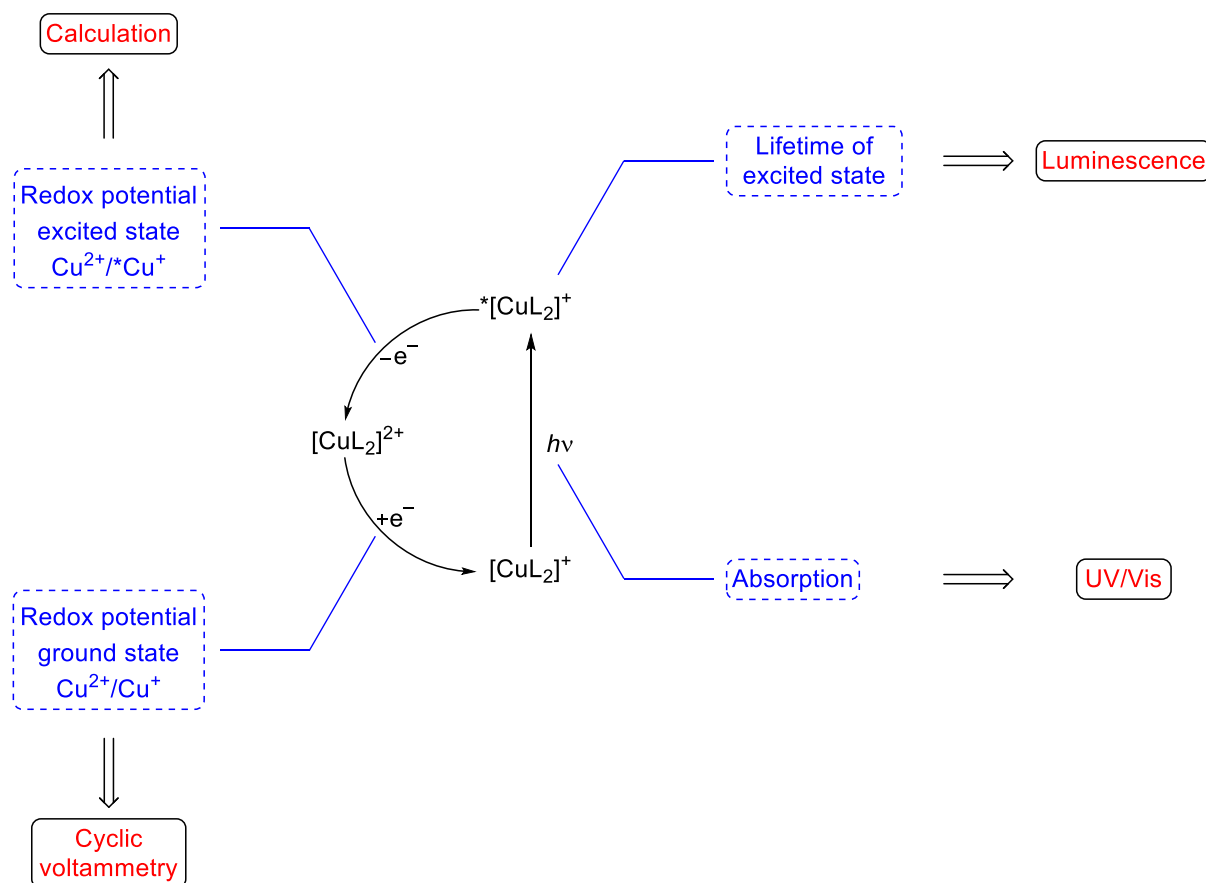


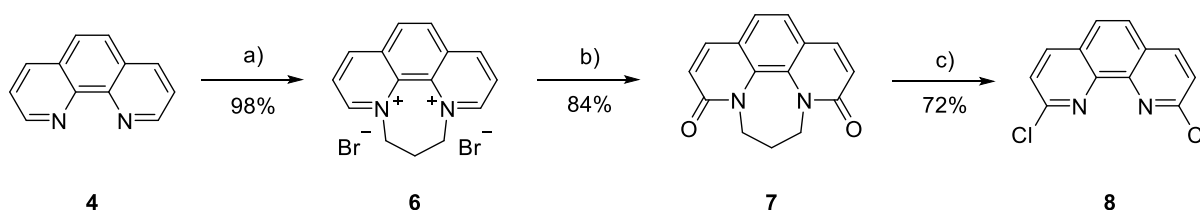
Figure 2. Key features of a photoredox catalyst and their determinations.

In literature, a variety of $[\text{Cu}(\text{NN})_2]^+$ complexes were studied regarding to their photophysical properties.^[5] However, less reports are known about their catalytic behaviour in photoredox catalysis.^[9] Since the first utilization of $[\text{Cu}(\text{dap})_2]\text{Cl}$ in visible light photoredox catalysis in 2012 as demonstrated by Reiser et al.^[10], it was decided to modify slightly the dap (2,9-bis(*para*-anisyl)-1,10-phenanthroline) core structure to compare the effects of substituents regarding to their photophysical and electrochemical properties as well as their catalytic activity. For this purpose, new copper complexes with different aryl substitution pattern in the 2,9-position of phenanthroline are synthesized, fully characterized and their catalytic performance in atom transfer radical addition (ATRA) reactions evaluated.

2. Synthesis of Copper(I) Phenanthroline Complexes

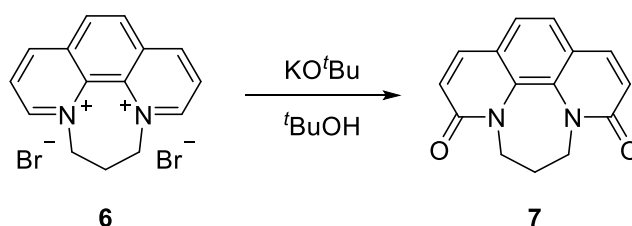
It was envisioned that aryl groups could be installed onto the 1,10-phenanthroline framework at the 2- and 9-position via Suzuki-Miyaura cross coupling. In literature, the synthesis of key intermediate **8** is mainly achieved by two routes. The first method leads to compound **8** in six steps by a monoalkylation/ oxidation/ chlorination-sequence in an overall yield of 44% as demonstrated by Lüning and co-workers.^[11] Sauvage et al. could successfully shorten the synthesis to yield 2,9-dichloro-1,10-phenanthroline (**8**) in a three step route, also starting from commercially available 1,10-phenanthroline (**4**).^[12] Therefore, the second approach was chosen and slightly modified for the synthesis of compound **8** as shown in Scheme 2.

Scheme 2. Synthesis of 2,9-dichloro-1,10-phenanthroline (**8**).^[a]



[a] Reaction conditions: a) 1,10-phenanthroline **4** (1.0 equiv), 1,3-dibromopropane (5.0 equiv), PhNO₂, 125 °C, 5 h, 98% b) KO^tBu (4.2 equiv), *t*-BuOH, 40 °C, 21 h, 84% c) PCl₅ (2.0 equiv), POCl₃, 150 °C, 21 h, 72%.

First, protection of 1,10-phenanthroline (**4**) with excess of 1,3-dibromopropane in nitrobenzene yielded quantitatively *N,N*-protected compound **6**. Initially, the oxidation of the salt **6** proved to be problematic and thus resulting in low yields. In general, the oxidation is performed using K₃[Fe(CN)₆] in basic aqueous solution.^[13] Unfortunately, even with an optimized workup best yield was obtained in 41% and the synthesis is limited for large scales. Recently, Guo and co-workers reported an improved oxidation protocol with potassium *tert*-butoxide and oxygen as oxidant in *tert*-butanol.^[14] Examination and optimization of the reaction parameters were explored using KO^tBu as the oxidizing agent and the phenanthroline salt **6** as the substrate in conjunction with various reaction conditions because no access of the mentioned paper was available (Table 1). The reactions were performed on a 2.0 mmol scale.

Table 1. Optimization for the oxidation step of *N,N*-protected compound **6**.^[a]


Entry	Base [equiv]	Temperature [°C]	Time [h]	Yield [%]
1	2.0	40	4.5	40
2	4.2	40	4.5	58
3	20.0	40	4.5	56
4	4.2	140	4.5	36
5	4.2	40	21	70
6 ^[b]	4.2	40	4.5	27
7 ^[c]	4.2	40	21	4
8 ^[d]	4.2	40	21	84

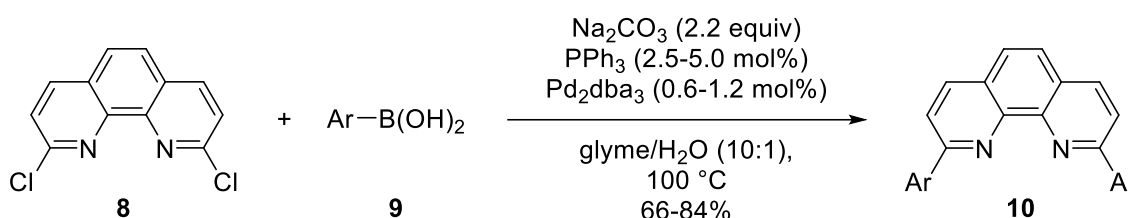
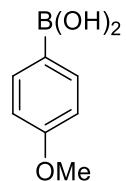
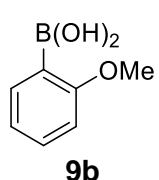
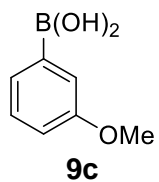
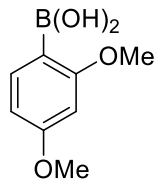
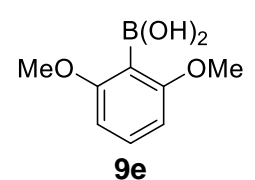
[a] Reaction conditions: *N,N*-protected compound **6** (2.0 mmol, 1.0 equiv), *t*-BuOH (1.0 mL); [b] anh. *t*-BuOH; [c] degassed *t*-BuOH; [d] 52 mmol scale.

The presence of 4.2 equivalent of potassium *tert*-butoxide proved to be slightly beneficial compared to 2.0 equivalent (Table 1, entries 1-2). Higher amounts of base had no influence (entry 3). Increasing the temperature from 40 °C to 140 °C led to lower yield resulting from competitive oxidation on different positions on the phenanthroline core (entry 4). When either anhydrous (entry 6) or degassed solvent (entry 7) were used, significantly lower yields were obtained. These results suggest that oxygen and traces of water are crucial in the oxidation step. With optimized conditions in hand, the reaction was performed on a 52 mmol scale resulting in product **7** in 84% yield (entry 8).

Then, the literature^[12] known reaction of *N,N*-annelated dione **7** with PCl_5 and POCl_3 gave rise to 2,9-dichloro-1,10-phenanthroline (**8**) in 72% yield. Subsequently, with key intermediate **8** in hand, the Suzuki-Miyaura cross coupling^[15] with boronic acid **9a-9e** were carried out yielding ligand **10a-10e** in moderate to good yields (Table 2). Reaction of halogen phenanthroline **8** with 2.2 equivalent of boronic acid **9a**, 2.0 equivalent of Na_2CO_3 , 2.5 mol% PPh_3 and 0.6 mol% Pd_2dba_3 in refluxing glyme/ H_2O (10:1) for 24 hours gave ligand **10a** directly on a 20 mmol scale in good yield (entry 1). Cross coupling of the other monosubstituted boronic acids **9b-9c** with dichlorophenanthroline **8**, under the same conditions, gave on a 1.0 mmol scale the expected coupling products **10b** and **10c** in 76% and 80% yield, respectively (entries 2-3). It is noteworthy that disubstituted ligand **10d-10e** needed a prolonged reaction time and higher amounts of palladium catalyst (entries 4-5).

It should be noted that the ligand **10a** is in literature commonly termed as “dap” instead of more precisely “*p*-dap”. For reasons of consistency, the ligand **10a** and its complex **11a** will be further termed as dap and $[\text{Cu}(\text{dap})_2]^+$, respectively.

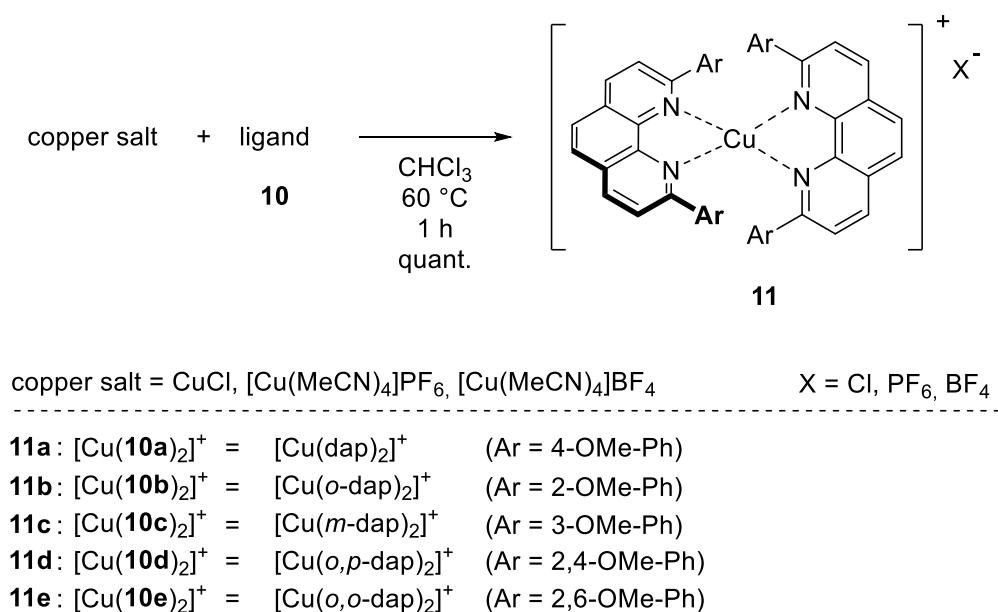
Table 2. Suzuki-Miyaura cross coupling for the synthesis of ligands **10a-10e**.^[a]

						
Entry	Boronic Acid	PPh ₃	Pd ₂ dba ₃	Time [h]	Product	Yield [%]
1 ^[b]	 9a	2.5 mol%	0.6 mol%	24	dap (Ar = <i>p</i> -OMe-Ph) 10a	84
2	 9b	2.5 mol%	0.6 mol%	24	<i>o</i> -dap (Ar = <i>o</i> -OMe-Ph) 10b	76
3	 9c	2.5 mol%	0.6 mol%	24	<i>m</i> -dap (Ar = <i>m</i> -OMe-Ph) 10c	80
4	 9d	5.0 mol%	1.2 mol%	48	<i>o,p</i> -dap (Ar = <i>o,p</i> -OMe-Ph) 10d	81
5	 9e	5.0 mol%	1.2 mol%	48	<i>o,o</i> -dap (Ar = <i>o,o</i> -OMe-Ph) 10e	66

[a] Reaction conditions: 2,9-dichloro-1,10-phenanthroline **8** (1.0 mmol, 1.0 equiv), boronic acid **9** (2.2 mmol, 2.2 equiv), Na₂CO₃ (2.2 mmol, 2.2 equiv), PPh₃ (2.5-5.0 mol%), Pd₂dba₃ (0.6-1.2 mol%), glyme/H₂O (10:1), 100 °C, 24-48 h, 66-81%; [b] 20 mmol scale: PPh₃ (5.0 mol%), Pd₂dba₃ (1.2 mol%), 48 h.

Finally, the novel homoleptic copper(I) complexes **11a-11e** were obtained in quantitative yield by reacting a solution of two equivalents of ligand **10a-10e** in chloroform with one equivalent of copper salt. After precipitation in diethyl ether or *n*-pentane, the yellowish beige to brown coloured complexes **11a-11e** could be stored for extended periods without any sign of decomposition (Scheme 3).

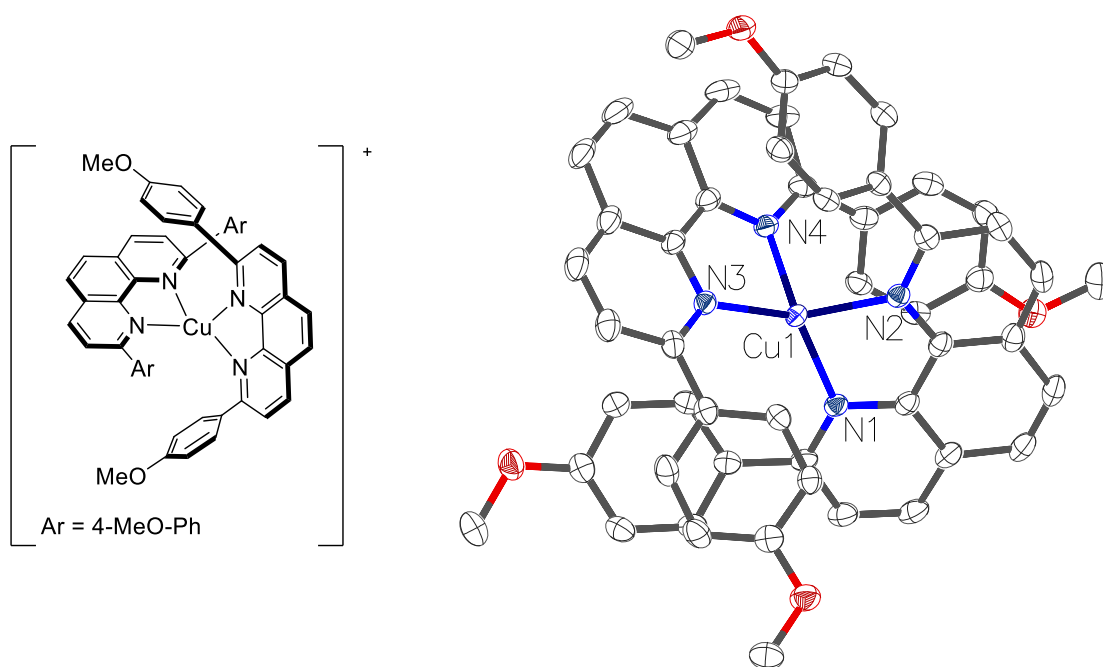
Scheme 3. Preparation of the homoleptic copper complexes **11a-11e**.



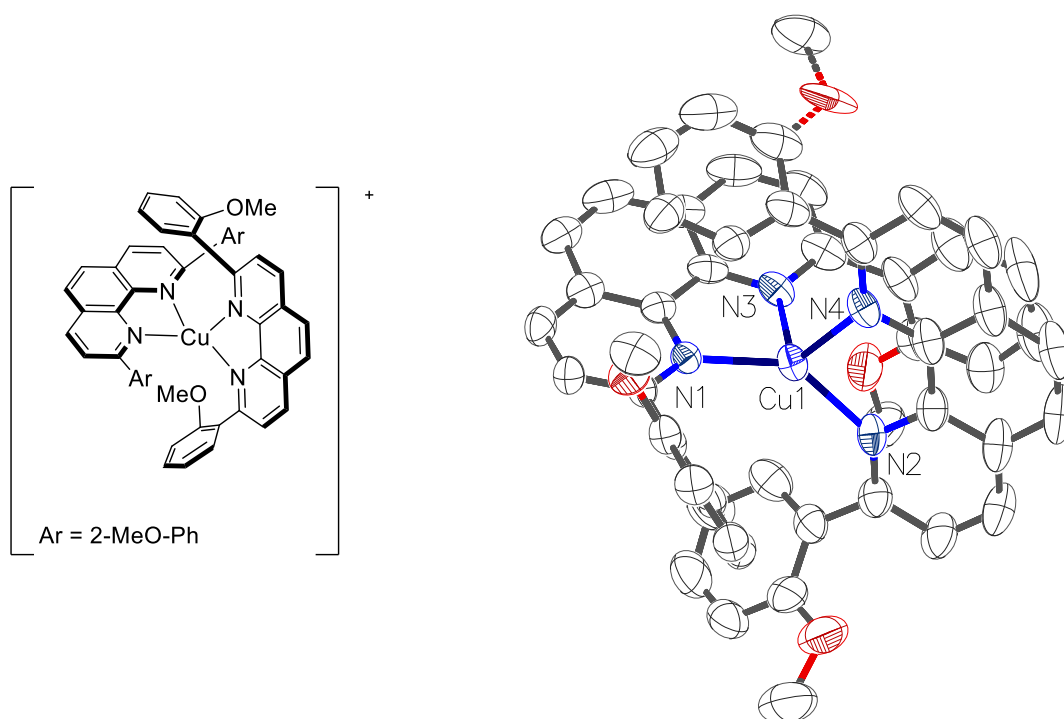
3. Characterization of Copper(I) Phenanthroline Complexes

3.1. X-ray Structures

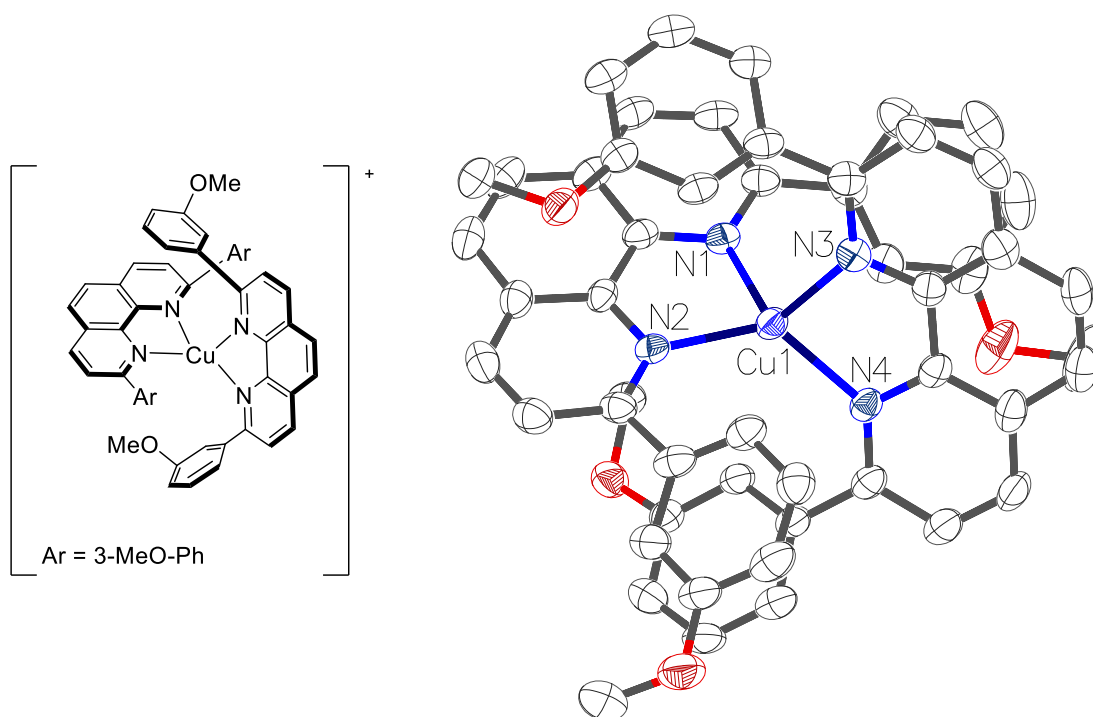
Single crystals suitable for X-ray analysis of copper catalysts **11a-11e** were obtained by vapor diffusion of Et₂O or *n*-pentane into CH₂Cl₂ solution containing [Cu(**10**)₂]X (X = BF₄, PF₆). The X-ray structures of complexes **11a-11e** and relevant distances and angles are depicted in Table 3-7. For better clarity the counterions have been removed. Compounds **11a** to **11e** are all mononuclear complexes, in which a single copper(I) atom is surrounded by two phenanthroline ligands **10a-10e**. Therefore, the geometries around the copper center are similar in all five complexes. The structural analysis of [Cu(**10a**)₂]⁺ to [Cu(**10e**)₂]⁺ indicates a flattened pseudotetrahedral coordination geometry with a dihedral angle of 70-81 ° between the mean planes of the respective ligands being in agreement with other literature reports.^[16] The bite angles are as expected in the range of 81-83 ° due to ligand rigidity and average Cu-N bond lengths are consistently around 2.054 Å.^[5b]

Table 3. X-ray structure of $[\text{Cu}(\text{dap})_2]^+$ (**11a**).

 $[\text{Cu}(\text{dap})_2]^+$ (11a**)**

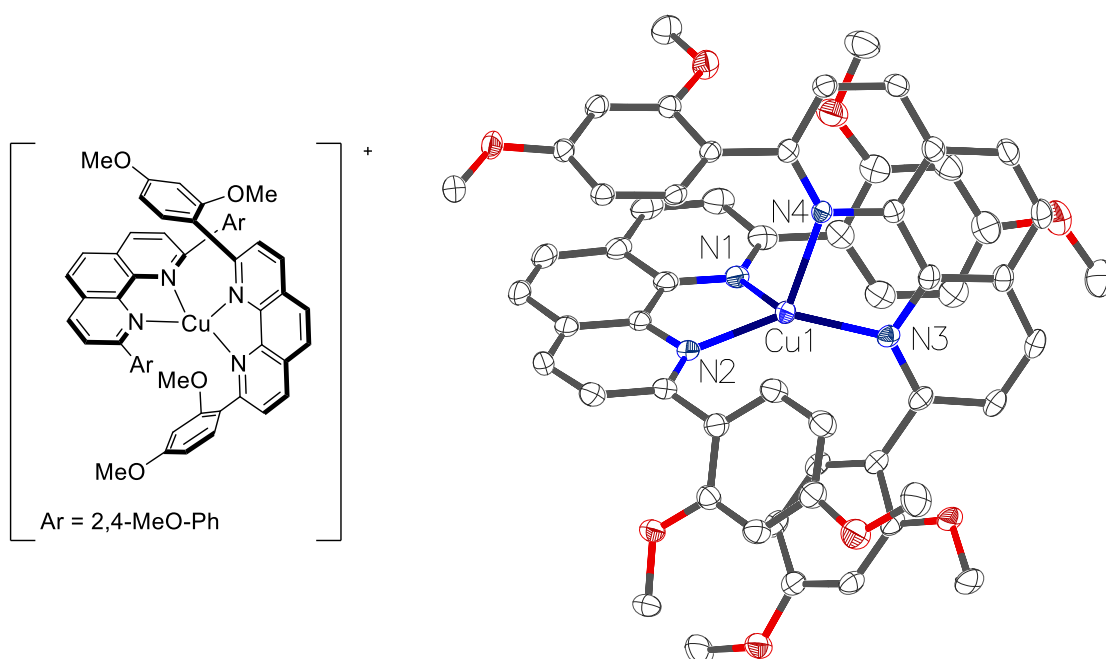
Bond Angle [deg]	
N1-Cu1-N2	83.2
N3-Cu1-N4	83.1
N3-Cu1-N1	102.6
N4-Cu1-N2	127.6
Dihedral Angle [deg]	
N1-Cu1-N2/N3-Cu1-N4	71.4
Bond Length [Å]	
Cu1-N1	2.048
Cu1-N2	2.030
Cu1-N3	2.028
Cu1-N4	2.053

Table 4. X-ray structure of $[\text{Cu}(\text{o-dap})_2]^+$ (**11b**).

 $[\text{Cu}(\text{o-dap})_2]^+$ (**11b**)

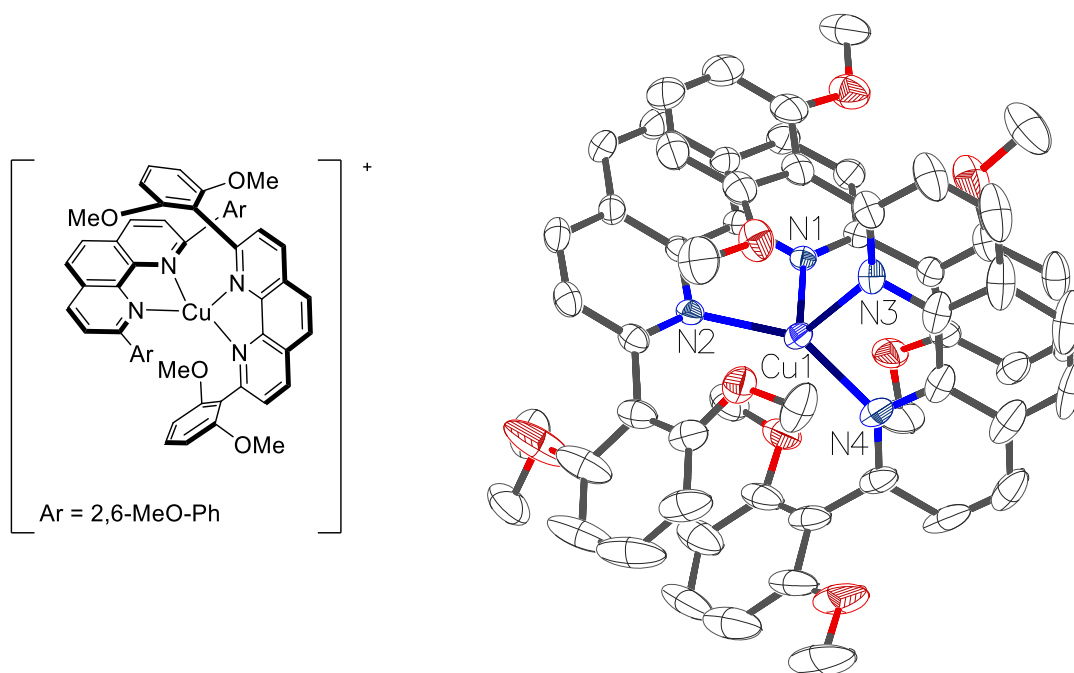
Bond Angle [deg]	
N1-Cu1-N2	82.8
N3-Cu1-N4	83.1
N3-Cu1-N1	101.2
N4-Cu1-N2	126.1
Dihedral Angle [deg]	
N1-Cu1-N2/N3-Cu1-N4	81.1
Bond Length [Å]	
Cu1-N1	2.009
Cu1-N2	2.086
Cu1-N3	2.019
Cu1-N4	2.069

Table 5. X-ray structure of $[\text{Cu}(m\text{-dap})_2]^+$ (**11c**).

 $[\text{Cu}(m\text{-dap})_2]^+$ (**11c**)

Bond Angle [deg]	
N1-Cu1-N2	82.5
N3-Cu1-N4	82.9
N3-Cu1-N1	102.4
N4-Cu1-N2	126.9
Dihedral Angle [deg]	
N1-Cu1-N2/N3-Cu1-N4	69.9
Bond Length [Å]	
Cu1-N1	2.062
Cu1-N2	2.031
Cu1-N3	2.040
Cu1-N4	2.059

Table 6. X-ray structure of $[\text{Cu}(\text{o},p\text{-dap})_2]^+$ (**11d**).

 $[\text{Cu}(\text{o},o\text{-dap})_2]^+$ (**11d**)

Bond Angle [deg]	
N1-Cu1-N2	66.8
N3-Cu1-N4	82.0
N3-Cu1-N1	142.5
N4-Cu1-N2	95.4
Dihedral Angle [deg]	
N1-Cu1-N2/N3-Cu1-N4	75.0
Bond Length [Å]	
Cu1-N1	2.016
Cu1-N2	2.117
Cu1-N3	2.022
Cu1-N4	2.101

Table 7. X-ray structure of $[\text{Cu}(\text{o,o-dap})_2]^+$ (**11e**).

 $[\text{Cu}(\text{o,o-dap})_2]^+$ (**11e**)

Bond Angle [deg]	
N1-Cu1-N2	82.6
N3-Cu1-N4	81.6
N3-Cu1-N1	95.2
N4-Cu1-N2	147.7
Dihedral Angle [deg]	
N1-Cu1-N2/N3-Cu1-N4	79.0
Bond Length [Å]	
Cu1-N1	2.118
Cu1-N2	2.016
Cu1-N3	2.160
Cu1-N4	2.005

3.2. Electronic Properties

The absorption and emission spectra of complexes **11a-11e** are depicted in Figure 3. The wavelengths and extinction coefficients are given in Table 8. The studied copper(I) phenanthroline complexes were dissolved in spectroscopic grade dichloromethane and recorded at ambient temperature for absorption spectra. The UV/Vis spectra of all complexes **11a-11e** display two intense high energy absorption bands with maxima in the wavelength range from 250 to 332 nm independent of their substitution pattern, which are assigned to $\pi\text{-}\pi^*$ ligand-centered (LC) transition of phenanthroline ligands. All complexes revealed a much less intense shoulder at longer wavelengths ($\lambda > 400$ nm) assigned to metal-to-ligand charge-transfer (MLCT), respectively. Moreover, the absorption spectra of all prepared complexes shows a geometry change on excitation, causing a more favorable (0,n)-transition state. These findings are in agreement with other homoleptic copper(I) phenanthroline complexes.^[5a]

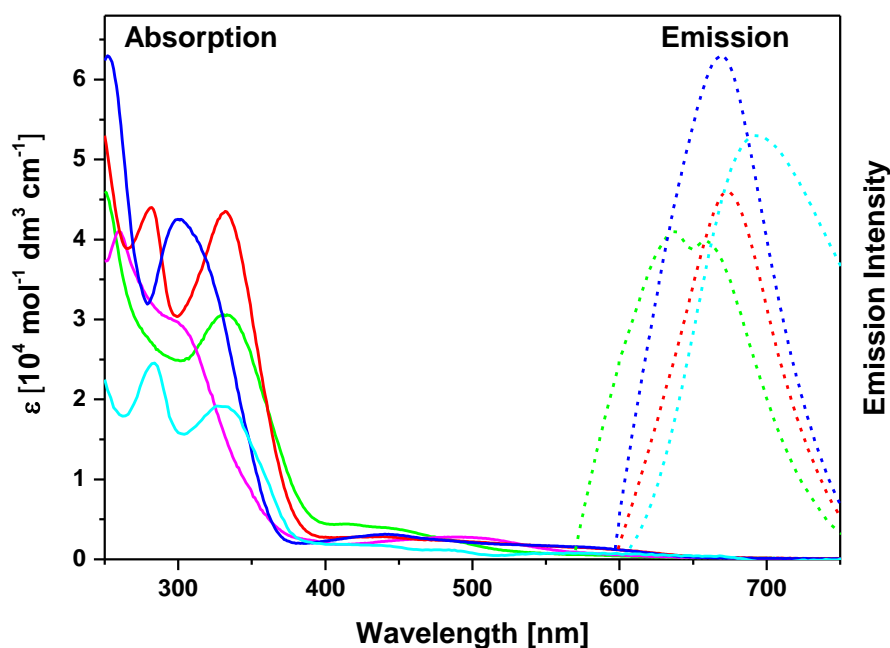


Figure 3. Absorption (full lines) and emission (dashed line) spectra of complexes **11a-11e** at ambient temperature (Cyan: $[\text{Cu}(\mathbf{10a})_2]^+$, Red: $[\text{Cu}(\mathbf{10b})_2]^+$, Blue: $[\text{Cu}(\mathbf{10c})_2]^+$, Green: $[\text{Cu}(\mathbf{10d})_2]^+$, Magenta: $[\text{Cu}(\mathbf{10e})_2]^+$).

Luminescence of complexes $[\text{Cu}(\mathbf{10a})_2]^+$ to $[\text{Cu}(\mathbf{10e})_2]^+$ were studied in PMMA (= poly(methyl methacrylate)). All investigated compounds **11a-11e** are weakly emissive at ambient temperature. They show a broad unstructured emission spectrum centered at around $\lambda_{\text{max}} = 670$ nm. An average excited state lifetime of around 0.46 μs is found for the novel complexes **11a-11d**. No emission spectra could be recorded of catalyst **11e** due to the limitation of detection of the used setup. Thus, providing an emission value lower than 600 nm and an excited state lifetime less than 0.37 μs .

Table 8. Photophysical properties of copper complexes [Cu(**10a**)₂]⁺ to [Cu(**10e**)₂]⁺.

Complex		Emission λ_{max} [nm]	Absorption λ_{Abs} [nm]	Molar Extinction Coefficient ϵ [dm ³ ·mol ⁻¹ ·cm ⁻¹]
[Cu(dap) ₂] ⁺ (11a)		690	245	4.7·10 ⁴
			331	2.3·10 ²
			455	1.6·10 ²
			530	1.3·10 ²
[Cu(o-dap) ₂] ⁺ (11b)		675	282	5.3·10 ⁴
			329	5.1·10 ⁴
			455	2.8·10 ²
			530	2.0·10 ²
[Cu(<i>m</i> -dap) ₂] ⁺ (11c)		670	252	6.3·10 ⁴
			299	4.4·10 ⁴
			455	3.3·10 ²
			530	1.6·10 ²
[Cu(o, <i>p</i> -dap) ₂] ⁺ (11d)		650	330	4.6·10 ⁴
			455	4.2·10 ³
			530	7.9·10 ²
[Cu(o, <i>o</i> -dap) ₂] ⁺ (11e)		<600	260	4.1·10 ⁴
			293	3.1·10 ⁴
			455	2.2·10 ³
			530	1.9·10 ²

All compounds **11a-11e** have allowed molar extinction coefficients in the range of $\epsilon \approx 5 \cdot 10^4 \text{ dm}^3 \cdot \text{mol}^{-1} \cdot \text{cm}^{-1}$ for $\lambda < 350 \text{ nm}$ and $\epsilon \approx 3 \cdot 10^2 \text{ dm}^3 \cdot \text{mol}^{-1} \cdot \text{cm}^{-1}$ for $\lambda > 450 \text{ nm}$ being in agreement with other literature reports.^[5a,7b,17] In principle, all complexes can be excited both with a blue as well as with a green light source. The charge-transfer (CT) absorptions are blue-shifted upon going from complex **11b** to **11c** compared to catalyst **11a** as a result of the incorporation of the electron donating methoxy group in the phenyl ring at the 2,9-positions of phenanthroline. In the case of disubstituted anisyl ring, the CT absorptions are red-shifted upon going from catalyst **11e** to **11d** compared to complex **11a**. The established [Cu(dap)₂]⁺ (**11a**) exhibits the most red-shifted absorption (331 nm) which could be a result of less interaction of the methoxy group with the copper center.

3.3. Electrochemistry

The electrochemical measurements were carried out in argon purged acetonitrile with 0.1 M tetrabutylammonium tetrafluoroborate as supporting electrolyte with use of a conventional undivided electrochemical cell, a glassy carbon working electrode, platinum wire as the counter electrode and silver wire as the reference electrode. Redox potentials were referenced against ferrocene as an internal standard and converted according to the SCE electrode.^[18] No influence of the anion ($X = \text{Cl}, \text{BF}_4, \text{PF}_6$) was observed during the measurements of copper complexes $[\text{Cu}(\mathbf{10})_2]\text{X}$.

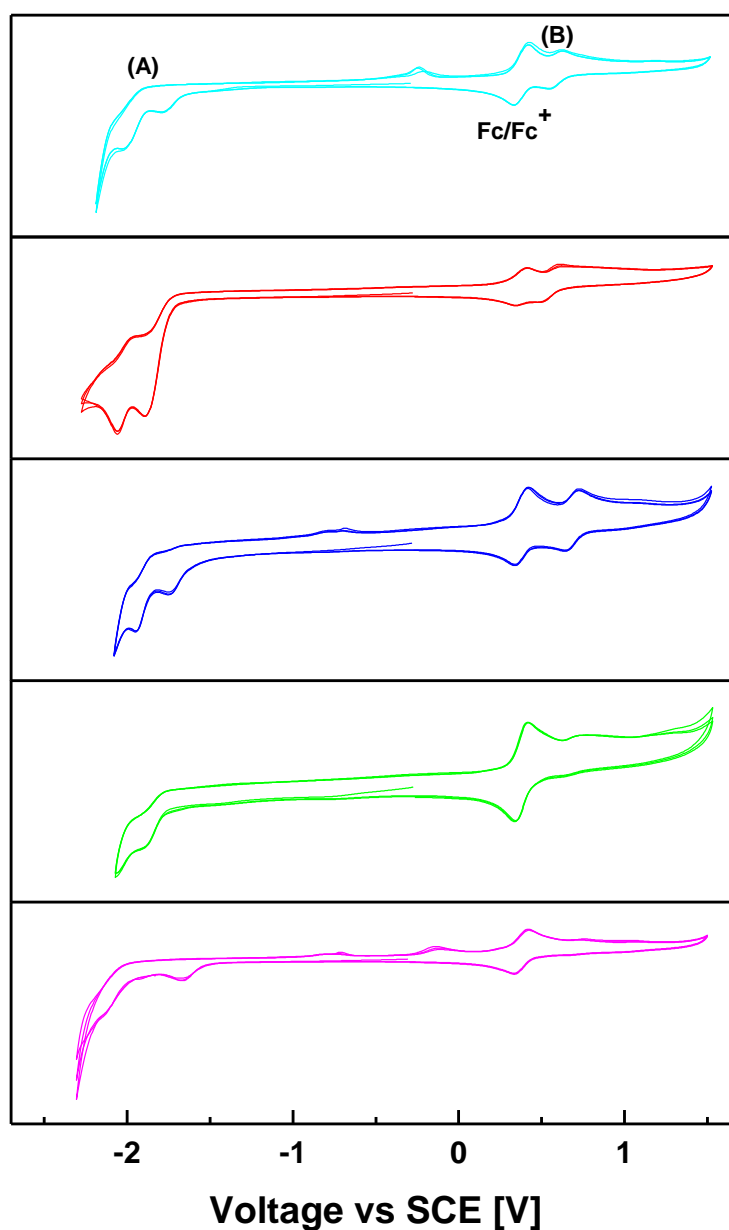


Figure 4. Cyclic voltammogram of $[\text{Cu}(\mathbf{10a})_2]\text{PF}_6$ to $[\text{Cu}(\mathbf{10e})_2]\text{PF}_6$ in MeCN using tetrabutyl ammonium tetrafluoroborate as supporting electrolyte and ferrocene as internal standard at a scan rate of $50 \text{ mV}\cdot\text{s}^{-1}$. Three cycles were run. (Cyan: $[\text{Cu}(\mathbf{10a})_2]^+$, Red: $[\text{Cu}(\mathbf{10b})_2]^+$, Blue: $[\text{Cu}(\mathbf{10c})_2]^+$, Green: $[\text{Cu}(\mathbf{10d})_2]^+$, Magenta: $[\text{Cu}(\mathbf{10e})_2]^+$).

The resulting cyclic voltammograms (Figure 4) of all five complexes **11a-11e** are consistent with a metal-based reversible oxidation step of the Cu(I)/Cu(II) couple (Wave B) and a ligand-based reduction step (Wave A). The half-wave potentials are highly dependent on the extent of the steric hindrance at the copper(I) core. Indeed, the latter undergoes a shift from tetrahedral to square planar geometry when Cu(I) changes formally to Cu(II). As a consequence, the larger the steric hindrance, the higher the potential of the metal centered oxidation.^[19] The oxidation potential of Cu(I) to Cu(II) in the disubstituted complexes **11d-11e** lie towards more positive values compared to Cu(I) to Cu(II) in complex **11a** ($E_{1/2} = 0.62$ V). Hence, they are slightly affected by the substitution pattern (vide infra). The values of the monosubstituted ligands are similar compared to [Cu(dap)₂]⁺ (**11a**). This suggests that the introduction of the methoxy group in the phenyl ring has a moderate influence on the metal-based ground state. The cathodic behavior revealed that for the monosubstituted complexes **11a-11c**, two well defined one electron reduction waves at -2.0 V vs SCE (reversible) and -1.80 V vs SCE (irreversible) are present. In contrast, disubstituted complexes [Cu(**10d**)₂]⁺ and [Cu(**10e**)₂]⁺ showed one irreversible reduction wave at -1.9 V and -2.1 V vs SCE, respectively. Therefore, these reduction waves are assigned to the addition of an extra electron in the phenanthroline moiety. To probe this assumption, independent electrochemical measurements of the ligands **10a-10e** were performed. Upon electrolysis, no further waves were monitored.

3.4. Summary of the Photophysical and Electrochemical Properties of New Copper(I) Phenanthroline Complexes

In photochemistry, the reduction potentials of the excited state are equal to the “strength” of a given photocatalyst, resulting in the success of a reaction. The excited state electrochemical potential $E^0(M^+/*M)$ [equal to $E_{1/2}(M^+/*M)$] can be approximated from the ground state electrochemical potential $E^0(M^+/M)$ and the spectroscopic energy $E_{0-0}(M \rightarrow *M)$, where M is the ground state molecule and $*M$ is the lowest excited state molecule (eq 1). $E^0(M^+/M)$ is obtained from cyclic voltammetry [equal to standard reduction potential $E_{1/2}(M^+/M)$] and given in Volt unit. $E_{0-0}(M \rightarrow *M)$ can be estimated from emission spectra and is given in eV unit. The redox couple $E^0(*M/M^-)$ can be approximated in the same way (eq 2).^[20]

$$E^0(M^+/*M) = E_{1/2}(M^+/*M) = E^0(M^+/M) - E_{0-0}(M \rightarrow *M) \quad (\text{eq 1})$$

$$E^0(*M/M^-) = E_{1/2}(*M/M^-) = E^0(M/M^-) + E_{0-0}(M \rightarrow *M) \quad (\text{eq 2})$$

For example, the value $E_{0-0}(\text{Cu}^+ \rightarrow *\text{Cu}^+)$ of $[\text{Cu}(\text{dap})_2]^+$ (**11a**) is 2.05 eV and $E_{1/2}(\text{Cu}^{2+}/\text{Cu}^+) = 0.62$ V. After conversion of eV to V, the redox potential of the excited complex $*[\text{Cu}(\text{dap})_2]^+$ (**11a**) can be calculated (eq 3):

$$E_{1/2}(\text{Cu}^{2+}/*\text{Cu}^+) = E_{1/2}(\text{Cu}^{2+}/\text{Cu}^+) - E_{0-0}(\text{Cu}^+ \rightarrow *\text{Cu}^+) = 0.62 \text{ V} - 2.05 \text{ V} = -1.43 \text{ V} \quad (\text{eq 3})$$

In analogy, the redox couple $E_{1/2}(\text{Cu}^{2+}/*\text{Cu}^+)$ of the other copper complexes **11b-11e** can be calculated. Based on the electrochemical and spectroscopic measurements *vide supra*, the photophysical properties (e.g. reduction potential, excited state life times) of copper complexes **11a-11e** are summarized in Table 9.

Table 9. Photophysical properties of copper complexes **11a-11e**.

Entry	Complex	Emission λ_{max} [nm]	Excitation λ_{max} [nm]	Excited state lifetime τ [μs]	$E_{1/2}$ ($\text{Cu}^{2+}/\text{Cu}^+$) [V]	$E_{1/2}$ ($\text{Cu}^{2+}/*\text{Cu}^+$) [V] ^[a]
1	$[\text{Cu}(\text{dap})_2]^+$ (11a)	690	434	0.50	0.62	-1.43
2	$[\text{Cu}(\text{o-dap})_2]^+$ (11b)	675	469	0.47	0.70	-1.26
3	$[\text{Cu}(\text{m-dap})_2]^+$ (11c)	670	441	0.44	0.69	-1.16
4	$[\text{Cu}(\text{o,p-dap})_2]^+$ (11d)	650	447	0.41	0.70	-1.20
5	$[\text{Cu}(\text{o,o-dap})_2]^+$ (11e)	<600	467	<0.37	0.71	-

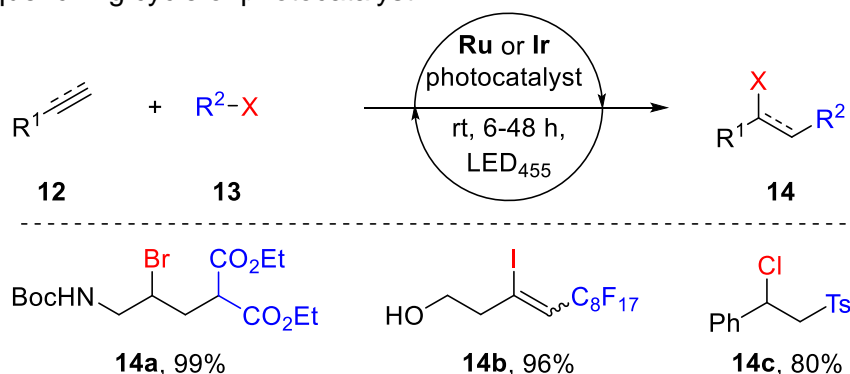
[a] calculated using equation 1.

Considering the obtained spectroscopic data with the electrochemical measurements, a reduction potential of $^*\text{Cu(II)}$ to Cu(I) is appraised to be -1.16 to -1.26 V vs SCE for catalysts **11b-11e**. The highest reduction potential in the excited state is still achieved by complex **11a** with -1.43 V vs SCE (entry 1). The new copper(I) phenanthroline complexes **11b** to **11e** are slightly stronger oxidants compared to established $[\text{Cu(dap)}_2]^+$ (**11a**) and are in the range of Ir(IV) to Ir(III) ($E_{1/2} = +0.77$ V vs SCE) in *fac*-Ir(ppy)₃. Importantly, the excited state of $^*[\text{Cu(10)}_2]^+$ is a much more potent electron donor towards most common used ruthenium or iridium catalysts, e.g. $^*\text{Ru(III)}$ to Ru(II) ($E_{1/2} = -0.81$ V vs SCE) in $[\text{Ru(bpy)}_3]^{2+}$.^[21] Other parameters like molar extinction coefficient ϵ or excited state lifetime τ seem to disfavor $[\text{Cu(10)}_2]^+$ vs $[\text{Ru(bpy)}_3]^{2+}$. However, this does not mean to be a severe drawback. Nevertheless, it is crucial to understand how modification of the phenanthroline ligand improve the photophysical properties and therefore the catalytic activity. Since copper(I) phenanthroline complexes cannot mediate photocatalyzed reactions via a reductive quenching cycle,^[1a,5a,22] this property facilitate both mechanistic investigations and side reactions. This suggests that copper(I) phenanthroline complexes can be an interesting alternative to well established ruthenium photocatalysts.

4. Catalysis

In the redox neutral atom transfer radical addition (ATRA) or also known as Kharasch addition, the atom transfer reagent, commonly haloalkanes, undergoes a σ -bond cleavage and is then added to a π -bond of an alkene or alkyne, respectively.^[21] This environmental friendly process forms simultaneously a carbon-carbon and a carbon-halogen bond without loss of atoms being in agreement with the concept of atom economy.^[23] Earlier procedures for this efficiently difunctionalization of alkenes/alkynes used radical initiators, UV light, or transition metal catalysts under thermal conditions.^[24] Recent effort have been made to develop an mild and efficient ATRA protocol with broad substrate scope.^[25] In 2012, Stephenson et al. developed the first visible light mediated atom transfer radical addition of haloalkanes **13** onto alkenes and alkynes **12** using the reductive or oxidative quenching cycle of $[\text{Ir}\{\text{dF}(\text{CF}_3)\text{ppy}\}_2(\text{dtbbpy})]\text{PF}_6$ and $[\text{Ru}(\text{bpy})_3]\text{Cl}_2$ (Scheme 4).^[26] The authors could demonstrate that careful selection and modification of parameters such as catalyst, additives, and solvent could predict the outcome of the reaction.

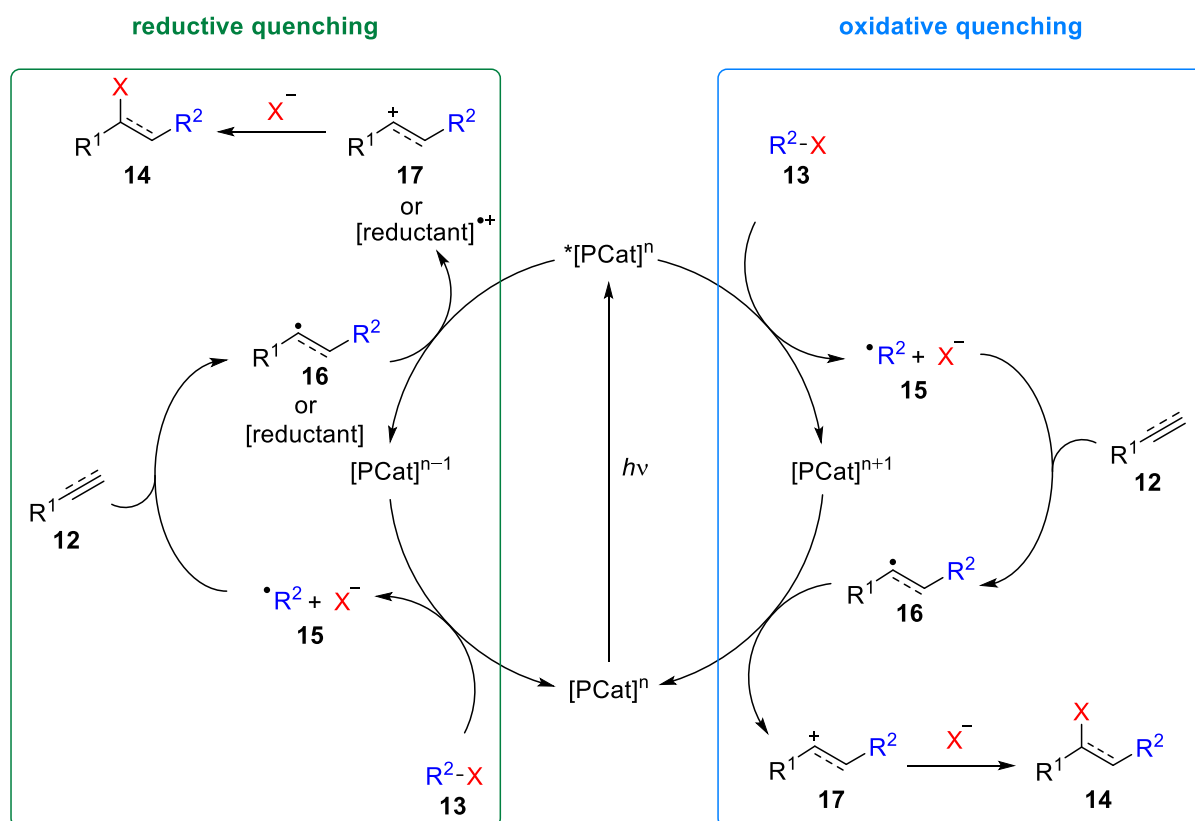
Scheme 4. First visible light mediated atom transfer radical addition reaction via an oxidative or reductive quenching cycle of photocatalyst.^[26]



The proposed mechanism for the visible light induced ATRA reaction is depicted in Scheme 5. In principle, the photoredox catalyst $[\text{PCat}]^n$ can undergo two productive pathways, an oxidative or a reductive quenching cycle in which single electron transfer (SET) steps can occur, respectively. After irradiation of the photocatalyst a stable and short-lived excited $^*[\text{PCat}]^n$ is populated followed by intersystem crossing (ISC) to form a more stable triplet state.^[21] The excited species transfer an electron to the ATRA reagent **13** giving rise to an oxidized metal species $[\text{PCat}]^{n+1}$, an alkyl radical and a halogen anion **15** which is in respect to the metal called oxidative quenching cycle. Trapping of the formed radical **15** with an alkene/alkyne **12** generates after an electron back transfer to the photocatalyst the carbocation **17** thus closing the catalytic cycle. Subsequently, nucleophilic attack of the halide produces the desired product **14**. Furthermore, radical **16** can alternatively abstract a halogen atom from the ATRA reagent **13** initiating a radical chain mechanism. In the reductive

quenching cycle a reductant also known as sacrificial electron donor, is necessary to start the cycle. In analogy, after single electron transfer to the haloalkane **13** followed by forming the radical **15**, this intermediate is trapped by an alkene/alkyne **12**. Depending on the reaction conditions both cycles can be utilized for chemical transformations.

Scheme 5. Mechanistic pathway for the visible light induced ATRA reaction.



4.1. Atom Transfer Radical Addition

Having addressed the synthesis, characterization, spectroscopic, and electrochemical properties of the new copper complexes **11b-11e**, their catalytic activity for the visible light mediated photoredox catalysis compared to established $[\text{Cu}(\text{dap})_2]\text{Cl}$ (**11a-Cl**) was investigated (Table 10). As model reaction the visible light induced atom transfer radical addition (ATRA) was chosen, for which previously the efficiency of $[\text{Cu}(\text{dap})_2]\text{Cl}$ (**11a-Cl**) upon irradiation at green light (530 nm) was demonstrated.^[10,27] The reactions were performed on a 1.0 mmol scale employing 1.0 mol% copper catalyst **11a-Cl** to **11e-Cl** and 2.0 equivalents of the ATRA reagent in anhydrous acetonitrile for 17-48 hours. For better comparison all reactions were irradiated with a green LED. Moreover, the potential carbon-halogen bond cleavage initiated by blue light, which is higher in energy than green light, is mainly ruled out. In addition, the alteration of light source (green to blue LED) resulted in no significant change of yield. Furthermore, other copper(I) phenanthroline salts such as $[\text{Cu}(\textbf{10})_2]\text{PF}_6$ and $[\text{Cu}(\textbf{10})_2]\text{BF}_4$ were similarly effective as $[\text{Cu}(\textbf{10})_2]\text{Cl}$.

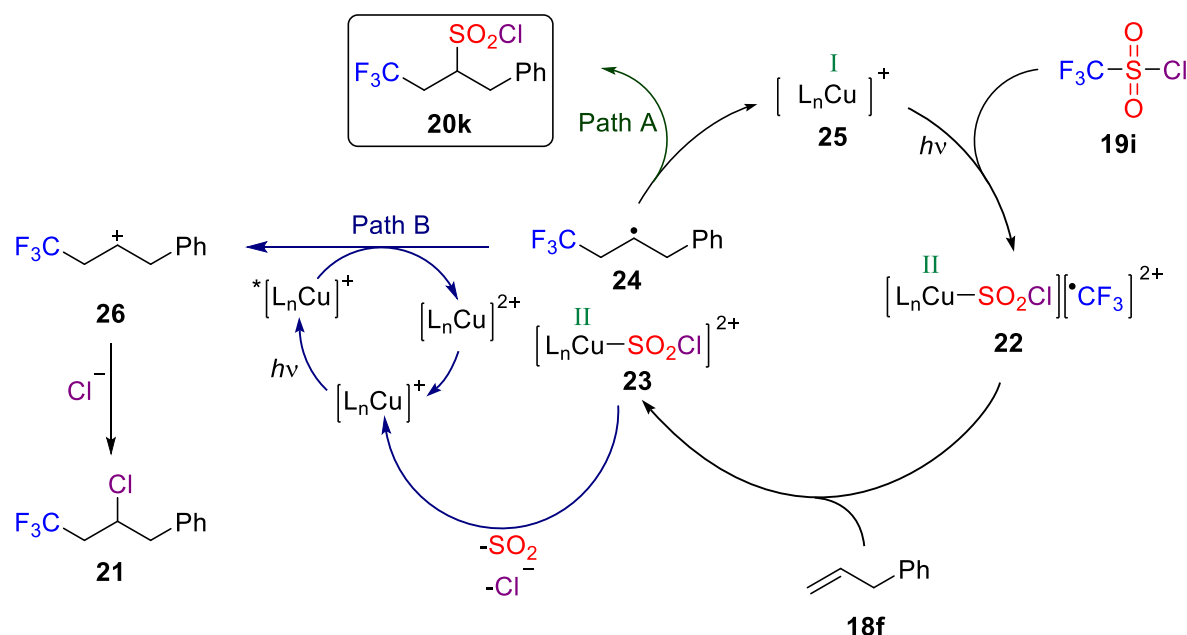
Tetrabromomethane (entry 1) and CBrCl_3 (entry 2) cleanly reacted with styrene (**18a**) or the radical clock **18b**, gave rise to the ATRA products **20a** and **20b** in good to excellent yields for all catalysts. Recently, Zeidler and co-workers reported a visible light mediated activation of polyhalomethanes where no photocatalyst is required.^[28] These results imply that already the highly activated carbon-halogen bond can be easily cleaved by means of visible light being in full agreement with the findings reported *vide supra*. Furthermore, applying *N*-Boc-allylamine (**18c**) afforded 1,2-adduct **20c** in good yields for all investigated monosubstituted complexes **11a-11c** (entry 3), albeit moderate yields for catalyst **11d** and **11e**. *De novo*, these results suggest that the carbon-halogen bond of diethyl bromomalonate (**19c**) can be already cleaved by light. Control experiments refuted this assumption.

The ATRA reaction between styrene (**18a**) and *para*-nitrobenzylbromide (**19d**) in the presence of $[\text{Cu}(\textbf{10a})_2]\text{Cl}$, $[\text{Cu}(\textbf{10b})_2]\text{Cl}$, or $[\text{Cu}(\textbf{10c})_2]\text{Cl}$ resulted in the smooth formation of product **20d** (entry 4). In contrast, no reaction was observed when catalyst **11d** or **11e** were employed. These results can be explained by the less excited state lifetime of complexes **11d** and **11e**. Attempts to use 4-cyano benzyl (**19e**) (entry 5) or 4-methylsulfonyl bromide (**19f**) (entry 6) as ATRA reagent resulted in complete recovery of the starting material, although based on the estimated reduction potential of novel copper catalysts, these substrates should be sufficiently activated for the initial C-Br bond cleavage ($E_{1/2} = -0.95$ V for NO_2 **19d**, -1.39 V for CN **19e** and -1.43 V for SO_2Me **19f** vs SCE). As expected, no reaction with benzylbromide (**19g**) itself was observed due to its high reduction potential (entry 7).^[29]

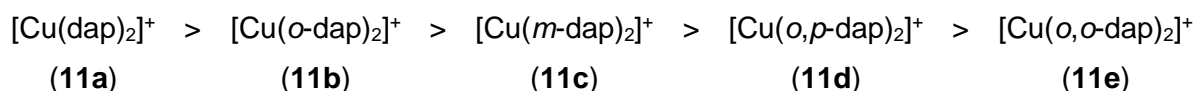
The addition of fluorine tag **19h** on styrene (**18a**) or phenylacetylene (**18d**) resulted in lower yield compared to known $[\text{Cu}(\text{dap})_2]\text{Cl}$ (**11a-Cl**) (entry 8 and 9) but showed the same *E/Z*-ratio of 92:08 (entry 11). The addition of diethyl bromomalonate (**19c**) to allyltrimethylsilane (**18e**) proceeded smoothly with $[\text{Cu}(\text{dap})_2]\text{Cl}$ (**11a-Cl**) (entry 10). A drop in yield by the factor of three was observed when catalyst **11b-Cl** and **11c-Cl** were employed. Even worse results were obtained when disubstituted complexes **11d-Cl** and **11e-Cl** were applied, showing again the low catalytic activity of these catalysts.

Intrestingly, when copper catalysts **11b-Cl** to **11e-Cl** were applied in the visible light mediated trifluoromethylchlorosulfonylation of allylbenzene (**18f**) with triflyl chloride (**19i**), the preference for the trifluoromethylsulfonylated product **20k** decreased dramatically from the ratio **20k/21** = 95:05 to ca. **20k/21** = 50:50 besides lower yields were obtained (entry 11). It is assumed that higher oxidation potential of catalyst $E_{1/2}(\text{Cu}^{2+}/\text{Cu}^+)$ results in faster oxidation of the formed radical **24** to its carbocation **26** (Scheme 6, Path B). Therefore, the catalyzed reaction is likely to proceed by an outer sphere mechanism in which upon electron transfer to the copper intermediate, the elusive SO_2Cl ligand fragments with concurrent loss of sulfur dioxide to yield trifluoromethylchlorination product **21** as already seen with $[\text{Ru}(\text{bpy})_3]\text{Cl}_2$ and *fac*- $\text{Ir}(\text{ppy})_3$.^[27a] Furthermore, $[\text{Cu}(\text{dap})_2]\text{Cl}$ (**11a-Cl**) can presumably coordinate SO_2Cl more efficiently due to less steric hindrance thus retaining the reactive intermediate in the inner coordination sphere and therefore slowing down the reaction (Path A). In addition, complex **11a** shows the lowest oxidation potential and cannot efficiently oxidize the alkyl radical **24** following an inner sphere mechanism. These observations suggest that catalysts **11b-Cl** to **11e-Cl** are preferable to perform the free radical addition pathway as competitive process which are established for the photoredox catalyzed ATRA reaction.^[21,26,30]

Scheme 6. Mechanistic explanation for the new ratio of products **20k/21**.



Finally, on the basis of the present results the following catalytic activity order can be written:



In all cases best results were achieved with established catalyst $[\text{Cu}(\text{dap})_2]\text{Cl}$ (**11a-Cl**). All catalysts **11a-11e** were in principle able to perform the ATRA reaction. The monosubstituted complexes **11a-11c** showed in contrast to disubstituted catalysts **11d-11e** in all investigated reactions higher yields due to longer excited state lifetimes and redox potentials. Moreover, $[\text{Cu}(\text{o-dap})_2]\text{Cl}$ (**11b-Cl**) was marginal better than $[\text{Cu}(\text{m-dap})_2]\text{Cl}$ (**11c-Cl**) being in good agreement with the measured photochemical and electrochemical data vide supra. When disubstituted catalysts $[\text{Cu}(\text{o,p-dap})_2]\text{Cl}$ (**11d-Cl**) and $[\text{Cu}(\text{o,o-dap})_2]\text{Cl}$ (**11e-Cl**) were employed in the ATRA protocol low yields or in worst case no reactions were obtained. These results showed that copper complexes bearing disubstituted anisyl pattern in the 2,9-position of phenanthroline have in contrast to monosubstituted ligands a low catalytic activity. Besides, the synthesis of ligand **10d** and **10e** which needed prolonged reaction time and higher catalyst loading, disfavor $[\text{Cu}(\text{10d})_2]\text{Cl}$ and $[\text{Cu}(\text{10e})_2]\text{Cl}$ for its application in photocatalysis. Unfortunately, no catalytic improvement was achieved by varying the phenanthroline ligand in respect to $[\text{Cu}(\text{dap})_2]\text{Cl}$ (**11a-Cl**). Therefore, no further investigations were performed in ligand modification.

4.2. Allyltrimethylsilane as Alkylating Agent

In order to increase the excited state lifetime of copper(I) phenanthroline complexes two approaches are known in literature thus providing better catalytic activities. Castellano et al. showed homoleptic copper(I) phenanthroline complexes with excited state lifetimes of 1.2 μ s using special designed ligands.^[31] Alternatively, heteroleptic copper(I) phenanthroline complexes have been proposed where one phenanthroline ligand is exchanged by a better π -acceptor ligand such as bidentate phosphine or isonitrile increasing the electron density at the metal center.^[32] For instance, the complex $[\text{Cu}(\text{dmp})(\text{DPEphos})]^+$ with a lifetime of 14.3 μ s was studied as sensitizer for the photocatalytic water reduction as demonstrated by McMillin and co-workers.^[32a] Nevertheless, rare catalytic applications are known in the literature although of their superior properties.^[5] In the course of further improvement and investigations of copper(I) phenanthroline complexes for the photoredox catalyzed ATRA reactions in the Reiser group, new heteroleptic complexes bearing one dap ligand **10a** were investigated.

In 2012, Reiser and co-workers could demonstrate the visible light mediated copper catalyzed reaction of allyl tributyltin with organohalides. Attempts to utilize allyltrimethylsilane (**18e**) as an ecologically more benign alternative was successfully in only one example.^[10] Therefore, in cooperation with M. Knorn, it was discussed the question whether the homoleptic $[\text{Cu}(\text{dap})_2]^+$ (**11a**) or the new heteroleptic complexes **27** and **28** could engage in this barley investigated process.

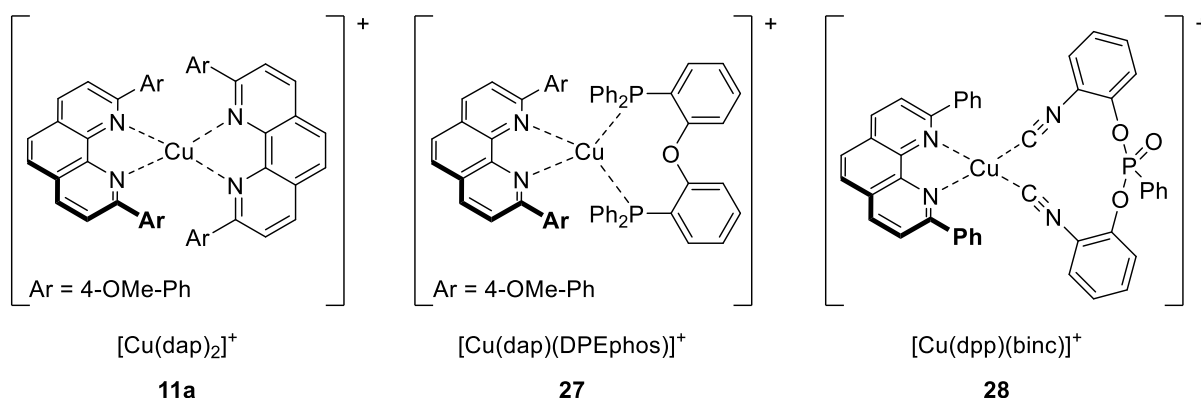


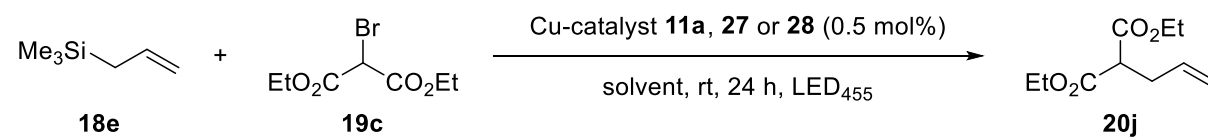
Figure 5. Homoleptic and heteroleptic copper(I) complexes.

The novel heteroleptic copper(I) complex **28** was obtained in quantitative yield by reacting an equimolar solution of two ligands in dichloromethane with $[\text{Cu}(\text{MeCN})_4]\text{BF}_4$ as demonstrated by M. Knorn.^[33] Screening of various phenanthroline ligands revealed that no catalytic improvement of the methoxy group in ligand **10a** was present. Therefore, commercially available 2,9-diphenyl-1,10-phenanthroline (dpp) as a replacement for dap (**10a**) was chosen.^[33] In contrast, $[\text{Cu}(\text{dap})(\text{DPEphos})]\text{BF}_4$ (**27-BF₄**) was prepared by stirring a solution of copper salt and bis(2-(diphenylphosphanyl)phenyl)ether (DPEphos) in CH_2Cl_2 for one hour at

room temperature followed by addition of ligand **10a** to yield the heteroleptic complex **27-BF₄**. When an equimolar amount of mixed ligands were reacted with [Cu(MeCN)₄]BF₄ homoleptic [Cu(dap)₂]BF₄ (**11a-BF₄**) was obtained being in agreement with other literature reports.^[34]

Having the new heteroleptic complexes **27** and **28** in hand, their catalytic activity was investigated for the visible light induced ATRA reaction between allyltrimethylsilane (**18e**) and diethyl bromomalonate (**19c**) where [Cu(dap)₂]⁺ (**11a**) proved to be a capable catalyst (vide supra). The reactions were performed on a 1.0 mmol scale employing 0.5 mol% of heteroleptic copper(I) catalyst **27-BF₄** and **28-BF₄** for 24 hours or rather 1.0 mol% of [Cu(dap)₂]BF₄ (**11a-BF₄**) for 48 hours. All reactions were irradiated with a blue LED. Yields were determined with dicyanobenzene as internal standard. The optimization of the alkylation process and the necessity of catalyst and light was already shown by the work of M. Knorn for [Cu(dpp)(binc)]BF₄ (**28-BF₄**).^[33] Analogue control experiments revealed that omission of light (entry 4) and catalyst **11a-BF₄** or **27-BF₄** (entry 5) resulted in no reaction (Table 11). Subsequently, when the literature reaction conditions of M. Pirtsch^[10] were applied only traces of product **20i** were obtained in the case of homoleptic complex **11a-BF₄** (entry 1) or low yields for [Cu(dap)(DPEphos)]BF₄ (**27-BF₄**) or [Cu(dpp)(binc)]BF₄ (**28-BF₄**). Moreover, acetonitrile showed slightly improved results (entry 2). In fact, it was found that 0.5 mol% (heteroleptic) or 1.0 mol% (homoleptic) of copper catalyst, three equivalents of allyltrimethylsilane (**19e**) in acetonitrile and irradiation with a blue LED for 24 hours (heteroleptic copper(I) complex) respectively 48 hours (homoleptic copper(I) complex) furnishes the allylated product **20j** in good yield (entry 3). The higher activity of the complex [Cu(dpp)(binc)]⁺ (**28**) and [Cu(dap)(DPEphos)]⁺ **27**) compared to the [Cu(dap)₂]⁺ (**11a**) is due to longer excited state lifetimes.^[22,32a,35] Hence, they promote photocatalytic reactions more efficient.

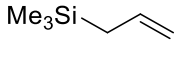
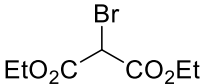
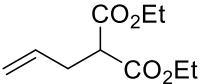
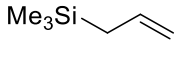
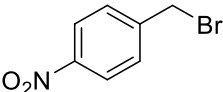
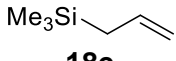
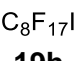
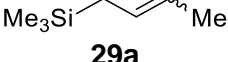
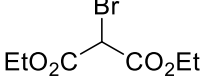
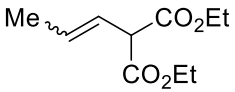
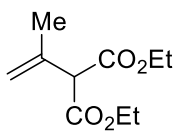
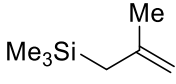
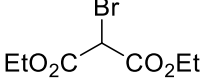
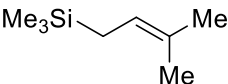
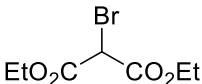
Table 11. Optimization and control experiments for the visible light mediated allylation of diethyl-bromomalonate, allyltrimethylsilane and various copper complexes.^[a]

					
Entry	Silane : Halide 18d : 19h	Solvent	Yield [%]		
			11a ^[b]	Cu-catalyst 27	28 ^[c]
1 ^[d]	1:1	DMF/H ₂ O (4:1)	5	23	30
2	1:1	MeCN	7	40	45
3	3:1	MeCN	67	75	77
4 ^[e]	3:1	MeCN	nr	nr	nr
5 ^[f]	3:1	MeCN	nr	nr	nr

[a] Reaction conditions: diethyl bromomalonate **19c** (1.0 mmol, 1.0 equiv), catalyst **11a-BF₄**, **27-BF₄** or **28-BF₄** (0.5 μmol, 0.5 mol%) in anh. solvent (1.0 mL), irradiation at 455 nm (blue LED), 24 h, rt, yield determined with 1,4-dicyanobenzene as internal standard; [b] catalyst loading 1.0 mol%, reaction time 48 h; [c] reaction performed by M. Knorn; [d] additive LiBr (1.0 mmol, 1.0 equiv); [e] dark reaction; [f] no catalyst.

Similar to the ATRA reaction, the performance of heteroleptic copper (I) phenanthroline catalysts **27** and **28** in the allylation of organohalides **19** with allyltrimethylsilane derivatives **29** were evaluated. Thus, the efficiency of the copper complexes [Cu(dap)₂]**BF**₄ (**11a-BF**₄), [Cu(dap)(DPEphos)]**BF**₄ (**27-BF**₄) and [Cu(dpp)(binc)]**BF**₄ (**28-BF**₄) was tested using 0.5 mol% of catalyst and three equivalents of silane **29** at room temperature under visible light conditions (Table 12).

Table 12. Visible light induced allylation of organohalides with allyltrimethylsilanes **29** and various copper complexes as photoredox catalyst.^[a]

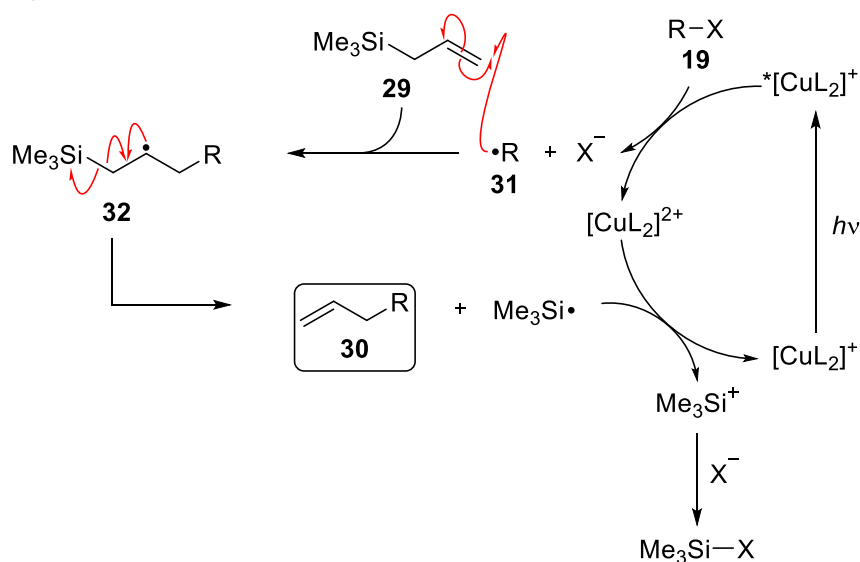
$ \begin{array}{c} \text{Me}_3\text{Si}-\text{CH}_2-\text{CH}=\text{CH}-\text{R}^1 \\ \mathbf{29} \end{array} + \begin{array}{c} \text{R}^2-\text{X} \\ \mathbf{19} \end{array} \xrightarrow[\text{anh. MeCN, rt, 24-48 h, LED}_{455}]{\text{Cu-catalyst } \mathbf{11a}, \mathbf{27} \text{ or } \mathbf{28} (0.5 \text{ mol}\%)} \begin{array}{c} \text{CH}_2=\text{CH}-\text{CH}(\text{R}^1)-\text{R}^2 \\ \mathbf{30} \end{array} $						
Entry	Alkene	Halide	Product	Yield [%]		
				Cu-catalyst 11a ^[b]	27	28
1	 18e	 19c	 20j	61	65	64 ^[c]
2	 18e	 19d	-	nr	nr	nr ^[c]
3	 18e	 19h	-	nr	nr	nr
4 ^[d]	 29a	 19c	 30a	74	78	80
			 30b	30a/30b = 84:16		
5	 29b	 19c	-	0	0	0
6	 29c	 19c	-	0	0	0

[a] Reaction conditions: halide **19** (1.0 mmol, 1.0 equiv), silane **29** (3.0 mmol, 3.0 equiv), catalyst **11a-BF**₄, **27-BF**₄ or **28-BF**₄ (0.5 μmol, 0.5 mol%) in anh. solvent (1.0 mL), irradiation at 455 nm (blue LED) for 24 h; [b] reaction time 48 h, catalyst loading 1.0 mol%; [c] reaction performed by M. Knorn; [d] in all cases, the ratio of **30a/30b** was equal.

In all reactions, the heteroleptic copper(I) phenanthroline complexes were more active than $[\text{Cu}(\text{dap})_2]^+$ (**11a**) and the reaction proceeded much faster. Comparable yields with homoleptic catalyst **11a** were obtained when the reactions were performed more prolonged. Best results were achieved with $[\text{Cu}(\text{dpp})(\text{binc})]^+$ (**28**). In contrast, $[\text{Cu}(\text{dap})(\text{DPEphos})]^+$ (**27**) proved to be a comparable competitor (entry 1 and 4). Attempts to utilize *para*-nitrobenzylbromine (**19d**) (entry 2) or perfluorooctyl iodide (**19h**) (entry 3) resulted in no conversion of the starting materials although already employed in the ATRA reaction *vide supra*. Furthermore, applying but-2-en-1-yltrimethylsilane (**29a**) gave rise to an inseparable mixture (**30a/30b** = 84:16) of the linear **30a** and branched isomer **30b** in good yields for all investigated complexes. Despite the success of this reaction, there are substitution patterns for which no allylation reaction was observed. As expected, sterically more hindered substrates resulted in complex reaction mixture due to regio- and diastereoselectivity (entries 5-6).

Again, an oxidative quenching cycle where the copper catalyst acts as an electron shuttle is assumed. First, photoexcited copper(I) catalyst reduces organohalide **19** by a single electron transfer (SET), which generates a Cu(II) species, a halide anion and an alkyl radical **31**, which adds to alkene **29** to form radical **32**. Upon forming the product **30**, a trimethylsilyl radical is released, which can be oxidized to its silyl cation by a back electron transfer to Cu(II) thus closing the catalytic cycle. Finally, a nucleophilic attack of the halide produces the volatile TMS-X (Scheme 7).

Scheme 7. Proposed mechanism.



5. Summary

In conclusion, the synthesis and characterization of a series of new homoleptic copper(I) phenanthroline complexes **11b-11e** was described. Subsequently, these photocatalysts were applied for the visible light induced atom transfer radical addition (ATRA) reaction. The correlation between substituent pattern in 2,9-position of the phenanthroline moiety compared to the known $[\text{Cu}(\text{dap})_2]\text{Cl}$ (**11a-Cl**) and its catalytic activity could be investigated by the addition of various alkyl halides, e.g. CBr_4 (**19a**), diethyl bromomalonate (**19c**), perfluorooctyl iodide (**19h**), or triflyl chloride (**19i**) to different olefins **18**. The new homoleptic complexes **11b-11e** showed low to good yields thus providing no enhanced properties compared to $[\text{Cu}(\text{dap})_2]\text{Cl}$ (**11a-Cl**).

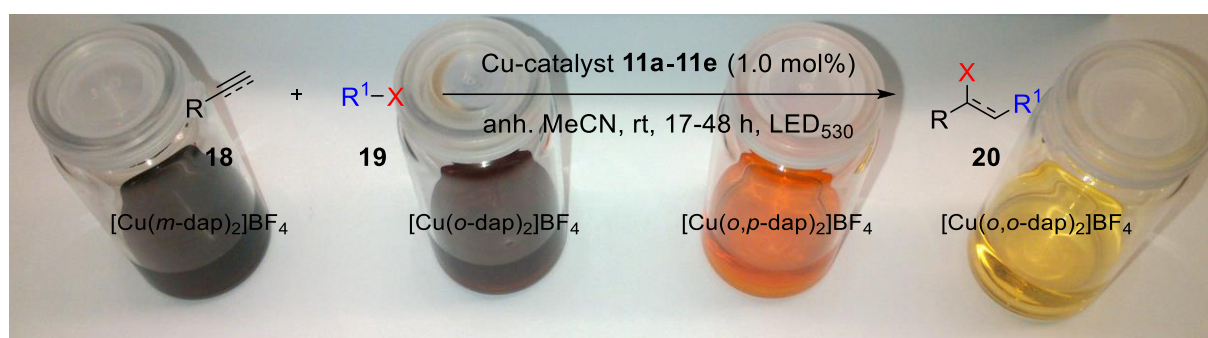
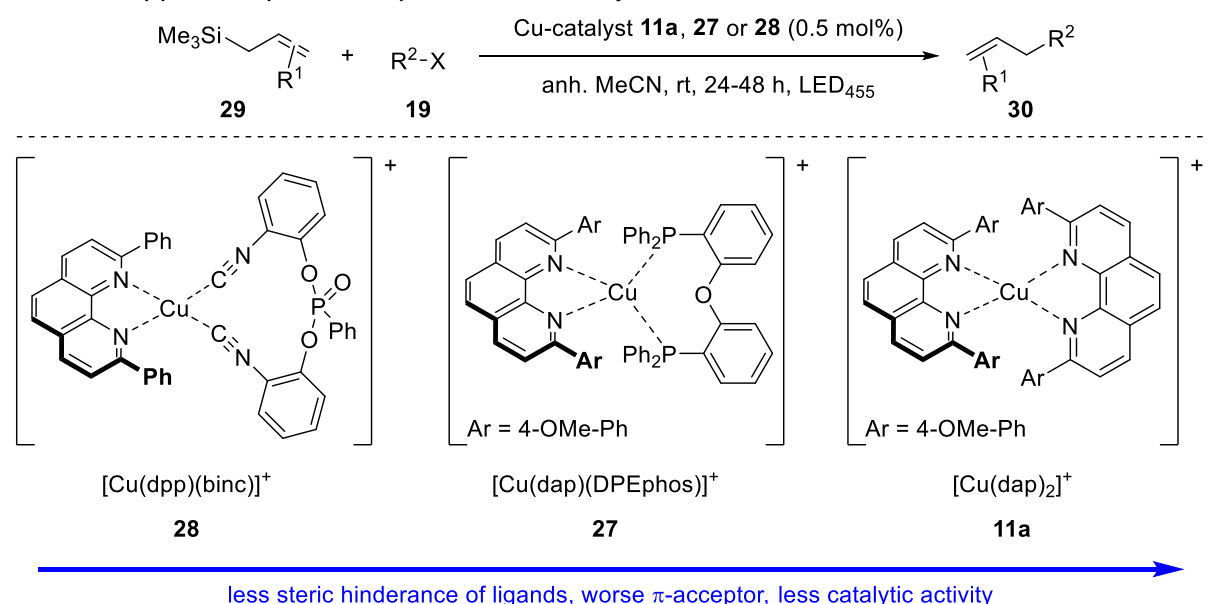


Figure 6. Catalytic activity of copper complexes.

Next, the two novel heteroleptic copper(I) complexes $[\text{Cu}(\text{dap})(\text{DPEphos})]\text{BF}_4$ (**27-BF₄**) and $[\text{Cu}(\text{dpp})(\text{binc})]\text{BF}_4$ (**28-BF₄**) were employed as photoredox catalysts in allylation reaction with allyltrimethylsilanes **29** (Scheme 8). They proved to be highly active owing to an enhanced excited state lifetime compared to established $[\text{Cu}(\text{dap})_2]\text{Cl}$ (**11a-Cl**).

Scheme 8. Visible light induced allylation of organohalides **19** with allyltrimethylsilanes **29** and various copper complexes as photoredox catalyst.



6. References

- [1] *Leading reviews on phenanthrolines:* a) Accorsi, G.; Listorti, A.; Yoosaf, K.; Armaroli, N. *Chem. Soc. Rev.* **2009**, 38, 1690-1700; b) Sammes, P. G.; Yahiolu, G. *Chem. Soc. Rev.* **1994**, 23, 327-334.
- [2] Gerdeissen *Ber. Dtsch. Chem. Ges.* **1889**, 22, 244-254.
- [3] Blau, F. *Monatsh. Chem.* **1898**, 19, 647-689.
- [4] a) Pfeiffer, P.; Christeleit, W. *J. Prakt. Chem.* **1938**, 151, 127-133; b) G. F. Smith, F. P. R. *Phenanthroline and Substituted Phenanthroline Indicators. Their Preparation, Properties, and Applications to Analysis*; The G. Frederick Smith Chemical Company: Columbus, 1944.
- [5] *Leading reviews on copper(I) phenanthrolines:* a) Armaroli, N. *Chem. Soc. Rev.* **2001**, 30, 113-124; b) Laviecampot, A.; Cantuel, M.; Leydet, Y.; Jonusauskas, G.; Bassani, D.; McClenaghan, N. *Coord. Chem. Rev.* **2008**, 252, 2572-2584; c) Lazorski, M. S.; Castellano, F. N. *Polyhedron* **2014**, 82, 57-70.
- [6] Listorti, A.; Esposti, A. D.; Kishore, R. S.; Kalsani, V.; Schmittel, M.; Armaroli, N. *J. Phys. Chem. A* **2007**, 111, 7707-7718.
- [7] a) Shinozaki, K.; Kaizu, Y. *Bull. Chem. Soc. Jpn* **1994**, 67, 2435-2439; b) Everly, R. M.; Ziessel, R.; Suffert, J.; McMillin, D. R. *Inorg. Chem.* **1991**, 30, 559-561; c) Eggleston, M. K.; McMillin, D. R.; Koenig, K. S.; Pallenberg, A. J. *Inorg. Chem.* **1997**, 36, 172-176; d) Cunningham, C. T.; Cunningham, K. L. H.; Michalec, J. F.; McMillin, D. R. *Inorg. Chem.* **1999**, 38, 4388-4392.
- [8] Masood, M. A.; Zacharias, P. S. *J. Chem. Soc., Dalton Trans.* **1991**, 111-114.
- [9] Paria, S.; Reiser, O. *ChemCatChem* **2014**, 6, 2477-2483.
- [10] Pirtsch, M.; Paria, S.; Matsuno, T.; Isobe, H.; Reiser, O. *Chem. Eur. J.* **2012**, 18, 7336-7340.
- [11] Eggers, F.; Lüning, U. *Eur. J. Org. Chem.* **2009**, 2009, 2328-2341.
- [12] Frey, J.; Kraus, T.; Heitz, V.; Sauvage, J. P. *Chem. Eur. J.* **2007**, 13, 7584-7594.
- [13] a) Frey, J.; Kraus, T.; Heitz, V.; Sauvage, J.-P. *Chem. Eur. J.* **2007**, 13, 7584-7594; b) Liu, B.; Pan, S.; Liu, B.; Chen, W. *Inorg. Chem.* **2014**, 53, 10485-10497.
- [14] Guo, H. C.; Zheng, R. H.; Jiang, H. J. *Org. Prep. Proced. Int.* **2012**, 44, 392-396.
- [15] Pirtsch, M. *Photokatalyse mit [Cu(dap)₂Cl] und sichtbarem Licht*, Dissertation, Universität Regensburg, **2013**.
- [16] a) Goodwin, K. V.; McMillin, D. R.; Robinson, W. R. *Inorg. Chem.* **1986**, 25, 2033-2036; b) Burke, P. J.; McMillin, D. R.; Robinson, W. R. *Inorg. Chem.* **1980**, 19, 1211-1214; c) Hoffmann, S. K.; Corvan, P. J.; Singh, P.; Sethulekshmi, C. N.; Metzger, R. M.; Hatfield, W. E. *J. Am. Chem. Soc.* **1983**, 105, 4608-4617; d) Cunningham, C. T.; Moore,

- J. J.; Cunningham, K. L. H.; Fanwick, P. E.; McMillin, D. R. *Inorg. Chem.* **2000**, 39, 3638-3644.
- [17] a) Gushurst, A. K. I.; McMillin, D. R.; Dietrich-Buchecker, C. O.; Sauvage, J. P. *Inorg. Chem.* **1989**, 28, 4070-4072; b) Blasse, G.; Breddels, P. A.; McMillin, D. R. *Chem. Phys. Lett.* **1984**, 109, 24-26; c) McMillin, D. R.; Kirchhoff, J. R.; Goodwin, K. V. *Coord. Chem. Rev.* **1985**, 64, 83-92.
- [18] a) Pavlishchuk, V. V.; Addison, A. W. *Inorg. Chim. Acta* **2000**, 298, 97-102; b) Smith, T. J.; Stevenson, K. J. Chapter 4: Reference Electrodes In *Handbook of Electrochemistry*, Elsevier: Amsterdam, 2007, p 73-110.
- [19] Miller, M. T.; Gantzel, P. K.; Karpishin, T. B. *Inorg. Chem.* **1999**, 38, 3414-3422.
- [20] Julliard, M.; Chanon, M. *Chem. Rev.* **1983**, 83, 425-506.
- [21] Prier, C. K.; Rankic, D. A.; MacMillan, D. W. *Chem. Rev.* **2013**, 113, 5322-5363.
- [22] Armaroli, N.; Accorsi, G.; Cardinali, F.; Listorti, A. *Top. Curr. Chem.* **2007**, 280, 69-115.
- [23] Trost, B. M. *Angew. Chem. Int. Ed.* **1995**, 34, 259-281.
- [24] a) Pintauer, T.; Matyjaszewski, K. *Chem. Soc. Rev.* **2008**, 37, 1087-1097; b) Minisci, F. *Acc. Chem. Res.* **1975**, 8, 165-171; c) Muñoz-Molina, J. M.; Belderrain, T. R.; Pérez, P. *J. Eur. J. Inorg. Chem.* **2011**, 2011, 3155-3164; d) Kharasch, M. S.; Skell, P. S.; Fisher, P. *J. Am. Chem. Soc.* **1948**, 70, 1055-1059.
- [25] a) Fernández-Zúmel, M. A.; Buron, C.; Severin, K. *Eur. J. Org. Chem.* **2011**, 2011, 2272-2277; b) Taylor, M. J.; Eckenhoff, W. T.; Pintauer, T. *Dalton Trans.* **2010**, 39, 11475-11482; c) Yorimitsu, H.; Shinokubo, H.; Matsubara, S.; Oshima, K.; Omoto, K.; Fujimoto, H. *J. Org. Chem.* **2001**, 66, 7776-7785.
- [26] Wallentin, C. J.; Nguyen, J. D.; Finkbeiner, P.; Stephenson, C. R. *J. Am. Chem. Soc.* **2012**, 134, 8875-8884.
- [27] a) Bagal, D. B.; Kachkovskiy, G.; Knorn, M.; Rawner, T.; Bhanage, B. M.; Reiser, O. *Angew. Chem. Int. Ed.* **2015**, 54, 6999-7002; b) Paria, S.; Pirtsch, M.; Kais, V.; Reiser, O. *Synthesis* **2013**, 45, 2689-2698.
- [28] Franz, J. F.; Kraus, W. B.; Zeitler, K. *Chem. Commun.* **2015**, 51, 8280-8283.
- [29] Koch, D. A. *J. Electrochem. Soc.* **1987**, 134, 3062-3067.
- [30] a) Narayanam, J. M.; Stephenson, C. R. *Chem. Soc. Rev.* **2011**, 40, 102-113; b) Nguyen, J. D.; Tucker, J. W.; Konieczynska, M. D.; Stephenson, C. R. *J. Am. Chem. Soc.* **2011**, 133, 4160-4163.
- [31] Khnayzer, R. S.; McCusker, C. E.; Olaiya, B. S.; Castellano, F. N. *J. Am. Chem. Soc.* **2013**, 135, 14068-14070.
- [32] a) Cuttell, D. G.; Kuang, S.-M.; Fanwick, P. E.; McMillin, D. R.; Walton, R. A. *J. Am. Chem. Soc.* **2002**, 124, 6-7; b) Kuang, S.-M.; Cuttell, D. G.; McMillin, D. R.; Fanwick, P. E.; Walton, R. A. *Inorg. Chem.* **2002**, 41, 3313-3322; c) Balzani, V.; Bergamini, G.;

- Campagna, S.; Puntoriero, F. *Top. Curr. Chem.* **2007**, *280*, 1-36; d) Smith, C. S.; Branham, C. W.; Marquardt, B. J.; Mann, K. R. *J. Am. Chem. Soc.* **2010**, *132*, 14079-14085; e) Smith, C. S.; Mann, K. R. *J. Am. Chem. Soc.* **2012**, *134*, 8786-8789; f) Czerwieniec, R.; Kowalski, K.; Yersin, H. *Dalton Trans.* **2013**, *42*, 9826-9830; g) Knorn, M.; Rawner, T.; Czerwieniec, R.; Reiser, O. *ACS Catalysis* **2015**, *5*, 5186-5193.
- [33] Knorn, M. *Metal-Isonitriles - Synthesis, Characterization and Application in Catalysis*, Dissertation, Universität Regensburg, **2015**.
- [34] Kaeser, A.; Mohankumar, M.; Mohanraj, J.; Monti, F.; Holler, M.; Cid, J. J.; Moudam, O.; Nierengarten, I.; Karmazin-Brelot, L.; Duhayon, C.; Delavaux-Nicot, B.; Armaroli, N.; Nierengarten, J. F. *Inorg. Chem.* **2013**, *52*, 12140-12151.
- [35] a) Hernandez-Perez, A. C.; Vlassova, A.; Collins, S. K. *Org. Lett.* **2012**, *14*, 2988-2991; b) Wallesch, M.; Volz, D.; Zink, D. M.; Schepers, U.; Nieger, M.; Baumann, T.; Brase, S. *Chem. Eur. J.* **2014**, *20*, 6578-6590; c) Hernandez-Perez, A. C.; Collins, S. K. *Angew. Chem. Int. Ed.* **2013**, *52*, 12696-12700; d) Tschierlei, S.; Karnahl, M.; Rockstroh, N.; Junge, H.; Beller, M.; Lochbrunner, S. *ChemPhysChem* **2014**, *15*, 3709-3713.

C. Photochemical Iodoperfluoroalkylation

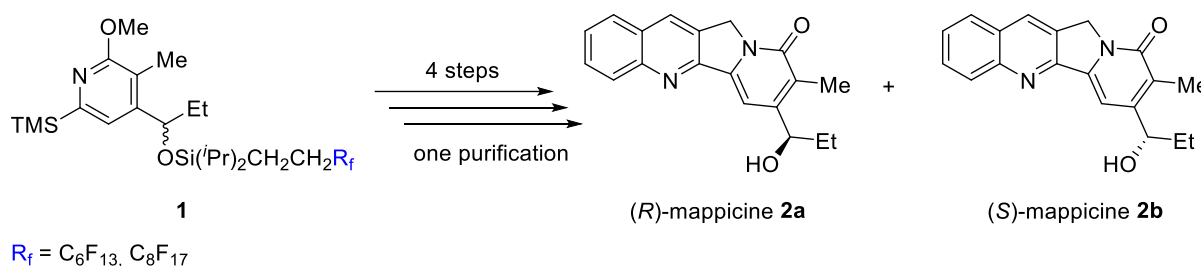
1. Introduction

Since the pioneering work^[1] in organofluorine chemistry in the 18th century by e.g. Scheele, Dumas, Péligré, Moissan, and Young much attention in the chemical and industrial community has attracted these compound class due to its intrinsic properties.^[2] The incorporation of fluorine onto organic molecules can dramatically change the chemical, physical or biological properties. Therefore, fluoroalkyl containing compounds play an important role in material science, medicinal chemistry and agrochemistry.^[3] For example, their high thermal stability, chemical resistance, and non-toxicity of hydrofluorocarbons led to the replacement of refrigerants based on chlorofluorocarbons such as CCl₃F and CCl₂F₂, which are involved in the depletion of the stratospheric ozone and are therefore responsible in global warming.^[4] Recent results in the progress of organic semiconductors showed that the installation of fluorinated alkyl chains increased the stability of the polymer films, thus leading to better performance at ambient conditions as demonstrated by Dodabalapur and co-workers.^[5] Moreover, approximately 20% of pharmaceuticals and 40% of agrochemicals that are commercially available contain fluorine or perfluoroalkyl groups as estimated by industry sources and top thirty drug sales.^[6] As a consequence, the development of efficient methods for the incorporation of fluorine are important. Taking into account the wide range of fluorinated motifs, this chapter will highlight recent examples in the perfluoroalkylation reaction of organic compounds. The interested reader is redirected to excellent reviews on the introduction of fluorine including fluorination, trifluoromethylation, trifluoromethylthiolation, triflation or asymmetric synthetic methods.^[6a,7]

Curran and co-workers introduced the concept of fluorous-tagging strategy for the fluorous mixture synthesis (FMS) and isolation of organic compounds demonstrating the benefits of longer perfluoroalkyl chains R_f than CF₃.^[8] On the contrary, perfluoroalkyl iodides R_f-I and related derivatives are e.g. less expensive than Togni, Umemoto or Ruppert's reagent and therefore more suitable for large scale synthesis.^[9] Moreover, in contrast to traditional solution phase and solid phase synthesis, fluorous synthesis offers many superior advantages.^[10] Fluorine tagged molecules can be easily separated and purified from non-fluorous molecules exploiting fluorophilicity by fluorous solid phase extraction (FSPE), fluorous liquid-liquid extraction (FLLE), fluorous high pressure liquid chromatography (F-HPLC), or by conventional methods such as extraction, column chromatography, distillation or recrystallization.^[8b,11] In addition, reactions can be monitored by standard analytical methods like TLC, IR, HPLC and NMR. In particular, the NMR activity of the ¹⁹F nuclei enables in vivo magnetic resonance imaging of biological probes and is therefore well established in medicinal chemistry.^[12]

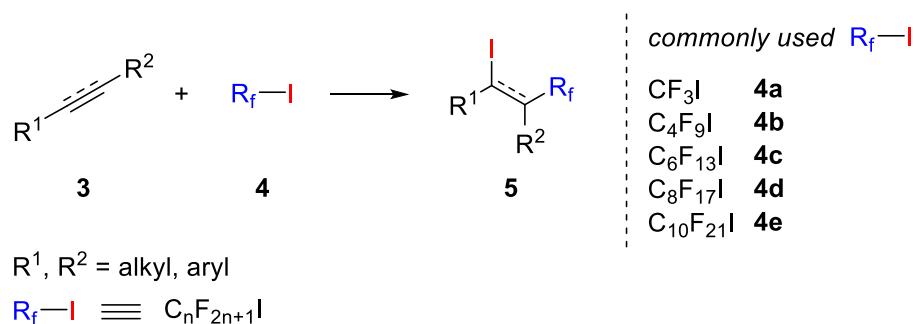
For example, the superiority of fluorine mixture synthesis was shown in the one pot total synthesis of both (*R*)- and (*S*)-mappicine as demonstrated by Curran and co-workers (Scheme 1).^[13] An equimolar mixture of prior synthesized fluorine tagged compound **1** was subjected to a four step sequence yielding a quasi-racemic mixture of the desired molecules. The separation and purification of the enantiomers were achieved by only one step via chiral F-HPLC. Enantiopure (*R*)- and (*S*)-mappicine (**2**) were obtained after deprotection of the corresponding fluorine tag in high yields. The natural products **2** are promising candidates against herpes viruses (HSV) and human cytomegalovirus (HCMV).^[14] In a similar way, the same authors reported the efficient and rapid synthesis of substituted mappicine library containing 560 analogues prepared by fluorine mixture synthesis.^[15]

Scheme 1. Quasi-racemic fluorine mixture synthesis of (*R*)- and (*S*)-mappicines **2**.^[13]



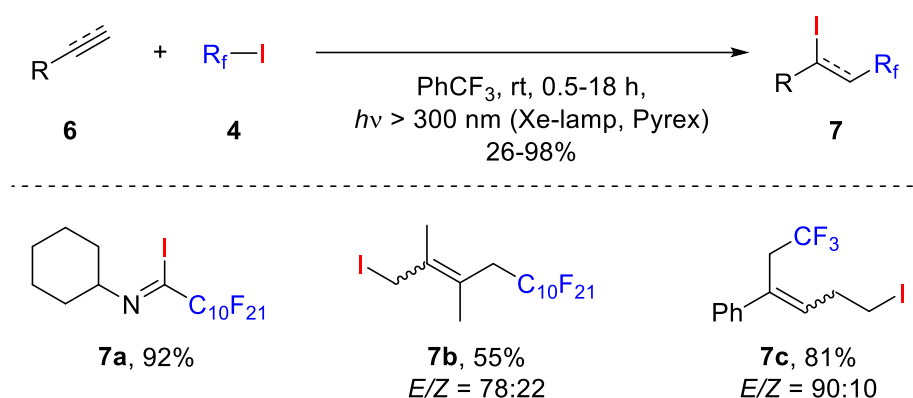
In literature, the addition of commercially available perfluoroalkyl iodides R_f-I (**4**) of various sizes to alkenes/alkynes **3** represent one of the most common means to synthesize perfluoroalkylated compounds **5** (Scheme 2). In general, many working groups have dedicated their research on the incorporation of the trifluoromethyl (CF_3) group while less studies were conducted to longer perfluoroalkyl chains. However, in the last 50 years, most synthetic procedures achieved the construction of the $C-R_f$ bond by UV-photolysis^[16], pyrolysis^[17], or electrolysis^[18]. Although significant progress has been made in this area, these processes suffer from the use of stoichiometric reagents, harsh reaction conditions, or special equipment. Furthermore, the use of alkynes usually proceed with low *E/Z* selectivity. As a result to circumvent these issues, mild and modern procedures were developed utilizing transition metal catalysis^[19], free radical initiators^[20] or visible light catalysis^[21].

Scheme 2. General scheme for the synthesis of perfluoroalkylated compounds.

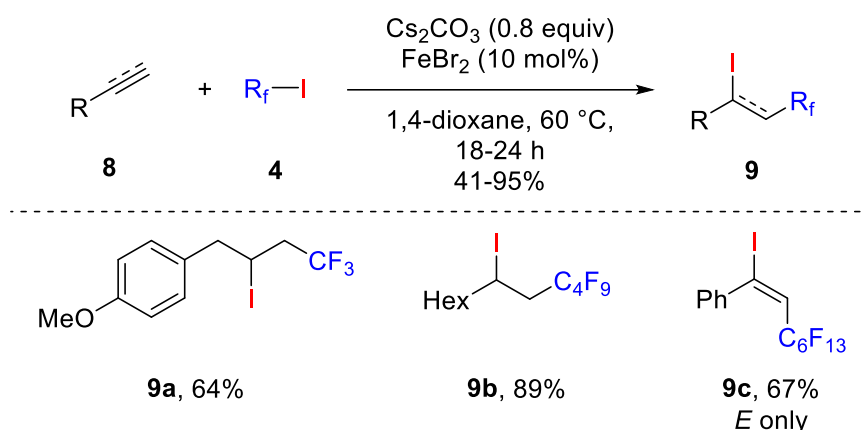


For instance, Ogawa et al. reported the photoinduced iodoperfluoroalkylation of various unsaturated compounds **6** e.g. alkenes, alkynes, allenes, dienes, and isocyanides with perfluoroalkyl iodides R_f-I (**4**) (Scheme 3).^[21a] The reactions were performed at room temperature in trifluorotoluene as organic solvent and irradiated with a xenon lamp ($\lambda > 300$ nm) through Pyrex. A variety of fluorine tagged molecules **7** were synthesized without the formation of polymerized byproducts. Nevertheless, only simple substrates bearing an isocyanide group or a π -bond were tested thus making the protocol unattractive for synthetic chemists. Very recently, the same working group expanded their protocol in the highly regioselective photoinduced iodoperfluoroalkylation of various vinylsilanes with perfluoroalkyl iodides $C_nF_{2n+1}I$ (**4b-4e**) ($n = 4, 6, 8, 10$).^[22] Moreover, the authors could demonstrate the preparation of a thin hydrophobic film coated on a glass plate via the introduction of a C_8 -fluorine tag into the vinyl groups of polysilane. Functionalized polysilanes are of great importance in material science e.g. solar cells or semiconductors due to its heat resistance and water-shedding properties.

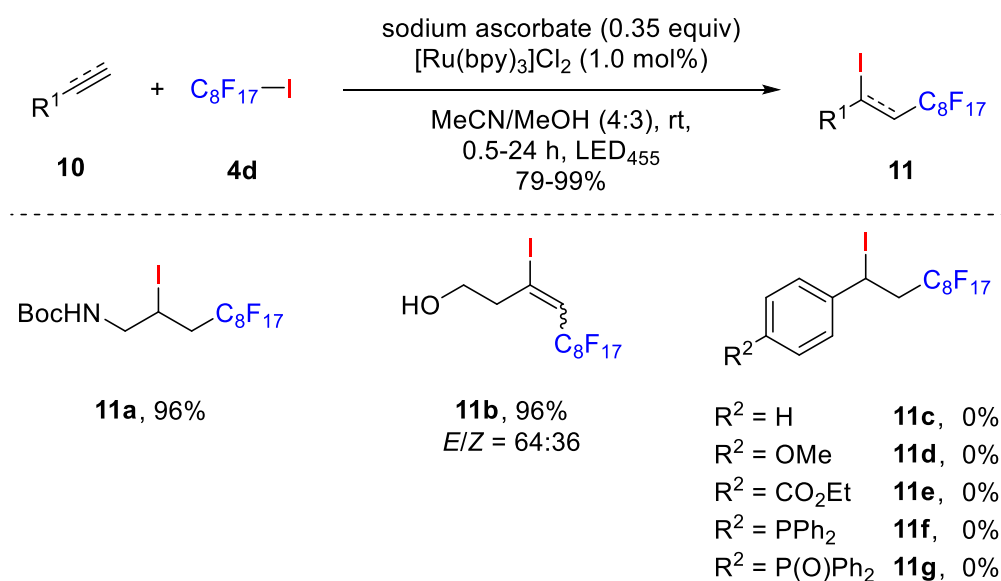
Scheme 3. Photoinitiated iodoperfluoroalkylation of unsaturated compounds **6**.^[21a]



In 2014, Hu et al. reported a simple and efficient iron-catalyzed iodoperfluoroalkylation method (Scheme 4) employing various perfluoroalkyl iodides $C_nF_{2n+1}I$ (**4a-4c**) ($n = 1, 4, 6$).^[23] The presented methodology has a wide substrate scope and functional group tolerance including alcohols, ether, thioether, nitrile, ester, keto, and aryl halides. Furthermore, the synthetic utility of the resulting atom transfer radical addition (ATRA) products **9** were demonstrated by a series of cross coupling reactions. Unfortunately, amines and styrenes proved to be incompatible in the desired transformation.

Scheme 4. Iron catalyzed ATRA reaction of R_f-I (**4**) to unsaturated compounds **8**.^[23]

In addition to the first visible light mediated atom transfer radical addition of haloalkanes onto alkenes and alkynes, Stephenson and co-workers also investigated the photoaddition of perfluoroalkyl iodides (Scheme 5).^[21d] Surprisingly, no conversion was observed when $C_8F_{17}I$ (**4d**) and substrate were reacted with ruthenium or iridium catalyst establishing the oxidative quenching cycle. Changing the reaction conditions to the reductive quenching cycle by the addition of sodium ascorbate yielded the desired product in high yield. The authors could demonstrate a wide substrate scope with good to excellent yields. Again, one exception was styrene and its derivatives, which are used in industry as crucial building blocks. All investigated styrenes produced complex reaction mixtures **11c-11g** resulting in 0% yield due to side reactions arising from decomposition of the starting material or product.

Scheme 5. Photoredox catalyzed ATRA reaction between perfluorooctyl iodides (**4d**) and unsaturated compounds **10**.^[21d]

However, the presented reactions *vide supra* have various drawbacks making them partly unattractive for e.g. synthetic chemists or industry. The mild and efficient visible light induced addition of perfluoroalkyl iodides to unsaturated compounds requires precious iridium or ruthenium photocatalysts. Even worse, crucial building blocks in industry like styrenes proved to be incompatible in the desired transformation. Nevertheless, the iodoperfluoroalkylation has been improved in recent years but is still underrepresented in literature. As part of an effort to broaden the range of transformations achieved by $[\text{Cu}(\text{dap})_2]\text{Cl}$ and encouraged by the synthetic gap in Stephenson's photoredox catalyzed reaction between perfluorooctyl iodides (**4d**) and unsaturated compounds, a new ATRA protocol within the field of fluorine chemistry was explored. In particular, it was envisioned that the unique properties of copper(I) phenanthroline catalyst and its consequential catalytic effects could produce the perfluorooctyl tagged styrenes. Indeed, the photoaddition of perfluoroalkyl iodides onto alkenes and alkynes was observed in the presence of $[\text{Cu}(\text{dap})_2]\text{Cl}$ (*vide infra*). Moreover, styrene and its derivatives proved to be compatible in this transformation.

2. Preliminary Studies with Styrene and Perfluorooctyl Iodide

This study starts by investigating the visible light mediated atom transfer radical addition (ATRA) between styrene (**12a**) and perfluorooctyl iodide (**4d**) (Table 1). Initially, when alkene **12a** and C₈F₁₇I (**4d**) was reacted in the presence of 1.0 mol% [Cu(dap)₂]Cl upon irradiation at 530 nm (green light), the iodoperfluorooctyl product **11c** was obtained in 60% yield after 48 h (entry 1). To improve the reaction efficiency, further screening of the reaction parameters was performed. Additional optimization indicated that the reaction proceeds faster upon higher concentration. Finally, it was found that 1.0 mol% [Cu(dap)₂]Cl promotes the visible light mediated ATRA reaction between styrene (**12a**) and two equivalents of C₈F₁₇I (**4d**) in 0.5 mL of anhydrous acetonitrile without any additives in high yield after 16 h (entry 2). Addressing the limitation of catalyst loading employing 0.3 mol% of [Cu(dap)₂]Cl gave 57% of the ATRA-product **11c** (entry 3). Variation of solvents (entries 4-6) resulted in a slight decrease in yield.

Employing only [Cu(MeCN)₄]BF₄ or CuCl as copper(I) salt, resulted in no turnover (entries 7-8). Also, no conversion was observed when reactions were run in the dark (entry 9) or in the absence of catalyst (entry 10). As reported for phenanthroline ligands, dap (dap = 2,9-bis(*para*-anisyl)-1,10-phenanthroline) alone promotes the reaction, but to a less extend than [Cu(dap)₂]Cl (entry 11).^[21g] The combination of CuCl/1,10-phen was somewhat effective (entry 12). Initiation of the reaction with the combination of CuCl and AIBN under thermal conditions led to a complex reaction mixture, thus providing poor yield (entry 13).

Surprisingly, well established photoredox catalysts such as [Ru(bpy)₃]Cl₂ and *fac*-Ir(ppy)₃ were ineffective resulting in very low yields (entries 14-15). These photocatalysts require irradiation at 455 nm. When [Cu(dap)₂]Cl was irradiated at this wavelength also low yield was observed indicating the instability of perfluorooctyl iodide (**4d**) or ATRA product **11c** (entry 16). Further test reactions revealed neither decomposition of photoadduct **11c** nor C₈F₁₇I (**4d**) upon irradiation at 455 nm. Stephenson et al. reported the [Ru(bpy)₃]Cl₂ catalyzed additions of C₈F₁₇I (**4d**) to alkenes, for which no product formation was observed in the case of styrene derivatives, being in full agreement with the findings reported herein.^[21d] Establishing the reductive quenching cycle of [Ru(bpy)₃]Cl₂ as well as the reaction conditions of Stephenson's protocol led to traces of product (entries 17-18).

Table 1. Optimization and control experiment for the visible light mediated copper-catalyzed iodoperfluoroalkylation.^[a]

Ph-CH=CH_2 (12a) + $\text{C}_8\text{F}_{17}\text{-I}$ (4d) $\xrightarrow[\text{solvent, 16 h, } h\nu]{\text{catalyst}}$ $\text{Ph-CH(I)-CH}_2\text{-C}_8\text{F}_{17}$ (11c)

Entry	Catalyst	Solvent	Yield [%]
1 ^[b]	[Cu(dap) ₂]Cl	MeCN	60
2	[Cu(dap) ₂]Cl	MeCN	84
3 ^[c]	[Cu(dap) ₂]Cl	MeCN	57
4	[Cu(dap) ₂]Cl	CH ₂ Cl ₂	49
5	[Cu(dap) ₂]Cl	DMF	35
6	[Cu(dap) ₂]Cl	DMSO	16
7	[Cu(MeCN) ₄]BF ₄	MeCN	nr
8	CuCl	MeCN	nr
9 ^[e]	[Cu(dap) ₂]Cl	MeCN	nr
10	no catalyst	MeCN	nr
11	dap	MeCN	11
12	CuCl/1,10-phen	MeCN	7
13 ^{[d],[e]}	CuCl/AIBN	MeCN	5
14 ^[f]	[Ru(bpy) ₃]Cl ₂	MeCN	10
15 ^[f]	<i>fac</i> -Ir(ppy) ₃	MeCN	16
16 ^[f]	[Cu(dap) ₂]Cl	MeCN	13
17 ^[f]	[Ru(bpy) ₃]Cl ₂	MeCN/H ₂ O (1:1)	2
18 ^{[f],[g]}	[Ru(bpy) ₃]Cl ₂	MeCN/H ₂ O (1:1)	3

[a] Reaction conditions: styrene **12a** (0.5 mmol, 1.0 equiv), C₈F₁₇I **4d** (1.0 mmol, 2.0 equiv), catalyst (0.5 μmol, 1.0 mol%) in anhydrous solvent (0.5 mL), irradiation at 530 nm (green LED) for 16 h; [b] reaction time of 48 h, anh. MeCN (1.0 mL); [c] catalyst loading 0.3 mol%; [d] AIBN (10 mol%), 100 °C; [e] dark reaction; [f] irradiation at 455 nm (blue LED); [g] sodium ascorbate (1.0 mmol, 2.0 equiv), reductive quenching cycle.

3. Variation of Perfluoroalkyl Iodide as Radical Source and Comparison of Various Photoredox Catalysts

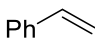
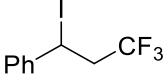
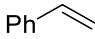
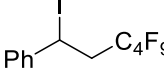
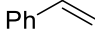
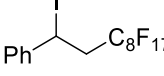
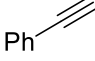
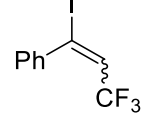
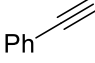
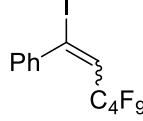
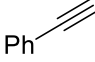
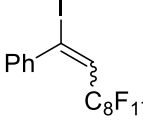
With the optimized conditions in hand, the reaction between styrene (**12a**) and various commercially available perfluoroalkyl iodides (**4**) were studied establishing 1.0 mol% of photoredox catalyst under irradiation for 16 hours (Table 2). As expected, high yields were obtained for $C_nF_{2n+1}I$ (**4a-4b**, **4d**) ($n = 1, 4, 8$) with a small decrease in yield shorter than perfluorooctyl iodide (**4d**) when copper photocatalyst was employed. Phenylacetylene (**12b**) was also a suitable substrate in this ATRA protocol yielding the desired products **13c-13e** in high yields with comparable diastereoselectivity in 16 hours.

Several literature reports^[24] indicate that for the photoaddition of the short fluorine tag CH_nF_{n+m} ($n = 0, 1, 2$; $n+m = 3$) onto unsaturated compounds, a reductive quenching cycle of photocatalyst is preferred. For example, Cho et al. demonstrated that only traces of product **13c** were observed when the oxidative quenching cycle of $[Ru(bpy)_3]Cl_2$ was employed in the reaction between phenylacetylene (**12b**) and CF_3I (**4a**). In contrast, high yields were obtained by the addition of *N,N,N',N'*-tetramethylethylenediamine (TMEDA) initiating the reductive quenching cycle.^[24a] Indeed, when styrene (**12a**) or phenylacetylene(**12b**) were subjected to the iodotrifluoromethylation reaction establishing 1.0 mol% $[Cu(dap)_2]Cl$ under optimized reaction conditions, the expected products **13a** and **13c** were isolated in 18% and 32% yield, respectively. It turned out that prolonged reaction time was necessary for full conversion. Hence, the reaction time was increased to 48 h leading to CF_3 tagged products **13a** and **13c** in moderate to good yield (entry 1 and 4). A plausible explanation for this drop in yield for CF_3I (**4a**) is that shorter perfluoroalkyl iodides have a more negative reduction potential and therefore are harder reduced to its carbo radical.^{[21d], [25]}

As a consequence, the comparison of widely established photoredox catalysts was investigated. For this purpose, irradiation of substrate **12a** with two equivalent of perfluoroalkane $C_nF_{2n+1}I$ (**4**) ($n = 1, 4, 8$) in the presence of 1.0 mol% catalyst was studied. As already indicated during the optimization for the visible light mediated copper catalyzed perfluorination, the reaction of styrene (**12a**) with perfluoroalkyl iodides (**4**) did not proceed effectively when iridium or ruthenium catalyst was utilized. When *fac*- $Ir(ppy)_3$ was employed, which has a much stronger excited state reduction potential ($E_{1/2} = -1.73$ V vs SCE) than $[Ru(bpy)_3]Cl_2$ ($E_{1/2} = -0.81$ V vs SCE)^[26], the fluorine tagged products **11c** and **13a-13e** were isolated in a slightly higher yield compared to the ruthenium based catalyst. The reduction of perfluoroalkane iodide (**4**)^[27] seems to approach the limit of $[Ru(bpy)_3]Cl_2$. However, this catalyst was applied in the ATRA reaction with low yield. It was assumed that photoadduct **11c** was unstable at the present reaction conditions. Therefore, to probe this hypothesis isolated fluorine tagged product **11c** was irradiated with a blue LED ($\lambda = 455$ nm) for 24 hours in the

presence of 1.0 mol% $[\text{Ru}(\text{bpy})_3]\text{Cl}_2$ in anhydrous acetonitrile- d_3 . After filtration through a short plug of silica, crude reaction mixture was analyzed by ^1H -NMR and ^{19}F -NMR. No decomposition or further side reactions were observed indicating that the product **11c** is photochemically stable. In the case of phenylacetylene lower yields with comparable diastereoselectivity were achieved. In all investigated reactions best results were obtained with $[\text{Cu}(\text{dap})_2]\text{Cl}$ whereas *fac*- $\text{Ir}(\text{ppy})_3$ was slightly more effective than $[\text{Ru}(\text{bpy})_3]\text{Cl}_2$. Nevertheless, both non copper catalysts proved to be less efficient.

Table 2. Substrate scope of photocatalyzed iodoperfluoroalkylation of various lengths.^[a]

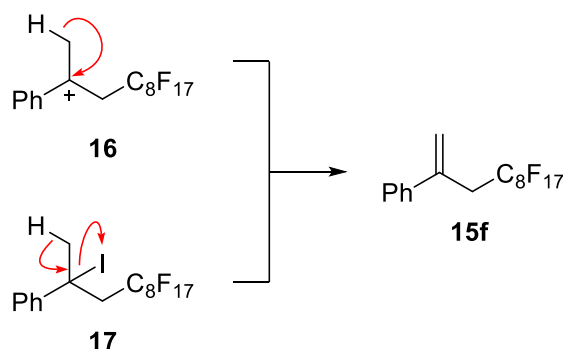
$ \begin{array}{c} \text{Ph}-\text{C}\equiv\text{C}-\text{H} + \text{F}_{2n+1}\text{C}_n-\text{I} \xrightarrow[\text{anh. MeCN, rt, 16-48 h, } h\nu]{\text{catalyst (1.0 mol\%)}} \text{Ph}-\text{C}(\text{I})=\text{C}(\text{H})-\text{C}_n\text{F}_{2n+1} \\ \text{12} \qquad \qquad \qquad \text{4} \qquad \qquad \qquad \qquad \qquad \qquad \qquad \qquad \qquad \qquad \qquad \qquad \qquad \qquad \text{13} \end{array} $						
Entry	Alkene / Alkyne	$\text{C}_n\text{F}_{2n+1}\text{I}$	Product	Yield [%]		
				$[\text{Cu}(\text{dap})_2]\text{Cl}$	$[\text{Ru}(\text{bpy})_3]\text{Cl}_2$	<i>fac</i> - $\text{Ir}(\text{ppy})_3$
1 ^[b]		CF_3I		45	2	3
	12a	4a	13a			
2		$\text{C}_4\text{F}_9\text{I}$		76	15	21
	12a	4b	13b			
3		$\text{C}_8\text{F}_{17}\text{I}$		84	10	16
	12a	4d	11c			
4 ^{[b], [c]}		CF_3I		69 $E/Z = 92:08$	14 $E/Z = 90:10$	23 $E/Z = 91:09$
	12b	4a	13c			
5 ^[c]		$\text{C}_4\text{F}_9\text{I}$		91 $E/Z = 82:18$	42 $E/Z = 81:19$	42 $E/Z = 82:18$
	12b	4b	13d			
6 ^[c]		$\text{C}_8\text{F}_{17}\text{I}$		89 $E/Z = 92:08$	46 $E/Z = 95:05$	55 $E/Z = 91:09$
	12b	4d	13e			

[a] Reaction conditions: alkene/alkyne **12** (1.0 mmol, 1.0 equiv), $\text{C}_n\text{F}_{2n+1}\text{I}$ **4** (2.0 mmol, 2.0 equiv), catalyst (1.0 μmol , 1.0 mol%) in anh. MeCN (1.0 mL), rt, 16 h, irradiation at 530 nm (green LED) for $[\text{Cu}(\text{dap})_2]\text{Cl}$, irradiation at 455 nm (blue LED) for $[\text{Ru}(\text{bpy})_3]\text{Cl}_2$ and $\text{Ir}(\text{ppy})_3$; [b] reaction time of 48 h; [c] *E/Z*-isomers obtained.

4. Substrate Scope

The scope of the reaction was explored using the optimized reaction conditions (Table 3). Notably, substrates containing both electron rich groups such as methyl **14a** (entry 2), and electron deficient groups like trifluoromethyl **14i** (entry 10) or methyl ester **14b** (entry 3), are well transformed into the corresponding fluorine tagged benzyl iodides **15**. In the case of *para*-methyl styrene (**14a**), the product **15a** was obtained in moderate yield with an almost equal amount of HI elimination product (entry 2). Attempts to increase the yield of the desired product **15a** failed. Furthermore, chlorine substitution at various positions of the aryl ring (*ortho*, *meta*, and *para*) did not alter the reactivity and yielded the products **15c**, **15g** and **15i** in good to very good yields (entries 4, 9 and 11). In literature, nitro compounds can act under photochemical conditions either as an electron acceptor leading to amines or as an effective triplet quencher.^[28] Indeed, when *para*-nitro styrene (**14d**) was subjected to the iodoperfluoroalkylation reaction, no turnover was observed and the starting material was reisolated in almost quantitatively yield (entry 5). As a consequence, the NO₂ group proved to be incompatible in the desired transformation. Furthermore, diphenyl(4-vinyl phenyl)phosphane (**14e**) underwent polymerization under the present conditions (entry 6). Neither the addition of perfluorooctyl iodide (**4d**) to the reaction mixture in several portions nor dilution prevented the polymerization. Therefore, no further optimization were followed. Methyl substitution in β -position of the styrene was possible giving rise to the 1,2-adduct **15e** in 77% yield with a diastereomeric ratio of *syn/anti* = 50:50 (entry 7). However, methyl substitution in α -position was not feasible for the ATRA reaction, resulting in product **15f** (entry 8) stemming from hydrogen abstraction **16** or HI elimination **17** (Scheme 6).

Scheme 6. Explanation for the formation of product **15f**.



As expected, the visible light induced reaction of 1-cyclopropylstyrene (**14k**) with C₈F₁₇I (**4d**) provided the ring opening product **15k** in excellent selectivity and good yield (entry 12). The ring opening process is much faster than the iodine abstraction being in agreement with the observations of Ogawa and co-workers.^[21a] Moreover, when methyl substituted cyclopropylstyrene **14l** was used as substrate, the perfluoroalkylation took place via the ring

opening of the cyclopropane, to give exclusively the higher substituted 1,5-adduct **15i** in good yield with a slightly decreased selectivity (entry 13).

Table 3. Substrate scope of copper catalyzed iodoperfluoroalkylation of styrene derivatives **14**.^[a]

$\text{Ar}-\text{CH}=\text{CH}_2 + \text{C}_8\text{F}_{17}-\text{I} \xrightarrow[\text{anh. MeCN, rt, 16-20 h, LED}_{530}]{[\text{Cu}(\text{dap})_2]\text{Cl} (1.0 \text{ mol}\%)} \text{Ar}-\text{CH}(\text{I})-\text{CH}_2-\text{C}_8\text{F}_{17}$			
<div style="display: flex; justify-content: space-around;"> 14 4d </div>		15	
Entry	Alkene	Product	Yield [%]
1	R = H 12a	R = H 11c	84
2 ^[b]	R = Me 14a	R = Me 15a	33
3	R = CO ₂ Me 14b	R = CO ₂ Me 15b	59
4	R = Cl 14c	R = Cl 15c	79
5	R = NO ₂ 14d	R = NO ₂ 15d	nr
6 ^[c]	R = PPh ₂ 14e	R = PPh ₂ 11f	0
7 ^[d]			77 <i>syn/anti</i> = 50:50
8			40
9			85
10			83
11			72
12 ^[d]			74 <i>E/Z</i> = 94:06
13 ^[d]			74 <i>E/Z</i> = 75:25

[a] Reaction conditions: Alkene **14** (1.0 mmol, 1.0 equiv), C₈F₁₇I **4d** (2.0 mmol, 2.0 equiv), [Cu(dap)₂]Cl (1.0 μmol, 1.0 mol%) in anh. MeCN (1.0 mL), irradiation at 530 nm (green LED) for 16-20 h; [b] besides HI elimination product in 20% isolated yield obtained; [c] polymerization of starting material; [d] *E/Z* isomers obtained.

Having addressed the substrate scope of aromatic alkenes, the attention to the aliphatic tolerance was examined. As already shown for the reaction between aliphatic alkene **16a** and nonafluorobutyl iodide (**4b**) by M. Pirtsch and S. Paria^[21g], *N*-Boc-allylamine (**16a**) was successfully employed in the ATRA reaction with very good yield (Table 4, entry 1). Unactivated alkene **16b** was transformed to give rise to 1,2-adduct **17a** in moderate yield showing the broad substrate tolerance (entry 2). Consistent with a radical pathway, diallyl ester **16d** underwent cyclization to form cyclopentane product **17c** in excellent yield and good selectivity (entry 4). The stereochemistry of cyclization product **17c** was assigned by 2D-NOESY NMR analysis. The NMR spectrum clearly showed the key cross diagonal peak between H_a and H_d confirming that the major diastereomer possesses a *Z*-configuration (Figure 1). Other important cross peaks are exemplarily shown in Figure 1. Besides, a syn to anti ratio of 74:26 was determined by ¹H-NMR.

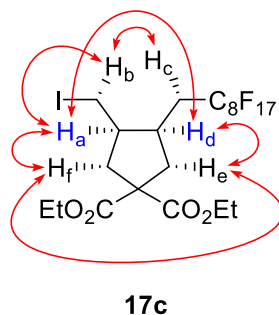
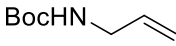
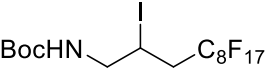
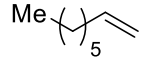
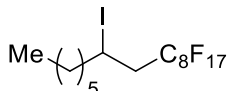
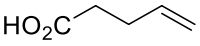
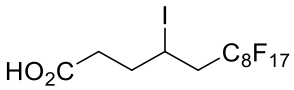
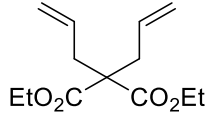
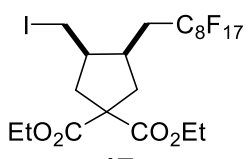
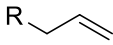
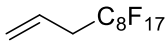




Figure 1. NOE correlations for the structural assignment of cyclopentane product **17c**.

Wu and co-workers reported the radical polyfluoroalkyl-lactonization cascade of pent-4-enoic acid (**16c**) and perfluorooctyl iodide (**4d**) initiated by sodium dithionite.^[29] It was shown that excess of strong bases like NaOH or Na₂CO₃ were crucial for the lactone formation. Attempts to use mild bases resulted at best in low yields or in the ATRA product. Indeed, no desired lactone formation was detected when pent-4-enoic acid (**16c**) was irradiated with C₈F₁₇I (**4d**) in the presence of K₂HPO₄ and copper catalyst. Instead, the ring opening product **17b** is formed in 62% yield implying that a stronger base is needed. Furthermore, sodium hydroxide was under the present reaction conditions incompatible. The addition of C₈F₁₇I (**4d**) to a solution containing either NaOH or Na₂CO₃, [Cu(dap)₂]Cl and solvent resulted instantly in polymerization of the ATRA reagent. On the other hand, the adduct **17b** was completely converted to the corresponding literature known lactone with the addition of two equivalents of sodium hydroxide in acetonitrile as determined by NMR. Unfortunately, potassium allyltrifluoroborate (**16e**) (entry 5) and allyltrimethylsilane (**16f**) (entry 6) appeared to be unsuitable as reaction partners. Under the present conditions no turnover was observed.

Table 4. Substrate scope of copper catalyzed iodoperfluoroalkylation of alkenes **16**.^[a]

$ \begin{array}{c} \text{R} \text{---} \text{CH}=\text{CH}_2 + \text{C}_8\text{F}_{17}\text{---I} \xrightarrow[\text{anh. MeCN, rt, 16-20 h, LED}_{530}]{[\text{Cu}(\text{dap})_2]\text{Cl (1.0 mol\%)}} \text{R} \text{---} \text{CH}(\text{I})\text{---CH}_2\text{---C}_8\text{F}_{17} \\ \text{16} \qquad \qquad \text{4d} \qquad \qquad \qquad \qquad \qquad \qquad \qquad \qquad \qquad \qquad \qquad \qquad \qquad \text{17} \end{array} $			
Entry	Alkene	Product	Yield [%]
1	 16a	 11a	85
2	 16b	 17a	41
3 ^[b]	 16c	 17b	62
4 ^[c]	 16d	 17c	91 <i>syn/anti</i> = 74:26
5	 16e	 17d	nr
6	 16f	 17e	nr

[a] Reaction conditions: alkene **16** (1.0 mmol, 1.0 equiv), C₈F₁₇I **4d** (2.0 mmol, 2.0 equiv), [Cu(dap)₂]Cl (1.0 μmol, 1.0 mol%) in anh. MeCN (1.0 mL), irradiation at 530 nm (green LED) for 16-20 h; [b] addition of K₂HPO₄ (2.0 mmol, 2.0 equiv); [c] diastereomers obtained.

To expand the scope of the present methodology, substituted aromatic alkynes including internal triple bonds were tested under the same reaction conditions (Table 5). In all cases the investigated substrates **18** furnished the desired photoproduct **19** in moderate to excellent yields. One exception was the internal alkyne **18f** (vide infra). Furthermore, excellent *E/Z*-stereoselectivities were observed with preferred formation of the *E*-isomer. The structure and configuration of all alkyne photoproducts **19** and **21** was confirmed by NMR spectroscopy (for more details see Chapter 5: Mechanistic Studies). The reactions between *para*-substituted phenylacetylene **18a-18c** and C₈F₁₇I (**4d**) gave the corresponding iodoperfluoro products **19a-19c** in good to excellent yields (entries 2-4). For example, phenylacetylene **18a** possessing the electron withdrawing group fluorine was a suitable substrate (entry 2). In a similar manner, 3-bromophenylacetylene (**18d**) reacted smoothly to afford the desired product **19d** in 74% yield (entry 5). Notably, when aromatic alkynes with electron donating groups such as 4-*tert*-butyl **18b** (entry 3) and 4-methoxy **18c** (entry 4) were used, products **19b** and **19c** were obtained in slightly lower yields. These results indicate that the ATRA reaction of aromatic alkynes with C₈F₁₇I (**4d**) are marginal favoured for electron withdrawing substrates. When the

terminal alkyne proton in phenylacetylene was substituted with another phenyl group to the symmetrical 1,2-diphenylethyne (**18e**) and subjected to the reaction conditions, no conversion was observed (entry 6). It was assumed that steric hinderance between the two phenyl groups prevented the turnover. Therefore, smaller methyl group was installed. Indeed, usage of substrate **18f** furnished the desired product **19f** in 40% yield and an *E/Z*-Ratio of 99:01 (entry 7). In literature is known that addition of carbon-centered alkyl radicals to internal alkynes proceeds usually slower than to terminal alkynes, thus less efficient.^[30] This fact is attributed by the lower steric hinderance in terminal alkynes. Moreover, it was envisioned to obtain allene product **19g** by the reaction of internal alkyne **18g** under the present reaction conditions. Unfortunately, no conversion of the starting material **18g** was observed indicating that electronic reasons play an important role in the planned transformation (entry 8).

Table 5. Substrate scope of copper catalyzed iodoperfluoroalkylation of aromatic alkynes **18**.^[a]

Entry	Alkyne	Product	<i>E/Z</i> -Ratio	Yield [%]
1			92:08	89
2	R = F 18a	R = F 19a	96:04	89
3	R = ^t Bu 18b	R = ^t Bu 19b	99:01	63
4	R = OMe 18c	R = OMe 19c	93:07	63
5			83:17	74
6	R = Ph 18e	R = Ph 19e	-	nr
7	R = Me 18f	R = Me 19f	99:01	40
8			-	nr

[a] Reaction conditions: alkyne **18** (1.0 mmol, 1.0 equiv), C₈F₁₇I **4d** (2.0 mmol, 2.0 equiv), [Cu(dap)₂]Cl (1.0 μmol, 1.0 mol%) in anh. MeCN (1.0 mL), irradiation at 530 nm (green LED), rt, 16-20 h.

As shown in Table 6, the iodoperfluoroalkylation proceeded at room temperature in modest to excellent yields with a variety of electronically diverse aliphatic alkynes **20**. In general, the stereoselectivities for the *E*-isomer were high for all investigated aliphatic alkynes, except for propargyl alcohol (**20b**). The ATRA reaction of protected amine **20a** yielded the iodoperfluorooctyl product **21a** in excellent stereoselectivity and good yield (entry 1). Moreover, the functional group tolerance is high. A free hydroxyl group like in propargyl alcohol (**20b**) is well tolerated showing no need of a protecting group for alcohols (entry 2). Remarkably, trimethylsilylacetylene (**20c**) participated successfully in the reaction thus giving the product **21c** in excellent yield (entry 3) implicating the higher reactivity of the triple bond. In contrast, the use of allyltrimethylsilane (**16f**) resulted in no conversion of the starting material (Table 4, entry 6). In addition, 1-hexyne (**20d**) reacted smoothly with perfluorooctyl iodide (**4d**) to give rise to fluorine tagged compound **21d** in 63% yield and an *E/Z*-ratio of 80:20 (entry 4). The symmetrical alkyne **20e** underwent radical addition with C₈F₁₇I (**4d**) in the presence of copper catalyst and provided the perfluorooctyl vinyl iodide **21e** with high stereoselectivity and excellent yield (entry 5). An effort to accomplish dimethyl acetylenedicarboxylate (**20f**) as a substrate failed to furnish the desired product **21f** (entry 6). No turnover was observed and the starting material was reisolated in almost quantitative yield. Again, it is assumed that the symmetrical electron distribution prevented the success of the iodoperfluorooctylation as already seen in the reaction between internal alkyne **18g** and C₈F₁₇I (**4d**) (Table 5, entry 8).

When cyclopropylacetylene (**20g**) was injected under standard reaction conditions, no ring opening product was observed. It was envisioned that addition of C₈F₁₇ radical onto unsaturated compound **20g** would give rise to vinyl radical. The following rearrangement would produce the corresponding allene radical. Subsequent iodine trapping should then yield the ATRA-allene product. Instead, the product **21g** was isolated in 52% yield (entry 7). It is assumed that two factors are responsible for this outcome. First, the arising vinyl radical has a considerably higher strain energy in the cyclopropylacetylene (**20g**) than in the cyclopropylstyrene (**14k**) thus leading to more favorable product **21g**. Warkentin and co-workers have demonstrated that the strain energy of the emerging radical in *tert*-butyl containing cyclopropylacetylene is about 14 kcal/mol higher than its alkene derivative.^[31] In addition, the obtained result also indicates that iodine trapping of the transient radical is presumably too fast. To probe the hypothesis that a slower reaction rate would facilitate the cyclopropyl ring opening, the reaction mixture was diluted by a factor of ten. Unfortunately, only formation of the trapped product **21g** was significantly slower. Moreover, it should be noted that trapping of the vinyl radical could already occur prior to ring opening. For example, Muralidharan and Back reported the addition of aryl sulfonyl radicals ArSO₂ to cyclopropylacetylene yielding trapped products before opening the cyclopropyl ring.^[32]

Table 6. Substrate scope of copper catalyzed iodoperfluoroalkylation of aliphatic alkynes **20**.^[a]

$$\text{R}-\text{C}\equiv\text{CH} + \text{C}_8\text{F}_{17}\text{I} \xrightarrow[\text{anh. MeCN, rt, 16-20 h, LED}_{530}]{[\text{Cu}(\text{dap})_2]\text{Cl (1.0 mol\%)}} \text{R}-\text{C}(\text{I})=\text{CH}-\text{C}_8\text{F}_{17}$$

20 **4d** **21**

Entry	Alkyne	Product	<i>E/Z</i> -Ratio	Yield [%]
1	 20a	 21a	99:01	77
2	 20b	 21b	50:50	84
3	 20c	 21c	71:29	89
4	 20d	 21d	80:20	63
5	 20e	 21e	95:05	88
6	 20f	 21f	-	nr
7	 20g	 21g	99:01	52

[a] Reaction conditions: alkyne **20** (1.0 mmol, 1.0 equiv), C₈F₁₇I **4d** (2.0 mmol, 2.0 equiv), [Cu(dap)₂]Cl (1.0 μmol, 1.0 mol%) in anh. MeCN (1.0 mL), irradiation at 530 nm (green LED), rt, 16-20 h.

5. Application

The great utility of coupling reactions in organic synthesis has lead to an increased emphasis on synthetic transformations and industrially usefull reactions. Therefore, organometallic chemistry has developed rapidly in the last 50 years and proved to be a powerful concept.^[33] In the beginning of the 19th century most reasearch on the metal-mediated coupling reaction was dedicated to copper and nickel. The pioneering work of e.g. Glaser, Ullmann, and Wurtz inspired chemists to evolve new protocols for the selective C-C bond formation. With time, a wide range of cross coupling reactions were developed like carbon-heteroatom coupling or arylation through C-H activation, at least since the important contributions in the 1970s from Sonogashira, Stille, Trost, Tsuji, Heck Negishi, Suzuki, and Kumada. It was demonstrated that carbon atoms in all hybridization states can efficiently undergo the C-C bond formation catalyzed by palladium.^[34] In 2010, the Nobel Prize was awarded to R. F. Heck, E. Negishi and A. Suzuki for the development of palladium-catalyzed cross coupling honoring the great effort made in this area.^[35] The most important substrates for the metal based cross coupling reactions are alkenyl and aryl triflates, bromides or iodides.^[36] The synthetic versatility of the obtained iodoperfluoroalkylated products **5** for further functionalization via metal-mediated coupling reaction is depicted in Figure 2.

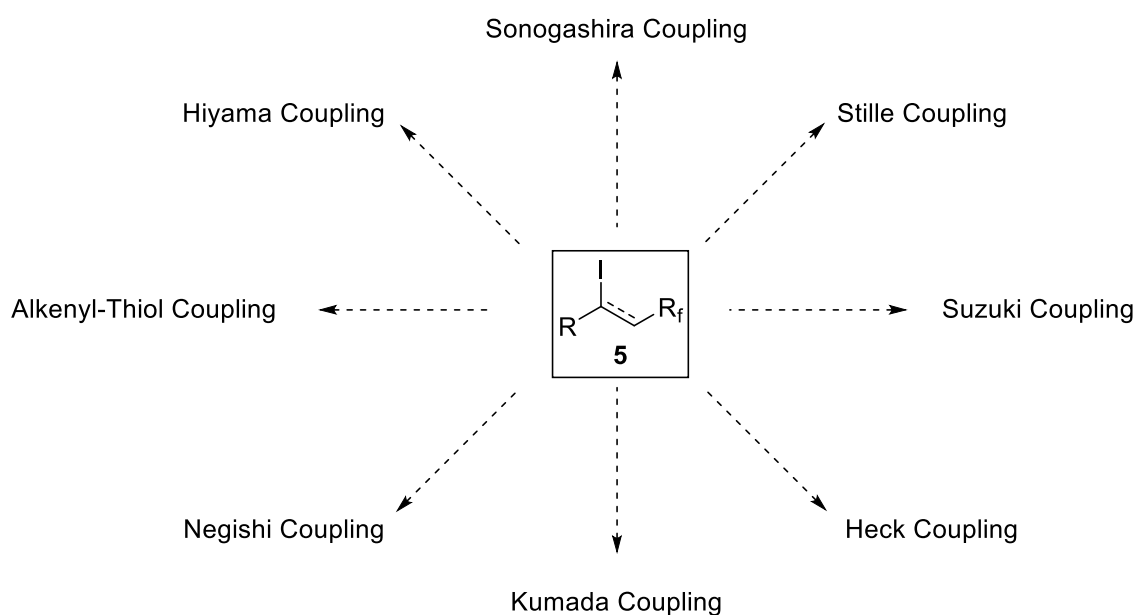
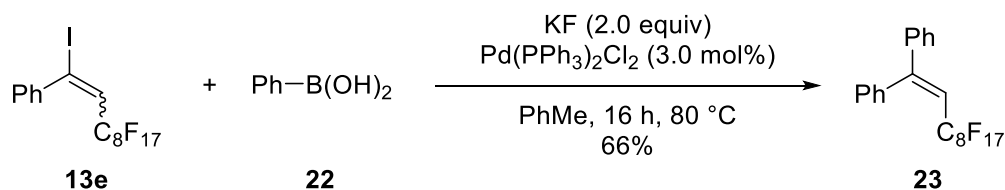


Figure 2. Possible transformations of fluorine tagged molecules using cross coupling reaction.

It is generally known that vinyl iodides have a broad utilization in organic transformations, especially in cross coupling reactions. Therefore, the Suzuki-Miyaura cross coupling of photoadduct **13e** was examined, exemplarily. When the reaction of vinyl iodide **13** and 2.2 equivalents of phenylboronic acid (**22**) in the presence of two equivalents of Na_2CO_3 , 2.5 mol% PPh_3 and 0.6 mol% Pd_2dba_3 in refluxing glyme/ H_2O (10:1) was carried out, the

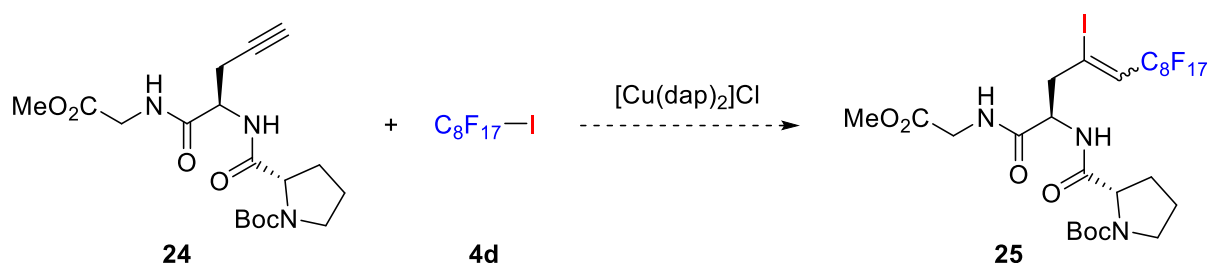
reaction was very complex as indicated by TLC and NMR (^1H , ^{19}F) and only traces of product **23** were identified. Changing the reaction conditions according to the procedure of Qing and co-workers^[37], the reaction of perfluorooctyl vinyl iodide **13e** with phenylboronic acid (**22**) in the presence of 3.0 mol% $\text{Pd}(\text{PPh}_3)_2\text{Cl}_2$ and two equivalent potassium fluoride in toluene proceeded smoothly to provide the corresponding trisubstituted olefin **23** within 16 h at 80 °C in good yield (Scheme 7).

Scheme 7. Suzuki-Miyaura cross coupling of perfluoroalkyl vinyl iodide **13e**.



In 1991, the bioactive tripeptide **24** was synthesized and its effects on the activity of prolyl 4-hydroxylase and collagen biosynthesis was studied by the group of Bayer.^[38] It was shown that in human skin fibroblast cultures the collagen biosynthesis was restricted by the use of tripeptide **24**. In order to obtain deeper understanding in the metabolism of tripeptide **24**, the concept of fluorine-tagging strategy can be applied and demonstrating the flexibility of the here presented methodology.

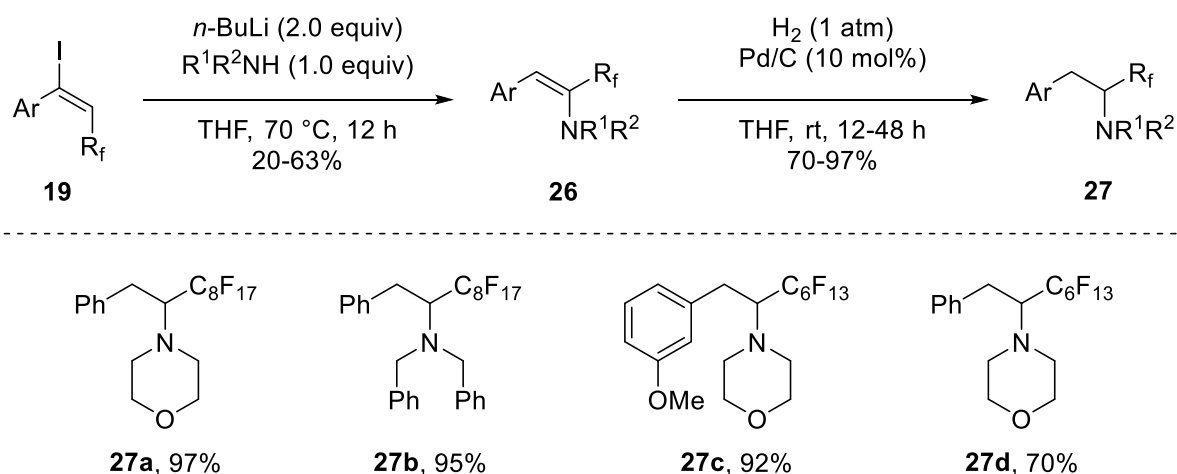
Scheme 8. Possible tagging of bioactive molecule **24**.



Therefore, first compound **24** has to be synthesized in overall nine steps and subsequently subjected to the photochemical addition of perfluorooctyl iodide yielding fluorine tagged tripeptide **25** (Scheme 8). Unfortunately, the synthesis of tripeptide **24** is very tedious and fault-prone. Moreover, it includes several time consuming purification steps, enzymatic resolution, and precaution in the synthesis due to racemization. Hence, the employment of compound **24** in the photochemical ATRA reaction with C₈F₁₇I (**4d**) was therefore not investigated any further. The similar compound *tert*-butyl phenyl(prop-2-yn-1-yl)carbamate (**20a**), which can be seen as model substrate, proved to be highly effective in the desired transformation (Table 6, entry 1) and demonstrating the use of the present method.

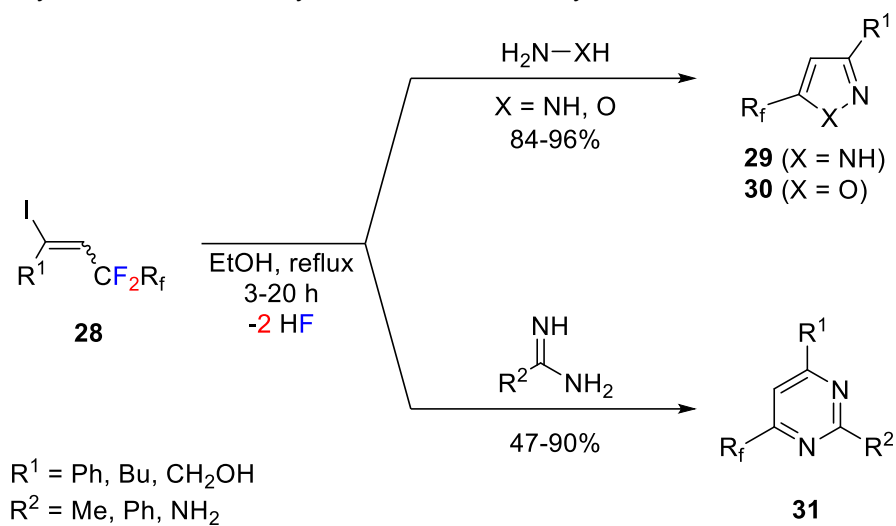
Other possible transformations of the fluorine tagged molecules **5** are known in literature. For example, in 2004 an easy and rapid synthesis of perfluorinated amphetamine analogues **27** was developed by Beller and co-workers (Scheme 9).^[39] The fluorinated acetylenes **19** were reacted with *n*-butyllithium solution to produce in situ the dehydroiodination product followed by the treatment with secondary amines to yield the corresponding enamines **26** in low to moderate yield. Subsequent hydrogenation under standard conditions gave rise to the desired amphetamine analogues **27** in good to excellent yields. Remarkably, higher yields were generally achieved in the synthesis of enamines **26** and amphetamine derivatives **27** when the longer fluorine tag C₈F₁₇ was applied. Until now, only one more publication^[40] deals with the synthesis of fluorinated amphetamine analogues despite the importance of this drug class and the positive effects of fluorine incorporation.

Scheme 9. Synthesis of amphetamine derivatives **27**.^[39]



Moreover, Hu et al. have demonstrated the versatility of 1-fluoroalkyl-2-iodoalkene **28** as building blocks for the synthesis of biological active fluoroalkyl substituted heterocycles such as pyrazoles (**29**), isoxazoles (**30**), or pyrimidines (**31**) (Scheme 10).^[41] The literature known reaction of alkynes initiated with sodium dithionite and perfluoroalkyl iodine (**4**) gave the starting material **28** in high yields as a mixture of *E/Z*-isomers in a 50:50 ratio.^[42] Subsequently, these compounds were reacted with hydrazine, hydroxylamine, amidines, or guanidine to yield heterocycles **29-31**.

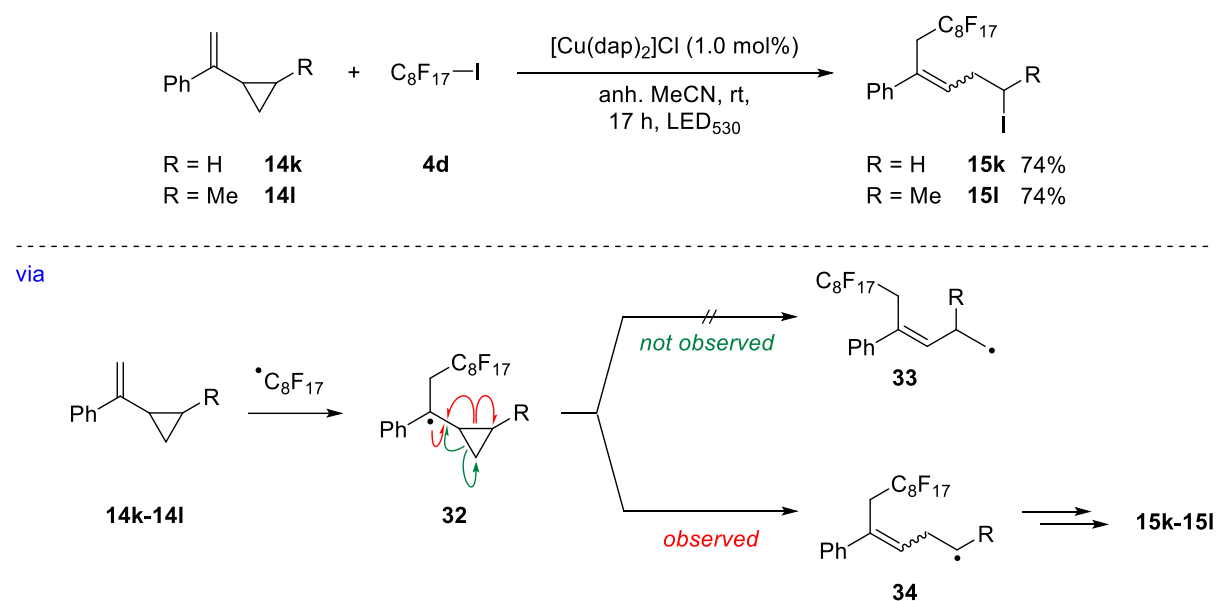
Scheme 10. Synthesis of fluoroalkyl substituted heterocycles.^[41]



6. Mechanistic Studies

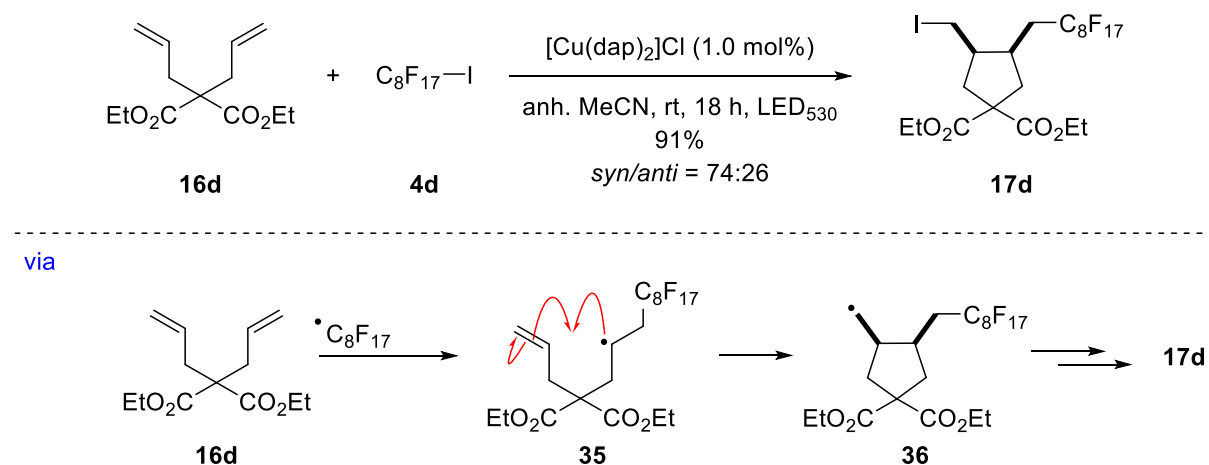
A series of experiments were carried out to gain more insight into the possible reaction mechanism. These findings *vide infra* clearly confirm the existence of radical intermediates. The implementation of the radical clocks **14k** and **14l** in the visible light induced reaction with $\text{C}_8\text{F}_{17}\text{I}$ (**4d**) catalyzed by $[\text{Cu}(\text{dap})_2]\text{Cl}$ provides an evidence for the existence of radicals. Indeed, when cyclopropylstyrene derivatives **14k** or **14l** were subjected to the iodoperfluorooctylation reaction, the ring opening products **15k** and **15l** were obtained in good yields (Scheme 11, see also Table 3, entries 12-13). The proposed mechanism is depicted in Scheme 11. After excitation of the copper catalyst and formation of the perfluorooctyl radical by a single electron transfer, the C_8F_{17} radical adds to the double bond of substrate resulting into intermediate **32**. Now, there are two variations for the C-C bond cleavage possible. One is the cleavage of the vicinal bond (red arrows) leading to the more stable secondary alkyl radical **34**. In contrast, the bond cleavage (green arrows) would result into the primary alkyl radical **33**. The following oxidation of the arising radical **34** to the corresponding carbocations and subsequently nucleophilic attack of iodine provides the products **15k** and **15l**. In all cases, no photoadducts which would result from the primary radical **33** were observed. Moreover, no indication of an 1,2-hydride shift to form an allyl radical was found being in agreement with other reports.^[43] In literature, the 1,2-hydride shift is known to be completely absent in free radical chemistry.^[44] Since no product formation resulting from allyl radical or its cation was detected a radical chain propagation mechanism cannot be excluded, completely.

Scheme 11. Mechanistic study: radical clock experiments.



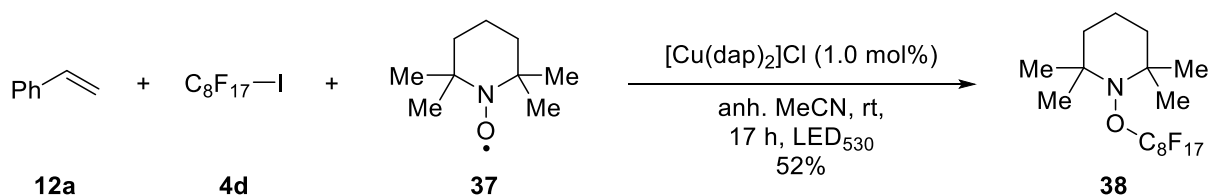
Moreover, consistent with a radical pathway, diallyl ester **16d** proved to be a superb example providing the desired cyclization product **17d** in excellent yield and good selectivity (Scheme 12, see also Table 4, entry 4). The stereochemistry was assigned by 2D-NOESY NMR analysis and by comparison with other literature reports.^[45] The suggested mechanism for the tandem radical cyclization is depicted in Scheme 12. The photochemical heterolysis of perfluorooctyl iodide (**4d**) mediated by [Cu(dap)₂]Cl generated a C₈F₁₇ radical which subsequently reacted with 1,6-diene **16d**. After the addition onto the double bond, the intramolecular 5-*exo-trig* ring closure leads to the primary radical **36**. The catalytic cycle is closed by the following oxidation of intermediate **36** to the corresponding carbocation and subsequent nucleophilic attack of iodine to provide the product **17d**.

Scheme 12. Mechanistic study: 5-*exo-trig* ring closure.



Furthermore, the perfluorination reaction was found to be completely inhibited by the addition of 2,2,6,6-tetramethyl-1-piperidinyloxy (TEMPO) (**37**) as a known radical scavenger (Scheme 13). Instead, the TEMPO addition to C₈F₁₇ radical was observed to give rise to photoadduct **38** in 52% yield, exclusively. Unfortunately, no other radicals were trapped when the amount of TEMPO (**37**) was increased or lowered. Only product **38** was obtained beside unreacted starting material.

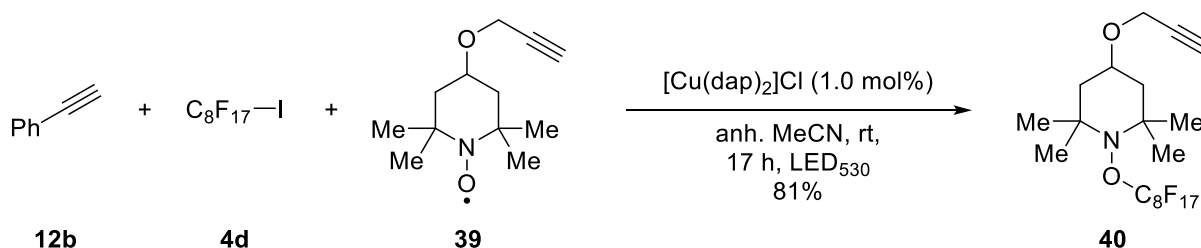
Scheme 13. Mechanistic study: trapping of intermediates by TEMPO (**37**).



Also, a competition experiment was performed to probe the reactivity of substrate **12b** (Scheme 14). The reaction between TEMPO derivative **39** and phenylacetylene (**12b**) resulted again only in the TEMPO addition of C₈F₁₇ radical forming

product **40** in 81% yield. A plausible reason may be that the reaction of the perfluorooctyl radical with nitroxyl radical occurs far more quickly than trapping of the formed benzyl or vinyl radical. To slow down the trapping reaction, the solution was irradiated with a green LED at constant -20 °C for 72 h in a second experiment. It was assumed that a slower reaction rate would facilitate the trapping of the vinyl radical. De novo, only TEMPO addition to C₈F₁₇ radical leading to product **40** was observed.

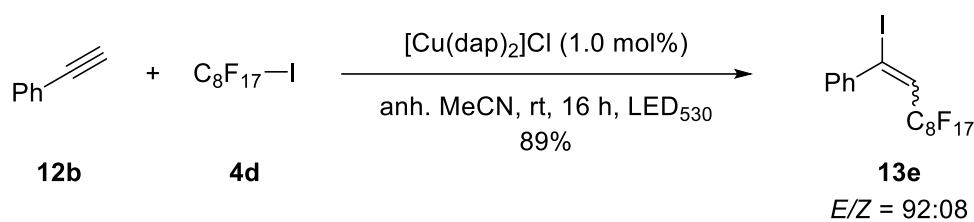
Scheme 14. Mechanistic study: competition experiment.



In addition, attempts to utilize perfluorooctyl bromide resulted in no conversion of the starting material styrene (**12a**), phenylacetylene (**12b**), allyltrimethylsilane (**16f**) or potassium allyltrifluoroborate (**16e**) which is in accordance with its higher reduction potential compared to perfluorooctyl iodide ($E_{1/2} = -1.57$ V for C₈F₁₇Br^[46] and -1.32 V for C₈F₁₇I^[21d] vs SCE in MeCN).

The structure and configuration of alkyne photoproducts **13c-13e**, **19a-19g** and **21a-21g** (Table 2 and Table 5-6) were confirmed by NMR spectroscopy. In all cases, the photoaddition of C_nF_{2n+1}I (**4**) onto alkynes resulted in an unseparable *E/Z*-mixture. The stereochemical assignment of the obtained perfluorinated phenylacetylene **13e** is exemplified.

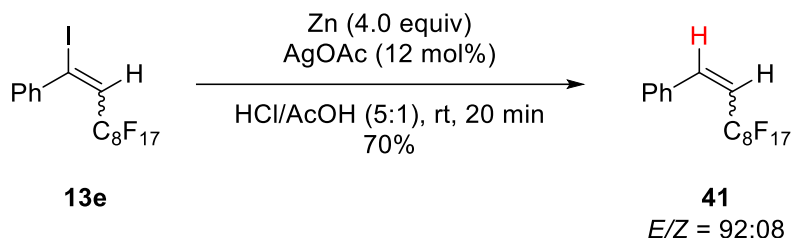
Scheme 15. Stereochemical assignment of alkyne photoproduct **13e**.



The vinyl hydrogen appears as a triplet in the ¹H-NMR spectra with a coupling constant of ³J_{FH} = 13.5 Hz (*E*-configuration) while the same proton has a coupling constant of ³J_{FH} = 13.2 Hz in the *Z*-configuration making the diastereochemical assignment difficult. In contrast, the -CF₂CF₃ group is a doublet of doublet of doublets in the ¹⁹F-NMR and the coupling constant is ³J_{FH} = 17.9 Hz. This is a typical value of Ar-CX=CHCF₂R where -CF₂R, with R = arbitrary rest, is in *E*-configuration to halide X.^[47] Moreover, when stereoselective reduction of the carbon-iodine bond was performed by the reaction of photoadduct **13e** with Zn/AgOAc

in acetic acid in the presence of concentrated hydrochloric acid, two isomers **41** were obtained in a ratio of $E/Z = 92:08$ as determined by $^1\text{H-NMR}$ (Scheme 16).

Scheme 16. Mechanistic study: stereoselective reduction of photoadduct **13e**.



For better clarity the $^1\text{H-NMR}$ spectrum is scaled from 5.40 ppm to 6.90 ppm showing the alkene protons from the starting material **13e** and the reduced product **41** (Figure 3). The spectrum was recorded after five minutes reaction time followed by standard work up in order to gain more mechanistic details about the selective reduction. When the reaction was stirred prolonged, full conversion was observed yielding product **41** in 70% overall yield with a ratio of $E/Z = 92:08$. The major reduced product **41a** has a vicinal coupling constant of $^3J_{\text{HH}} = 12.8 \text{ Hz}$ being typical for *cis* isomers.^[48] Whereas, the coupling constant of the *trans* isomer **41b** is $^3J_{\text{HH}} = 16.0 \text{ Hz}$. Therefore, the photoadducts **13c-13e**, **19a-19g** and **21a-21g** were stereochemically assigned to be *E*-configuration based on the obtained results vide supra.

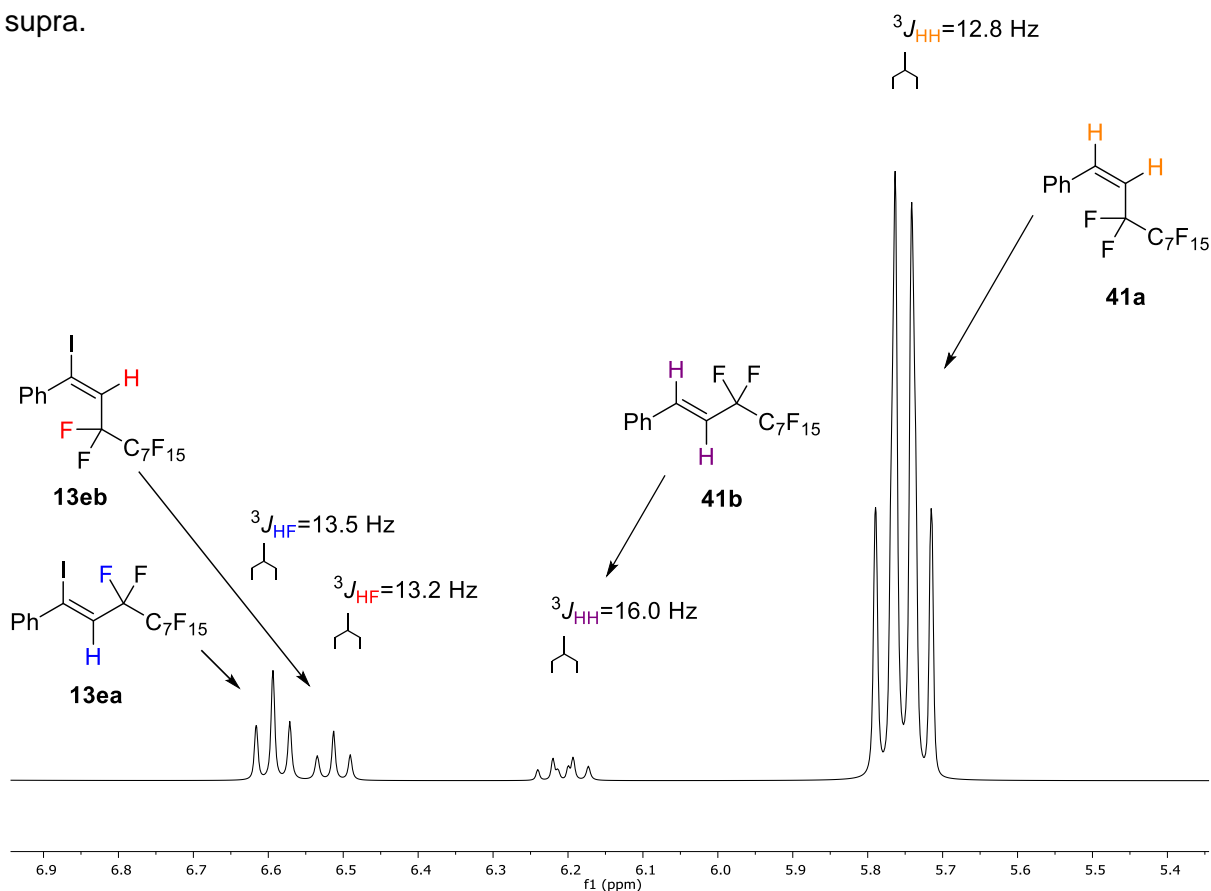
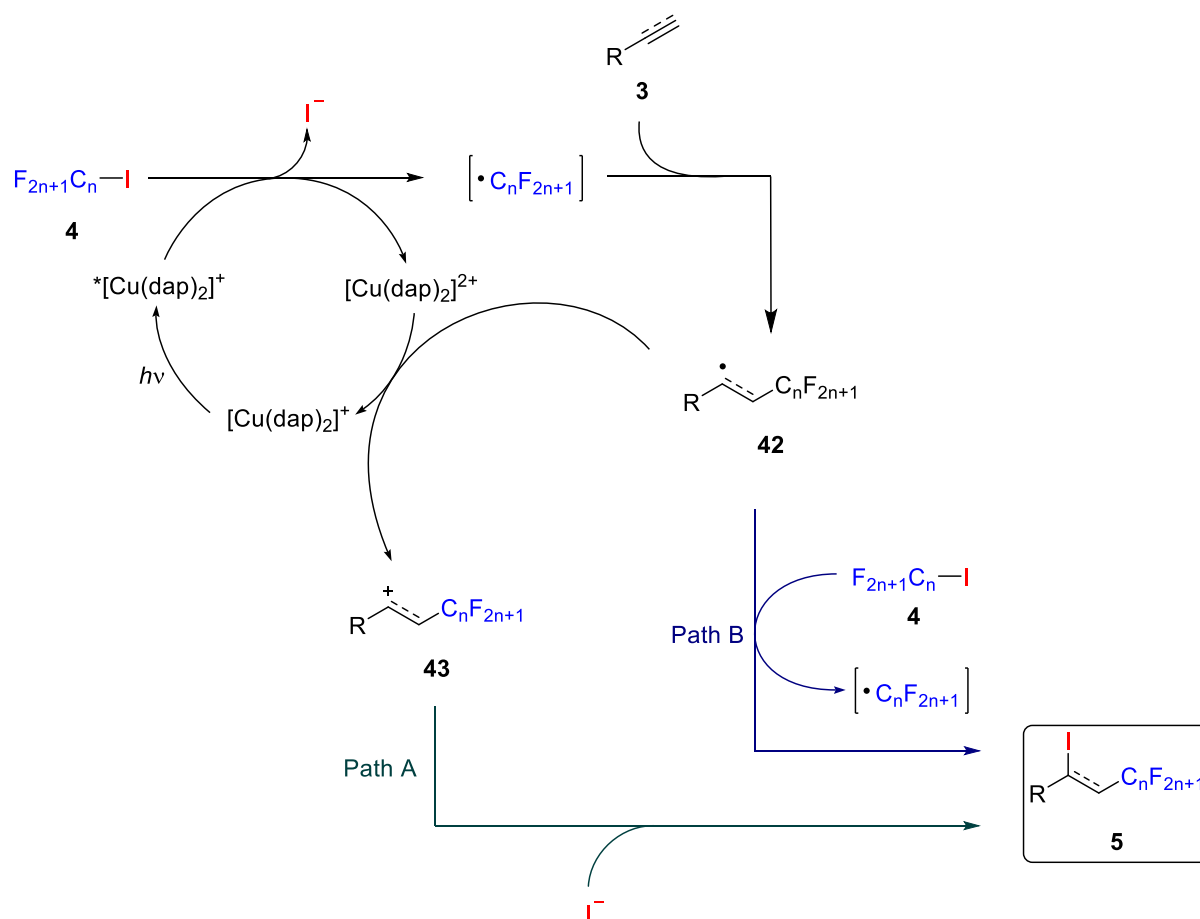


Figure 3. $^1\text{H-NMR}$ of stereoselective reduction of perfluorinated phenylacetylene **13e** after 5 min reaction time.

7. Proposed Mechanism

Finally, on the basis of these results above, a plausible mechanism is proposed as follows: first, photoexcited $[\text{Cu}(\text{dap})_2]^+$ reduces $\text{C}_n\text{F}_{2n+1}\text{I}$ (**4**) by a single electron transfer (SET), which generates a $\text{Cu}(\text{II})$ species, perfluoroalkyl radical **42** and iodine anion. The $\text{C}_n\text{F}_{2n+1}$ radical reacts with the alkene/alkyne **3** to generate a benzyl/vinyl radical **42**, which can be oxidized to its carbocation **43** by a back electron transfer to $[\text{Cu}(\text{dap})_2]^{2+}$ thus closing the catalytic cycle. Finally, a nucleophilic substitution reaction of the iodine produces the desired fluorine tagged product **5** (Path A). Alternatively, the benzyl/vinyl radical **33** can abstract an iodine atom rapidly from the perfluoroalkyl iodide **4** initiated through a radical chain propagation mechanism (Path B).

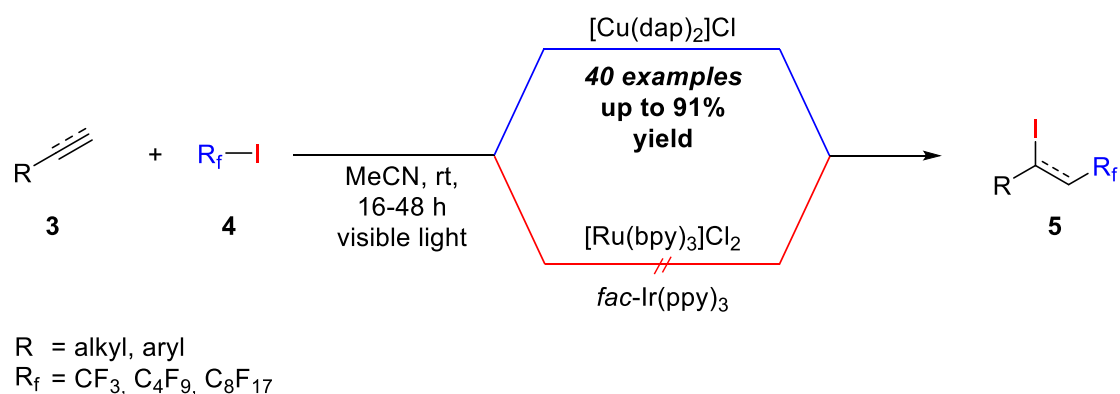
Scheme 17. Proposed mechanism.



8. Summary

In conclusion, a practical and straightforward method for the radical addition of perfluoroalkyl iodides **4** to a variety of alkenes and alkynes (**3**) utilizing the oxidative quenching cycle of $[\text{Cu}(\text{dap})_2]\text{Cl}$ was developed. In particular, it was shown that the fluorine chain C_8F_{17} achieved higher yields than shorter R_f tags like C_4F_9 and CF_3 . Moreover, no special precautions for handling were necessary due to lower volatility of perfluorooctyl iodide (**4d**) compared to gaseous trifluoromethyl iodide (**4a**). In addition, well established photocatalysts such as $[\text{Ru}(\text{bpy})_3]\text{Cl}_2$ and *fac*- $\text{Ir}(\text{ppy})_3$ failed to furnish the desired products **5** in reasonable yields. A series of experiments were carried out to obtain deeper understanding into the possible reaction mechanism. Exemplary, the Suzuki-Miyaura cross coupling of one photoadduct was examined to demonstrate the synthetic versatility of these compound class.

Scheme 18. Photoredox catalyzed ATRA reaction between perfluoroalkyl iodides (**4**) and unsaturated compounds **3**.



9. References

- [1] Banks, R. E.; Tatlow, J. C. *J. Fluorine Chem.* **1986**, *33*, 71-108.
- [2] O'Hagan, D. *Chem. Soc. Rev.* **2008**, *37*, 308-319.
- [3] a) J. A. Gladysz; D. P. Curran; Horváth, I. T. *Handbook of Fluorous Chemistry*; Wiley-VCH: Weinheim, 2004; b) Kirsch, P. *Modern Fluoroorganic Chemistry - Synthesis, Reactivity, Applications*; Wiley-VCH: Weinheim, 2013.
- [4] Siegemund, G.; Schwertfeger, W.; Feiring, A.; Smart, B.; Behr, F.; Vogel, H.; McKusick, B.; Kirsch, P. Fluorine Compounds, Organic In *Ullmann's Encyclopedia of Industrial Chemistry* 2016, p 1-56.
- [5] Katz, H. E.; Lovinger, A. J.; Johnson, J.; Kloc, C.; Siegrist, T.; Li, W.; Lin, Y. Y.; Dodabalapur, A. *Nature* **2000**, *404*, 478-481.
- [6] a) Champagne, P. A.; Desroches, J.; Hamel, J. D.; Vandamme, M.; Paquin, J. F. *Chem. Rev.* **2015**, *115*, 9073-9174; b) O'Hagan, D. *J. Fluorine Chem.* **2010**, *131*, 1071-1081.
- [7] *Leading reviews*: a) Ni, C.; Hu, M.; Hu, J. *Chem. Rev.* **2015**, *115*, 765-825; b) Liang, T.; Neumann, C. N.; Ritter, T. *Angew. Chem. Int. Ed.* **2013**, *52*, 8214-8264; c) Ma, J. A.; Cahard, D. *Chem. Rev.* **2004**, *104*, 6119-6146; d) Wilkinson, J. A. *Chem. Rev.* **1992**, *92*, 505-519; e) Campbell, M. G.; Ritter, T. *Chem. Rev.* **2015**, *115*, 612-633; f) Alonso, C.; Martinez de Marigorta, E.; Rubiales, G.; Palacios, F. *Chem. Rev.* **2015**, *115*, 1847-1935; g) Yang, X.; Wu, T.; Phipps, R. J.; Toste, F. D. *Chem. Rev.* **2015**, *115*, 826-870; h) Umemoto, T. *Chem. Rev.* **1996**, *96*, 1757-1778; i) Xu, X. H.; Matsuzaki, K.; Shibata, N. *Chem. Rev.* **2015**, *115*, 731-764; j) Besset, T.; Poisson, T.; Pannecoucke, X. *Eur. J. Org. Chem.* **2015**, *2015*, 2765-2789.
- [8] a) D. P. Curran, S. H., A. Studer, M. He, S.-Y. Kim, Z. Luo, M. Larhed, A. Hallberg, and B. Linclau In *Combinatorial Chemistry: A Practical Approach*; H. Fenniri 1.ed.; Oxford Univ. Press: Oxford, 2000; Vol. 2, p 327-352; b) Luo, Z.; Zhang, Q.; Oderaotoshi, Y.; Curran, D. P. *Science* **2001**, *291*, 1766-1769.
- [9] For more information see price list of Sigma Aldrich: <http://www.sigmaaldrich.com>.
- [10] Zhang, W. *Chem. Rev.* **2004**, *104*, 2531-2556.
- [11] a) Nakajima, Y.; Arinami, Y.; Yamamoto, K. *J. Chrom. A* **2014**, *1374*, 231-237; b) Hayama, T.; Yoshida, H.; Yamaguchi, M.; Nohta, H. *J. Pharm. Biomed. Anal.* **2014**, *101*, 151-160.
- [12] a) Zhu, L.; Ploessl, K.; Kung, H. F. *Science* **2013**, *342*, 429-430; b) Tirota, I.; Dichiarante, V.; Pigliacelli, C.; Cavallo, G.; Terraneo, G.; Bombelli, F. B.; Metrangolo, P.; Resnati, G. *Chem. Rev.* **2015**, *115*, 1106-1129; c) Ametamey, S. M.; Honer, M.; Schubiger, P. A. *Chem. Rev.* **2008**, *108*, 1501-1516.
- [13] Zhang, Q.; Rivkin, A.; Curran, D. P. *J. Am. Chem. Soc.* **2002**, *124*, 5774-5781.
- [14] Pendrak, I.; Wittrock, R.; Kingsbury, W. D. *J. Org. Chem.* **1995**, *60*, 2912-2915.

- [15] Zhang, W.; Luo, Z.; Chen, C. H.-T.; Curran, D. P. *J. Am. Chem. Soc.* **2002**, *124*, 10443-10450.
- [16] a) Haszeldine, R. N. *J. Chem. Soc.* **1950**, 2789-2792; b) Qiu, Z.-M.; Burton, D. J. *J. Org. Chem.* **1995**, *60*, 3465-3472.
- [17] a) Cady, G.; Grosse, A.; Barber, E.; Burger, L.; Sheldon, Z. *Ind. Eng. Chem.* **1947**, *39*, 290-292; b) Fowler, R.; Buford, W.; Hamilton, J. J.; Sweet, R.; Weber, C.; Kasper, J.; Litant, I. *Ind. Eng. Chem.* **1947**, *39*, 292-298; c) Leedham, K.; Haszeldine, R. N. *J. Chem. Soc.* **1954**, 1634-1638.
- [18] a) Fox, H. M.; Ruehlen, F. N.; Childs, W. V. *J. Electrochem. Soc.* **1971**, *118*, 1246-1249; b) Calas, P.; Moreau, P.; Commeyras, A. *J. Chem. Soc., Chem. Commun.* **1982**, 433-434; c) Calas, P.; Commeyras, A. *J. Fluorine Chem.* **1980**, *16*, 553-554.
- [19] a) Burton, D. J.; Kehoe, L. J. *J. Org. Chem.* **1970**, *35*, 1339-1342; b) Hu, C.; Qiu, Y. *J. Org. Chem.* **1992**, *57*, 3339-3342; c) Zeng, R.; Fu, C.; Ma, S. *Angew. Chem. Int. Ed.* **2012**, *51*, 3888-3891; d) Nenajdenko, V. G.; Muzalevskiy, V. M.; Shastin, A. V. *Chem. Rev.* **2015**, *115*, 973-1050; e) Zhang, B.; Studer, A. *Org. Lett.* **2014**, *16*, 3990-3993; f) He, L.; Natte, K.; Rabeah, J.; Taeschler, C.; Neumann, H.; Bruckner, A.; Beller, M. *Angew. Chem. Int. Ed.* **2015**, *54*, 4320-4324.
- [20] a) Antonietti, F.; Gambarotti, C.; Mele, A.; Minisci, F.; Paganelli, R.; Punta, C.; Recupero, F. *Eur. J. Org. Chem.* **2005**, *2005*, 4434-4440; b) Bravo, A.; Bjørsvik, H.-R.; Fontana, F.; Liguori, L.; Mele, A.; Minisci, F. *J. Org. Chem.* **1997**, *62*, 7128-7136; c) Bazhin, D. N.; Gorbunova, T. I.; Zapevalov, A. Y.; Saloutin, V. I. *J. Fluorine Chem.* **2009**, *130*, 438-443; d) Xiao, Z.; Hu, H.; Ma, J.; Chen, Q.; Guo, Y. *Chin. J. Chem.* **2013**, *31*, 939-944; e) Yang, B.; Shi, L.; Wu, J.; Fang, X.; Yang, X.; Wu, F. *Tetrahedron* **2013**, *69*, 3331-3337; f) Lazzari, D.; Cassani, M. C.; Solinas, G.; Pretto, M. *J. Fluorine Chem.* **2013**, *156*, 34-37; g) Yoshioka, E.; Kohtani, S.; Sawai, K.; Kentefu, Tanaka, E.; Miyabe, H. *J. Org. Chem.* **2012**, *77*, 8588-8604; h) Itoh, Y.; Mikami, K. *Org. Lett.* **2005**, *7*, 4883-4885.
- [21] a) Tsuchii, K.; Imura, M.; Kamada, N.; Hirao, T.; Ogawa, A. *J. Org. Chem.* **2004**, *69*, 6658-6665; b) Nagib, D. A.; Scott, M. E.; MacMillan, D. W. *J. Am. Chem. Soc.* **2009**, *131*, 10875-10877; c) Nguyen, J. D.; Tucker, J. W.; Konieczynska, M. D.; Stephenson, C. R. *J. Am. Chem. Soc.* **2011**, *133*, 4160-4163; d) Wallentin, C. J.; Nguyen, J. D.; Finkbeiner, P.; Stephenson, C. R. *J. Am. Chem. Soc.* **2012**, *134*, 8875-8884; e) Kim, E.; Choi, S.; Kim, H.; Cho, E. *J. Chem. Eur. J.* **2013**, *19*, 6209-6212; f) Wozniak, L.; Murphy, J. J.; Melchiorre, P. *J. Am. Chem. Soc.* **2015**, *137*, 5678-5681; g) Pirtsch, M.; Paria, S.; Matsuno, T.; Isobe, H.; Reiser, O. *Chem. Eur. J.* **2012**, *18*, 7336-7340.
- [22] Yoshimura, A.; Nomoto, A.; Uchida, M.; Kusano, H.; Saeki, T.; Ogawa, A. *Res. Chem. Intermed.* **2016**, 1-11.
- [23] Xu, T.; Cheung, C. W.; Hu, X. *Angew. Chem. Int. Ed.* **2014**, *53*, 4910-4914.

- [24] a) Iqbal, N.; Jung, J.; Park, S.; Cho, E. J. *Angew. Chem. Int. Ed.* **2014**, *53*, 539-542; b) Li, L.; Huang, M.; Liu, C.; Xiao, J. C.; Chen, Q. Y.; Guo, Y.; Zhao, Z. G. *Org. Lett.* **2015**, *17*, 4714-4717; c) Park, S.; Joo, J. M.; Cho, E. J. *Eur. J. Org. Chem.* **2015**, 4093-4097.
- [25] Dolbier, W. R. *Chem. Rev.* **1996**, *96*, 1557-1584.
- [26] Prier, C. K.; Rankic, D. A.; MacMillan, D. W. *Chem. Rev.* **2013**, *113*, 5322-5363.
- [27] Typical oxidation potentials are in the range of -1.0 to -2.0 V.
- [28] a) Yang, X.-J.; Chen, B.; Zheng, L.-Q.; Wu, L.-Z.; Tung, C.-H. *Green Chem.* **2014**, *16*, 1082-1086; b) E Crespo-Hernandez, C. *Mod. Chem. Appl.* **2013**, *1*, 106-113; c) Arce, R.; Pino, E. F.; Valle, C.; Negron-Encarnacion, I.; Morel, M. *J. Phys. Chem. A* **2011**, *115*, 152-160.
- [29] Zou, X.; Wu, F.; Shen, Y.; Xu, S.; Huang, W. *Tetrahedron* **2003**, *59*, 2555-2560.
- [30] Wille, U. *Chem. Rev.* **2013**, *113*, 813-853.
- [31] Ingold, K. U.; Warkentin, J. *Can. J. Chem.* **1980**, *58*, 348-352.
- [32] Back, T. G.; Muralidharan, K. R. *J. Org. Chem.* **1989**, *54*, 121-125.
- [33] a) Fiandanese, V. *Pure Appl. Chem.* **1990**, *62*, 1987-1992; b) Rossi, R.; Bellina, F. *Org. Prep. Proced. Int.* **1997**, *29*, 137-176.
- [34] Johansson Seechurn, C. C.; Kitching, M. O.; Colacot, T. J.; Snieckus, V. *Angew. Chem. Int. Ed.* **2012**, *51*, 5062-5085.
- [35] The Nobel Prize in Chemistry 2010, *nobelprize.org.*, Nobel Media AB 2014, http://www.nobelprize.org/nobel_prizes/chemistry/laureates/2010/ (April 2016)
- [36] Miyaura, N. *Cross-Coupling Reactions - A Practical Guide*; Springer Verlag: Heidelberg, Deutschland, 2002.
- [37] Liu, S. Q.; Wang, S. W.; Qing, F.-L. *J. Fluorine Chem.* **2005**, *126*, 771-778.
- [38] Willisch, H.; Hiller, W.; Hemmasi, B.; Bayer, E. *Tetrahedron* **1991**, *47*, 3947-3958.
- [39] Tewari, A.; Hein, M.; Zapf, A.; Beller, M. *Tetrahedron Lett.* **2004**, *45*, 7703-7707.
- [40] Uno, H.; Shiraishi, Y.; Shimokawa, K.; Suzuki, H. *Chem. Lett.* **1988**, *17*, 729-732.
- [41] Guan, H.-P.; Tang, X.-Q.; Luo, B.-H.; Hu, C.-M. *Synthesis* **1997**, 1997, 1489-1494.
- [42] Wei-Yuan, H.; Long, L.; Yuan-Fa, Z. *Chin. J. Chem.* **1990**, *8*, 350-354.
- [43] a) Feldman, K. S.; Parvez, M. *J. Am. Chem. Soc.* **1986**, *108*, 1328-1330; b) Griller, D.; Ingold, K. U. *Acc. Chem. Res.* **1980**, *13*, 317-323; c) Ogawa, A.; Ogawa, I.; Sonoda, N. *J. Org. Chem.* **2000**, *65*, 7682-7685; d) Tanko, J. M.; Gillmore, J. G.; Friedline, R.; Chahma, M. *J. Org. Chem.* **2005**, *70*, 4170-4173.
- [44] Anslyn, E. V.; Dougherty, D. A. *Modern Physical Organic Chemistry*; Univ. Science Books: Sausalito, USA, 2006.
- [45] Huang, W.-Y.; Zhao, G.; Ding, Y. *J. Chem. Soc., Perkin Trans. 1* **1995**, 1729-1731.
- [46] CV measurement in degassed MeCN

- [47] Dolbier, W. R. *Guide to Fluorine NMR for Organic Chemists*; 1. ed.; John Wiley & Sons: Hoboken, N.J., 2009.
- [48] Manfred Hesse; Herbert Meier; Zeeh, B. *Spektroskopische Methoden in der organischen Chemie*; 7. ed.; Georg Thieme Verlag: Stuttgart, Deutschland, 2006.

D. Synthesis of Trifluoromethylated Sultones From Alkenols Using a Copper Photoredox Catalyst

1. Introduction

The incorporation of the trifluoromethyl (CF_3) group into organic compounds and transition metal complexes can profoundly change their chemical^[1], physical^[2] and biological^[3] properties. Consequently, various approaches including nucleophilic^[4], electrophilic^[5] or radical^[6] strategies, for installing a CF_3 moiety into organic molecules have been reported. Moreover, recent examples utilize the environmental friendly and mild visible light mediated redox photocatalysis.^[7] Photocatalysts, such as $[\text{Ru}(\text{bpy})_3]\text{Cl}_2$, *fac*- $\text{Ir}(\text{ppy})_3$, Rose Bengal or $[\text{Cu}(\text{dap})_2]\text{Cl}$ can effectively generate the CF_3 radical from precursors like Togni reagent (**1**)^[8], CF_3I (**2**)^[9], triflyl chloride (**3a**)^[10], Ruppert-Prakash reagent (**4**)^[11], pyridine *N*-oxide derivative (**5**)^[12], or Umemoto reagent (**6**)^[8a,13] (Figure 1).

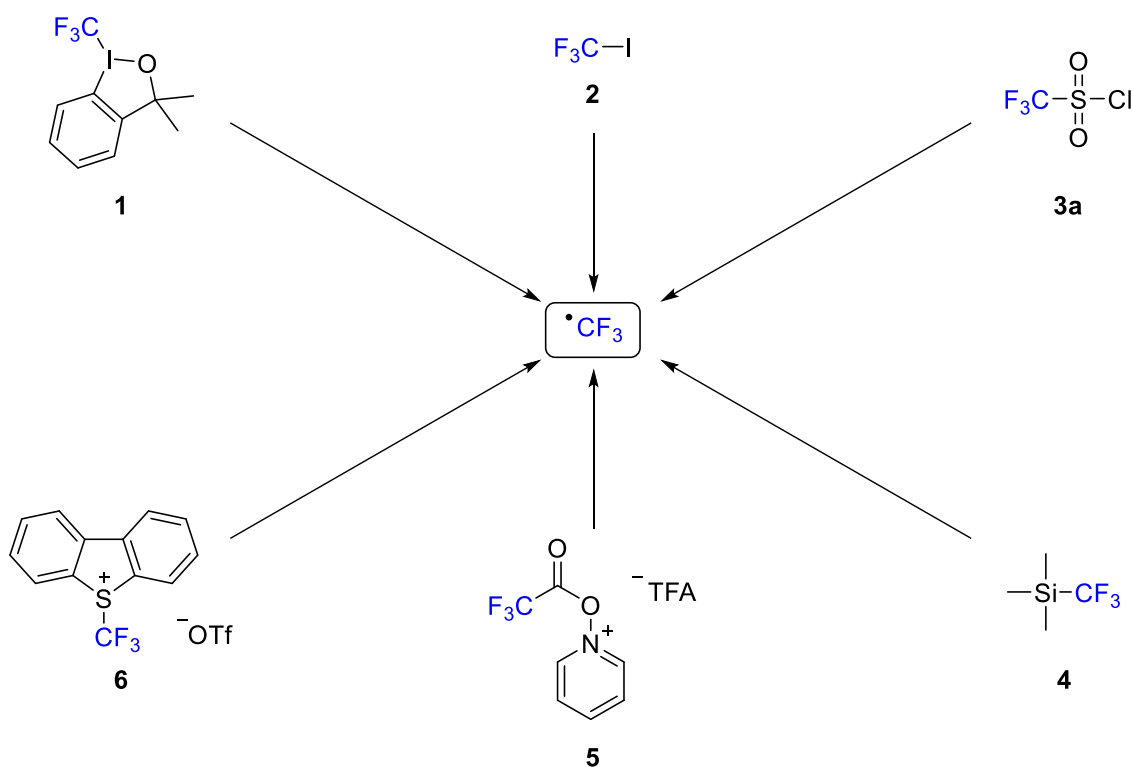
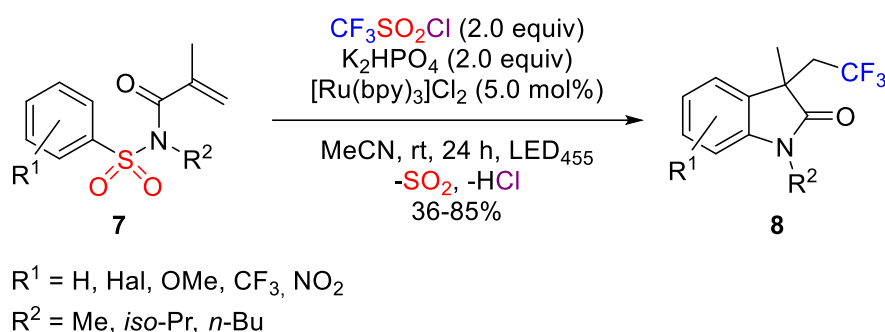
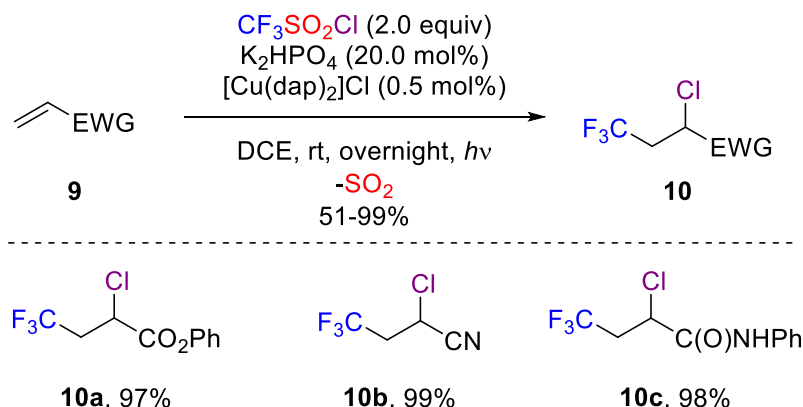


Figure 1. Representative examples for the generation of CF_3 radical.

For instance, Xia and co-workers^[14] demonstrated an elegant approach for the synthesis of α -aryl- β -trifluoromethyl amides **8** initiated by a visible light induced trifluoromethylarylation/ 1,4-aryl shift/ desulfonylation-cascade (Scheme 1). Different CF_3 radical precursors such as Togni reagent (**1**), trifluoromethane iodide (**2**) or triflyl chloride (**3a**) were screened. However, best results were obtained with $\text{CF}_3\text{SO}_2\text{Cl}$ (**3a**).

Scheme 1. Visible light induced cascade catalyzed by $[\text{Ru}(\text{bpy})_3]\text{Cl}_2$.^[14]


In 2015, the working group of Dolbier^[10c] showed a simple and highly effective copper catalyzed trifluoromethylchlorination reaction between $\text{CF}_3\text{SO}_2\text{Cl}$ (**3a**) and electron deficient alkenes **9** under visible light conditions (Scheme 2). The authors could demonstrate the net addition of CF_3Cl with α,β -unsaturated ketones, amides, esters, carboxylic acids, sulfones, and phosphonates. Furthermore, higher fluoroalkylsulfonyl chlorides $\text{R}_f\text{SO}_2\text{Cl}$ (i.e. $\text{R}_f = \text{C}_4\text{F}_9, \text{CF}_2\text{H}, \text{CH}_2\text{F}$, and CF_3CH_2) were successfully applied in this protocol by increasing the temperature to 100°C .

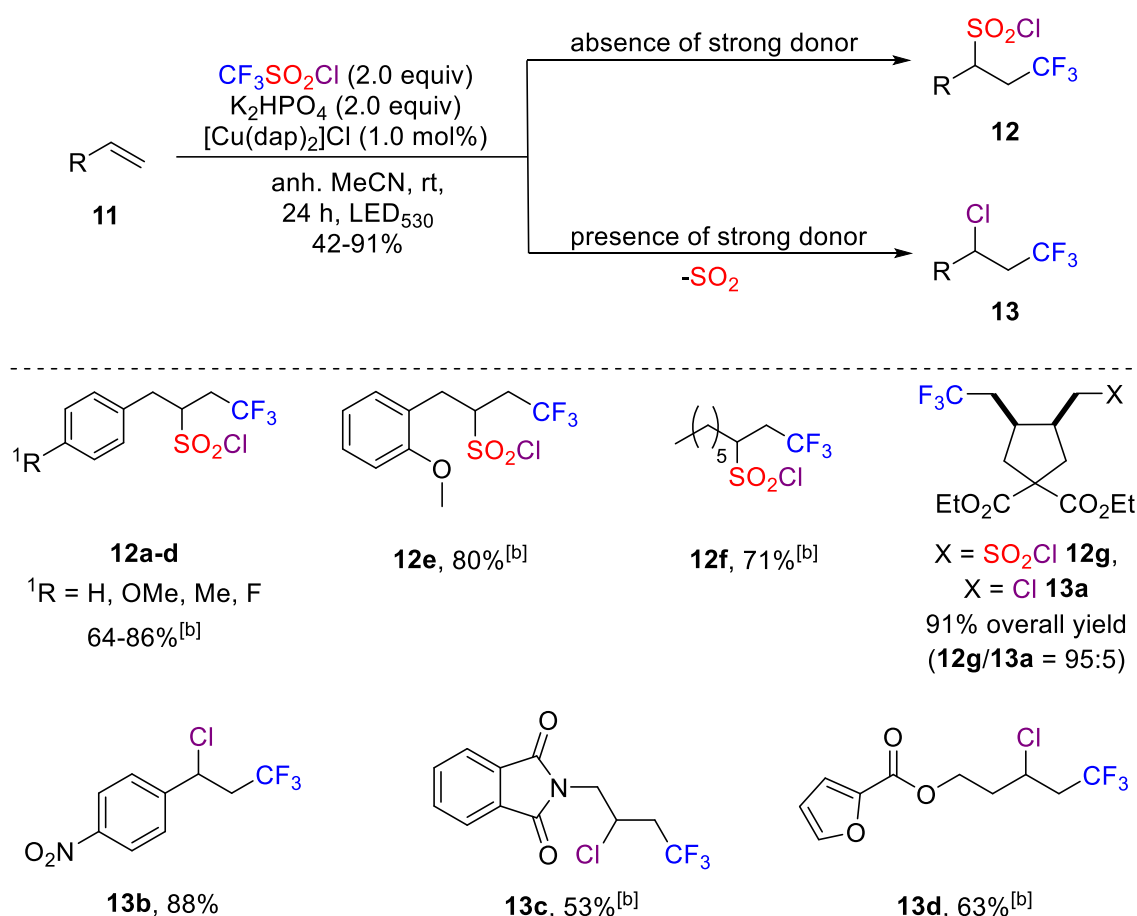
Scheme 2. $[\text{Cu}(\text{dap})_2]\text{Cl}$ catalyzed reaction between $\text{CF}_3\text{SO}_2\text{Cl}$ (**3a**) and electron deficient alkenes **9**.^[10c]


Moreover, the same process can be also achieved by photoredox catalysis^[10b] using the oxidative quenching cycle of $[\text{Ru}(\text{phen})_3]\text{Cl}_2$ or by thermal cleavage of $\text{CF}_3\text{SO}_2\text{Cl}$ (**3a**) catalyzed by $[\text{RuCl}_2(\text{PPh}_3)_3]$ as demonstrated by Kamigata et al.^[15] These examples illustrate that triflyl chloride (**3a**) commonly forms under photochemical or thermal conditions the trifluorochlorination product with concurrent loss of sulfurdioxide.

2. Trifluoromethylchlorosulfonylation

Very recently, an unprecedented visible light mediated trifluoromethylchlorosulfonylation of unactivated alkenes **11** with triflyl chloride (**3a**) in the presence of [Cu(dap)₂]Cl developed by Reiser et al. was published (Scheme 3).^[16] In contrast to ruthenium and iridium based photocatalysts, no SO₂ extrusion was observed in the absence of strong donor atoms leading to trifluoromethylsulfonylated products **12a-12g**.

Scheme 3. Representative examples for the [Cu(dap)₂]Cl catalyzed trifluoromethylchlorosulfonylation of alkenes **11**.^[a]

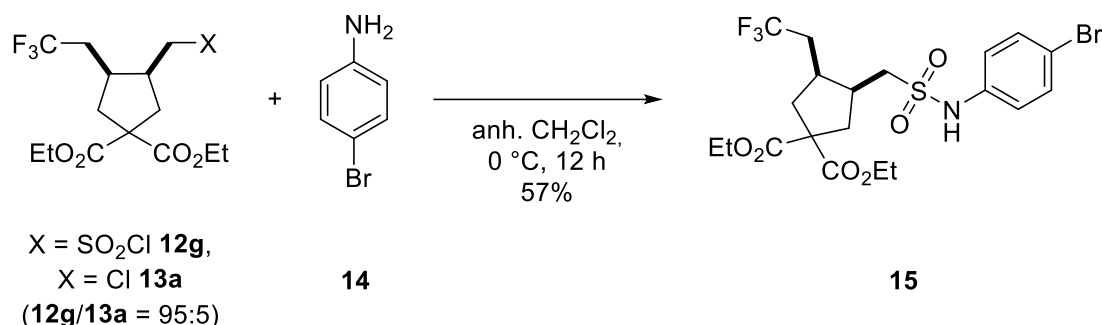


[a] Reaction conditions: alkene **11** (1.0 mmol, 1.0 equiv), CF₃SO₂Cl **3a** (2.0 mmol, 2.0 equiv), K₂HPO₄ (2.0 mmol, 2.0 equiv), [Cu(dap)₂]Cl (1.0 mol%), anh. MeCN (3.0 mL), irradiation at 530 nm (green LED), 24 h; [b] reaction performed by D. B. Bagal.

The labile sulfonyl chlorides **12a-12g** were reacted with aniline derivatives to form relevant trifluoromethylated sulfonamides for medicinal chemistry.^[17] When heteroatoms were present net CF₃Cl addition **13b-13d** was observed being in agreement with other literature reports.^[10c,18] Diethyl 2,2-diallylmalonate proved to be an excellent substrate for the trifluoromethylchlorosulfonylation, giving rise to an inseparable mixture of the ATRA product **12g** and chlorine adduct **13a** in 91% overall yield (**12g/13a** = 95:5). Afterwards, this mixture was treated with 1.2 equivalent of 4-bromo aniline **14** in anhydrous dichloromethane at 0 °C yielding sulfonamide **15** in 57% yield (Scheme 4). The stereochemistry was confirmed by

2D-NOESY NMR analysis and by comparison with other literature reports.^[8b] Again in contrast to related $[\text{Ru}(\text{bpy})_3]\text{Cl}_2$ catalyzed trifluoromethylations with the same substrate, which proceed only in moderate yield, the unique properties of $[\text{Cu}(\text{dap})_2]\text{Cl}$ could be demonstrated.^[8b]

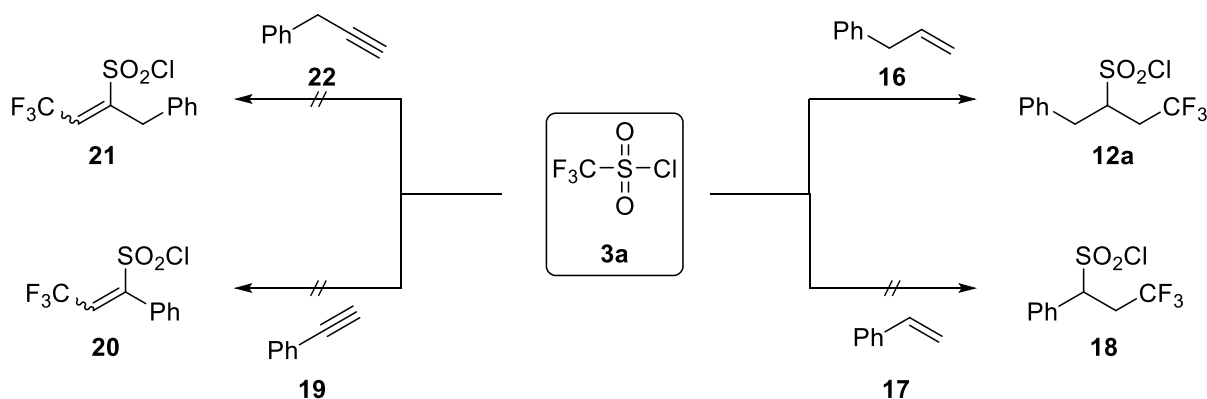
Scheme 4. Substrate screening for the copper-catalyzed trifluoromethylchlorosulfonylation.



Screening of various reaction parameters revealed that initiation of the reaction between allyl benzene (**16**) and triflyl chloride (**3a**) with the combination of CuCl and AIBN under thermal conditions exclusively led to the chlorine adduct in 35% yield. Also, the quantum yield Φ of the photocatalytic addition of trifluoromethanesulfonyl chloride (**3a**) to allyl benzene (**16**) was determined by a method developed by Riedle et al.^[19] being 12%, ruling out a free radical chain mechanism.

Attempts to use styrenes such as 4-methoxy, 4-methyl, 4-chloro styrene, or styrene (**17**) itself as reaction partner resulted mainly in trifluoromethylchlorination adduct. However, mixtures of products that result from subsequent elimination of HCl were generally obtained in low yield. An exception was the electron deficient *para*-nitrostyrene that was converted exclusively into product **13b** in high yield. Moreover, when phenylacetylene (**19**) or propargyl benzene (**22**) were subjected to photochemical trifluoromethylchlorosulfonylation reaction, a conversion of approximately 10% was observed after two days where no desired product could be identified. This results indicate that styrenes and especially acetylenes are not feasible for this transformation (Scheme 5).

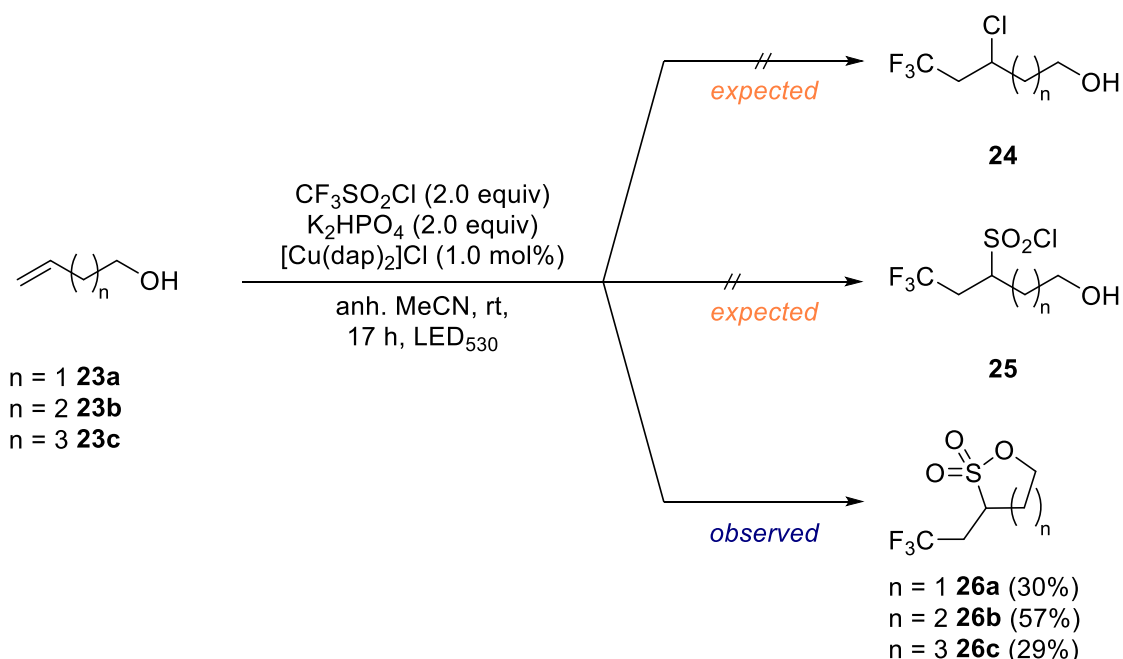
Scheme 5. Substrate screening for the copper-catalyzed trifluoromethylchlorosulfonylation.



3. Preliminary Studies with Alkenols

Initially performed screening for new substrates for the copper catalyzed trifluoromethylchlorosulfonylation of alkenes exhibited that irradiation of alkenols **23a-23c** in the presence of triflyl chloride (**3a**), K_2HPO_4 and copper catalyst resulted in no desired product. NMR, IR and mass spectroscopy analysis quickly revealed that instead of chlorine adduct **24** or ATRA product **25**, cyclization **26a-26c** occurred (Scheme 6).

Scheme 6. Initial study performed in cooperation with M. Knorn.^[a]



[a] Reaction conditions: alkene (1.0 mmol, 1.0 equiv), CF_3SO_2Cl (2.0 mmol, 2.0 equiv), K_2HPO_4 (2.0 mmol, 2.0 equiv), $[Cu(dap)_2]Cl$ (1.0 mol%), anhydrous MeCN (3.0 mL), irradiation at 530 nm (green LED), 24 h; equal contribution of author and M. Knorn.

Since the discovery of internal esters of hydroxy sulfonic acids commonly known as “sultones” by Erdmann in 1888,^[20] this compound class is attractive for a variety of research fields including natural product synthesis and biologically active compounds, medicinal chemistry, and material science.^[21] Several types of nomenclature have been found in the literature due to the fact that sultones can be also seen as sulfur analogues of lactones.^[22] For example, the aliphatic sultone **29b** can be named as 4-hydroxybutane-1-sulfonic acid, 1,4-butane-sultone or δ -sultone (Figure 2).

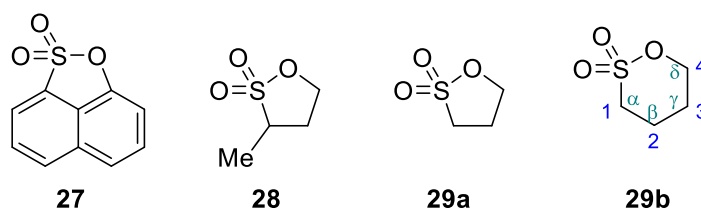


Figure 2. Representative sultone structure.

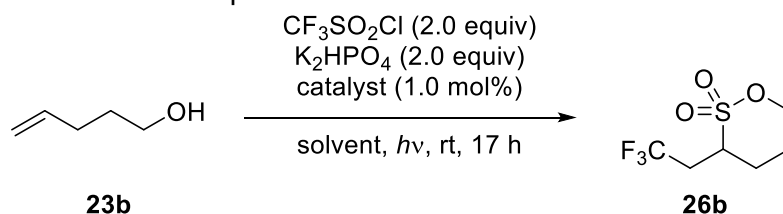
Metz and co-workers^[23] could successfully demonstrate the application of sultones as key intermediates in natural product synthesis. Moreover, promising results against human cytomegalovirus (HCMV), varicellazoster virus (VZV), and human immunodeficiency virus type 1 (HIV-1) were demonstrated by Velázquez and co-workers.^[24] Furthermore, sultones are applied in lithium-ion batteries (LIB) as an electrolyte additive^[25] to overcome problems such as low-temperature performance and calendar life performance, and safety issues for their application in electric vehicles. Especially in this context, the virtue of fluorine containing sultone (FPS) additives have been recognized.^[26] In particular, it was demonstrated that FPS exhibits cycle performance superior to 1,3-propane sultone (**29a**) and vinylene carbonate (VC). Besides, an increased number of patent registration from battery manufactures such as Sony Corp., Samsung SDI Co, Ltd., Dow Chemical, JCI, and BYD Company is observed for substituted γ - and δ -sultone.^[27] Less attention in the scientific community was given to 1,4-butane sultone (**29b**) although similar results were obtained. For example, the capacity loss of the battery with BS (**29b**) is equal to the value of a battery containing PS (**29a**) (after 100 cycles: 2.9%).^[25b,25c] Early approaches for sultone synthesis utilize the sulfonation of olefins with SO_3 and its adducts^[28], carbanion-mediated sulfonate coupling reactions^[29], or heating of the corresponding hydroxysulfonic acids in vacuum^[30]. In the last decade, milder methodologies have been developed including ring-closing metathesis (RCM), Diels-Alder reactions, or rhodium-catalyzed C-H insertion.^[21b]

In the last years, rapid progress was made in the field of visible light mediated redox photocatalysis and has established itself as a powerful technique for conducting free radical transformations.^[7] In this context, the visible light induced photocatalytic difunctionalization of alkenes proved to be an efficient approach for CF_xR -containing heterocycles.^[14,31] Recently, a variety of pyrrolidines and lactones were efficiently synthesized by photoredox catalysis employing $[\text{Cu}(\text{dap})_2]\text{Cl}$ and $\text{CHF}_2\text{SO}_2\text{Cl}$ as demonstrated by Dolbier and co-workers.^[18] In this cases however the reaction proceed with loss of sulfur dioxide without any sign of sultone or sulfonamide formation. Expanding the scope of the copper-catalyzed trifluoromethylchlorosulfonylation of alkenes (vide supra), the one-step visible mediated synthesis of α -substituted trifluoromethylated sultones from α,ω -alkenols is presented.

4. Optimization and Control Experiments

To optimize the reaction conditions, different parameters i.e. solvent, catalyst loading, and various photocatalysts using 4-penten-1-ol (**23b**) as a benchmark substrate were screened (Table 1). Indeed, the reaction with triflyl chloride (**3a**) in the presence of $[\text{Cu}(\text{dap})_2]\text{Cl}$ (1.0 mol%) results in the smooth formation of sultone **26b** (entry 1). Omitting the base, which is assumed to act as a scavenger for hydrochloric acid that is formed in the course of the reaction, leads to a significant decrease in yield (entry 2). While the reaction proceeds well in CH_2Cl_2 , DMF or DMSO (entries 3-5), acetonitrile appears to be the optimal solvent (entry 1). Reducing the amount of $[\text{Cu}(\text{dap})_2]\text{Cl}$ to 0.5 mol% (entry 6) was met with a reduction in yield: it is assumed that this is not a result of catalyst deactivation but rather due to deep coloring of the reaction solution with time that blocks the photoprocess. In contrast, net addition of CF_3Cl was mainly observed besides unidentified side products and low yields of sultone **26b** when well established photoredox catalysts such as $[\text{Ru}(\text{bpy})_3]\text{Cl}_2$ or *fac*- $\text{Ir}(\text{ppy})_3$ were used (entries 11-12). These photocatalysts require irradiation at 455 nm. To rule out that the failure to form photoadduct **26b** with these catalyst was due to the higher light energy, $[\text{Cu}(\text{dap})_2]\text{Cl}$ was also tested at this wavelength, which proceeded cleanly but resulted in a slightly lower yield of product **26b** (entry 13).

Table 1: Optimization of reaction parameters for the sultone formation.^[a]



Entry	Catalyst	Solvent	Yield [%]
1	$[\text{Cu}(\text{dap})_2]\text{Cl}$	MeCN	88
2 ^[b]	$[\text{Cu}(\text{dap})_2]\text{Cl}$	MeCN	34
3	$[\text{Cu}(\text{dap})_2]\text{Cl}$	CH_2Cl_2	71
4	$[\text{Cu}(\text{dap})_2]\text{Cl}$	DMF	50
5	$[\text{Cu}(\text{dap})_2]\text{Cl}$	DMSO	61
6 ^[c]	$[\text{Cu}(\text{dap})_2]\text{Cl}$	MeCN	49
7 ^[d]	$[\text{Cu}(\text{dap})_2]\text{Cl}$	MeCN	4
8	CuCl	MeCN	2
9	dap	MeCN	nr
10	no catalyst	MeCN	nr
11 ^[e]	$[\text{Ru}(\text{bpy})_3]\text{Cl}_2$	MeCN	10
12 ^[e]	<i>fac</i> - $\text{Ir}(\text{ppy})_3$	MeCN	18
13 ^[e]	$[\text{Cu}(\text{dap})_2]\text{Cl}$	MeCN	66

[a] Reaction conditions: 4-penten-1-ol **23b** (0.5 mmol, 1.0 equiv), $\text{CF}_3\text{SO}_2\text{Cl}$ **3a** (1.0 mmol, 2.0 equiv), K_2HPO_4 (1.0 mmol, 2.0 equiv), catalyst (1.0 mol%) in anh. solvent (1.5 mL), irradiation at 530 nm (green LED) for 17 h. All yields were based on using benzo-trifluoride as the internal standard; [b] absence of K_2HPO_4 ; [c] catalyst loading 0.5 mol%; [d] dark reaction; [e] irradiation at 455 nm (blue LED).

5. Substrate Scope

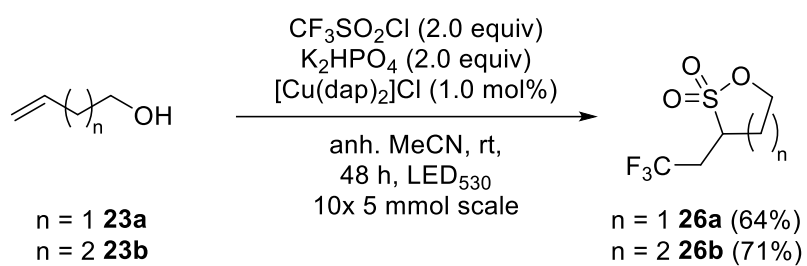
With optimized conditions in hand, the scope of the reaction was examined (Table 2). Attempts to use allyl alcohol **23d** gave rise to a complex reaction mixture with only trace amounts of the desired β -sultone **26d** detectable (entry 1), a compound class that is known to have low stability.^[32] The γ - and δ -sultones **26a** and **26b** were obtained in good to excellent yields, while a drop of yield was observed for the ε -sultone **26c** (entries 2-4). Focusing on δ -sultones, readily available pent-4-en-1-ols **23e-23i** being substituted in 2- and/or 3-position gave rise to sultones **26e-26i**. However, methyl or phenyl substitution either in 4- or 5-position led to complex mixtures containing regio- and diastereomeric sultones, and in addition, trifluoromethylchlorination of the alkene was observed (entries 11-13). In general, it should be noted that the developed trifluoromethylchlorosulfonylation of alkenes is sensitive to steric effects: substitution at the double bond or next to it leads to increasing amounts of CF_3Cl addition, which is the general reaction mode for ruthenium- or iridium-based photocatalysts. An X-ray structure of product **26f** confirmed the general structure of the cyclic sultones formed. Embedding a phenol moiety into the substrate was also possible as demonstrated with the transformation of substrate **23n** to sultone **26n**, being especially relevant for the synthesis of drug-like sultones (vide infra).

To demonstrate the viability of the method for preparative purposes, scale-up of sultones **26b** and **26c** to gram quantities was also demonstrated. The setup for the small scale and scale-up reaction is depicted in Figure 3. Initially, irradiation was ensured by a high power green LED (A) with $\lambda = 530$ nm bundled through a glass rod (B) directly into the degassed reaction solution (C) using a Schlenk tube (D) and a lockable screw cap including a Teflon inlet (E). Since higher amount of solvent was needed and unfortunately a continuous flow microreactor was not usable due to the heterogeneous system, the reaction was performed ten times on a 5 mmol scale in an appropriate bigger Schlenk pressure tube (F). Also, higher light density achieved by installing two additional LED plates (G) was necessary for full conversion of the starting material. Afterwards, the reaction solutions were combined, quenched with water, followed by extracting with CH_2Cl_2 . The residue was purified by distillation. This sequence yielded overall 64% and 71% for the 5- and 6-membered product **26a** and **26b**, respectively. This method allows rapid access to α -substituted sultones in good yield on a larger scale employing mild reaction conditions, facile reaction setup and low catalyst loading. Efforts to prepare sultones in higher purity (>94%) failed. For example, multiple fractional distillation using vigreux column with different lengths beside column chromatography resulted in no improvement.

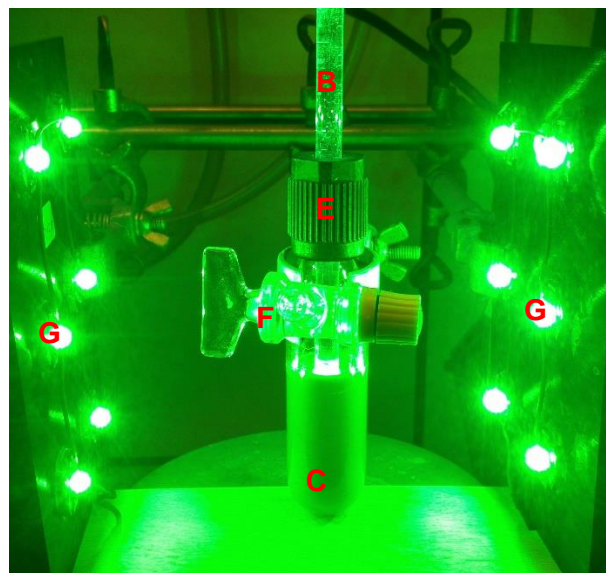
Table 2: Substrate scope of photoredox catalyzed intramolecular formation of sultone.^[a]

$ \begin{array}{c} \text{CF}_3\text{SO}_2\text{Cl (2.0 equiv),} \\ \text{K}_2\text{HPO}_4 \text{ (2.0 equiv),} \\ \text{[Cu(dap)}_2\text{]Cl (1.0 mol\%)} \\ \text{anh. MeCN, rt, 17 h, LED}_{530} \end{array} $			
Entry	Alkene	Product	Yield [%]
1	n = 1 23d	n = 1 26d	<5
2	n = 2 23a	n = 2 26a	64
3	n = 3 23b	n = 3 26b	90
4 ^[b]	n = 4 23c	n = 4 26c	32
5	 23e	 26m	73
6	R = Ph 23f	R = Ph 26f	73
7	R = CO ₂ Et 23g	R = CO ₂ Et 26g	50
8	 23h	 26h	74
9 ^[c]	 23i	 26i	90
10	 23j	 26j	67
11	R ¹ = H, R ² = Me 23k	R ¹ = H, R ² = Me 26k	0
12	R ¹ = Me, R ² = H 23l	R ¹ = Me, R ² = H 26l	0
13	R ¹ = Ph, R ² = H 23m	R ¹ = Ph, R ² = H 26m	0

[a] Reaction conditions: alkene **23** (1.0 mmol, 1.0 equiv), CF₃SO₂Cl **3a** (2.0 mmol, 2.0 equiv), K₂HPO₄ (2.0 mmol, 2.0 equiv), [Cu(dap)₂]Cl (1.0 μmol, 1.0 mol%) in anh. MeCN (3.0 mL), irradiation at 530 nm (green LED), rt, 17 h; [b] reaction performed by M. Knorn; [c] diastereomeric ratio **26i** *syn/anti* = 44:56.



1.0 mmol scale



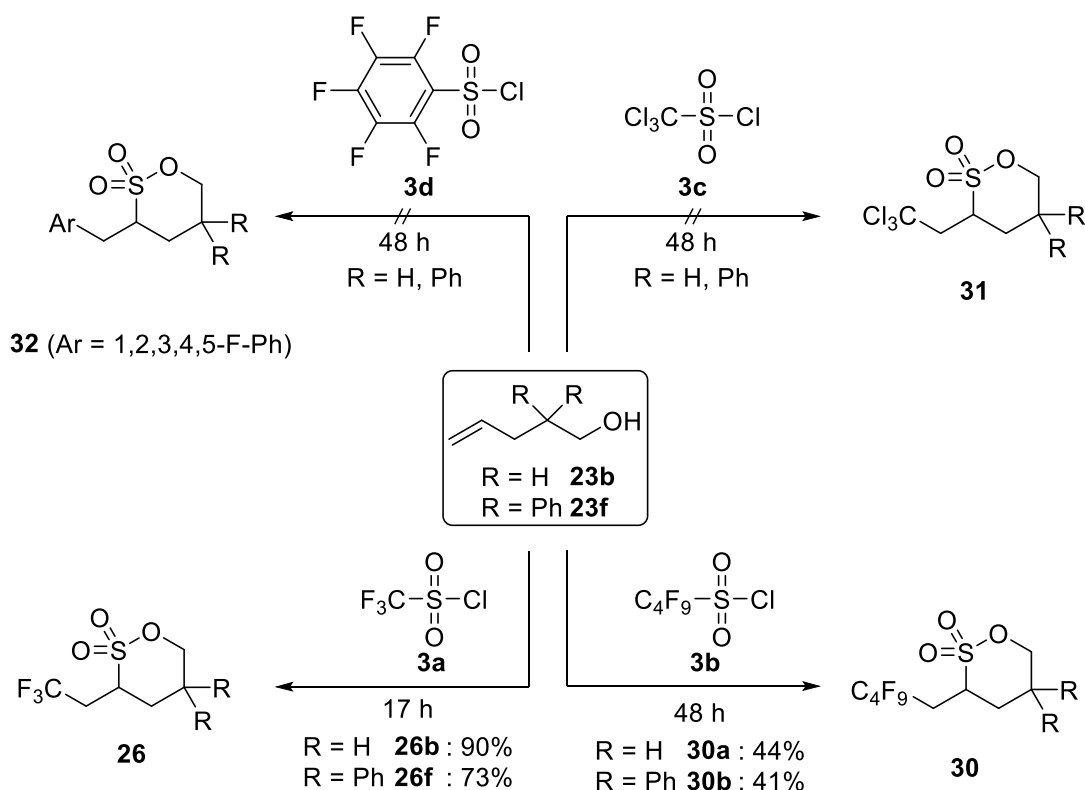
5.0 mmol scale

Figure 3. Setup-overview for scale up.

6. Variation of Sulfonyl Chlorides as Radical Source

In the photoredox catalyzed intramolecular aminodifluoromethylation of unactivated alkenes Dolbier et al. employed photocatalyst $[\text{Cu}(\text{dap})_2]\text{Cl}$ and $\text{CHF}_2\text{SO}_2\text{Cl}$ as radical source (for more details see Chapter A, Scheme 6).^[18] As already mentioned, no sultone or sulfamide formation was observed. Moreover, the use of $\text{CF}_3\text{SO}_2\text{Cl}$ (**3a**) or $\text{C}_4\text{F}_9\text{SO}_2\text{Cl}$ (**3b**) led to the simple ATRA addition products. The authors claim that the oxidation of the formed carboradical to its cation is inhibited when more electronegative groups (e.g. CF_3 or C_4F_9) than CHF_2 were present. Encouraged by the positive results *vide supra*, different commercially available sulfonyl chlorides were tested for the introduction of various side chains (Scheme 7). Indeed, cyclization was observed for alkenol **23b** and **23f** when $\text{C}_4\text{F}_9\text{SO}_2\text{Cl}$ (**3b**) was employed yielding perfluorobutane-containing sultones **30a** and **30b** in 41% and 44% yield, respectively, but longer reaction times were necessary to obtain full conversion. No conversion of the starting materials **23b** and **23f** were observed with pentafluorobenzenesulfonyl chloride (**3d**). Use of $\text{CCl}_3\text{SO}_2\text{Cl}$ (**3c**) as radical source led to a complex reaction mixture in which the desired product **31** could not be identified.

Scheme 7. Various sulfonyl chlorides tested for sultone synthesis.^[a]



[a] Reaction conditions: alkene **23** (1.0 mmol, 1.0 equiv), sulfonyl chloride (**3**) (2.0 mmol, 2.0 equiv), K_2HPO_4 (2.0 mmol, 2.0 equiv), $[\text{Cu}(\text{dap})_2]\text{Cl}$ (1.0 μmol , 1.0 mol%) in anhyd. MeCN (3.0 mL), irradiation at 530 nm (green LED), rt, 17–48 h.

7. Application of Methodology in Pharmaceutical Chemistry

Inspired by the successful intermolecular formation of sultone utilizing the oxidative quenching cycle of $[\text{Cu}(\text{dap})_2]\text{Cl}$, its application in pharmaceutical drug synthesis was envisioned. In 1985, Suntory Ltd. reported in a patent the preparation and pharmaceutical decomposition of novel benzoxathiin derivatives **33** (Figure 4).^[33]

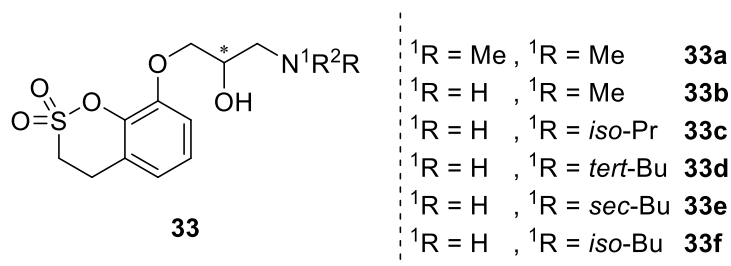
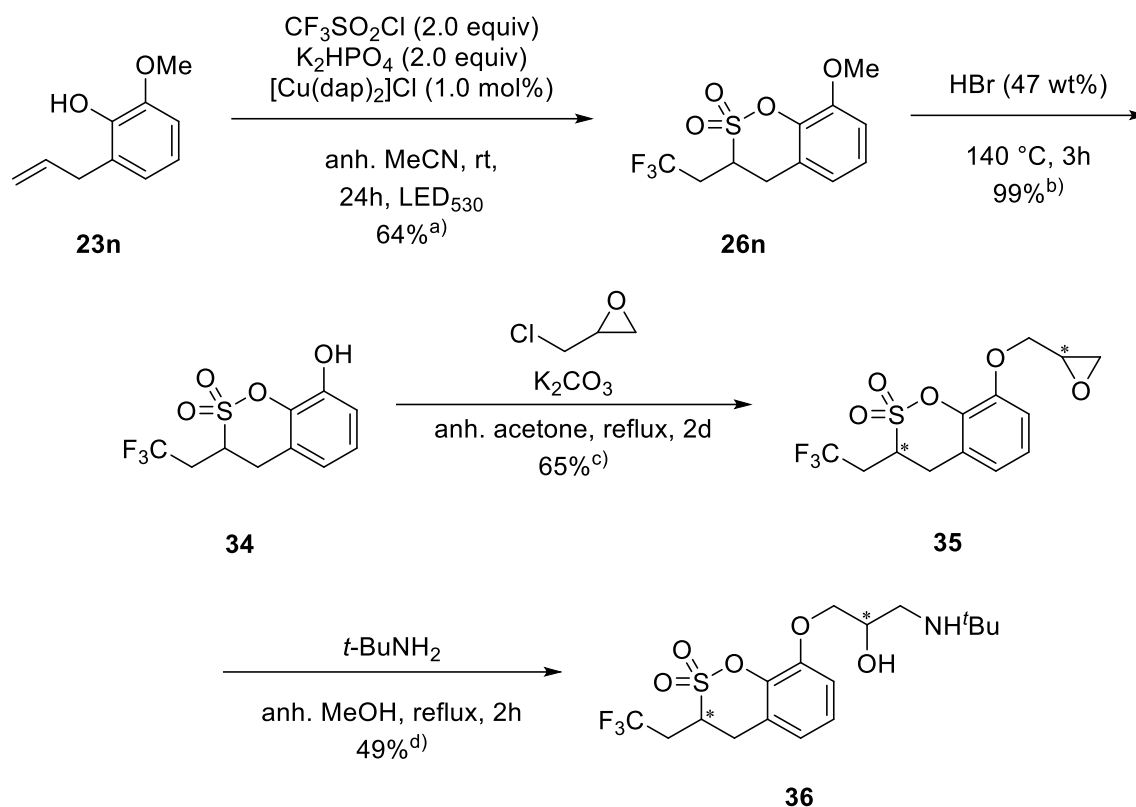


Figure 4. Pharmaceutical important benzoxathiin derivatives **33** prepared by Suntory Ltd.^[33]

Benzoxathiins have been recognized as lead structures in medicinal chemistry due to their excellent pharmacological properties. In particular, sultone **33d**, being available in a seven step sequence from *o*-vanillin, showed at a concentration of 1 μmol 96.3% β -receptor blocking inhibition and anti-arrhythmic activity of 0.03 mg/kg (ED_{50}), while its toxicity is very low (LD_{50} : 59.2 mg/kg intravenous, >500 mg/kg in stomach) compared to other commercial available β -blockers.^[33] These drugs are used in the medical field for disorders of the cardiovascular system such as arrhythmia, angina pectoris or hypertension.

Considering the benefits of fluoroalkyl group introduction into biologically active molecules,^[34] based on the methodology reported here, the CF_3CH_2 analogue **39** could be efficiently synthesized in only four steps from commercially available *o*-eugenol (**23n**) (Scheme 8). The latter was converted under the standard conditions to sultone **26n** on a 3 mmol scale in 64% yield. Cleavage of the methoxy group with HBr and etherification with racemic epichlorohydrine gave rise to epoxid **38**, which upon treatment with *tert*-butylamine resulted in compound **39** as a 1:1 mixture of diastereomers in an overall yield of 20% over four steps. Finally, the synthesized benzoxathiin derivative **39** has to be tested in order to identify the influence of the side chain. Unfortunately, these tests can be only achieved by mice tests which are therefore not investigated any further.

Scheme 8. Synthesis of novel benzoxathiin derivative derived from visible light mediated intramolecular formation of sultone as key step.^[a]

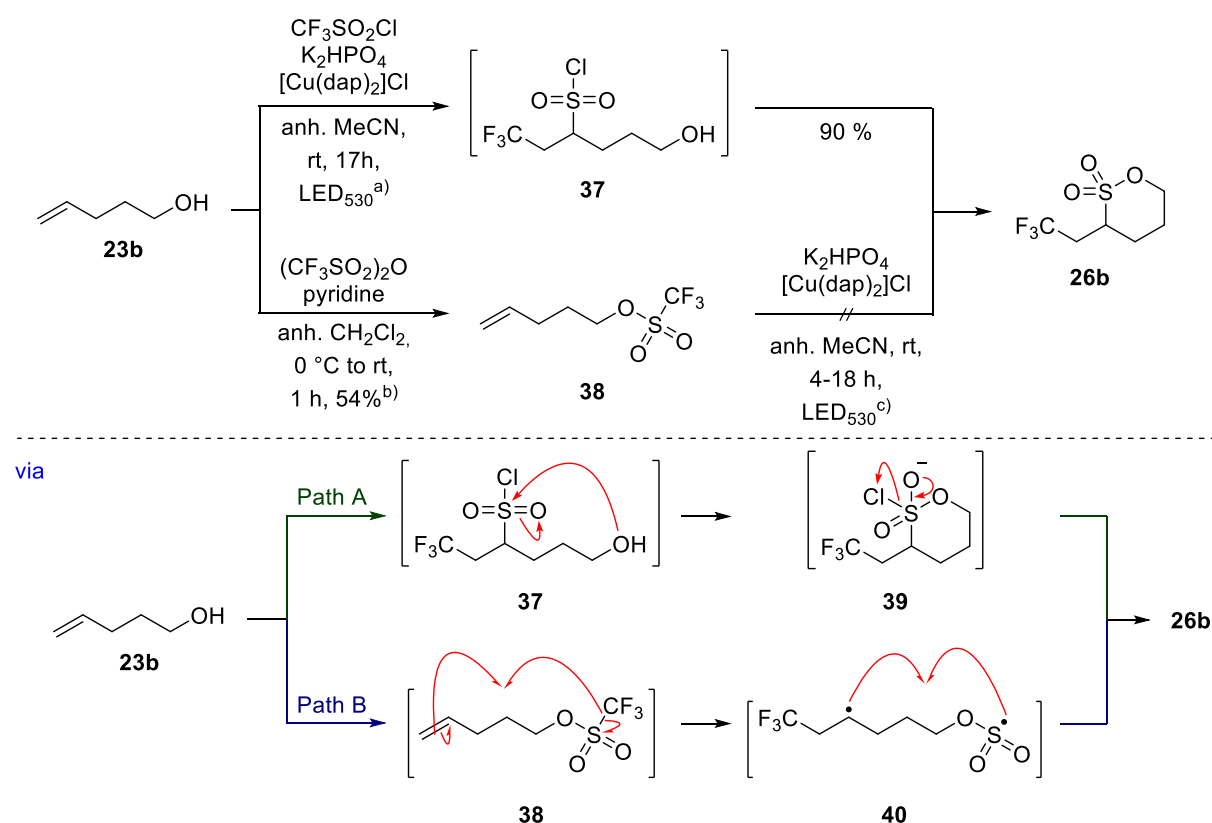


[a] Reaction conditions: 1.Step: 2-allyl-6-methoxyphenol **23n** (3.0 mmol, 1.0 equiv), $\text{CF}_3\text{SO}_2\text{Cl}$ **3a** (6.0 mmol, 2.0 equiv), K_2HPO_4 (6.0 mmol, 2.0 equiv), $[\text{Cu}(\text{dap})_2]\text{Cl}$ (3.0 μmol , 1.0 mol%), anhydrous MeCN (9.0 mL), irradiation at 530 nm (green LED), rt, 48 h, 64%; b) HBr (30 mL, 47 wt%), 140 °C, 3 h, 99%; c) epichlorohydrin (25.5 mmol, 18.2 equiv), K_2CO_3 (3.1 mmol, 2.2 equiv), anhydrous acetone (20 mL), reflux, 2 d, 65% (d.r. = 50:50); $t\text{-BuNH}_2$ (7.7 mmol, 12.9 equiv), anhydrous MeOH (40 mL), reflux, 2 h, 49% (d.r. = 50:50), 20% overall yield after four steps.

8. Mechanistic Studies

In order to gain a deeper insight to the mechanism, a series of experiments were carried out. Taking alcohol **23b** as model compound, it was tested if initially trifluorochlorosulfonylation to compound **37** followed by cyclization takes place (Path A) or if first the triflate **38** is formed, which is subsequently photochemical cleaved with concurrent cyclization to sultone **26b** (Scheme 9). The latter was ruled out by the independent synthesis of triflyl protected alcohol **38**, which resulted upon irradiation under the standard reaction conditions only in polymerization of the starting material. Both Greene et al. and Veal and co-workers reported that the prepared triflate derivative **38** is moisture, heat and light sensitive and therefore tend to polymerize being in full agreement with the findings reported herein.^[35] Moreover, the reaction of alkenol **23b** with $\text{CF}_3\text{SO}_2\text{Cl}$ (**3a**) is sluggish, even in the presence of a base such as pyridine. A conversion of 12% was determined by $^1\text{H-NMR}$ after 36 hours. Therefore, it is concluded that trifluoromethylsulfonylation of alkene precedes through sultone formation.

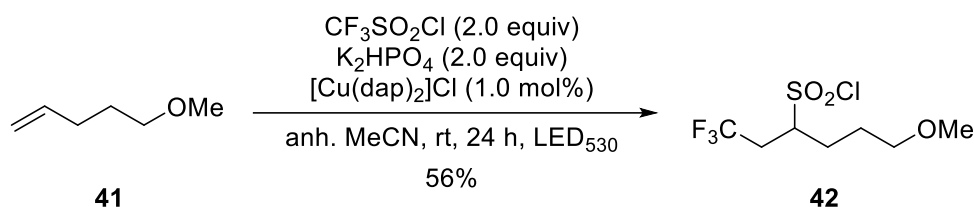
Scheme 9. Mechanistic studies: trifluoromethylchlorosulfonylation vs triflate formation.^[a]



[a] Reaction conditions: a) 4-penten-1-ol **23b** (1.0 mmol, 1.0 equiv), $\text{CF}_3\text{SO}_2\text{Cl}$ (**3a**) (2.0 mmol, 2.0 equiv), K_2HPO_4 (2.0 mmol, 2.0 equiv), $[\text{Cu}(\text{dap})_2]\text{Cl}$ (1.0 μmol , 1.0 mol%), anhyd. MeCN (3.0 mL), irradiation at 530 nm (green LED), rt, 18 h, 90%; b) 4-penten-1-ol **23b** (5.0 mmol, 1.0 equiv), Tf_2O (5.0 mmol, 1.0 equiv), pyridine (5.0 mmol, 1.0 equiv), anhyd. CH_2Cl_2 (20.0 mL), 0 °C to rt, 1 h, 54%; c) pent-4-en-1-yl trifluoromethanesulfonate **38** (1.0 mmol, 1.0 equiv), K_2HPO_4 (2.0 mmol, 2.0 equiv), $[\text{Cu}(\text{dap})_2]\text{Cl}$ (1.0 μmol , 1.0 mol%), anhyd. MeCN (3.0 mL), irradiation at 530 nm (green LED), rt, 4-18 h, 0%.

In agreement with these findings, reacting protected alcohol **41** under the standard reaction conditions, trifluoromethylchlorosulfonylation to adduct **42** was observed (Scheme 10). A similar outcome was already noticed in the reaction between triflyl chloride (**3a**) and 1-allyl-2-methoxybenzene leading to compound **12e** as already seen in the trifluoromethylchlorosulfonylation *vide supra*.

Scheme 10. Trifluoromethylchlorosulfonylation of protected α,ω -alkenol **41**.^[a]



[a] Reaction conditions: 5-methoxypent-1-ene **41** (1.0 mmol, 1.0 equiv), $\text{CF}_3\text{SO}_2\text{Cl}$ **3a** (2.0 mmol, 2.0 equiv), K_2HPO_4 (2.0 mmol, 2.0 equiv), $[\text{Cu}(\text{dap})_2]\text{Cl}$ (1.0 μmol , 1.0 mol%), anh. MeCN (3.0 mL), irradiation at 530 nm (green LED), rt, 24 h, 56%.

While the overall process to sultones **26** proceeded cleanly, minor impurities were identified such as the corresponding sultines (SO_2 instead of SO_3), which could not be removed in the case of product **26h**. The sultines could arise by reduction of the sultones. Therefore, the isolated δ -sultone **26b** was subjected again under the reaction condition of its formation: no decomposition or further side reactions were observed indicating that the sultones are photochemically stable. Most likely, the sultines arise from CF_3SOCl that is present in commercially available trifluoromethanesulfonyl chloride (**3a**) due to incomplete oxidation of the corresponding sodium sulfinate, acid, or sulfinyl derivatives.^[36]

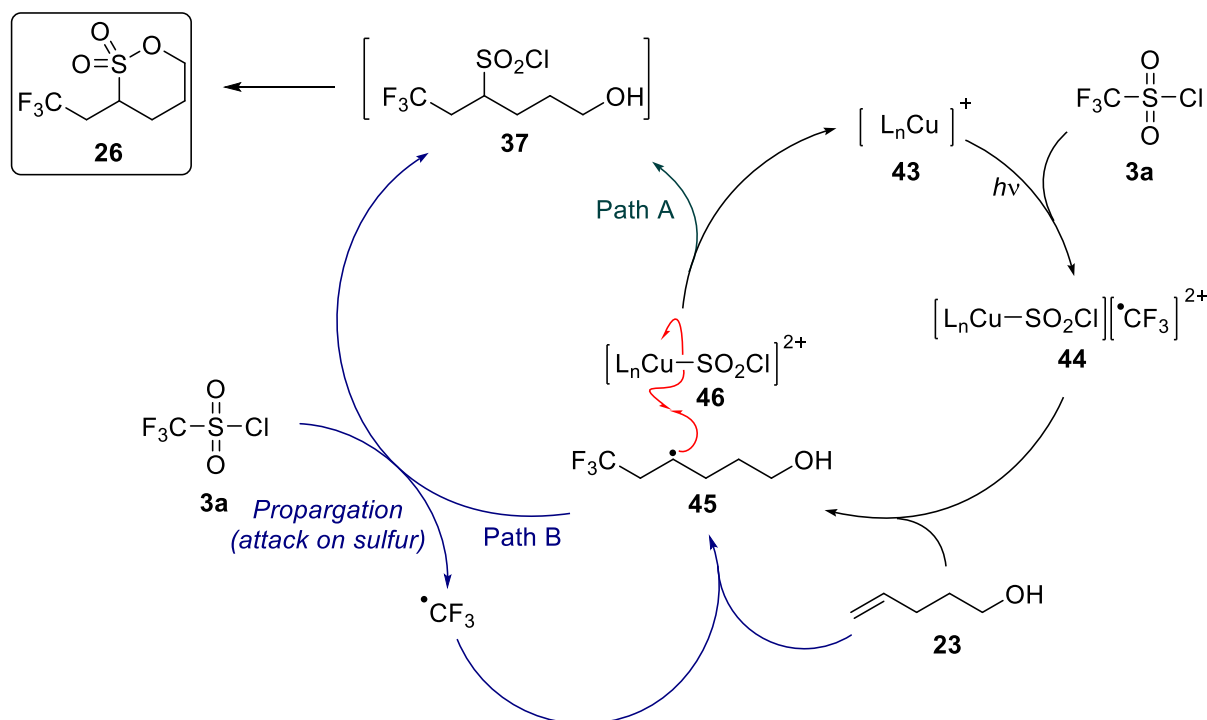
A second impurity that was identified with the generation of photoproduct **26g** is a sultone having a chlorine instead of a trifluoromethyl group incorporated, suggesting that under the photoredox conditions chlorine radicals are also generated that initiate sultone formation by addition to the alkene in alcohol **23**.

9. Proposed Mechanism

Taking these observations *vide supra* into account, the following mechanistic picture arises: photoexcited $^*[\text{Cu}(\text{dap})_2]^+$ **43** reduces triflyl chloride (**3a**) by a single electron transfer (SET), thus generating a trifluoromethyl radical, which adds to alkene **23** to form the radical **45**. The Cu(II) species **46** formed concurrently in this process might coordinate and thus stabilize SO_2Cl^- , which then combines with radical **45** by a back electron transfer to regenerate the Cu(I) catalyst **43** and to form trifluoromethylchlorosulfonylation product **37**. The involvement of nucleophiles bound to Cu(II) has been recently shown by Fu et al. for the copper-mediated cross coupling of an aryl thiol with an aryl halide induced by visible light.^[37] Finally, an intramolecular cyclization of the free alcohol **37** produces the desired sultone **26** (Scheme 11).

Alternatively, radical **45** might initiate a radical chain process with $\text{CF}_3\text{SO}_2\text{Cl}$ (**3a**) to produce trifluoromethylchlorosulfonylation product **37** and CF_3 radical. This proposal would call for a rather unusual attack of **45** at sulfur in $\text{CF}_3\text{SO}_2\text{Cl}$ (**3a**). It should be noted that when $[\text{Ru}(\text{bpy})_3]\text{Cl}_2$ is used instead of $[\text{Cu}(\text{dap})_2]\text{Cl}$, trifluoromethyl *chlorination* instead of *chlorosulfonylation* is observed, which was explained by the attack of radicals of the type **45** onto chloride in $\text{CF}_3\text{SO}_2\text{Cl}$ (**3a**).^[10b] Given the lower oxidation potential of Cu(II) to Cu(I) ($E_{1/2} = 0.62$ V vs SCE) compared to Ru(III) to Ru(II) ($E_{1/2} = 0.77$ V vs SCE), in the ruthenium catalyzed process a more facile oxidation of **45** to its corresponding cation might be the key intermediate that takes up chloride.

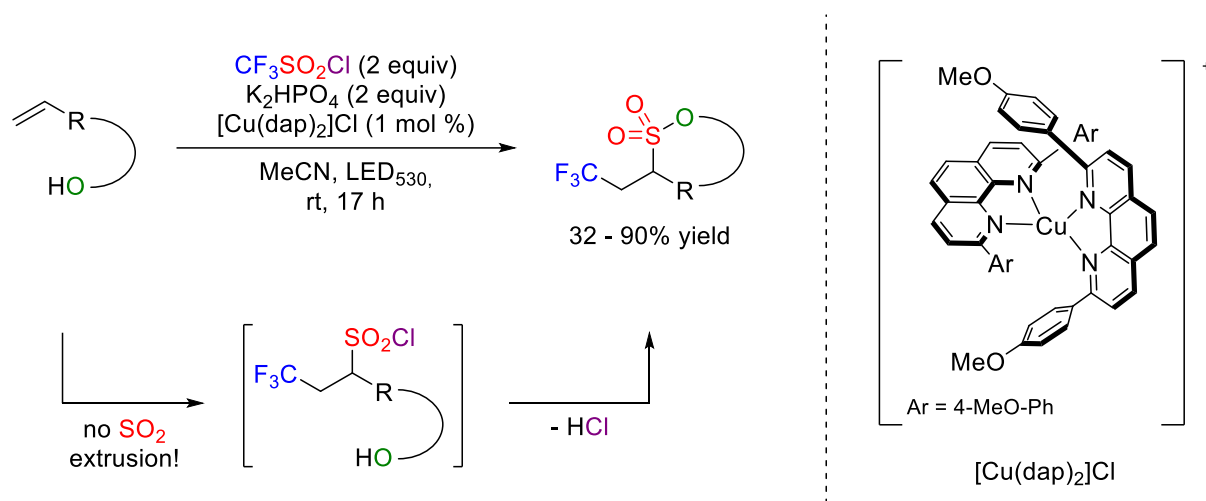
Scheme 11. Proposed mechanism.



10. Summary

In conclusion, a simple photoredox catalyzed procedure for the one-step synthesis of sultones **26** with trifluoroethyl substitution in the 3-position^[38] from readily available α,ω -alkenols **23** in moderate to excellent yield using an inexpensive copper catalyst with low loading. The resulting sultones might have potential as lithium battery additives, which is currently under investigation. Moreover, the trifluoroethyl substituted benzoxathiin derivate **36** could be synthesized, which is an analogue of the highly potent β -blocker **33**.

Scheme 12. Synthesis of trifluoromethylated sultones from alkenols using $[\text{Cu}(\text{dap})_2]\text{Cl}$ as photoredox catalyst.



11. References

- [1] a) Prakash, G. K.; Wang, F.; Ni, C.; Shen, J.; Haiges, R.; Yudin, A. K.; Mathew, T.; Olah, G. A. *J. Am. Chem. Soc.* **2011**, *133*, 9992-9995; b) Prakash, G. K.; Wang, F.; Rahm, M.; Zhang, Z.; Ni, C.; Shen, J.; Olah, G. A. *J. Am. Chem. Soc.* **2014**, *136*, 10418-10431.
- [2] a) Schlosser, M. *Angew. Chem. Int. Ed.* **1998**, *37*, 1496-1513; b) Siodla, T.; Oziminski, W. P.; Hoffmann, M.; Koroniak, H.; Krygowski, T. M. *J. Org. Chem.* **2014**, *79*, 7321-7331.
- [3] a) Purser, S.; Moore, P. R.; Swallow, S.; Gouverneur, V. *Chem. Soc. Rev.* **2008**, *37*, 320-330; b) Yale, H. L. *J. Med. Chem.* **1959**, *1*, 121-133; c) Muller, K.; Faeh, C.; Diederich, F. *Science* **2007**, *317*, 1881-1886.
- [4] a) Langlois, B. R.; Billard, T.; Roussel, S. *J. Fluorine Chem.* **2005**, *126*, 173-179; b) Liu, X.; Xu, C.; Wang, M.; Liu, Q. *Chem. Rev.* **2015**, *115*, 683-730; c) Prakash, G. K. S.; Yudin, A. K. *Chem. Rev.* **1997**, *97*, 757-786; d) Miyake, Y.; Ota, S.; Shibata, M.; Nakajima, K.; Nishibayashi, Y. *Org. Biomol. Chem.* **2014**, *12*, 5594-5596; e) Prakash, G. K.; Jog, P. V.; Batamack, P. T.; Olah, G. A. *Science* **2012**, *338*, 1324-1327.
- [5] a) Shibata, N.; Matsnev, A.; Cahard, D. *Beilstein J. Org. Chem.* **2010**, *6*, No. 65; b) Brand, J. P.; Fernandez Gonzalez, D.; Nicolai, S.; Waser, J. *Chem. Commun.* **2011**, *47*, 102-115; c) He, Z.; Tan, P.; Hu, J. *Org. Lett.* **2016**, *18*, 72-75; d) Macé, Y.; Magnier, E. *Eur. J. Org. Chem.* **2012**, *2012*, 2479-2494; e) Charpentier, J.; Fruh, N.; Togni, A. *Chem. Rev.* **2015**, *115*, 650-682.
- [6] a) Beatty, J. W.; Douglas, J. J.; Cole, K. P.; Stephenson, C. R. *Nat. Commun.* **2015**, *6*, 7919; b) Studer, A. *Angew. Chem. Int. Ed.* **2012**, *51*, 8950-8958; c) Sato, A.; Han, J.; Ono, T.; Wzorek, A.; Acena, J. L.; Soloshonok, V. A. *Chem. Commun.* **2015**, *51*, 5967-5970; d) Cao, X. H.; Pan, X.; Zhou, P. J.; Zou, J. P.; Asekun, O. T. *Chem. Commun.* **2014**, *50*, 3359-3362; e) Presset, M.; Oehlrich, D.; Rombouts, F.; Molander, G. A. *J. Org. Chem.* **2013**, *78*, 12837-12843.
- [7] *Leading reviews*: a) Prier, C. K.; Rankic, D. A.; MacMillan, D. W. *Chem. Rev.* **2013**, *113*, 5322-5363; b) Narayanam, J. M.; Stephenson, C. R. *Chem. Soc. Rev.* **2011**, *40*, 102-113; c) Zeitler, K. *Angew. Chem. Int. Ed.* **2009**, *48*, 9785-9789; d) Paria, S.; Reiser, O. *ChemCatChem* **2014**, *6*, 2477-2483; e) Ravelli, D.; Protti, S.; Fagnoni, M. *Chem. Rev.* **2016**, ASAP, DOI: 10.1021/acs.chemrev.5b00662; f) Skubi, K. K.; Blum, T. R.; Yoon, T. P. *Chem. Rev.* **2016**, ASAP, DOI: 10.1021/acs.chemrev.6b00018.
- [8] a) Lin, Q. Y.; Xu, X. H.; Qing, F. L. *J. Org. Chem.* **2014**, *79*, 10434-10446; b) Mizuta, S.; Verhoog, S.; Engle, K. M.; Khotavivattana, T.; O'Duill, M.; Wheelhouse, K.; Rassias, G.; Medebielle, M.; Gouverneur, V. *J. Am. Chem. Soc.* **2013**, *135*, 2505-2508.
- [9] a) Wallentin, C. J.; Nguyen, J. D.; Finkbeiner, P.; Stephenson, C. R. *J. Am. Chem. Soc.* **2012**, *134*, 8875-8884; b) Ye, Y.; Sanford, M. S. *J. Am. Chem. Soc.* **2012**, *134*,

- 9034-9037; c) Pham, P. V.; Nagib, D. A.; MacMillan, D. W. *Angew. Chem. Int. Ed.* **2011**, *50*, 6119-6122.
- [10] a) Nagib, D. A.; MacMillan, D. W. *Nature* **2011**, *480*, 224-228; b) Oh, S. H.; Malpani, Y. R.; Ha, N.; Jung, Y. S.; Han, S. B. *Org. Lett.* **2014**, *16*, 1310-1313; c) Tang, X. J.; Dolbier, W. R., Jr. *Angew. Chem. Int. Ed.* **2015**, *54*, 4246-4249.
- [11] Fu, W.; Guo, W.; Zou, G.; Xu, C. *J. Fluorine Chem.* **2012**, *140*, 88-94.
- [12] Beatty, J. W.; Douglas, J. J.; Cole, K. P.; Stephenson, C. R. *Nat. Commun.* **2015**, *6*, 7919-7925.
- [13] a) Asano, M.; Tomita, R.; Koike, T.; Akita, M. *J. Fluorine Chem.* **2015**, *179*, 83-88; b) Wang, H.; Cheng, Y.; Yu, S. *Sci. China Chem.* **2015**, *59*, 195-198; c) Tomita, R.; Yasu, Y.; Koike, T.; Akita, M. *Beilstein J. Org. Chem.* **2014**, *10*, 1099-1106.
- [14] Zheng, L.; Yang, C.; Xu, Z.; Gao, F.; Xia, W. *J. Org. Chem.* **2015**, *80*, 5730-5736.
- [15] Kamigata, N.; Fukushima, T.; Yoshida, M. *J. Chem. Soc., Chem. Commun.* **1989**, 1559-1560.
- [16] Bagal, D. B.; Kachkovskyi, G.; Knorn, M.; Rawner, T.; Bhanage, B. M.; Reiser, O. *Angew. Chem. Int. Ed.* **2015**, *54*, 6999-7002.
- [17] Carta, F.; Scozzafava, A.; Supuran, C. T. *Expert Opin. Ther. Patents* **2012**, *22*, 747-758.
- [18] Zhang, Z.; Tang, X.; Thomoson, C. S.; Dolbier, W. R., Jr. *Org. Lett.* **2015**, *17*, 3528-3531.
- [19] Megerle, U.; Lechner, R.; König, B.; Riedle, E. *Photochem. Photobiol. Sci.* **2010**, *9*, 1400-1406.
- [20] Erdmann, H. *Justus Liebigs Ann. Chem.* **1888**, *247*, 306-366.
- [21] *Leading Reviews*: a) Mustafa, A. *Chem. Rev.* **1954**, *54*, 195-223; b) Mondal, S. *Chem. Rev.* **2012**, *112*, 5339-5355; c) Roberts, D. W.; Williams, D. L. *Tetrahedron* **1987**, *43*, 1027-1062; d) Metz, P. *J. Prakt. Chem.* **1998**, *340*, 1-10.
- [22] a) Morel, T.; Verkade, P. E. *Recl. Trav. Chim. Pays-Bas* **2010**, *68*, 619-638; b) Crane, E. J.; Patterson, A. M. *Chem. Abstr.* **1945**, *39*, 5934.
- [23] a) Metz, P.; Stölting, J.; Läge, M.; Krebs, B. *Angew. Chem. Int. Ed.* **1994**, *33*, 2195-2197; b) Wang, Y.; Bernsmann, H.; Gruner, M.; Metz, P. *Tetrahedron Lett.* **2001**, *42*, 7801-7804; c) Merten, J.; Fröhlich, R.; Metz, P. *Angew. Chem. Int. Ed.* **2004**, *43*, 5991-5994; d) Merten, J.; Hennig, A.; Schwab, P.; Fröhlich, R.; Tokalov, S. V.; Gutzeit, H. O.; Metz, P. *Eur. J. Org. Chem.* **2006**, *2006*, 1144-1161; e) Merten, J.; Wang, Y.; Krause, T.; Kataeva, O.; Metz, P. *Chem. Eur. J.* **2011**, *17*, 3332-3334.
- [24] a) de Castro, S.; Lobaton, E.; Perez-Perez, M. J.; San-Felix, A.; Cordeiro, A.; Andrei, G.; Snoeck, R.; De Clercq, E.; Balzarini, J.; Camarasa, M. J.; Velazquez, S. *J. Med. Chem.* **2005**, *48*, 1158-1168; b) Camarasa, M.-J.; San-Felix, A.; Velazquez, S.; Perez-Perez, M.-J.; Gago, F.; Balzarini, J. *Curr. Top. Med. Chem.* **2004**, *4*, 945-963; c) Velazquez, S.; Lobaton, E.; De Clercq, E.; Koontz, D. L.; Mellors, J. W.; Balzarini, J.; Camarasa, M. J.

- J. Med. Chem.* **2004**, *47*, 3418-3426; d) Rodríguez-Barrios, F.; Pérez, C.; Lobatón, E.; Velázquez, S.; Chamorro, C.; San-Félix, A.; Pérez-Pérez, M.-J.; Camarasa, M.-J.; Pelemans, H.; Balzarini, J.; Gago, F. *J. Med. Chem.* **2001**, *44*, 1853-1865; e) de Castro, S.; Peromingo, M. T.; Naesens, L.; Andrei, G.; Snoeck, R.; Balzarini, J.; Velázquez, S.; Camarasa, M. J. *J. Med. Chem.* **2008**, *51*, 5823-5832.
- [25] *Sultones in electrochemistry*: a) Lee, H.; Choi, S.; Choi, S.; Kim, H.-J.; Choi, Y.; Yoon, S.; Cho, J.-J. *Electrochem. Commun.* **2007**, *9*, 801-806; b) Zuo, X.; Xu, M.; Li, W.; Su, D.; Liu, J. *Electrochem. Solid-State Lett.* **2006**, *9*, A196; c) Xu, M. Q.; Li, W. S.; Zuo, X. X.; Liu, J. S.; Xu, X. *J. Power Sources* **2007**, *174*, 705-710; d) Park, G.; Nakamura, H.; Lee, Y.; Yoshio, M. *J. Power Sources* **2009**, *189*, 602-606; e) Xu, M.; Li, W.; Lucht, B. L. *J. Power Sources* **2009**, *193*, 804-809; f) Leggesse, E. G.; Jiang, J.-C. *RSC Adv.* **2012**, *2*, 5439-5446; g) Li, B.; Xu, M.; Li, T.; Li, W.; Hu, S. *Electrochem. Commun.* **2012**, *17*, 92-95; h) Zhang, B.; Metzger, M.; Solchenbach, S.; Payne, M.; Meini, S.; Gasteiger, H. A.; Garsuch, A.; Lucht, B. L. *J. Phys. Chem. C* **2015**, *119*, 11337-11348.
- [26] Jung, H. M.; Park, S.-H.; Jeon, J.; Choi, Y.; Yoon, S.; Cho, J.-J.; Oh, S.; Kang, S.; Han, Y.-K.; Lee, H. *J. Mater. Chem. A* **2013**, *1*, 11975-11981.
- [27] a) Xiao, F.; Wang, M., BYD Co, Ltd., PCT/CN2005/002389, 2006; b) Coley, S. M.; Wilson, D. R.; Timmers, F. J., Rohm and Haas Electronic Materials LLC, US 2010-428996, 2012; c) Hallac, P. B.; Jiang, H.; Fell, C., Johnson Controls Technology Corporation, PCT/US2013/044456, 2013; d) Lee, S. T.; Yu, J. Y.; Shin, W. C.; Han, S. I.; Kim, S. H.; Chung, B.; Kim, D. H.; Jeong, M. H.; Bae, T. H.; Lee, M., Samsung SDI CO LTD, US201414162705 20140123 2014; e) Misawa, M.; Odani, T.; Nishi, T., Sony Cooperation, WO/2014/112420 A1, 2014
- [28] a) Bordwell, F. G.; Peterson, M. L. *J. Am. Chem. Soc.* **1954**, *76*, 3957-3961; b) Bordwell, F. G.; Rondestvedt, C. S. *J. Am. Chem. Soc.* **1948**, *70*, 2429-2433; c) Bordwell, F. G.; Suter, C. M.; Webber, A. J. *J. Am. Chem. Soc.* **1945**, *67*, 827-832.
- [29] Postel, D.; Van Nhien, Albert N.; Marco, José L. *Eur. J. Org. Chem.* **2003**, *2003*, 3713-3726.
- [30] a) Smith, C. W.; Norton, D. G.; Ballard, S. A. *J. Am. Chem. Soc.* **1953**, *75*, 748-749; b) Helberger, J. H. D.; Manecke, G. D.; Lantermann, H. D.; Fischer, H. M. D., Boehme Fettchemie GmbH, DE1940B005802D 19401010 1953; c) Helferich, B.; Böllert, V. *Chem. Ber.* **1961**, *94*, 505-509.
- [31] a) Liu, C.; Zhao, W.; Huang, Y.; Wang, H.; Zhang, B. *Tetrahedron* **2015**, *71*, 4344-4351; b) Yasu, Y.; Arai, Y.; Tomita, R.; Koike, T.; Akita, M. *Org. Lett.* **2014**, *16*, 780-783.
- [32] a) Knunyants, I. L.; Sokolski, G. A. *Angew. Chem. Int. Ed.* **1972**, *11*, 583-595; Lepoittevin et al. showed that the half life of β -sultones is 1.5 min at room temperature until polymerization occurs, found in b) Roberts, D. W. *Org. Proc. Res. Dev.* **1998**, *2*, 194-202.

- [33] Hori, M., Suntory Limited, EP19850102644 19850308, 1985
- [34] a) Kang, J.; Yue, X. L.; Chen, C. S.; Li, J. H.; Ma, H. J. *Molecules* **2015**, 21, E39;
b) Cornut, D.; Lemoine, H.; Kanishchev, O.; Okada, E.; Albrieux, F.; Beavogui, A. H.; Bienvenu, A. L.; Picot, S.; Bouillon, J. P.; Medebielle, M. *J. Med. Chem.* **2013**, 56, 73-83;
c) Ojima, I.; Lin, S.; Slater, J. C.; Wang, T.; Pera, P.; Bernacki, R. J.; Ferlini, C.; Scambia, G. *Bioorg. Med. Chem.* **2000**, 8, 1619-1628.
- [35] Triflate derivative **38** is reported to be moisture, heat and light sensitive, see: a) Dobbs, A. P.; Jones, K.; Veal, K. T. *Tetrahedron Lett.* **1997**, 38, 5383-5386; b) Kanazawa, A.; Muniz, M. N.; Greene, A. E. *Synlett* **2005**, 1328-1330.
- [36] a) Langlois, B.; Forat, G., Rhone Poulenc Chimie, WO 2000FR02848 20001012, 2000;
b) Gharda, K. H., Gharda, Keki Hormusji, WO2011IN00106 20110223, 2011
- [37] Johnson, M. W.; Hannoun, K. I.; Tan, Y.; Fu, G. C.; Peters, J. C. *Chem. Sci.* **2016**, ASAP, DOI: 10.1039/c5sc04709a.
- [38] For the synthesis of alkyl-3-substituted sultones from the corresponding unsubstituted sultones by deprotonation with stoichiometric amounts of n-BuLi and trapping with alkylhalides, see: a) Schmitt, S.; Bouteiller, C.; Barre, L.; Perrio, C. *Chem. Commun.* **2011**, 47, 11465–11467. b) Margelefsky, E. L.; Zeidan, R. K.; Dufaud, V.; Davis, M. E. *J. Am. Chem. Soc.* **2007**, 129, 13691–13697. c) Smith, M. B.; Wolinsky, J. *J. Org. Chem.* **1981**, 46, 101–106

E. Summary

1. Summary in English

The present PhD thesis demonstrates the development of new environmental friendly, efficient, and mild methodologies for visible light mediated atom transfer radical addition reactions establishing a copper based photoredox catalyst. Moreover, unique photochemical transformations were presented whereas ruthenium and iridium catalysts failed to furnish the product.

First, a brief introduction to visible light mediated photoredox catalysis presenting recent publications in the area of copper(I) phenantroline based photoredox catalysts is shown (Chapter A). Afterwards, the synthesis of new homoleptic copper(I) phenanthroline complexes were demonstrated and their photophysical properties were characterized by spectroscopic analysis, X-ray and cyclovoltammetry. As a consequence, their catalytic activity in atom transfer radical addition reactions was examined and compared to established $[\text{Cu}(\text{dap})_2]\text{Cl}$ (Chapter B).

In the chapter C “Photochemical Iodoperfluoroalkylation”, the photocatalytic addition of perfluoroalkyl iodides onto various alkenes and alkynes utilizing the oxidative quenching cycle of $[\text{Cu}(\text{dap})_2]\text{Cl}$ without any additive is presented. After optimization of the reaction conditions and discussion of a plausible reaction mechanism, the substrate scope and limitations are described. Compared to previous reports with ruthenium and iridium based photocatalysts, $[\text{Cu}(\text{dap})_2]\text{Cl}$ proved to be an excellent catalyst for the proposed transformation. Remarkably, great difference between copper and noble-metal photocatalysts such as $[\text{Ru}(\text{bpy})_3]\text{Cl}_2$ or *fac*- $\text{Ir}(\text{ppy})_3$ was also demonstrated. At the end of the chapter, possible transformations of the obtained perfluoroalkylated vinyl iodides are shown and the Suzuki-Miyaura cross coupling of one photoadduct was examined, exemplarily.

The last chapter “Trifluoromethylated Sultones From Alkenols Using a Copper Photoredox Catalyst” demonstrate the unique role of $[\text{Cu}(\text{dap})_2]\text{Cl}$ as photocatalyst in two new developed transformations. In cooperation with D. B. Bagal, M. Knorn and G. Kachkovskyi the unprecedented trifluoromethylchlorosulfonylation of unactivated alkenes is presented. Thereby, only own results contributing to the publication are shown (*Angew. Chem. Int. Ed.* **2015**, 54, 6999 – 7002). The second part deals with the photoredox catalyzed procedure for the intramolecular formation of trifluoromethyl containing sultones using alkenols and triflyl chloride as reagents. After optimization of the reaction conditions, the substrate scope and limitations are mentioned. Also, a series of mechanistic experiments were carried out. The study ends with the synthesis of a novel benzoxathiin derivative (Chapter D).

2. Summary in German (Zusammenfassung)

Die vorliegende Arbeit ist in fünf Kapitel unterteilt und zeigt die Entwicklung neuartiger „Atom Transfer Radikal Addition“ (ATRA)-Reaktionen mithilfe eines Kupferkatalysators unter sichtbarem Licht. Im Gegensatz zu etablierten Photokatalysatoren wie zum Beispiel $\text{Ru}(\text{bpy})_3\text{Cl}_2$ oder *fac*- $\text{Ir}(\text{ppy})_3$ zeigte $[\text{Cu}(\text{dap})_2]\text{Cl}$ einzigartige Eigenschaften in den vorgestellten Photoreaktionen. Nach einer kurzen Einführung in die Photoredox-Katalyse mit sichtbarem Licht, werden in Kapitel A „Copper(I) Phenanthrolines in Photochemistry“ aktuelle Veröffentlichungen auf dem Gebiet der Photochemie mit Kupfer(I)-Phenanthrolin Komplexen vorgestellt. Dazu werden neben der Atom Transfer Radikal Addition Reaktion auch bisher unbekannte Umwandlungen vorgestellt, in denen vor allem $[\text{Cu}(\text{dap})_2]\text{Cl}$ Anwendung findet.

In Kapitel B „Synthesis of New Copper(I) Phenanthroline Complexes and Their Catalytic Activity“ wird die Synthese verschiedener homoleptischer $[\text{Cu}(\text{phenanthroline})_2]^+$ Komplexe und deren photophysikalische und elektrochemische Eigenschaften beschrieben. Anschließend wurde deren katalytische Aktivität in der lichtinduzierten ATRA Reaktion gezeigt und miteinander verglichen. Trotz vielversprechender Resultate konnten in keinem Fall bessere Ergebnisse als mit dem etablierten $[\text{Cu}(\text{dap})_2]\text{Cl}$ erzielt werden. In Kooperation mit M. Knorrn wurden zwei heteroleptische Kupfer(I)-Komplexe basierend auf einem Phenanthrolin und einem Phosphin bzw. Isonitril Ligand synthetisiert. Dabei zeigen beide Katalysatoren verglichen mit $[\text{Cu}(\text{dap})_2]\text{Cl}$ deutlich höhere Lebenszeiten des angeregten Zustandes und dadurch eine erhöhte katalytische Aktivität. Diese wurde in der milden lichtinduzierten Allylierung mit Trimethylallylsilanen exemplarisch präsentiert.

Im darauffolgenden Kapitel wird erstmals die photochemische Iodoperfluoroalkylierung an Styrolen und Derivaten mithilfe des Kupferkatalysators $[\text{Cu}(\text{dap})_2]\text{Cl}$ beschrieben. Nach Optimierung der Reaktionsbedingungen und der Diskussion des möglichen Reaktionsmechanismus, wird sowohl die Substratbreite, als auch die Limitierungen der vorgestellten Reaktion aufgezeigt. Dabei konnte das neuentwickelte ATRA Protokoll erfolgreich auf aromatische und aliphatische Alkine erweitert werden. Abschließend werden mögliche Transformationen der erhaltenen Photoprodukte aufgezeigt und exemplarisch die Suzuki-Miyaura Kreuzkupplung durchgeführt.

Im letzten Kapitel D „Trifluoromethylated Sulfones From Alkenols Using a Copper Photoredox Catalyst“ wird die besondere Rolle von $[\text{Cu}(\text{dap})_2]\text{Cl}$ als Katalysator in zwei photochemischen Reaktionstypen dargestellt. In beiden vorgestellten Umwandlungen zeigt der Kupferkatalysator im Gegensatz zu anderen etablierten Photoredoxkatalysatoren die Unterbindung von SO_2 -Eliminierung aus Triflylchlorid. In Zusammenarbeit mit D. B. Bagal, M. Knorrn und G. Kachkovskyi wurde ein neues Verfahren für die

Trifluoromethylchlorsulfonylierung von nicht aktivierten Alkenen vorgestellt. Dabei werden nur die zur Veröffentlichung beigetragenen Ergebnisse präsentiert (*Angew. Chem. Int. Ed.* **2015**, *54*, 6999 – 7002). Darüber hinaus wird ein photochemisches Verfahren zur Bildung von cyclischen Sulfonestern, auch bekannt als Sultone, vorgestellt. Nach Optimierung der Reaktionsbedingungen und mechanistischer Studien, wird die Substratbreite der vorgestellten Reaktion aufgezeigt. Abschließend konnte mithilfe der vorgestellten Methode als Schlüsselschritt ein neuartiges Benzoxathiin-Derivat synthetisiert werden.

F. Experimental Part

1. General Comments

Commercially available chemicals were used as received, without any further purification. All reactions were carried out in oven dried glassware under atmospheric conditions unless otherwise stated. Reactions with moisture or oxygen sensitive reagents were carried out in flame dried glassware under an atmosphere of predried nitrogen. Anhydrous solvents were prepared by established laboratory procedures.^[1] All photochemical reactions were carried out in oven-dried glassware applying three consecutive freeze-pump-thaw cycles. Solvents for column chromatography were distilled prior to use. The reported yields are referred to the isolated compounds unless otherwise stated.

Chromatography

Analytical thin layer chromatography was performed with TLC precoated aluminium sheets (Merck silica gel 60 F₂₅₄, 0.2 mm layer thickness). Visualization was done with UV light ($\lambda = 254$ nm) and staining with vanillin (6 g vanillin in 100 mL EtOH and 5 mL H₂SO₄), sodium permanganate (1 g KMnO₄ and 2 g Na₂CO₃ in 100 mL H₂O), PMA (1 g ceric ammonium sulphate and 2.5 g ammonium molybdate in 10 mL H₂SO₄ and 90 mL H₂O) or anisaldehyde (5 mL *p*-anisaldehyde in 5 mL H₂SO₄ and 100 mL EtOH) followed by heating. Column chromatography was performed with silica gel (Merck, Geduran 60, 0.063 - 0.200 mm particle size). Flash column chromatography was performed with silica gel (Merck, Geduran 60, 0.040 - 0.063 mm particle size)

¹H-, ¹³C- and ¹⁹F-NMR

NMR-spectra were recorded on a FT-NMR-spectrometer of the type BRUKER Avance 300 (300 MHz for ¹H, 75 MHz for ¹³C, 282 MHz for ¹⁹F), BRUKER Avance III 400 "Nanobay" (400 MHz for ¹H, 100 MHz for ¹³C, 386 MHz for ¹⁹F) or BRUKER Avance III 600 (600 MHz for ¹H, 151 MHz for ¹³C, 565 MHz for ¹⁹F) at ambient temperature. All spectra were recorded in CDCl₃ unless otherwise stated. Chemical shift δ for ¹H-NMR were reported in ppm relative to the signal of CDCl₃ at 7.26 ppm. Spectra were evaluated in 1st order and coupling constants *J* were reported in Hz. Splitting patterns for the spin multiplicity in the spectra are given as follows: s = singlet, d = doublet, t = triplet, q = quartet, dd = doublet of a doublet, ddd = doublet of a doublet of a doublet, dt = doublet of a triplet, b = broad and m = multiplet. Chemical shift δ for ¹³C-NMR were reported in ppm relative to the signal of CDCl₃ at 77.2 ppm.

IR-Spectroscopy

ATR-IR spectroscopy was carried out on a Biorad Excalibur FTS 3000 spectrometer, equipped with a Specac Golden Gate Diamond Single Reflection ATR-System. Solid and liquid compounds were measured neatly and the wave numbers are reported as cm^{-1} . FTIR spectroscopy was carried out on a Cary 630 FTIR Spectrometer. Solid and liquid compounds were measured neatly and the wave numbers are reported as cm^{-1} .

Gas Chromatography

Gas chromatography was performed on a Fisons GC 8000 Series with a flame ionization detector (FID). DB1 (100% Dimethylpolysiloxan, 30 m, ID 0.25 mm, 0.25 μm Film) was used as stationary phase.

Mass Spectroscopy

Mass spectroscopy was performed using a Jeol AccuTOF GCX, Agilent Q-TOF 6540 UHD, Finnigan MAT SSQ 710 A, Varian MAT 311 A, Finnigan MAT 95 or Thermoquest Finnigan TSQ 7000 at the Central Analytical Laboratory (University of Regensburg). High-resolution mass spectra were measured using atmospheric pressure chemical ionization (APCI), chemical ionization (CI), electron ionization (EI), electrospray ionization (ESI), field desorption (FD) or field ionization (FI) with a quadrupole time-of-flight (Q-TOF) detector.

Microwave

Microwave was performed using a CEM Discover S-Class.

Karl-Fischer-Titration

Karl-Fischer-Titration was performed using a Metrohm 899 Coulometer.

Cyclic Voltammetry

Cyclic voltammetry measurements were carried out on an Autolab PGSTAT 302N set-up at 20 °C in the stated solvent containing tetrabutyl ammonium tetrafluoroborate (0.1 M) as the supporting electrolyte under an argon atmosphere with use of a conventional undivided electrochemical cell, a glassy carbon working electrode, platinum wire as the counter electrode and silver wire as the reference electrode. The solvent was degassed by vigorous argon bubbling prior to the measurements. Redox potentials were referenced against ferrocene as an internal standard. For better comparison all values are reported in reference to the SCE electrode. The values were converted according to reference.^[2]

Melting Point

Melting point measurements were carried out on a SRS MPA 100 OptiMelt at a heating rate of 1 °C/min.

X-ray

X-ray analysis of single crystals was performed using a Agilent Technologies SuperNova, Agilent Technologies Gemini R Ultra, Agilent GV 50 or Rigaku GV 50 at the Central Analytical Laboratory (University of Regensburg). The ellipsoid contour percent probability level is set to 50%.

Light Sources

Photochemical reactions were performed using a LED-plate or a LED-stick.

Green LED-plate LED ₅₃₀	six green light emitting diodes (3 W, λ_{max} = 530 nm, produced by LUXEON Lumiled, purchased from Conrad Electronic SE) mounted on a heat sink. A LUMOtech LEDlight 1 -20 VA Universal was used as power supply unit.
Blue LED-plate LED ₄₅₅	six blue light emitting diodes (3 W, λ_{max} = 455 nm, produced by LUXEON Lumiled, purchased from Conrad Electronic SE) mounted on a heat sink. A LUMOtech LEDlight 1 -20 VA Universal was used as power supply unit.
Green LED-stick LED ₅₃₀	One green light emitting diode Cree XP-E (3 W, λ_{max} = 520-535 nm).
Blue LED-stick LED ₄₅₅	One blue light emitting diode Cree XP-E (3 W, λ_{max} = 450-465 nm).

2. Chapter B: Synthesis of New Copper(I) Phenanthroline Complexes and Their Catalytic Activity

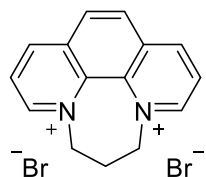
2.1. Synthesis of Literature Known Compounds and Reagents

The following compounds were synthesized according to the reported procedures. The spectral data are consistent with the data reported:

(4-methoxyphenyl)boronic acid (**9a**)^[3], (2-methoxyphenyl)boronic acid (**9b**)^[4], (3-methoxyphenyl)boronic acid (**9c**)^[5], (2,4-dimethoxyphenyl)boronic acid (**9d**)^[6], (2,6-dimethoxyphenyl)boronic acid (**9e**)^[7], *tert*-butyl allylcarbamate (**18c**)^[8], (1-cyclopropylvinyl)benzene (**18e**)^[9], ethynylbenzene (**18f**)^[1b], 1-(bromomethyl)-4-nitrobenzene (**19d**)^[10], but-2-en-1-yltrimethylsilane (**29a**)^[11], trimethyl(2-methylallyl)silane (**29b**)^[12], trimethyl(3-methylbut-2-en-1-yl)silane (**29c**)^[13].

2.2. Compound Characterization

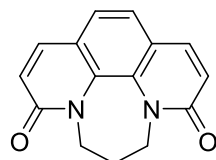
6,7-Dihydro-5*H*-[1,4]diazepino[1,2,3,4-*lmn*][1,10]phenanthroline-4,8-diium bromide (**6**)^[14]



A three-neck flask equipped with a magnetic stirring bar, dropping funnel and a reflux condenser was charged with 1,10-phenanthroline (10.6 g, 58.8 mmol, 1.0 equiv) and dissolved in nitrobenzene (80 mL). Afterwards, 1,3-dibromopropane (31 mL, 306 mmol, 5.2 equiv) was dropwise added and the mixture was stirred at 130 °C for 5 h. During the reaction, the product precipitated from the reaction mixture. Then, the mixture was allowed to cool to room temperature and the precipitate was collected by filtration, washed with hexanes and dried over CaCl₂ in a desiccator overnight to yield **6** as a yellowish solid (22.5 g, 98%).

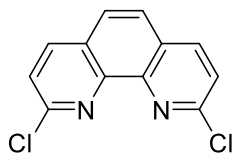
¹H-NMR (300 MHz, D₂O) δ = 9.55 (dd, J = 5.8, 1.2 Hz, 2H), 9.35 (dd, J = 8.5, 1.3 Hz, 2H), 8.48 (s, 2H), 8.43 (dd, J = 8.4, 5.8 Hz, 2H), 5.03 (t, J = 7.0 Hz, 4H), 3.31 (p, J = 7.0 Hz, 2H). **¹³C-NMR** (101 MHz, D₂O) δ = 150.9, 147.4, 134.2, 133.6, 130.4, 127.4, 60.5, 31.0.

6,7-Dihydro-5*H*-[1,4]diazepino[1,2,3,4-*lmn*][1,10]phenanthroline-3,9-dione (**7**)^[14]



A mixture of compound **6** (30.0 g, 78.5 mmol, 1.0 equiv) and KO^{*t*}Bu (37.0 g, 329.7 mmol, 4.2 equiv) in *tert*-butyl alcohol (400 mL) was stirred at 40 °C overnight in an open flask. Afterwards, oxygen was bubbled once to the suspension via a balloon. Then, water (100 mL) and CHCl₃ (100 mL) was added and extracted with CHCl₃ (5x 50 mL). The combined organic layers were washed with brine (2x 100 mL), dried over anhydrous Na₂SO₄ and the solvent was removed under reduced pressure to yield the pure product **7** as a brown solid (18.8 g, 95%).

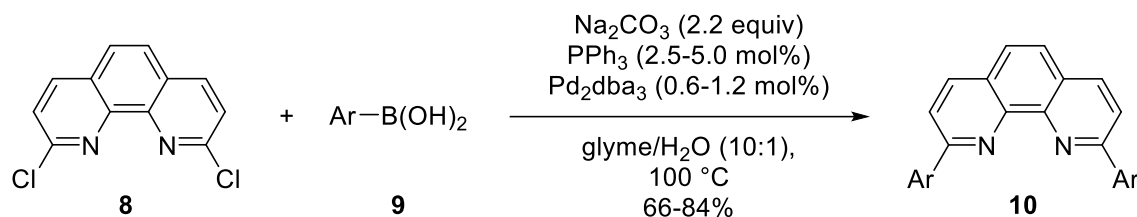
¹H-NMR (300 MHz, CDCl₃) δ = 7.72 (d, J = 9.5 Hz, 2H), 7.36 (s, 2H), 6.80 (d, J = 9.5 Hz, 2H), 4.32 (s, 4H), 2.46 (p, J = 6.6 Hz, 2H). **¹³C-NMR** (75 MHz, CDCl₃) δ = 162.7, 138.8, 132.1, 123.1, 122.8, 122.8, 45.8, 25.7.

2,9-Dichloro-1,10-phenanthroline (8)^[14]

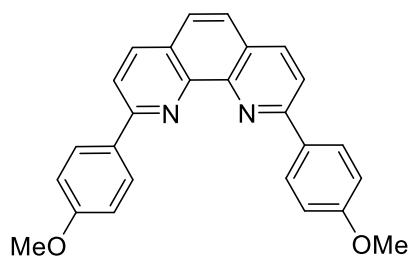
A flame dried three-neck flask equipped with a magnetic stirring bar and a reflux condenser was charged with compound **7** (18.8 g, 74.5 mmol, 1.0 equiv.) and PCl_5 (31.0 g, 149 mmol, 2.0 equiv) under nitrogen atmosphere. After addition of POCl_3 (300 mL) the mixture was stirred overnight at 145 °C. The excess of POCl_3 was removed by distillation. The resulting brown residue was cooled to 0 °C and quenched carefully by the addition of ice followed by aqueous NH_3 (1 M) until neutral pH. Then, the dark solution was extracted with CH_2Cl_2 (4x 75 mL). The combined organic layers were washed with brine (1x 100 mL), dried over anhydrous MgSO_4 and the solvent was removed under reduced pressure. The residue was purified by column chromatography on silica gel (CH_2Cl_2) to afford **8** as a yellowish solid (13.4 g, 72%).

R_f (CH_2Cl_2) = 0.55. **Staining:** KMnO_4 (UV active). **$^1\text{H-NMR}$** (300 MHz, CDCl_3) δ = 8.21 (d, J = 8.4 Hz, 2H), 7.81 (s, 2H), 7.64 (d, J = 8.4 Hz, 2H). **$^{13}\text{C-NMR}$** (101 MHz, CDCl_3) δ = 152.0, 144.9, 138.8, 127.7, 126.3, 124.9.

General Procedure for Suzuki-Miyaura Cross Coupling (GP-A)

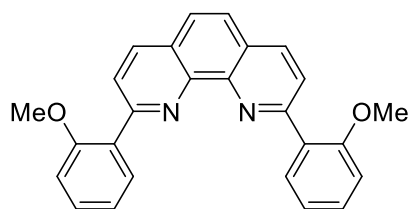


A flame dried three-neck round-bottom flask equipped with a reflux condenser was charged with 2,9-dichloro-1,10-phenanthroline (**8**) (1.0 equiv), boronic acid **9** (2.2 equiv), PPh_3 (2.5-5.0 mol%) and Pd_2dba_3 (0.6 - 1.2 mol%) in freshly distilled glyme under nitrogen atmosphere. The reaction mixture was degassed by three freeze-pump-thaw cycles. Afterwards, a solution of K_2CO_3 (2.2 equiv) in water was added and the mixture was degassed by one freeze-pump-thaw cycle. The resulting solution was stirred for 24-48 h at 100°C . Then, the mixture was allowed to cool to room temperature and extracted with CH_2Cl_2 (4x 50 mL). The combined organic layers were washed with brine (4x 50 mL), dried over anhydrous Na_2SO_4 and the solvent was removed under reduced pressure. The residue was purified by flash column chromatography on silica gel (CH_2Cl_2 followed by CH_2Cl_2 -MeOH, 95:5) followed by recrystallization from hot toluene to afford the entitled product **10**.

2,9-Bis(4-methoxyphenyl)-1,10-phenanthroline (10a)^[14]

Following GP-A, **10a** was prepared using 2,9-dichloro-1,10-phenanthroline (**8**) (2.49 g, 10.0 mmol, 1.0 equiv), (4-methoxyphenyl)boronic acid (**9a**) (3.34 g, 22.0 mmol, 2.2 equiv), PPh₃ (131 mg, 500 μ mol, 5.0 mol%), Pd₂dba₃ (100 mg, 109 μ mol, 1.2 mol%) and K₂CO₃ (3.04 g, 22.0 mmol, 2.2 equiv) in glyme-H₂O (10:1, 88 mL). Column chromatography on silica gel (CH₂Cl₂ followed by CH₂Cl₂-MeOH, 95:5) followed by recrystallization from hot toluene (50 mL) afforded **10a** as a yellowish solid (3.31 g, 84%).

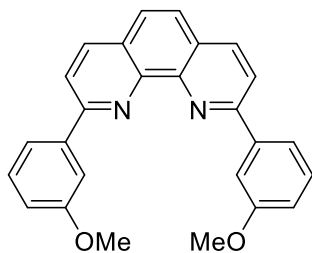
R_f (CH₂Cl₂-MeOH, 9:1) = 0.80. **Staining:** KMnO₄ (UV active). **¹H-NMR** (300 MHz, CDCl₃) δ = 8.46 – 8.42 (m, 4H), 8.26 (d, *J* = 8.4 Hz, 2H), 8.08 (d, *J* = 8.4 Hz, 2H), 7.75 (s, 2H), 7.15 – 7.09 (m, 4H), 3.93 (s, 6H). **¹³C-NMR** (101 MHz, CDCl₃) δ = 161.1, 156.5, 146.1, 136.9, 132.3, 129.1, 128.4, 127.7, 125.8, 119.5, 114.3, 55.5.

2,9-Bis(2-methoxyphenyl)-1,10-phenanthroline (10b)

Following GP-A, **10b** was prepared using 2,9-dichloro-1,10-phenanthroline (**8**) (249 mg, 1.0 mmol, 1.0 equiv), (2-methoxyphenyl)boronic acid (**9b**) (334 mg, 2.2 mmol, 2.2 equiv), PPh₃ (7 mg, 25 μ mol, 2.5 mol%), Pd₂dba₃ (5 mg, 5.5 μ mol, 0.6 mol%) and K₂CO₃ (304 mg, 2.2 mmol, 2.2 equiv) in glyme-H₂O (10:1, 11 mL). Column chromatography on silica gel (CH₂Cl₂ followed by CH₂Cl₂-MeOH, 95:5) followed by recrystallization from hot toluene (7 mL) afforded **10b** as a dark orange solid (298 mg, 76%).

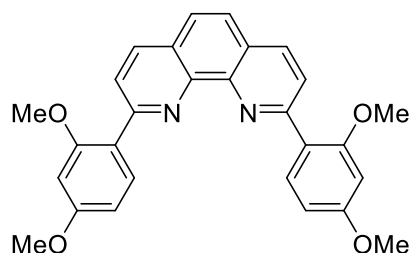
R_f (CH₂Cl₂-MeOH, 9:1) = 0.81. **Staining:** KMnO₄ (UV active). **¹H-NMR** (400 MHz, CDCl₃) δ = 8.36 (dd, J = 7.6, 1.8 Hz, 2H), 8.27 – 8.19 (m, 4H), 7.76 (s, 2H), 7.43 (ddd, J = 8.3, 7.4, 1.8 Hz, 2H), 7.21 (td, J = 7.5, 1.1 Hz, 2H), 7.04 (dd, J = 8.4, 1.0 Hz, 2H), 3.89 (s, 6H). **¹³C-NMR** (101 MHz, CDCl₃) δ = 157.6, 156.3, 146.3, 135.3, 132.5, 130.2, 129.9, 127.4, 126.0, 124.9, 121.4, 111.6, 55.9. **IR** (neat, cm⁻¹): 3042, 3004, 2960, 2837, 2087, 1580, 1506, 1357, 1305, 1260, 1182, 1021, 891, 846, 753. **HRMS** (ESI) exact mass calc. for C₂₆H₂₁N₂O₂: m/z 393.1598, found: m/z 393.1607 [M+H]⁺. **mp**: 197 °C.

2,9-Bis(3-methoxyphenyl)-1,10-phenanthroline (**10c**)



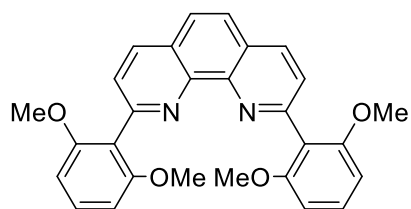
Following GP-A, **10c** was prepared using 2,9-dichloro-1,10-phenanthroline (**8**) (249 mg, 1.0 mmol, 1.0 equiv), (3-methoxyphenyl)boronic acid (**9c**) (334 mg, 2.2 mmol, 2.2 equiv), PPh₃ (7 mg, 25 μmol, 2.5 mol%), Pd₂dba₃ (5 mg, 5.5 μmol, 0.6 mol%) and K₂CO₃ (304 mg, 2.2 mmol, 2.2 equiv) in glyme-H₂O (10:1, 11 mL). Column chromatography on silica gel (CH₂Cl₂ followed by CH₂Cl₂-MeOH, 95:5) followed by recrystallization from hot toluene (10 mL) afforded **9c** as a orange solid (314 mg, 80%).

R_f (CH₂Cl₂-MeOH, 9:1) = 0.82. **Staining:** KMnO₄ (UV active). **¹H-NMR** (300 MHz, CDCl₃) δ = 8.34 – 8.27 (m, 4H), 8.15 (d, *J* = 8.4 Hz, 2H), 7.94 (dt, *J* = 7.8, 1.2 Hz, 2H), 7.79 (s, 2H), 7.45 (t, *J* = 8.0 Hz, 2H), 7.07 – 7.01 (m, 2H), 4.04 (s, 6H). **¹³C-NMR** (75 MHz, CDCl₃) δ = 160.4, 156.2, 146.0, 140.8, 137.0, 129.8, 128.1, 126.1, 119.9, 119.8, 115.7, 113.0, 55.5. **IR** (neat, cm⁻¹): 3004, 2937, 2833, 2080, 1908, 1830, 1595, 1487, 1368, 1293, 1215, 1170, 1103, 954, 898, 850, 824, 682. **HRMS** (ESI) exact mass calc. for C₂₆H₂₁N₂O₂: *m/z* 393.1598, found: *m/z* 393.1597 [M+H]⁺. **mp**: 194 °C.

2,9-Bis(2,4-dimethoxyphenyl)-1,10-phenanthroline (10d)

Following GP-A, **10d** was prepared using 2,9-dichloro-1,10-phenanthroline (**8**) (249 mg, 1.0 mmol, 1.0 equiv), (2,4-dimethoxyphenyl)boronic acid (**9d**) (400 mg, 2.2 mmol, 2.2 equiv), PPh_3 (13 mg, 50 μmol , 5.0 mol%), Pd_2dba_3 (10 mg, 10.9 μmol , 1.2 mol%) and K_2CO_3 (304 mg, 2.2 mmol, 2.2 equiv) in glyme- H_2O (10:1, 11 mL). Column chromatography on silica gel (CH_2Cl_2 followed by CH_2Cl_2 -MeOH, 95:5) followed by recrystallization from hot toluene (10 mL) afforded **10d** as a white solid (366 mg, 81%).

R_f (CH_2Cl_2 -MeOH, 9:1) = 0.80. **Staining:** vanilin (UV active). **$^1\text{H-NMR}$** (300 MHz, CDCl_3) δ = 8.39 (d, J = 8.6 Hz, 2H), 8.25 (d, J = 8.4 Hz, 2H), 8.18 (d, J = 8.5 Hz, 2H), 7.74 (s, 2H), 6.75 (dd, J = 8.6, 2.4 Hz, 2H), 6.60 (d, J = 2.3 Hz, 2H), 3.90 (s, 12H). **$^{13}\text{C-NMR}$** (75 MHz, CDCl_3) δ = 161.7, 158.8, 155.9, 146.1, 135.3, 133.4, 127.1, 125.6, 124.4, 122.8, 105.5, 99.0, 55.8, 55.5, 50.9;. **IR** (neat, cm^{-1}): 3001, 2938, 2833, 2117, 1920, 1584, 1502, 1469, 1424, 1357, 1282, 1245, 1100, 1021, 895, 850, 775, 731. **HRMS** (ESI) exact mass calc. for $\text{C}_{28}\text{H}_{25}\text{N}_2\text{O}_4$: m/z 453.1809, found: m/z 453.1811 $[\text{M}+\text{H}]^+$. **mp:** 201 $^\circ\text{C}$.

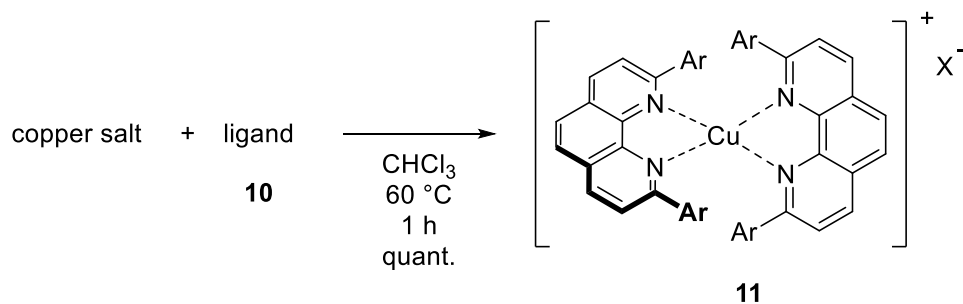
2,9-Bis(2,6-dimethoxyphenyl)-1,10-phenanthroline (10e)

Following GP-A, **10e** was prepared using 2,9-dichloro-1,10-phenanthroline (**8**) (249 mg, 1.0 mmol, 1.0 equiv), (2,6-dimethoxyphenyl)boronic acid (**9e**) (400 mg, 2.2 mmol, 2.2 equiv), PPh₃ (13 mg, 50 μ mol, 5.0 mol%), Pd₂dba₃ (10 mg, 10.9 μ mol, 1.2 mol%) and K₂CO₃ (304 mg, 2.2 mmol, 2.2 equiv) in glyme-H₂O (10:1, 11 mL). Column chromatography on silica gel (CH₂Cl₂ followed by CH₂Cl₂-MeOH, 95:5) followed by recrystallization from hot toluene (10 mL) afforded **10e** as a white solid (299 mg, 66%).

R_f (CH₂Cl₂-MeOH, 9:1) = 0.80. **Staining**: vanilin (UV active). **¹H-NMR** (400 MHz, CDCl₃) δ = 8.27 (d, J = 7.9 Hz, 2H), 7.82 (s, 2H), 7.66 (d, J = 8.3 Hz, 2H), 7.30 (t, J = 8.4 Hz, 2H), 6.66 (d, J = 8.4 Hz, 4H), 3.73 (s, 12H). **¹³C-NMR** (101 MHz, CDCl₃) δ = 158.8, 154.9, 135.6, 129.9, 127.6, 126.4, 126.2, 105.4, 56.7. **IR** (neat, cm⁻¹): 3075, 3008, 2945, 2837, 2371, 2110, 1946, 1580, 1469, 1353, 1279, 1245, 1096, 1018, 865, 716. **HRMS** (ESI) exact mass calc. for C₂₈H₂₅N₂O₄: m/z 453.1809, found: m/z 453.1819 [M+H]⁺. **mp**: 200 °C.

General Procedure for Complex Formation (GP-B)

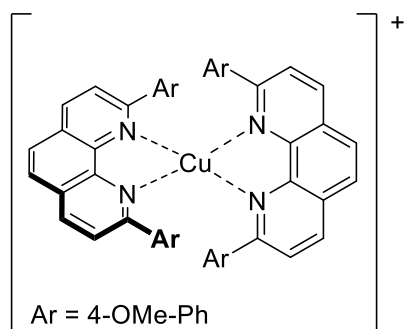
A suspension of copper salt (1.0 equiv) in CHCl_3 was added to a solution of ligand **10** (2.0 equiv) in CHCl_3 . The solution immediately changed its yellowish colour to red to brown depending on the used ligand. The reaction mixture was stirred for 1 h at room temperature followed by stirring at 60 °C for another hour. Afterwards, the mixture was allowed to cool down to room temperature followed by precipitation in Et_2O to give pure complex **11** in quantitative yield.



copper salt = CuCl , $[\text{Cu}(\text{MeCN})_4]\text{PF}_6$, $[\text{Cu}(\text{MeCN})_4]\text{BF}_4$ $\text{X} = \text{Cl}, \text{PF}_6, \text{BF}_4$

- 11a**: $[\text{Cu}(\textbf{10a})_2]^+ = [\text{Cu}(\text{dap})_2]^+$ (Ar = 4-OMe-Ph)
11b: $[\text{Cu}(\textbf{10b})_2]^+ = [\text{Cu}(\text{o-dap})_2]^+$ (Ar = 2-OMe-Ph)
11c: $[\text{Cu}(\textbf{10c})_2]^+ = [\text{Cu}(\text{m-dap})_2]^+$ (Ar = 3-OMe-Ph)
11d: $[\text{Cu}(\textbf{10d})_2]^+ = [\text{Cu}(\text{o,p-dap})_2]^+$ (Ar = 2,4-OMe-Ph)
11e: $[\text{Cu}(\textbf{10e})_2]^+ = [\text{Cu}(\text{o,o-dap})_2]^+$ (Ar = 2,6-OMe-Ph)

[Cu(dap)₂]⁺ (11a)



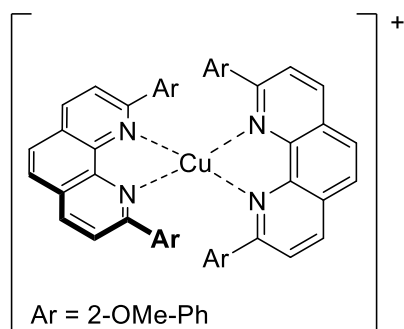
Following GP-B, **11a-Cl** was prepared using CuCl (252 mg, 2.5 mmol, 1.0 equiv) and 2,9-bis(4-methoxyphenyl)-1,10-phenanthroline (**10a**) (2.0 g, 5.1 mmol, 2.0 equiv) in CHCl₃ (50 mL) to yield **11a-Cl** as a purple solid (2.25 g, quantitative).

Following GP-B, **11a-PF₆** was prepared using [Cu(MeCN)₄]PF₆ (5.7 mg, 15.3 μmol, 1.0 equiv) and 2,9-bis(4-methoxyphenyl)-1,10-phenanthroline (**10a**) (12 mg, 30.6 μmol, 2.0 equiv) in CHCl₃ (1 mL) to yield **11a-PF₆** as a purple solid (15 mg, quantitative).

Single crystals suitable for X-ray analysis of [Cu(dap)₂]PF₆ (**11a-PF₆**) (15 mg) was obtained by vapor diffusion of pentane into CH₂Cl₂ solution (2.0 mL).

¹H-NMR (400 MHz, CDCl₃) δ = 8.55 (d, *J* = 8.3 Hz, 4H), 8.05 (s, 4H), 7.84 (d, *J* = 8.3 Hz, 4H), 7.42 – 7.32 (m, 8H), 6.09 – 5.94 (m, 8H), 3.45 (s, 12H). **¹³C-NMR** (101 MHz, CDCl₃) δ = 160.2, 156.4, 143.5, 137.4, 131.2, 129.2, 128.0, 126.3, 124.5, 112.6, 55.3. **IR** (neat, cm⁻¹): 3347, 3008, 2956, 2833, 2110, 1875, 1603, 1573, 1521, 1487, 1424, 1305, 1249, 1174, 1115, 1018, 828, 794, 749. **HRMS** (ESI) exact mass calc. for C₅₂H₄₀CuN₄O₄: *m/z* 847.2340, found: *m/z* 847.2336 [M]⁺. **mp**: 229 °C.

[Cu(o-dap)₂]⁺ (11b)



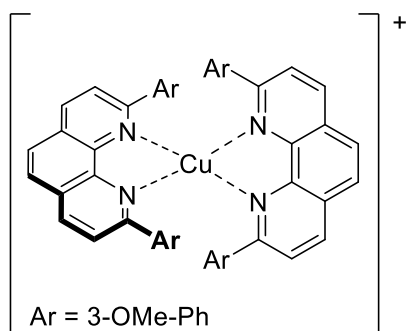
Following GP-B, **11b-Cl** was prepared using CuCl (25 mg, 253 μ mol, 1.0 equiv) and 2,9-bis(4-methoxyphenyl)-1,10-phenanthroline (**10b**) (200 mg, 510 μ mol, 2.0 equiv) in CHCl₃ (20 mL) to yield **11b-Cl** as a red solid (223 mg, quantitative).

Following GP-B, **11b-BF₄** was prepared using [Cu(MeCN)₄]BF₄ (4.8 mg, 15.3 μ mol, 1.0 equiv) and 2,9-bis(2-methoxyphenyl)-1,10-phenanthroline (**10b**) (12 mg, 30.6 μ mol, 2.0 equiv) in CHCl₃ (1 mL) to yield **11b-BF₄** as a red solid (15 mg, quantitative).

Single crystals suitable for X-ray analysis of [Cu(o-dap)₂]BF₄ (**11b-BF₄**) (15 mg) was obtained by vapor diffusion of pentane into CH₂Cl₂ solution (2.0 mL).

¹H-NMR (400 MHz, CDCl₃) δ = 8.41 (d, J = 8.4 Hz, 4H), 7.96 (s, 4H), 7.88 (d, J = 8.4 Hz, 4H), 7.09 (dd, J = 7.5, 1.7 Hz, 4H), 6.71 (ddd, J = 8.3, 7.4, 1.7 Hz, 4H), 6.35 (dd, J = 8.4, 1.0 Hz, 4H), 5.88 (td, J = 7.5, 1.0 Hz, 4H), 3.49 (s, 12H). **¹³C-NMR** (101 MHz, CDCl₃) δ = 155.7, 154.9, 143.5, 135.7, 130.2, 129.7, 128.0, 127.9, 127.2, 126.5, 119.1, 109.6, 55.1. **IR** (neat, cm⁻¹): 3075, 2941, 2840, 2102, 1983, 1603, 1487, 1357, 1245, 1152, 1018, 906, 861, 746, 682. **HRMS** (ESI) exact mass calc. for C₅₂H₄₀CuN₄O₄: m/z 847.2340, found: m/z 847.2351 [M]⁺. **mp**: 227 °C.

[Cu(*m*-dap)₂]⁺ (11c**)**



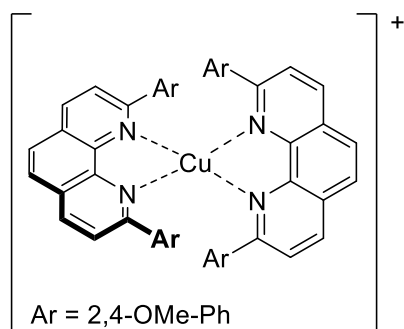
Following GP-B, **11c-Cl** was prepared using CuCl (32 mg, 323 μ mol, 1.0 equiv) and 2,9-bis(4-methoxyphenyl)-1,10-phenanthroline (**10c**) (250 mg, 637 μ mol, 2.0 equiv) in CHCl₃ (25 mL) to yield **11c-Cl** as a brown solid (282 mg, quantitative).

Following GP-B, **11c-BF₄** was prepared using [Cu(MeCN)₄]BF₄ (4.8 mg, 15.3 μ mol, 1.0 equiv) and 2,9-bis(2-methoxyphenyl)-1,10-phenanthroline (**10c**) (12 mg, 30.6 μ mol, 2.0 equiv) in CHCl₃ (1 mL) to yield **11c-BF₄** as a brown solid (15 mg, quantitative).

Single crystals suitable for X-ray analysis of [Cu(*m*-dap)₂]BF₄ (**11c-BF₄**) (15 mg) was obtained by vapor diffusion of pentane into CH₂Cl₂ solution (3.0 mL).

¹H-NMR (400 MHz, CDCl₃) δ = 8.54 (d, *J* = 8.0 Hz, 4H), 8.13 (s, 8H), 7.23 – 6.82 (m, 8H), 6.56 (t, *J* = 6.1 Hz, 4H), 6.28 (d, *J* = 8.0 Hz, 4H), 3.18 (s, 12H). **¹³C-NMR** (101 MHz, CDCl₃) δ = 158.4, 137.4, 128.6, 126.7, 120.2, 114.4, 113.0, 54.8. **IR** (neat, cm⁻¹): 2982, 2941, 2102, 1990, 1580, 1485, 1454, 1357, 1316, 1282, 1215, 1174, 1115, 1036, 831, 775, 746, 693. **HRMS** (ESI) exact mass calc. for C₅₂H₄₀CuN₄O₄: *m/z* 847.2340, found: *m/z* 847.2336 [M]⁺. **mp**: 252 °C.

[Cu(*o,p*-dap)₂]⁺ (11d**)**



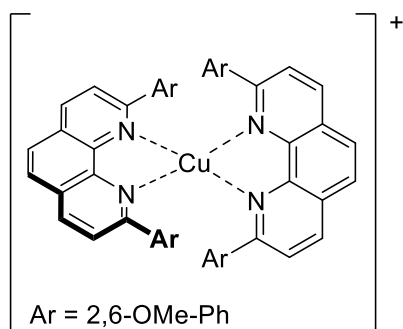
Following GP-B, **11d-Cl** was prepared using CuCl (33 mg, 331 μ mol, 1.0 equiv) and 2,9-bis(2,4-methoxyphenyl)-1,10-phenanthroline (**10d**) (300 mg, 663 μ mol, 2.0 equiv) in CHCl₃ (30 mL) to yield **11d-Cl** as a beige solid (333 mg, quantitative).

Following GP-B, **11d-PF₆** was prepared using [Cu(MeCN)₄]PF₆ (4.9 mg, 13.3 μ mol, 1.0 equiv) and 2,9-bis(2,4-methoxyphenyl)-1,10-phenanthroline (**10d**) (12 mg, 26.5 μ mol, 2.0 equiv) in CHCl₃ (1 mL) to yield **11d-PF₆** as a beige solid (15 mg, quantitative).

Single crystals suitable for X-ray analysis of [Cu(*o,p*-dap)₂]PF₆ (**11d-PF₆**) (15 mg) was obtained by vapor diffusion of Et₂O into CH₂Cl₂ solution (1.0 mL).

¹H-NMR (400 MHz, CDCl₃) δ = 8.30 (d, *J* = 43.8 Hz, 4H), 7.84 (d, *J* = 24.8 Hz, 4H), 7.64 (s, 4H), 7.30 (s, 4H), 6.77 – 6.55 (m, 8H), 3.74 (s, 24H). **¹³C-NMR** (101 MHz, CDCl₃) δ = 158.6, 158.0, 154.9, 135.5, 131.1, 129.8, 127.6, 126.3, 126.1, 105.2, 104.5, 56.5, 56.0. **IR** (neat, cm⁻¹): 2937, 2837, 2117, 1908, 1584, 1502, 1469, 1424, 1357, 1248, 1100, 1021, 850, 775, 731. **HRMS** (ESI) exact mass calc. for C₅₆H₄₈CuN₄O₈: *m/z* 967.2763, found: *m/z* 967.2773 [M]⁺. **mp**: 262 °C.

[Cu(o,o-dap)₂]⁺ (11e)



Following GP-B, **11e-Cl** was prepared using CuCl (21.9 mg, 221 μ mol, 1.0 equiv) and 2,9-bis(2,6-dimethoxyphenyl)-1,10-phenanthroline (**10e**) (200 mg, 442 μ mol, 2.0 equiv) in CHCl₃ (20 mL) to yield **11e** as a yellowish beige solid (222 mg, quantitative).

Following GP-B, **11e-BF₄** was prepared using [Cu(MeCN)₄]BF₄ (4.5 mg, 14.4 μ mol, 1.0 equiv) and 2,9-bis(2,6-methoxyphenyl)-1,10-phenanthroline (**10e**) (13 mg, 28.7 μ mol, 2.0 equiv) in CHCl₃ (1 mL) to yield **11e-BF₄** as a yellowish beige solid (15 mg, quantitative).

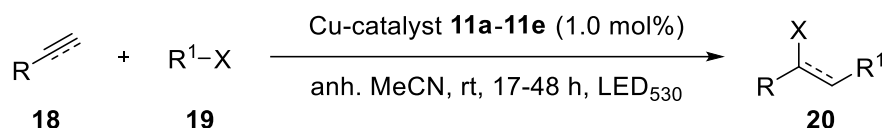
Single crystals suitable for X-ray analysis of [Cu(o,o-dap)₂]BF₄ (**11e-BF₄**) (15 mg) was obtained by vapor diffusion of Et₂O into CH₂Cl₂ solution (0.8 mL).

¹H-NMR (400 MHz, CDCl₃) δ = 8.46 – 8.34 (m, 6H), 8.25 (d, J = 8.3 Hz, 4H), 7.90 (d, J = 3.4 Hz, 4H), 7.44 (d, J = 8.3 Hz, 4H), 5.88 (d, J = 8.4 Hz, 6H), 3.03 (s, 24H).

¹³C-NMR (101 MHz, CDCl₃) δ = 157.0, 135.2, 130.2, 128.9, 127.6, 126.5, 102.6, 54.4.

IR (neat, cm⁻¹): 3004, 2945, 2840, 1920, 1584, 1510, 1472, 1431, 1364, 1252, 1103, 1021, 906, 835, 787, 738. **HRMS** (ESI) exact mass calc. for C₅₆H₄₈CuN₄O₈: m/z 967.2763, found: m/z 967.2782 [M]⁺. **mp**: 258 °C.

General Procedure for ATRA Reaction with Various Photocatalysts (GP-C)



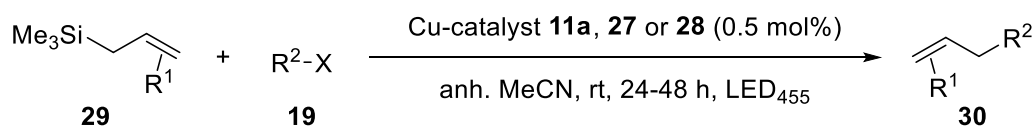
Method A

A Schlenk tube equipped with a magnetic stir bar was charged with alkene or alkyne **18** (1.0 mmol, 1.0 equiv), alkyl halide **19** (1.0 mmol, 1.0 equiv), copper photocatalyst **11a-Cl** to **11e-Cl** (0.3 - 1.0 mol%) and dissolved in anh. solvent (1.0 mL). The reaction mixture was degassed by three freeze-pump-thaw cycles, set under nitrogen and irradiated with a green LED (530 nm) at room temperature. After completion of the reaction (judged by TLC) the reaction mixture was concentrated in vacuo. The residue was purified by flash column chromatography on silica gel to yield the entitled product **20**.

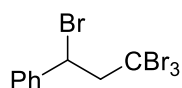
Method B

A Schlenk tube equipped with a magnetic stir bar was charged with alkene or alkyne **18** (1.0 mmol, 1.0 equiv), alkyl halide **19** (2.0 mmol, 2.0 equiv), copper photocatalyst **11a-Cl** to **11e-Cl** (0.3 - 1.0 mol%), additive (2.0 mmol, 2.0 equiv) and dissolved in anh. solvent (1.0 mL). The reaction mixture was degassed by three freeze-pump-thaw cycles, set under nitrogen and irradiated with a green LED (530 nm) at room temperature. After completion of the reaction (judged by TLC), water (5 mL) was added and the reaction mixture was extracted with CH₂Cl₂ (3x 10 mL). The combined organic layers were washed once with brine (20 mL), dried over anhydrous Na₂SO₄, filtered and the solvent was evaporated under reduced pressure. The residue was purified by flash column chromatography on silica gel to yield the entitled product **20**.

General Procedure for Allylation Reaction with Various Photocatalysts (GP-D)



A Schlenk tube equipped with a magnetic stir bar was charged with alkyl halide **19** (0.5 mmol, 1.0 equiv), copper photocatalyst **11a-BF₄**, **27-BF₄** or **28-BF₄** (0.5 mol%) and dissolved in anh. MeCN (1.0 mL). The reaction mixture was degassed by three freeze-pump-thaw cycles. Allyltrimethylsilane derivative **29** (1.5 mmol, 3.0 equiv) was added under nitrogen and the reaction mixture irradiated with a blue LED (455 nm) at room temperature. After completion of the reaction (judged by TLC), water (5 mL) was added and the reaction mixture was extracted with CH₂Cl₂ (3x 10 mL). The combined organic layers were washed with brine (3x 10 mL), dried over anhydrous Na₂SO₄, filtered and the solvent was evaporated under reduced pressure. The residue was purified by flash column chromatography on silica gel to yield the entitled product **30**.

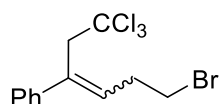
(1,3,3,3-Tetrabromopropyl)benzene (20a)^[15]

Following GP-C (Method A), **20a** was prepared using styrene (**18a**) (115 μ L, 1.0 mmol, 1.0 equiv), CBr₄ (**19a**) (331 mg, 1.0 mmol, 1.0 equiv) and copper photocatalyst **11a-Cl** to **11e-Cl** (0.3 μ mol, 0.3 mol%) in anh. CH₂Cl₂ (1 mL). Flash column chromatography on silica gel (hexanes) afforded **20a** as a white solid (Table 1).

Table 1. Yields of copper-catalyzed ATRA between styrene (**18a**) and CBr₄ (**19a**).

Entry	Catalyst	Isolated Mass [mg]	Yield [%]
1	[Cu(dap) ₂]Cl 11a-Cl	373	88
2	[Cu(o-dap) ₂]Cl 11b-Cl	357	85
3	[Cu(m-dap) ₂]Cl 11c-Cl	371	88
4	[Cu(o,p-dap) ₂]Cl 11d-Cl	328	78
5	[Cu(o,o-dap) ₂]Cl 11e-Cl	321	76

R_f (hexanes-EtOAc, 19:1) = 0.60. **Staining:** vanilin (UV active). **¹H-NMR** (300 MHz, CDCl₃) δ = 7.54 – 7.27 (m, 5H), 5.33 (dd, *J* = 7.5, 4.3 Hz, 1H), 4.18 – 3.99 (m, 2H). **¹³C-NMR** (75 MHz, CDCl₃) δ = 140.9, 129.1, 129.0, 128.3, 66.6, 50.2, 35.2.

(6-Bromo-1,1,1-trichlorohex-3-en-3-yl)benzene (20b)

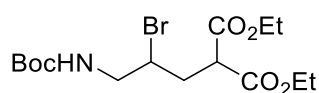
Following GP-C (Method A), **20b** was prepared using (1-cyclopropylvinyl)benzene (**18b**) (144 mg 1.0 mmol, 1.0 equiv), CBrCl₃ (**19b**) (100 μ L, 1.0 mmol, 1.0 equiv) and copper photocatalyst **11a-Cl** to **11e-Cl** (1.0 μ mol, 1.0 mol%) in anh. MeCN (1 mL). Flash column chromatography on silica gel (hexanes) afforded **20b** as a colourless liquid (Table 2).

Table 2. Yields and *E/Z*-Ratio of copper-catalyzed ATRA between (1-cyclopropylvinyl)benzene (**18b**) and CBrCl₃ (**19b**).^[a]

Entry	Catalyst		<i>E/Z</i> -Ratio	Isolated Mass [mg]	Yield [%]
1	[Cu(dap) ₂]Cl	11a-Cl	94:06	278	81
2	[Cu(o-dap) ₂]Cl	11b-Cl	93:07	261	76
3	[Cu(m-dap) ₂]Cl	11c-Cl	93:07	268	78
4	[Cu(o,p-dap) ₂]Cl	11d-Cl	94:06	240	70
5	[Cu(o,o-dap) ₂]Cl	11e-Cl	91:09	238	69

[a] *E/Z*-ratio determined by ¹H-NMR.

R_f (hexanes) = 0.25. **Staining:** vanilin (UV active). **¹H-NMR** (300 MHz, CDCl₃) δ = 7.40 – 7.24 (m, 5H), 5.94 (t, *J* = 7.3 Hz, 1H), 3.99 (s, 2H), 3.50 (t, *J* = 6.8 Hz, 2H), 2.95 (q, *J* = 7.0 Hz, 2H). **¹³C-NMR** (75 MHz, CDCl₃) δ = 142.6, 136.4, 134.2, 128.4, 127.4, 127.0, 98.5, 54.0, 33.2, 31.8. **IR** (neat, cm⁻¹): 3064, 3022, 2960, 2926, 2885, 2113, 1722, 1159, 1431, 1264, 1215, 947, 757, 697. **HRMS** (EI) exact mass calc. for C₁₂H₁₂Cl₃Br: *m/z* 339.9188, found: *m/z* 339.9187 [M]⁺.

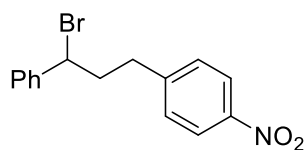
Diethyl 2-(2-bromo-3-((*tert*-butoxycarbonyl)amino)propyl)malonate (20c)^[15]

Following GP-C (Method B), **20c** was prepared using *tert*-butyl allylcarbamate (**18c**) (157 mg, 1.0 mmol, 1.0 equiv), diethyl 2-bromomalonate (**19c**) (340 μ L, 2.0 mmol, 2.0 equiv), LiBr (174 mg, 2.0 mmol, 2.0 equiv) and copper photocatalyst **11a-Cl** to **11e-Cl** (0.3 μ mol, 0.3 mol%) in DMF-H₂O (4:1, 1 mL). Flash column chromatography on silica gel (hexanes-EtOAc, 6:1) afforded **20c** as a yellow oil (Table 3).

Table 3. Yields of copper-catalyzed ATRA between *tert*-butyl allylcarbamate (**18c**) and diethyl 2-bromomalonate (**19c**).

Entry	Catalyst	Isolated Mass [mg]	Yield [%]
1	[Cu(dap) ₂]Cl 11a-Cl	299	75
2	[Cu(<i>o</i> -dap) ₂]Cl 11b-Cl	275	69
3	[Cu(<i>m</i> -dap) ₂]Cl 11c-Cl	259	65
4	[Cu(<i>o,p</i> -dap) ₂]Cl 11d-Cl	167	42
5	[Cu(<i>o,o</i> -dap) ₂]Cl 11e-Cl	150	38

R_f (hexanes-EtOAc, 4:1) = 0.42. **Staining:** ninhydrin (UV active). **¹H-NMR** (300 MHz, CDCl₃) δ = 5.04 (t, *J* = 6.3 Hz, 1H), 4.21 – 4.12 (m, 4H), 4.12 – 4.03 (m, 1H), 3.69 (dd, *J* = 9.4, 5.0 Hz, 1H), 3.47 (t, *J* = 6.4 Hz, 2H), 2.43 (ddd, *J* = 14.9, 9.6, 3.7 Hz, 1H), 1.39 (s, 9H), 1.22 (td, *J* = 7.2, 1.7 Hz, 6H). **¹³C-NMR** (75 MHz, CDCl₃) δ = 169.0, 168.6, 155.7, 80.0, 62.0, 61.9, 53.4, 50.3, 47.2, 34.8, 28.5, 14.2, 14.2.

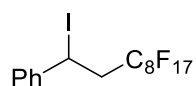
1-(3-Bromo-3-phenylpropyl)-4-nitrobenzene (20d)^[16]

Following GP-C (Method A), **20d** was prepared using styrene (**18a**) (115 μ L, 1.0 mmol, 1.0 equiv), 1-(bromomethyl)-2-nitrobenzene (**19d**) (216 mg, 1.0 mmol, 1.0 equiv) and copper photocatalyst **11a-Cl** to **11e-Cl** (1.0 μ mol, 1.0 mol%) in anh. MeCN (1 mL). Flash column chromatography on silica gel (hexanes-EtOAc, 9:1) afforded **20d** as a colourless oil (Table 4).

Table 4. Yields of copper-catalyzed ATRA between styrene (**18a**) and 1-(bromomethyl)-2-nitrobenzene (**19d**).

Entry	Catalyst	Isolated Mass [mg]	Yield [%]
1	[Cu(dap) ₂]Cl 11a-Cl	289	90
2	[Cu(o-dap) ₂]Cl 11b-Cl	211	66
3	[Cu(m-dap) ₂]Cl 11c-Cl	196	61
4	[Cu(o,p-dap) ₂]Cl 11d-Cl	-	nr
5	[Cu(o,o-dap) ₂]Cl 11e-Cl	-	nr

R_f (hexanes-EtOAc, 9:1) = 0.50. **Staining:** vanilin (UV active). **¹H-NMR** (300 MHz, CDCl₃) δ = 8.19 – 8.11 (m, 2H), 7.45 – 7.28 (m, 7H), 4.93 (dd, J = 8.6, 6.2 Hz, 1H), 2.95 (ddd, J = 14.4, 9.2, 5.7 Hz, 1H), 2.87 – 2.74 (m, 1H), 2.64 (dtd, J = 14.3, 8.7, 5.6 Hz, 1H), 2.46 (ddt, J = 14.2, 9.3, 6.3 Hz, 1H). **¹³C-NMR** (75 MHz, CDCl₃) δ = 148.3, 146.4, 141.3, 129.3, 128.8, 128.5, 127.2, 123.6, 54.2, 40.6, 34.1.

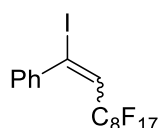
(3,3,4,4,5,5,6,6,7,7,8,8,9,9,10,10,10-Heptadecafluoro-1-iododecyl)benzene (20h)

Following GP-C (Method A), **20h** was prepared using styrene (**18a**) (115 μ L, 1.0 mmol, 1.0 equiv), $C_8F_{17}I$ (**19h**) (530 μ L, 2.0 mmol, 2.0 equiv) and copper photocatalyst **11a-Cl** to **11e-Cl** (1.0 μ mol, 1.0 mol%) in anh. MeCN (1 mL). Flash column chromatography on silica gel (hexanes) afforded **20h** as a white solid (Table 5).

Table 5. Yields of copper-catalyzed ATRA between styrene (**18a**) and $C_8F_{17}I$ (**19h**).

Entry	Catalyst	Isolated Mass [mg]	Yield [%]
1	$[Cu(dap)_2]Cl$ 11a-Cl	549	84
2	$[Cu(o-dap)_2]Cl$ 11b-Cl	115	18
3	$[Cu(m-dap)_2]Cl$ 11c-Cl	111	17
4	$[Cu(o,p-dap)_2]Cl$ 11d-Cl	21	3
5	$[Cu(o,o-dap)_2]Cl$ 11e-Cl	-	nr

R_f (hexanes) = 0.51. **Staining:** $KMnO_4$ (UV active). **1H -NMR** (400 MHz, $CDCl_3$) δ = 7.45 – 7.41 (m, 2H), 7.35 – 7.25 (m, 3H), 5.45 (dd, J = 9.6, 5.2 Hz, 1H), 3.36 – 3.10 (m, 2H). **^{19}F -NMR** (376 MHz, $CDCl_3$) δ = -81.30 (t, J = 10.1 Hz, 3F), -112.48 – -115.56 (m, 2F), -122.27 (d, J = 121.2 Hz, 6F), -123.24 (s, 2F), -124.02 (s, 2F), -126.63 (s, 2F). **^{13}C -NMR** (101 MHz, $CDCl_3$) δ = 142.7, 128.9, 128.6, 126.7, 118.6 – 103.5 (m), 42.5 (t, J = 20.5 Hz), 16.5 (t, J = 2.5 Hz). **IR** (neat, cm^{-1}): 3025, 1495, 1457, 1372, 1293, 1238, 1200, 1144, 962, 872, 831, 742, 693. **LRMS** (EI) m/z (%): 523.1 ($[M-I]^+$, 63), 177.1 (90), 153.1 (85), 109.1 (90), 104.1 (100), 91.1 (30). **HRMS** (EI) exact mass calc. for $C_{16}H_7F_{17}$: m/z 648.9312, found: m/z 648.9315 $[M-H]^+$. **mp:** 69 $^{\circ}C$.

(3,3,4,4,5,5,6,6,7,7,8,8,9,9,10,10,10-Heptadecafluoro-1-iododec-1-en-1-yl)benzene (20i)

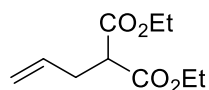
Following GP-C (Method A), **20i** was prepared using phenylacetylene (**18d**) (102 mg, 1.0 mmol, 1.0 equiv), C₈F₁₇I (**19h**) (530 μ L, 1.0 mmol, 2.0 equiv) and copper photocatalyst **11a-Cl** to **11e-Cl** (1.0 μ mol, 1.0 mol%) in anh. MeCN (1 mL). Chromatography on silica (hexanes) afforded **20i** as a white solid (Table 6).

R_f (hexanes) = 0.74. **Staining**: vanilin (UV active). **¹H-NMR** (400 MHz, CDCl₃) δ = 7.45 – 7.27 (m, 5H), 6.61 (t, J = 13.5 Hz, 1H). **¹⁹F-NMR** (376 MHz, CDCl₃) δ = -80.91 (t, J = 10.1 Hz, 3F), -105.12 – -109.00 (m, 2F), -121.48 – -121.61 (m, 2F), -121.96 (t, J = 19.4 Hz, 4F), -122.83 (dt, J = 17.4, 7.6 Hz, 4F), -126.20 (ddd, J = 18.7, 9.3, 4.1 Hz, 2F). **¹³C-NMR** (101 MHz, CDCl₃) δ = 141.5, 129.4, 128.7, 128.2, 127.12 – 126.88 (m), 117.8 - 107.0 (m). **IR** (neat, cm⁻¹): 3065, 2926, 1640, 1352, 1220, 1138, 1031, 920, 890, 701. **HRMS** (EI) exact mass calc. for C₁₆H₅F₁₇I: m/z 647.9164, found: m/z 647.9199 [M-H]⁺. **mp**: 60 °C.

Table 6: Yields and *E/Z*-Ratio of copper-catalyzed ATRA between phenylacetylene (**18d**) and C₈F₁₇I (**19h**).^[a]

Entry	Catalyst	<i>E/Z</i> -Ratio	Isolated Mass [mg]	Yield [%]
1	[Cu(dap) ₂]Cl 11a-Cl	92:08	450	69
2	[Cu(<i>o</i> -dap) ₂]Cl 11b-Cl	92:08	108	17
3	[Cu(<i>m</i> -dap) ₂]Cl 11c-Cl	92:08	102	16
4	[Cu(<i>o,p</i> -dap) ₂]Cl 11d-Cl	-	-	nr
5	[Cu(<i>o,o</i> -dap) ₂]Cl 11e-Cl	-	-	nr

[a] *E/Z*-ratio determined by ¹H-NMR.

Diethyl 2-allylmalonate (20j)^[17]

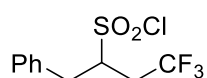
Following GP-C (Method B), **20j** was prepared using allyltrimethylsilane (**18e**) (159 μ L, 1.0 mmol, 1.0 equiv), diethyl bromomalonate (**19c**) (340 μ L, 2.0 mmol, 2.0 equiv) and copper photocatalyst **11a-Cl** to **11e-Cl** (1.0 μ mol, 1.0 mol%) in anh. MeCN (3 mL). Flash column chromatography on silica gel (hexanes-EtOAc, 9:1) afforded **20j** as a colourless liquid (Table 7, entries 1-5).

Following GP-D, **20j** was prepared using diethyl bromomalonate (**19c**) (170 μ L, 1.0 mmol, 1.0 equiv), allyltrimethylsilane (**18e**) (477 μ L, 3.0 mmol, 3.0 equiv) and copper photocatalyst **11a-BF₄**, **27-BF₄** or **28-BF₄** (0.5 μ mol, 0.5 mol%) in anh. MeCN (3 mL). Flash column chromatography on silica gel (hexanes-EtOAc, 9:1) afforded **20j** as a colourless liquid (Table 7, entries 6-8).

Table 7. Yields of copper-catalyzed ATRA between allyltrimethylsilane (**18e**) and diethyl 2-bromomalonate (**19c**).

Entry	Catalyst		Isolated Mass [mg]	Yield [%]
1	[Cu(dap) ₂]Cl	11a-Cl	135	67
2	[Cu(<i>o</i> -dap) ₂]Cl	11b-Cl	47	23
3	[Cu(<i>m</i> -dap) ₂]Cl	11c-Cl	34	17
4	[Cu(<i>o,p</i> -dap) ₂]Cl	11d-Cl	10	5
5	[Cu(<i>o,o</i> -dap) ₂]Cl	11e-Cl	8	4
6	[Cu(dap) ₂]BF ₄	11a-BF₄	122	61
7	[Cu(dap)(DPEphos)]BF ₄	27-BF₄	130	65
8	[Cu(dpp)(binc)]BF ₄	28-BF₄	129	64

R_f (hexanes-EtOAc, 4:1) = 0.60. **Staining:** KMnO₄ (UV inactive). **¹H-NMR** (300 MHz, CDCl₃) δ = 5.74 (dtd, J = 17.0, 6.7, 3.5 Hz, 1H), 5.13 – 4.98 (m, 2H), 4.16 (qd, J = 7.2, 2.9 Hz, 4H), 3.38 (td, J = 7.6, 2.7 Hz, 1H), 2.65 – 2.56 (m, 2H), 1.23 (td, J = 7.2, 2.7 Hz, 6H). **¹³C-NMR** (75 MHz, CDCl₃) δ = 170.8, 168.9, 134.1, 132.4, 119.2, 117.5, 61.4, 61.3, 57.3, 51.7, 36.8, 32.9, 14.2, 14.1.

4,4,4-Trifluoro-1-phenylbutane-2-sulfonyl chloride (20k)^[18]

Following GP-C (Method B), **20k** was prepared using allylbenzene (**18f**) (132 μ L, 1.0 mmol, 1.0 equiv), $\text{CF}_3\text{SO}_2\text{Cl}$ (**19i**) (210 μ L, 2.0 mmol, 2.0 equiv), K_2HPO_4 (348 mg, 2.0 mmol, 2.0 equiv) and copper photocatalyst **11a-Cl** to **11e-Cl** (1.0 μ mol, 1.0 mol%) in anh. MeCN (3 mL). Flash column chromatography on silica gel (hexanes-EtOAc, 99:1) afforded an mixture of **20k:21** as a colourless liquid (Table 8).

Table 8. Yields and selectivity of copper-catalyzed ATRA between allylbenzene (**18f**) and $\text{CF}_3\text{SO}_2\text{Cl}$ (**19i**).^[a]

Entry	Catalyst	Selectivity		Isolated Mass [mg]	Yield [%]
		20k	21		
1	[Cu(dap) ₂] Cl 11a-Cl	95	5	244	86
2	[Cu(o-dap) ₂] Cl 11b-Cl	52	48	39	15
3	[Cu(m-dap) ₂] Cl 11c-Cl	53	47	25	10
4	[Cu(o,p-dap) ₂] Cl 11d-Cl	52	48	17	6
5	[Cu(o,o-dap) ₂] Cl 11e-Cl	50	50	11	4

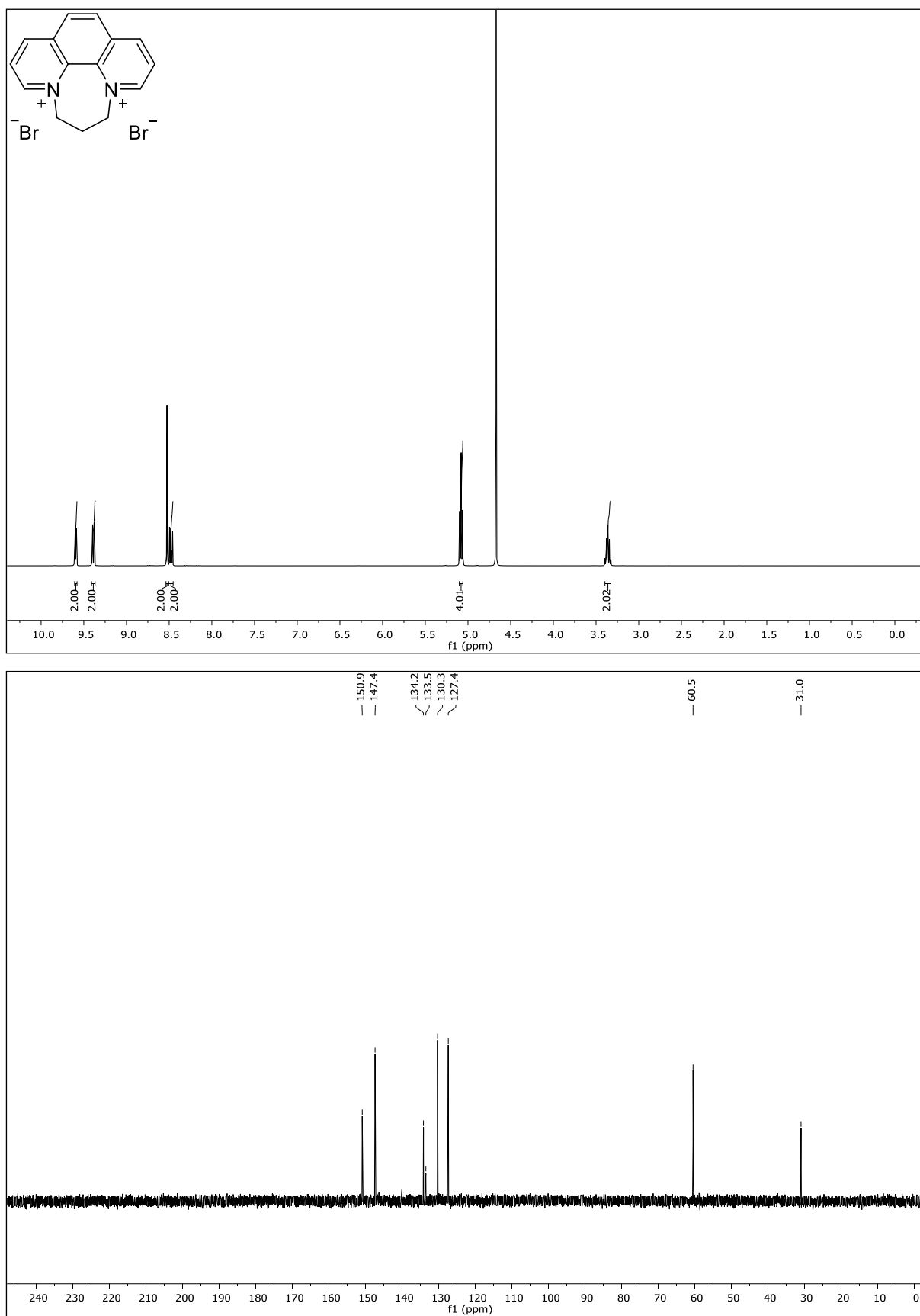
[a] Selectivity determined by ^{19}F -NMR.

R_f (hexanes-EtOAc, 9:1) = 0.70. **Staining:** KMnO_4 (UV active). ^1H -NMR (300 MHz, CDCl_3) δ = 7.42 – 7.24 (m, 5H), 4.06 (qd, J = 7.0, 3.5 Hz, 1H), 3.57 (dd, J = 14.9, 5.6 Hz, 1H), 3.26 (dd, J = 14.8, 6.9 Hz, 1H), 3.10 – 2.94 (m, 1H), 2.66 (dq, J = 15.6, 9.7, 7.3 Hz, 1H). ^{19}F -NMR (376 MHz, CDCl_3) δ = -63.95 (s, 3F). ^{13}C -NMR (75 MHz, CDCl_3) δ = 133.9, 129.5, 129.1, 128.1, 124.7 (q, J = 277.6 Hz), 70.9 (q, J = 2.4 Hz), 36.2, 34.0 (q, J = 31.1 Hz).

2.3. NMR Spectra

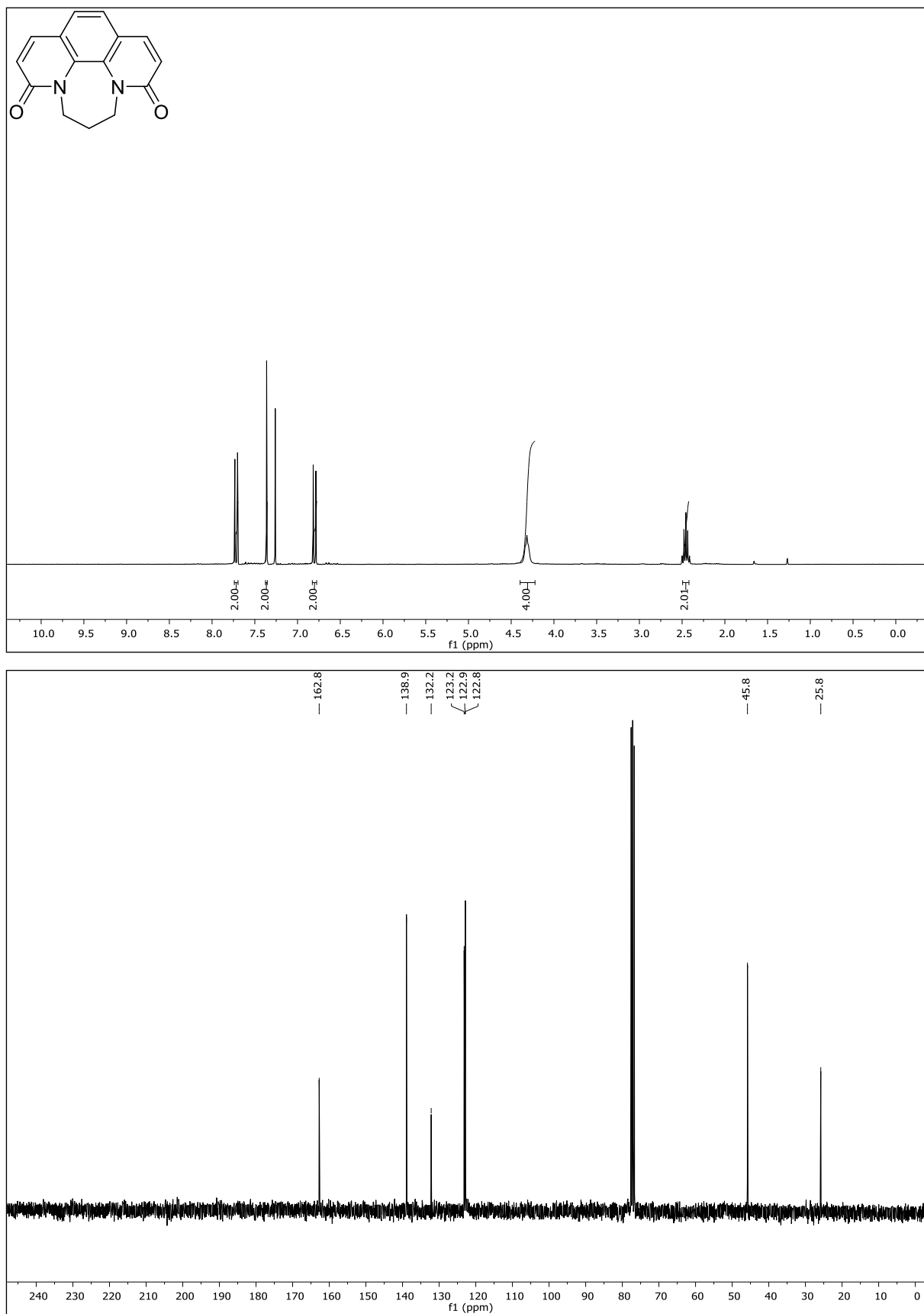
^1H -NMR	first image
^{13}C -NMR	second image
^{19}F -NMR	third image

6,7-Dihydro-5*H*-[1,4]diazepino[1,2,3,4-*lmn*][1,10]phenanthroline-4,8-diium bromide (6)



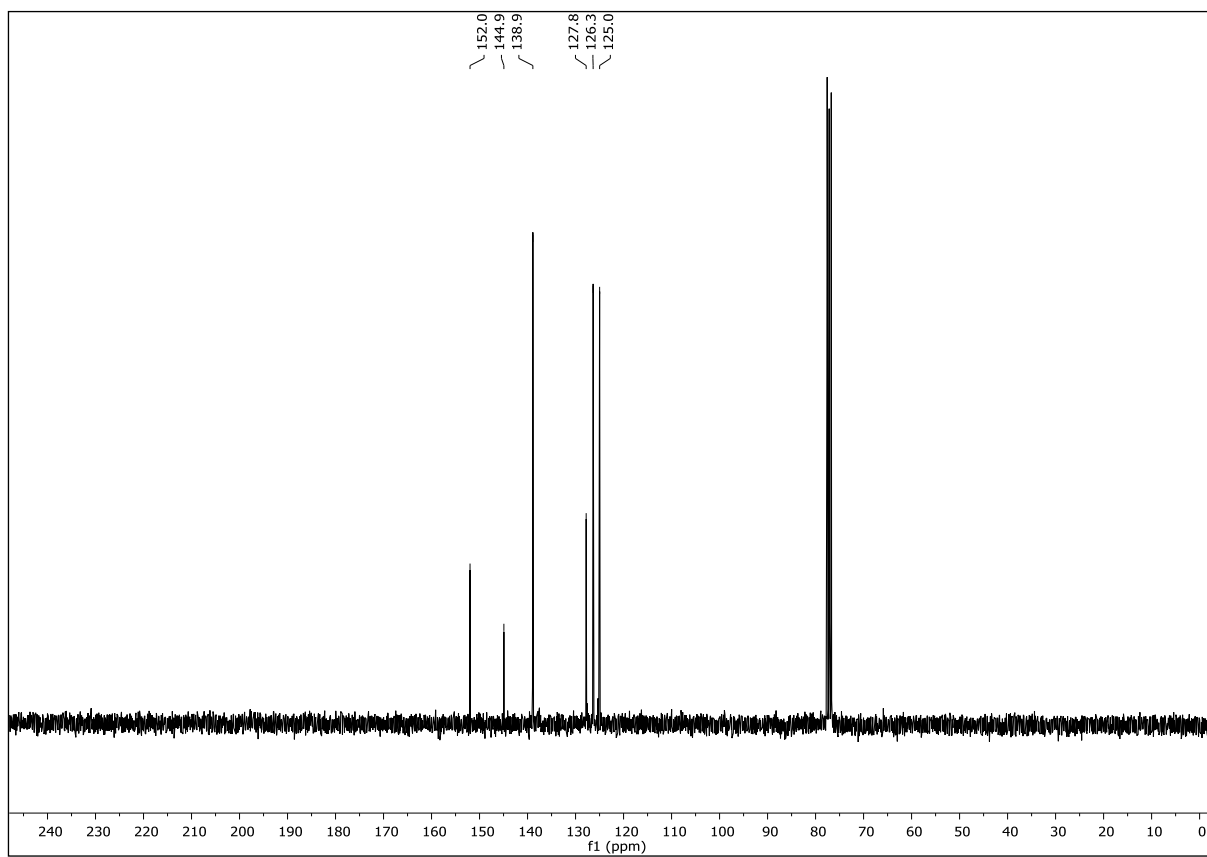
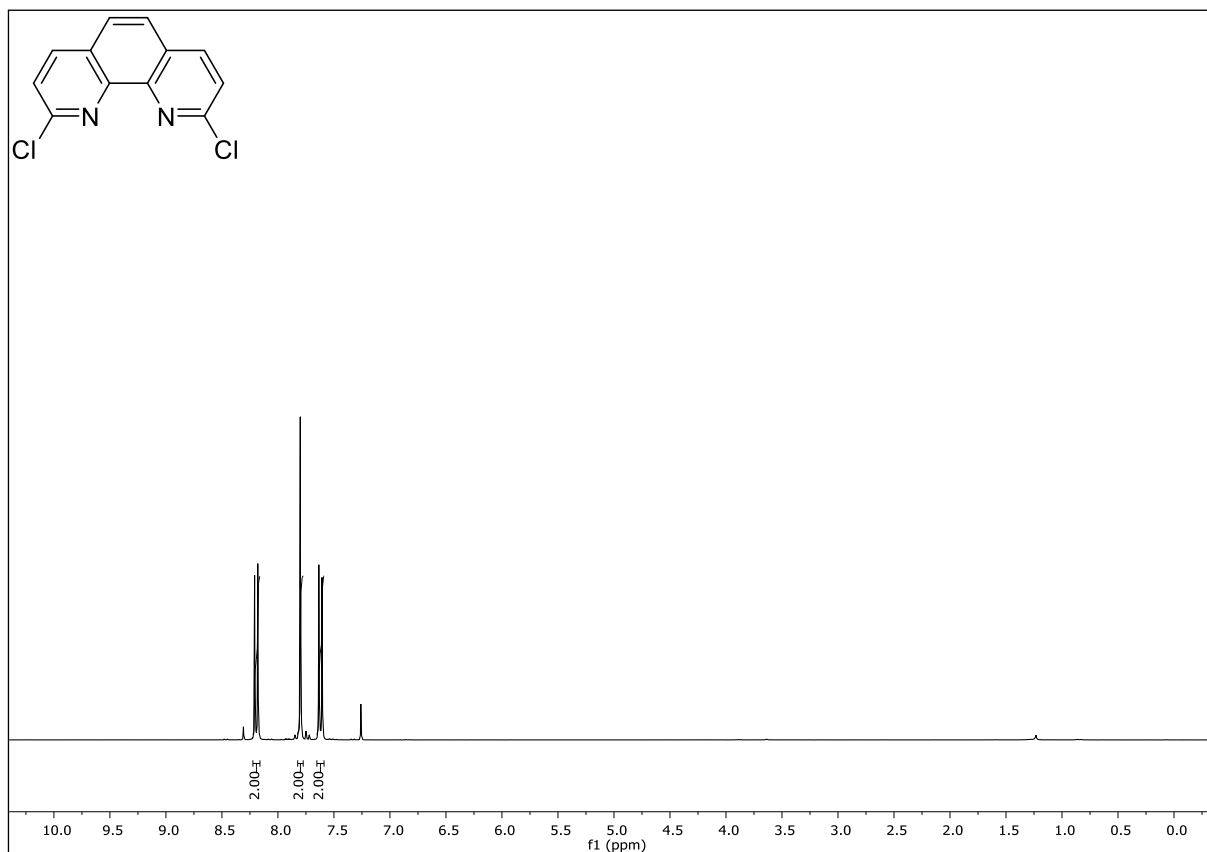
NMR-Solvent: D₂O

6,7-Dihydro-5*H*-[1,4]diazepino[1,2,3,4-*lmn*][1,10]phenanthroline-3,9-dione (7)



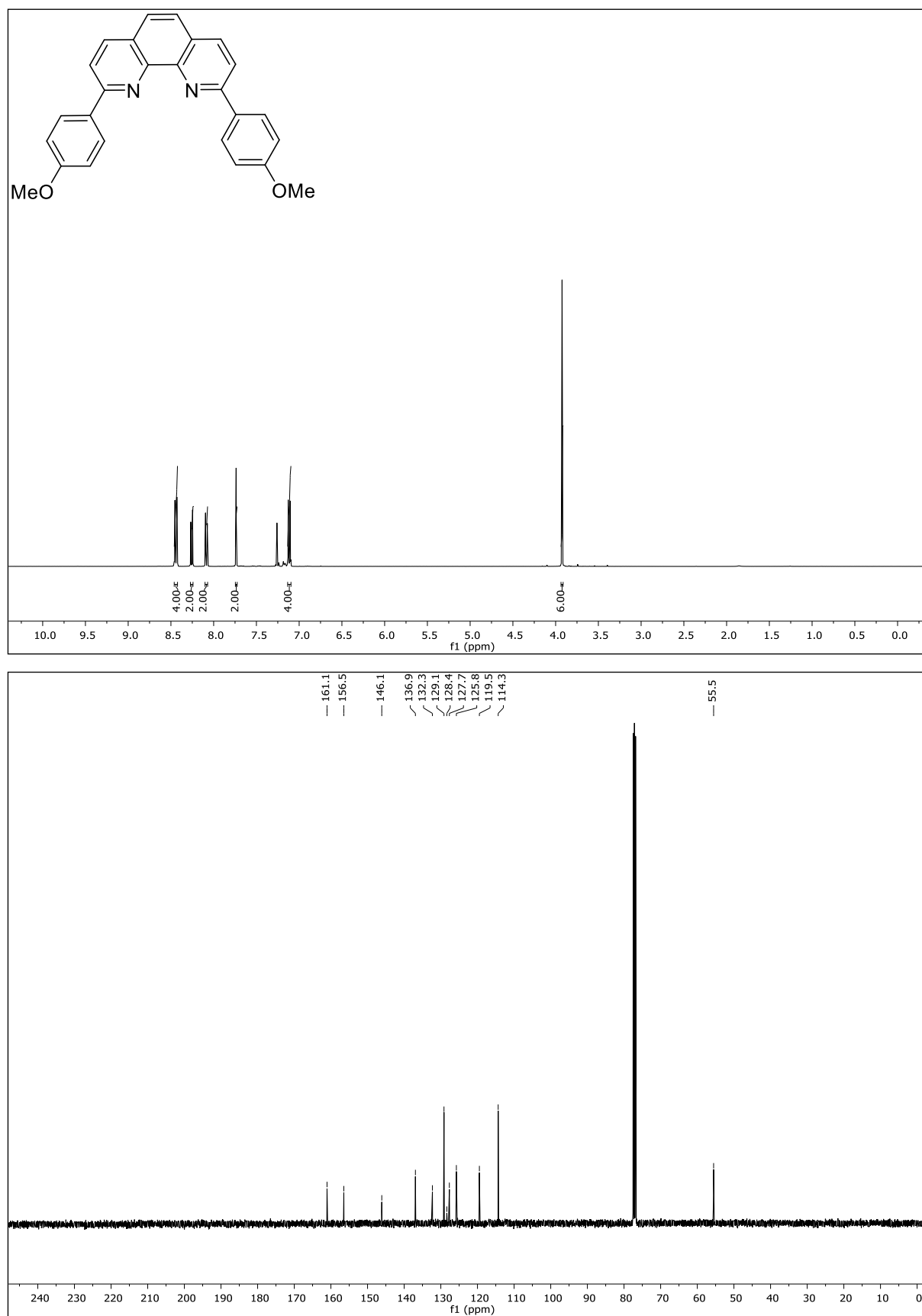
NMR-Solvent: CDCl₃

2,9-Dichloro-1,10-phenanthroline (8)



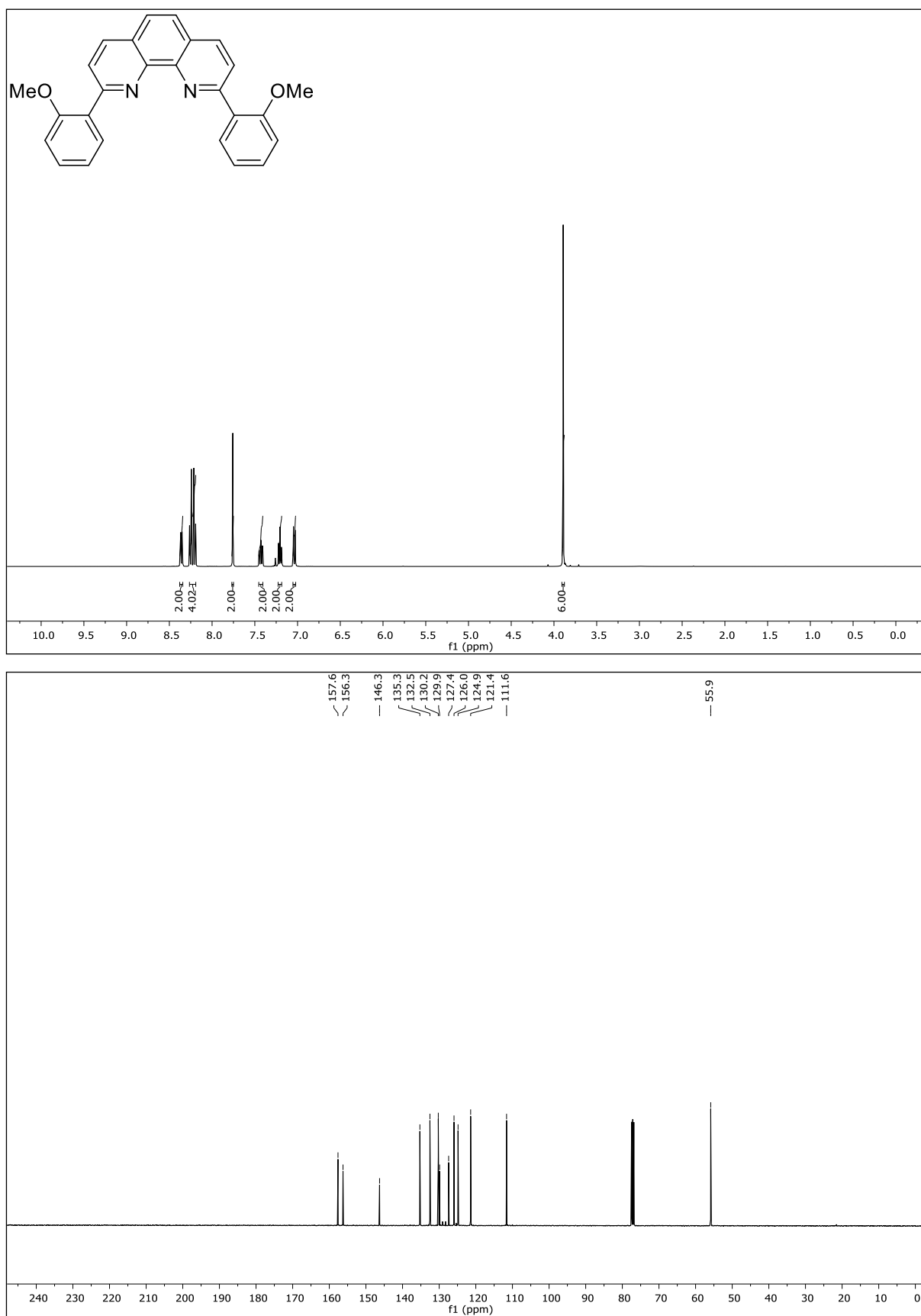
NMR-Solvent: CDCl₃

2,9-Bis(4-methoxyphenyl)-1,10-phenanthroline (10a)



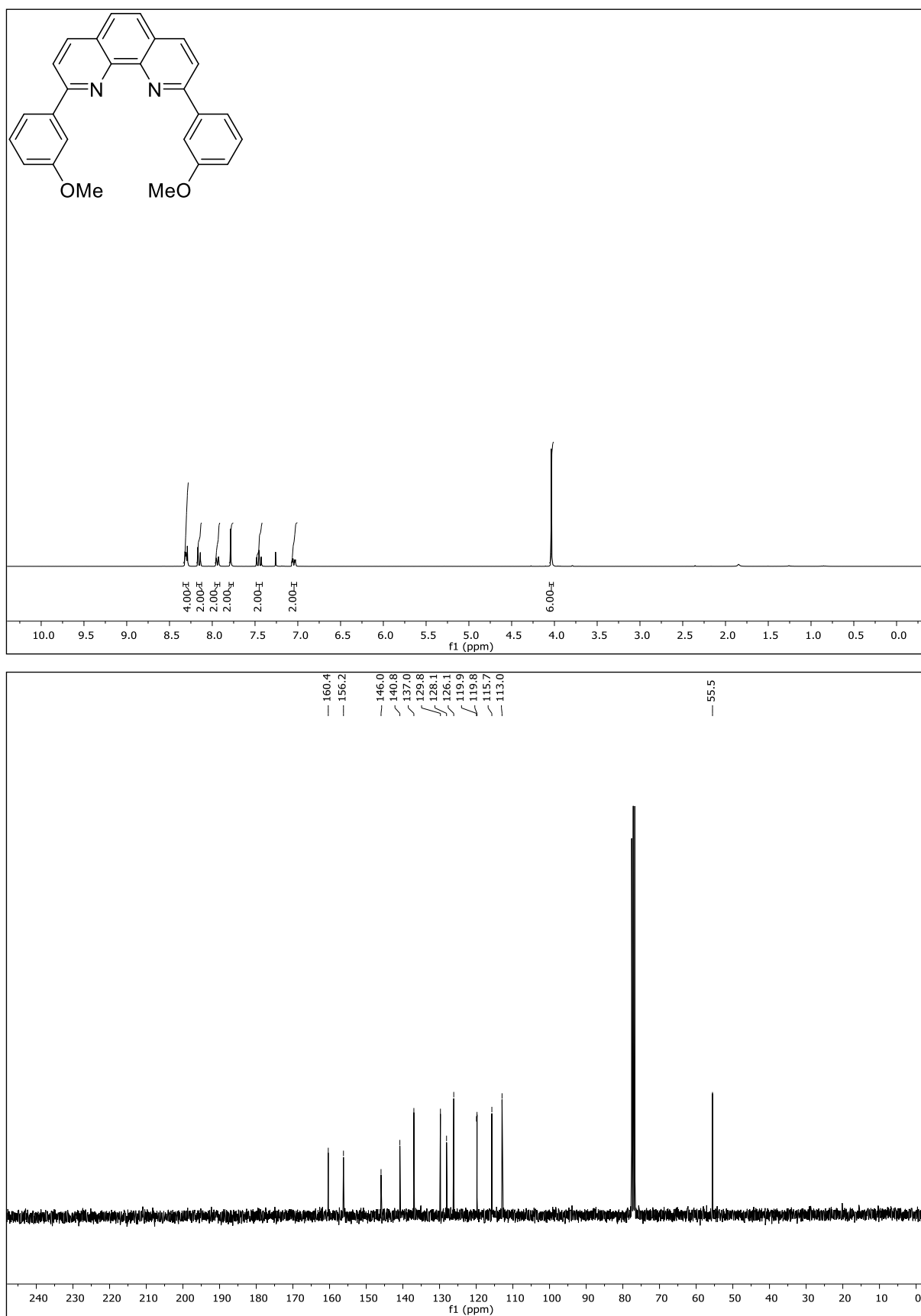
NMR-Solvent: CDCl₃

2,9-Bis(2-methoxyphenyl)-1,10-phenanthroline (10b)



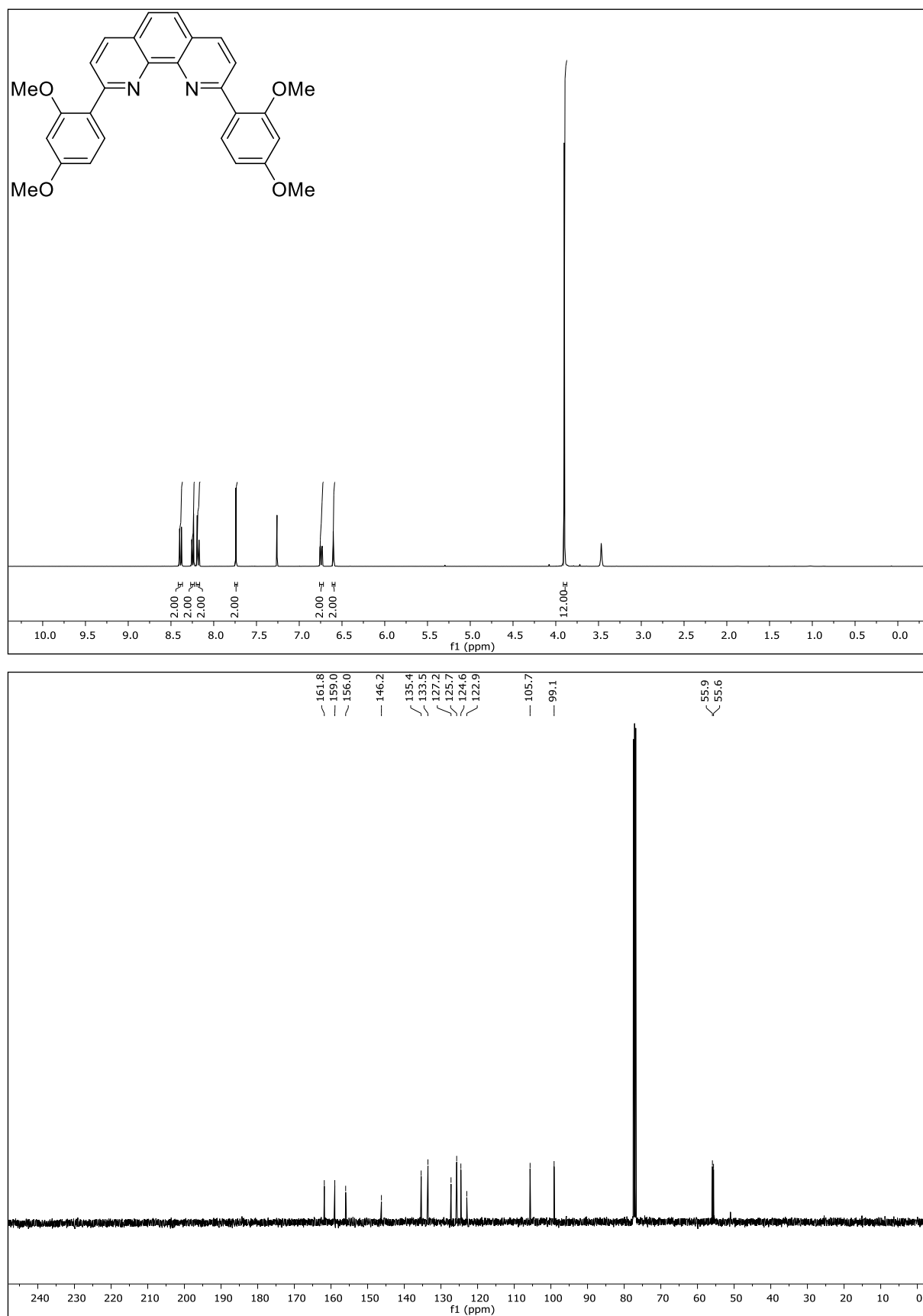
NMR-Solvent: CDCl₃

2,9-Bis(3-methoxyphenyl)-1,10-phenanthroline (10c)



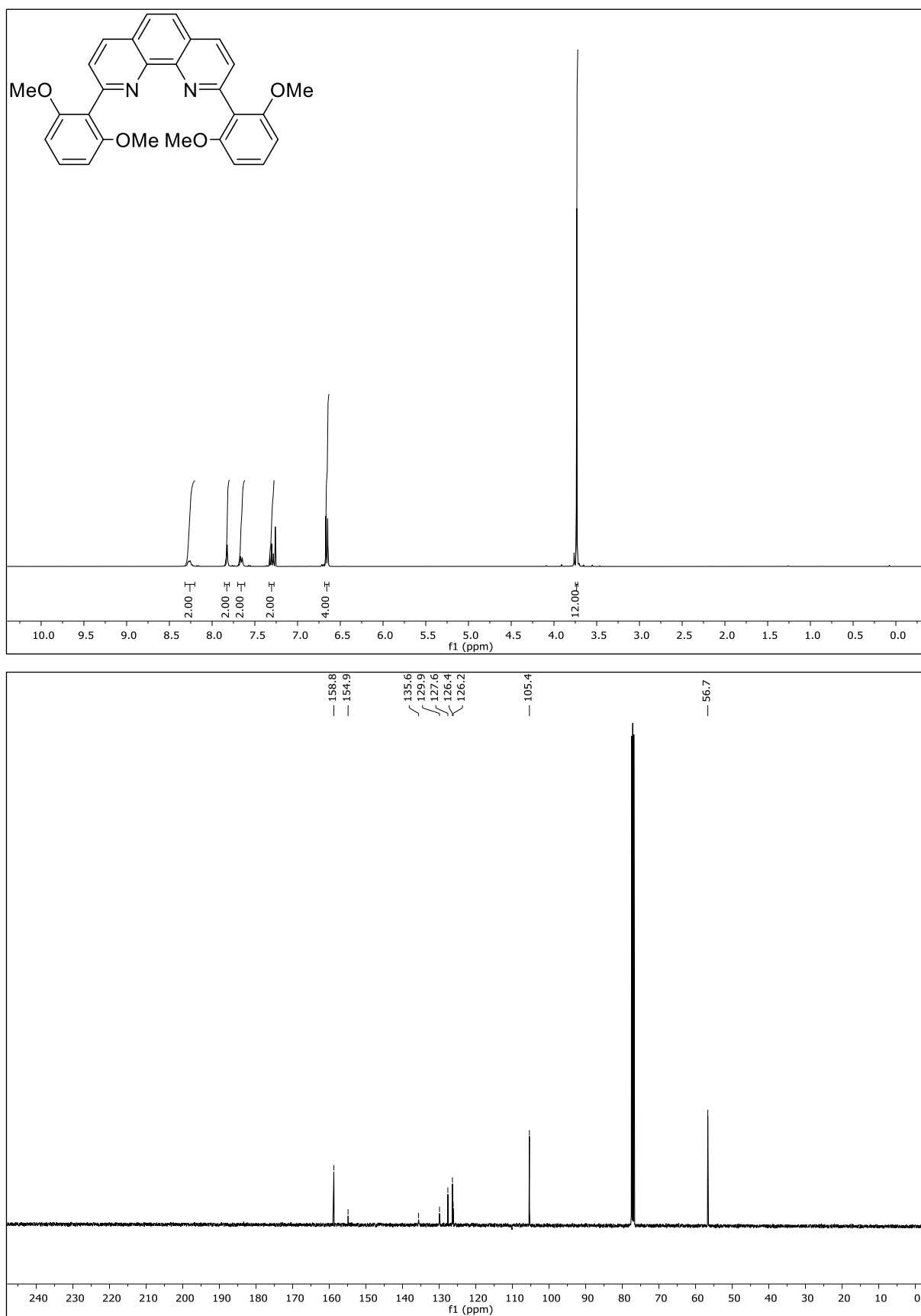
NMR-Solvent: CDCl₃

2,9-Bis(2,4-dimethoxyphenyl)-1,10-phenanthroline (10d)



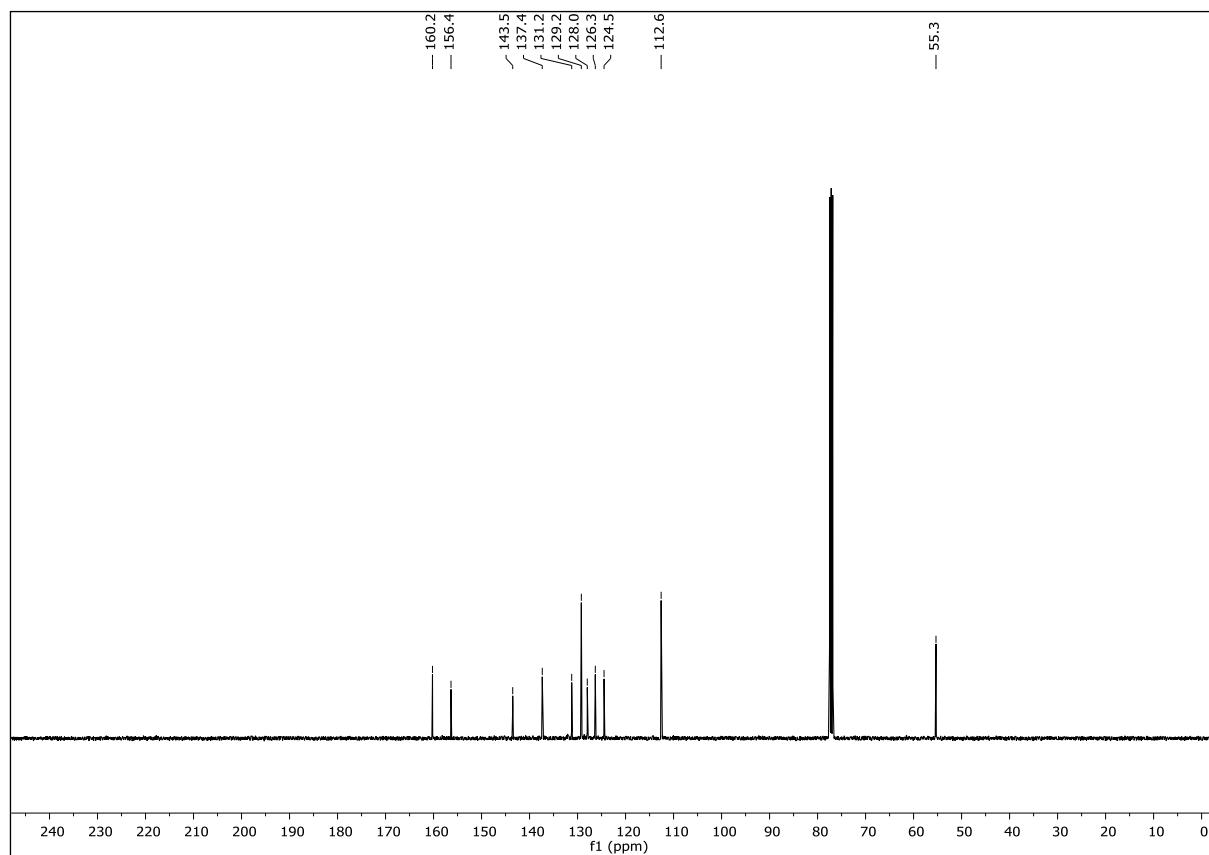
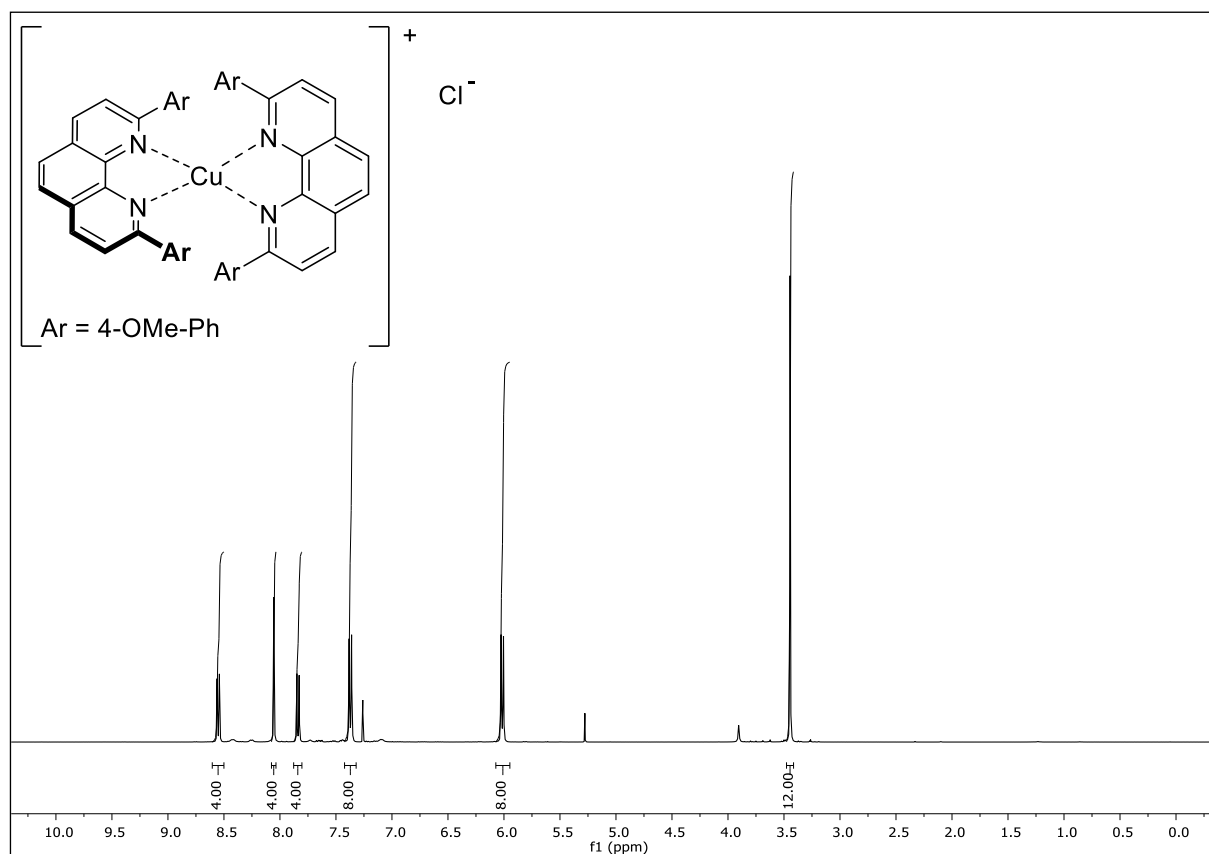
NMR-Solvent: CDCl₃

2,9-Bis(2,6-dimethoxyphenyl)-1,10-phenanthroline (10e)



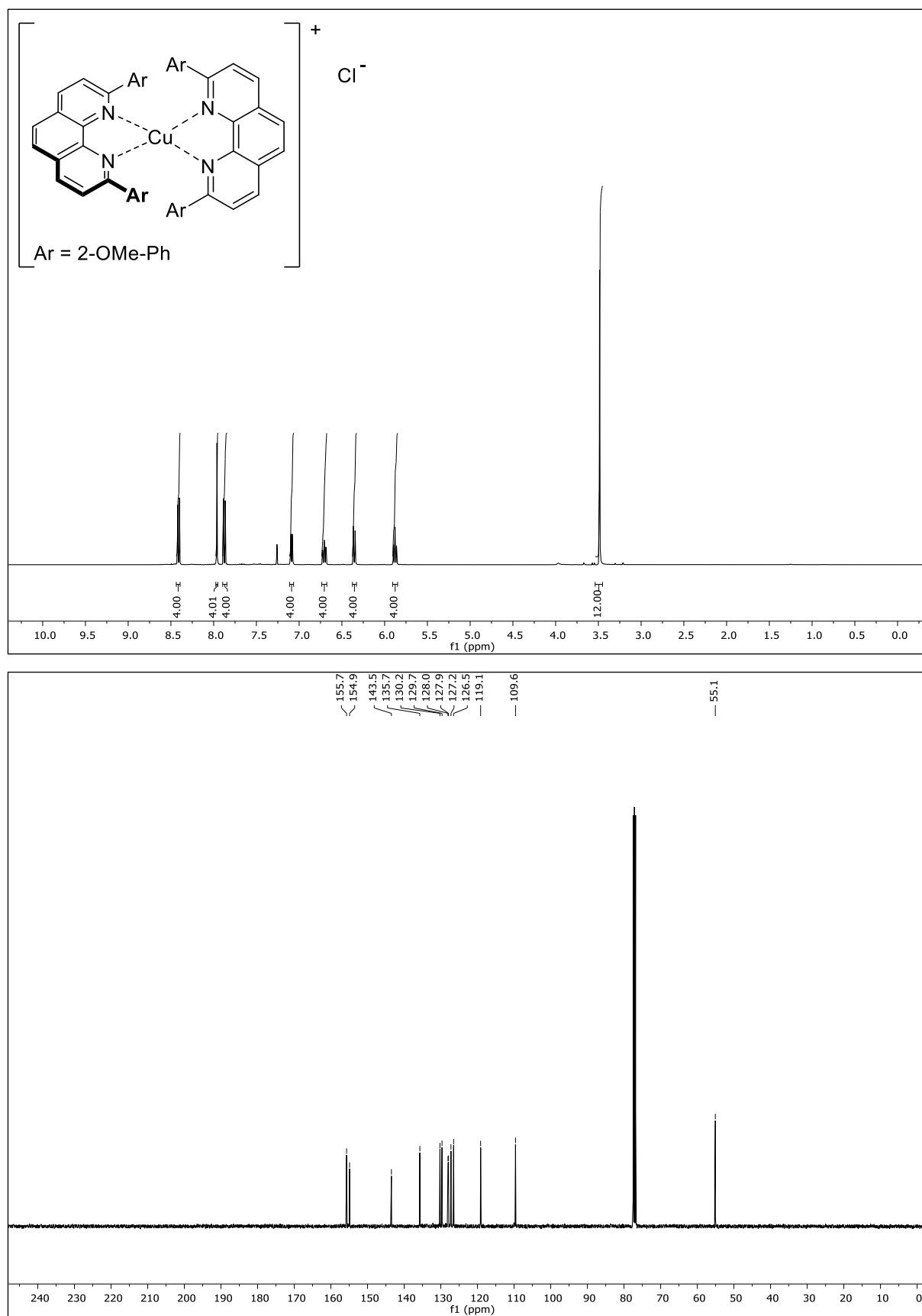
NMR-Solvent: CDCl₃

[Cu(dap)₂]⁺Cl⁻ (11a-Cl)



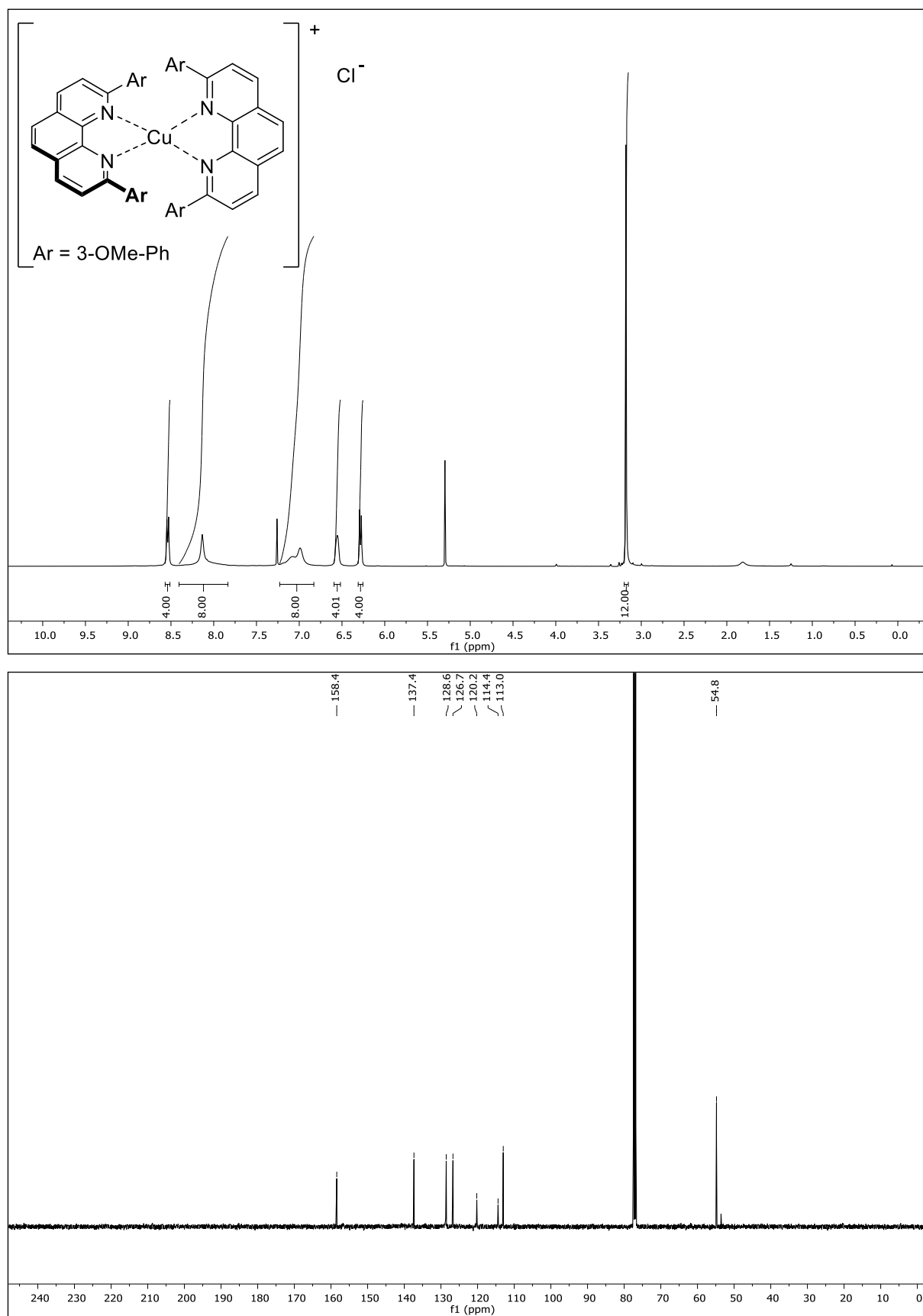
NMR-Solvent: CDCl₃

[Cu(o-dap)₂]Cl (11b-Cl)



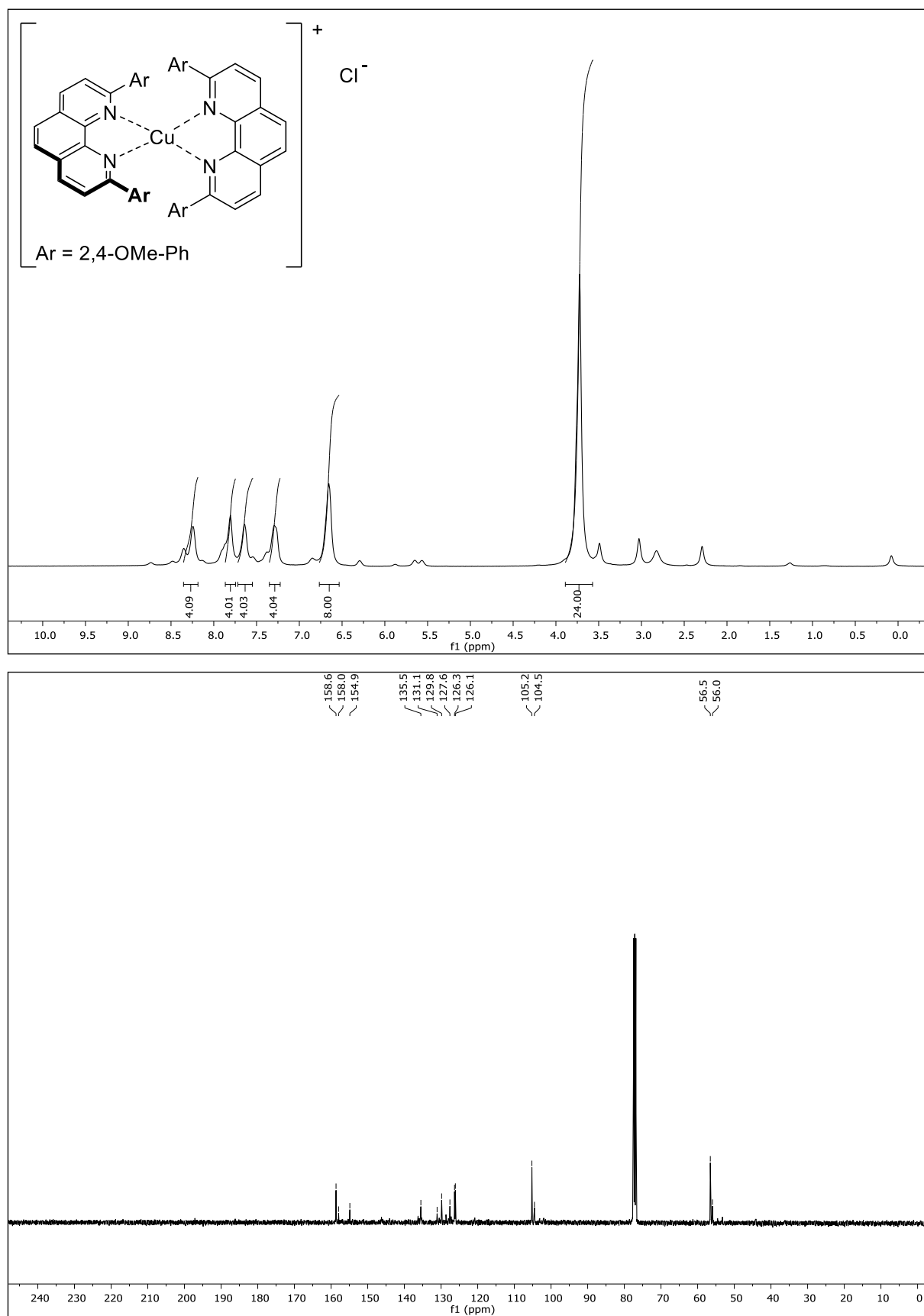
NMR-Solvent: CDCl₃

[Cu(*m*-dap)₂]Cl (11c-Cl)



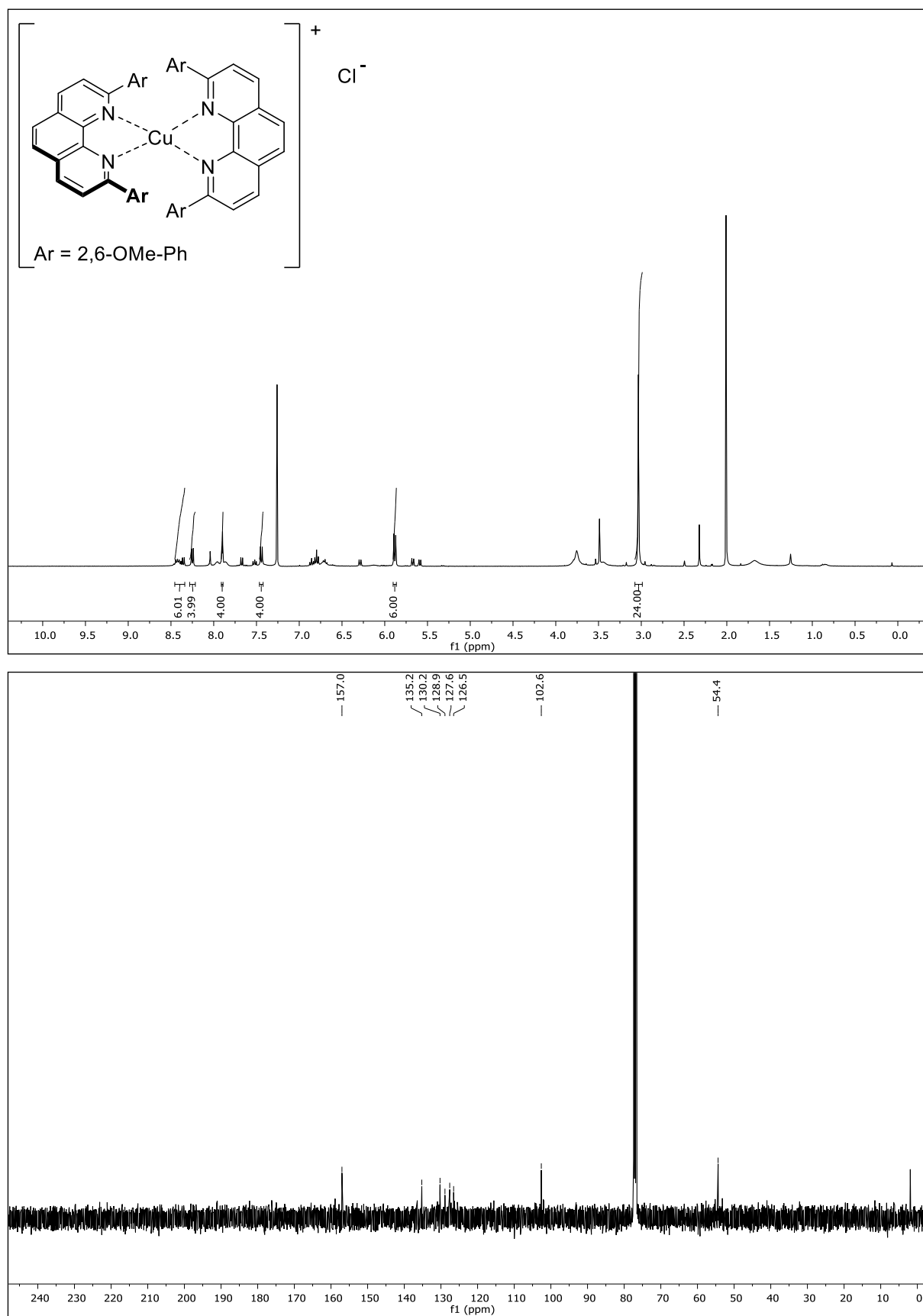
NMR-Solvent: CDCl₃

[Cu(*o,p*-dap)₂Cl] (11d-Cl)



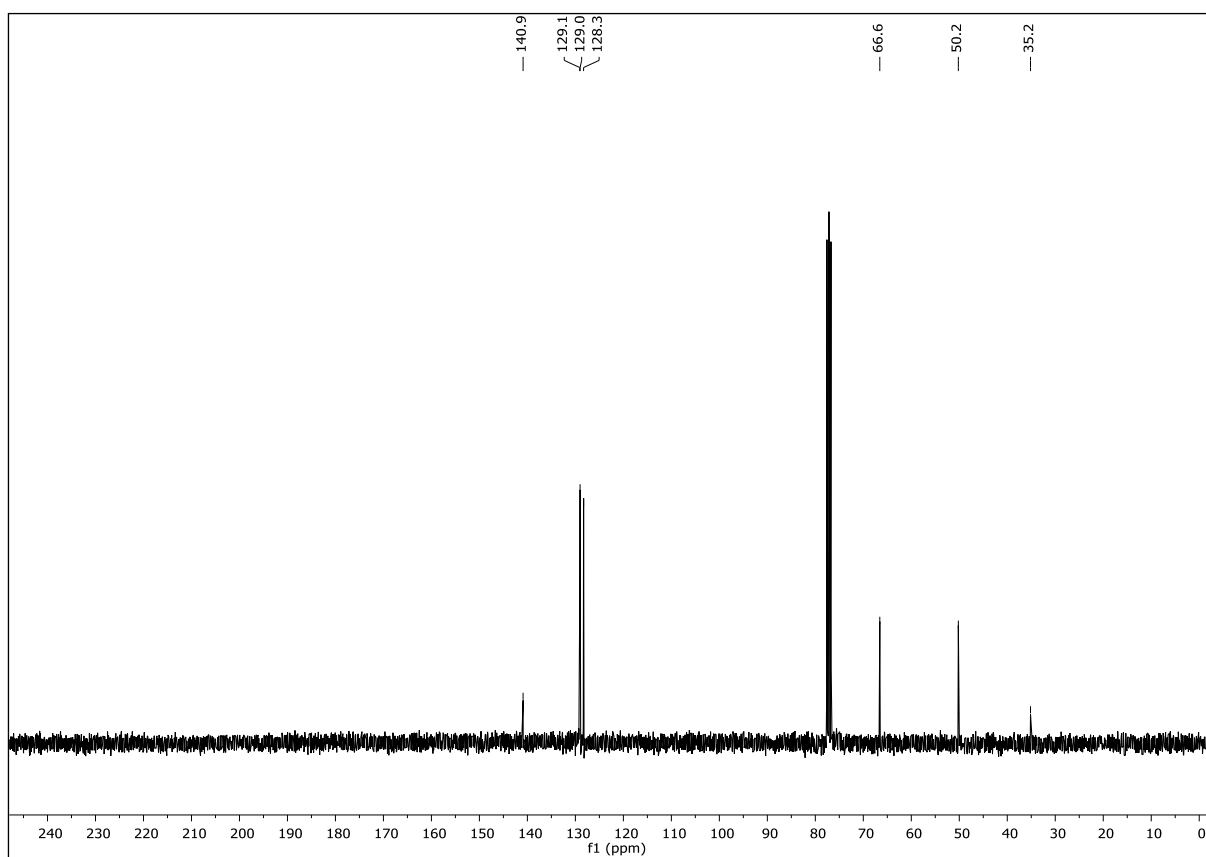
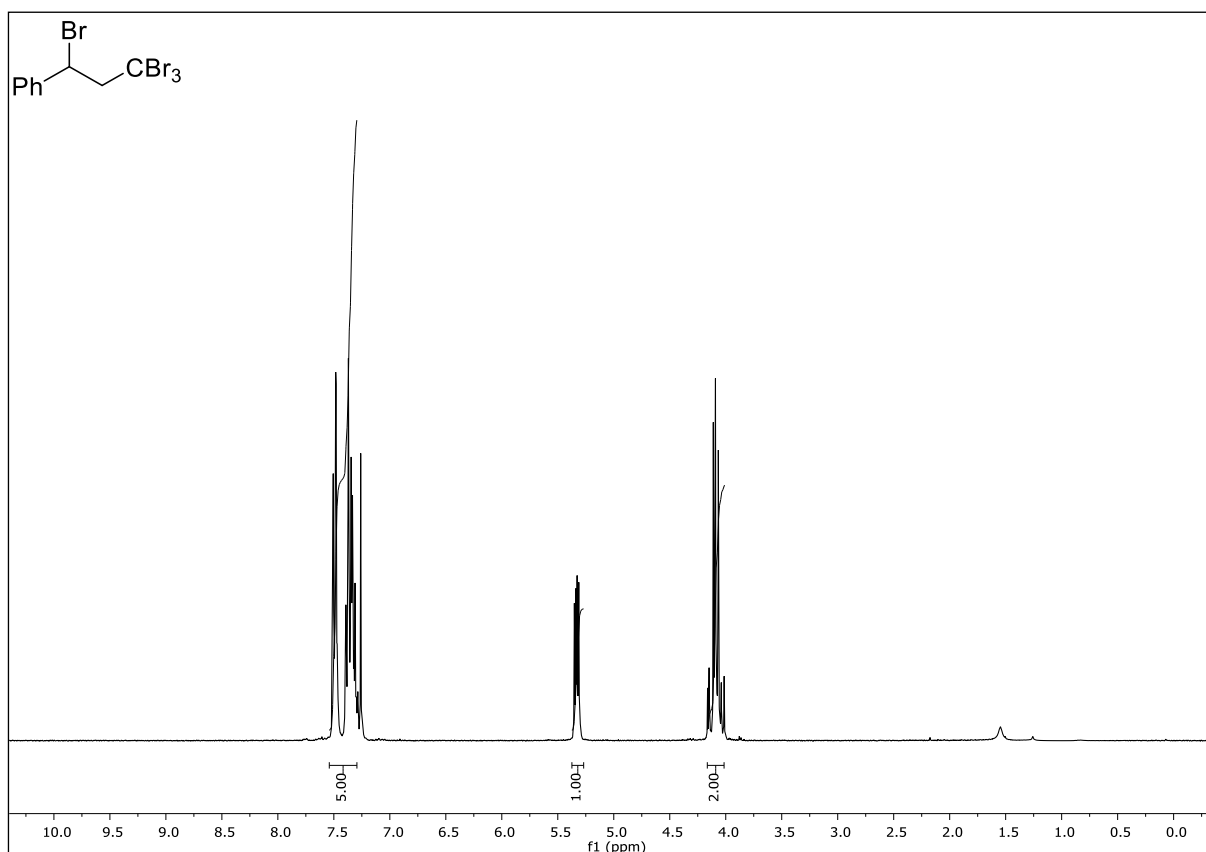
NMR-Solvent: CDCl₃

[Cu(o,o-dap)₂]⁺Cl⁻ (11e-Cl)



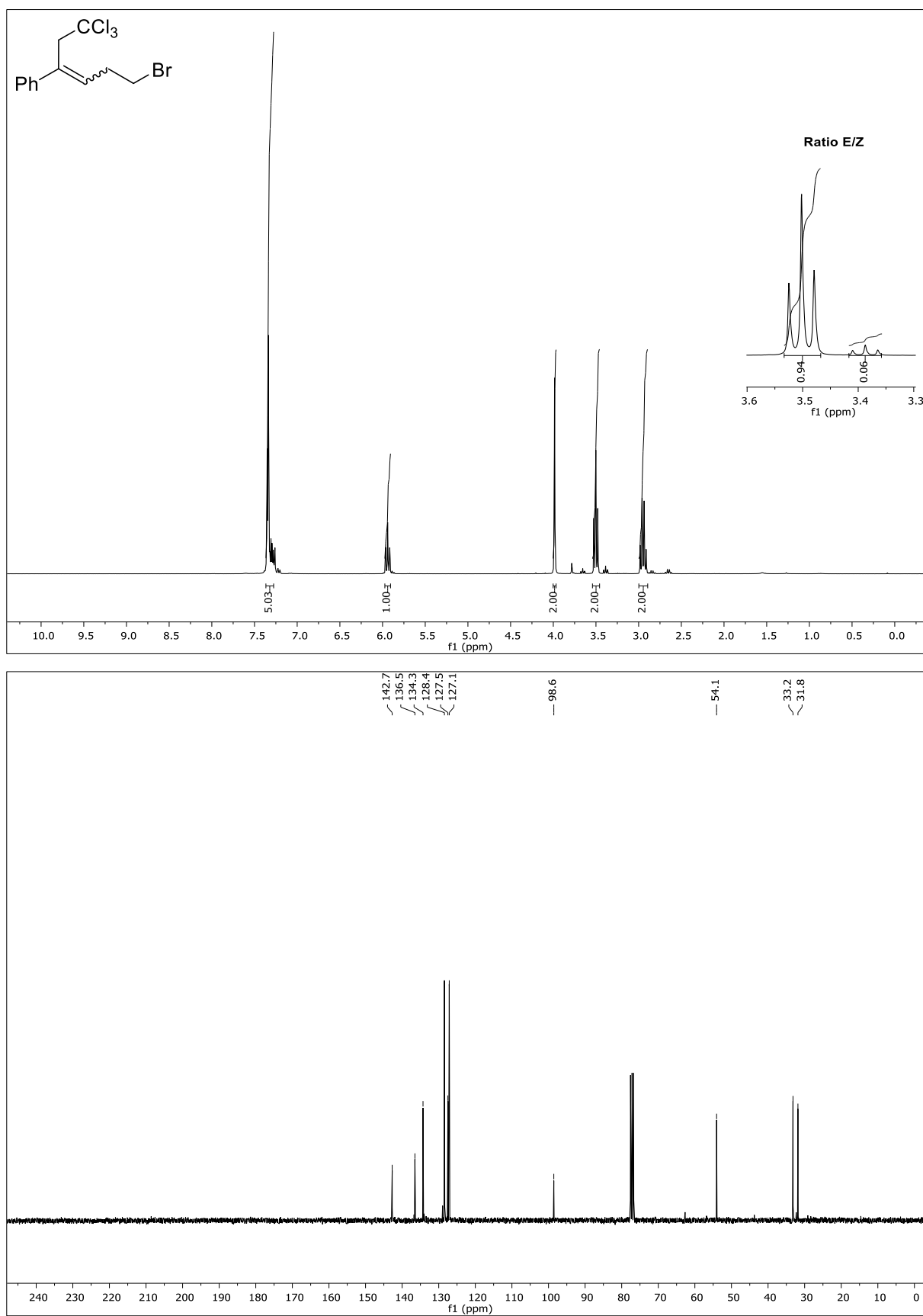
NMR-Solvent: CDCl₃

(1,3,3,3-Tetrabromopropyl)benzene (20a)



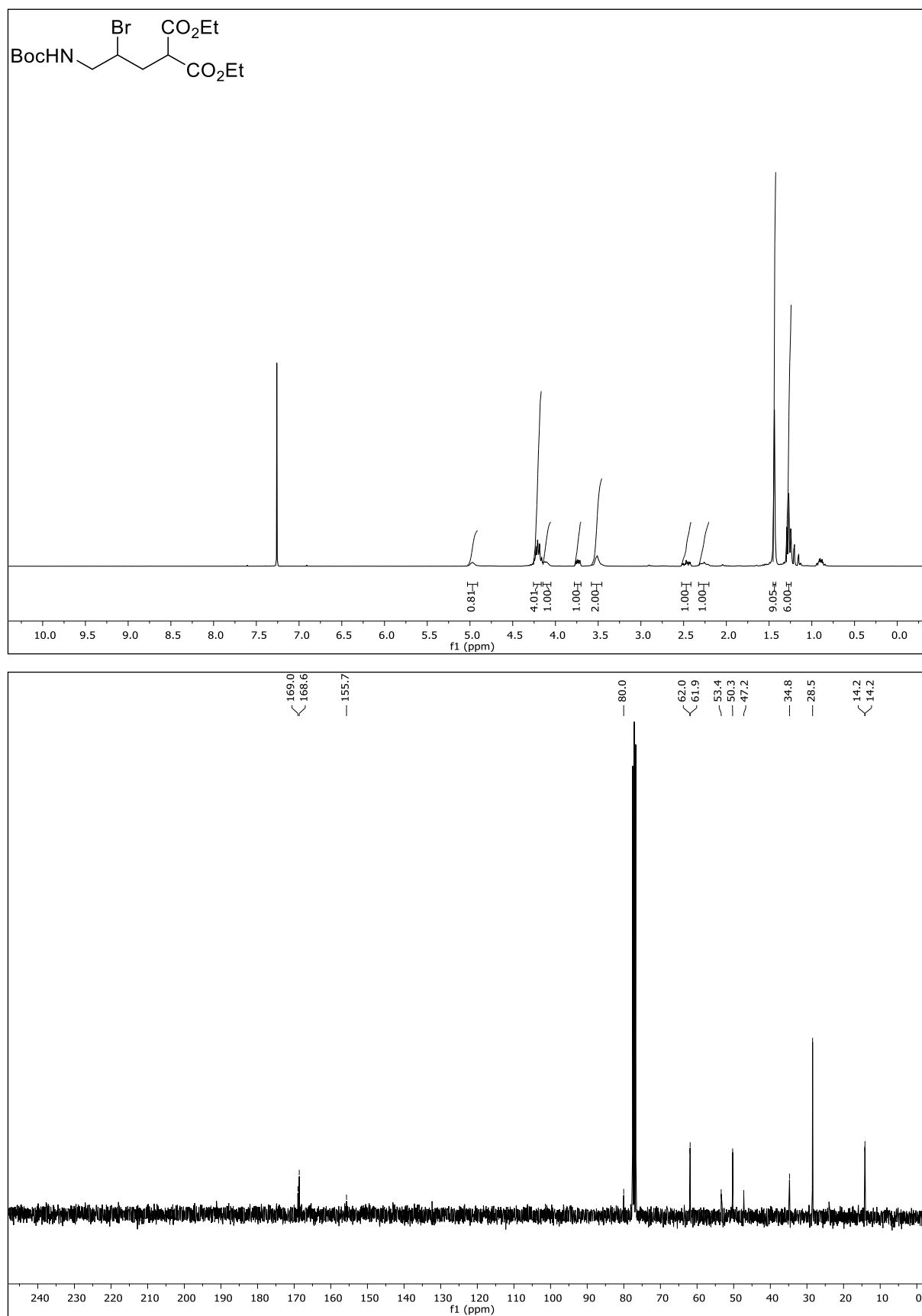
NMR-Solvent: CDCl₃

(6-Bromo-1,1,1-trichlorohex-3-en-3-yl)benzene (20b)



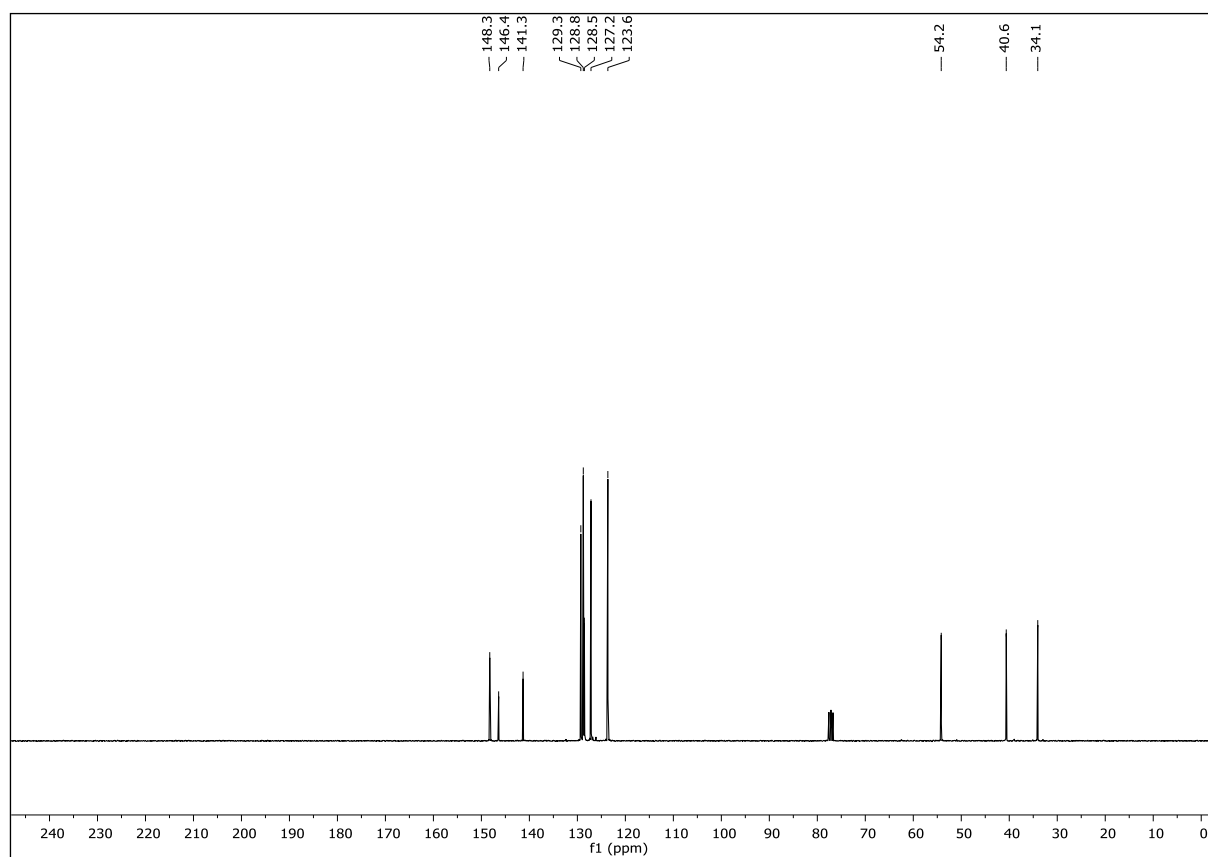
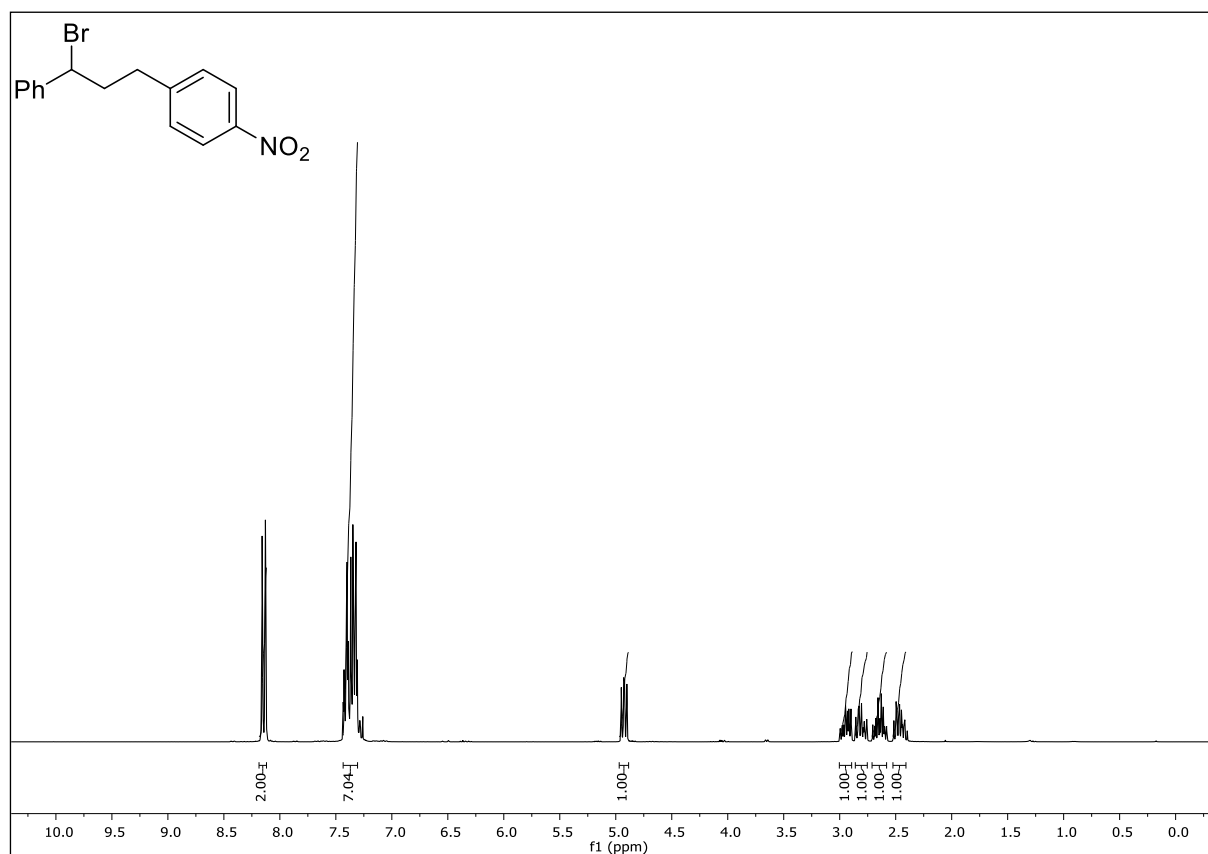
NMR-Solvent: CDCl₃

Diethyl 2-(2-bromo-3-((*tert*-butoxycarbonyl)amino)propyl)malonate (20c)



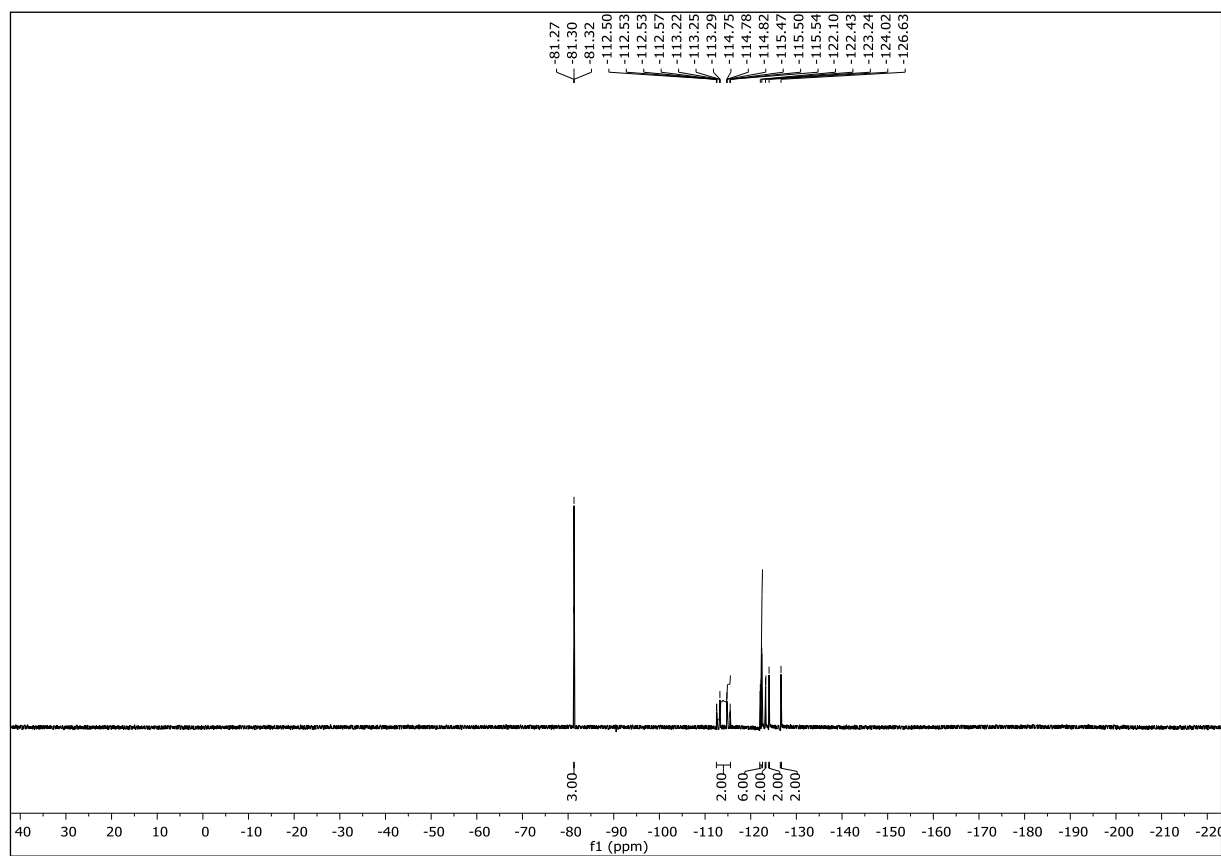
NMR-Solvent: CDCl₃

1-(3-Bromo-3-phenylpropyl)-4-nitrobenzene (20d)



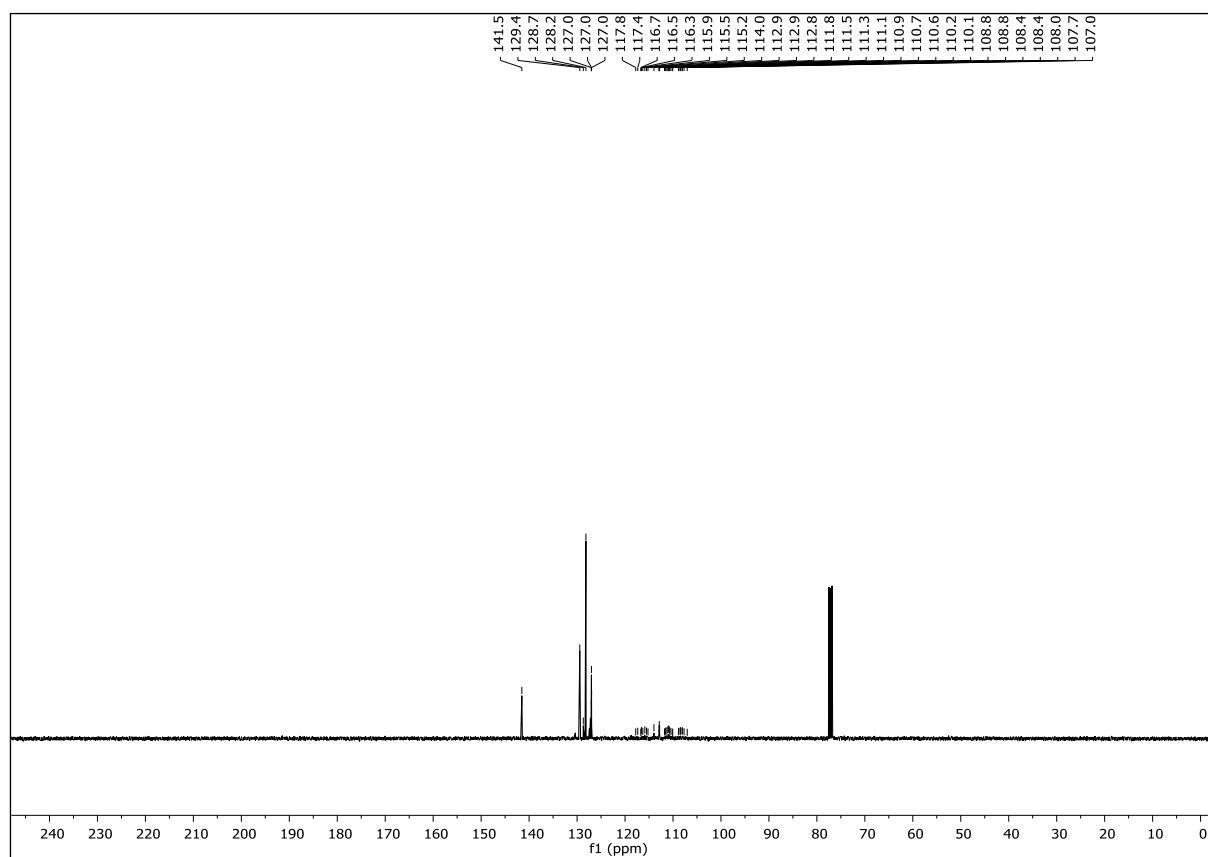
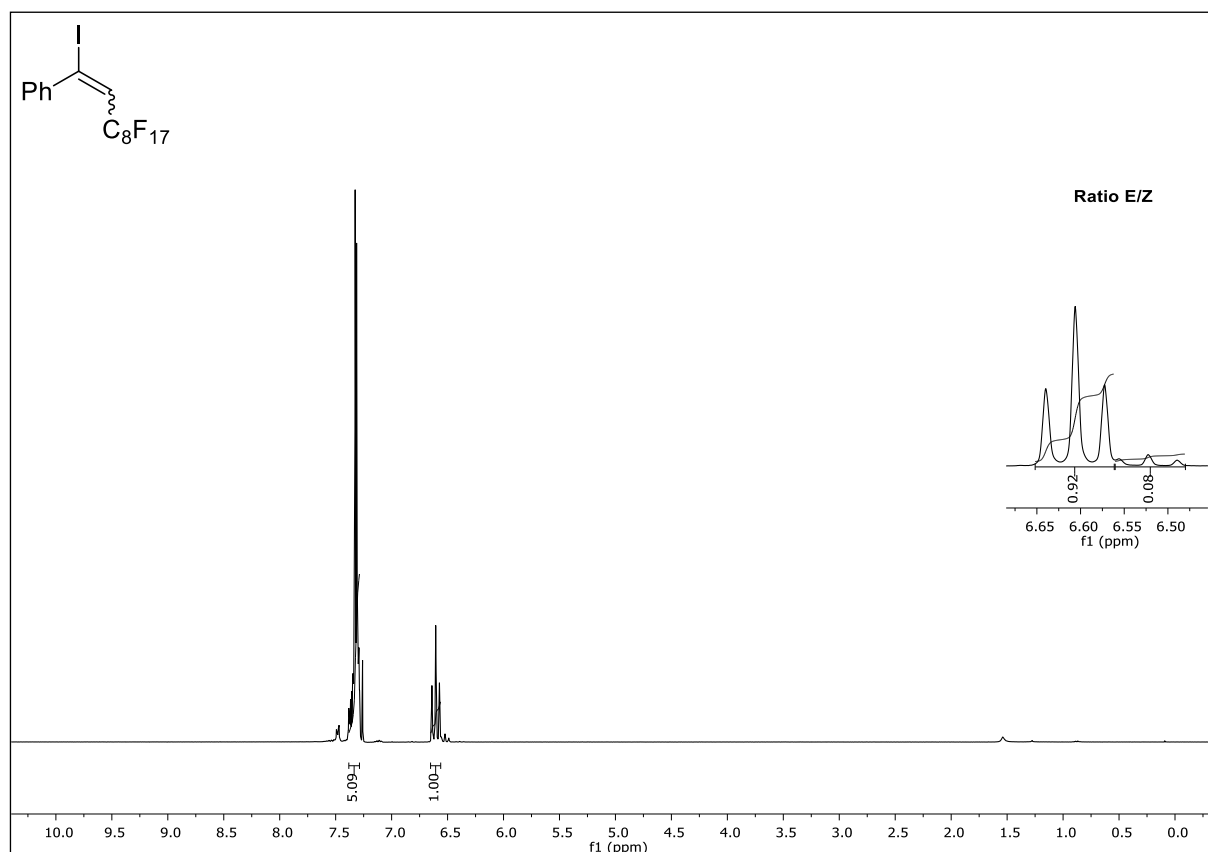
NMR-Solvent: CDCl₃

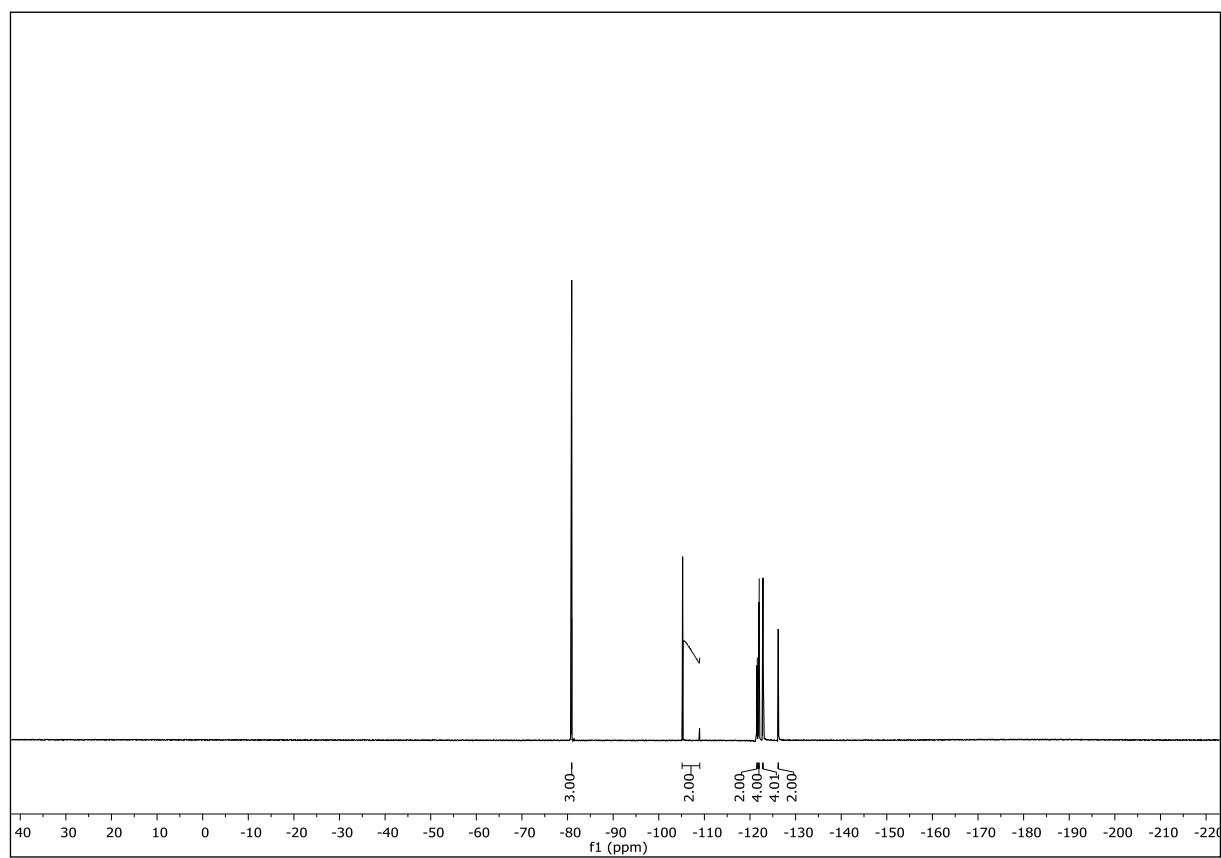




NMR-Solvent: CDCl_3

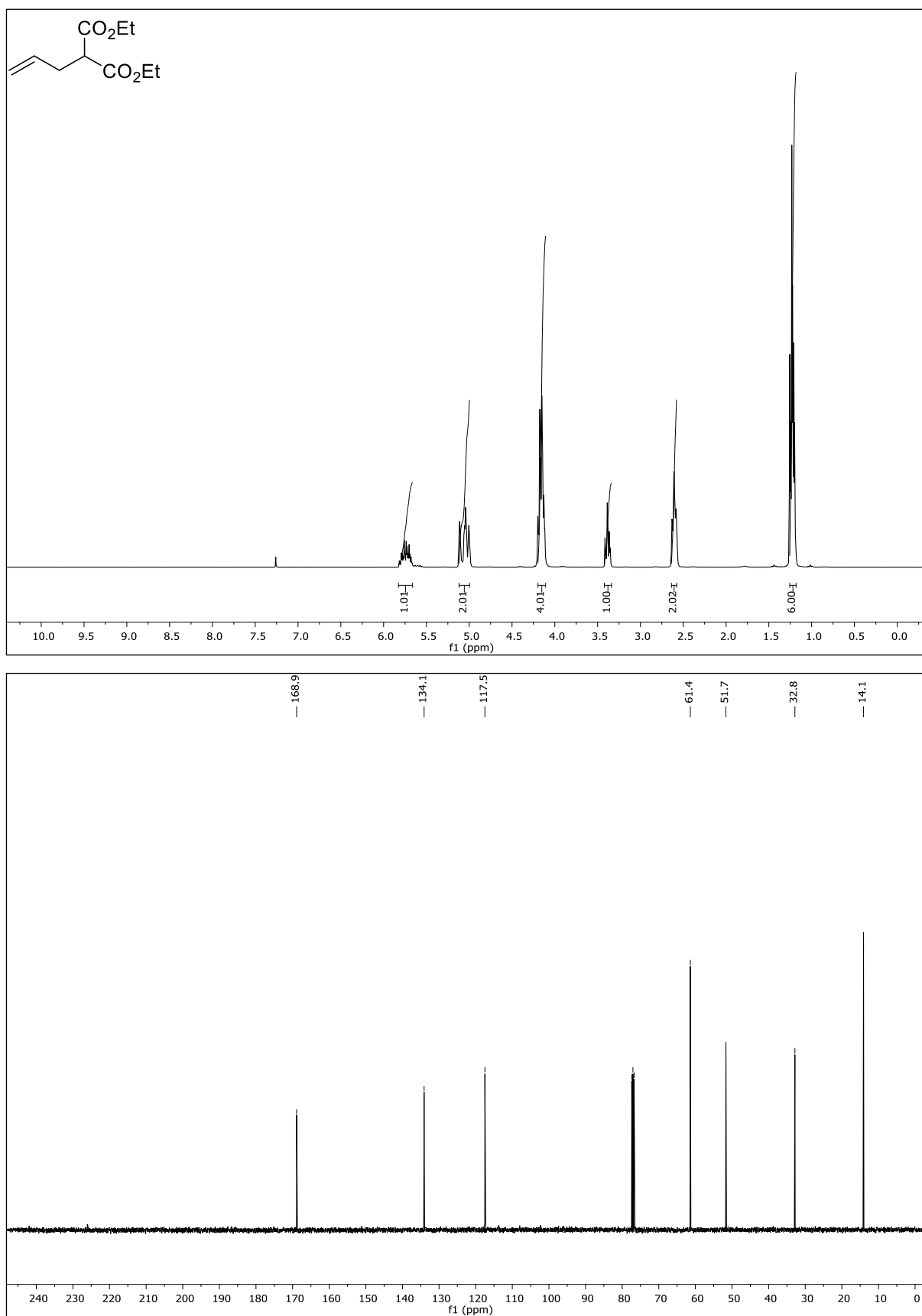
(3,3,4,4,5,5,6,6,7,7,8,8,9,9,10,10,10-Heptadecafluoro-1-iododec-1-en-1-yl)benzene (20i)





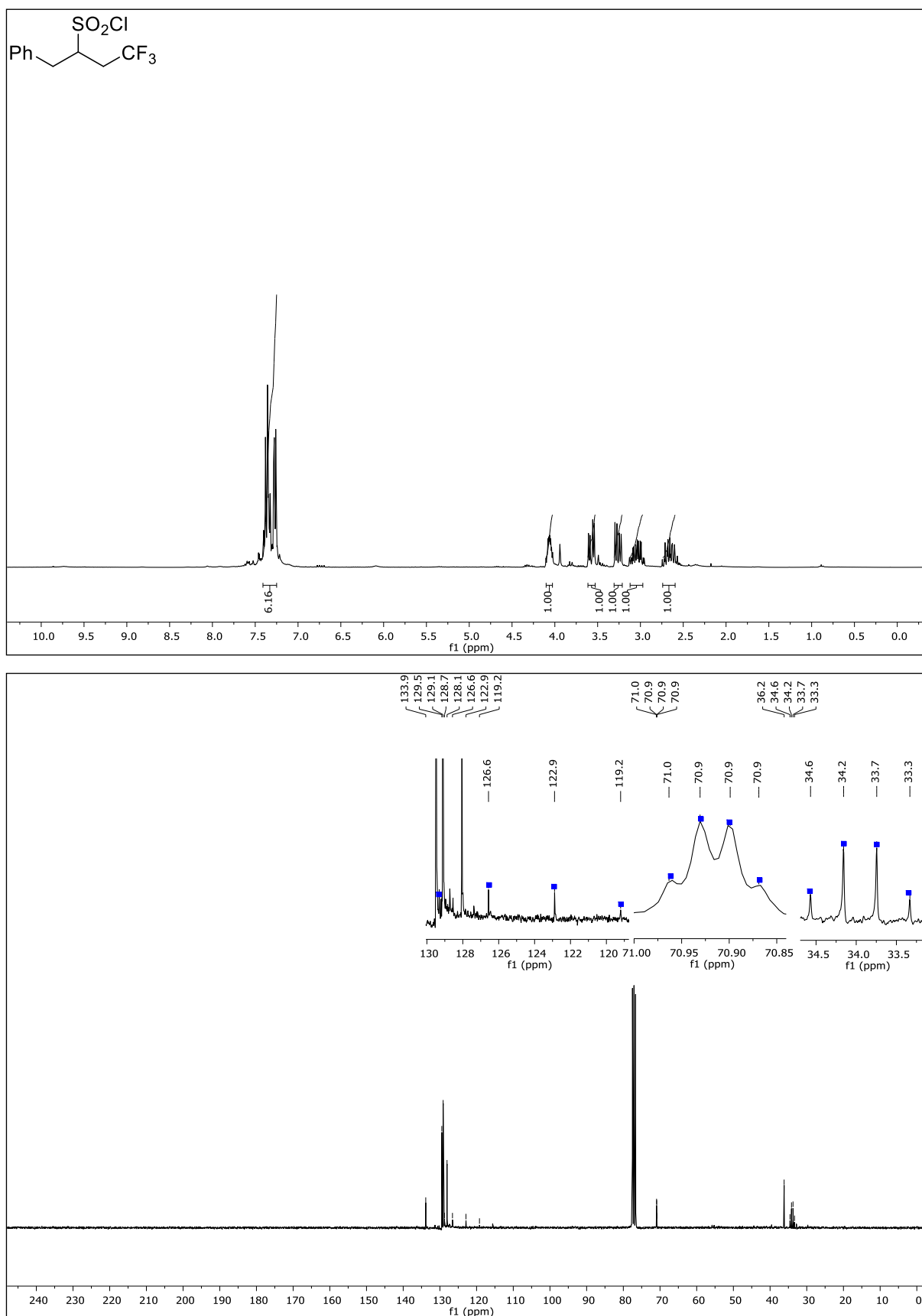
NMR-Solvent: CDCl_3

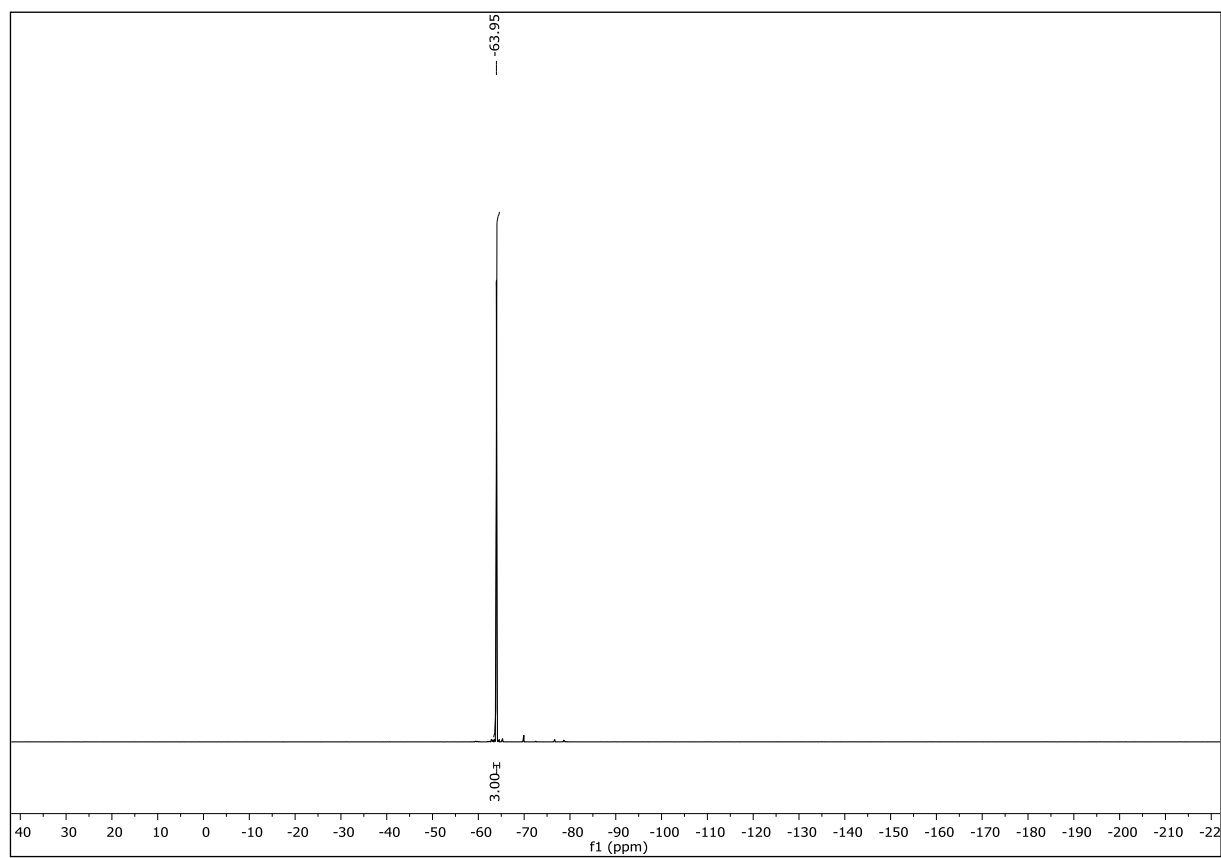
Diethyl 2-allylmalonate (20j)



NMR-Solvent: CDCl₃

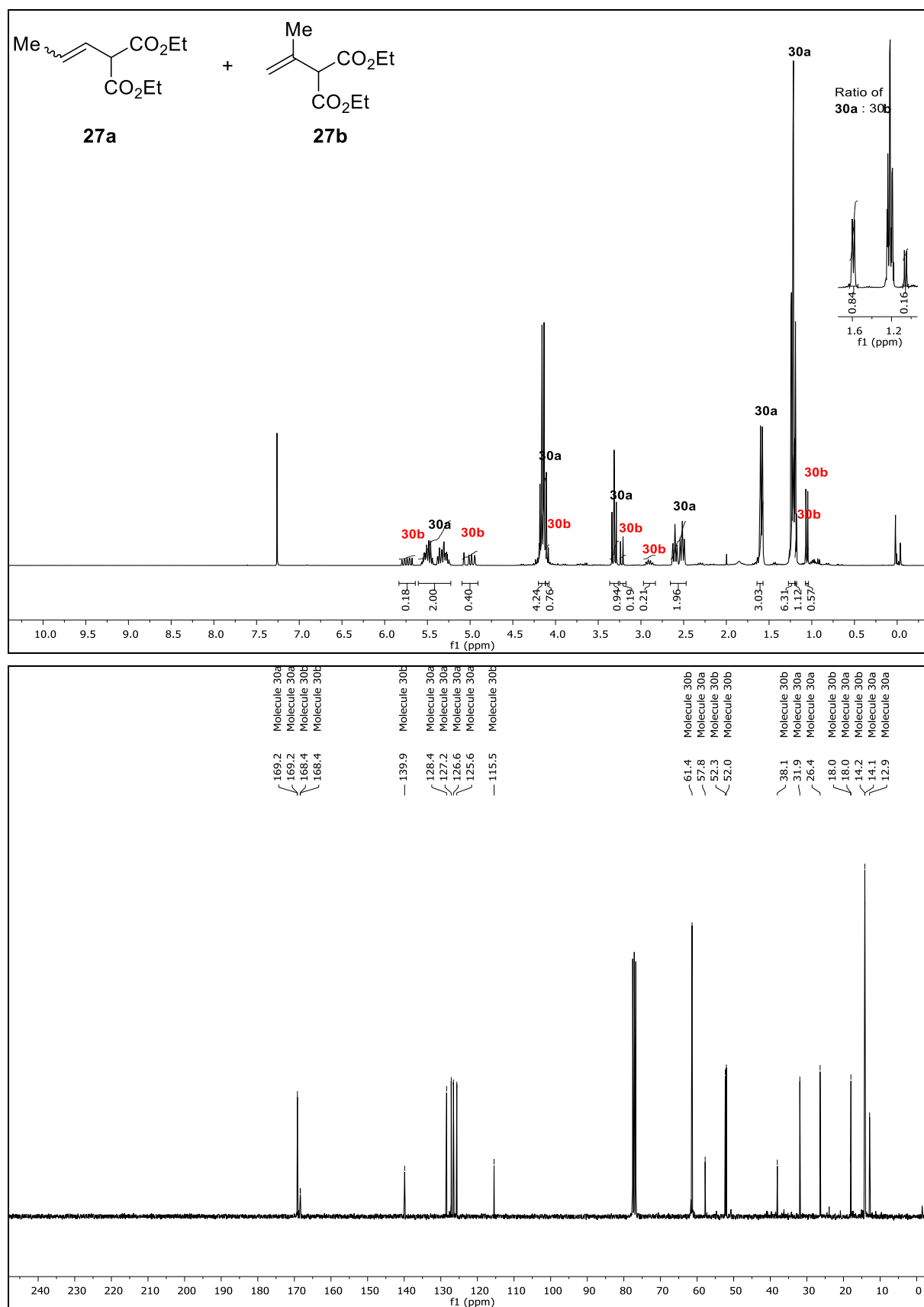
4,4,4-Trifluoro-1-phenylbutane-2-sulfonyl chloride (20k)





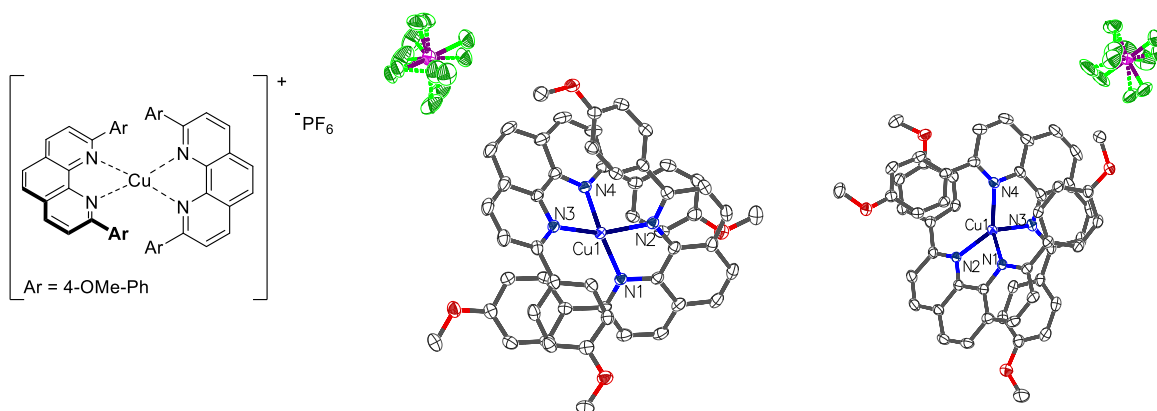
NMR-Solvent: CDCl_3

Diethyl 2-(prop-1-en-1-yl)malonate (30a) and diethyl 2-(prop-1-en-2-yl)malonate (30b)



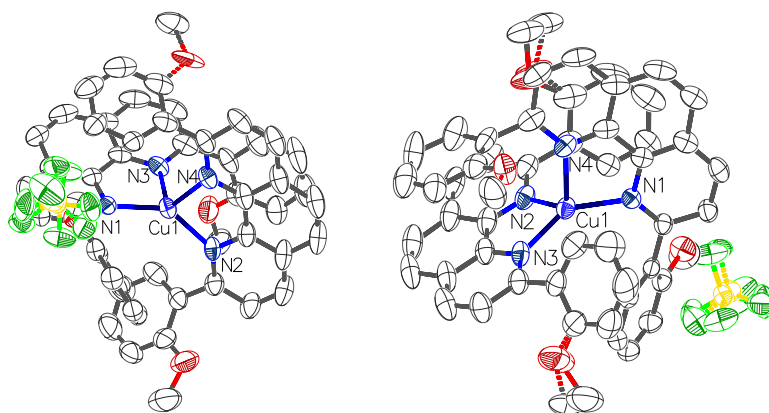
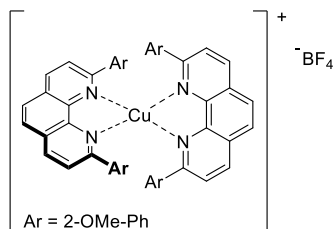
NMR-Solvent: CDCl₃

2.4. X-ray

[Cu(dap)₂]PF₆ (11a-PF₆)

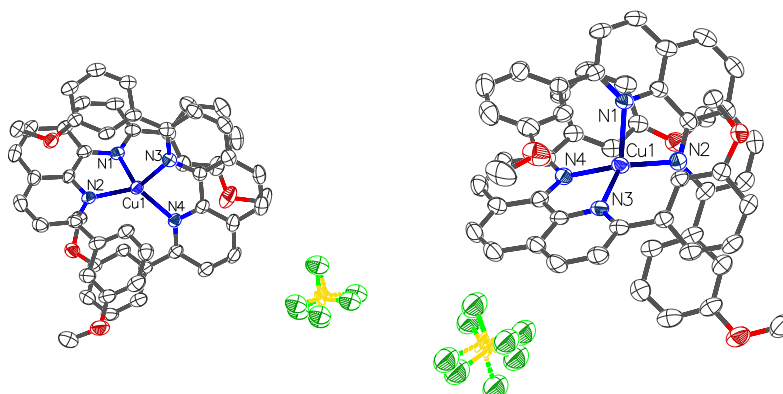
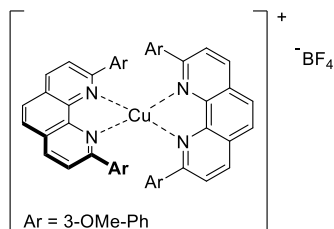
formula	C ₅₂ H ₄₀ CuF ₆ N ₄ O ₄ P
$D_{\text{calc.}}$ / g cm ⁻³	1.520
μ /mm ⁻¹	1.746
formula weight	993.39
colour	dark red
shape	prism
max size/mm	0.29
mid size/mm	0.20
min size/mm	0.12
T /K	123.1(3)
crystal system	triclinic
space group	P-1
$a/\text{\AA}$	13.7826(3)
$b/\text{\AA}$	14.2150(3)
$c/\text{\AA}$	14.2236(3)
$\alpha/^\circ$	100.0320(16)
$\beta/^\circ$	106.6474(18)
$\gamma/^\circ$	118.836(2)
$V/\text{\AA}^3$	2170.80(9)
Z	2
Z'	1
$\theta_{\text{min}}/^\circ$	3.494
$\theta_{\text{max}}/^\circ$	66.807
measured refl.	67964
independent refl.	7652
reflections used	7236
R_{int}	0.0352
parameters	636
restraints	0
largest peak	0.605
deepest hole	-0.440
GooF	1.022
wR_2 (all data)	0.0901
wR_2	0.0889
R_1 (all data)	0.0343
R_1	0.0327

[Cu(o-dap)₂BF₄ (11b-BF₄)



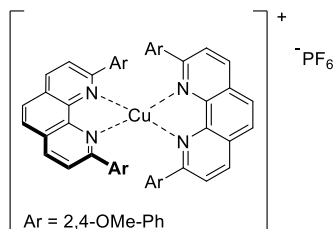
formula	C ₅₂ H ₄₀ BCuF ₄ N ₄ O ₄
$D_{\text{calc.}}/\text{g cm}^{-3}$	1.430
μ/mm^{-1}	1.300
formula weight	935.23
colour	clear colourless
shape	block
max size/mm	0.21
mid size/mm	0.11
min size/mm	0.02
T/K	122.99(17)
crystal system	trigonal
space group	P3 ₂
$a/\text{\AA}$	14.7198(3)
$b/\text{\AA}$	14.7198(3)
$c/\text{\AA}$	17.3594(4)
$\alpha/^\circ$	90
$\beta/^\circ$	90
$\gamma/^\circ$	120
$V/\text{\AA}^3$	3257.37(13)
Z	3
Z'	1
$\theta_{\text{min}}/^\circ$	3.467
$\theta_{\text{max}}/^\circ$	73.627
measured refl.	11342
independent refl.	5891
reflections used	5562
R_{int}	0.0259
parameters	683
restraints	287
largest peak	0.510
deepest hole	-0.296
GooF	1.047
wR_2 (all data)	0.1070
wR_2	0.1047
R_1 (all data)	0.0432
R_1	0.0404

[Cu(*m*-dap)₂]BF₄ (11c-BF₄)

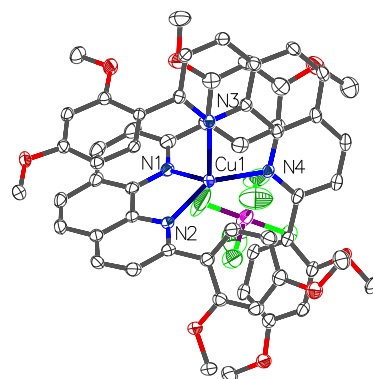
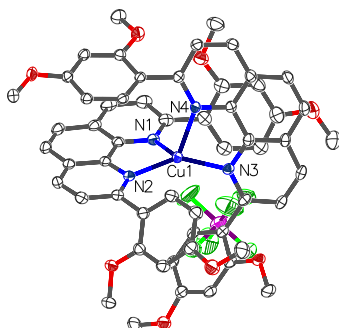


formula	C ₅₂ H ₄₀ BCuF ₄ N ₄ O ₄
<i>D</i> _{calc.} / g cm ⁻³	1.497
<i>μ</i> /mm ⁻¹	2.358
formula weight	1020.15
colour	clear brownish red
shape	plank
max size/mm	0.33
mid size/mm	0.07
min size/mm	0.02
<i>T</i> /K	122.97(13)
crystal system	orthorhombic
space group	P2 ₁ 2 ₁ 2 ₁
<i>a</i> /Å	7.8835(2)
<i>b</i> /Å	23.0294(4)
<i>c</i> /Å	24.9360(6)
<i>α</i> /°	90
<i>β</i> /°	90.000(2)
<i>γ</i> /°	90
<i>V</i> /Å ³	4527.16(19)
<i>Z</i>	4
<i>Z</i> '	1
<i>θ</i> _{min} /°	3.545
<i>θ</i> _{max} /°	73.729
measured refl.	93517
independent refl.	9101
reflections used	7797
<i>R</i> _{int}	0.0704
parameters	625
restraints	0
largest peak	0.611
deepest hole	-0.553
GooF	1.034
<i>wR</i> ₂ (all data)	0.1688
<i>wR</i> ₂	0.1553
<i>R</i> ₁ (all data)	0.0760
<i>R</i> ₁	0.0624

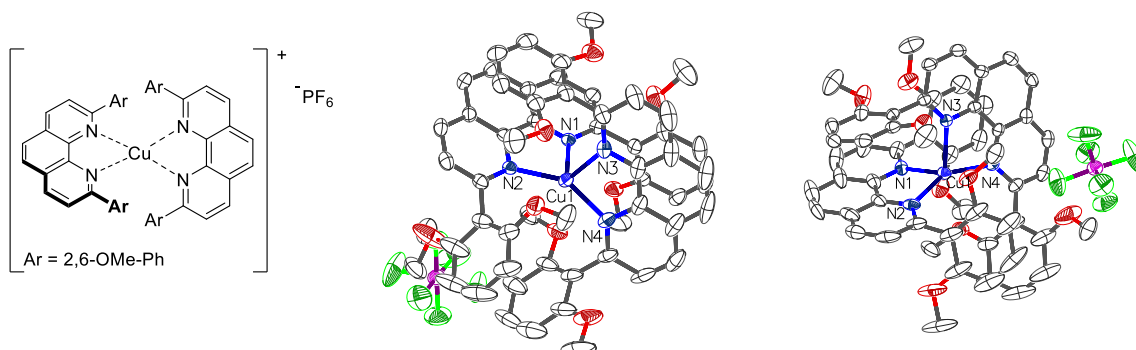
[Cu(o,p-dap)₂PF₆] (11d-PF₆)



⁻PF₆



formula	C ₅₆ H ₄₈ CuF ₆ N ₄ O ₈ P
<i>D</i> _{calc.} / g cm ⁻³	1.551
<i>μ</i> /mm ⁻¹	2.580
formula weight	1198.42
colour	clear intense red
shape	plate
max size/mm	0.11
mid size/mm	0.05
min size/mm	0.03
<i>T</i> /K	122.98(17)
crystal system	monoclinic
space group	P2 ₁ /c
<i>a</i> /Å	14.63723(17)
<i>b</i> /Å	13.87541(17)
<i>c</i> /Å	25.3163(4)
<i>α</i> /°	90
<i>β</i> /°	93.5970(12)
<i>γ</i> /°	90
<i>V</i> /Å ³	5131.55(11)
<i>Z</i>	4
<i>Z</i> '	1
<i>θ</i> _{min} /°	3.025
<i>θ</i> _{max} /°	70.781
measured refl.	28062
independent refl.	9578
reflections used	8101
<i>R</i> _{int}	0.0255
parameters	712
restraints	0
largest peak	1.069
deepest hole	-0.843
GooF	1.019
<i>wR</i> ₂ (all data)	0.1014
<i>wR</i> ₂	0.0946
<i>R</i> ₁ (all data)	0.0473
<i>R</i> ₁	0.0378

[Cu(o,o-dap)₂]PF₆ (11e-PF₆)

formula	C ₅₆ H ₄₈ CuF ₆ N ₄ O ₈ P
$D_{\text{calc.}}/\text{g cm}^{-3}$	1.492
μ/mm^{-1}	1.656
formula weight	1113.49
colour	brownish
shape	n/a
max size/mm	0.36
mid size/mm	0.18
min size/mm	0.01
T/K	122.97(19)
crystal system	monoclinic
space group	P2 ₁ /n
$a/\text{\AA}$	11.63864(13)
$b/\text{\AA}$	25.0255(2)
$c/\text{\AA}$	17.5225(2)
$\alpha/^\circ$	90
$\beta/^\circ$	103.7677(13)
$\gamma/^\circ$	90
$V/\text{\AA}^3$	4957.02(11)
Z	4
Z'	1
$\theta_{\text{min}}/^\circ$	3.140
$\theta_{\text{max}}/^\circ$	73.339
measured refl.	56282
independent refl.	9712
reflections used	8699
R_{int}	0.0288
parameters	696
restraints	0
largest peak	0.713
deepest hole	-0.743
GooF	1.029
wR_2 (all data)	0.1480
wR_2	0.1435
R_1 (all data)	0.0633
R_1	0.0579

3. Chapter C: Photochemical Iodoperfluoroalkylation

3.1. Synthesis of Literature Known Compounds and Reagents

The following compounds were prepared according to literature and spectroscopic data were in accordance with literature:

tert-butyl phenyl(prop-2-yn-1-yl)carbamate (**20a**)^[21], 1-nitro-4-vinylbenzene (**14d**)^[22], diphenyl(4-vinylphenyl)phosphane (**14e**)^[23], (1-cyclopropylvinyl)benzene (**14k**)^[9], (1-(2-methylcyclopropyl)vinyl)benzene (**14l**)^[9], *tert*-butyl allylcarbamate(**16a**)^[8], diethyl 2,2-diallylmalonate (**16d**)^[24], prop-1-yn-1-ylbenzene (**18f**)^[25]

3.2. Preparation of Trifluoromethyl Iodide Stock Solution

Note: CF_3I is a gas and the bottle is under pressure! Compressed gas cylinder should be handled carefully and safety precautions should be met before using! Take time for the preparation and inform your colleagues! Trifluoromethyl iodide is suspected of causing genetic defects. All operations were performed at -78°C . Protect the stock solution from sunlight and store in a refrigerator at -5°C .

Trifluoroiodomethane was condensed into a Schlenk flask (B) cooled at -78°C (F) by opening the valve of the gas cylinder (A) with one turn. The exact amount of the condensed gas was measured by weighting the empty Schlenk flask (B) and the sealed Schlenk flask (B) filled with CF_3I at -78°C (F). Excess of trifluoromethyl iodide was collected by condensation into another Schlenk tubes (C-E) with the aid of cooling traps kept at -78°C (F). The gas valve was closed after obtaining sufficient condensed CF_3I . Then, Schlenk flask (B) was connected to the nitrogen line and MeCN was added dropwise at -78°C (F). During the addition, some precipitate was observed, which dissolved upon warming. The mixture was allowed to warm slowly to room temperature under a gentle stream of nitrogen. Afterwards, the Schlenk flask was placed under N_2 -atmosphere and sealed. The resulting stock solution (2 M) was obtained in quantitative yield, protected from light and stored in a refrigerator at -5°C . The trifluoromethyl iodide stock solution could be stored for extended periods without any sign of decomposition.

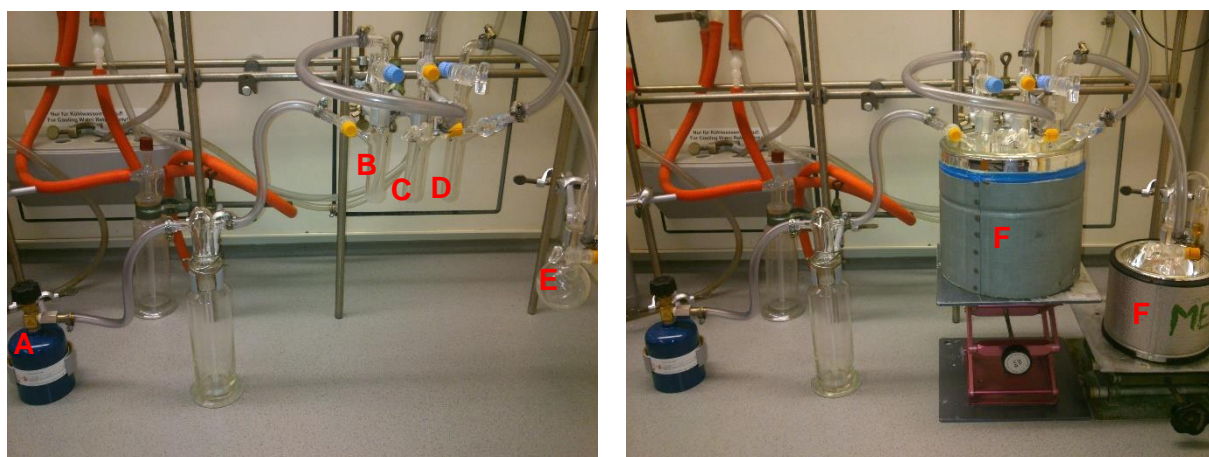
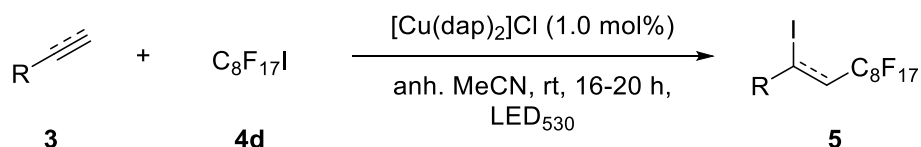


Figure 1. Setup overview.

3.3. Compound Characterization

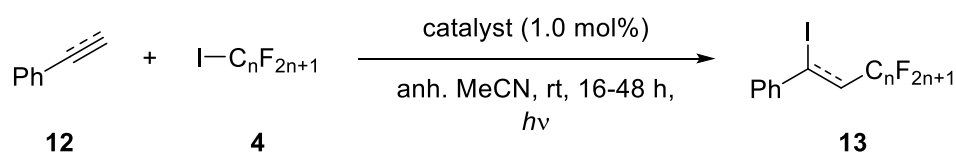
General Procedure for Iodoperfluoroalkylation of Alkenes/Alkynes with [Cu(dap)₂]Cl (GP-A)



A Schlenk tube equipped with a magnetic stir bar was charged with alkene/alkyne **3** (1.0 mmol, 1.0 equiv), perfluorooctyl iodide (**4d**) (530 μL , 2.0 mmol, 2.0 equiv) and [Cu(dap)₂]Cl (8.8 mg, 1.0 μmol , 1.0 mol%) in anh. MeCN (1.0 mL). The reaction mixture was degassed by three freeze-pump-thaw cycles, placed under N₂-atmosphere and irradiated with a green LED (530 nm) at room temperature. After completion of the reaction (judged by TLC), the solvent was evaporated under reduced pressure and the residue was purified by flash column chromatography on silica gel to yield pure product **5**.

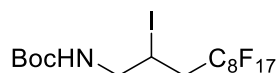
Note: Styrene products are sensitive to heat. Also, slow decomposition is noticeable in solution if oxygen or acid is present (colour change from colourless to purple)! Column chromatography should be performed immediately and the solvent evaporated as soon as possible.

General Procedure for Iodoperfluoroalkylation of Alkenes/Alkynes with Various Photocatalysts (GP-B)



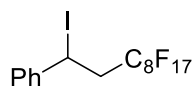
A Schlenk tube equipped with a magnetic stir bar was charged with styrene (**12a**) (104 mg, 1.0 mmol, 1.0 equiv) or phenylacetylene (**12b**) (102 mg, 1.0 mmol, 1.0 equiv), perfluoroalkyl iodides (**4**) (2.0 mmol, 2.0 equiv) and photocatalyst (1.0 μmol , 1.0 mol%) in anh. MeCN (1.0 mL). The reaction mixture was degassed by three freeze-pump-thaw cycles, placed under N₂-atmosphere and irradiated with a green LED (530 nm) for [Cu(dap)₂]Cl or a blue LED (455 nm) for [Ru(bpy)₃]Cl₂ and *fac*-Ir(ppy)₃ at room temperature. After completion of the reaction (judged by TLC), the solvent was evaporated under reduced pressure and the residue was purified by flash column chromatography on silica gel to yield pure product **13**.

***tert*-Butyl (4,4,5,5,6,6,7,7,8,8,9,9,10,10,11,11,11-heptadecafluoro-2-iodoundecyl) carbamate (**11a**)**



Following GP-A, **11a** was prepared using *tert*-butyl allylcarbamate (**16a**) (235 mg, 1.5 mmol, 1.0 equiv), C₈F₁₇I (**4d**) (796 μ L, 3.0 mmol, 2.0 equiv) and [Cu(dap)₂]Cl (8.8 mg, 1.0 μ mol, 1 mol%). Chromatography on silica gel (hexanes) afforded **11a** as a brown solid (891 mg, 85%, rotamere present).

R_f (hexanes-EtOAc, 5:1) = 0.75. **Staining:** KMnO₄ (UV active). **¹H-NMR** (300 MHz, CDCl₃) δ = 5.11 (d, *J* = 5.5 Hz, 1H), 4.30 (p, *J* = 6.5 Hz, 1H), 3.60 – 3.28 (m, 2H), 2.92 – 2.59 (m, 2H), 1.37 (s, 9H). **¹⁹F-NMR** (282 MHz, CDCl₃) δ = -81.83 (t, *J* = 10.0 Hz, 3F), -113.33 – -115.67 (m, 2F), -122.15 – -122.63 (m, 2F), -122.77 (s, 4F), -123.62 (s, 2F), -124.42 (s, 2F), -126.94 – -127.22 (m, 2F). **¹³C-NMR** (75 MHz, CDCl₃) δ = 155.7, 125.1 – 100.9 (m), 80.1, 48.9, 38.5 (t, *J* = 21.2 Hz), 28.1, 18.4. **IR** (neat, cm⁻¹): 3370, 2986, 2941, 1733, 1685, 1603, 1521, 1454, 1394, 1372, 1334, 1275, 1197, 1144, 1088, 992, 857, 783, 738. **HRMS** (ESI) exact mass calc. for C₁₆H₁₅F₁₇INNaO₂: *m/z* 725.9773, found: *m/z* 725.9768 [M+Na]⁺. **mp**: 64 °C.

(3,3,4,4,5,5,6,6,7,7,8,8,9,9,10,10,10-Heptadecafluoro-1-iododecyl)benzene (11c)

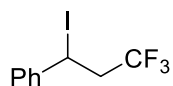
Following GP-A, **11c** was prepared using styrene (**12a**) (104 mg, 1.0 mmol, 1.0 equiv), C₈F₁₇I (**4d**) (530 μ L, 2.0 mmol, 2.0 equiv) and [Cu(dap)₂]Cl (8.8 mg, 1.0 μ mol, 1.0 mol%). Chromatography on silica (hexanes) afforded **11c** as a white solid (546 mg, 84%).

Following GP-B, **11c** was prepared using styrene (**12a**) (104 mg, 1.0 mmol, 1.0 equiv), C₈F₁₇I (**4d**) (530 μ L, 2.0 mmol, 2.0 equiv) and photocatalyst (1.0 μ mol, 1.0 mol%). Chromatography on silica (hexanes) afforded **11c** as a white solid (Table 1).

Table 1: Comparison of photocatalyst for the visible light mediated iodoperfluorooctylation between styrene (**12a**) and C₈F₁₇I (**4d**).

Entry	Catalyst	Isolated Mass [mg]	Yield [%]
1	[Cu(dap) ₂]Cl	546	84
2	[Ru(bpy) ₃]Cl ₂	68	10
3	fac-Ir(ppy) ₃	107	16

R_f (hexanes) = 0.51. **Staining:** KMnO₄ (UV active). **¹H-NMR** (400 MHz, CDCl₃) δ = 7.45 – 7.41 (m, 2H), 7.35 – 7.25 (m, 3H), 5.45 (dd, J = 9.6, 5.2 Hz, 1H), 3.36 – 3.10 (m, 2H). **¹⁹F-NMR** (376 MHz, CDCl₃) δ = -81.30 (t, J = 10.1 Hz, 3F), -112.48 – -115.56 (m, 2F), -122.27 (d, J = 121.2 Hz, 6F), -123.24 (s, 2F), -124.02 (s, 2F), -126.63 (s, 2F). **¹³C-NMR** (101 MHz, CDCl₃) δ = 142.7, 128.9, 128.6, 126.7, 118.6 – 103.5 (m), 42.5 (t, J = 20.5 Hz), 16.5 (t, J = 2.5 Hz). **IR** (neat, cm⁻¹): 3025, 1495, 1457, 1372, 1293, 1238, 1200, 1144, 962, 872, 831, 742, 693. **LRMS** (EI) m/z (%): 523.1 ([M-I]⁺, 63), 177.1 (90), 153.1 (85), 109.1 (90), 104.1 (100), 91.1 (30). **HRMS** (EI) exact mass calc. for C₁₆H₇F₁₇I: m/z 648.9312, found: m/z 648.9315 [M-H]⁺. **mp:** 69 °C.

(3,3,3-Trifluoro-1-iodopropyl)benzene (13a)

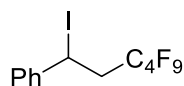
Following GP-A, **13a** was prepared using styrene (**12a**) (104 mg, 1.0 mmol, 1.0 equiv), CF₃I (**4a**) (1.0 mL, 2.0 mmol, 2.0 equiv, 2 M MeCN) and [Cu(dap)₂]Cl (8.8 mg, 1.0 μmol, 1.0 mol%). Chromatography on silica (hexanes) afforded **13a** as a white solid (135 mg, 45%).

Following GP-B, **13a** was prepared using styrene (**12a**) (104 mg, 1.0 mmol, 1.0 equiv), CF₃I (**4a**) (1.0 mL, 2.0 mmol, 2.0 equiv, 2 M MeCN) and photocatalyst (1.0 μmol, 1.0 mol%). Chromatography on silica (hexanes) afforded **13a** as a white solid (Table 2).

Table 2: Comparison of photocatalyst for the visible light mediated iodotrifluoromethylation between styrene (**12a**) and CF₃I (**4a**).

Entry	Catalyst	Isolated Mass [mg]	Yield [%]
1	[Cu(dap) ₂]Cl	135	45
2	[Ru(bpy) ₃]Cl ₂	5	2
3	<i>fac</i> -Ir(ppy) ₃	10	3

R_f (hexanes) = 0.52. **Staining:** KMnO₄ (UV active). **¹H-NMR** (300 MHz, CDCl₃) δ = 7.45 – 7.40 (m, 2H), 7.37 – 7.25 (m, 3H), 5.33 (dd, *J* = 9.0, 6.1 Hz, 1H), 3.33 – 3.14 (m, 2H). **¹⁹F-NMR** (282 MHz, CDCl₃) δ = -64.91 (s, 3F). **¹³C-NMR** (75 MHz, CDCl₃) δ = 142.4, 129.0, 128.7, 127.1 – 126.9 (m), 125.0 (q, *J* = 279.5 Hz), 45.8 (q, *J* = 28.4 Hz), 17.8 (q, *J* = 3.2 Hz). **IR** (neat, cm⁻¹): 3068, 3034, 1703, 1599, 1495, 1454, 1372, 1349, 1245, 1126, 1100, 1074, 929, 835, 760, 693. **HRMS** (EI) exact mass calc. for C₉H₈F₃: *m/z* 173.0573, found: *m/z* 173.0573 [M-I]⁺. **mp:** 29 °C.

(3,3,4,4,5,5,6,6,6-Nonafluoro-1-iodohexyl)benzene (13b)

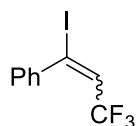
Following GP-A, **13b** was prepared using styrene (**12a**) (104 mg, 1.0 mmol, 1.0 equiv), C₄F₉I (**4b**) (346 μ L, 2.0 mmol, 2.0 equiv) and [Cu(dap)₂]Cl (8.8 mg, 1.0 μ mol, 1.0 mol%). Chromatography on silica (hexanes) afforded **13b** as a white solid (342 mg, 76%).

Following GP-B, **13b** was prepared using styrene (**12a**) (104 mg, 1.0 mmol, 1.0 equiv), C₄F₉I (**4b**) (346 μ L, 2.0 mmol, 2.0 equiv) and photocatalyst (1.0 μ mol, 1.0 mol%). Chromatography on silica (hexanes) afforded **13b** as a white solid (Table 3).

Table 3: Comparison of photocatalyst for the visible light mediated iodoperfluorobutylation between styrene (**12a**) and C₄F₉I (**4b**).

Entry	Catalyst	Isolated Mass [mg]	Yield [%]
1	[Cu(dap) ₂]Cl	342	76
2	[Ru(bpy) ₃]Cl ₂	68	15
3	<i>fac</i> -Ir(ppy) ₃	96	21

R_f (hexanes) = 0.50. **Staining:** KMnO₄ (UV active). **¹H-NMR** (300 MHz, CDCl₃) δ = 7.45 – 7.27 (m, 5H), 5.44 (dd, *J* = 9.6, 5.3 Hz, 1H), 3.40 – 3.06 (m, 2H). **¹⁹F-NMR** (282 MHz, CDCl₃) δ = -81.52 (tt, *J* = 9.9, 3.3 Hz, 3F), -112.58 – -115.96 (m, 2F), -124.98 (dtd, *J* = 15.6, 9.7, 8.7, 4.0 Hz, 2F), -126.44 (tp, *J* = 13.6, 5.2, 4.7 Hz, 2F). **¹³C-NMR** (75 MHz, CDCl₃) δ = 142.9, 129.1, 128.7, 126.9, 42.8, 42.5, 42.2, 16.7. **IR** (neat, cm⁻¹): 3065, 1638, 1489, 1445, 1350, 1223, 1130, 1109, 1028, 920, 887, 860, 762, 741, 692, 667, 650, 590, 528. **HRMS** (EI) exact mass calc. for C₁₂H₈F₉: *m/z* 323.0482, found: *m/z* 323.0480 [M-I]⁺. **mp**: 43 °C.

(3,3,3-Trifluoro-1-iodoprop-1-en-1-yl)benzene (13c)

Following GP-A, **13c** was prepared using phenylacetylene (**12b**) (102 mg, 1.0 mmol), CF₃I (**4a**) (1.0 mL, 2.0 mmol, 2.0 equiv, 2 M MeCN) and [Cu(dap)₂]Cl (8.8 mg, 1.0 μmol, 1.0 mol%). Chromatography on silica (hexanes) afforded **13c** as a white solid (205 mg, 69%) in a diastereomeric ratio of *E/Z* = 92:08.

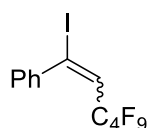
Following GP-B, **13c** was prepared using phenylacetylene (**12b**) (102 mg, 1.0 mmol), CF₃I (**4a**) (1.0 mL, 2.0 mmol, 2.0 equiv, 2 M MeCN) and photocatalyst (1.0 μmol, 1.0 mol%). Chromatography on silica (hexanes) afforded **13c** as a white solid (Table 4).

Table 4: Comparison of photocatalyst for the visible light mediated iodotrifluoromethylation between phenylacetylene (**12b**) and CF₃I (**4a**).^[a]

Entry	Catalyst	<i>E/Z</i> -Ratio	Isolated Mass [mg]	Yield [%]
1	[Cu(dap) ₂]Cl	92:08	205	69
2	[Ru(bpy) ₃]Cl ₂	90:10	43	14
3	<i>fac</i> -Ir(ppy) ₃	91:09	68	23

[a] *E/Z*-ratio determined by ¹H-NMR.

R_f (hexanes) = 0.58. **Staining:** KMnO₄ (UV active). **¹H-NMR** (400 MHz, CDCl₃) δ = 7.41 – 7.29 (m, 5H), 6.66 (q, *J* = 7.3 Hz, 1H). **¹⁹F-NMR** (376 MHz, CDCl₃) δ = -57.67 (s, 3F). **¹³C-NMR** (101 MHz, CDCl₃) δ = 140.8, 132.2, 129.5, 128.2, 127.3 (q, *J* = 1.7 Hz), 121.3 (d, *J* = 273.9 Hz), 111.2 (q, *J* = 6.3 Hz). **IR** (neat, cm⁻¹): 3064, 2926, 1759, 1640, 1491, 1446, 1346, 1264, 1174, 1118, 924, 805, 764, 723, 693. **LRMS** (EI) *m/z* (%): 171.0 ([M-I]⁺, 100), 151.1 ([M-I, -HF]⁺, 87), 102.1 (40), 76.1 (14), 298.0 (11), 50.1 (7), 279.1 ([M-F, 3]). **HRMS** (EI) exact mass calc. for C₉H₆F₃I: *m/z* 297.9461, found: *m/z* 297.9449 [M-H]⁺. **mp**: 31 °C.

(3,3,4,4,5,5,6,6,6-Nonafluoro-1-iodohex-1-en-1-yl)benzene (13d)

Following GP-A, **13d** was prepared using phenylacetylene (**12b**) (102 mg, 1.0 mmol, 1.0 equiv), C₄F₉I (**4b**) (346 μ L, 1.0 mmol, 2.0 equiv) and [Cu(dap)₂]Cl (8.8 mg, 1.0 μ mol, 1.0 mol%). Chromatography on silica (hexanes) afforded **13d** as a yellowish oil (408 mg, 91%) in a diastereomeric ratio of *E/Z* = 82:18.

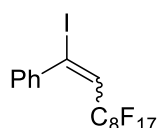
Following GP-B, **13d** was prepared using phenylacetylene (**12b**) (102 mg, 1.0 mmol, 1.0 equiv), C₄F₉I (**4b**) (346 μ L, 1.0 mmol, 2.0 equiv) and photocatalyst (1.0 μ mol, 1.0 mol%). Chromatography on silica (hexanes) afforded **13d** as a yellowish oil (Table 5).

Table 5: Comparison of photocatalyst for the visible light mediated iodotrifluoromethylation between phenylacetylene (**12b**) and C₄F₉I (**4b**).^[a]

Entry	Catalyst	<i>E/Z</i> -Ratio	Isolated Mass [mg]	Yield [%]
1	[Cu(dap) ₂]Cl	82:18	408	91
2	[Ru(bpy) ₃]Cl ₂	81:19	190	42
3	<i>fac</i> -Ir(ppy) ₃	82:18	188	42

[a] *E/Z*-ratio determined by ¹H-NMR.

R_f (hexanes) = 0.60. **Staining:** KMnO₄ (UV active). **¹H-NMR** (300 MHz, CDCl₃) δ = 7.53 – 7.34 (m, 5H), 6.66 (t, *J* = 13.4 Hz, 1H). **¹⁹F-NMR** (282 MHz, CDCl₃) δ = -81.56 – -81.81 (m, 3F), -105.23 – -109.93 (m, 2F), -124.40 (q, *J* = 9.4, 8.4 Hz, 2F), -126.27 – -126.57 (m, 2F). **¹³C-NMR** (75 MHz, CDCl₃) δ = 141.4, 130.2, 129.3, 128.0, 128.8 – 126.5 (m), 124.0 (t, *J* = 23.7 Hz), 124.7 – 106.0 (m). **IR** (neat, cm⁻¹): 3064, 1636, 1353, 1223, 1133, 1029, 924, 887, 700. **LRMS** (EI) *m/z* (%): 321.0 ([M-I]⁺, 100), 102.1 (42), 182.1 (40), 151.1 (33), 133.1 (17), 76.1 (8), 448.0 (3). **HRMS** (EI) exact mass calc. for C₁₂H₆F₉I: *m/z* 447.9352, found: *m/z* 447.9360 [M-H]⁺.

(3,3,4,4,5,5,6,6,7,7,8,8,9,9,10,10,10-Heptadecafluoro-1-iododec-1-en-1-yl)benzene (13e)

Following GP-A, **13e** was prepared using phenylacetylene (**12b**) (102 mg, 1.0 mmol), C₈F₁₇I (**4d**) (530 μ L, 1.0 mmol, 2.0 equiv) and [Cu(dap)₂]Cl (8.8 mg, 1.0 μ mol, 1.0 mol%). Chromatography on silica (hexanes) afforded **13e** as a white solid (577 mg, 89%) in a diastereomeric ratio of *E/Z* = 92:08.

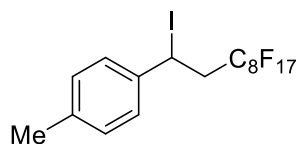
Following GP-B, **13e** was prepared using phenylacetylene (**12b**) (102 mg, 1.0 mmol), C₈F₁₇I (**4d**) (530 μ L, 1.0 mmol, 2.0 equiv) and photocatalyst (1.0 μ mol, 1.0 mol%). Chromatography on silica (hexanes) afforded **13e** as a white solid (Table 6).

Table 6: Comparison of photocatalyst for the visible light mediated iodotrifluoromethylation between phenylacetylene (**12b**) and C₈F₁₇I (**4d**).^[a]

Entry	Catalyst	<i>E/Z</i> -Ratio	Isolated Mass [mg]	Yield [%]
1	[Cu(dap) ₂]Cl	92:08	577	89
2	[Ru(bpy) ₃]Cl ₂	95:05	295	46
3	<i>fac</i> -Ir(ppy) ₃	91:09	259	55

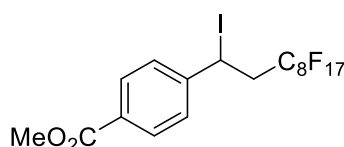
[a] *E/Z*-ratio determined by ¹H-NMR.

R_f (hexanes) = 0.74. **Staining:** vanilin (UV active). **¹H-NMR** (400 MHz, CDCl₃) δ = 7.45 – 7.27 (m, 5H), 6.61 (t, *J* = 13.5 Hz, 1H). **¹⁹F-NMR** (376 MHz, CDCl₃) δ = -80.91 (t, *J* = 10.1 Hz, 3F), -105.12 – -109.00 (m, 2F), -121.48 – -121.61 (m, 2F), -121.96 (t, *J* = 19.4 Hz, 4F), -122.83 (dt, *J* = 17.4, 7.6 Hz, 4F), -126.20 (ddd, *J* = 18.7, 9.3, 4.1 Hz, 2F). **¹³C-NMR** (101 MHz, CDCl₃) δ = 141.5, 129.4, 128.7, 128.2, 127.12 – 126.88 (m), 117.8 - 107.0 (m). **IR** (neat, cm⁻¹): 3065, 2926, 1640, 1352, 1220, 1138, 1031, 920, 890, 701. **HRMS** (EI) exact mass calc. for C₁₆H₅F₁₆I: *m/z* 628.9253, found: *m/z* 628.9237 [M-F]⁺. **mp**: 60 °C.

1-(3,3,4,4,5,5,6,6,7,7,8,8,9,9,10,10,10-Heptafluoro-1-iododecyl)-4-methylbenzene (15a)


Following GP-A, **15a** was prepared using 1-methyl-4-vinylbenzene (**14a**) (132 μ L, 1.0 mmol, 1.0 equiv), $C_8F_{17}I$ (**4d**) (530 μ L, 2.0 mmol, 2.0 equiv) and $[Cu(dap)_2]Cl$ (8.8 mg, 1.0 μ mol, 1.0 mol%). Chromatography on silica (hexanes) afforded **15a** as a white solid (219 mg, 33%).

R_f (hexanes) = 0.58. **Staining:** $KMnO_4$ (UV active). **1H -NMR** (300 MHz, $CDCl_3$) δ = 7.37 – 7.31 (m, 2H), 7.17 – 7.12 (m, 2H), 5.48 (dd, J = 9.7, 5.2 Hz, 1H), 3.44 – 3.07 (m, 2H), 2.33 (s, 3H). **^{19}F -NMR** (282 MHz, $CDCl_3$) δ = -81.29 (t, J = 9.7 Hz, 3F), -111.36 – -115.83 (m, 2F), -121.98 – -122.30 (s, 2F), -122.45 (s, 4F), -123.29 (s, 2F), -123.61 – -124.31 (m, 2F), -126.65 (s, 2F). **^{13}C -NMR** (75 MHz, $CDCl_3$) δ = 139.8, 129.6, 126.8 – 126.4 (m), 129.5, 127.7 – 126.6 (m), 126.6, 42.5 (t, J = 20.9 Hz), 21.2, 17.2 (t, J = 3.5 Hz). **IR** (neat, cm^{-1}): 3000, 2933, 1590, 1381, 1200, 804. **LRMS** (EI) m/z (%): 537.3 ($[M-I]^+$, 100), 118.2 ($[M-I-C_8F_{17}]^+$, 95), 123.1 (56), 147.1 (17), 91.1 (17), 69.1 (12), 231.0 (4). **HRMS** (EI) exact mass calc. for $C_{17}H_9F_{17}$: m/z 536.0427, found: m/z 536.0417 $[M-HI]^+$. **mp**: 31 $^{\circ}C$.

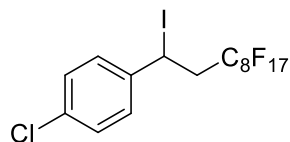
Methyl-4-(3,3,4,4,5,5,6,6,7,7,8,8,9,9,10,10,10-heptafluoro-1-iododecyl)benzoate (15b)


Following GP-A, **15b** was prepared using methyl 4-vinylbenzoate (**14b**) (162 mg, 1.0 mmol, 1.0 equiv), $C_8F_{17}I$ (**4d**) (530 μ L, 2.0 mmol, 2.0 equiv) and $[Cu(dap)_2]Cl$ (8.8 mg, 1.0 μ mol, 1.0 mol%). Chromatography on silica (hexanes) afforded **15b** as a colourless oil (416 mg, 59%).

R_f (hexanes-EtOAc, 5:1) = 0.50. **Staining:** vanilin (UV active). **1H -NMR** (400 MHz, $CDCl_3$) δ = 8.03 – 7.93 (m, 2H), 7.40 – 7.30 (m, 2H), 5.42 – 5.23 (m, 1H), 4.45 (dddd, J = 13.1, 8.4, 5.6 Hz, 1H), 3.91 (dd, J = 2.9, 1.5 Hz, 3H), 2.68 – 2.35 (m, 1H). **^{19}F -NMR** (376 MHz, $CDCl_3$) δ = -81.34 (t, J = 10.0 Hz, 3F), -111.54 – -113.82 (m, 2F), -122.07 (s, 2F), -122.43 (s, 4F), -123.24 (s, 2F), -123.87 (s, 2F), -126.65 (t, J = 13.6 Hz, 2F). **^{13}C -NMR** (101 MHz, $CDCl_3$) δ = 145.0, 143.4, 130.0 (d, J = 2.0 Hz), 127.9, 126.6 (d, J = 3.6 Hz), 52.2, 35.7 (t, J = 21.2 Hz), 25.6. **IR** (neat, cm^{-1}): 3001, 2956, 1722, 1610, 1577, 1510, 1439, 1282, 1238, 1200, 1148,

1111, 1021, 910, 857, 772, 705. **HRMS** (EI) exact mass calc. for $C_{18}H_{11}F_{17}O_2$: m/z 582.0482, found: m/z 582.0473 $[M+H-I]^+$.

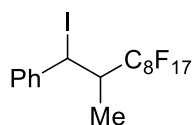
1-Chloro-4-(3,3,4,4,5,5,6,7,7,8,8,9,9,10,10,10-heptafluoro-1-iododecyl)benzene (15c)



Following GP-A, **15c** was prepared using 1-chloro-4-vinylbenzene (**14c**) (120 μ L, 1.0 mmol, 1.0 equiv), $C_8F_{17}I$ (**4d**) (530 μ L, 2.0 mmol, 2.0 equiv) and $[Cu(dap)_2]Cl$ (8.8 mg, 1.0 μ mol, 1.0 mol%). Chromatography on silica (hexanes) afforded **15c** as a white solid (539 mg, 79%).

R_f (hexanes) = 0.53. **Staining**: $KMnO_4$ (UV active). **1H -NMR** (300 MHz, $CDCl_3$) δ = 7.43 – 7.24 (m, 5H), 5.41 (dd, J = 9.9, 5.1 Hz, 1H), 3.38 – 3.03 (m, 2H). **^{19}F -NMR** (282 MHz, $CDCl_3$) δ = -81.5 (t, J = 10.0 Hz, 3F), -111.9 – -116.6 (m, 2F), -122.3 (m, 2F), -122.6 (m, 4F), -123.4 (m, 2F), -124.1 (m, 2F), -126.8 (m, 2F). **^{13}C -NMR** (75 MHz, $CDCl_3$) δ = 141.4, 134.4, 129.3, 125.8 – 96.9 (m), 42.7 (t, J = 20.5 Hz), 15.3. **IR** (neat, cm^{-1}): 1595, 1493, 1343, 1414, 1369, 1354, 1331, 1234, 1198, 1144, 1115, 1092, 1034, 1013, 962, 954, 920, 831, 777, 476, 706, 660, 638, 625, 596, 575, 557, 527, 461, 419, 405. **LRMS** (EI) m/z (%): 557.1 ($[M-I]^+$, 100), 138.0 (48), 143.1 (34), 559.3 (28), 187.1 (24), 558.3 (18), 140.1 (14), 103.1 (13), 145.1 (11), 133.1 (9), 126.9 (5), 153.1 (5), 144.1 (3), 76.2 (2), 684.8 (2). **HRMS** (EI) exact mass calc. for $C_{16}H_6ClF_{17}I$: m/z 682.8926, found: m/z 682.8929 $[M-H]^+$. **mp**: 39 $^{\circ}C$.

(3,3,4,4,5,5,6,7,7,8,8,9,9,10,10,10-Heptafluoro-1-iodo-2-methyldecyl)benzene (15e)

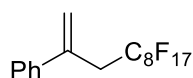


Following GP-A, **15e** was prepared using *trans*- β -methylstyrene (**14f**) (118 mg, 1.0 mmol, 1.0 equiv), $C_8F_{17}I$ (**4d**) (530 μ L, 2.0 mmol, 2.0 equiv) and $[Cu(dap)_2]Cl$ (8.8 mg, 1.0 μ mol, 1.0 mol%). Chromatography on silica (hexanes) afforded **15e** as a white solid (509 mg, 77%) in a diastereomeric mixture of *cis/trans* = 47:53.

R_f (hexanes) = 0.49. **Staining**: $KMnO_4$ (UV active). **1H -NMR** (400 MHz, $CDCl_3$) δ = 7.48 – 7.25 (m, 10H), 5.78 (d, J = 3.6 Hz, 1H), 5.56 (d, J = 3.9 Hz, 1H), 3.20 – 2.98 (m, 1H), 2.50 – 2.35 (m, 1H), 1.50 (d, J = 6.8 Hz, 3H), 1.43 (d, J = 6.7 Hz, 3H). **^{19}F -NMR** (376 MHz, $CDCl_3$) δ = -80.82 (t, J = 9.9 Hz, 3F), -111.64 – -118.30 (m, 1F), -119.93 – -120.75 (m, 2F), -121.70

(d, $J = 132.9$ Hz, 6F), -122.71 (s, 2F), -125.93 – -126.29 (m, 2F). **^{13}C -NMR** (101 MHz, CDCl_3) $\delta = 141.9, 139.4, 129.4, 128.6, 128.5, 128.4, 128.2, 128.1, 46.5, 46.3, 46.1, 43.4, 43.2, 43.0, 29.5$. **IR** (neat, cm^{-1}): 3030, 1491, 1394, 1372, 1327, 1200, 1147, 1033, 962, 865, 805, 738; **LRMS** (EI) m/z (%): 537.0 ($[\text{M}-\text{I}]^+$, 68), 167.1 (16), 118.0 (20), 91.0 (100). **HRMS** (FD) exact mass calc. for $\text{C}_{17}\text{H}_{10}\text{F}_{17}$: m/z 663.9550, found: m/z 663.9563 $[\text{M}]^+$. **mp**: 33 °C.

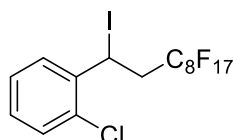
(4,4,5,5,6,6,7,7,8,8,9,9,10,10,11,11,11-Heptadecafluoroundec-1-en-2-yl) benzene (15f)



Following GP-A, **15f** was prepared using α -methylstyrene (**14g**) (118 mg, 1.0 mmol, 1.0 equiv), $\text{C}_8\text{F}_{17}\text{I}$ (**4d**) (530 μL , 2.0 mmol, 2.0 equiv) and $[\text{Cu}(\text{dap})_2]\text{Cl}$ (8.8 mg, 1.0 μmol , 1.0 mol%). Chromatography on silica (hexanes) afforded **15f** as a white solid (214 mg, 40%).

R_f (hexanes) = 0.39. **Staining**: KMnO_4 (UV active). **^1H -NMR** (400 MHz, CDCl_3) $\delta = 7.42 - 7.30$ (m, 5H), 5.65 (s, 1H), 5.38 (s, 1H), 3.29 (t, $J = 18.6$ Hz, 2H). **^{19}F -NMR** (376 MHz, CDCl_3) $\delta = -81.36$ (t, $J = 10.0$ Hz), -112.88 (t, $J = 14.5$ Hz), -122.13, -122.28 – -122.64 (m), -123.26, -123.57 (d, $J = 16.1$ Hz), -125.46 – -127.77 (m). **^{13}C -NMR** (101 MHz, CDCl_3) $\delta = 140.5, 137.2, 128.6, 128.1, 126.2, 120.7, 36.4$ (t, $J = 22.1$ Hz). **IR** (neat, cm^{-1}): 3099, 3078, 3023, 3000, 2911, 1632, 1491, 1353, 1200, 1144, 921, 805, 734. **HRMS** (EI) exact mass calc. for $\text{C}_{17}\text{H}_9\text{F}_{17}$: m/z 536.0427, found: m/z 536.0413 $[\text{M}]^+$. **mp**: 30 °C.

1-Chloro-2-(3,3,4,4,5,5,6,6,7,7,8,8,9,9,10,10-heptadecafluoro-1-iododecyl)benzene (15g)

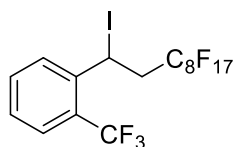


Following GP-A, **15g** was prepared using 1-chloro-2-vinylbenzene (**14h**) (128 μL , 1.0 mmol, 1.0 equiv), $\text{C}_8\text{F}_{17}\text{I}$ (**4d**) (530 μL , 2.0 mmol, 2.0 equiv) and $[\text{Cu}(\text{dap})_2]\text{Cl}$ (8.8 mg, 1.0 μmol , 1.0 mol%). Chromatography on silica (hexanes) afforded **15g** as a white solid (581 mg, 85%).

R_f (hexanes) = 0.50. **Staining**: KMnO_4 (UV active). **^1H -NMR** (400 MHz, CDCl_3) $\delta = 7.71 - 7.46$ (m, 1H), 7.49 - 7.14 (m, 3H), 5.94 (dd, $J = 9.3, 5.8$ Hz, 1H), 3.55 - 3.07 (m, 2H). **^{19}F -NMR** (376 MHz, CDCl_3) $\delta = -80.94$ (t, $J = 9.9$ Hz, 3F), -112.28 – -114.95 (m, 2F), -121.62 (s, 2F), -121.98 (s, 4F), -122.80 (s, 2F), -123.55 (s, 2F), -126.21 (s, 2F). **^{13}C -NMR** (101 MHz, CDCl_3) $\delta = 139.6, 130.3, 129.6, 128.5, 127.6, 120.7 - 104.2$ (m), 41.21 (t, $J = 19.7$ Hz), 11.4 – 10.9 (m). **IR** (neat, cm^{-1}): 1477, 1441, 1369, 1346, 1329, 1290, 1238, 1198, 1144, 1132, 1115, 1094, 1072, 1053, 1038, 1028, 978, 961, 924, 869, 831, 785, 756, 743, 704, 683, 658,

602, 573, 559, 527, 469. **LRMS** (EI) m/z (%): 143.1 (100), 557.1 ($[M-I]^+$, 77), 187.0 (77), 140.1 (58), 133.1 (46), 152.1 (43), 138.0 (38), 103.1 (38), 145.1 (34), 69.1 (21), 559.2 (17), 558.3 (11), 76.2 (10), 144.1 (9), 126.9 (2). **HRMS** (EI) exact mass calc. for $C_{16}H_7ClF_{16}I$: m/z 664.9020, found: m/z 664.9019 $[M-F]^+$. **mp**: 60 °C.

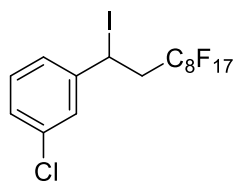
1-(3,3,4,4,5,5,6,6,7,7,8,8,9,9,10,10,10-Heptadecafluoro-1-iododecyl)-2-(trifluoromethyl)benzene (15h)



Following GP-A, **15h** was prepared using 1-(trifluoromethyl)-2-vinylbenzene (**14i**) (172 mg, 1.0 mmol, 1.0 equiv), $C_8F_{17}I$ (**4d**) (530 μ L, 2.0 mmol, 2.0 equiv) and $[Cu(dap)_2]Cl$ (8.8 mg, 1.0 μ mol, 1.0 mol%). Chromatography on silica (hexanes) afforded **15h** as a colourless oil (596 mg, 83%).

R_f (hexanes) = 0.53. **Staining**: $KMnO_4$ (UV active). **1H -NMR** (300 MHz, $CDCl_3$) δ = 7.81 (d, J = 8.3 Hz, 1H), 7.58 (ddd, J = 7.1, 4.1, 2.6 Hz, 2H), 7.42 – 7.34 (m, 1H), 5.82 (dd, J = 9.5, 5.2 Hz, 1H), 3.48 – 3.06 (m, 2H). **^{19}F -NMR** (282 MHz, $CDCl_3$) δ = -60.38 (s, 3F), -81.30 (t, J = 10.1 Hz, 3F), -114.15 – -115.65 (m, 2F), -122.10 (dt, J = 25.1, 11.0 Hz, 2F), -122.45 (dt, J = 21.8, 10.7 Hz, 4F), -123.23 (d, J = 18.5 Hz, 2F), -124.06 (d, J = 15.3 Hz, 2F), -126.57 – -126.73 (m, 2F). **^{13}C -NMR** (75 MHz, $CDCl_3$) δ = 144.6, 134.6, 130.1, 128.7, 127.0, 124.9, 119.0-106.6 (m), 42.7, 42.4 (J = 20.6 Hz), 42.1, 14.5. **IR** (neat, cm^{-1}): 1314, 1238, 1202, 1171, 1144, 1128, 1115, 1061, 1036, 980, 962, 872, 764, 721, 704, 652, 598, 559. **LRMS** (EI) m/z (%): 591.1 ($[M-I]^+$, 100), 221.1 (50), 177.1 (90), 172.1 (65), 151.1 (25), 127.1 (20). **HRMS** (EI) exact mass calc. for $C_{17}H_7F_{19}I$: m/z 698.9284, found: m/z 698.9285 $[M-F]^+$.

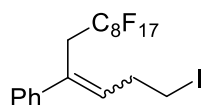
1-Chloro-3-(3,3,4,4,5,5,6,6,7,7,8,8,9,9,10,10,10-heptafluoro-1-iododecyl)benzene (15i)



Following GP-A, **15i** was prepared using 1-chloro-3-vinylbenzene (**14j**) (128 μ L, 1.0 mmol, 1.0 equiv), $C_8F_{17}I$ (**4d**) (530 μ L, 2.0 mmol, 2.0 equiv) and $[Cu(dap)_2]Cl$ (8.8 mg, 1.0 μ mol, 1.0 mol%). Chromatography on silica (hexanes) afforded **15i** as a white solid (492 mg, 72%).

R_f (hexanes) = 0.50. **Staining**: $KMnO_4$ (UV active). **1H -NMR** (300 MHz, $CDCl_3$) δ = 7.45 – 7.41 (m, 1H), 7.35 – 7.21 (m, 3H), 5.38 (dd, J = 9.6, 5.3 Hz, 1H), 3.38 – 3.03 (m, 2H). **^{19}F -NMR** (282 MHz, $CDCl_3$) δ = -81.69 (t, J = 10.0 Hz, 3F), -111.95 – -116.09 (m, 2F), -122.31 (d, J = 7.7 Hz, 2F), -122.64 (d, J = 7.3 Hz, 4F), -123.49 (s, 2F), -124.01 – -124.32 (m, 2F), -126.94 (m, J = 13.8 Hz, 2F). **^{13}C -NMR** (75 MHz, $CDCl_3$) δ = 144.8, 134.8, 130.3, 129.0, 127.2, 125.1, 120.9 - 106.8 (m), 42.6 (t, J = 20.6 Hz), 14.7. **IR** (neat, cm^{-1}): 1593, 1576, 1476, 1435, 1368, 1331, 1279, 1234, 1198, 1146, 1115, 1103, 1080, 1032, 997, 962, 935, 880, 841, 826, 793, 775, 746, 704, 692, 685, 654, 603, 573, 559, 517, 451. **LRMS** (EI) m/z (%): 557.1 ($[M-I]^+$, 100), 138.0 (38), 143.1 (69), 559.2 (28), 187.0 (29), 558.3 (17), 140.1 (11), 103.1 (19), 145.1 (21), 133.1 (15), 126.9 (6), 153.1 (8), 144.1 (6), 76.2 (2), 684.4 (2). **HRMS** (EI) exact mass calc. for $C_{16}H_6ClF_{17}I$: m/z 682.8926, found: m/z 682.8914 $[M-H]^+$. **mp**: 60 $^{\circ}C$.

(6,6,7,7,8,8,9,9,10,10,11,11,12,12,13,13,13-Heptafluoro-1-iodotridec-3-en-4-yl)benzene (15j)

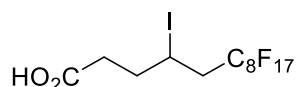


Following GP-A, **15j** was prepared using (1-cyclopropylvinyl)benzene (**14k**) (150 μ L, 1.0 mmol, 1.0 equiv), $C_8F_{17}I$ (**4d**) (530 μ L, 2.0 mmol, 2.0 equiv) and $[Cu(dap)_2]Cl$ (8.8 mg, 1.0 μ mol, 1 mol%). Chromatography on silica (hexanes) afforded **15j** as a white solid (509 mg, 74%) in a diastereomeric ratio of E/Z = 94:06.

R_f (hexanes) = 0.30. **Staining**: vanilin (UV active). **1H -NMR** (300 MHz, $CDCl_3$) δ = 7.40 – 7.30 (m, 5H), 6.02 (t, J = 7.3 Hz, 1H), 3.36 (t, J = 18.7 Hz, 2H), 3.27 (t, J = 6.9 Hz, 2H), 2.86 (q, J = 7.0 Hz, 2H). **^{19}F -NMR** (282 MHz, $CDCl_3$) δ = -81.61 (t, J = 10.0 Hz, 3F), -111.85 – -112.95 (m, 2F), -122.10 – -122.37 (m, 2F), -122.61 (tt, J = 18.9, 8.8 Hz, 4F), -123.46 (tdq, J = 24.0, 18.1, 8.4 Hz, 2F), -123.77 (dq, J = 23.9, 11.0, 8.5 Hz, 2F), -126.89 (td, J = 13.7, 13.0, 5.1 Hz,

CDCl_3) δ = -80.91 (t, J = 10.0 Hz, 3F), -111.15 – -112.46 (m, 1F), -114.67 (dt, J = 269.9, 13.5 Hz, 1F), -121.63 (d, J = 7.9 Hz, 2F), -121.97 (s, 4F), -122.79 (s, 2F), -123.66 (s, 2F), -126.22 (d, J = 13.3 Hz, 2F). **^{13}C -NMR** (101 MHz, CDCl_3) δ = 123.4 – 106.2 (m), 41.7 (t, J = 20.8 Hz), 40.4 (d, J = 1.9 Hz), 31.6, 29.5, 28.2, 22.5, 20.8, 13.9. **IR** (neat, cm^{-1}): 2967, 2940, 2913, 2874, 1633, 1470, 1369, 1325, 1238, 1200, 1146, 1105, 1061, 982, 704, 654, 629, 555, 528. **LRMS** (EI): m/z (%): 57.1 (100), 489.0 ($[\text{M}-\text{I}-\text{C}_3\text{H}_6]^+$, 46), 69.1 (34), 84.0 (28), 531.1 ($[\text{M}-\text{I}]^+$, 28). **HRMS** (EI) exact mass calc. for $\text{C}_{16}\text{H}_{16}\text{F}_{17}$: m/z 531.0977, found: m/z 531.0990 $[\text{M}-\text{I}]^+$.

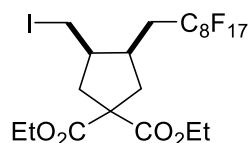
6,6,7,7,8,8,9,9,10,10,11,11,12,12,13,13,13-Heptadecafluoro-4-iodotridecanoic acid (17b)



Following GP-A, **17b** was prepared using pent-4-enoic acid (**16c**) (100 mg, 1.0 mmol, 1.0 equiv), $\text{C}_8\text{F}_{17}\text{I}$ (**4d**) (530 μL , 1.0 mmol, 2.0 equiv) and $[\text{Cu}(\text{dap})_2]\text{Cl}$ (8.8 mg, 0.5 μmol , 1 mol%). Chromatography on silica (CH_2Cl_2 , followed by CH_2Cl_2 -MeOH, 9:1) afforded **17b** as a yellowish solid (403 mg, 62%).

R_f (CH_2Cl_2 -MeOH, 9:1) = 0.56. **Staining**: KMnO_4 (UV active). **^1H -NMR** (300 MHz, CDCl_3) δ = 10.65 (br, 1H), 4.40 (dddd, J = 12.0, 9.0, 5.3, 3.5 Hz, 1H), 3.05 – 2.54 (m, 4H), 2.25 – 2.01 (m, 2H). **^{19}F -NMR** (282 MHz, CDCl_3) δ = -81.31 (t, J = 10.0 Hz, 3F), -111.38 – -115.62 (m, 2F), -121.98 – -122.24 (m, 2F), -122.31 – -122.63 (m, 4F), -123.27 (dt, J = 22.0, 10.2 Hz, 2F), -124.08 (t, J = 13.9 Hz, 2F), -126.54 – -126.79 (m, 2F). **^{13}C -NMR** (75 MHz, CDCl_3) δ = 178.2, 41.9 (t, J = 20.7 Hz), 35.1 (d, J = 1.8 Hz), 34.5, 18.9. **IR** (neat, cm^{-1}): 3038, 2922, 1700, 1435, 1372, 1331, 1290, 1200, 1148, 1115, 1074, 1018, 958, 910, 828, 768, 705. **HRMS** (EI) exact mass calc. for $\text{C}_{13}\text{H}_9\text{F}_{17}\text{IO}_2$: m/z 646.9370, found: m/z 646.9371 $[\text{M}+\text{H}]^+$. **mp**: 79 $^\circ\text{C}$.

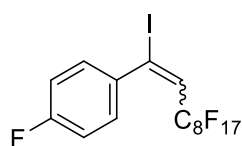
Diethyl (3*R*,4*R*)-3-(2,2,3,3,4,4,5,5,6,6,7,7,8,8,9,9,9-heptafluorononyl)-4-(iodomethyl)cyclopentane-1,1-dicarboxylate (17c)



Following GP-A, **17c** was prepared using diethyl 2,2-diallylmalonate (**16d**) (240 mg, 1.0 mmol, 1.0 equiv), C₈F₁₇I (**4d**) (530 μ L, 2.0 mmol, 2.0 equiv) and [Cu(dap)₂]Cl (8.8 mg, 1.0 μ mol, 1 mol%). Chromatography on silica (hexanes/EtOAc = 7:1) afforded **17c** as a colourless oil (718 mg, 91%) in a diastereomeric ratio of cis/trans = 74:11.

R_f (hexanes-EtOAc, 5:1) = 0.63. **Staining**: KMnO₄ (UV active). **¹H-NMR** (300 MHz, CDCl₃) δ = 4.20 (qd, J = 7.1, 3.4 Hz, 4H), 3.16 (dd, J = 9.8, 5.6 Hz, 1H), 3.05 (t, J = 9.8 Hz, 1H), 2.66 – 2.44 (m, 4H), 2.36 – 1.99 (m, 4H), 1.26 (q, J = 7.0 Hz, 6H). **¹⁹F-NMR** (282 MHz, CDCl₃) δ = -81.56 (t, J = 10.0 Hz, 3F), -113.83 (m, 2F), -122.42 (d, 6F), -123.42 (s, 2F), -124.08 (s, 2F), -126.88 (s, 2F). **¹³C-NMR** (75 MHz, CDCl₃) δ = 172.4, 172.1, 121.9 – 106.7 (m), 62.0, 61.9, 58.4, 45.6, 39.8, 38.5 (d, J = 2.3 Hz), 29.8 (t, J = 21.7 Hz), 14.1, 14.0, 5.7. **IR** (neat, cm⁻¹): 2886, 1730, 1446, 1368, 1238, 1200, 1059, 1029, 980, 865, 790, 705. **LRMS** (ESI): m/z (%): 809.0 ([M+Na]⁺, 100), 788.0 ([M+H]⁺, 13), 659.1 ([M-I]⁺, 3), 741.0 ([M-C₂H₅O]⁺, 1). **HRMS** (ESI) exact mass calc. for C₂₁H₂₁F₁₇IO₄: m/z 787.0208, found: m/z 787.0209 [M+H]⁺.

1-Fluoro-4-(3,3,4,4,5,5,6,6,7,7,8,8,9,9,10,10,10-heptafluoro-1-iododec-1-en-1-yl)benzene (19a)

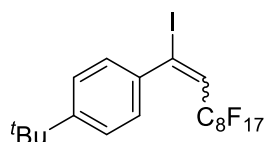


Following GP-A, **19a** was prepared using 1-bromo-3-ethynylbenzene (**18a**) (115 μ L, 1.0 mmol, 1.0 equiv.), C₈F₁₇I (**4d**) (530 μ L, 2.0 mmol, 2.0 equiv.) and [Cu(dap)₂]Cl (8.8 mg, 1.0 μ mol, 1.0 mol%). Chromatography on silica (hexanes) afforded **19a** as a colourless oil (593 mg, 89%) in a diastereomeric ratio of *E/Z* = 96:04.

R_f (hexanes) = 0.61. **Staining**: vanilin (UV active). **¹H-NMR** (300 MHz, CDCl₃) δ = 7.33 – 7.26 (m, 2H), 7.07 – 6.99 (m, 2H), 6.61 (t, J = 13.4 Hz, 1H). **¹⁹F-NMR** (282 MHz, CDCl₃) δ = -81.43 (dd, J = 11.2, 8.9 Hz), -105.63 – -105.89 (m), -111.47, -121.98 – -122.25 (m), -122.50 (dq, J = 30.2, 12.9, 10.7 Hz), -123.24 – -123.48 (m), -126.75 (ddtd, J = 17.9, 11.0, 7.0, 3.6 Hz). **¹³C-NMR** (75 MHz, CDCl₃) δ = 164.7, 161.4, 137.5 (d, J = 3.7 Hz), 129.9 – 128.6 (m), 127.8 (t,

$J = 22.1$ Hz), 115.5, 115.2, 114.9 – 107.6 (m). **IR** (neat, cm^{-1}): 3069, 1645, 1597, 1504, 1371, 1325, 1236, 1196, 1144, 1113, 1072, 976, 841, 797, 754, 704, 660, 606, 554, 527. **LRMS** (EI) m/z (%): 539.1 ($[\text{M-I}]^+$, 100), 120.1 (82), 169.1 ($[\text{M-I-C}_3\text{F}_7]^+$, 69), 200.1 ($[\text{M-I-C}_4\text{F}_8]^+$, 52), 69.1 (13). **HRMS** (EI) exact mass calc. for $\text{C}_{16}\text{H}_5\text{F}_{18}\text{I}$: m/z 665.9148, found: m/z 665.9150 $[\text{M}]^+$.

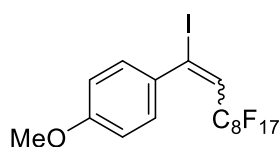
1-(*tert*-Butyl)-4-(3,3,4,4,5,5,6,6,7,7,8,8,9,9,10,10,10-heptafluoro-1-iododec-1-en-1-yl)benzene (19b)



Following GP-A, **19b** was prepared using 1-(*tert*-butyl)-4-ethynylbenzene (**18b**) (180 μL , 1.0 mmol, 1.0 equiv.), $\text{C}_8\text{F}_{17}\text{I}$ (**4d**) (530 μL , 2.0 mmol, 2.0 equiv.) and $[\text{Cu}(\text{dap})_2]\text{Cl}$ (8.8 mg, 1.0 μmol , 1.0 mol%). Chromatography on silica (hexanes) afforded **19b** as white solid (442 mg, 63%) in a diastereomeric ratio of $E/Z = 99:01$.

R_f (hexanes) = 0.66. **Staining**: KMnO_4 (UV active). **$^1\text{H-NMR}$** (300 MHz, CDCl_3) $\delta = 7.36 - 7.31$ (m, 2H), 7.26 – 7.21 (m, 2H), 6.57 (t, $J = 13.6$ Hz, 1H), 1.32 (s, 9H). **$^{19}\text{F-NMR}$** (282 MHz, CDCl_3) $\delta = -81.28$ (t, $J = 9.9$ Hz), -105.52 (t, $J = 13.1$ Hz), -122.00 (d, $J = 8.4$ Hz), -122.42 (d, $J = 7.7$ Hz), -123.09 – -123.52 (m), -126.52 – -126.79 (m). **$^{13}\text{C-NMR}$** (75 MHz, CDCl_3) $\delta = 152.7$, 138.4, 126.9, 126.6, 126.4, 125.0, 34.9, 31.3. **IR** (neat, cm^{-1}): 2967, 2876, 1638, 1505, 1466, 1404, 1370, 1327, 1240, 1198, 1146, 1108, 1070, 1021, 970, 841, 819, 737, 705, 688, 659, 602, 555, 525, 492. **LRMS** (EI) m/z (%): 577.2 ($[\text{M-I}]^+$, 100), 143.2 (24), 578.2 (20), 57.2 (16), 115.1 (8), 579.2 (2). **HRMS** (EI) exact mass calc. for $\text{C}_{20}\text{H}_{14}\text{F}_{17}\text{I}$: m/z 703.9869, found: m/z 703.9856 $[\text{M}]^+$. **mp**: 49 $^\circ\text{C}$.

1-(3,3,4,4,5,5,6,6,7,7,8,8,9,9,10,10,10-Heptafluoro-1-iododec-1-en-1-yl)-4-methoxybenzene (19c)

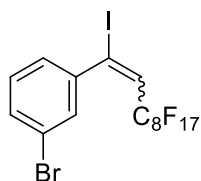


Following GP-A, **19c** was prepared using 1-ethynyl-4-methoxybenzene (**18c**) (132 μL , 1.0 mmol, 1.0 equiv.), $\text{C}_8\text{F}_{17}\text{I}$ (**4d**) (530 μL , 2.0 mmol, 2.0 equiv.) and $[\text{Cu}(\text{dap})_2]\text{Cl}$ (8.8 mg, 1.0 μmol , 1.0 mol%). Chromatography on silica (hexanes) afforded **19c** as white solid (427 mg, 63%) in a diastereomeric ratio of $E/Z = 93:07$.

R_f (hexanes-EtOAc, 4:1) = 0.76. **Staining**: vanilin (UV active). **$^1\text{H-NMR}$** (300 MHz, CDCl_3) $\delta = 7.53$ (d, $J = 2.2$ Hz, 1H), 7.26 – 7.20 (m, 1H), 6.83 (d, $J = 8.5$ Hz, 1H), 6.57 (t,

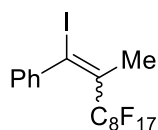
$J = 13.4$ Hz, 1H), 3.91 (s, 3H). **^{19}F -NMR** (282 MHz, CDCl_3) $\delta = -81.36$ (t, $J = 10.0$ Hz, 3F), -105.54 (t, $J = 13.2$ Hz, 2F), $-121.94 - -122.17$ (m, 2F), -122.46 (dq, $J = 19.9, 11.4, 10.0$ Hz, 4F), -123.33 (ddt, $J = 27.6, 20.8, 10.1$ Hz, 4F), -126.70 (tt, $J = 13.4, 5.2$ Hz, 2F). **^{13}C -NMR** (75 MHz, CDCl_3) $\delta = 156.6, 134.8, 132.3, 128.0 - 127.4$ (m), $127.2, 111.2, 111.0, 56.4$. **IR** (neat, cm^{-1}): 3021, 2967, 2868, 1636, 1595, 1494, 1460, 1371, 1324, 1286, 1257, 1243, 1202, 1143, 1121, 1055, 1021, 978, 891, 830, 814, 787, 725, 705, 642, 525. **HRMS** (EI) exact mass calc. for $\text{C}_{17}\text{H}_8\text{F}_{17}\text{IO}$: m/z 677.9348, found: m/z 677.9340 $[\text{M}]^+$. **mp**: 70 °C.

1-Bromo-3-(3,3,4,4,5,5,6,6,7,7,8,8,9,9,10,10,10-heptafluoro-1-iododec-1-en-1-yl)benzene (19d)



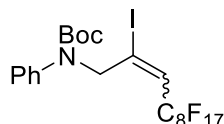
Following GP-A, **19d** was prepared using 1-bromo-3-ethynylbenzene (**18d**) (182 mg, 1.0 mmol, 1.0 equiv.), $\text{C}_8\text{F}_{17}\text{I}$ (**4d**) (530 μL , 2.0 mmol, 2.0 equiv.) and $[\text{Cu}(\text{dap})_2]\text{Cl}$ (8.8 mg, 1.0 μmol , 1.0 mol%). Chromatography on silica (hexanes) afforded **19d** as white solid (539 mg, 74%) in a diastereomeric ratio of $E/Z = 83:17$.

R_f (hexanes) = 0.69. **Staining**: KMnO_4 (UV active). **^1H -NMR** (300 MHz, CDCl_3) $\delta = 7.49 - 7.41$ (m, 2H), $7.25 - 7.16$ (m, 2H), 6.63 (t, $J = 13.4$ Hz, 1H). **^{19}F -NMR** (282 MHz, CDCl_3) $\delta = -81.23$ (t, $J = 10.1$ Hz, 3F), -105.23 (dt, $J = 13.4$ Hz, 2F), -121.98 (s, 2F), -122.44 (d, $J = 20.7$ Hz, 4F), $-122.71 - -123.48$ (m, 4F), -126.61 (qd, $J = 11.8, 9.7, 4.6$ Hz, 2F). **^{13}C -NMR** (75 MHz, CDCl_3) $\delta = 143.2, 135.1 - 108.8$ (m), $132.5, 129.9$ (t, $J = 2.2$ Hz), $129.7, 128.2$ (t, $J = 22.4$ Hz), 125.5 (t, $J = 2.5$ Hz), $122.0, 78.6$. **IR** (neat, cm^{-1}): 3071, 1644, 1588, 1562, 1469, 1402, 1372, 1327, 1215, 1141, 1115, 973, 913, 872, 824, 768, 705. **HRMS** (EI) exact mass calc. for $\text{C}_{16}\text{H}_5\text{F}_{17}\text{BrI}$: m/z 725.8342, found: m/z 725.8340 $[\text{M}]^+$. **mp**: 52 °C.

(3,3,4,4,5,5,6,6,7,7,8,8,9,9,10,10,10-Heptadecafluoro-1-iodo-2-methyldec-1-en-1-yl) benzene (19f)

Following GP-A, **19f** was prepared using prop-1-yn-1-ylbenzene (**18f**) (117 mg, 1.0 mmol, 1.0 equiv), C₈F₁₇I (**4d**) (530 μ L, 2.0 mmol, 2.0 equiv) and [Cu(dap)₂]Cl (8.8 mg, 1.0 μ mol, 1.0 mol%). Chromatography on silica (hexanes) afforded **19f** as a white solid (268 mg, 40%) in a diastereomeric ratio of *E/Z* = 99:01.

R_f (hexanes) = 0.69. **Staining:** KMnO₄ (UV active). **¹H-NMR** (300 MHz, CDCl₃) δ = 7.34 – 7.17 (m, 5H), 2.30 (s, 3H). **¹⁹F-NMR** (282 MHz, CDCl₃) δ = -81.53 (t, *J* = 10.0 Hz, 3F), -103.83 (qd, *J* = 9.1, 8.7, 4.2 Hz, 2F), -120.11 (dt, *J* = 20.2, 8.7 Hz, 2F), -122.40 – -122.69 (m, 6F), -123.42 (ddt, *J* = 28.6, 20.1, 8.1 Hz, 2F), -126.85 (dq, *J* = 13.2, 6.7 Hz, 2F). **¹³C-NMR** (75 MHz, CDCl₃) δ = 144.3, 128.8, 128.3, 127.8, 126.9, 119.2 - 103.3 (m), 26.73 (p, *J* = 3.1 Hz). **IR** (neat, cm⁻¹): 1636, 1487, 1443, 1372, 1327, 1290, 1197, 1144, 1111, 1018, 954, 857, 824, 764, 697, 664. **HRMS** (EI) exact mass calc. for C₁₇H₈F₁₇: *m/z* 535.0349, found: *m/z* 535.0326 [M-I]⁺. **mp**: 79 °C.

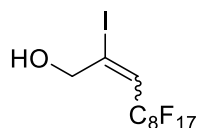
tert-Butyl-(4,4,5,5,6,6,7,7,8,8,9,9,10,10,11,11,11-heptadecafluoro-2-iodoundec-2-en-1-yl)(phenyl)carbamate (21a)

Following GP-A, **21a** was prepared using *tert*-butyl phenyl(prop-2-yn-1-yl)carbamate (**20a**) (231 mg, 1.0 mmol), C₈F₁₇I (**4d**) (530 μ L, 2.0 mmol, 2.0 equiv) and [Cu(dap)₂]Cl (8.8 mg, 1.0 μ mol, 1 mol%). Chromatography on silica (hexanes/EtOAc = 95:05) afforded **21a** as a colourless oil (598 mg, 77%, rotamere present) in a diastereomeric ratio of *E/Z* = 75:25.

R_f (hexanes-EtOAc, 5:1) = 0.76. **Staining:** vanilin (UV inactive). **¹H-NMR** (400 MHz, CDCl₃) δ = 7.37 – 7.30 (m, 2H), 7.27 – 7.18 (m, 3H), 6.49 (t, *J* = 13.4 Hz, 1H), 4.64 (s, 2H), 1.46 (s, 9H). **¹⁹F-NMR** (376 MHz, CDCl₃) δ = -80.97 (t, *J* = 9.9 Hz, 3F), -108.40 (s, 2F), -121.49 (s, 2F), -121.98 (s, 4F), -123.00 (m, 4F), -126.24 (s, 2F). **¹³C-NMR** (101 MHz, CDCl₃) δ = 154.0, 141.8, 129.1, 128.9, 127.4, 126.9, 126.6, 126.0, 121.6 (t, *J* = 24.8 Hz), 118.7 – 106.7 (m), 81.9, 64.1, 28.4, 28.2. **IR** (neat, cm⁻¹): 3412, 3322, 3234, 2977, 2189, 1706, 1598, 1496, 1369, 1236, 1202, 1146, 1114, 1051, 1003, 860, 706, 532, 502, 467. **LRMS** (ESI): *m/z* (%): 721.9 ([MH⁺-C₄H₈], 100), 799.9 ([M+Na]⁺, 52), 722.9 (18), 723.9 (3), 709.1 (1).

HRMS (ESI) exact mass calc. for $C_{22}H_{17}F_{17}INNaO_2$: m/z 799.9925, found: m/z 799.9902 $[M+Na]^+$.

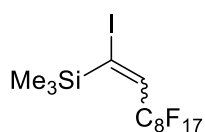
4,4,5,5,6,6,7,7,8,8,9,9,10,10,11,11,11-Heptadecafluoro-2-iodoundec-2-en-1-ol (21b)



Following GP-A, **21b** was prepared using prop-2-yn-1-ol (**20b**) (60 μ L, 1.0 mmol, 1.0 equiv), $C_8F_{17}I$ (**4d**) (530 μ L, 2.0 mmol, 2.0 equiv) and $[Cu(dap)_2]Cl$ (8.8 mg, 1.0 μ mol, 1 mol%). Chromatography on silica (hexanes/EtOAc 7:1) afforded **21b** as yellow solid (506 mg, 84%) in a diastereomeric ratio of E/Z = 51:49.

R_f (hexanes-EtOAc, 7:1) = 0.24. **Staining**: $KMnO_4$ (UV active). **1H -NMR** (300 MHz, $CDCl_3$) δ = 6.79 (t, J = 13.4 Hz, 1H), 6.47 (t, J = 14.6 Hz, 1H), 4.35 (q, J = 3.8 Hz, 4H), 2.46 (s, 2H). **^{19}F -NMR** (282 MHz, $CDCl_3$) δ = -81.31 (t, J = 9.9 Hz, 6F), -105.53 (t, J = 13.3 Hz, 2F), -108.69 (t, J = 13.1 Hz, 2F), -121.99 (s, J = 4.3 Hz, 4F), -122.19 – -122.67 (m, 8F), -123.09 – -123.51 (m, 6F), -123.54 – -123.81 (m, 2F), -126.53 – -126.82 (m, 4F). **^{13}C -NMR** (75 MHz, $CDCl_3$) δ = 127.6 (t, J = 24.9 Hz), 120.1 (t, J = 24.1 Hz), 122.8, 120.4, 111.5 - 103.3 (m), 72.7, 65.0 (t, J = 4.8 Hz). **IR** (neat, cm^{-1}): 3272, 1639, 1437, 1371, 1333, 1239, 1011, 1199, 1146, 1116, 1068, 1052, 987, 949, 866, 834, 777, 746, 723, 707, 656, 558, 525, 517, 420. **LRMS** (EI): m/z (%): 106.1 (100), 602.2 ($[M]^+$, 59), 69.1 (55), 595.4 (34), 475.2 ($[M-I]^+$, 31), 77.1 (28), 137.1 (27), 119.1 (25), 55.2 (21). **HRMS** (EI) exact mass calc. for $C_{11}H_4F_{17}IO$: m/z 601.9035, found: m/z 601.9034 $[M]^+$. **mp**: 56 $^{\circ}C$.

(3,3,4,4,5,5,6,6,7,7,8,8,9,9,10,10,10-Heptadecafluoro-1-iododec-1-en-1-yl)trimethylsilane (21c)

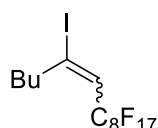


Following GP-A, **21c** was prepared using ethynyltrimethylsilane (**20c**) (141 μ L, 1.0 mmol, 1.0 equiv), $C_8F_{17}I$ (**4d**) (530 μ L, 1.0 mmol, 2.0 equiv) and $[Cu(dap)_2]Cl$ (8.8 mg, 1.0 μ mol, 1.0 mol%). Chromatography on silica (hexanes) afforded **21c** as a colourless oil (573 mg, 89%) in a diastereomeric ratio of E/Z = 71:29.

R_f (hexanes) = 0.83. **Staining**: $KMnO_4$ (UV active). **1H -NMR** (300 MHz, acetone- d_6) δ = 7.51 (t, J = 15.6 Hz, 1H, *major*), 7.02 (t, J = 13.3 Hz, 1H, *minor*), 0.36 (s, 9H, *major*), 0.30 (s, 9H, *minor*). **^{19}F -NMR** (282 MHz, acetone- d_6) δ = -80.76 (q, J = 9.9, 9.3 Hz, 3F), -99.55 – -113.72

(m, 2F), -121.04 (s, 2F), -121.46 (s, 4F), -121.80 – -122.74 (m, 4F), -125.82 (d, $J = 17.2$ Hz, 2F). **$^{13}\text{C-NMR}$** (75 MHz, acetone- d_6) $\delta = 139.3$ (t, $J = 23.2$ Hz, *major*), 131.9 (t, $J = 23.2$ Hz, *minor*), 129.2, 129.0 – 128.9 (m), 126.2 – 102.3 (m), 1.2 (*major*), -1.8 (*minor*). **IR** (neat, cm^{-1}): 2963, 1588, 1416, 1368, 1327, 1238, 1200, 1148, 1115, 1059, 984, 846, 764, 738, 705. **HRMS** (EI) exact mass calc. for $\text{C}_{13}\text{H}_{10}\text{F}_{17}\text{I}$ Si: m/z 643.9301, found: m/z 643.9300 $[\text{M}]^+$.

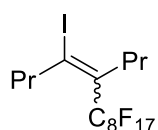
7,7,8,8,9,9,10,10,11,11,12,12,13,13,14,14,14-Heptadecafluoro-5-iodotetradec-5-ene (21d)



Following GP-A, **21d** was prepared using hex-1-yne (**20d**) (114 μL , 1.0 mmol, 1.0 equiv), $\text{C}_8\text{F}_{17}\text{I}$ (**4d**) (530 μL , 1.0 mmol, 2.0 equiv) and $[\text{Cu}(\text{dap})_2]\text{Cl}$ (8.8 mg, 1.0 μmol , 1 mol%). Chromatography on silica (hexanes) afforded **21d** as a colourless oil (396 mg, 63%) in a diastereomeric ratio of $E/Z = 80:20$.

R_f (hexanes) = 0.80. **Staining**: vanilin (UV active). **$^1\text{H-NMR}$** (300 MHz, CDCl_3) $\delta = 6.32$ (t, $J = 14.5$ Hz, 1H), 2.63 (t, $J = 7.5$ Hz, 2H), 1.56 (ddd, $J = 9.6, 4.8, 2.4$ Hz, 2H), 1.40 – 1.31 (m, 2H), 0.94 (t, $J = 7.2$ Hz, 3H). **$^{19}\text{F-NMR}$** (282 MHz, CDCl_3) $\delta = -81.32$ (t, $J = 10.0$ Hz, 3F), -103.71 – -115.04 (m, 2F), -121.08 – -122.91 (m, 6F), -122.93 – -124.32 (m, 4F), -126.68 (tt, $J = 11.6, 5.8$ Hz, 2F). **$^{13}\text{C-NMR}$** (75 MHz, CDCl_3) $\delta = 126.6$ (t, $J = 23.9$ Hz), 41.1, 32.3, 21.8, 13.9. **IR** (neat, cm^{-1}): 2963, 2930, 2860, 1464, 1433, 1364, 1234, 1200, 1146, 1115, 974, 878, 721, 704, 656. **HRMS** (EI) exact mass calc. for $\text{C}_{14}\text{H}_{10}\text{F}_{17}\text{I}$: m/z 627.9555, found: m/z 627.8999 $[\text{M}]^+$.

6,6,7,7,8,8,9,9,10,10,11,11,12,12,13,13,13-Heptadecafluoro-4-iodo-5-propyltridec-4-ene (21e)

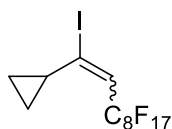


Following GP-A, **21e** was prepared using 4-octyne (**20e**) (147 μL , 1.0 mmol, 1.0 equiv), $\text{C}_8\text{F}_{17}\text{I}$ (**4d**) (530 μL , 2.0 mmol, 2.0 equiv) and $[\text{Cu}(\text{dap})_2]\text{Cl}$ (8.8 mg, 1.0 μmol , 1.0 mol%). Chromatography on silica (hexanes) afforded **21e** as colourless oil (578 mg, 88%) in a diastereomeric ratio of $E/Z = 96:04$.

R_f (hexanes) = 0.80. **Staining**: KMnO_4 (UV active). **$^1\text{H-NMR}$** (400 MHz, CDCl_3) $\delta = 2.71$ (t, $J = 6.4$ Hz, 1H), 2.40 – 2.33 (m, 1H), 1.71 – 1.49 (m, 2H), 0.95 (dt, $J = 16.6, 7.4$ Hz, 3H). **$^{19}\text{F-NMR}$** (376 MHz, CDCl_3) $\delta = -81.85$ (t, $J = 10.0$ Hz, 3F), -103.56 (t, $J = 13.0$ Hz,

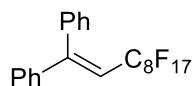
2F), -122.06 (d, $J = 8.1$ Hz, 2F), -122.37 – -122.95 (m, 6F), -123.60 (s, 2F), -126.96 – -127.20 (m, 2F). $^{13}\text{C-NMR}$ (101 MHz, CDCl_3) $\delta = 132.7$ (t, $J = 20.9$ Hz), 125.371 – 125.1 (m), 119.3 – 107.3 (m), 52.8, 46.8, 45.6, 42.2, 24.6, 22.1, 14.0, 13.9, 12.8, 12.7. **IR** (neat, cm^{-1}): 3320, 3202, 2968, 2939, 2878, 2180, 1613, 1468, 1367, 1239, 1201, 1147, 1107, 1006, 887, 777, 713, 674, 655, 632, 533, 496, 419. **HRMS** (EI) exact mass calc. for $\text{C}_{16}\text{H}_{14}\text{F}_{17}\text{I}$: m/z 655.9869, found: m/z 655.9885 $[\text{M}]^+$.

(3,3,4,4,5,5,6,6,7,7,8,8,9,9,10,10,10-Heptafluoro-1-iododec-1-en-1-yl)cyclopropane (21g)



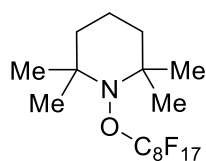
Following GP-A, **21g** was prepared using ethynylcyclopropane (**20g**) (66 mg, 1.0 mmol, 1.0 equiv), $\text{C}_8\text{F}_{17}\text{I}$ (**4d**) (530 μL , 1.0 mmol, 2.0 equiv) and $[\text{Cu}(\text{dap})_2]\text{Cl}$ (8.8 mg, 1.0 μmol , 1.0 mol%). Chromatography on silica (hexanes) afforded **21g** as a colourless oil (318 mg, 52%) in a diastereomeric ratio of $E/Z = 99:01$.

R_f (hexanes) = 0.80. **Staining**: KMnO_4 (UV inactive). $^1\text{H-NMR}$ (300 MHz, CDCl_3) $\delta = 6.39$ (t, $J = 14.7$ Hz, 1H), 1.50 (q, $J = 6.3$ Hz, 1H), 0.88 – 0.82 (m, 4H). $^{19}\text{F-NMR}$ (282 MHz, CDCl_3) $\delta = -81.67$ (t, $J = 10.1$ Hz), -105.21 (td, $J = 13.3$, 3.0 Hz), -122.23 (tdd, $J = 17.1$, 10.5, 5.2 Hz), -122.64 (qd, $J = 18.4$, 16.6, 8.3 Hz), -123.39 – -123.62 (m), -123.86 (dq, $J = 15.1$, 8.8, 7.2 Hz), -126.94 (tdd, $J = 18.1$, 7.5, 4.3 Hz). $^{13}\text{C-NMR}$ (75 MHz, CDCl_3) $\delta = 130.0$ (t, $J = 6.3$ Hz), 125.9 (t, $J = 24.3$ Hz), 121.9 – 98.9 (m), 18.1 (t, $J = 4.7$ Hz), 11.2. **IR** (neat, cm^{-1}): 3019, 1618, 1368, 1454, 1428, 1320, 1197, 1148, 1103, 984, 951, 883, 824, 705. **HRMS** (EI) exact mass calc. for $\text{C}_{13}\text{H}_{60}\text{F}_{17}\text{I}$: m/z 611.9237, found: m/z 611.9248 $[\text{M}]^+$.

(3,3,4,4,5,5,6,6,7,7,8,8,9,9,10,10,10-Heptadecafluorodec-1-ene-1,1-diyl)dibenzene (23)

A Schlenk flask was charged with photoadduct **13e** (162 mg, 0.25 mmol, 1.0 equiv), potassium fluoride (30 mg, 0.5 mmol, 2.0 equiv), phenylboronic acid (**22**) (50 mg, 0.40 mmol, 1.6 equiv) and Pd₂dba₃ (5.4 mg, 7.5 μmol, 3.0 mol%) in anh. toluene (1 mL). The reaction mixture was stirred at 80 °C for 16 hours. Afterwards, the yellow solution was diluted with diethyl ether, water was added and the product was extracted with Et₂O (3x 10 mL). The combined organic layers were washed with saturated aqueous Na₂CO₃ (2x 10 mL), followed by brine (1x 10 mL), dried over Na₂SO₄ and concentrated in vacuo. The residue was purified by column chromatography on silica (hexanes) to obtain the product **23** as a white solid (98 mg, 66%).

R_f (hexanes) = 0.56. **Staining**: vanilin (UV active). **¹H-NMR** (300 MHz, CDCl₃) δ = 7.42 – 7.21 (m, 10H), 6.11 (t, *J* = 14.7 Hz, 1H). **¹⁹F-NMR** (282 MHz, CDCl₃) δ = -81.33 (t, *J* = 9.9 Hz, 3F), -104.06 (t, *J* = 11.7 Hz, 2F), -121.78 – -121.91 (m, 2F), -122.33 – -122.68 (m, 4F), -123.18 – -123.74 (m, 4F), -126.22 – -126.98 (m, 2F). **¹³C-NMR** (75 MHz, CDCl₃) δ = 154.4, 140.7, 137.5, 129.5, 129.0, 128.5, 128.3, 127.9, 127.9, 112.8. **IR** (neat, cm⁻¹): 3071, 1653, 1601, 1580, 1493, 1447, 1369, 1327, 1244, 1194, 1144, 1099, 1030, 978, 864, 785, 754, 704, 694, 652. **HRMS** (EI) exact mass calc. for C₂₂H₁₁F₁₇: *m/z* 598.0589, found: *m/z* 598.0596 [M]⁺. **mp**: 67 °C.

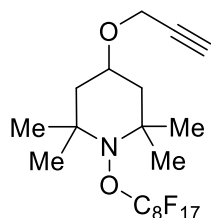
1-((2,2,3,3,4,4,5,5,6,6,7,7,8,8,9,9,9-Heptadecafluorononyl)oxy)-2,2,6,6-tetramethylpiperidine (38)

Following GP-A, **38** was prepared using 2,2,6,6-tetramethylpiperidinyloxyl (**37**) (39 mg, 0.3 mmol), styrene (**12a**) (28 μL, 0.3 mmol, 1.0 equiv), C₈F₁₇I (**4d**) (132 μL, 0.5 mmol, 2.0 equiv) and [Cu(dap)₂]Cl (2.2 mg, 0.3 μmol, 1.0 mol%). Chromatography on silica (hexanes) afforded **38** as white solid (90 mg, 52%).

R_f (hexanes) = 0.55. **Staining**: KMnO₄ (UV active). **¹H-NMR** (300 MHz, CDCl₃) δ = 1.64 – 1.56 (m, 5H), 1.37 (qd, *J* = 5.7, 4.7, 3.1 Hz, 1H), 1.18 (s, 12H). **¹⁹F-NMR** (282 MHz, CDCl₃) δ = -79.02 (p, *J* = 6.2, 5.3 Hz, 2F), -81.30 (t, *J* = 9.9 Hz, 3F), -122.26 (dp, *J* = 11.5, 4.0 Hz, 2F), -122.35 – -122.52 (m, 4F), -122.98 – -123.43 (m, 2F), -124.13 (ddt, *J* = 14.5, 9.2, 4.3 Hz, 2F), 126.66 (dq, *J* = 14.3, 6.7, 5.1 Hz, 2F). **¹³C-NMR** (75 MHz, CDCl₃) δ = 62.1, 40.6, 33.6 (t,

$J = 5.3$ Hz), 20.8, 17.0. **IR** (neat, cm^{-1}): 2986, 2945, 1681, 1469, 1372, 1334, 1238, 1200, 1133, 999, 880, 815, 775, 723. **HRMS** (ESI) exact mass calc. for $\text{C}_{18}\text{H}_{21}\text{F}_{17}\text{NO}$: m/z 589.1190, found: m/z 589.1183 $[\text{M}+\text{H}]^+$. **mp**: 40 °C.

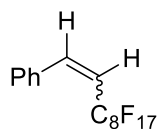
2,2,6,6-Tetramethyl-1-((perfluorooctyl)oxy)-4-(prop-2-yn-1-yloxy)piperidine (40)



Following GP-A, **40** was prepared using 1-piperidinyloxy-2,2,6,6-tetramethyl-4-(2-propynyloxy) (**39**) (105 mg, 0.5 mmol, 1.0 equiv), phenylacetylene (**12b**) (51 mg, 0.5 mmol, 1.0 equiv), $\text{C}_8\text{F}_{17}\text{I}$ (**4d**) (265 μL , 1.0 mmol, 2.0 equiv) and $[\text{Cu}(\text{dap})_2]\text{Cl}$ (4.4 mg, 0.5 μmol , 1.0 mol%). Chromatography on silica (hexanes/EtOAc 9:1) afforded **40** as yellow solid (252 mg, 81%, rotamere present).

R_f (hexanes-EtOAc, 3:1) = 0.85. **Staining**: vanilin (UV active). **$^1\text{H-NMR}$** (300 MHz, CDCl_3) δ = 4.19 (dd, $J = 8.9, 1.5$ Hz, 2H), 3.76 (dtt, $J = 66.5, 11.5, 4.2$ Hz, 1H), 2.43 (t, $J = 2.4$ Hz, 1H), 2.07 – 1.90 (m, 2H), 1.72 – 1.33 (m, 3H), 1.22 (dd, $J = 6.0, 2.3$ Hz, 12H). **$^{19}\text{F-NMR}$** (282 MHz, CDCl_3) δ = -79.37 (t, $J = 7.2$ Hz, 2F), -81.22 (t, $J = 9.9$ Hz, 3F), -122.07 – -122.52 (m, 6F), -123.24 (s, 2F), -124.08 (p, $J = 9.4, 8.3$ Hz, 2F), -126.62 (tq, $J = 10.5, 5.2, 4.6$ Hz, 2F). **$^{13}\text{C-NMR}$** (75 MHz, CDCl_3) δ = 81.7, 79.8, 74.9, 74.4, 68.7, 68.6, 62.2, 62.1, 55.5, 55.4, 45.4, 45.1, 33.6 (t, $J = 5.2$ Hz), 21.7, 21.6. **IR** (neat, cm^{-1}): 3230, 3014, 2984, 2943, 1447, 1387, 1373, 1354, 1332, 1201, 1182, 1150, 1135, 1000, 880, 728, 667. **HRMS** (ESI) exact mass calc. for $\text{C}_{21}\text{H}_{23}\text{F}_{17}\text{NO}_2$: m/z 644.1403, found: m/z 644.1295 $[\text{M}+\text{H}]^+$. **mp**: 46 °C.

(3,3,4,4,5,5,6,6,7,7,8,8,9,9,10,10,10-Heptafluorodec-1-en-1-yl)benzene (41)^[26]



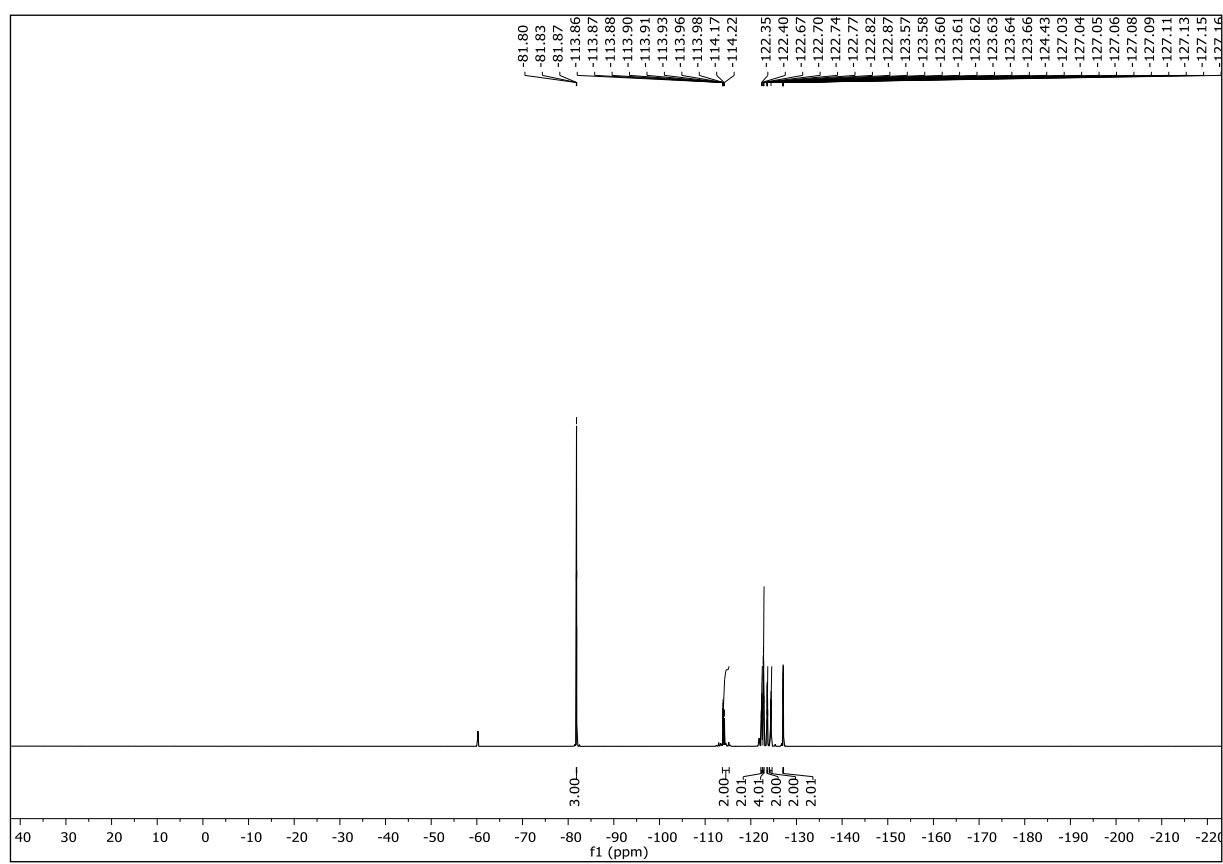
To a mixture of photoadduct **13e** (324 mg, 0.5 mmol, 1.0 equiv), zinc (131 mg, 2.0 mmol, 4.0 equiv) and AgOAc (10 mg, 60 μ mol, 12 mol%) in acetic acid (1 mL) was added dropwise concentrated HCl (0.1 mL, 37 wt%) at room temperature. During the addition of hydrochloric acid, a black solid precipitated from the reaction mixture. The reaction mixture was further stirred for 30 min. Afterwards, the beige suspension was quenched with water (5 mL), and CH_2Cl_2 (10 mL) was added. The product was extracted with CH_2Cl_2 (3x 10 mL). The combined organic layers were washed with saturated aqueous Na_2CO_3 (3x 10 mL), followed by brine (1x 10 mL), dried over Na_2SO_4 and concentrated in vacuo. The residue was purified by column chromatography on silica (hexanes) to obtain the product **41** as a white solid (184 mg, 70%) in a diastereomeric ratio of $E/Z = 92:08$.

R_f (hexanes) = 0.89. **Staining:** KMnO_4 (UV active). **$^1\text{H-NMR}$** (600 MHz, CDCl_3) δ = 7.39 – 7.28 (m, 5H, *Z*-isomer), 7.44 – 7.17 (m, 6H, *E*-isomer), 7.14 (dt, J = 12.8, 3.0 Hz, 1H, *Z*-isomer), 6.21 (dt, J = 16.2, 12.2 Hz, 1H, *E*-isomer), 5.75 (q, J = 12.8 Hz, 1H, *Z*-isomer).

3.4. NMR Spectra

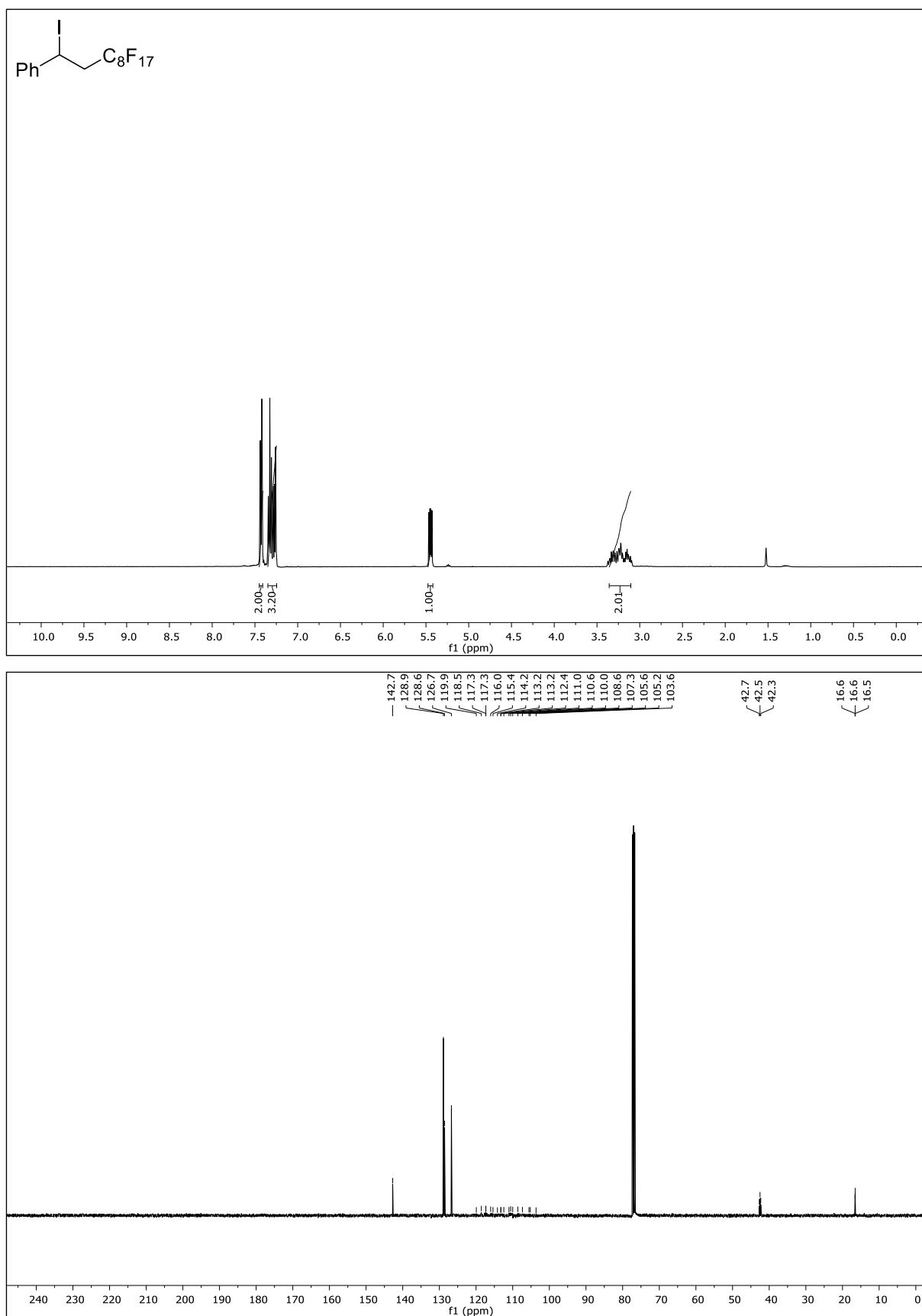
^1H -NMR	first image
^{13}C -NMR	second image
^{19}F -NMR	third image

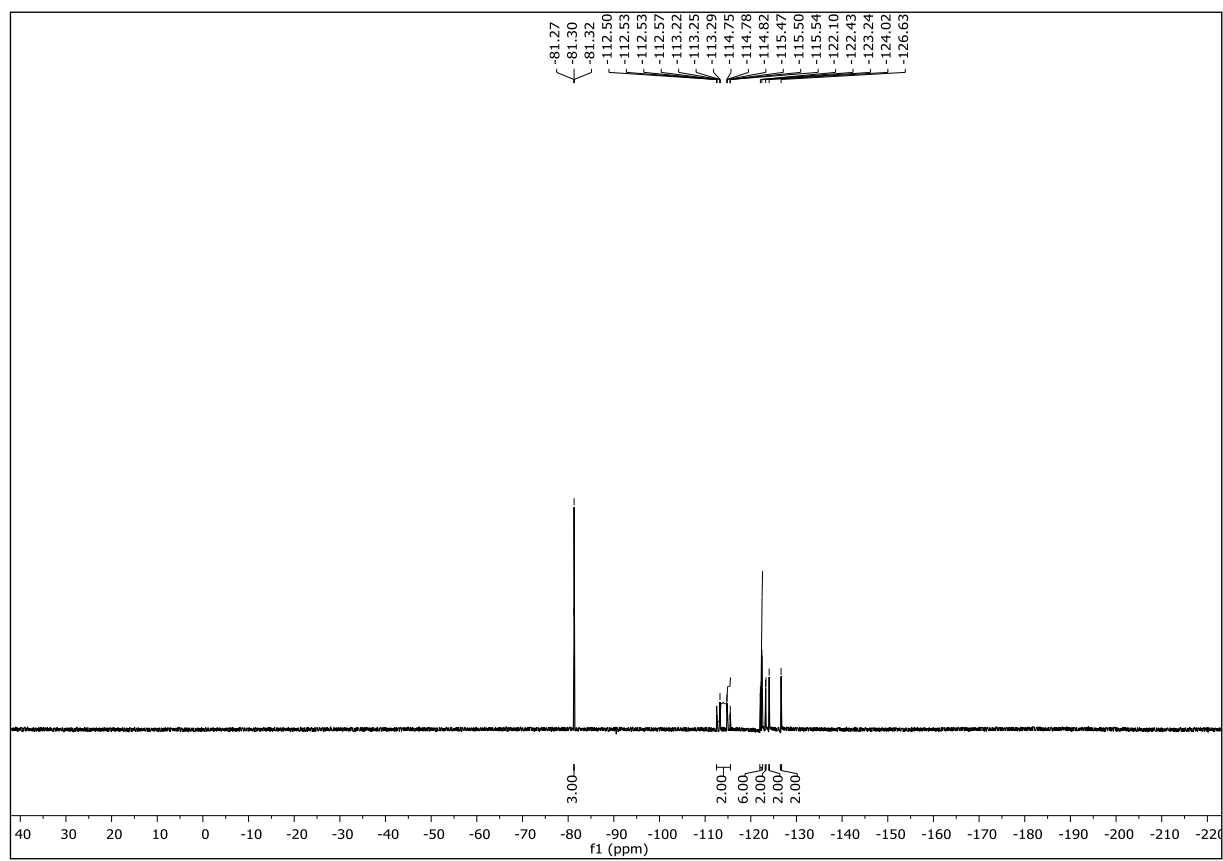




NMR-Solvent: CDCl₃

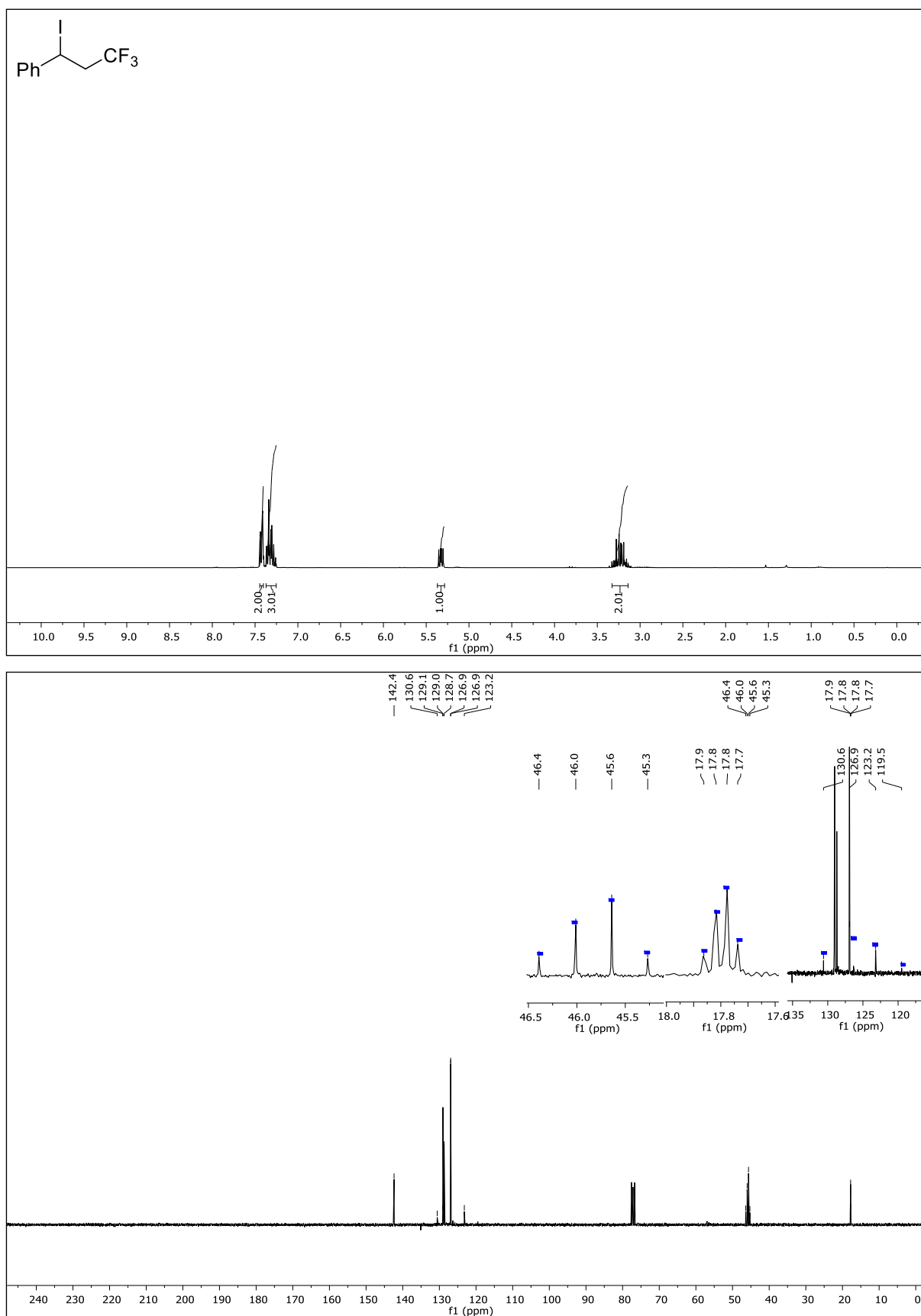
(3,3,4,4,5,5,6,6,7,7,8,8,9,9,10,10,10-Heptadecafluoro-1-iododecyl)benzene (11c)

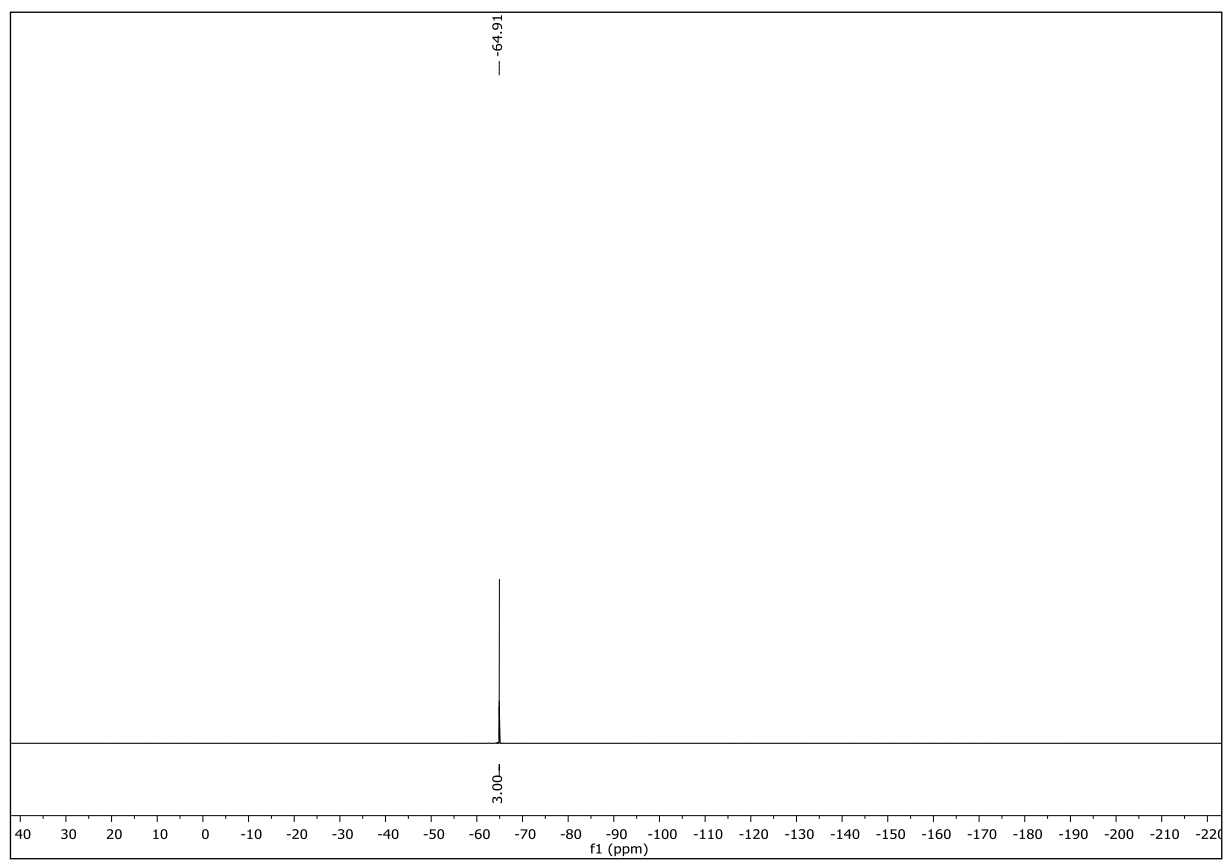




NMR-Solvent: CDCl_3

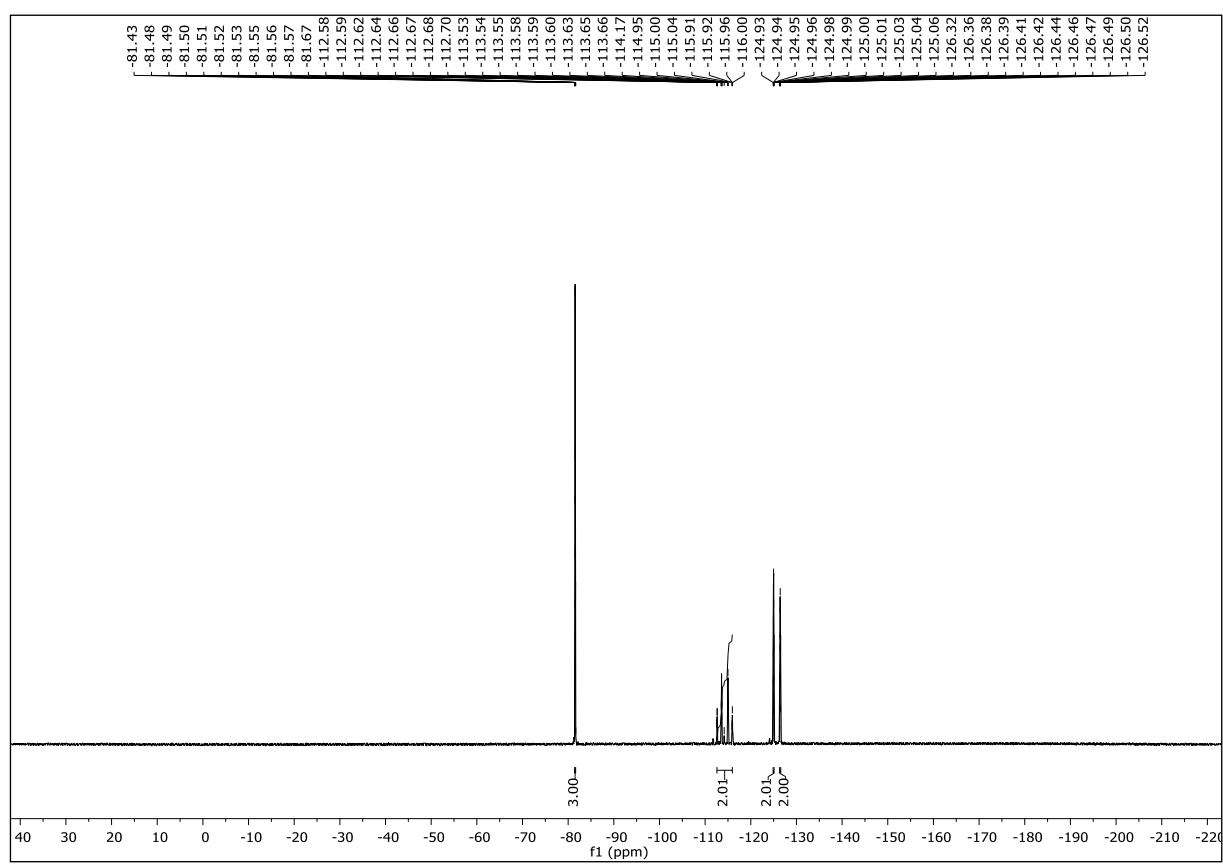
(3,3,3-Trifluoro-1-iodopropyl)benzene (13a)





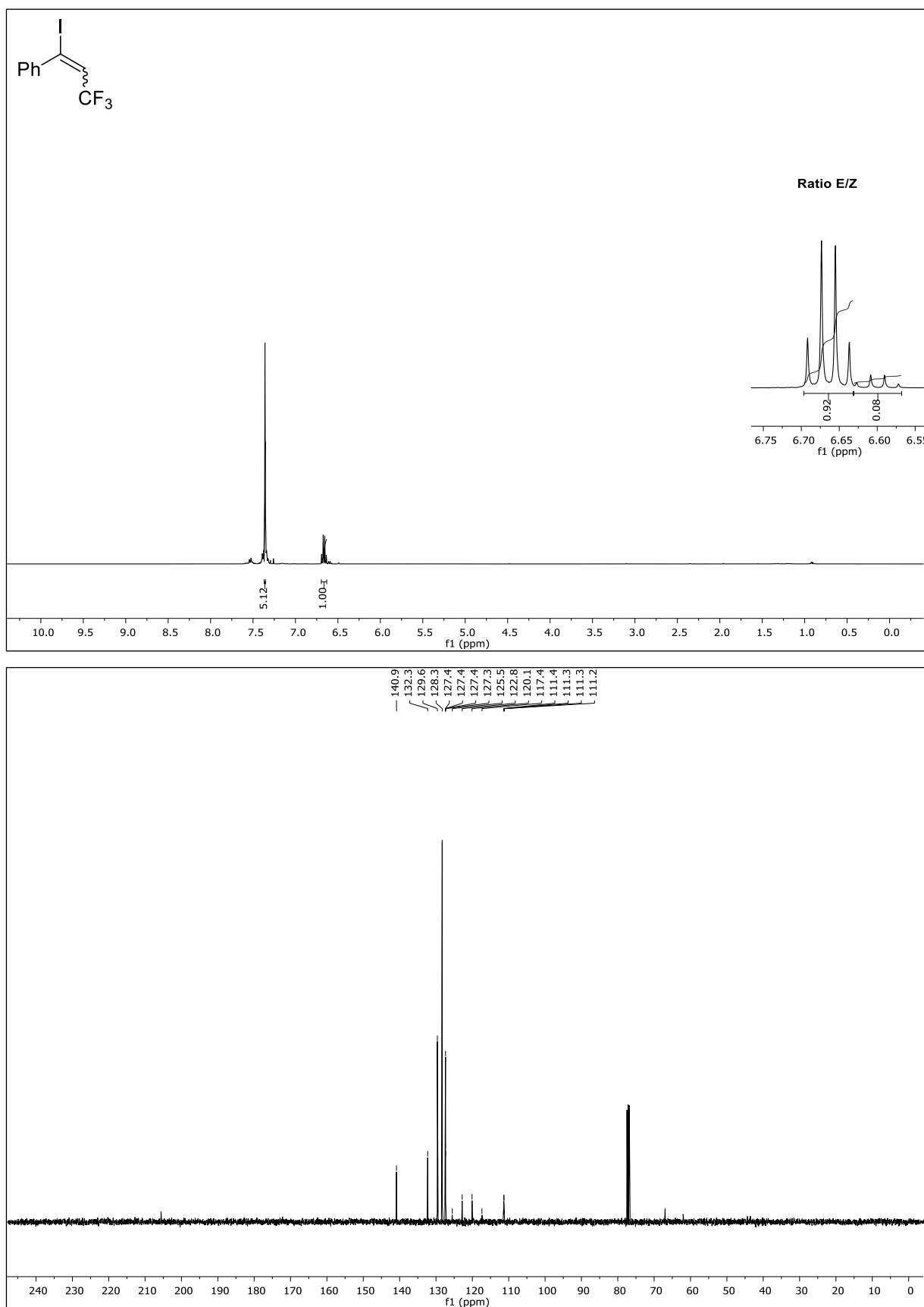
NMR-Solvent: CDCl_3

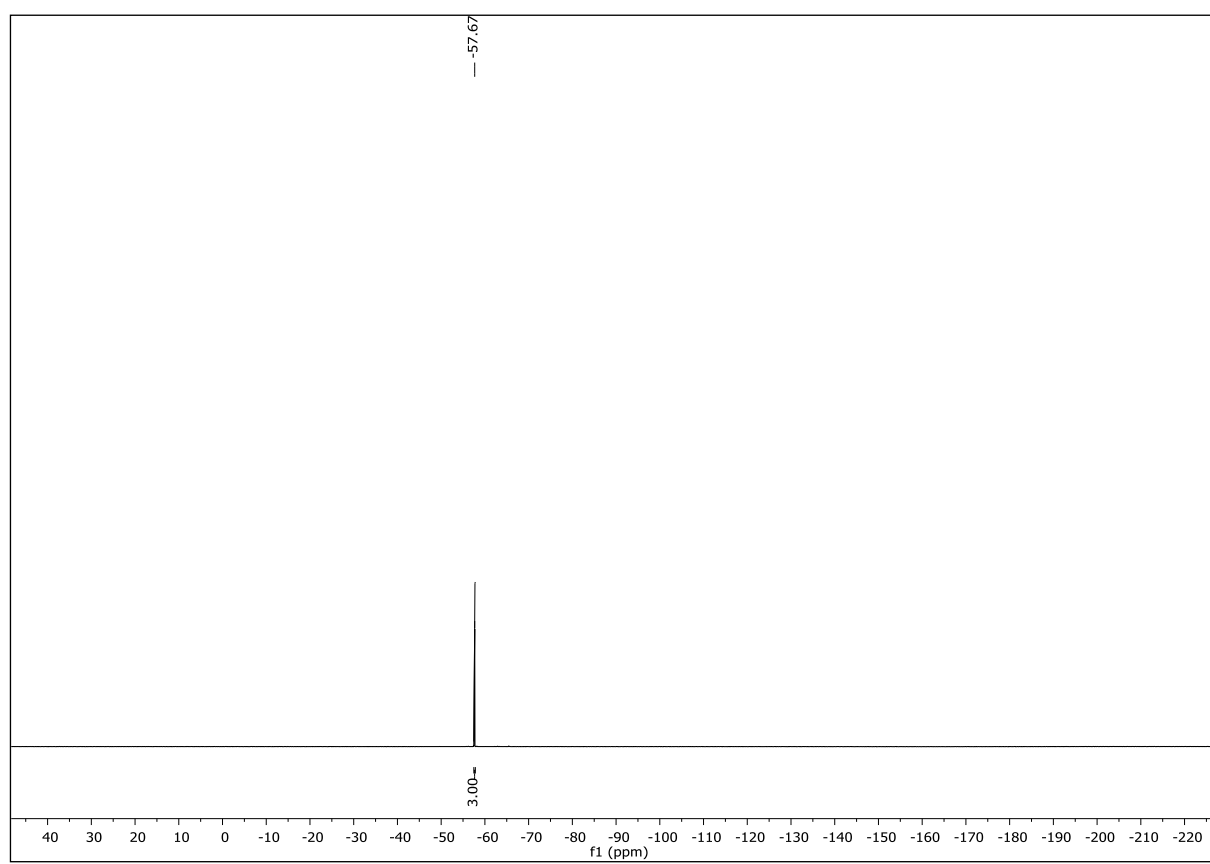




NMR-Solvent: CDCl_3

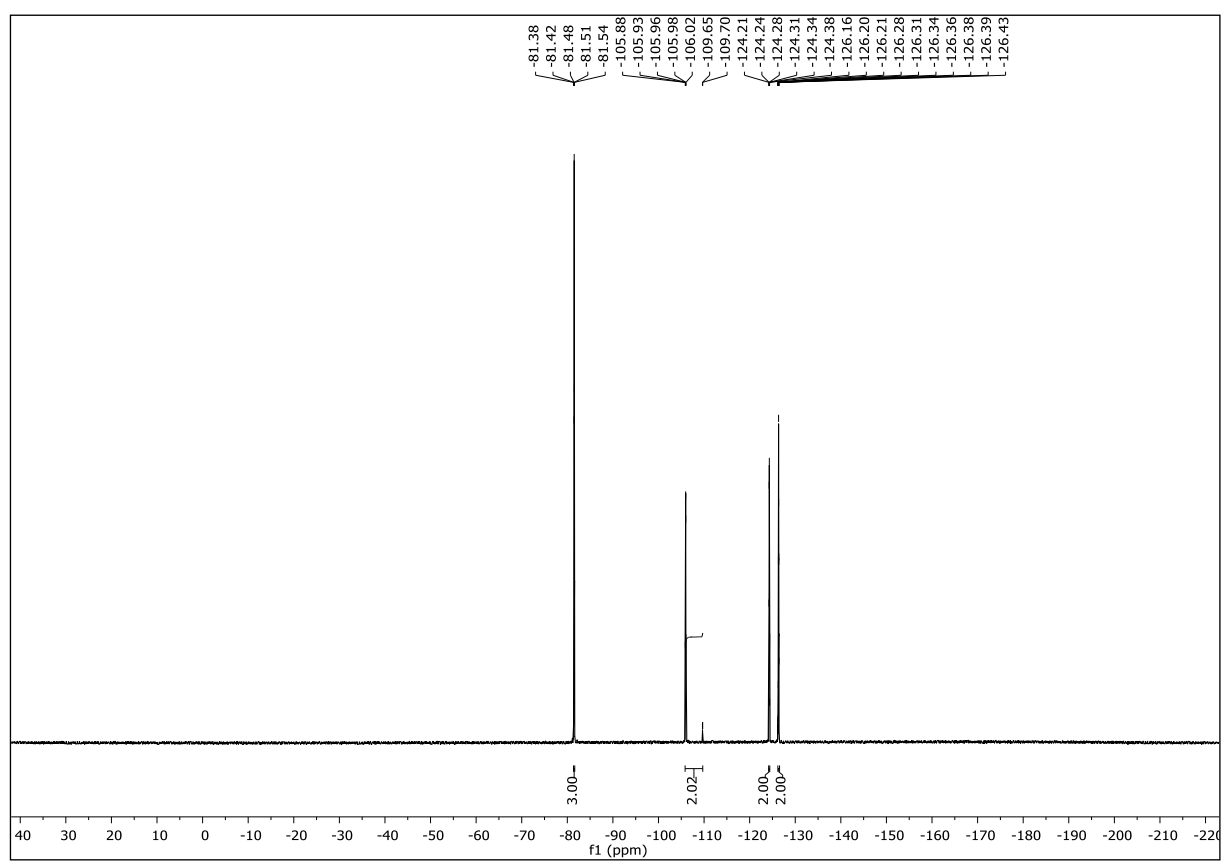
(3,3,3-Trifluoro-1-iodoprop-1-en-1-yl)benzene (13c)





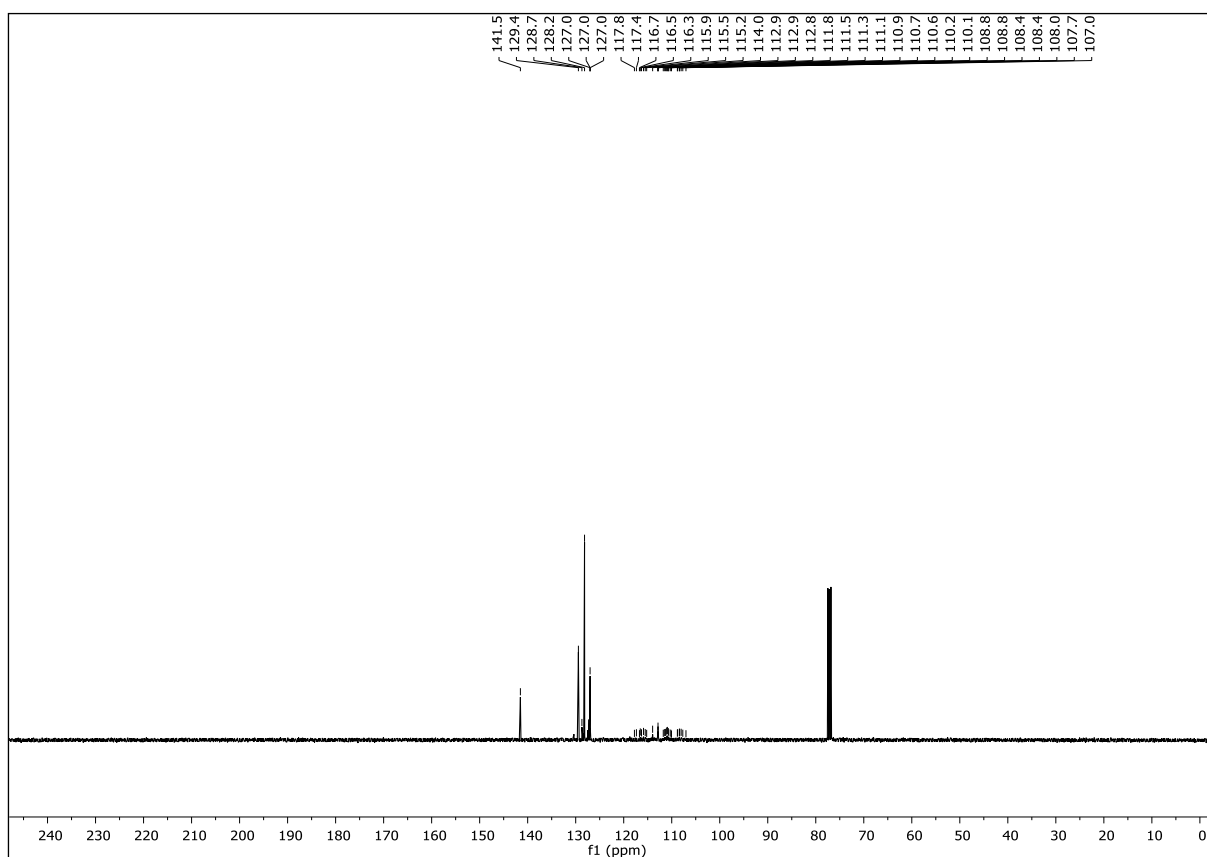
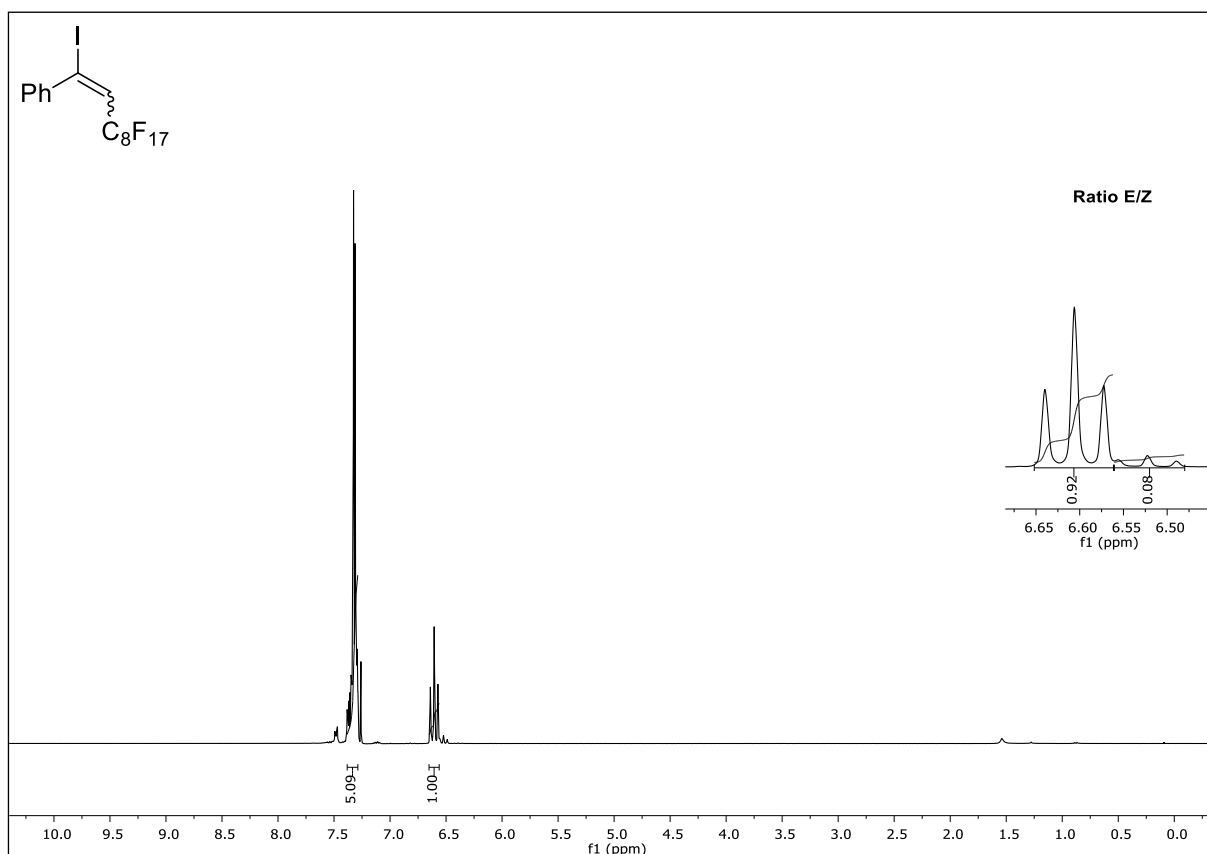
NMR-Solvent: CDCl_3

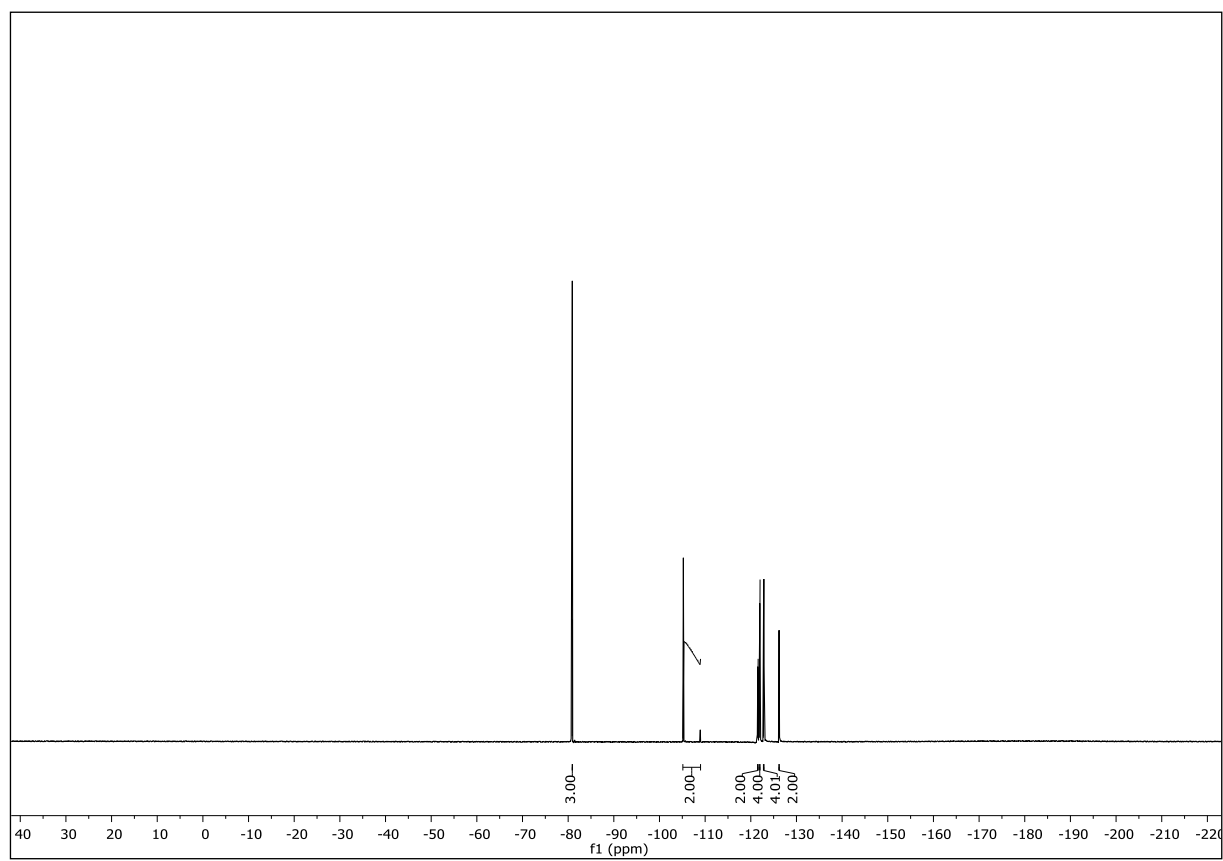




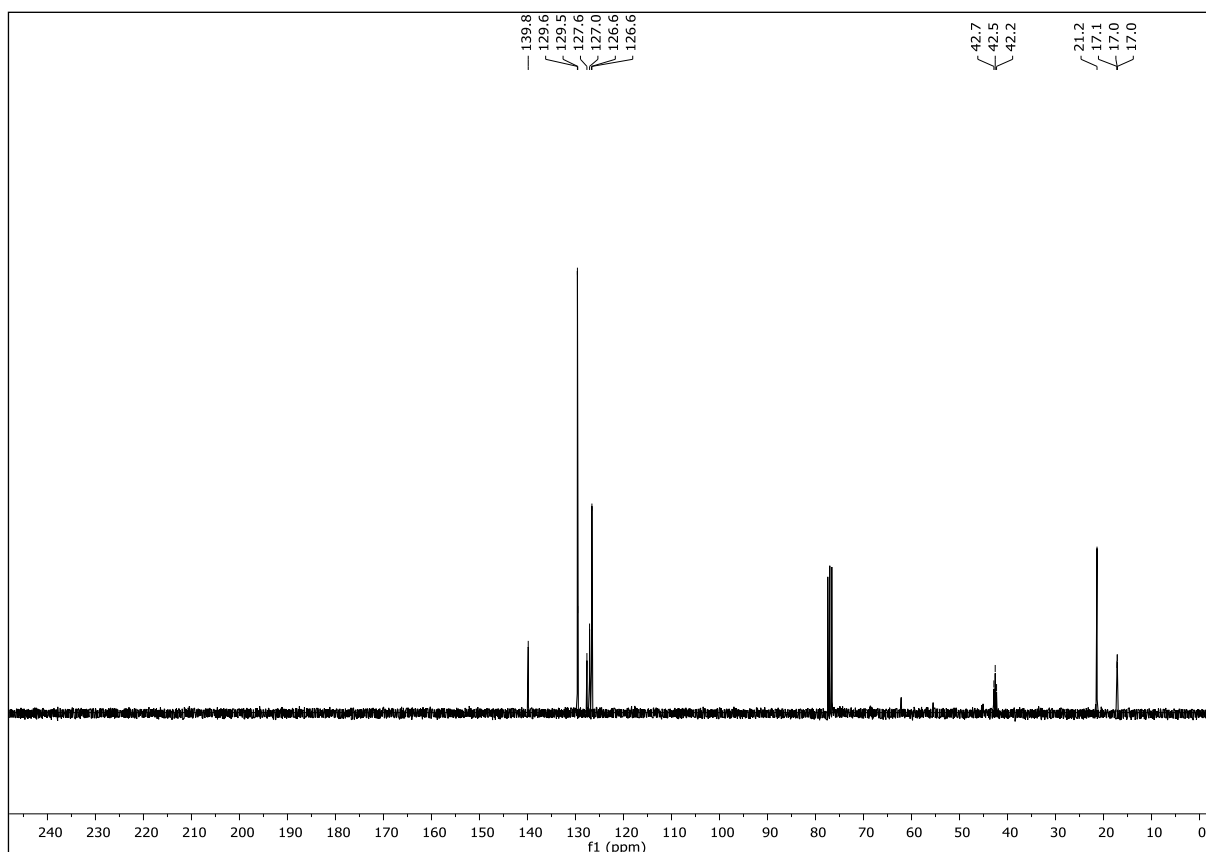
NMR-Solvent: CDCl₃

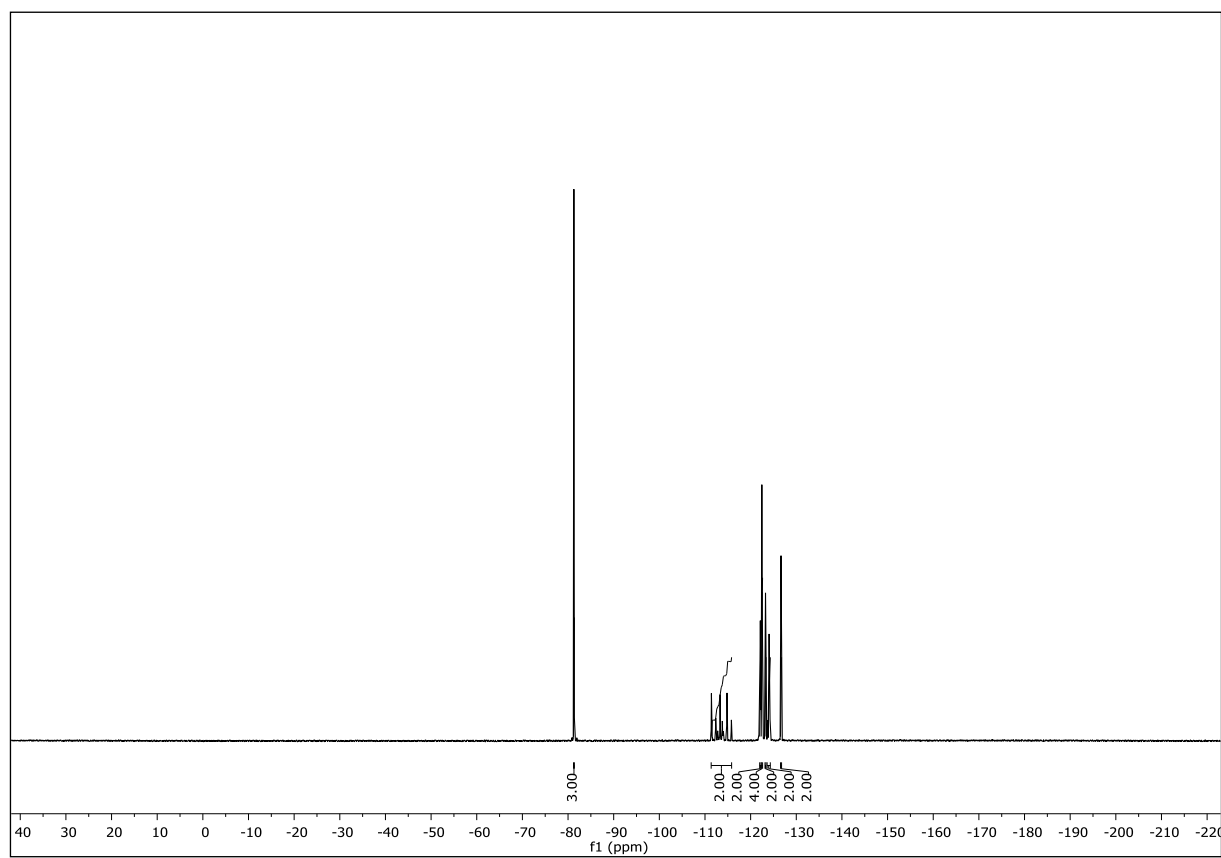
(3,3,4,4,5,5,6,6,7,7,8,8,9,10,10,10-Heptafluoro-1-iododec-1-en-1-yl)benzene (13e)





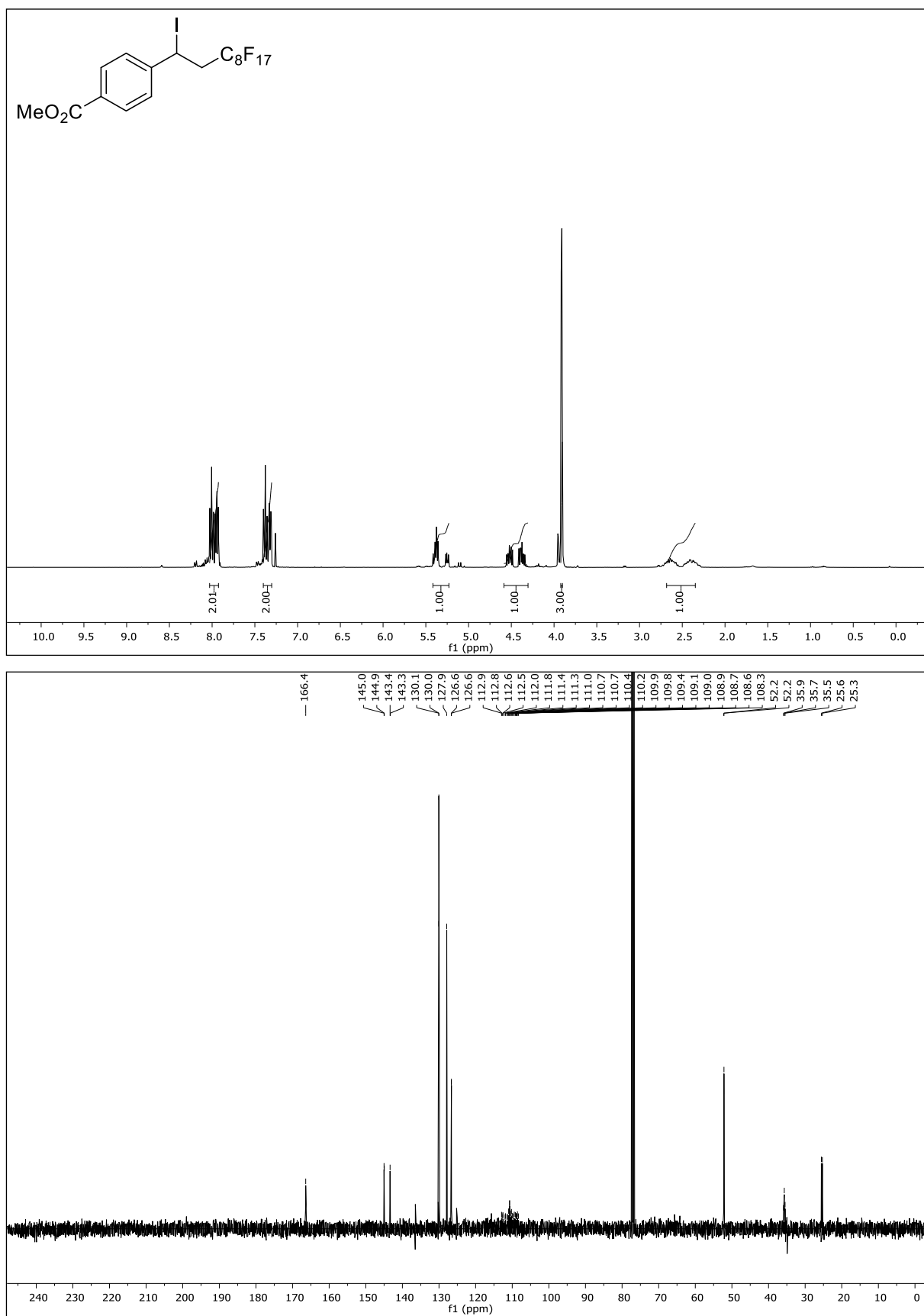
NMR-Solvent: CDCl_3

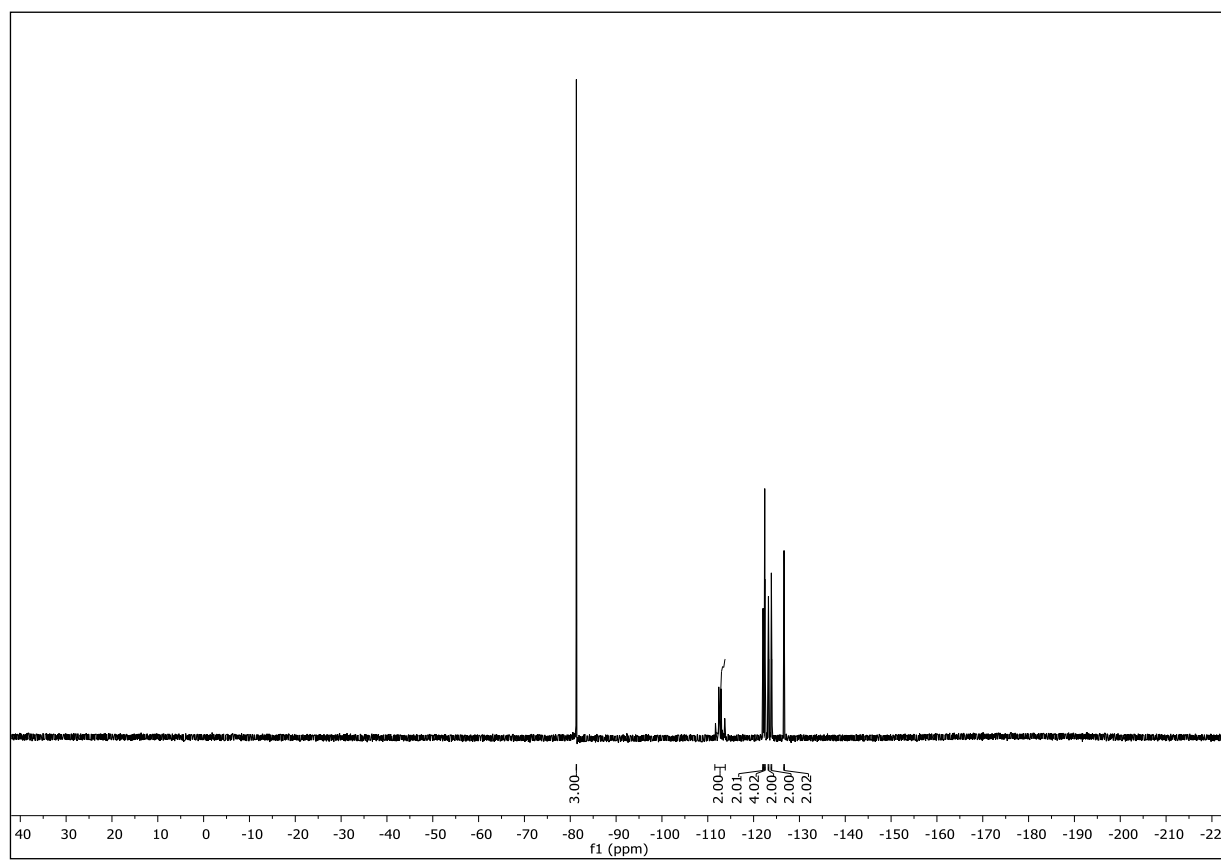




NMR-Solvent: CDCl_3

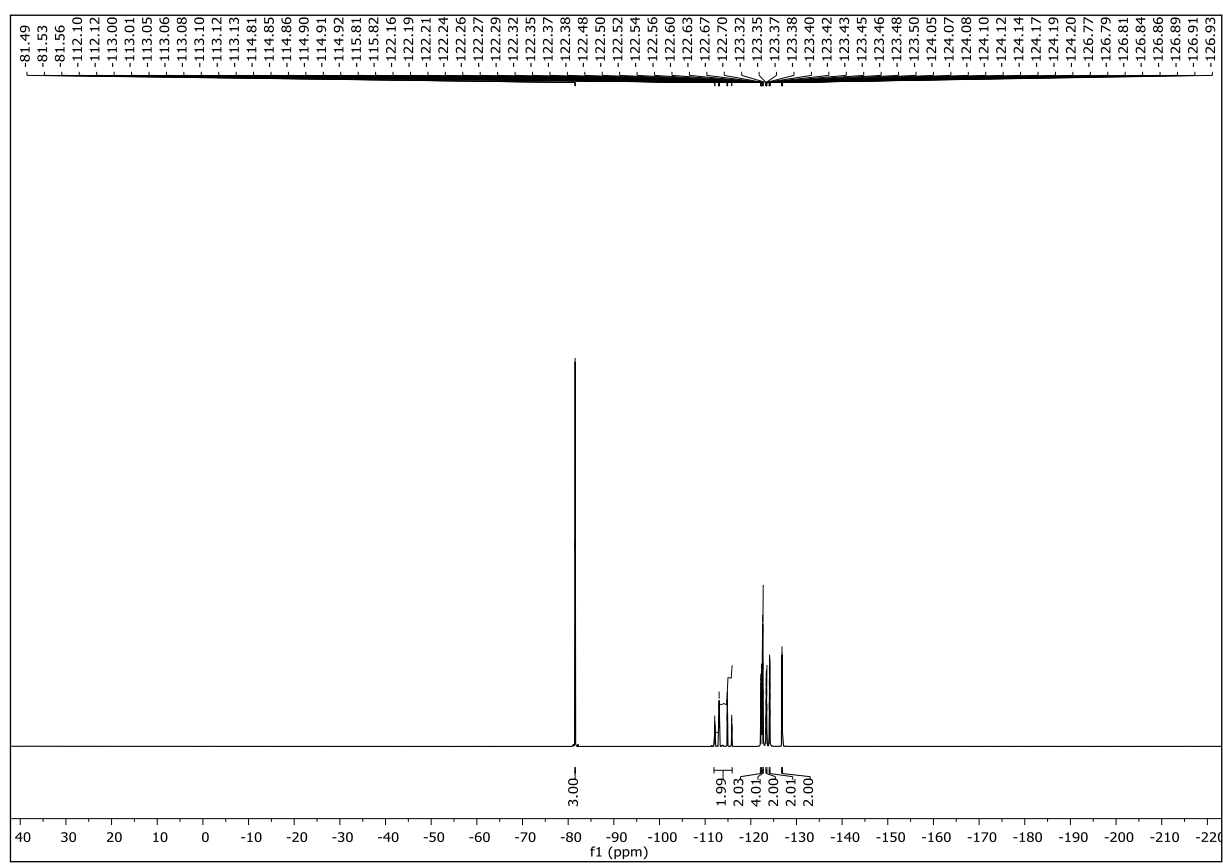
Methyl 4-(3,3,4,4,5,5,6,6,7,7,8,8,9,9,10,10,10-heptafluoro-1-iododecyl)benzoate (15b)





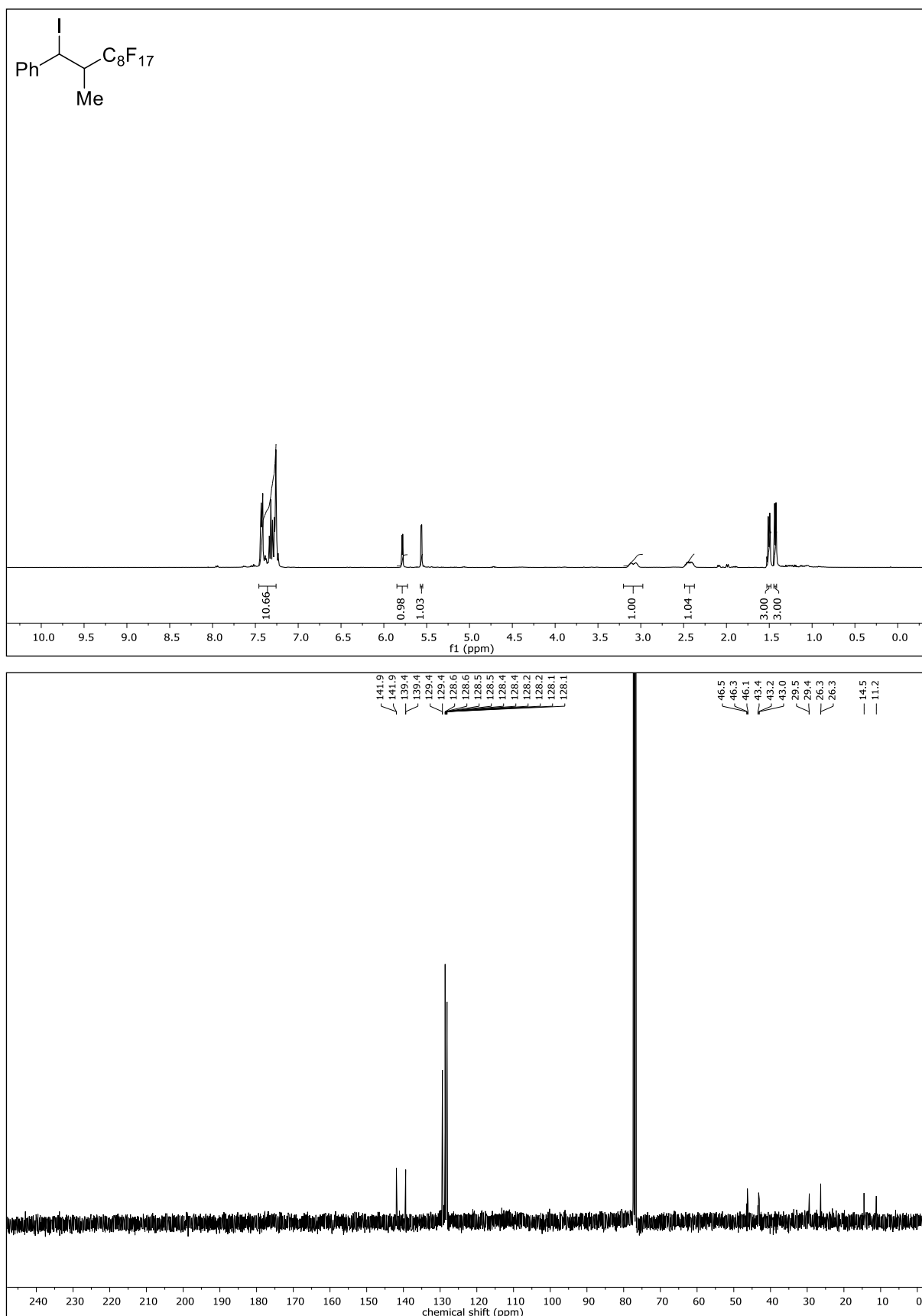
NMR-Solvent: CDCl_3

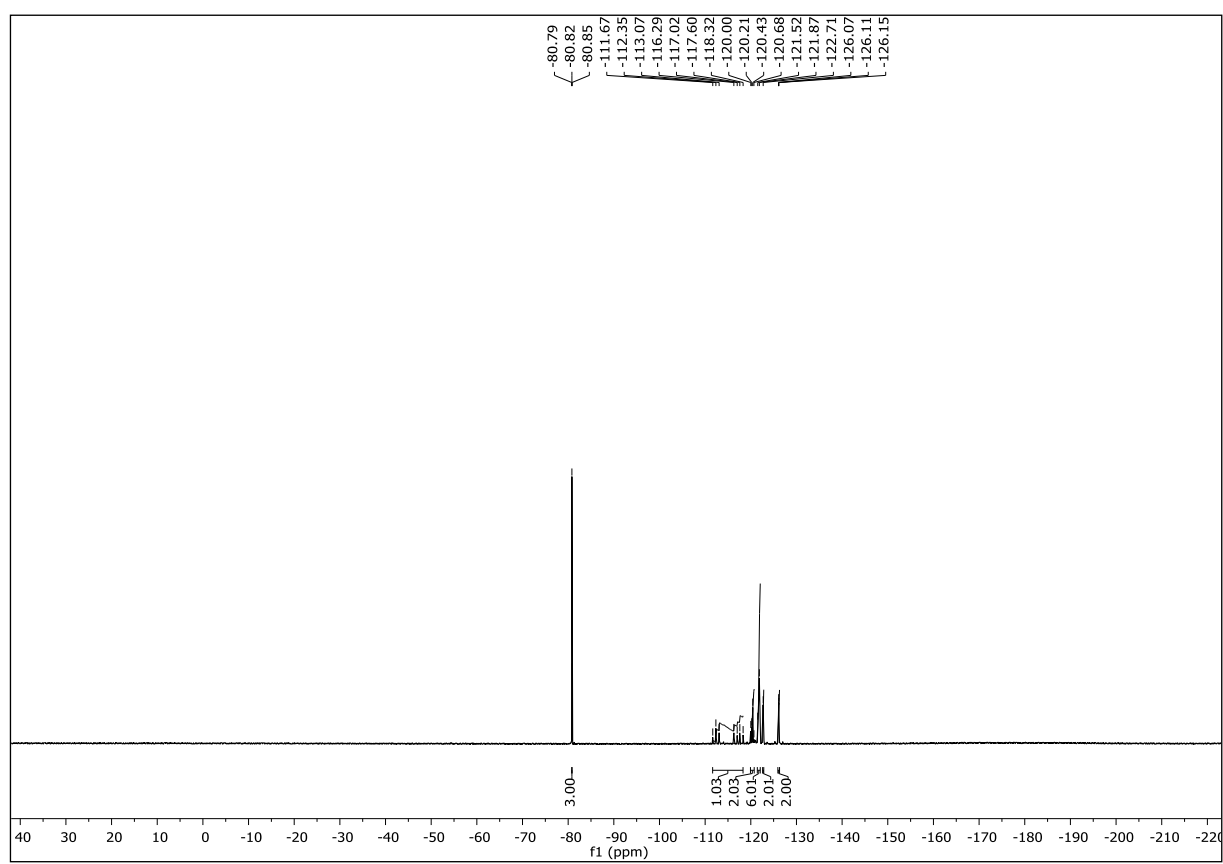




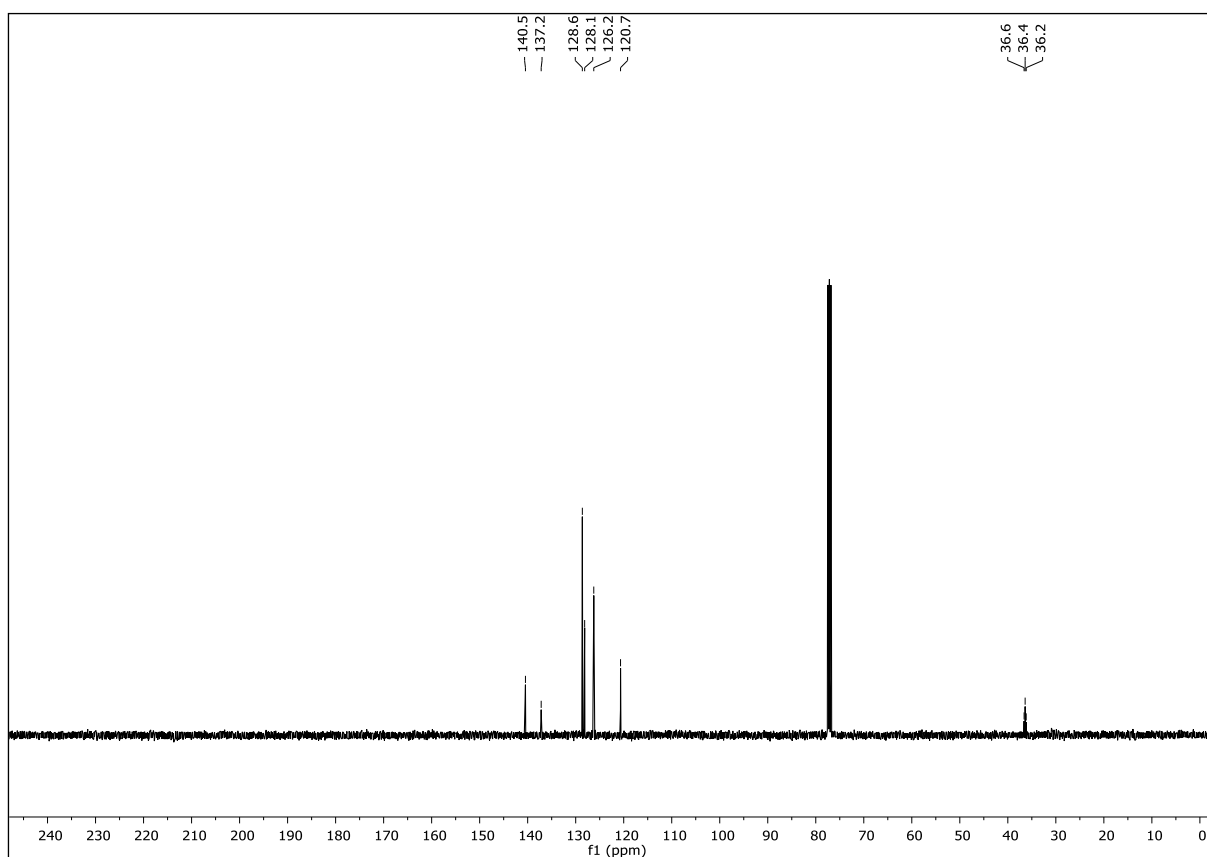
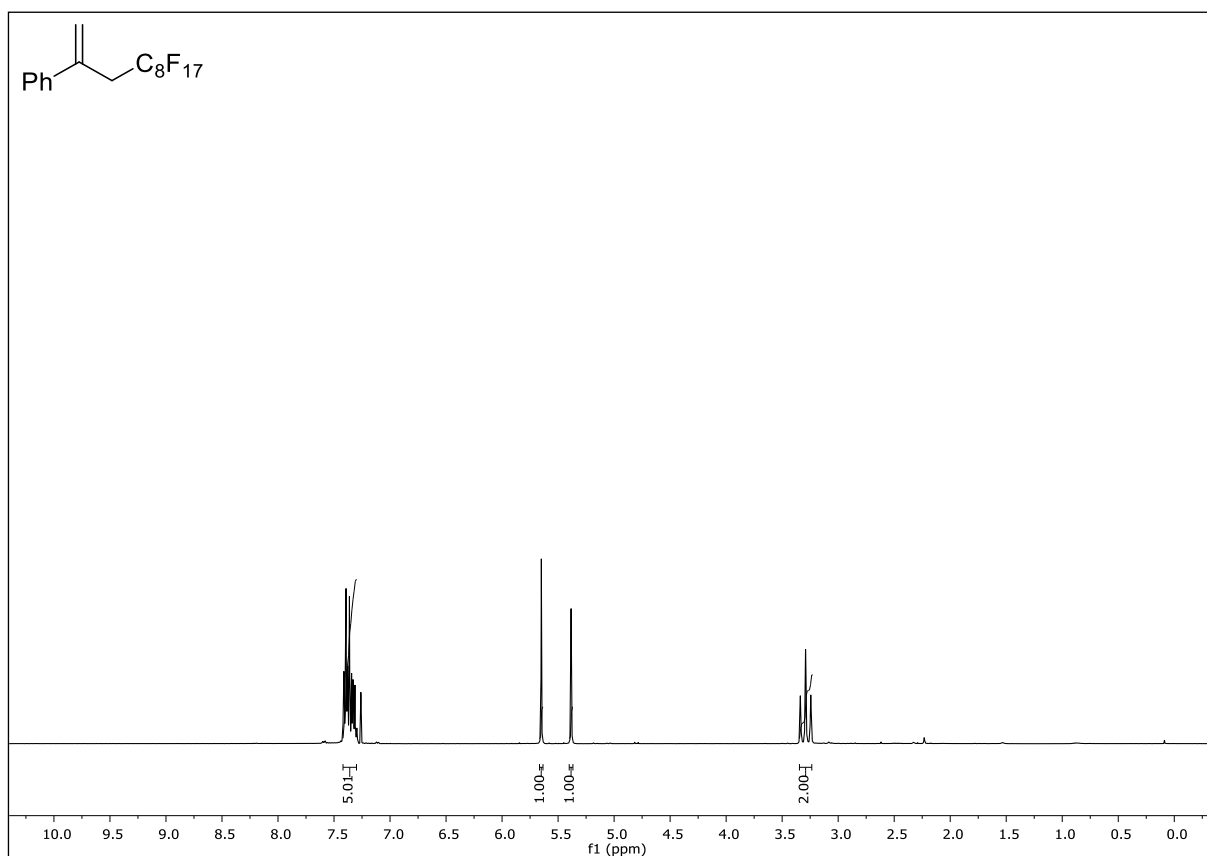
NMR-Solvent: CDCl_3

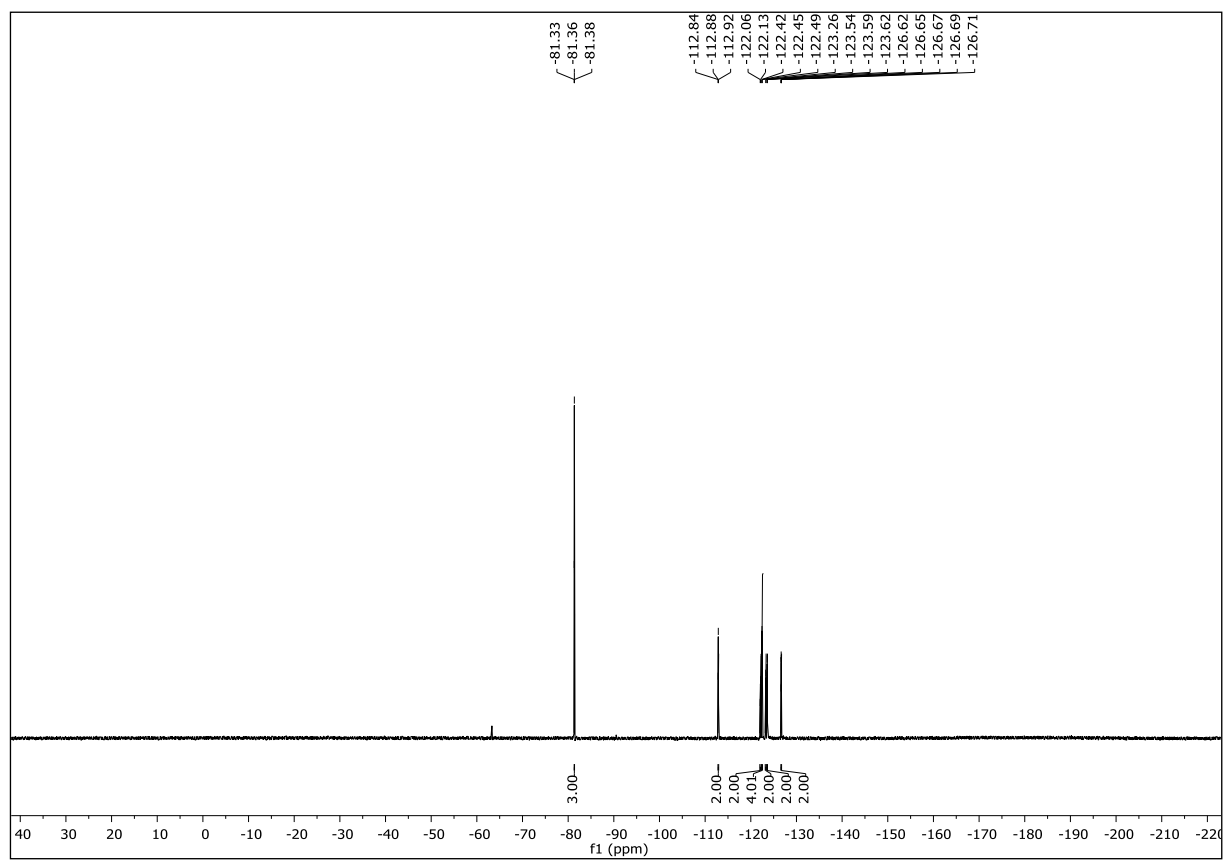
(3,3,4,4,5,5,6,6,7,7,8,8,9,10,10,10-Heptadecafluoro-1-iodo-2-methyldecyl)benzene (15e)





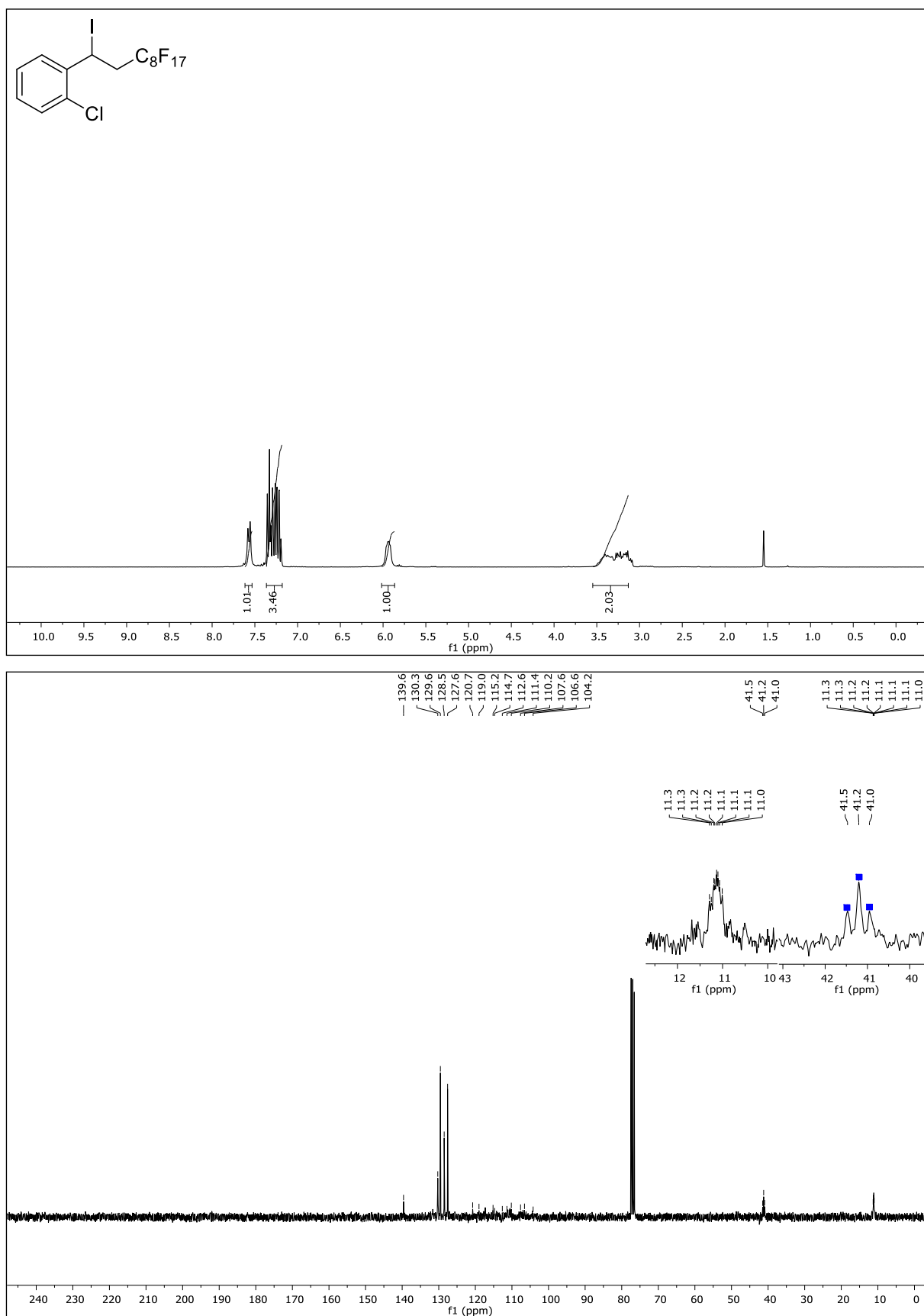
NMR-Solvent: CDCl_3

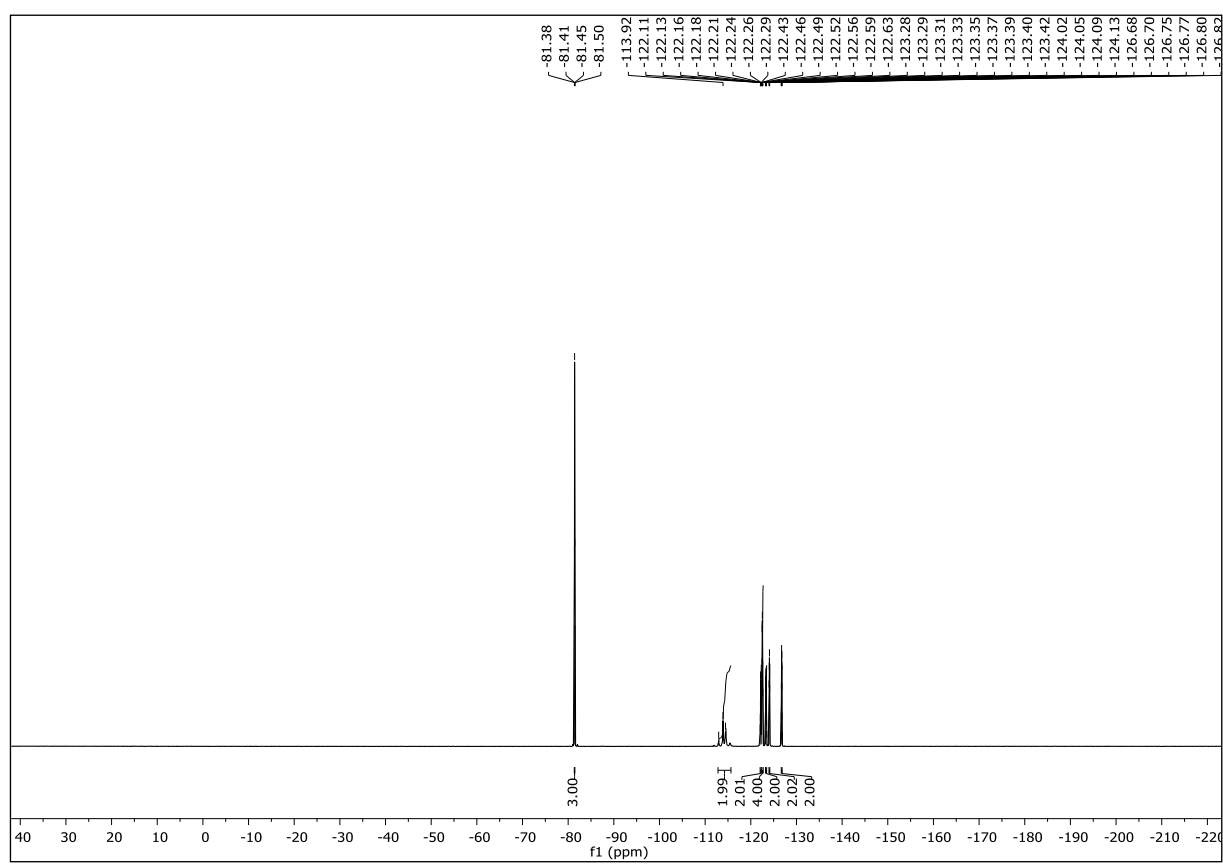




NMR-Solvent: CDCl₃

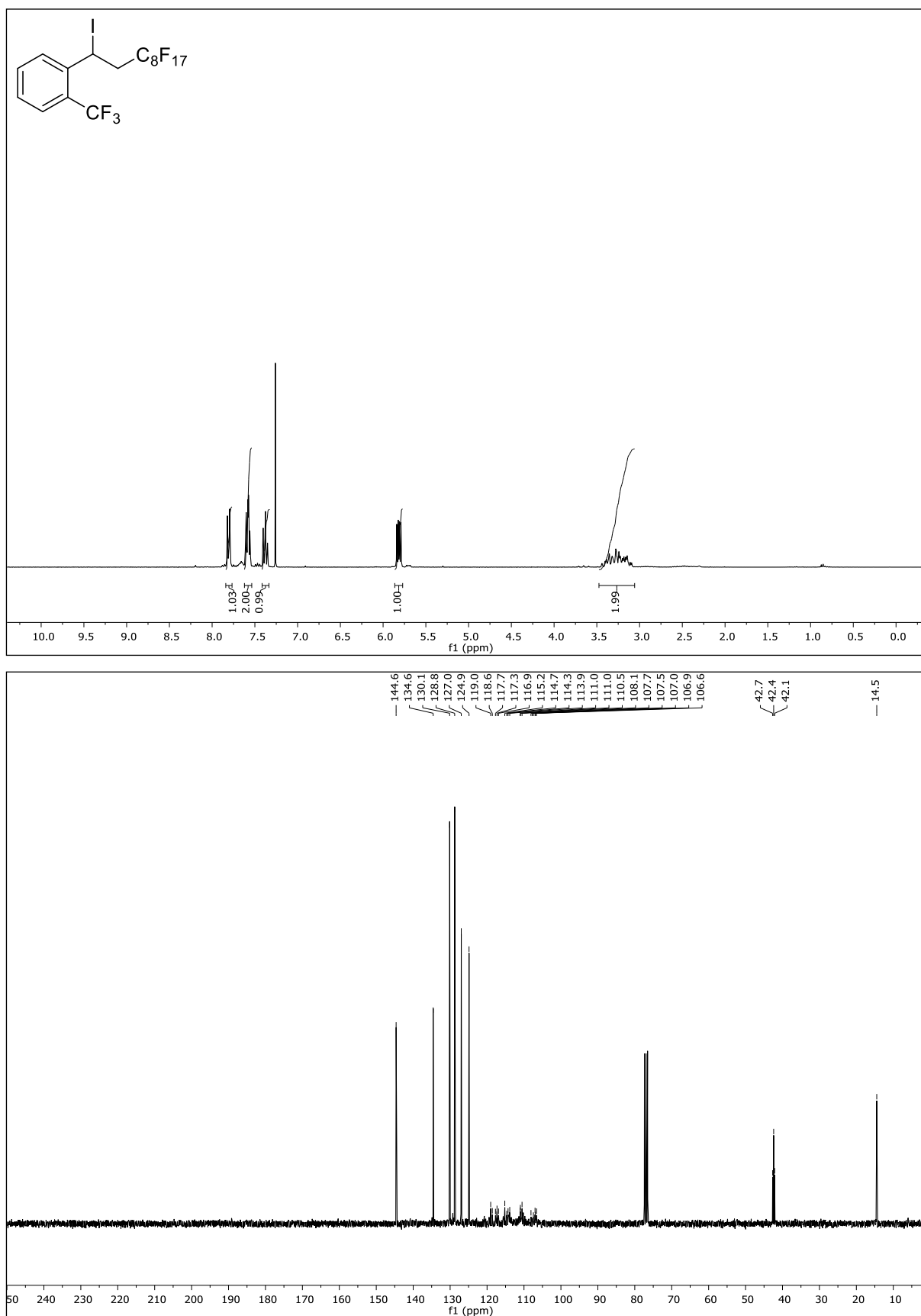
1-Chloro-2-(3,3,4,4,5,5,6,6,7,7,8,8,9,9,10,10,10-heptafluoro-1-iododecyl)benzene (15g)

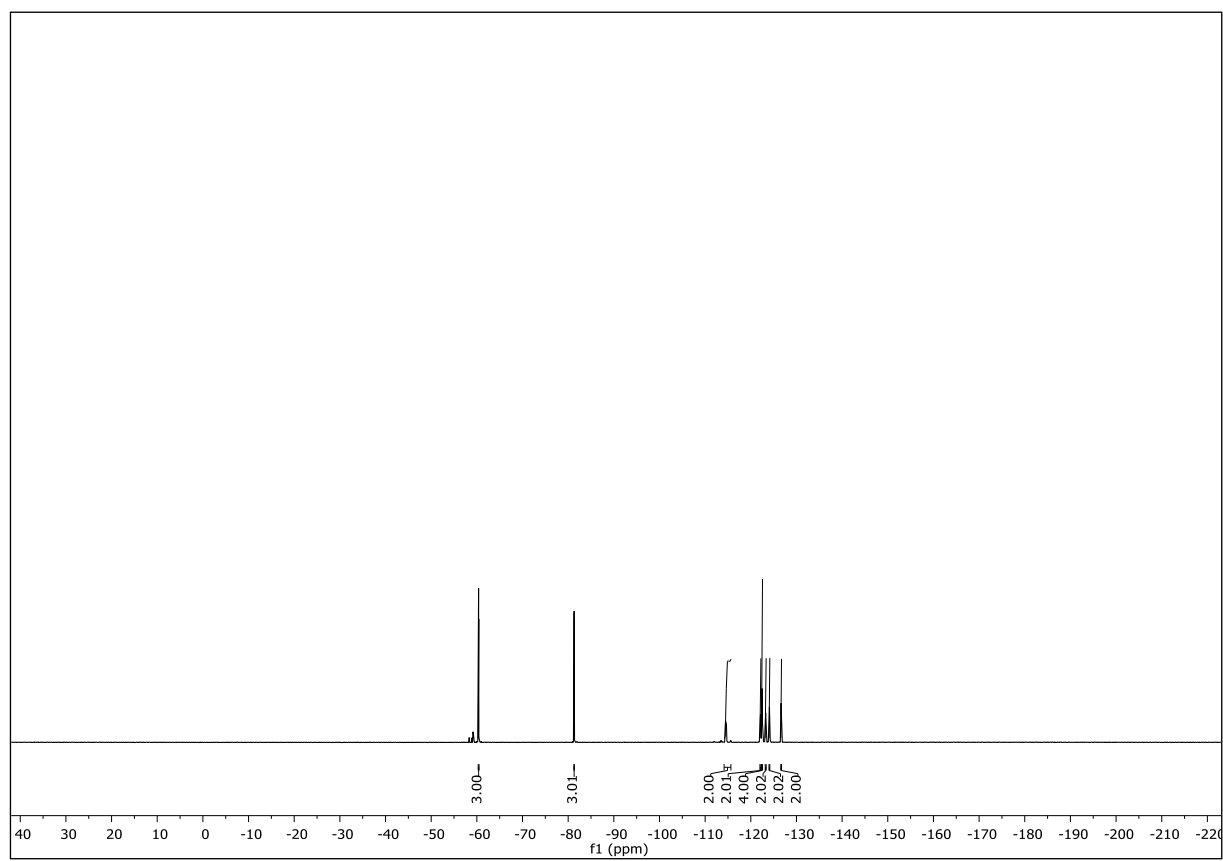




NMR-Solvent: CDCl_3

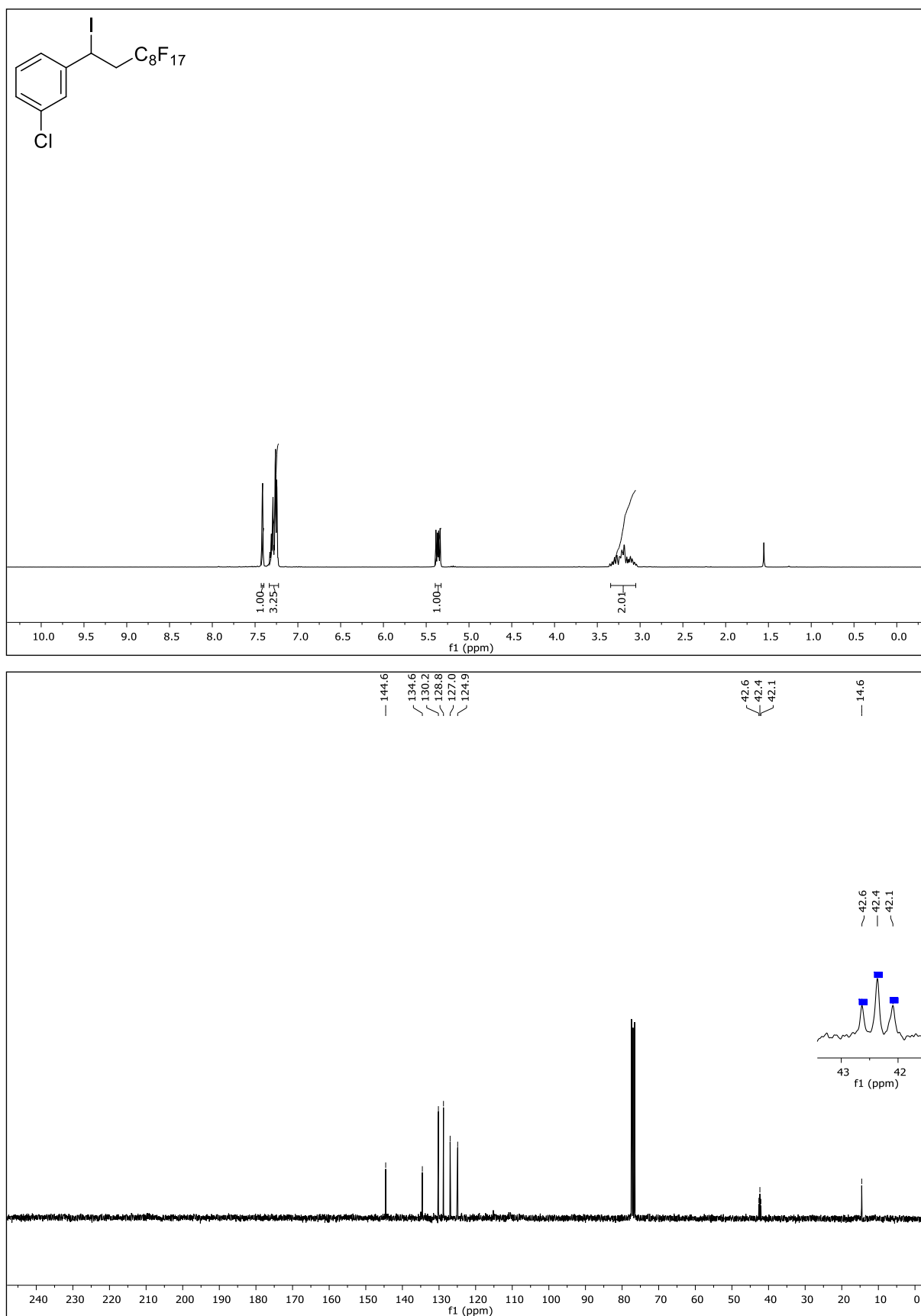
1-(3,3,4,4,5,5,6,6,7,7,8,8,9,9,10,10,10-Heptafluoro-1-iododecyl)-2-(trifluoromethyl) benzene (15h)

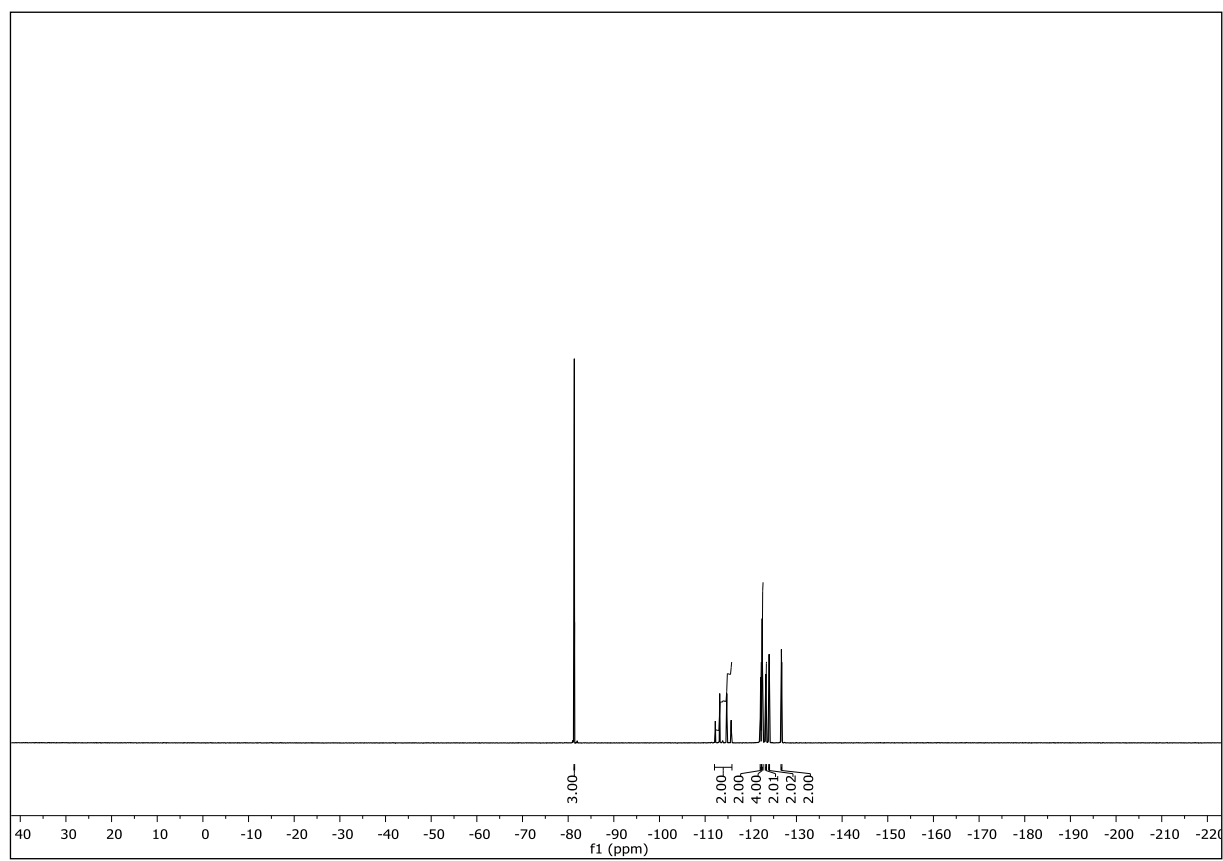




NMR-Solvent: CDCl_3

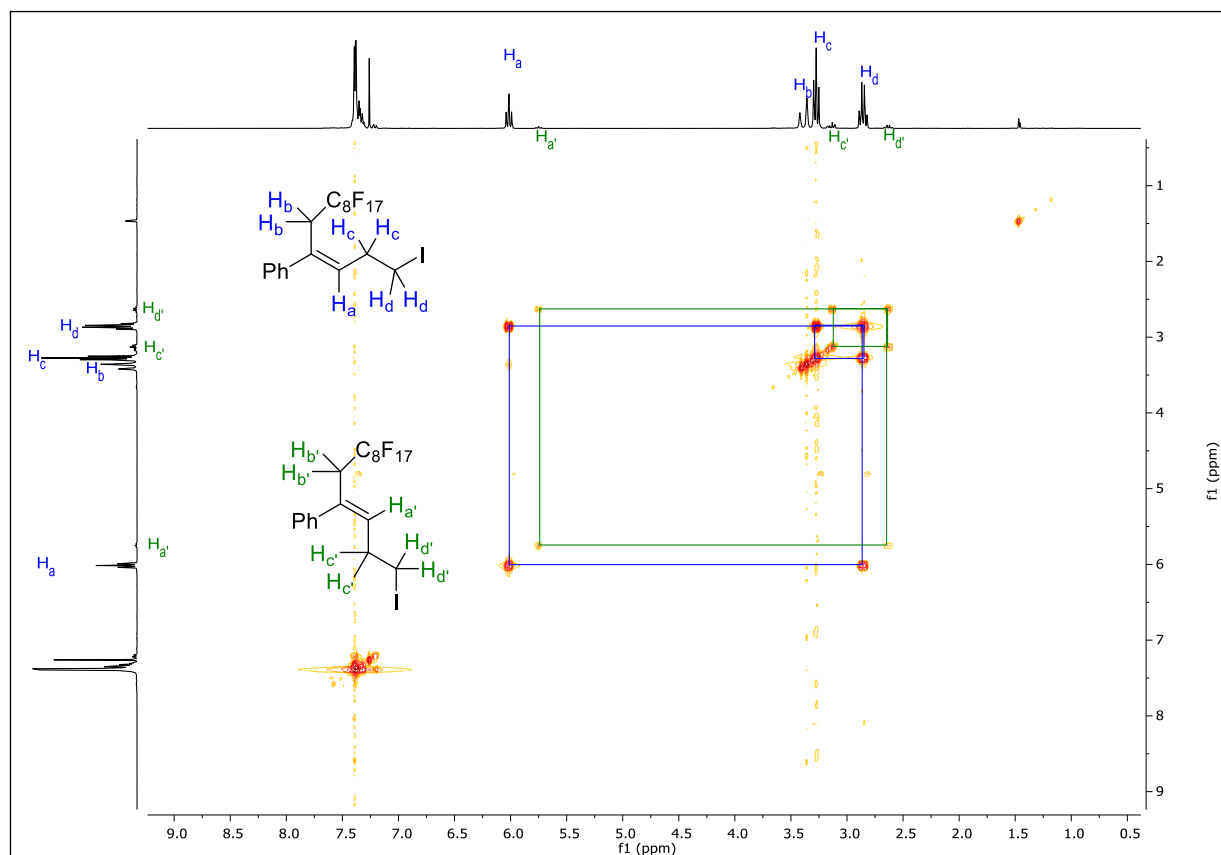
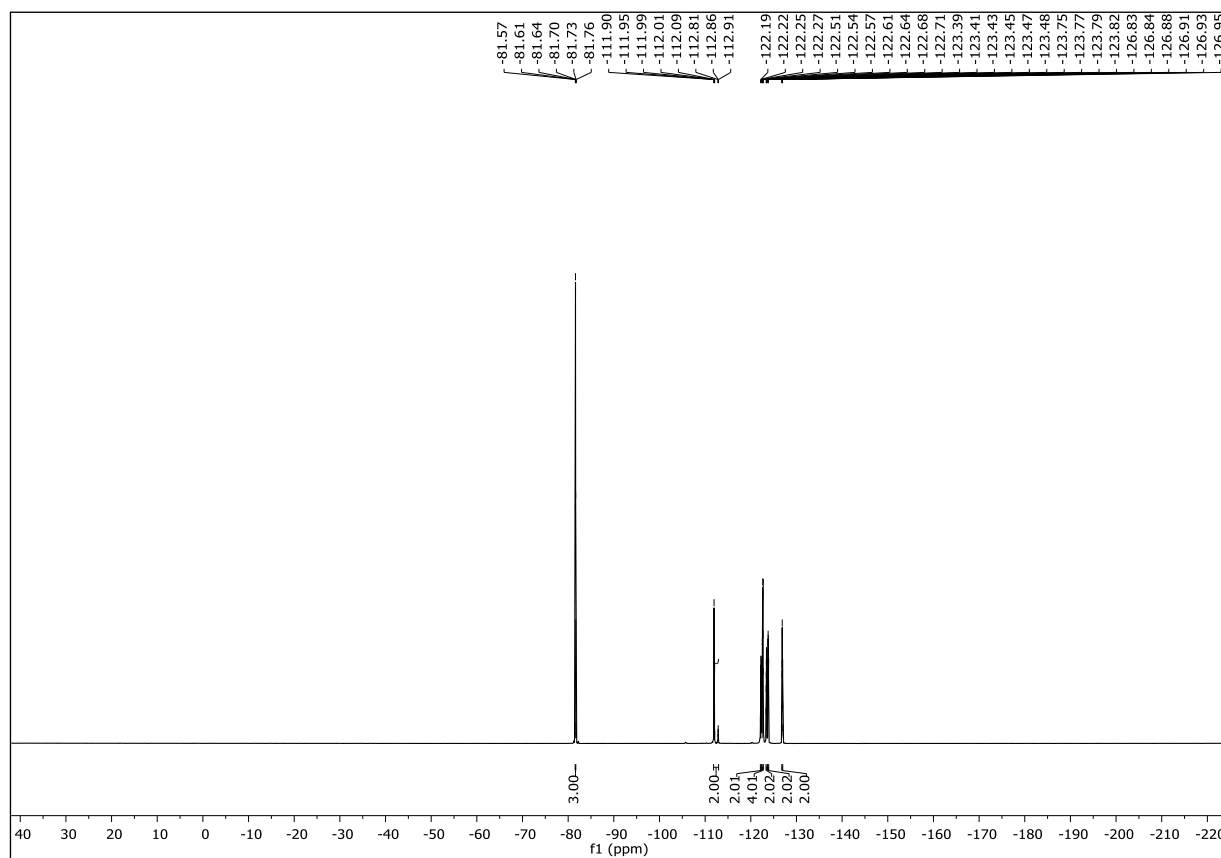
1-Chloro-3-(3,3,4,4,5,5,6,6,7,7,8,8,9,9,10,10,10-heptafluoro-1-iododecyl)benzene (15i)





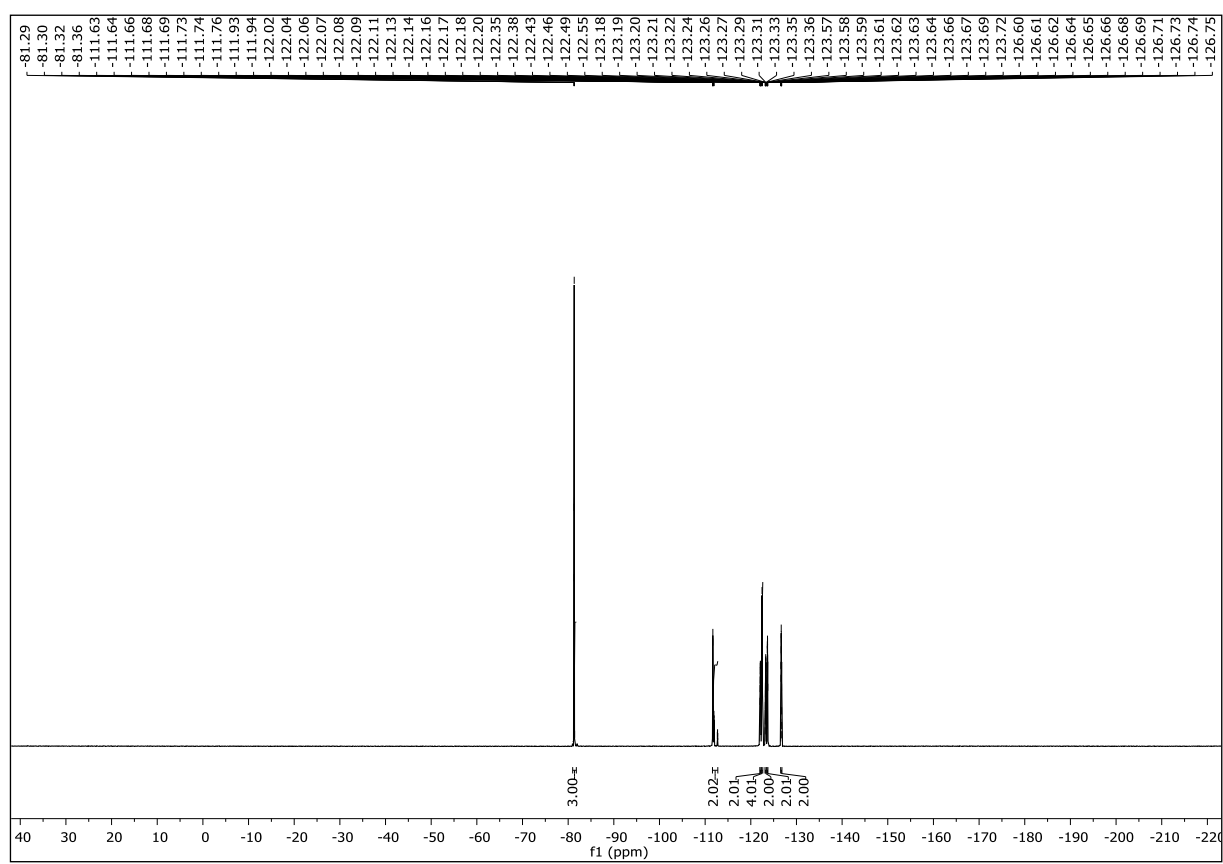
NMR-Solvent: CDCl_3





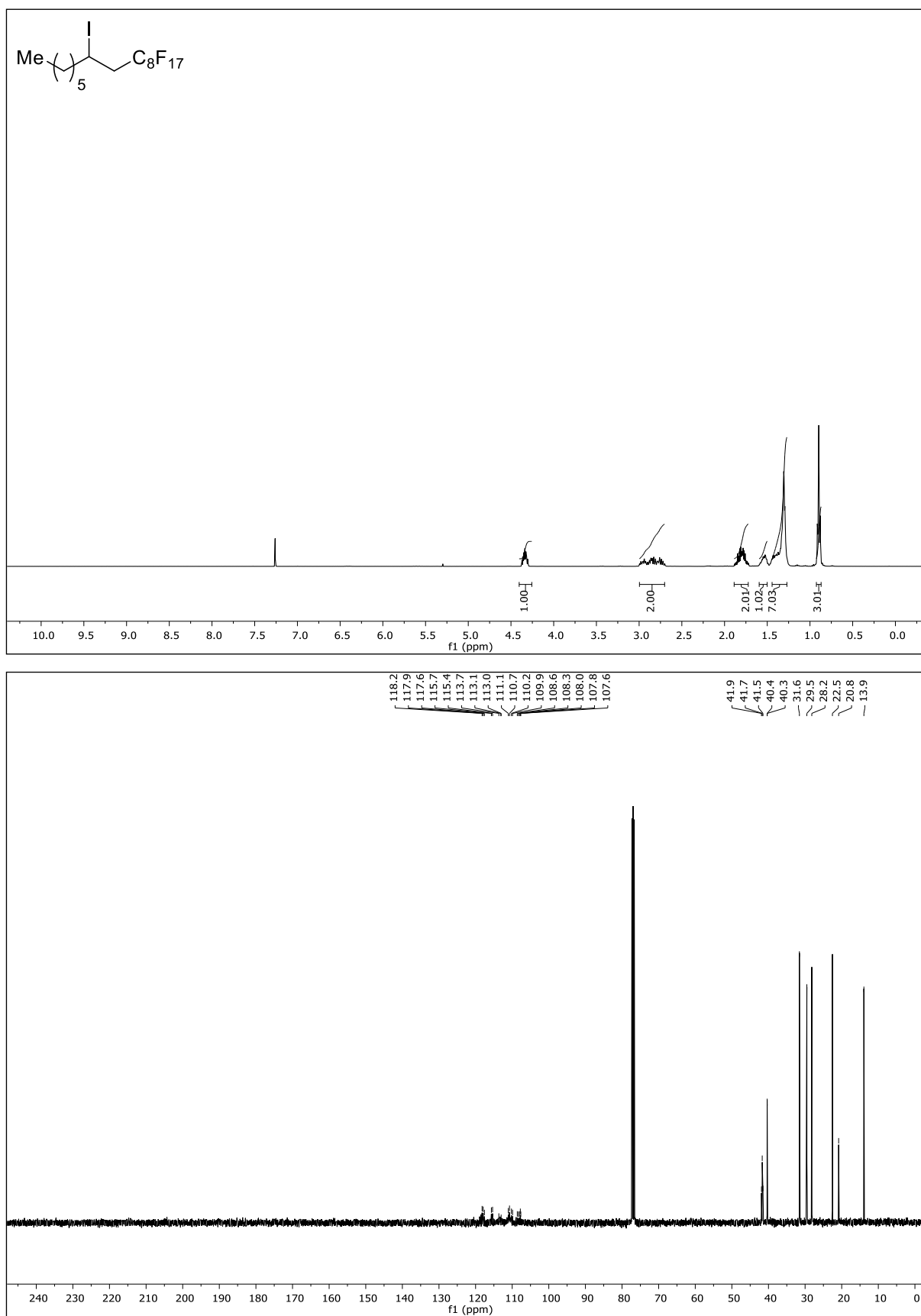
NMR-Solvent: CDCl_3

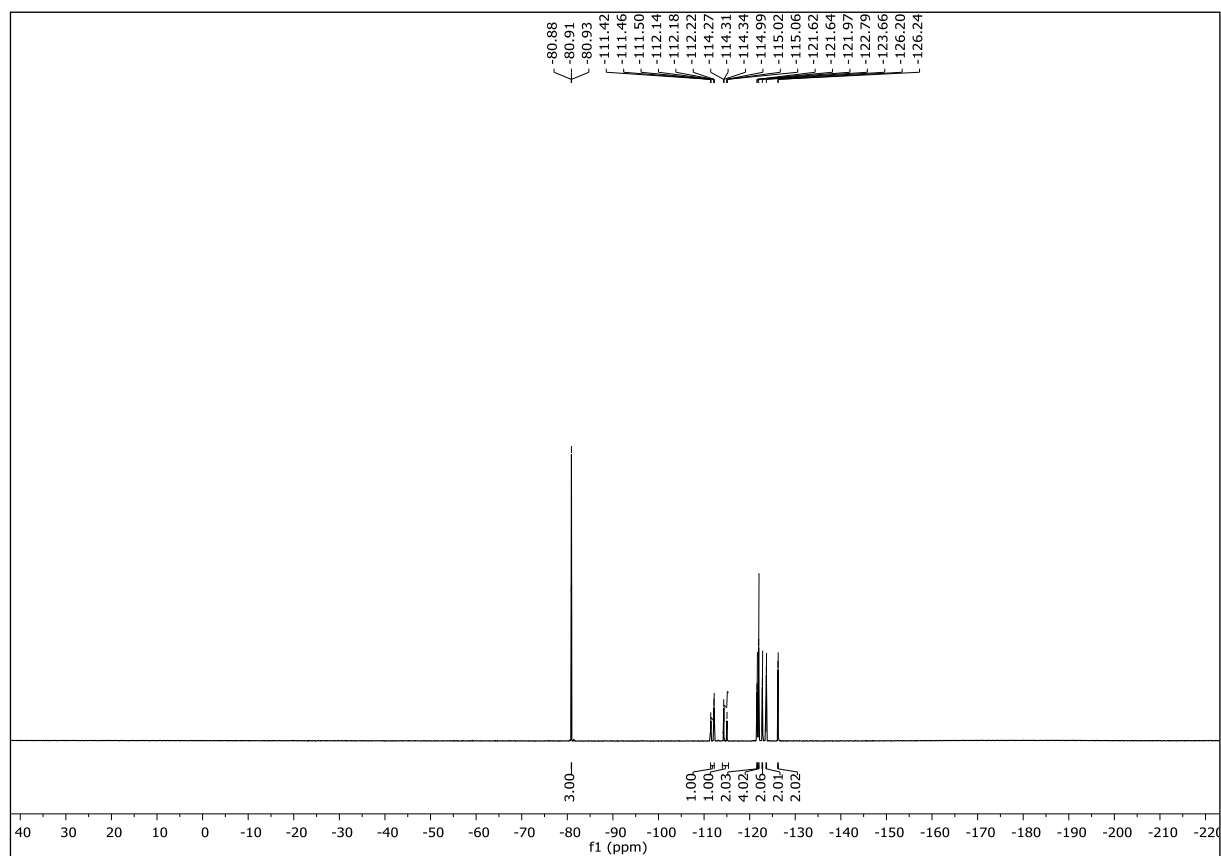




NMR-Solvent: CDCl_3

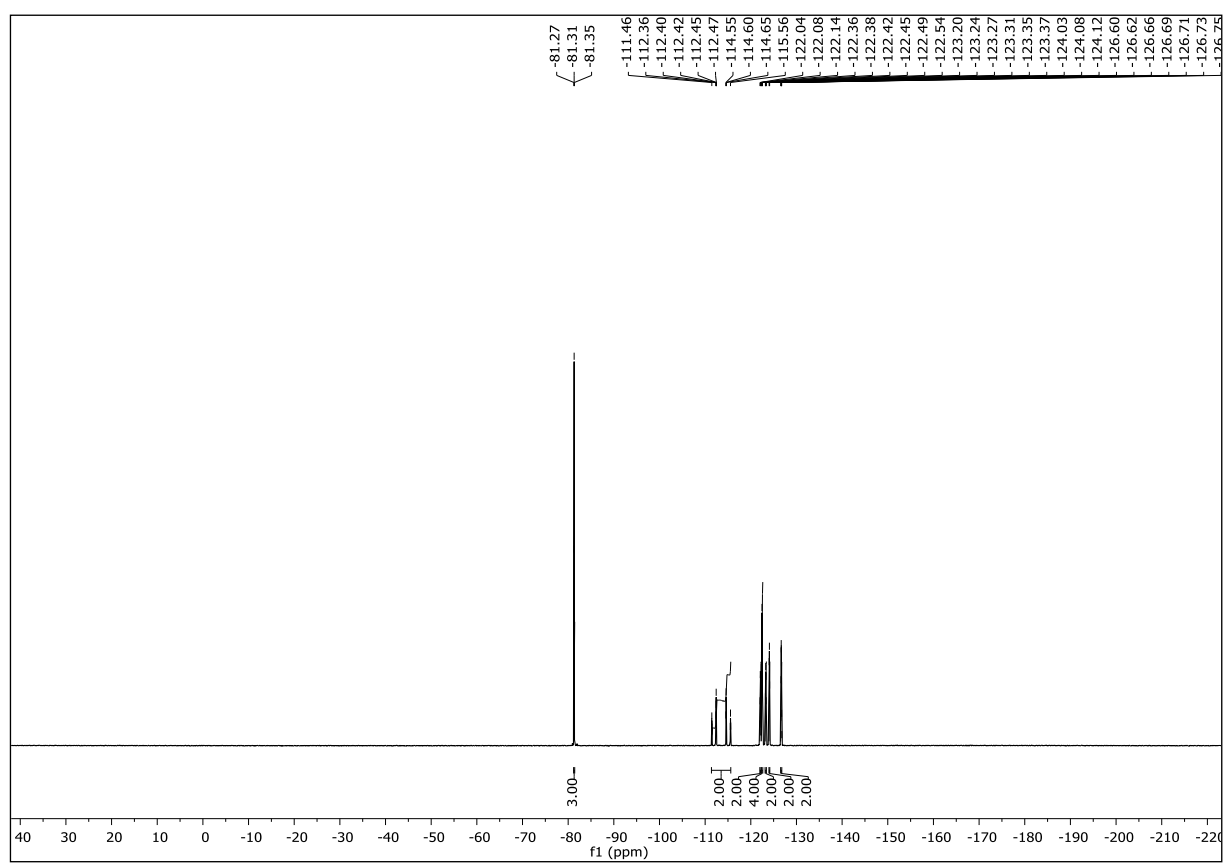
1,1,1,2,2,3,3,4,4,5,5,6,6,7,7,8,8-Heptafluoro-10-iodohexadecane (17a)



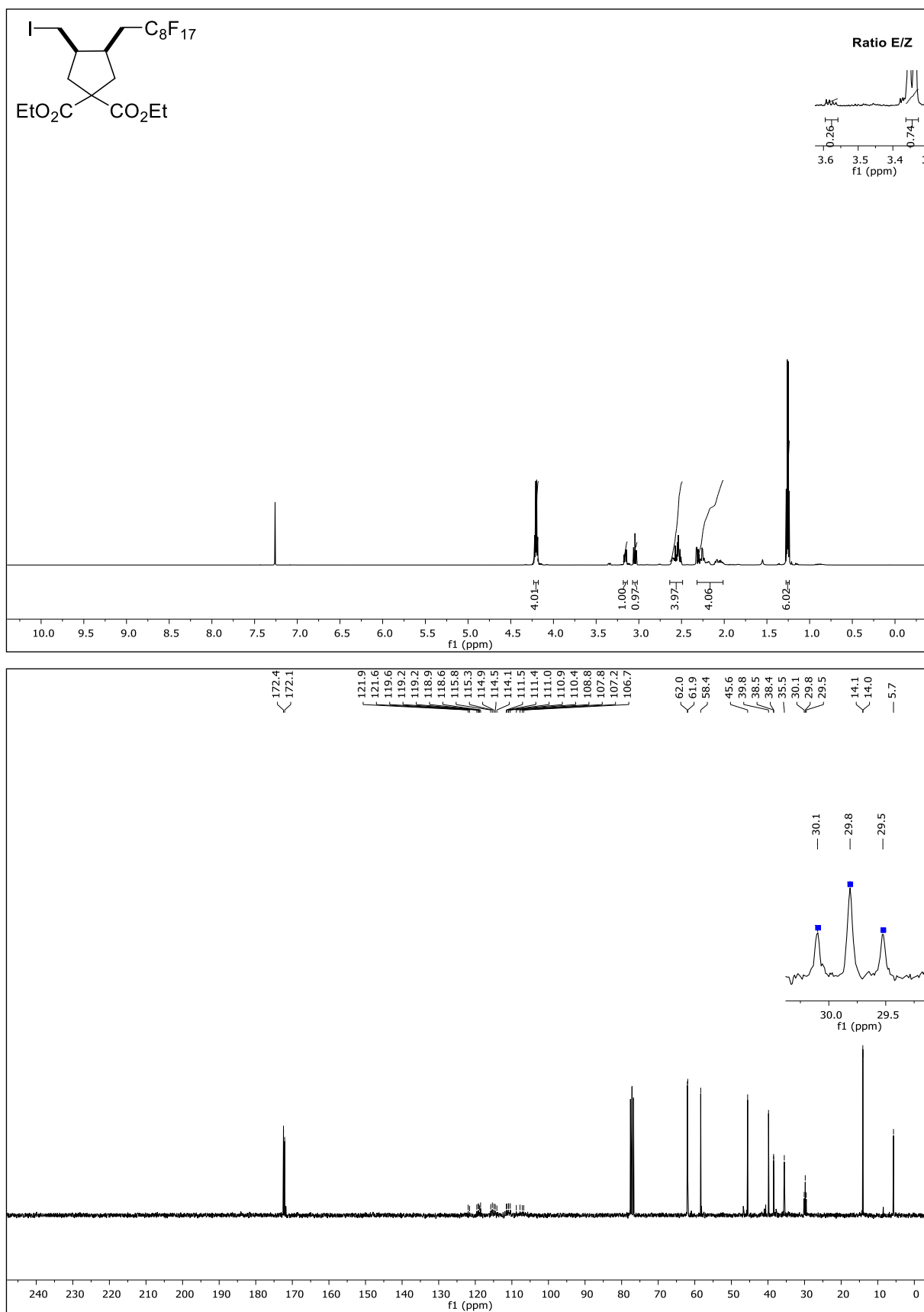


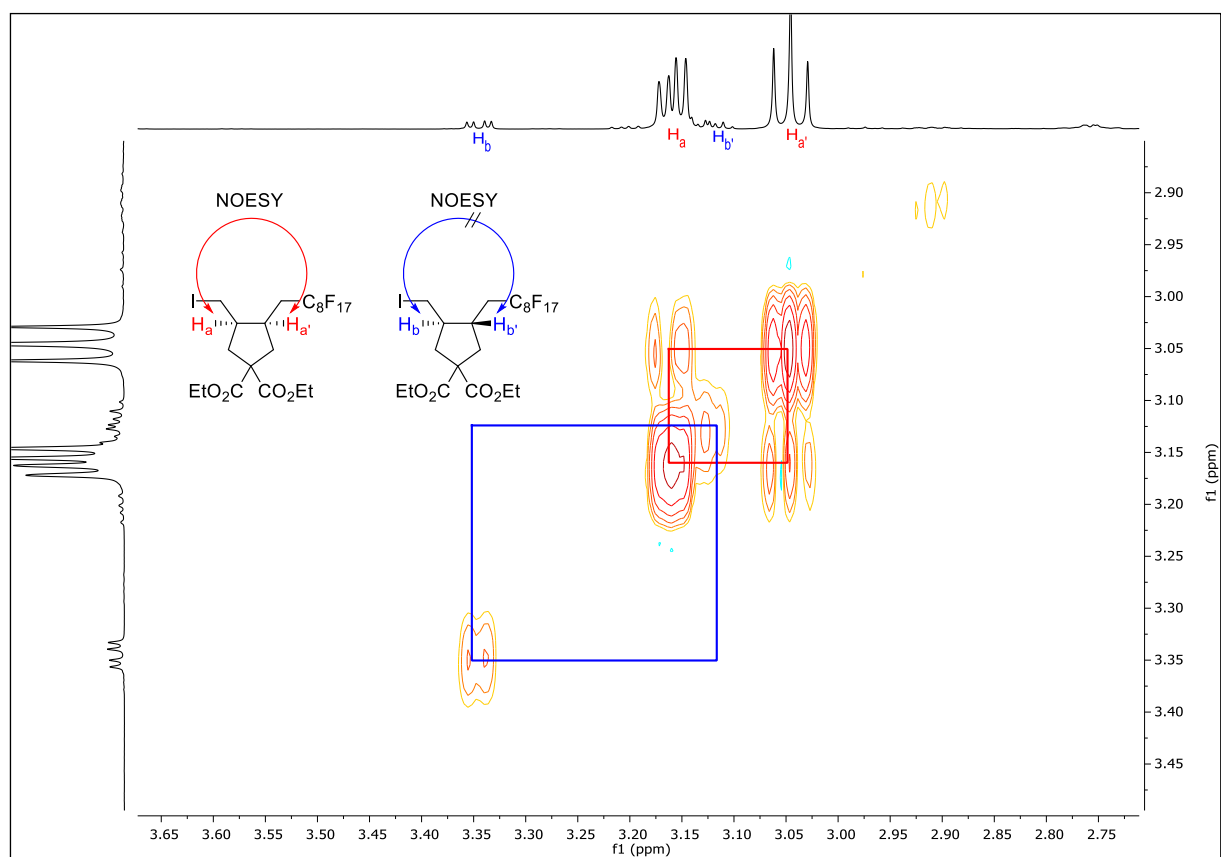
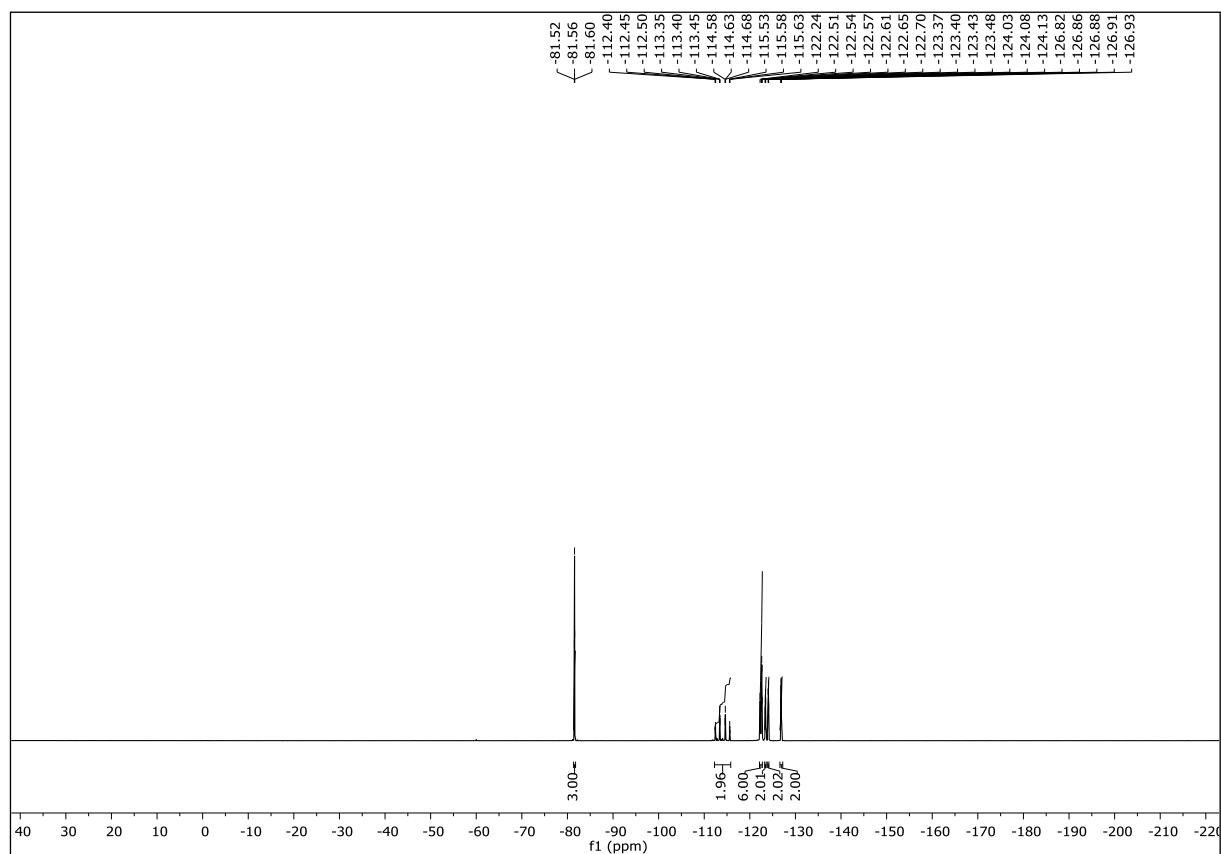
NMR-Solvent: CDCl_3





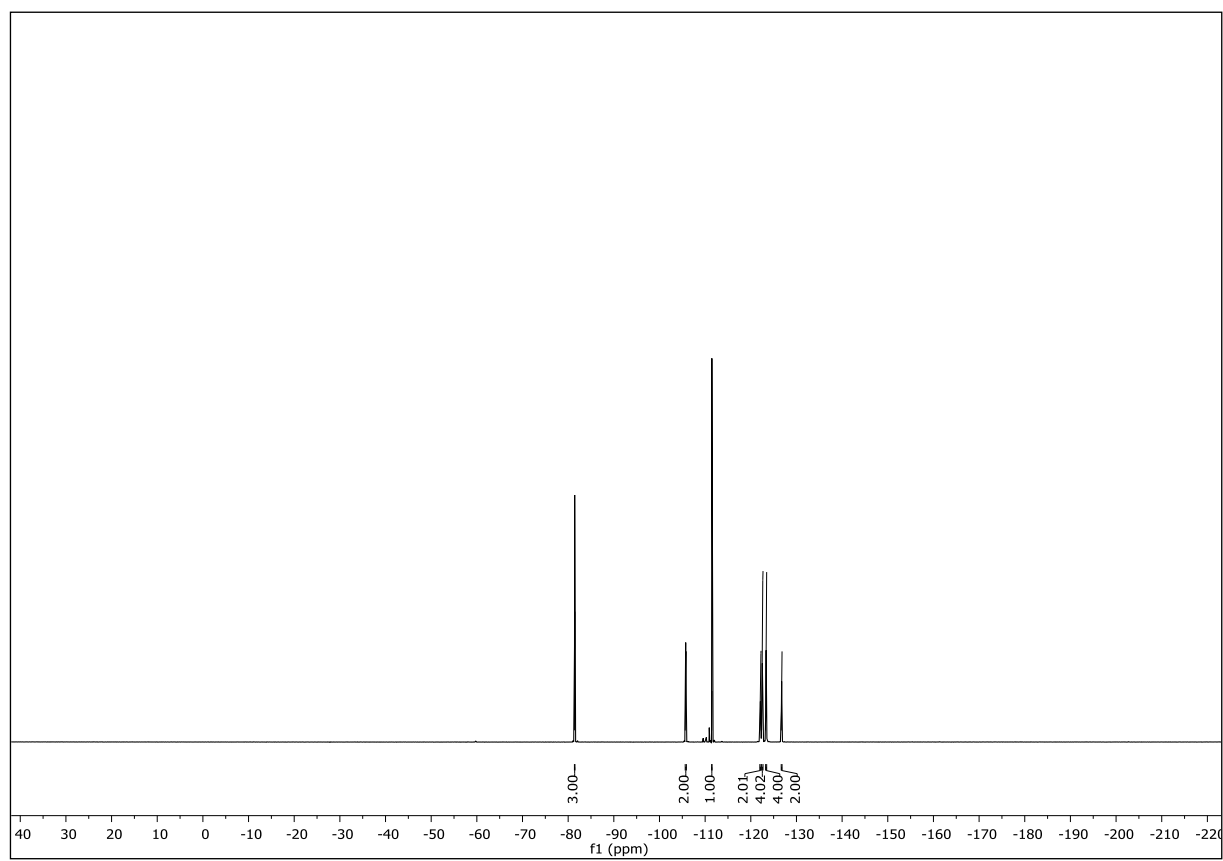
NMR-Solvent: CDCl_3

Diethyl (3*R*,4*R*)-3-(2,2,3,3,4,4,5,5,6,6,7,7,8,8,9,9,9-heptafluorononyl)-4-(iodomethyl)cyclopentane-1,1-dicarboxylate (17c)



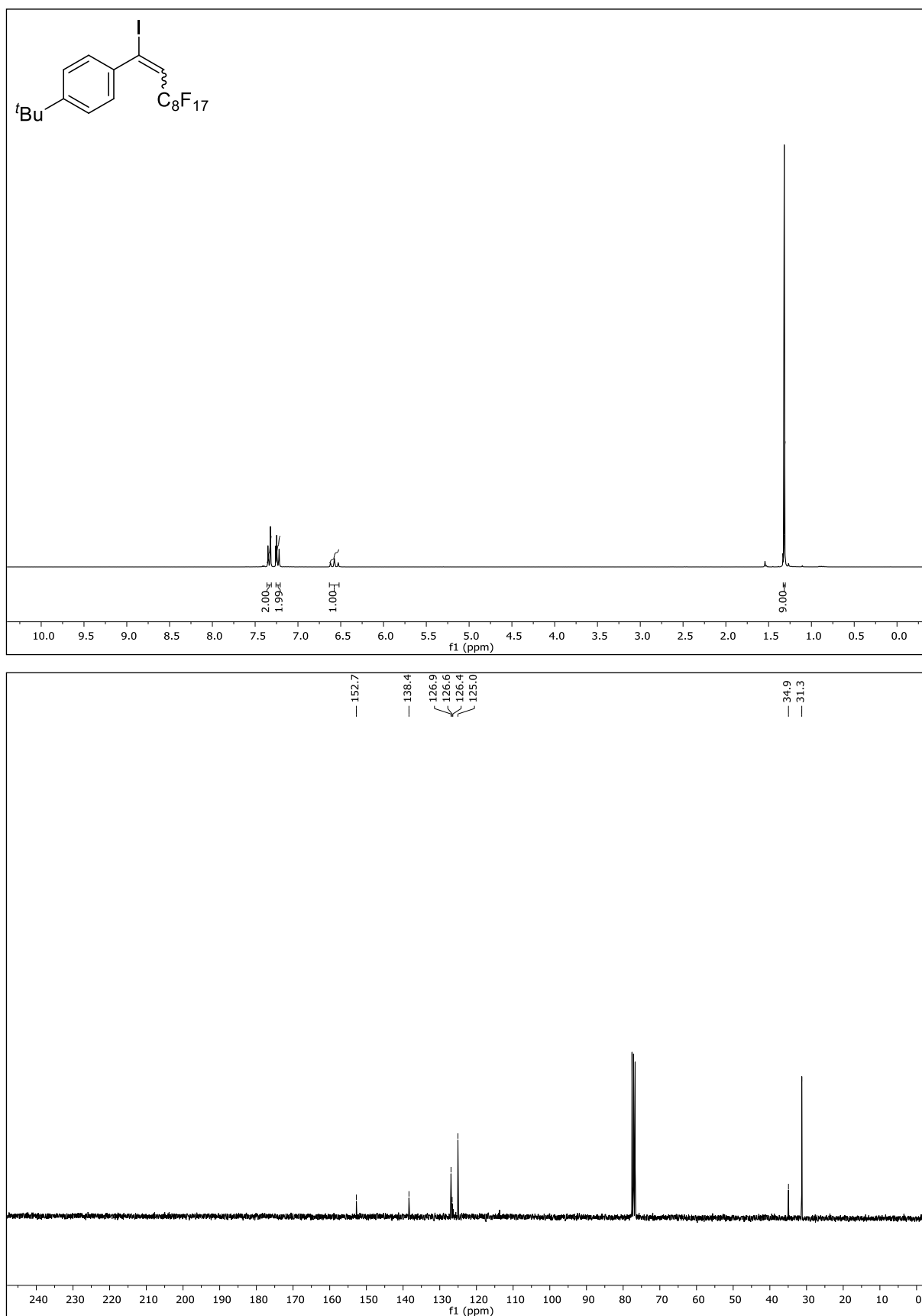
NMR-Solvent: CDCl₃

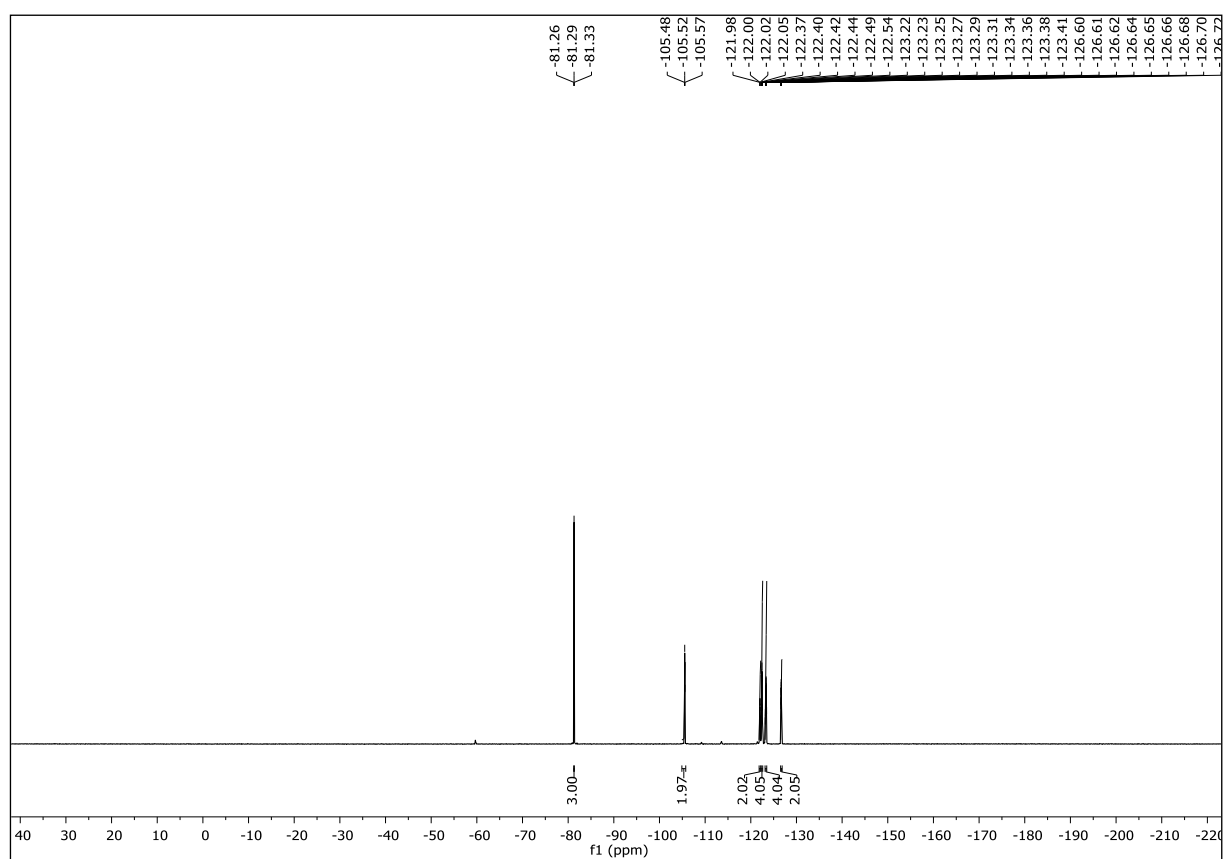




NMR-Solvent: CDCl_3

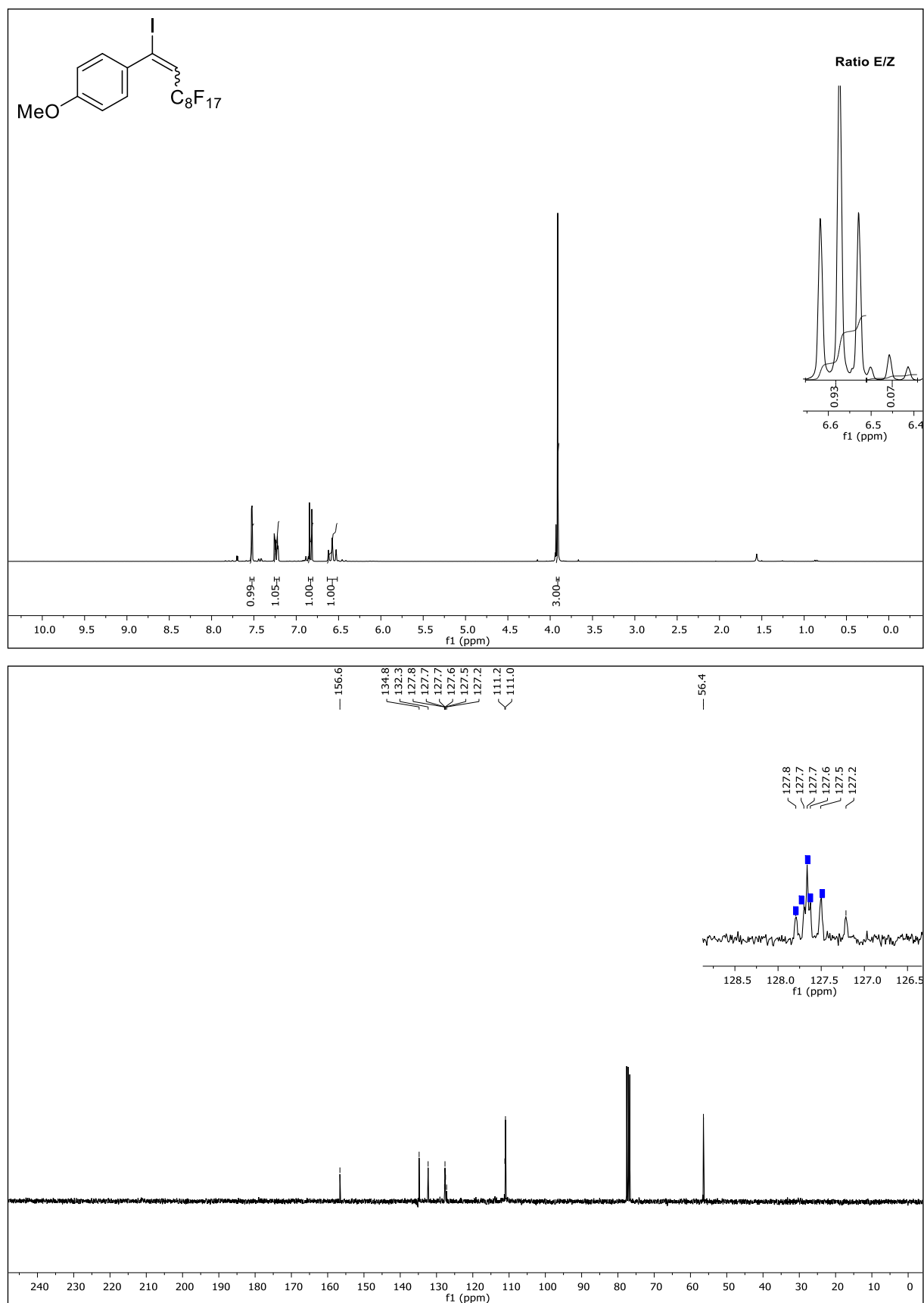
1-(*tert*-Butyl)-4-(3,3,4,4,5,5,6,6,7,7,8,8,9,9,10,10,10-heptafluoro-1-iododec-1-en-1-yl)benzene (19b)

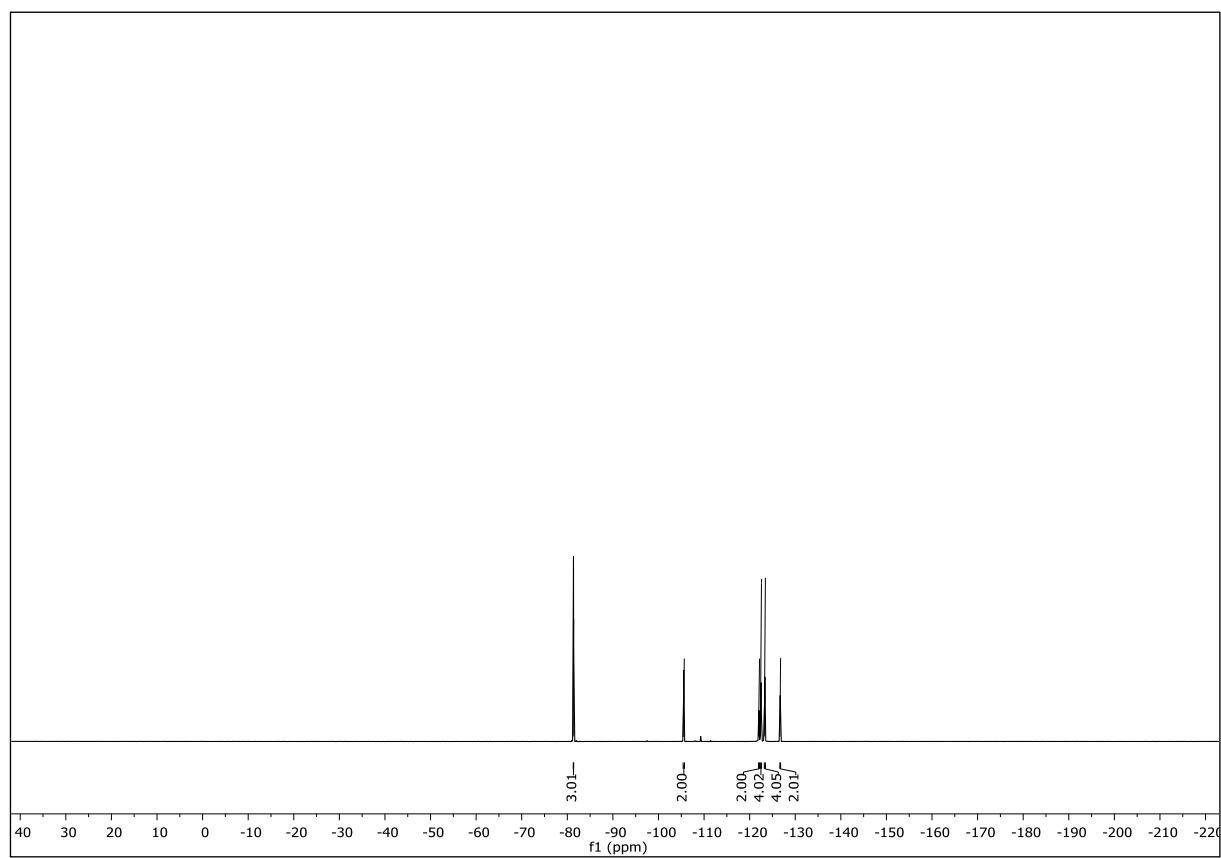




NMR-Solvent: CDCl₃

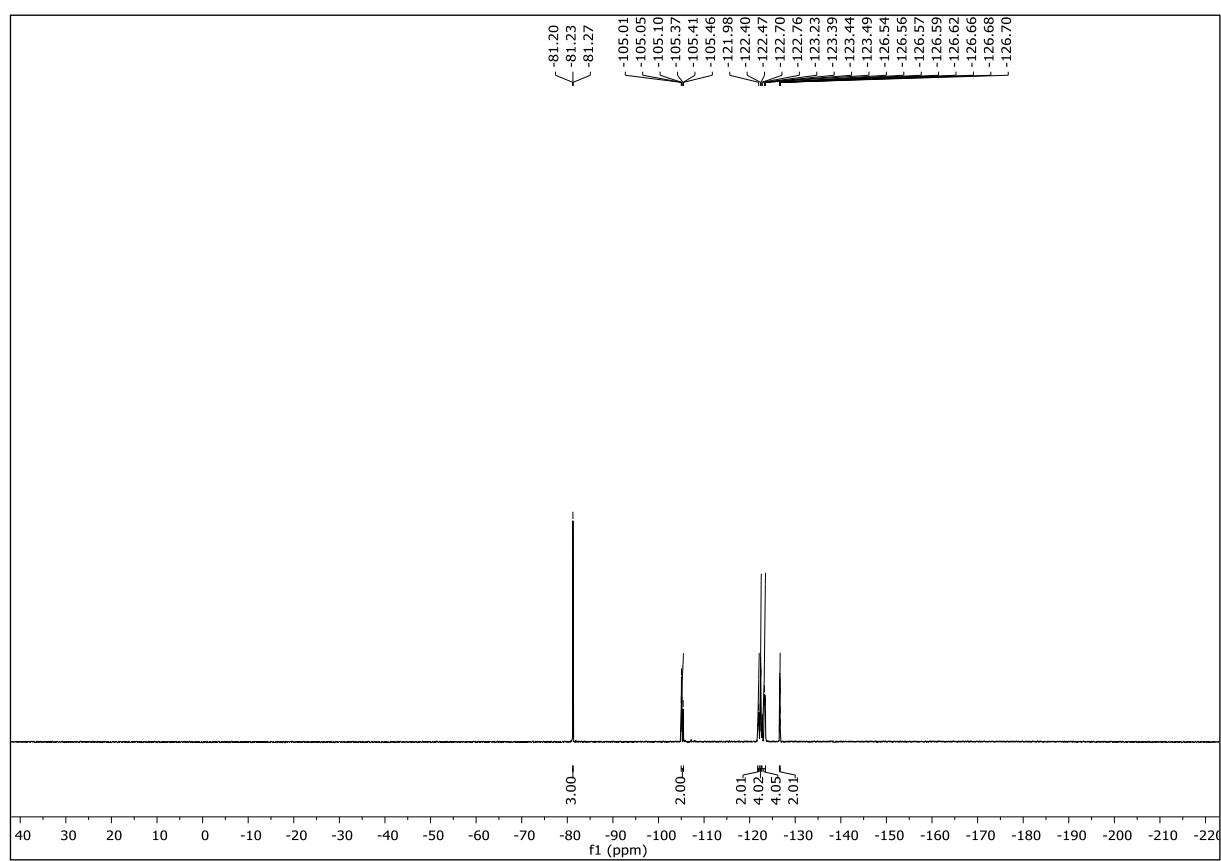
1-(3,3,4,4,5,5,6,6,7,7,8,8,9,9,10,10,10-Heptafluoro-1-iododec-1-en-1-yl)-4-methoxy benzene (19c)





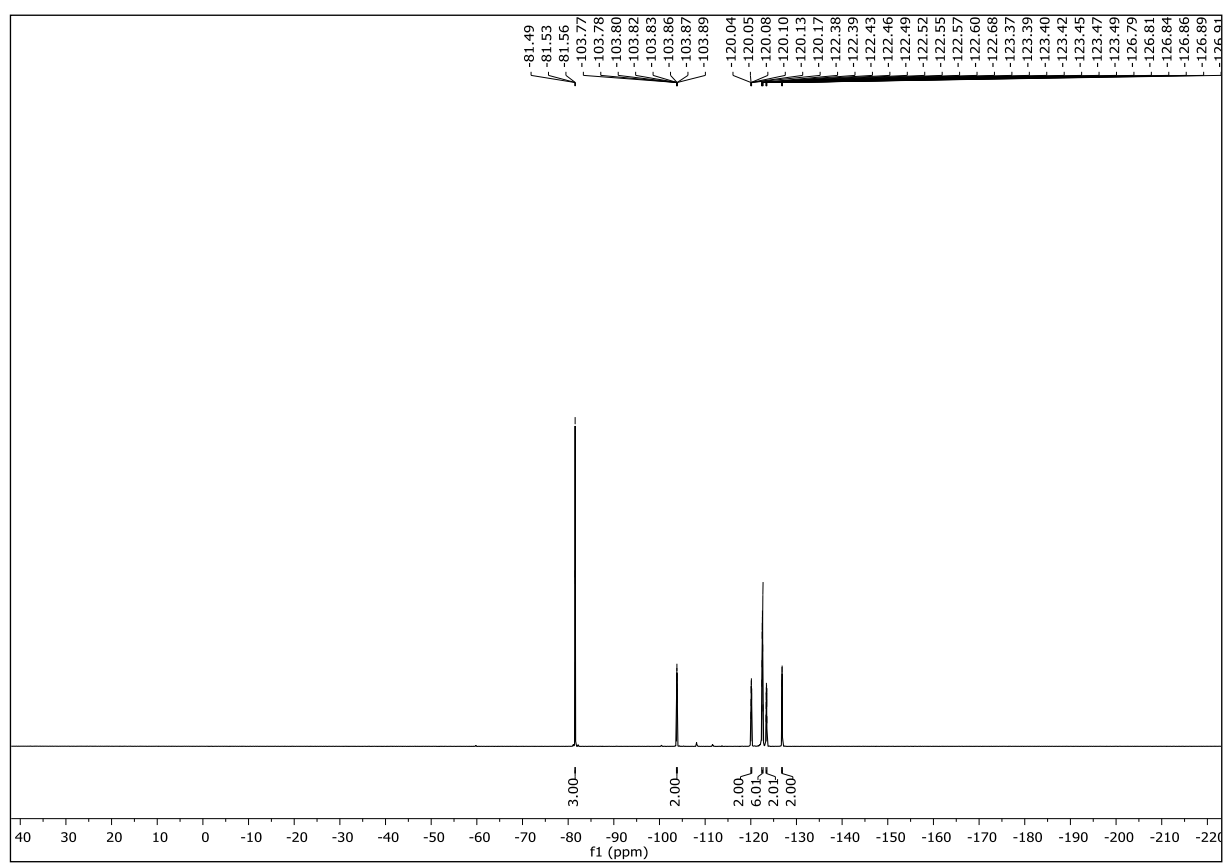
NMR-Solvent: CDCl_3





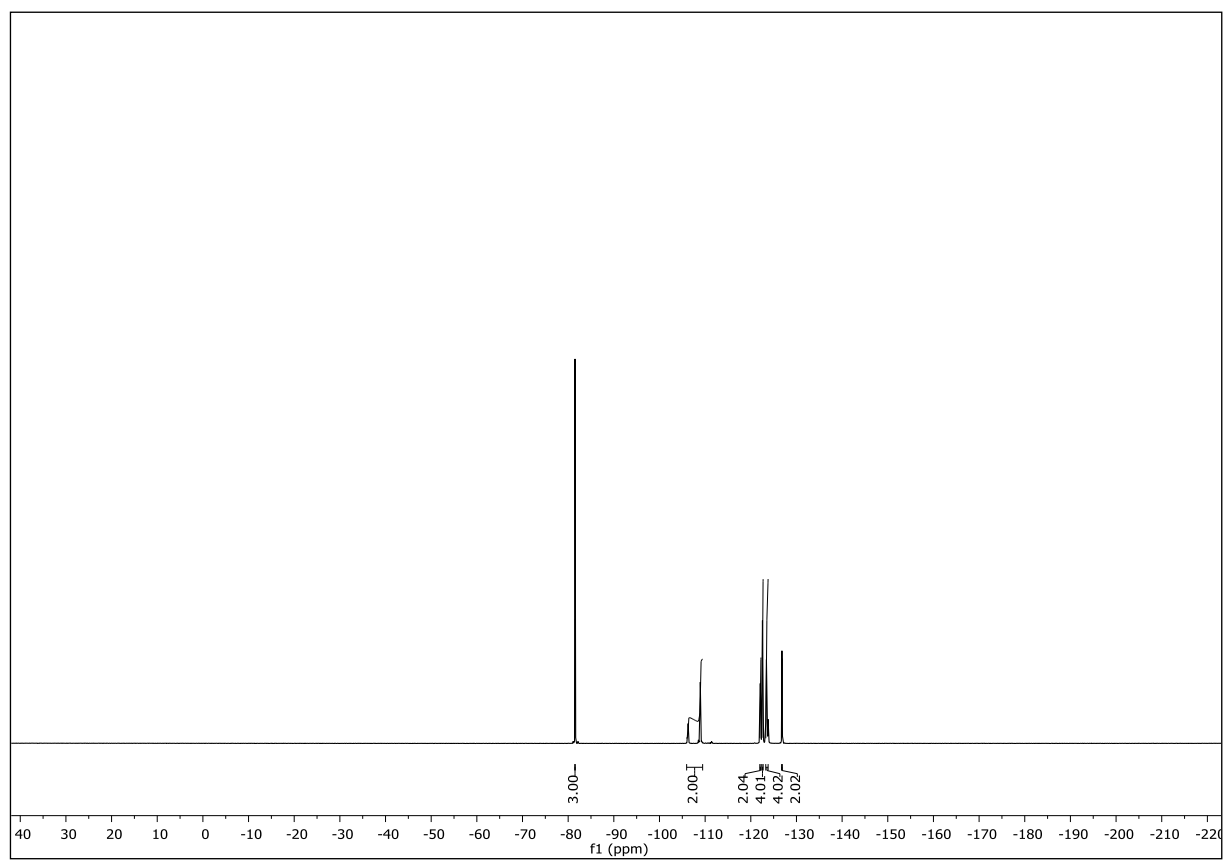
NMR-Solvent: CDCl_3





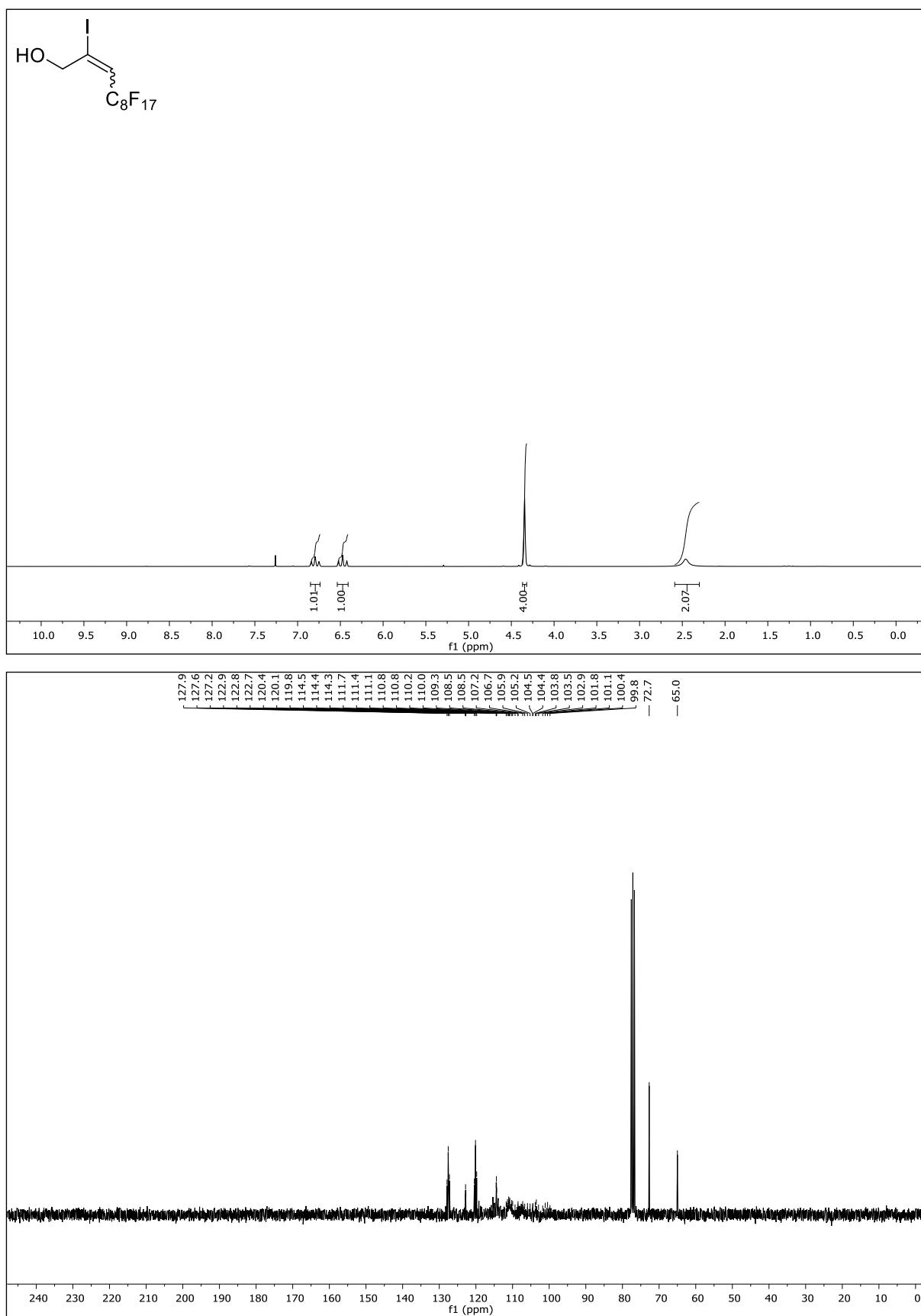
NMR-Solvent: CDCl₃

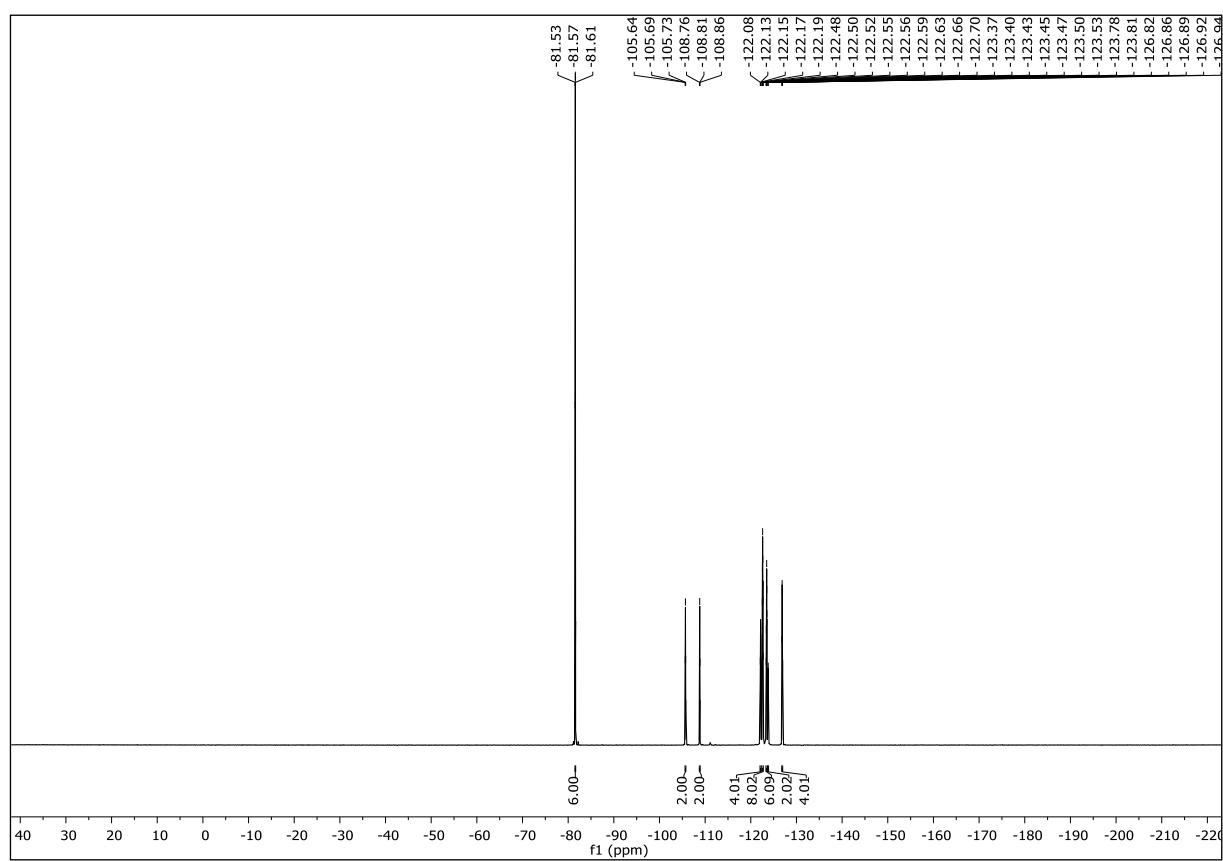




NMR-Solvent: CDCl_3

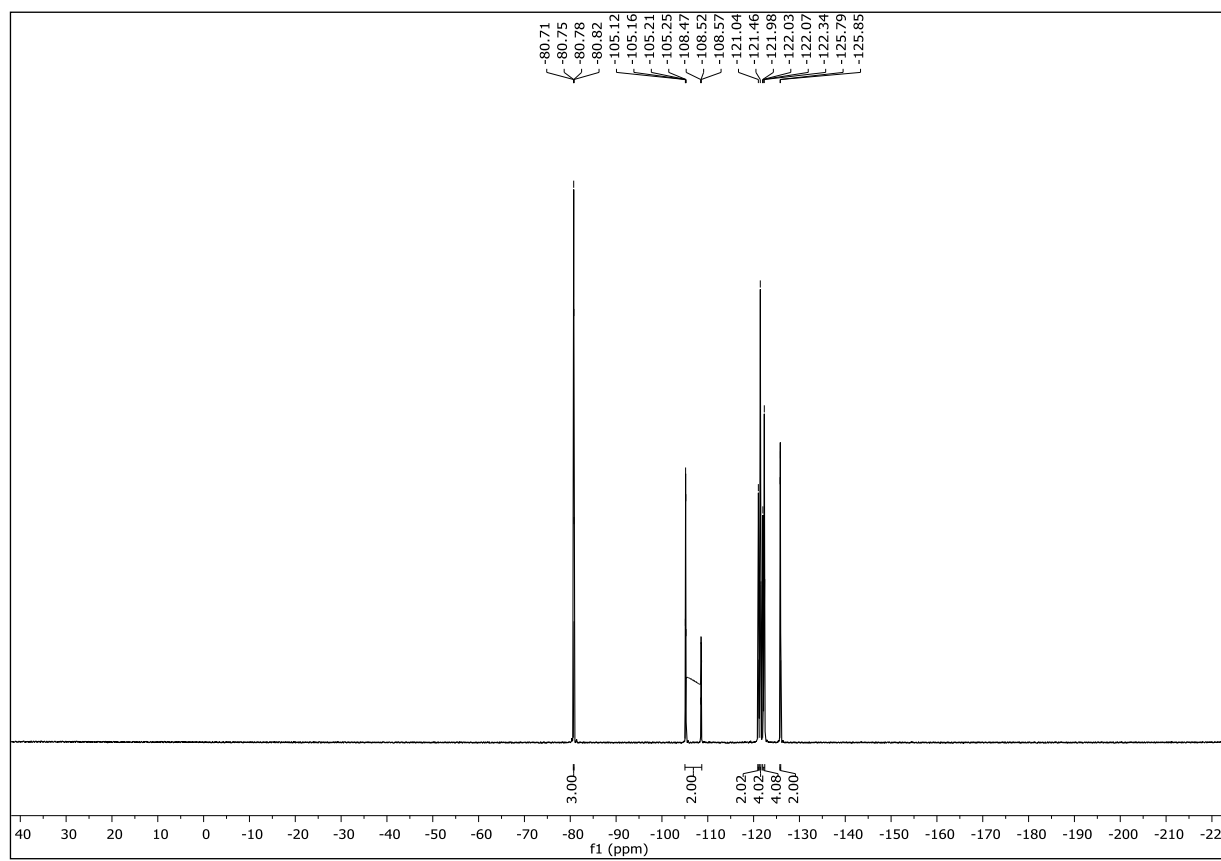
4,4,5,5,6,6,7,7,8,8,9,9,10,10,11,11,11-Heptadecafluoro-2-iodoundec-2-en-1-ol (21b)





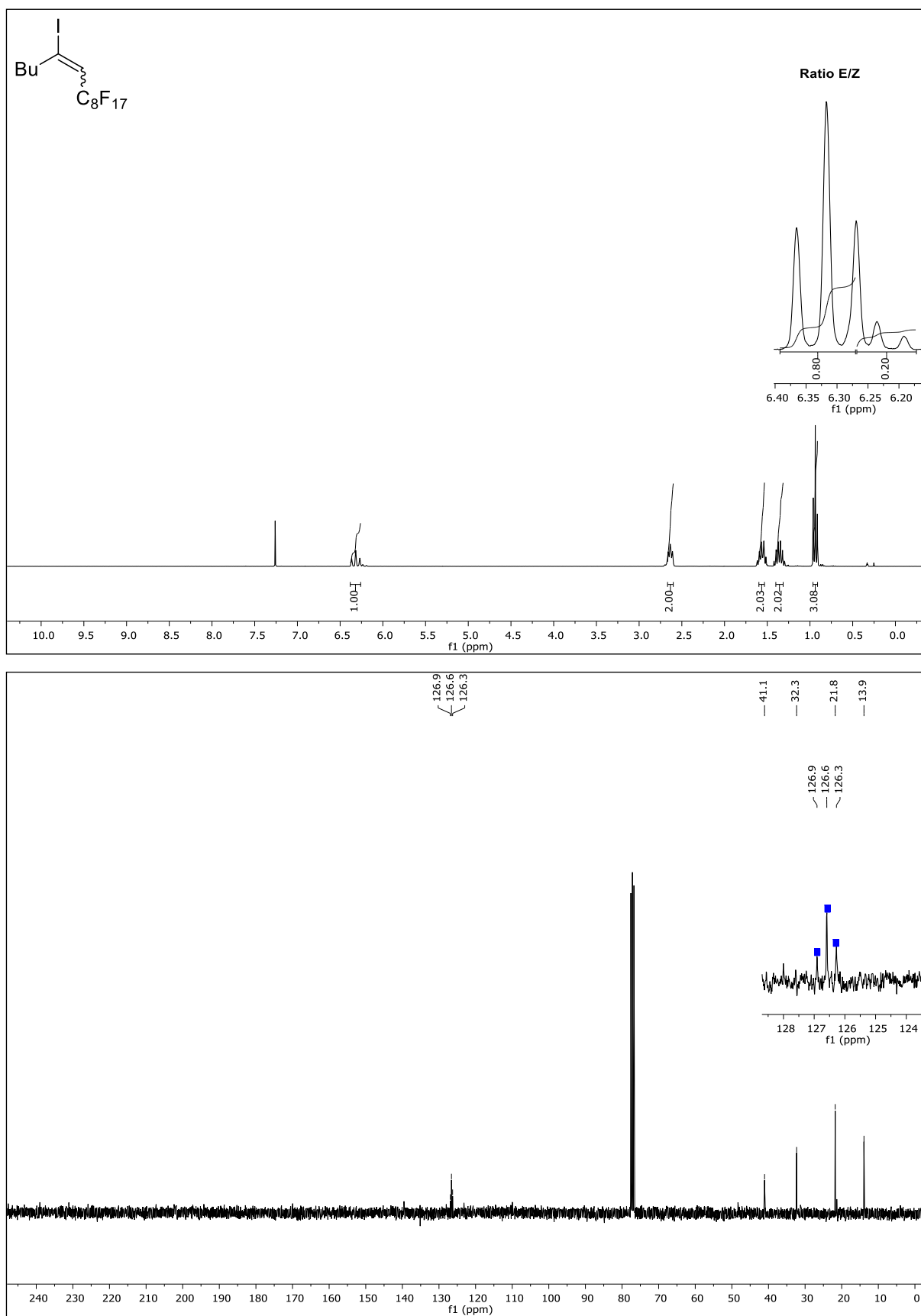
NMR-Solvent: CDCl₃

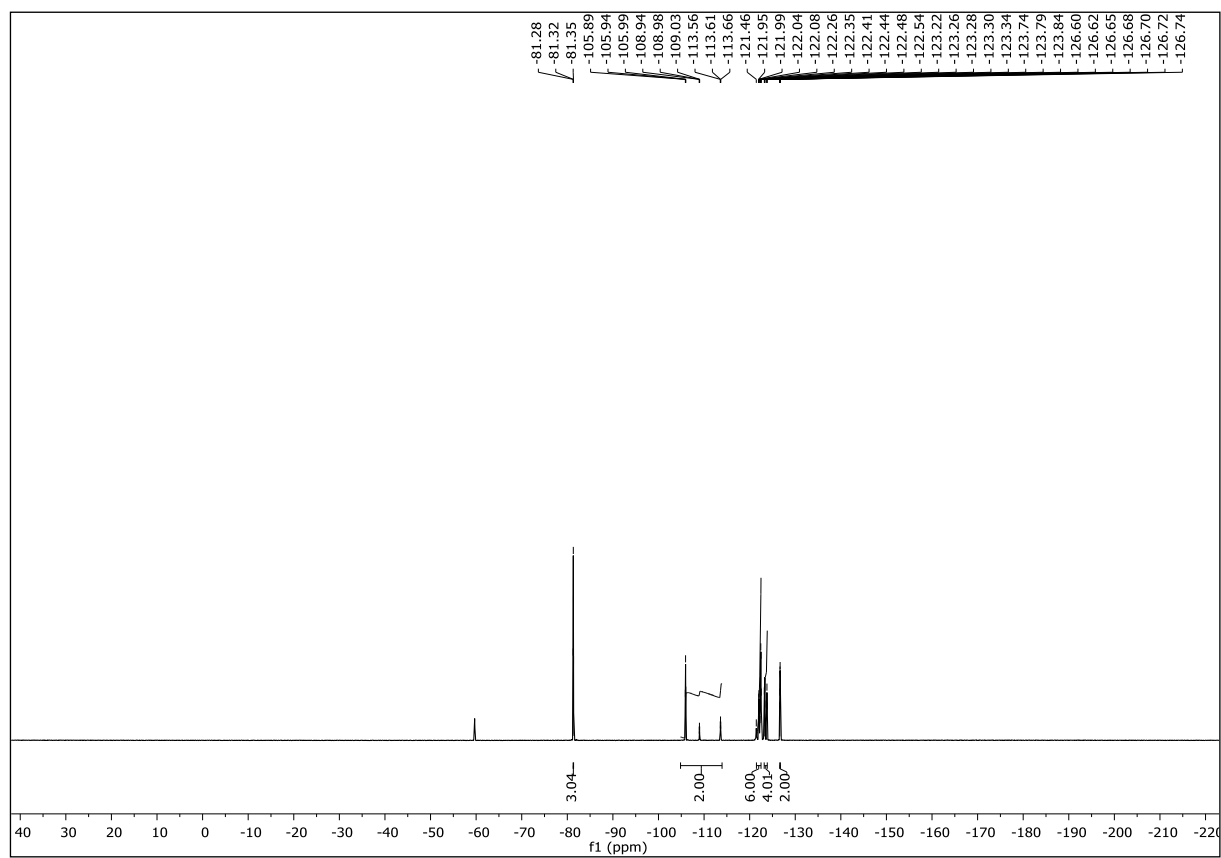




NMR-Solvent: Acetone- d_6

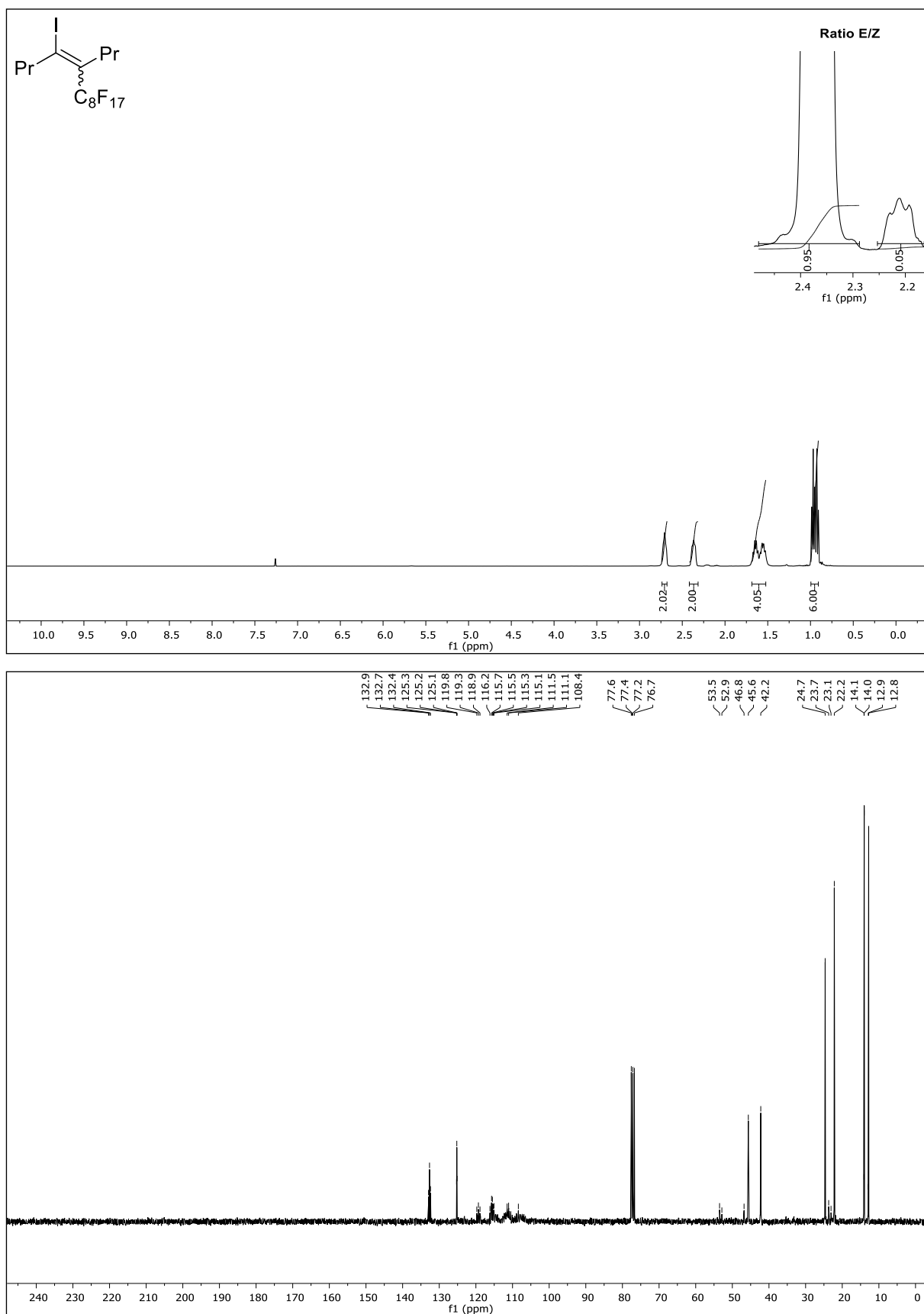
7,7,8,8,9,10,10,11,11,12,12,13,13,14,14,14-Heptafluoro-5-iodotetradec-5-ene (21d)

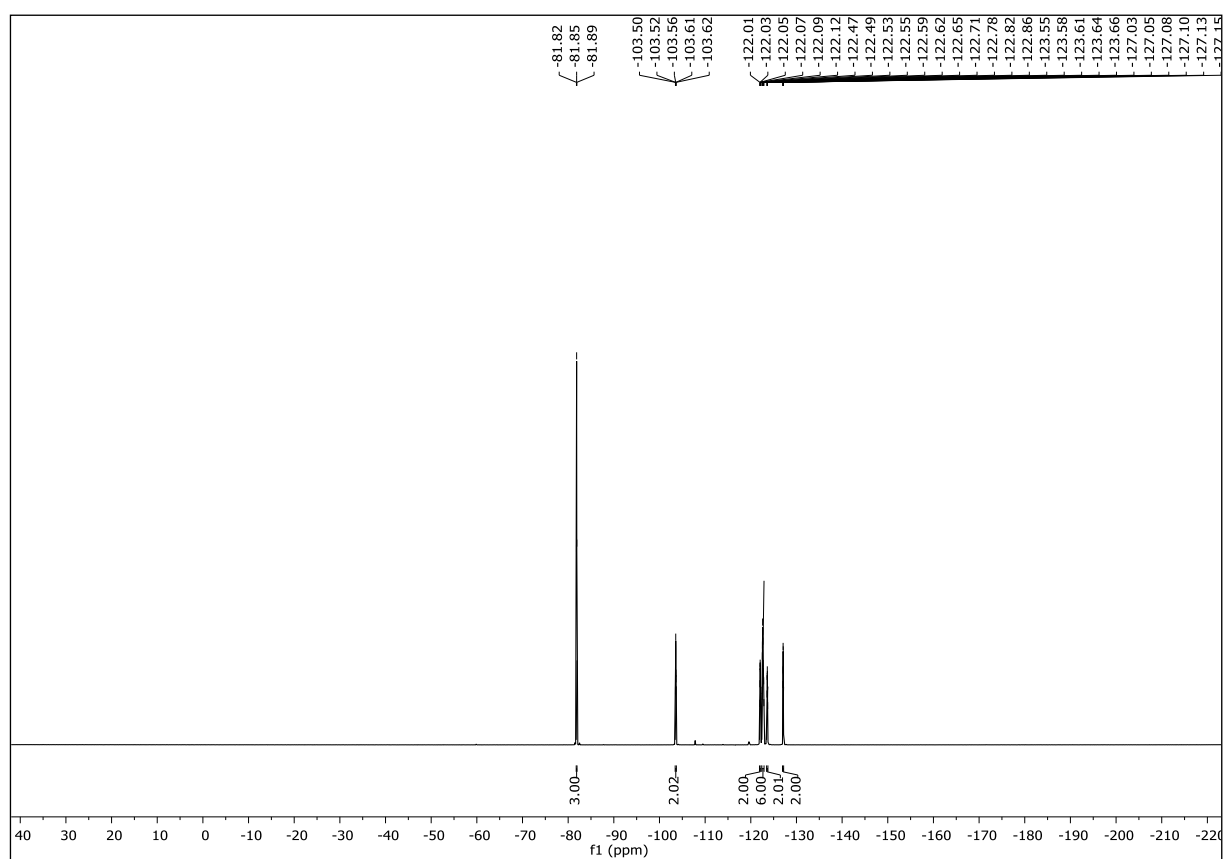




NMR-Solvent: CDCl_3

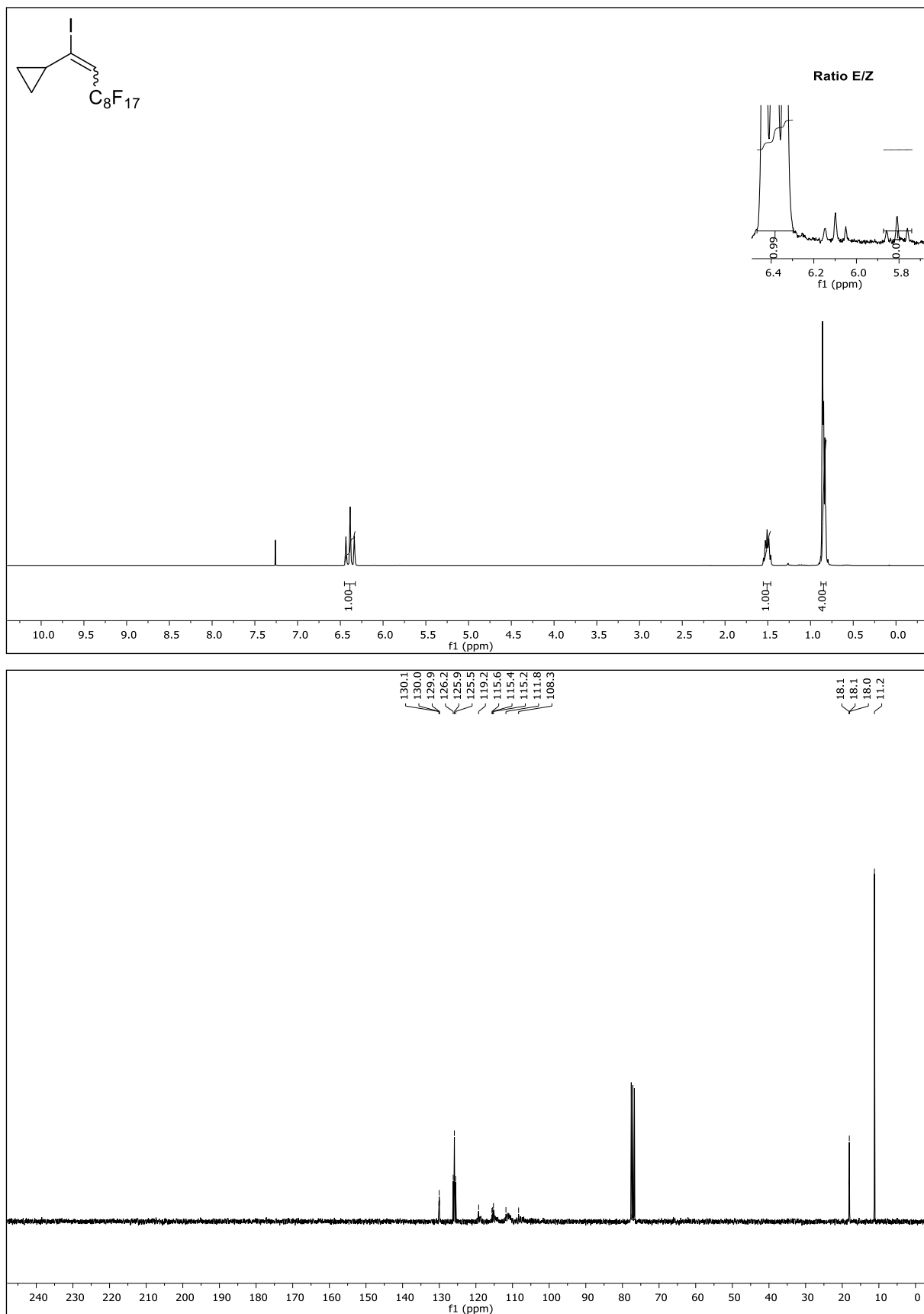
6,6,7,7,8,8,9,9,10,10,11,11,12,12,13,13,13-Heptafluoro-4-iodo-5-propyltridec-4-ene (21e)

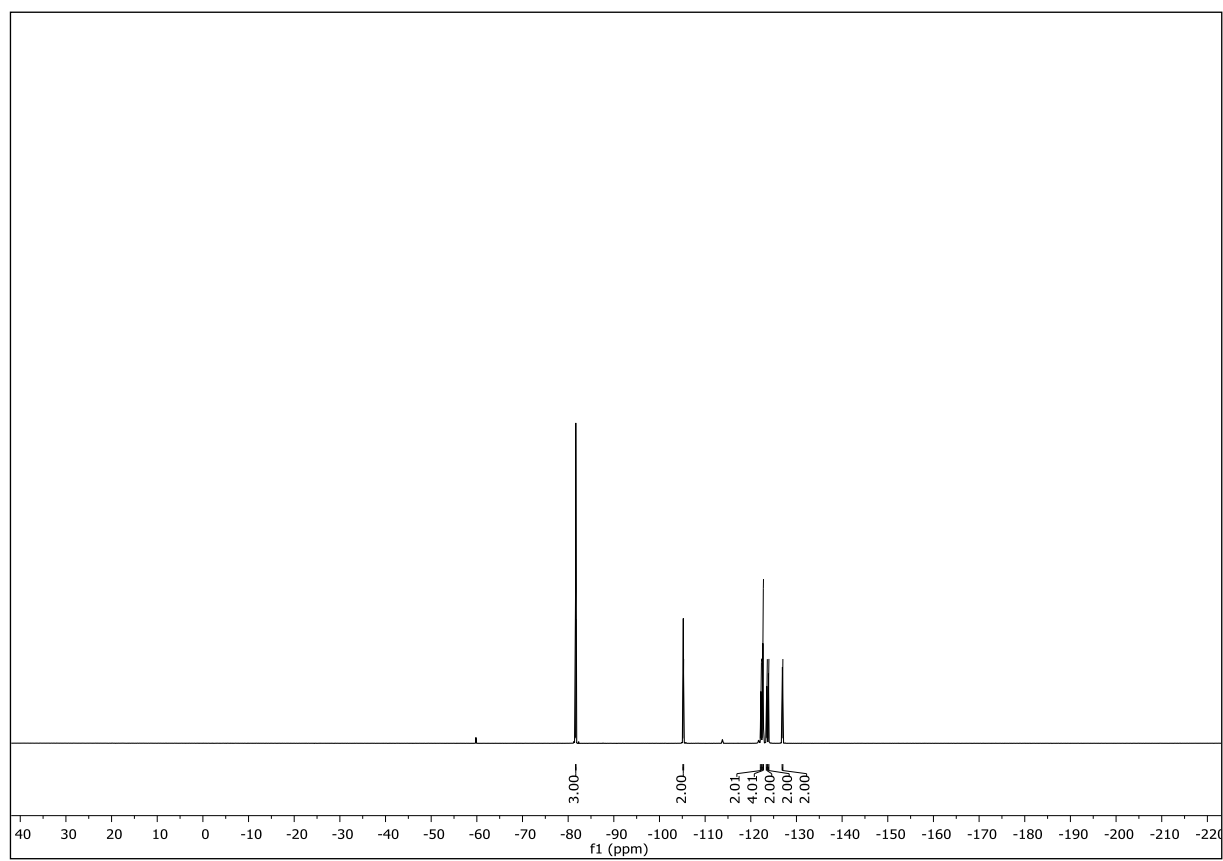




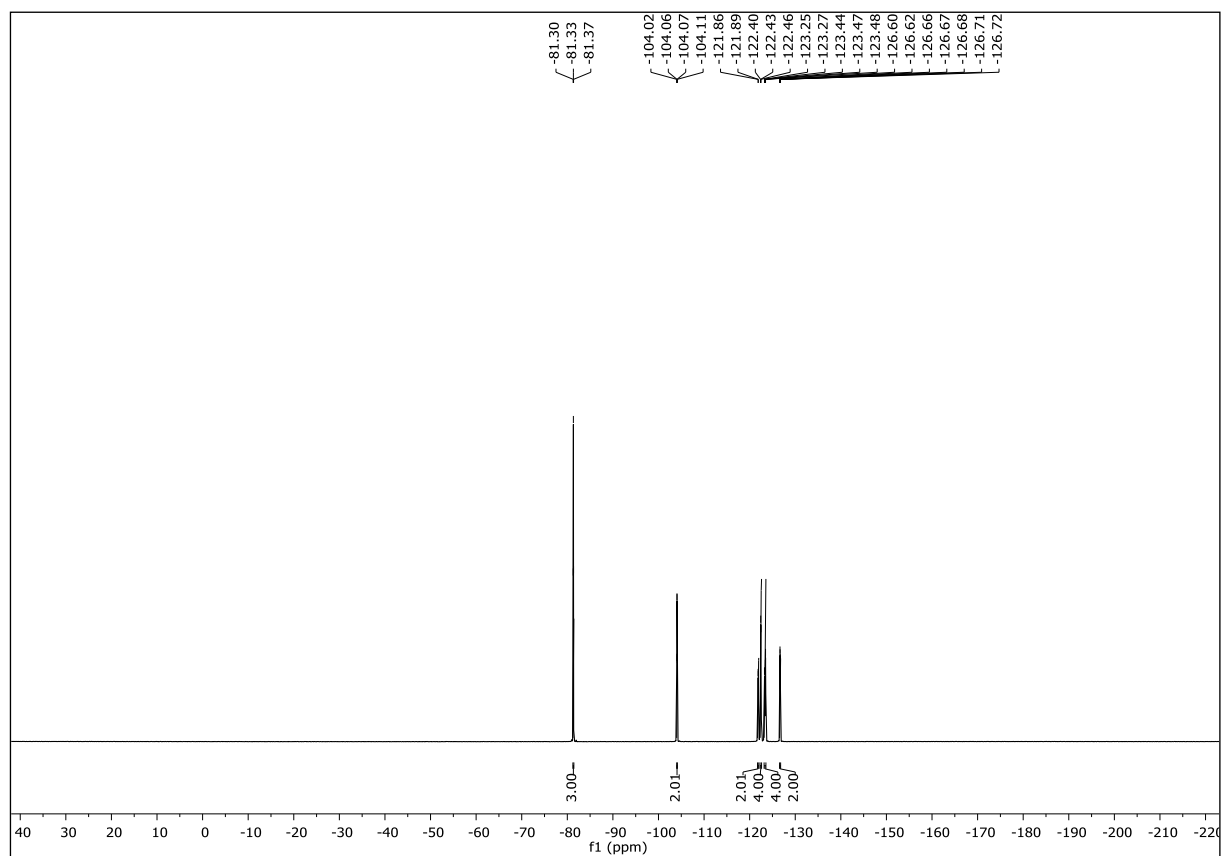
NMR-Solvent: CDCl_3

(3,3,4,4,5,5,6,7,7,8,8,9,9,10,10,10-Heptafluoro-1-iododec-1-en-1-yl)cyclopropane (21g)



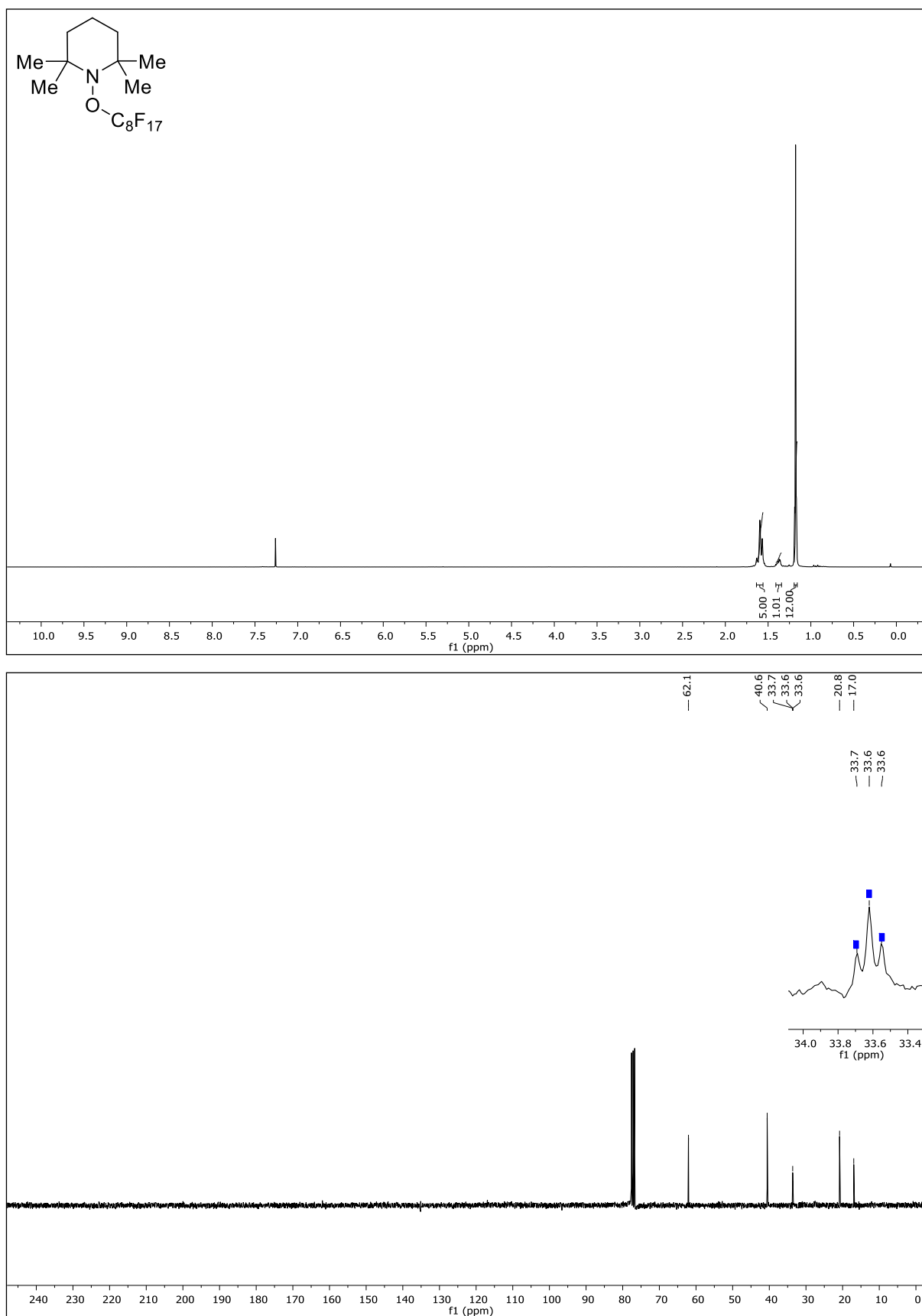


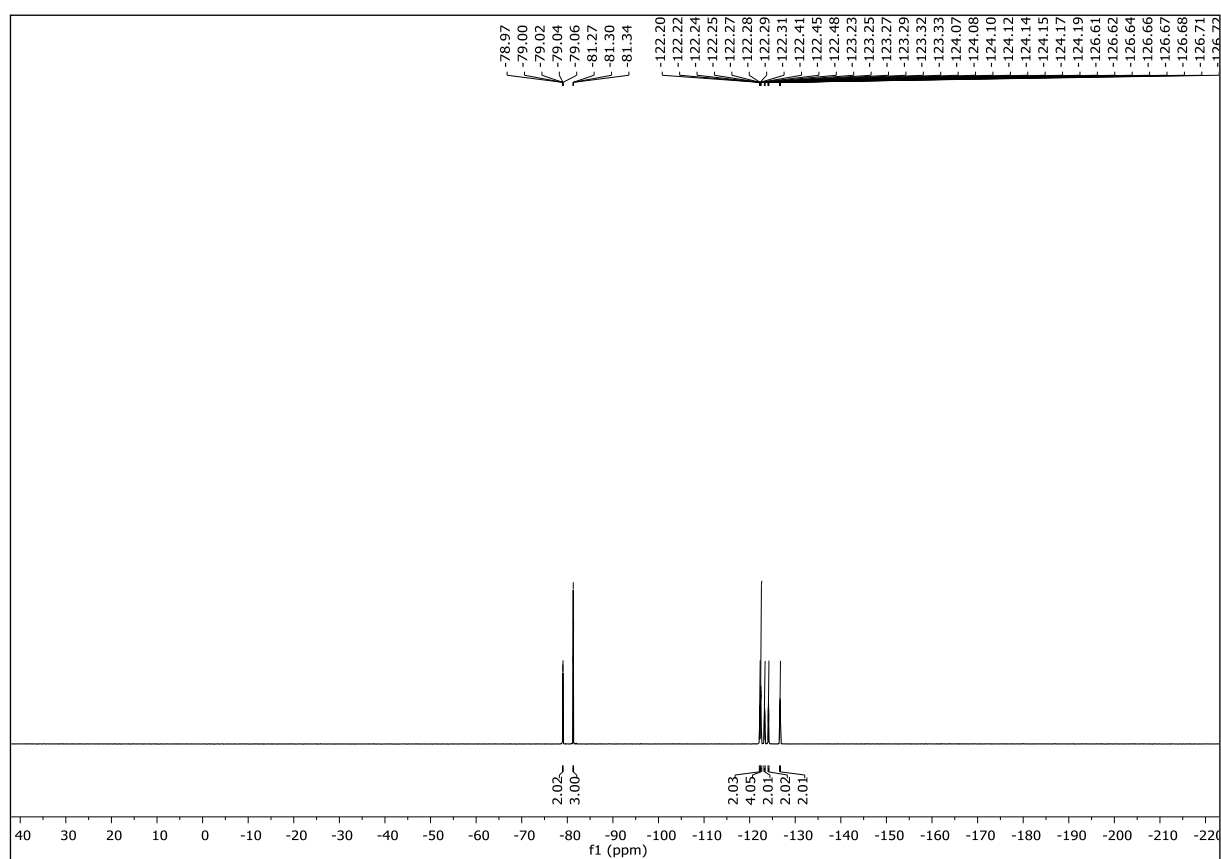
NMR-Solvent: CDCl_3



NMR-Solvent: CDCl₃

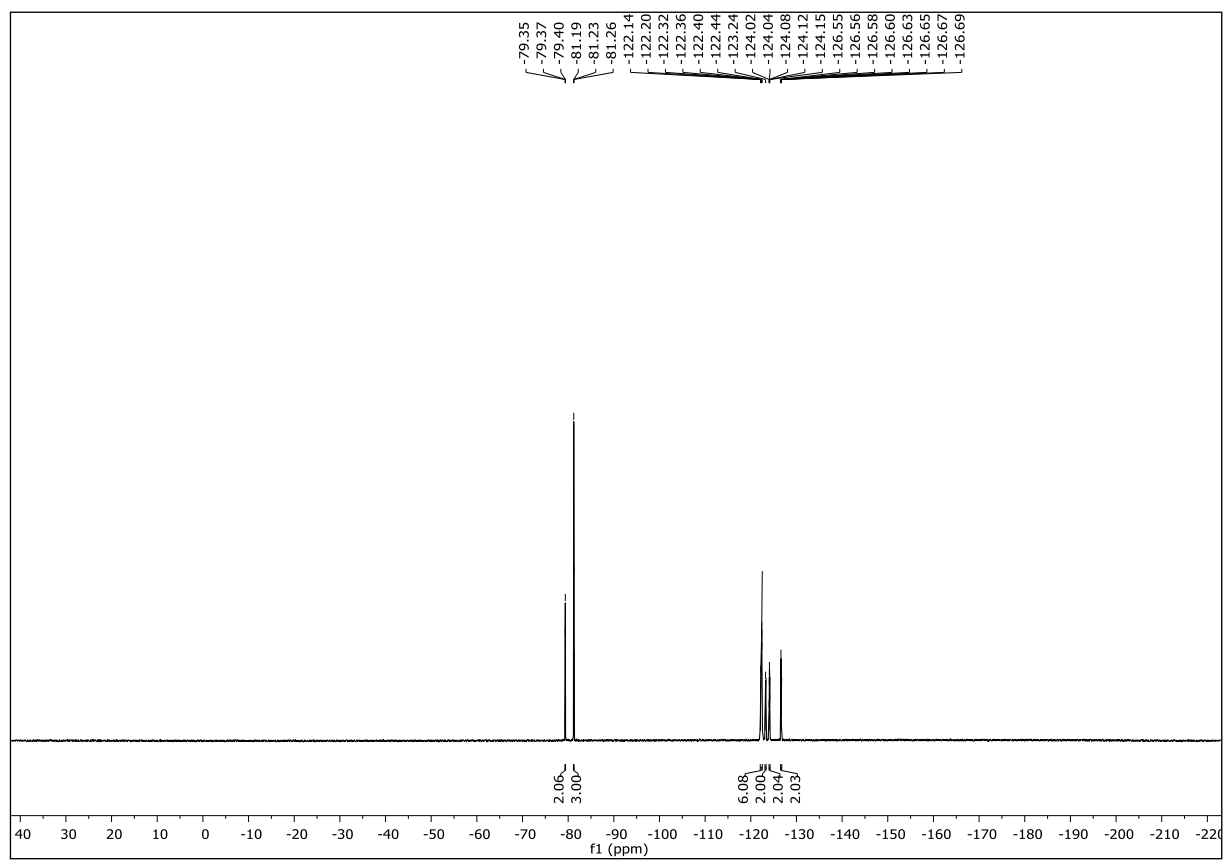
1-((2,2,3,3,4,4,5,5,6,6,7,7,8,8,9,9,9-Heptafluorononyl)oxy)-2,2,6,6-tetramethyl piperidine (38)





NMR-Solvent: CDCl₃





NMR-Solvent: CDCl_3

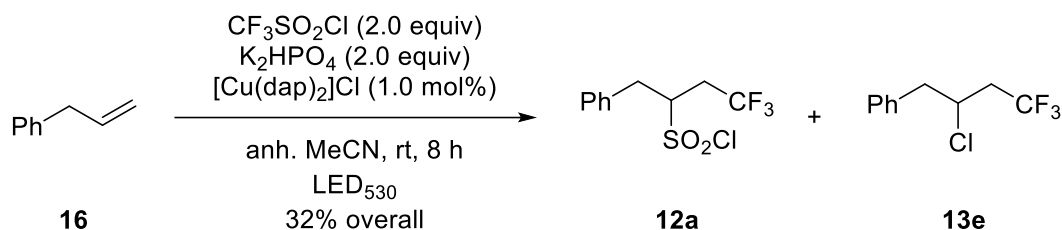
4. Chapter D: Synthesis of Trifluoromethylated Sultones From Alkenols Using a Copper Photoredox Catalyst

4.1. Synthesis of Literature Known Compounds and Reagents

The following compounds were synthesized according to the reported procedures. The spectral data are consistent with the data reported:

1-nitro-4-vinylbenzene^[22], diethyl 2,2-diallylmalonate^[24], 2-methylhex-5-en-2-ol (**23e**)^[27], 2,2-diphenylpent-4-en-1-ol (**23f**)^[28], diethyl 2-allyl-2-(hydroxymethyl)malonate (**23g**)^[17,29], (1-allylcyclohexyl)methanol (**23h**)^[30], *rel*-(1*R*,6*S*)-7-Oxabicyclo [4.1.0]-heptane^[31], *rel*-(1*S*,2*R*)-2-allylcyclohexan-1-ol (**23i**)^[32], 4-methylpent-4-en-1-ol (**23k**)^[33], hex-4-en-1-ol (**23l**)^[34], 2-allyl-6-methoxyphenol (**23m**)^[35], pent-4-en-1-yl trifluoromethanesulfonate (**41**)^[36], 2-(chloromethyl)tetrahydrofuran^[37], 5-methoxypent-1-ene (**44**)^[38].

4.2. Quantum Yield Determination



The quantum yield Φ of the photocatalytic addition of trifluoromethanesulfonyl chloride (**3a**) to allyl benzene (**16**) was determined by a method developed by Riedle et al.^[39] An oven-dried fluorescence cuvette equipped with a stirring bar and septum was charged with K_2HPO_4 (177 mg, 1.0 mmol, 2.0 equiv) and $[\text{Cu}(\text{dap})_2]\text{Cl}$ (4.4 mg, 5.0 μmol , 1.0 mol%) under a nitrogen atmosphere. Previously degassed MeCN (1.5 mL) by three freeze-pump-thaw cycles was added, followed by the addition of allylbenzene (**16**) (66 μL , 0.5 mmol, 1.0 equiv) and $\text{CF}_3\text{SO}_2\text{Cl}$ (**3a**) (106 μL , 1.0 mmol, 2.0 equiv).

The measurement was accomplished in a dark room to minimize the ambient light. The radiant power of light transmitted by the cuvette with a blank solution containing K_2HPO_4 (177 mg, 1.0 mmol, 2.0 equiv) in degassed MeCN (1.5 mL) was measured ($U_{\text{Ref}} = 0.186 \text{ V}$) and the transmitted power ($P_{\text{Ref}} = U_{\text{Ref}}/10 = 18.6 \text{ mW}$) was noted. The cuvette with blank was changed by the cuvette with the reaction mixture and the transmitted power ($P_{\text{Sample}} = 8.7 \text{ mW}$) was noted. The transmitted radiant power was monitored during the irradiation and remained constant.

The sample was irradiated for eight hours to reach 26% yield of the $\text{SO}_2\text{Cl}/\text{CF}_3$ product **12a** (37 mg, 0.13 mmol) respectively 6% yield for the Cl/CF_3 product **13e** (7 mg, 0.03 mmol) determined by ^1H -NMR using 1,4-Dicyanobenzene as internal standard. The quantum yield Φ was calculated from equation 1:

$$\Phi = \frac{N_{\text{Product}}}{N_{\text{Photons}}} = \frac{N_A * n_{\text{Product}}}{\frac{E_{\text{Light}}}{E_{\text{Photons}}}} = \frac{N_A * n_{\text{Product}}}{\frac{P_{\text{absorbed}} * t}{\frac{h * c}{\lambda}}} = \frac{h * c * N_A * n_{\text{Product}}}{\lambda * (P_{\text{Ref}} - P_{\text{Sample}}) * t} \quad (\text{eq 1})$$

where Φ is the quantum yield, N_{Product} is the number of molecules created, N_{Photons} is the number of absorbed photons, N_A is Avogadro's constant in moles⁻¹, n_{Product} is the molar amount of molecules created in moles, E_{Light} is the energy of light absorbed in joule, E_{Photons} is the energy of a single photon in joule, P_{absorbed} is the radiant power absorbed in Watt, t is the irradiation time in seconds, h is the Planck's constant in joule seconds, c is the speed of light in meter per second, λ is the wavelength of irradiation source in meter, P_{Ref} is the radiant

power transmitted by a blank cuvette in Watt and P_{Sample} is the radiant power transmitted by the cuvette with the reaction mixture in Watts.

This results in:

$$\begin{aligned}\Phi &= \frac{h * c * N_A * n_{\text{Product}}}{\lambda * (P_{\text{Ref}} - P_{\text{Sample}}) * t} = \\ &= \frac{6.626 * 10^{-34} \text{ Js} * 2.998 * 10^8 \frac{\text{m}}{\text{s}} * 6.022 * 10^{23} \frac{1}{\text{mol}} * 0.13 * 10^{-3} \text{ mol}}{435 * 10^{-9} \text{ m} * (18.6 - 8.7) * 10^{-3} \frac{\text{J}}{\text{s}} * 28800 \text{ s}} = \\ &= \frac{1.5551 * 10^{-5} \text{ Jm}}{1.2631 * 10^{-4} \text{ Jm}} = 0.1231 \approx 12\%\end{aligned}$$

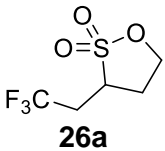
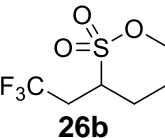
The quantum yield for the $\text{SO}_2\text{Cl}/\text{CF}_3$ product **12a** was determined to be $\Phi = 12\%$ respectively be $\Phi = 3\%$ for the Cl/CF_3 product **13e**.

4.3. Karl Fischer Titration

The water contamination of the photocatalytic ring closure of trifluoromethanesulfonyl chloride (**3a**) to but-3-en-1-ol (**23a**) and pent-4-en-1-ol (**23b**) was determined by Karl Fischer titration. The water contamination of a blank solution of anhydrous Et₂O (1.5 mL) respectively a sample containing sultone in anhydrous Et₂O (1.5 mL) was measured and the mass fraction of H₂O of the injected sample calculated (eq 2).

$$wt_{Sample}(H_2O) = \frac{m_{Sample}(H_2O)}{m(Sample)} \quad (\text{eq 2})$$

Table 1: Results of Karl-Fischer Titration.

Entry	Sample	m(Sample) [g]	m _{Sample} (H ₂ O) [μg]	wt _{Sample} (H ₂ O) [ppm]
1	Et ₂ O	0.982	11.6	11.8
2 ^[a]	 26a	0.657	103.1	156.9
3 ^[b]	 26b	0.993	50.0	50.3

Measurement conditions: [a] solution containing 3-(2,2,2-trifluoroethyl)-1,2-oxathiolane 2,2-dioxide (**26a**) (m_{Sulton} = 225 mg) in anh. anhydrous Et₂O (1.5 mL); [b] solution containing 3-(2,2,2-trifluoroethyl)-1,2-oxathiane 2,2-dioxide (**26b**) (m_{Sulton} = 286 mg) in anh. anhydrous Et₂O (1.5 mL).

The water contamination wt_{Sulton}(H₂O) of the pure product was calculated after subtraction of the blank value for anh. Et₂O (m_{Sample}(H₂O) = 11.6 μg) using equation 3 and 4.

$$\Delta m_{Sulton}(H_2O) = m_{Sample}(H_2O) - m_{Et_2O}(H_2O) \quad (\text{eq 3})$$

$$wt_{Sulton}(H_2O) = \frac{\Delta m_{Sulton}(H_2O)}{m_{Sulton}} \quad (\text{eq 4})$$

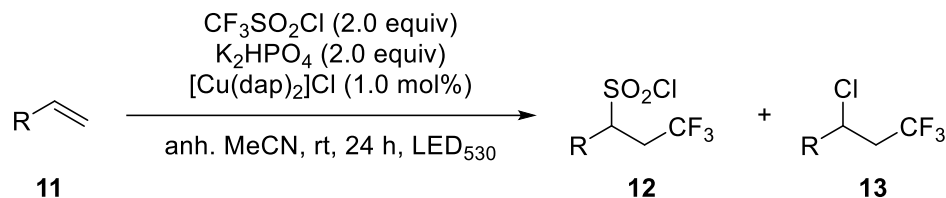
For example, the water contamination of the 5-ring **26a** can be calculated (eq 5):

$$wt_{Sulton, 5-ring}(H_2O) = \frac{\Delta m_{Sulton, 5-ring}(H_2O)}{m_{Sulton, 5-ring}} = \frac{91.5 \cdot 10^{-6} \text{ g}}{0.225 \text{ g}} \approx 407 \cdot 10^{-6} \quad (\text{eq 5})$$

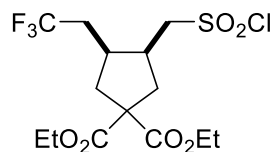
Finally, the water contamination for 3-(2,2,2-trifluoroethyl)-1,2-oxathiolane 2,2-dioxide (**26a**) was determined to be 407 ppm respectively 134 ppm for 3-(2,2,2-trifluoroethyl)-1,2-oxathiane 2,2-dioxide (**26b**).

4.5. Compound Characterization

General Procedure for the Trifluoromethylchlorosulfonylation Catalyzed by [Cu(dap)₂]Cl Under Visible Light (GP-A)

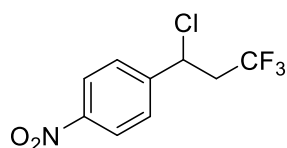


An oven-dried Schlenk tube equipped with a magnetic stirring bar was charged with alkene **11** (1.0 mmol, 1.0 equiv), K₂HPO₄ (348 mg, 2.0 mmol, 2.0 equiv) and [Cu(dap)₂]Cl (8.8 mg, 1.0 μmol, 1.0 mol%) in anhydrous MeCN (3 mL). The resulting suspension was degassed by three freeze-pump-thaw cycles followed by the addition of CF₃SO₂Cl (**3a**) (210 μL, 2.0 mmol, 2.0 equiv). The reaction mixture was irradiated under stirring for 24 hours with a green light LED, ($\lambda_{\text{max}} = 530 \text{ nm}$) at room temperature. The reaction mixture was quenched with water (3 mL) and the product was extracted with CH₂Cl₂ (3x 10 mL). The combined organic layers were dried over anhydrous Na₂SO₄ and concentrated in vacuum. The residue was purified by column chromatography on silica.

Diethyl (3S,4S)-3-((chlorosulfonyl)methyl)-4-(2,2,2-trifluoroethyl)cyclopentane-1,1-dicarboxylate (12g)^[18]

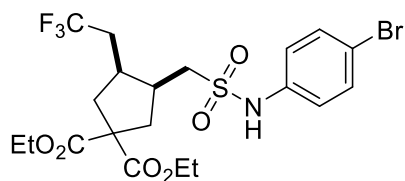
Following GP-A, **12g** was prepared using diethyl 2,2-diallylmalonate (240 mg, 1.0 mmol), K_2HPO_4 (352 mg, 2.0 mmol, 2.0 equiv), CF_3SO_2Cl (**3a**) (210 μ L, 2.0 mmol, 2.0 equiv) and $[Cu(dap)_2]Cl$ (8.8 mg, 1.0 μ mol, 1 mol%). Chromatography on silica (hexanes-EtOAc, 9:1) afforded an unseparable mixture of SO_2Cl **12g** and Cl/CF_3 adduct **13a** in a ratio of 95:05 as a colorless oil (367 mg, 91% overall yield).

R_f (hexanes-EtOAc, 9:1) = 0.21. **Staining:** $KMnO_4$ (UV inactive). **1H -NMR** (300 MHz, $CDCl_3$) δ = 4.20 (qd, J = 7.1, 1.5 Hz, 4H), 3.86 – 3.62 (m, 2H), 2.92 (ddd, J = 10.3, 6.4, 4.4 Hz, 1H), 2.73 – 2.45 (m, 4H), 2.28 – 2.01 (m, 3H), 1.25 (t, J = 7.1 Hz, 6H). **^{19}F -NMR** (282 MHz, $CDCl_3$) δ = -64.75 (s, 3F). **^{13}C -NMR** (101 MHz, $CDCl_3$) δ = 172.5, 171.5, 126.5 (q, J = 276.9 Hz), 65.1, 62.4, 62.1, 58.0, 38.4, 38.3, 37.8, 36.8 (q, J = 2.2 Hz), 33.4 (q, J = 28.7 Hz), 14.0, 14.0. **IR** (neat, cm^{-1}): 2985, 2943, 1991, 1721, 1447, 1367, 1256, 1150, 1117, 1097, 1056, 1026, 1010, 860, 760, 662, 631, 581, 538. **HRMS** (ESI) exact mass calc. for $C_{14}H_{21}ClF_3O_6S$: m/z 409.0694, found: m/z 409.00696 $[M+H]^+$.

1-(1-Chloro-3,3,3-trifluoropropyl)-4-nitrobenzene (13b)^[18]

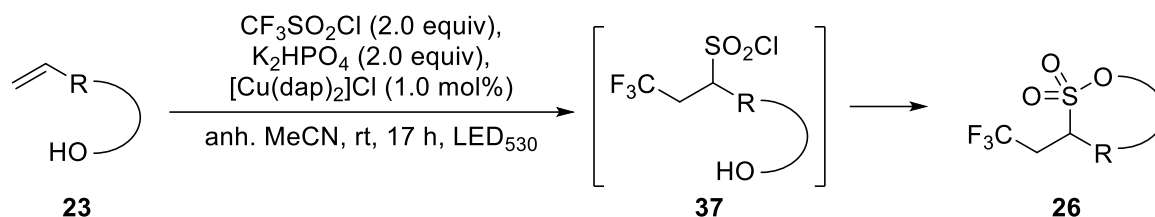
Following GP-A, **13b** was prepared using 1-nitro-4-vinylbenzene (149 mg, 1.0 mmol, 1.0 equiv), K_2HPO_4 (352 mg, 2.0 mmol, 2.0 equiv), CF_3SO_2Cl (**3a**) (210 μ L, 2.0 mmol, 2.0 equiv) and $[Cu(dap)_2]Cl$ (8.8 mg, 1.0 μ mol, 1 mol%). Chromatography on silica (pentane-Et₂O, 3:1) afforded **13b** as a colorless oil (224 mg, 88%).

R_f (pentane-Et₂O, 3:1) = 0.55. **Staining:** $KMnO_4$ (UV active). **1H -NMR** (300 MHz, $CDCl_3$) δ = 8.33 – 8.20 (m, 2H), 7.66 – 7.54 (m, 2H), 5.18 (t, J = 7.1 Hz, 1H), 3.15 – 2.77 (m, 2H). **^{19}F -NMR** (282 MHz, $CDCl_3$) δ = -64.32 (s, 3F). **^{13}C -NMR** (75 MHz, $CDCl_3$) δ = 148.2, 146.3, 128.1, 124.5 (q, J = 278.0 Hz), 124.4, 53.3 (q, J = 3.6 Hz), 43.6 (q, J = 28.7 Hz). **IR** (neat, cm^{-1}): 3085, 2867, 1610, 1524, 1427, 1348, 1318, 1254, 1229, 1139, 1098, 1044, 1015, 934, 859, 845, 812, 784, 700, 644. **HRMS** (ESI) exact mass calc. for $C_9H_8ClF_3NO_2$: m/z 254.0190, found: m/z 254.0191 $[M+H]^+$.

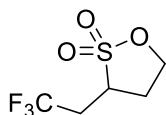
Diethyl-(3*S*,4*S*)-3-((*N*-(4-bromophenyl)sulfamoyl)methyl)-4(2,2,2-trifluoroethyl)cyclopentane-1,1-dicarboxylate (15**)**^[18]

To an ice cooled solution of the mixture containing sulfonylchloride derivative **12g** and chlorine adduct **13a** (100 mg, 0.24 mmol, 1.0 equiv) in anh. CH₂Cl₂ (5 mL) was added 4-bromoaniline **14** (51 mg, 0.29 mmol, 1.2 equiv). The resulting reaction mixture was stirred overnight. After completion as judged by TLC, the reaction mixture was quenched with HCl (10 mL, 1 M) and extracted with CH₂Cl₂ (3x 20 mL). The combined organic layers were washed with sat. NaHCO₃ solution until neutral pH followed by brine (2x 20 mL). The organic layer was dried over anhydrous Na₂SO₄, filtered and concentrated in vacuo. The resulting crude product was purified by column chromatography (pentane-Et₂O, 1:1) to afford **15** as a beige solid (76 mg, 57%).

R_f (pentane-Et₂O, 1:1) = 0.22. **Staining:** KMnO₄ (UV active). **¹H-NMR** (300 MHz, CDCl₃) δ = 7.48 – 7.40 (m, 2H), 7.36 (br, s, 1H), 7.14 – 7.07 (m, 2H), 4.25 – 4.06 (m, 4H), 3.16 – 3.03 (m, 2H), 2.70 (dq, *J* = 12.9, 6.2 Hz, 1H), 2.48 (dtd, *J* = 20.7, 14.6, 6.6 Hz, 4H), 2.19 – 1.94 (m, 3H), 1.21 (q, *J* = 7.2 Hz, 6H). **¹⁹F-NMR** (282 MHz, CDCl₃) δ = -64.56 (s, 3F). **¹³C-NMR** (75 MHz, CDCl₃) δ = 172.6, 171.9, 135.9, 132.8, 132.5 – 121.9 (q, *J* = 277.2 Hz), 121.8, 118.3, 62.2, 62.1, 58.2, 51.3, 38.2, 38.0, 37.6, 36.5 (dd, *J* = 4.7, 2.1 Hz), 33.2 (q, *J* = 28.4 Hz). **IR** (neat, cm⁻¹): 3243, 2984, 2939, 2907, 1720, 1591, 1489, 1449, 1390, 1319, 1257, 1142, 1114, 1058, 1009, 920, 822, 796, 709, 659, 582. **HRMS** (ESI) exact mass calc. for C₂₀H₂₅BrF₃NO₆S: *m/z* 544.0611, found: *m/z* 544.0609 [M+H]⁺. **mp**: 109 °C.

General Procedure for the Preparation of Sultones Catalyzed by [Cu(dap)₂]Cl Under Visible Light (GP-B)

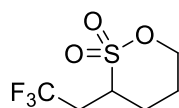
An oven-dried Schlenk tube equipped with a magnetic stirring bar was charged with alkene **23** (1.0 mmol, 1.0 equiv), K_2HPO_4 (348 mg, 2.0 mmol, 2.0 equiv) and $[\text{Cu}(\text{dap})_2]\text{Cl}$ (8.8 mg, 1.0 μmol , 1.0 mol%) in anhydrous MeCN (3 mL). The resulting suspension was degassed by three freeze-pump-thaw cycles followed by the addition of $\text{CF}_3\text{SO}_2\text{Cl}$ (**3a**) (210 μL , 2.0 mmol, 2.0 equiv). The reaction mixture was irradiated under stirring for 17 hours with a green light LED ($\lambda_{\text{max}} = 530 \text{ nm}$) at room temperature. The reaction mixture was quenched with water (3 mL) and the product was extracted with CH_2Cl_2 . The combined organic layers were dried over anhydrous Na_2SO_4 and concentrated in vacuum. The residue was purified by filtration through a silica plug with CH_2Cl_2 as the eluent or by column chromatography on silica gel to yield the desired product **26**.

3-(2,2,2-Trifluoroethyl)-1,2-oxathiolane 2,2-dioxide (26a)

Following GP-B, **26a** was prepared using but-3-en-1-ol (**23a**) (86 μ L, 1.0 mmol, 1.0 equiv), K_2HPO_4 (352 mg, 2.0 mmol, 2.0 equiv), CF_3SO_2Cl (**3a**) (210 μ L, 2.0 mmol, 2.0 equiv) and $[Cu(dap)_2]Cl$ (8.8 mg, 1.0 μ mol, 1.0 mol%). The reaction solution was filtered through a silica plug with CH_2Cl_2 as the eluent. The filtrate was concentrated under reduced pressure to afford **26a** as a colorless oil (102 mg, 50%).

Scale-Up: The reaction was performed ten times on a 5 mmol scale (=50 mmol). Following GP-B, **26a** was prepared using but-3-en-1-ol (**23a**) (430 μ L, 5.0 mmol, 1.0 equiv), K_2HPO_4 (1.76 g, 10.0 mmol, 2.0 equiv), CF_3SO_2Cl (**3a**) (1.1 mL, 10.0 mmol, 2.0 equiv) and $[Cu(dap)_2]Cl$ (44 mg, 5.0 μ mol, 1.0 mol%) in anh. MeCN (15 mL). The reaction mixture was irradiated under stirring for 48 hours with a green light plate LED (λ_{max} = 530 nm) at room temperature. The combined reaction solutions of the overall ten reactions was filtered through a silica plug with CH_2Cl_2 as the eluent and concentrated in vacuo. The residue was purified by distillation under reduced pressure (1.4 mbar, oilbath temperature 150-170 $^{\circ}C$, boiling point at 87-89 $^{\circ}C$) to yield **26a** as a colorless oil (6.53 g, 64%).

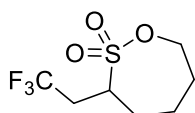
R_f = not determinable. **Staining:** not determinable (UV inactive). **1H -NMR** (600 MHz, $CDCl_3$) δ = 4.51 (ddd, J = 9.2, 8.2, 3.3 Hz, 1H), 4.43 (td, J = 9.1, 7.0 Hz, 1H), 3.50 (tdd, J = 10.1, 7.9, 3.9 Hz, 1H), 2.95 – 2.87 (m, 1H), 2.83 – 2.78 (m, 1H), 2.51 – 2.41 (m, 2H). **^{19}F -NMR** (282 MHz, $CDCl_3$) δ = -64.99 (s, 3F). **^{13}C -NMR** (75 MHz, $CDCl_3$) δ = 125.3 (d, J = 277.1 Hz), 67.2, 49.7 (q, J = 2.8 Hz), 33.5 (q, J = 30.8 Hz), 29.6. **IR** (neat, cm^{-1}): 2966, 2926, 1350, 1315, 1258, 1165, 1137, 1077, 993, 914, 792, 661, 631, 609, 496. **HRMS** (APCI) exact mass calc. for $C_5H_8F_3O_3S$: m/z 205.0141, found: m/z 205.0140 $[M+H]^+$. **GC-Analysis:** purity 94%, t_R = 5.276 min. **wt(H_2O)** = 407 ppm.

3-(2,2,2-Trifluoroethyl)-1,2-oxathiane 2,2-dioxide (26b)

Following GP-B, **26b** was prepared using pent-4-en-1-ol (**23b**) (102 μ L, 1.0 mmol, 1.0 equiv), K_2HPO_4 (352 mg, 2.0 mmol, 2.0 equiv) and CF_3SO_2Cl (**3a**) (210 μ L, 2.0 mmol, 2.0 equiv) and $[Cu(dap)_2]Cl$ (8.8 mg, 1.0 μ mol, 1.0 mol%). The reaction solution was filtered through a silica plug with CH_2Cl_2 as the eluent. The filtrate was concentrated under reduced pressure to afford **26b** as a colorless oil (207 mg, 94%).

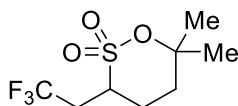
Scale-Up: The reaction was performed ten times on a 5 mmol scale (=50 mmol). Following GP-B, **26b** was prepared using pent-4-en-1-ol (**23b**) (510 μ L, 5.0 mmol, 1.0 equiv), K_2HPO_4 (1.76 g, 10.0 mmol, 2.0 equiv), CF_3SO_2Cl (**3a**) (1.1 mL, 10.0 mmol, 2.0 equiv) and $[Cu(dap)_2]Cl$ (44 mg, 5.0 μ mol, 1.0 mol%) in anh. MeCN (15 mL). The reaction mixture was irradiated under stirring for 48 hours with a green light plate LED (λ_{max} = 530 nm) at room temperature. The combined reaction solutions of the overall ten reactions was filtered through a silica plug with CH_2Cl_2 as the eluent and concentrated in vacuo. The residue was purified by distillation under reduced pressure (0.7 mbar, oilbath temperature 120°C, boiling point at 83-84 °C) to yield **26b** as a colorless oil (7.72 g, 71%).

R_f = not determinable. **Staining:** not determinable (UV inactive). **1H -NMR** (600 MHz, $CDCl_3$) δ = 4.61 (td, J = 11.1, 2.9 Hz, 1H), 4.55 (dtd, J = 11.4, 4.2, 1.8 Hz, 1H), 3.40 (tt, J = 10.6, 3.5 Hz, 1H), 2.94 (dq, J = 15.3, 11.1, 2.9 Hz, 1H), 2.50 – 2.38 (m, 2H), 2.11 (dtd, J = 14.4, 10.9, 3.7 Hz, 1H), 2.03 – 1.95 (m, 1H), 1.90 (ddq, J = 15.2, 5.2, 3.5 Hz, 1H). **^{19}F -NMR** (282 MHz, $CDCl_3$) δ = -63.86 (s, 3F). **^{13}C -NMR** (75 MHz, $CDCl_3$) δ = 125.4 (q, J = 277.2 Hz), 74.5, 53.7 (q, J = 2.3 Hz), 32.5 (q, J = 30.8 Hz), 28.3, 23.2. **IR** (neat, cm^{-1}): 2987, 1439, 1353, 1327, 1252, 1223, 1170, 1133, 1062, 1014, 939, 872, 794, 738. **HRMS** (ESI) exact mass calc. for $C_6H_{13}F_3NO_3S$: m/z 236.0563, found: m/z 236.0565 $[M+NH_4]^+$. **GC-Analysis:** purity 95%, t_R = 6.821 min. **wt(H₂O)** = 134 ppm.

3-(2,2,2-Trifluoroethyl)-1,2-oxathiepane 2,2-dioxide (26c)

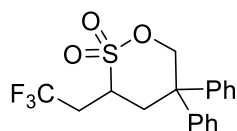
Following GP-B, **26c** was prepared using hex-5-en-1-ol (**23c**) (120 μ L, 1.0 mmol, 1.0 equiv), K_2HPO_4 (352 mg, 2.0 mmol, 2.0 equiv), CF_3SO_2Cl (**3a**) (210 μ L, 2.0 mmol, 2.0 equiv) and $[Cu(dap)_2]Cl$ (8.8 mg, 1.0 μ mol, 1.0 mol%). The reaction solution was filtered through a silica plug with CH_2Cl_2 as the eluent. The filtrate was concentrated under reduced pressure to afford **26c** as a colorless oil (74 mg, 32%).

R_f = not determinable. **Staining**: not determinable (UV inactive). **1H -NMR** (300 MHz, $CDCl_3$) δ = 4.45 – 4.23 (m, 2H), 3.50 – 3.39 (m, 1H), 3.06 – 2.87 (m, 1H), 2.52 – 2.31 (m, 1H), 2.30 – 2.18 (m, 1H), 2.16 – 2.05 (m, 2H), 2.05 – 1.92 (m, 1H), 1.86 – 1.66 (m, 2H). **^{19}F -NMR** (282 MHz, $CDCl_3$) δ = -63.89 (s, 3F). **^{13}C -NMR** (75 MHz, $CDCl_3$) δ = 125.7 (q, J = 277.4 Hz), 71.1, 57.7 (q, J = 2.2 Hz), 34.1 (q, J = 30.2 Hz), 28.9, 28.5, 22.8. **IR** (neat, cm^{-1}): 2961, 2923, 2853, 1458, 1357, 1261, 1133, 1096, 1022, 800, 633. **HRMS** (APCI) exact mass calc. for $C_7H_{11}F_3O_3S$: m/z 233.0454, found: m/z 233.0450 $[M+H]^+$.

6,6-Dimethyl-3-(2,2,2-trifluoroethyl)-1,2-oxathiane 2,2-dioxide (26e)

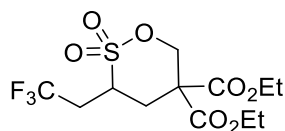
Following GP-B, **26e** was prepared using 2-methylhex-5-en-2-ol (**23e**) (115 mg, 1.0 mmol, 1.0 equiv), K_2HPO_4 (352 mg, 2.0 mmol, 2.0 equiv) and CF_3SO_2Cl (**3a**) (210 μ L, 2.0 mmol, 2.0 equiv) and $[Cu(dap)_2]Cl$ (8.8 mg, 1.0 μ mol, 1.0 mol%). The reaction solution was filtered through a silica plug with CH_2Cl_2 as the eluent. The filtrate was concentrated under reduced pressure to afford **26e** as a yellowish solid (179 mg, 73%).

R_f = not determinable. **Staining**: not determinable (UV inactive). **1H -NMR** (600 MHz, $CDCl_3$) δ = 3.27 (tt, J = 10.7, 3.4 Hz, 1H), 2.97 – 2.89 (m, 1H), 2.40 (ddt, J = 15.2, 12.6, 10.0 Hz, 2H), 2.26 – 2.19 (m, 1H), 1.94 (ddd, J = 15.2, 11.8, 3.6 Hz, 1H), 1.87 (ddd, J = 14.7, 5.5, 3.4 Hz, 1H), 1.63 (s, 3H), 1.53 (s, 3H). **^{19}F -NMR** (376 MHz, $CDCl_3$) δ = -63.59 (s, 3F). **^{13}C -NMR** (101 MHz, $CDCl_3$) δ = 125.6 (q, J = 277.3 Hz), 93.2, 52.6 (q, J = 2.3 Hz), 35.1, 32.6 (q, J = 30.4 Hz), 30.4, 25.4, 25.1 (dd, J = 2.5, 1.1 Hz). **IR** (neat, cm^{-1}): 2994, 2955, 1446, 1396, 1342, 1291, 1243, 1174, 1132, 1097, 1078, 1032, 875, 848, 778, 696, 545. **HRMS** (ESI) exact mass calc. for $C_8H_{14}F_3O_3S$: m/z 247.0610, found: m/z 247.0610 $[M+H]^+$. **mp**: 68 $^{\circ}C$.

5,5-Diphenyl-3-(2,2,2-trifluoroethyl)-1,2-oxathiane 2,2-dioxide (26f)

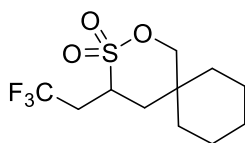
Following GP-B, **26f** was prepared using 2,2-diphenylpent-4-en-1-ol (**23f**) (238 mg, 1.0 mmol, 1.0 equiv), K_2HPO_4 (352 mg, 2.0 mmol, 2.0 equiv), CF_3SO_2Cl (**3a**) (210 μL , 2.0 mmol, 2.0 equiv) and $[Cu(dap)_2]Cl$ (8.8 mg, 1.0 μmol , 1.0 mol%). Chromatography on silica gel (pentane- CH_2Cl_2 , 2:1) afforded **26f** as a white solid (269 mg, 73%).

R_f (pentane- CH_2Cl_2 , 3:1) = 0.25. **Staining:** PMA (UV active). **1H -NMR** (600 MHz, $CDCl_3$) δ = 7.45 – 7.24 (m, 8H), 7.13 – 7.07 (m, 2H), 5.04 (dd, J = 12.3, 2.7 Hz, 1H), 4.79 (d, J = 12.4 Hz, 1H), 3.22 (tdd, J = 10.5, 4.8, 2.8 Hz, 1H), 3.12 – 3.02 (m, 2H), 2.87 (dq, J = 15.2, 10.9, 2.8 Hz, 1H), 2.51 – 2.42 (m, 1H). **^{19}F -NMR** (376 MHz, $CDCl_3$) δ = -63.22 (s, 3F). **^{13}C -NMR** (101 MHz, $CDCl_3$) δ = 141.4, 140.3, 129.4, 129.1, 128.0, 127.9, 127.6, 127.1, 125.4 (d, J = 277.5 Hz), 78.4, 50.9 (q, J = 2.6 Hz), 32.4 (q, J = 30.5 Hz). **IR** (neat, cm^{-1}): 3064, 3030, 2960, 2874, 1739, 1603, 1495, 1448, 1361, 1316, 1260, 1174, 1141, 1014, 954, 928. **HRMS** (ESI) exact mass calc. for $C_{18}H_{17}F_3O_3S$: m/z 370.0845, found: m/z 370.0847 $[M]^+$. **mp**: 187 $^{\circ}C$.

Diethyl 3-(2,2,2-trifluoroethyl)-1,2-oxathiane-5,5-dicarboxylate 2,2-dioxide (26g)

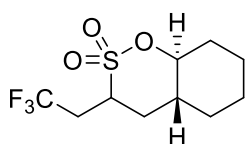
Following GP-B, **26g** was prepared using diethyl 2-allyl-2-(hydroxymethyl)malonate (**23g**) (230 mg, 1.0 mmol, 1.0 equiv), K_2HPO_4 (352 mg, 2.0 mmol, 2.0 equiv), CF_3SO_2Cl (**3a**) (210 μL , 2.0 mmol, 2.0 equiv) and $[Cu(dap)_2]Cl$ (8.8 mg, 1.0 μmol , 1.0 mol%). Chromatography on silica gel (pentane- CH_2Cl_2 , 5:1) afforded **26g** as a colourless oil (181 mg, 50%).

R_f (pentane- CH_2Cl_2 , 5:1) = 0.42. **Staining:** $KMnO_4$ (UV inactive). **1H -NMR** (600 MHz, $CDCl_3$) δ = 5.01 – 4.88 (m, 2H), 4.40 – 4.20 (m, 4H), 3.84 – 3.75 (m, 1H), 3.20 – 2.88 (m, 2H), 2.43 – 2.22 (m, 2H), 1.34 – 1.25 (m, 6H). **^{19}F -NMR** (282 MHz, $CDCl_3$) δ = -63.57 (s, 3F). **^{13}C -NMR** (75 MHz, $CDCl_3$) δ = 166.9, 166.3, 125.2 (q, J = 277.7 Hz), 74.5, 63.2, 63.1, 57.1, 50.7 (q, J = 2.2 Hz), 39.9, 34.1, 32.7 (q, J = 31.0 Hz), 14.0. **IR** (neat, cm^{-1}): 2989, 1733, 1439, 1368, 1320, 1252, 1178, 1141, 1014, 965, 846, 801, 742, 697. **HRMS** (ESI) exact mass calc. for $C_{12}H_{18}F_3O_7S$: m/z 363.0720, found: m/z 363.0721 $[M+H]^+$. **GC-Analysis:** purity 88%, t_R = 11.526 min.

4-(2,2,2-Trifluoroethyl)-2-oxa-3-thiaspiro[5.5]undecane 3,3-dioxide (26h)

Following GP-B, **26h** was prepared using (1-allylcyclohexyl)methanol (**23h**) (154 mg, 1.0 mmol, 1.0 equiv), K_2HPO_4 (352 mg, 2.0 mmol, 2.0 equiv), CF_3SO_2Cl (**3a**) (210 μL , 2.0 mmol, 2.0 equiv) and $[Cu(dap)_2]Cl$ (8.8 mg, 1.0 μmol , 1.0 mol%). Chromatography on silica gel (pentane- CH_2Cl_2 , 1:1) afforded **26h** as a yellowish oil (213 mg, 74%).

R_f (pentane- CH_2Cl_2 , 2:1) = 0.40. **Staining:** PMA (UV inactive). **1H -NMR** (600 MHz, $CDCl_3$) δ = 4.35 (d, J = 11.4 Hz, 1H), 3.47 (ddt, J = 13.4, 10.3, 3.5 Hz, 1H), 2.90 (dq, J = 15.3, 11.0, 2.9 Hz, 1H), 2.42 – 2.24 (m, 2H), 1.86 – 1.31 (m, 12H). **^{19}F -NMR** (376 MHz, $CDCl_3$) δ = -64.00 (s, 3F). **^{13}C -NMR** (101 MHz, $CDCl_3$) δ = 125.5 (q, J = 277.4 Hz), 80.7, 49.7 (q, J = 2.7 Hz), 39.4, 34.2, 33.9, 32.9 (q, J = 30.4 Hz), 30.5, 26.0, 21.4, 20.9. **IR** (neat, cm^{-1}): 2933, 2863, 1454, 1361, 1320, 1267, 1170, 1003, 954, 910, 846, 805, 731. **HRMS** (ESI) exact mass calc. for $C_{11}H_{18}F_3O_3S$: m/z 287.0923, found: m/z 287.0928 $[M+H]^+$. **GC-Analysis:** purity 88%, t_R = 10.945 min.

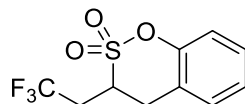
rel-(4aR,8aS)-3-(2,2,2-Trifluoroethyl)octahydrobenzo[e][1,2]oxathiine 2,2-dioxide (26i)

Following GP-B, **26i** was prepared using *rel*-(1S,2R)-2-allylcyclohexan-1-ol (**23i**) (140 mg, 1.0 mmol, 1.0 equiv), K_2HPO_4 (352 mg, 2.0 mmol, 2.0 equiv), CF_3SO_2Cl (**3a**) (210 μL , 2.0 mmol, 2.0 equiv) and $[Cu(dap)_2]Cl$ (8.8 mg, 1.0 μmol , 1.0 mol%). The reaction solution was filtered through a silica plug with CH_2Cl_2 as the eluent. The filtrate was concentrated under reduced pressure to afford **26i** as a mixture of diastereomers as a yellowish oil (245 mg, *syn/anti* = 44:56, 90% overall yield).

R_f = not determinable. **Staining:** not determinable (UV inactive). **1H -NMR** (600 MHz, $CDCl_3$) δ = 4.38 – 4.29 (m, 2H), 3.53 – 3.48 (m, 1H), 3.38 (ddt, J = 12.3, 7.0, 3.3 Hz, 1H), 2.91 – 2.87 (m, 1H), 2.62 (dd, J = 10.2, 5.1 Hz, 1H), 2.36 – 2.31 (m, 1H), 2.26 – 2.18 (m, 2H), 2.06 (ddt, J = 16.4, 8.3, 3.6 Hz, 3H), 1.84 (q, J = 3.2 Hz, 2H), 1.81 – 1.66 (m, 8H), 1.56 – 1.48 (m, 2H), 1.30 – 1.22 (m, 4H), 1.14 – 1.04 (m, 2H). **^{19}F -NMR** (376 MHz, $CDCl_3$) δ = -63.53 (s, 3F, *minor*), -64.42 (s, 3F, *major*). **^{13}C -NMR** (101 MHz, $CDCl_3$) δ = 125.6 (q, J = 277.3 Hz), 125.5 (q, J = 277.4 Hz), 89.2, 89.0, 54.2 (q, J = 2.5 Hz), 52.0 (q, J = 2.4 Hz),

40.7, 35.4, 34.7, 32.4, 32.8 (q, $J = 30.5$ Hz), 32.0 (q, $J = 30.0$ Hz), 31.6, 31.5, 30.2, 30.0, 24.9, 24.7, 24.0, 23.9. **IR** (neat, cm^{-1}): 2941, 2866, 1454, 1357, 1256, 1137, 977, 910, 883, 831, 753, 667. **HRMS** (APCI) exact mass calc. for $\text{C}_{10}\text{H}_{19}\text{F}_3\text{NO}_3\text{S}$: m/z 290.1032, found: m/z 290.1036 $[\text{M}+\text{NH}_4]^+$. **GC-Analysis**: purity 90%, $t_R = 10.496$ min (two diastereomers).

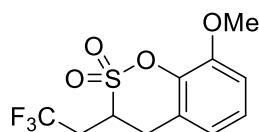
3-(2,2,2-Trifluoroethyl)-3,4-dihydrobenzo[e][1,2]oxathiine 2,2-dioxide (26j)



Following GP-B, **26j** was prepared using 2-allylphenol (**23j**) (134 mg, 1.0 mmol, 1.0 equiv), K_2HPO_4 (352 mg, 2.0 mmol, 2.0 equiv), $\text{CF}_3\text{SO}_2\text{Cl}$ (**3a**) (210 μL , 2.0 mmol, 2.0 equiv) and $[\text{Cu}(\text{dap})_2]\text{Cl}$ (8.8 mg, 1.0 μmol , 1.0 mol%). The reaction solution was filtered through a silica plug with CH_2Cl_2 as the eluent. The filtrate was concentrated under reduced pressure to afford **26j** as a yellowish oil (178 mg, 67% yield).

R_f (pentane- CH_2Cl_2 , 3:1) = 0.20. **Staining**: PMA (UV active). **$^1\text{H-NMR}$** (300 MHz, CDCl_3) $\delta = 7.39 - 7.05$ (m, 4H), 3.83 (dddd, $J = 10.8, 8.0, 5.3, 2.6$ Hz, 1H), 3.70 (dd, $J = 17.0, 5.4$ Hz, 1H), 3.41 (dd, $J = 17.1, 8.3$ Hz, 1H), 3.09 (dq, $J = 15.1, 10.8, 2.6$ Hz, 1H), 2.61 – 2.43 (m, 1H). **$^{19}\text{F-NMR}$** (282 MHz, CDCl_3) $\delta = -63.81$ (s, 3F). **$^{13}\text{C-NMR}$** (75 MHz, CDCl_3) $\delta = 151.1, 129.9, 129.2, 126.2, 125.4$ (q, $J = 277.3$ Hz), 119.3, 118.9, 50.4 (q, $J = 2.6$ Hz), 32.5 (q, $J = 28.9$ Hz), 32.3. **IR** (neat, cm^{-1}): 3071, 2960, 1618, 1584, 1457, 1491, 1375, 1327, 1260, 1186, 1148, 1096, 1010, 924, 876, 816, 790, 757, 719, 670. **HRMS** (EI) exact mass calc. for $\text{C}_{10}\text{H}_9\text{F}_3\text{O}_3\text{S}$: m/z 266.0219, found: m/z 266.0208 $[\text{M}]^+$. **GC-Analysis**: purity 89%, $t_R = 10.004$ min.

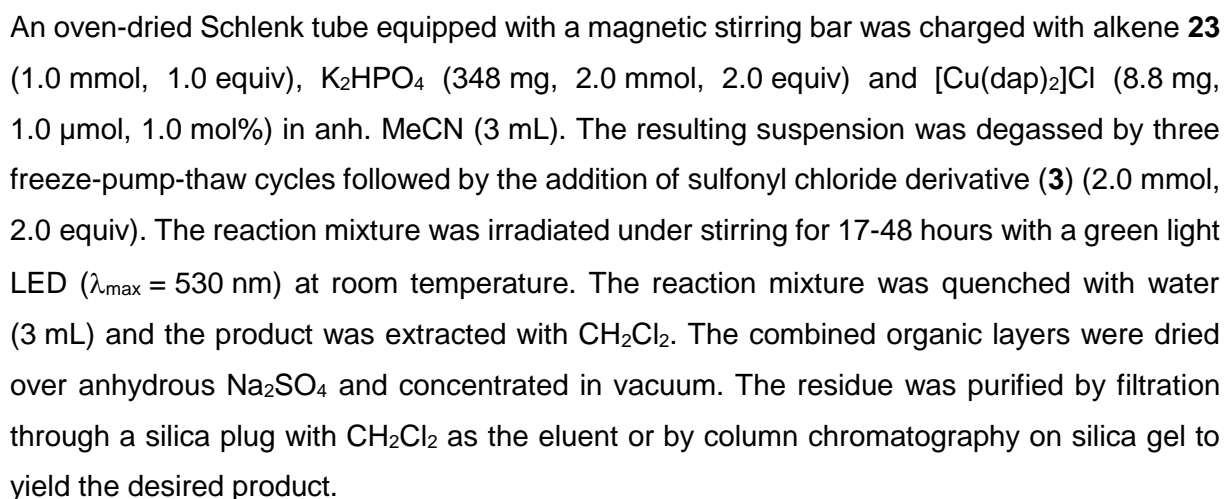
8-Methoxy-3-(2,2,2-trifluoroethyl)-3,4-dihydrobenzo[e][1,2]oxathiine 2,2-dioxide (26n)

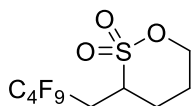


Following GP-B, **26m** was prepared using 2-allyl-6-methoxyphenol (**23n**) (492 mg, 3.0 mmol, 1.0 equiv), K_2HPO_4 (1.06 g, 6.0 mmol, 2.0 equiv), $\text{CF}_3\text{SO}_2\text{Cl}$ (**3a**) (630 μL , 6.0 mmol, 2.0 equiv) and $[\text{Cu}(\text{dap})_2]\text{Cl}$ (26 mg, 3.0 μmol , 1.0 mol%). Chromatography on silica gel (pentane- CH_2Cl_2 , 7:1) afforded **26n** as a yellowish solid (566 mg, 64%).

R_f (hexanes-EtOAc, 5:1) = 0.36. **Staining**: anisaldehyde (UV active). **$^1\text{H-NMR}$** (300 MHz, CDCl_3) $\delta = 7.13$ (t, $J = 8.0$ Hz, 1H), 6.89 (dd, $J = 8.4, 1.4$ Hz, 1H), 6.81 – 6.75 (m, 1H), 3.86 (d, $J = 1.5$ Hz, 3H), 3.78 (ddt, $J = 10.6, 5.3, 2.6$ Hz, 1H), 3.66 (dd, $J = 17.2, 5.4$ Hz, 1H), 3.36 (dd,

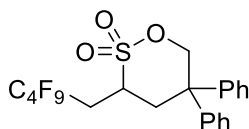
$J = 17.1, 8.0$ Hz, 1H), 3.12 – 2.96 (m, 1H), 2.56 – 2.39 (m, 1H). **^{19}F -NMR** (282 MHz, CDCl_3) $\delta = -63.84$ (s, 3F). **^{13}C -NMR** (75 MHz, CDCl_3) $\delta = 149.0, 140.5, 126.0, 125.4$ (q, $J = 277.6$ Hz), 120.8, 120.5, 111.5, 56.2, 50.3 (q, $J = 2.6$ Hz), 32.6 (q, $J = 30.8$ Hz), 32.4. **IR** (neat, cm^{-1}): 3019, 2982, 2948, 2844, 1618, 1588, 1480, 1372, 1323, 1279, 1204, 1144, 1111, 999, 954, 869, 801, 716, 686. **HRMS** (ESI) exact mass calc. for $\text{C}_{11}\text{H}_{11}\text{F}_3\text{O}_4\text{S}$: m/z 296.0325, found: m/z 296.0319 $[\text{M}]^+$. **mp**: 97 °C.



3-(2,2,3,3,4,4,5,5,5-Nonafluoropentyl)-1,2-oxathiane 2,2-dioxide (33a)

Following GP-C, **33a** was prepared using pent-4-en-1-ol (**23b**) (102 μ L, 1.0 mmol, 1.0 equiv), K_2HPO_4 (352 mg, 2.0 mmol, 2.0 equiv), $C_4F_9SO_2Cl$ (**3b**) (636 mg, 2.0 mmol, 2.0 equiv) and $[Cu(dap)_2]Cl$ (8.8 mg, 1.0 μ mol, 1.0 mol%). The reaction solution was filtered through a silica plug with CH_2Cl_2 as the eluent. The filtrate was concentrated under reduced pressure to afford **33a** as a white solid (162 mg, 44%).

R_f = not determinable. **Staining**: not determinable (UV inactive). **1H -NMR** (300 MHz, $CDCl_3$) δ = 4.70 – 4.49 (m, 2H), 3.52 (tdd, J = 10.3, 3.9, 2.7 Hz, 1H), 3.01 – 2.79 (m, 1H), 2.54 – 2.26 (m, 2H), 2.22 – 2.11 (m, 1H), 2.11 – 1.96 (m, 1H), 1.91 (dtt, J = 11.2, 5.4, 3.0 Hz, 1H). **^{19}F -NMR** (282 MHz, $CDCl_3$) δ = -81.56 (td, J = 9.6, 4.9 Hz, 3F), -109.36 – -117.15 (m, 2F), -124.74 (tq, J = 9.5, 4.7, 4.2 Hz, 2F), -126.42 (dtd, J = 24.7, 13.1, 12.1, 4.5 Hz, 2F). **^{13}C -NMR** (75 MHz, $CDCl_3$) δ = 74.6, 53.0 (d, J = 3.9 Hz), 29.4 (t, J = 21.9 Hz), 29.1 (d, J = 3.7 Hz), 23.5. **IR** (neat, cm^{-1}): 3088, 3031, 2996, 2962, 1600, 1584, 1497, 1448, 1376, 1337, 1227, 1193, 1172, 1133, 1111, 1081, 971, 931, 802, 738, 696, 513. **HRMS** (ESI) exact mass calc. for $C_9H_{10}F_9O_3S$: m/z 369.0201, found: m/z 369.0200 $[M+H]^+$. **mp**: 66 $^{\circ}C$.

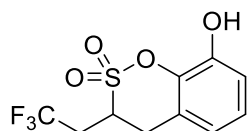
3-(2,2,3,3,4,4,5,5,5-Nonafluoropentyl)-5,5-diphenyl-1,2-oxathiane 2,2-dioxide (33b)

Following GP-C, **33b** was prepared using 2,2-diphenylpent-4-en-1-ol (**23f**) (238 mg, 1.0 mmol, 1.0 equiv), K_2HPO_4 (352 mg, 2.0 mmol, 2.0 equiv), $C_4F_9SO_2Cl$ (**3b**) (636 mg, 2.0 mmol, 2.0 equiv) and $[Cu(dap)_2]Cl$ (8.8 mg, 1.0 μ mol, 1.0 mol%). Chromatography on silica gel (pentane- CH_2Cl_2 , 2:1) afforded **33b** as a white solid (218 mg, 41%).

R_f (pentane- CH_2Cl_2 , 3:1) = 0.29. **Staining**: PMA (UV active). **1H -NMR** (600 MHz, $CDCl_3$) δ = 7.47 – 7.24 (m, 8H), 7.15 – 7.06 (m, 2H), 5.06 (dd, J = 12.4, 2.8 Hz, 1H), 4.82 (d, J = 12.4 Hz, 1H), 3.34 (tdd, J = 10.3, 4.8, 2.5 Hz, 1H), 3.17 – 3.05 (m, 2H), 2.86 (dddd, J = 33.1, 16.9, 6.4, 2.4 Hz, 1H), 2.49 – 2.38 (m, 1H). **^{19}F -NMR** (282 MHz, $CDCl_3$) δ = -81.50 (td, J = 9.7, 4.8 Hz, 3F), -105.42 – -118.36 (m, 2F), -124.69 (dt, J = 11.4, 4.4 Hz, 2F), -126.41 (ddd, J = 26.1, 16.5, 11.8 Hz, 2F). **^{13}C -NMR** (75 MHz, $CDCl_3$) δ = 141.4, 140.2, 129.4, 129.1, 128.0, 127.9, 127.6, 127.0, 78.4, 50.1 (d, J = 3.7 Hz), 47.7, 40.3 (d, J = 3.6 Hz), 29.2 (t, J = 21.6 Hz). **IR** (neat, cm^{-1}): 2951, 2931, 2868, 2332, 2164, 2053, 1435, 1385, 1350,

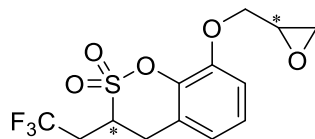
1292, 1276, 1221, 1188, 1166, 1131, 1072, 1040, 1023, 1008, 931, 877, 855, 808, 786, 741, 696, 513. **HRMS** (ESI) exact mass calc. for $C_{21}H_{18}F_9O_3S$: m/z 521.0827, found: m/z 521.0825 $[M+H]^+$. **mp**: 111 °C.

8-Hydroxy-3-(2,2,2-trifluoroethyl)-3,4-dihydrobenzo[e][1,2]oxathiine 2,2-dioxide (37)



A mixture of sultone **26n** (500 mg, 1.7 mmol, 1.0 equiv) and hydrobromic acid (30 mL, 47wt%) was heated at 140 °C for three hours. After completion of the reaction as monitored by TLC, the mixture was cooled to room temperature and extracted with Et_2O (3x 30 mL). The combined organic layers were washed with brine (1x 50 mL), dried over anhydrous Na_2SO_4 and concentrated under reduced pressure. The residue was recrystallized from pentane- CH_2Cl_2 (1:1) to obtain the entitled product **37** as a white solid (470 mg, 99%)

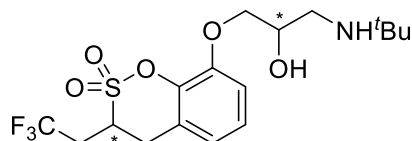
R_f (hexanes- $EtOAc$, 5:1) = 0.32. **Staining**: anisaldehyde (UV active). **1H -NMR** (300 MHz, $CDCl_3$) δ = 7.10 (t, J = 7.9 Hz, 1H), 6.96 (dd, J = 8.2, 1.5 Hz, 1H), 6.76 (dt, J = 7.8, 1.2 Hz, 1H), 5.43 (s, 1H), 3.85 (dddd, J = 10.7, 8.0, 5.2, 2.6 Hz, 1H), 3.68 (dd, J = 17.0, 5.2 Hz, 1H), 3.40 (dd, J = 17.2, 8.1 Hz, 1H), 3.13 – 2.99 (m, 1H), 2.52 (ddt, J = 15.1, 10.7, 9.6 Hz, 1H). **^{19}F -NMR** (282 MHz, $CDCl_3$) δ = -63.80 (s, 3F). **^{13}C -NMR** (75 MHz, $CDCl_3$) δ = 145.1, 139.2, 126.5, 125.3 (q, J = 277.3 Hz), 120.7, 119.9, 116.1, 51.0 (q, J = 2.3 Hz), 32.6 (q, J = 31.0 Hz), 32.4. **IR** (neat, cm^{-1}): 3452, 2922, 2851, 2117, 1946, 1737, 1633, 1592, 1502, 1476, 1394, 1361, 1320, 1267, 1118, 1006, 939, 895, 790, 682. **HRMS** (EI) exact mass calc. for $C_{10}H_9F_3O_4S$: m/z 282.0168, found: m/z 282.0166 $[M]^+$. **mp**: 112 °C.

8-(Oxiran-2-ylmethoxy)-3-(2,2,2-trifluoroethyl)-3,4-dihydrobenzo[e][1,2]oxathiine 2,2-dioxide (38)


To a solution of alcohol **37** (400 mg, 1.4 mmol, 1.0 equiv) and epichlorohydrin (2 mL, 25.5 mmol, 18.2 equiv) in anh. acetone (20 mL) was added K_2CO_3 (433 mg, 3.1 mmol, 2.2 equiv) and the mixture was heated at reflux for two days. Afterwards, the solvent was removed in vacuo and the residue extracted with $CHCl_3$ (3x 50 mL). The combined organic layers were washed with water (1x 50 mL) followed by brine (1x 50 mL), dried over anh. Na_2SO_4 and concentrated under reduced pressure. The residue was purified by chromatography on silica gel (CH_2Cl_2) to afford **38** as a white solid (312 mg, 65%) in a diastereomeric mixture of *syn/anti* = 50:50.

R_f (CH_2Cl_2) = 0.43. **Staining:** $KMnO_4$ (UV active). **1H -NMR** (400 MHz, $CDCl_3$) δ = 7.12 (t, J = 8.0 Hz, 1H), 6.94 (dd, J = 8.3, 1.3 Hz, 1H), 6.81 (dd, J = 7.8, 1.2 Hz, 1H), 4.28 (dt, J = 11.3, 2.7 Hz, 1H), 4.02 (ddd, J = 11.3, 5.5, 2.2 Hz, 1H), 3.79 (dddt, J = 10.4, 7.8, 5.0, 2.4 Hz, 1H), 3.66 (dd, J = 17.0, 5.4 Hz, 1H), 3.47 – 3.31 (m, 2H), 3.06 (dq, J = 15.2, 10.8, 2.6 Hz, 1H), 2.91 (t, J = 4.5 Hz, 1H), 2.77 (ddd, J = 4.9, 2.7, 0.9 Hz, 1H), 2.59 – 2.38 (m, 1H). **^{19}F -NMR** (376 MHz, $CDCl_3$) δ = -63.84 (s, 3F), -63.85 (s, 3F). **^{13}C -NMR** (101 MHz, $CDCl_3$) δ = 148.1, 148.1, 141.1, 126.1, 125.4 (q, J = 277.5 Hz), 121.7, 121.7, 120.8, 120.8, 113.7, 113.7, 70.4, 70.3, 50.4 (ddd, J = 5.4, 2.6, 1.5 Hz), 50.3 (ddd, J = 5.8, 2.6, 1.3 Hz), 50.1, 44.8, 44.8, 33.6 (q, J = 28.0 Hz), 33.2 (q, J = 28.0 Hz), 32.5, 32.5. **IR** (neat, cm^{-1}): 3097, 3004, 2933, 1621, 1588, 1480, 1372, 1327, 1267, 1193, 1152, 1118, 1010, 939, 887, 790, 719. **HRMS** (ESI) exact mass calc. for $C_{13}H_{17}F_3NO_5S$: m/z 356.0774, found: m/z 356.0777 $[M+NH_4]^+$. **mp**: 80 °C.

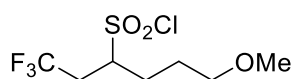
8-(3-(*tert*-Butylamino)-2-hydroxypropoxy)-3-(2,2,2-trifluoroethyl)-3,4-dihydrobenzo[e][1,2]oxathiane 2,2-dioxide (39)



To a solution of epoxid **38** (200 mg, 0.6 mmol, 1.0 equiv) in anh. MeOH (40 mL) was added freshly distilled *tert*-butylamine (0.8 mL, 7.7 mmol, 12.9 equiv) and the mixture was heated at reflux for two hours. Afterwards, the solvent and the amine was removed in vacuo. The residue was purified by chromatography on silica gel (CH₂Cl₂) followed by recrystallized from pentane-CH₂Cl₂ (1:1) to obtain the entitled product **39** as a white solid (202 mg, 49%) in a diastereomeric mixture of *syn/anti* = 50:50.

R_f (CH₂Cl₂) = 0.13. **Staining:** KMnO₄ (UV active). **¹H-NMR** (600 MHz, CDCl₃) δ = 7.10 (t, *J* = 7.9 Hz, 1H), 6.92 (d, *J* = 8.0 Hz, 1H), 6.79 (d, *J* = 7.7 Hz, 1H), 4.27 (dt, *J* = 7.4, 3.4 Hz, 1H), 4.19 (td, *J* = 9.0, 8.5, 4.4 Hz, 1H), 4.09 – 4.02 (m, 2H), 3.77 (dtd, *J* = 10.7, 7.9, 5.1 Hz, 2H), 3.63 (dd, *J* = 17.0, 5.4 Hz, 1H), 3.37 – 3.33 (m, 1H), 3.10 (dt, *J* = 12.2, 3.3 Hz, 1H), 3.05 – 2.97 (m, 1H), 2.47 (ddd, *J* = 24.9, 19.5, 9.6 Hz, 2H), 1.28 (s, 9H). **¹⁹F-NMR** (376 MHz, CDCl₃) δ = -63.82 (s, 3F), -63.84 (s, 3F). **¹³C-NMR** (151 MHz, CDCl₃) δ = 148.0, 140.8, 140.7, 126.0, 125.2 (q, *J* = 277.4 Hz), 121.4, 121.3, 120.6, 120.6, 113.4, 113.4, 73.9, 73.8, 71.8, 71.7, 50.4 – 50.2 (m), 44.7, 44.7, 32.5 (q, *J* = 30.9 Hz), 32.4, 27.2, 25.7. **IR** (neat, cm⁻¹): 3327, 2971, 2937, 2873, 2618, 1742, 1618, 1585, 1477, 1379, 1322, 1271, 1236, 1192, 1155, 1119, 1039, 1009, 945, 886, 841, 784, 769, 732, 664, 623, 581, 548. **HRMS** (ESI) exact mass calc. for C₁₇H₂₄F₃NO₅S: *m/z* 412.1400, found: *m/z* 412.1404 [M+H]⁺. **mp**: 88 °C.

3-(2,2,2-Trifluoroethyl)-1,2-oxathiane 2,2-dioxide (45)



Following GP-B, **45** was prepared using 5-methoxypent-1-ene (**44**) (100 mg, 1.0 mmol, 1.0 equiv), K₂HPO₄ (352 mg, 2.0 mmol, 2.0 equiv), CF₃SO₂Cl (**3a**) (210 μL, 2.0 mmol, 2.0 equiv) and [Cu(dap)₂]Cl (8.8 mg, 1.0 μmol, 1.0 mol%). Chromatography on silica gel (pentane-Et₂O, 5:1) afforded **45** as a colourless oil (150 mg, 56%).

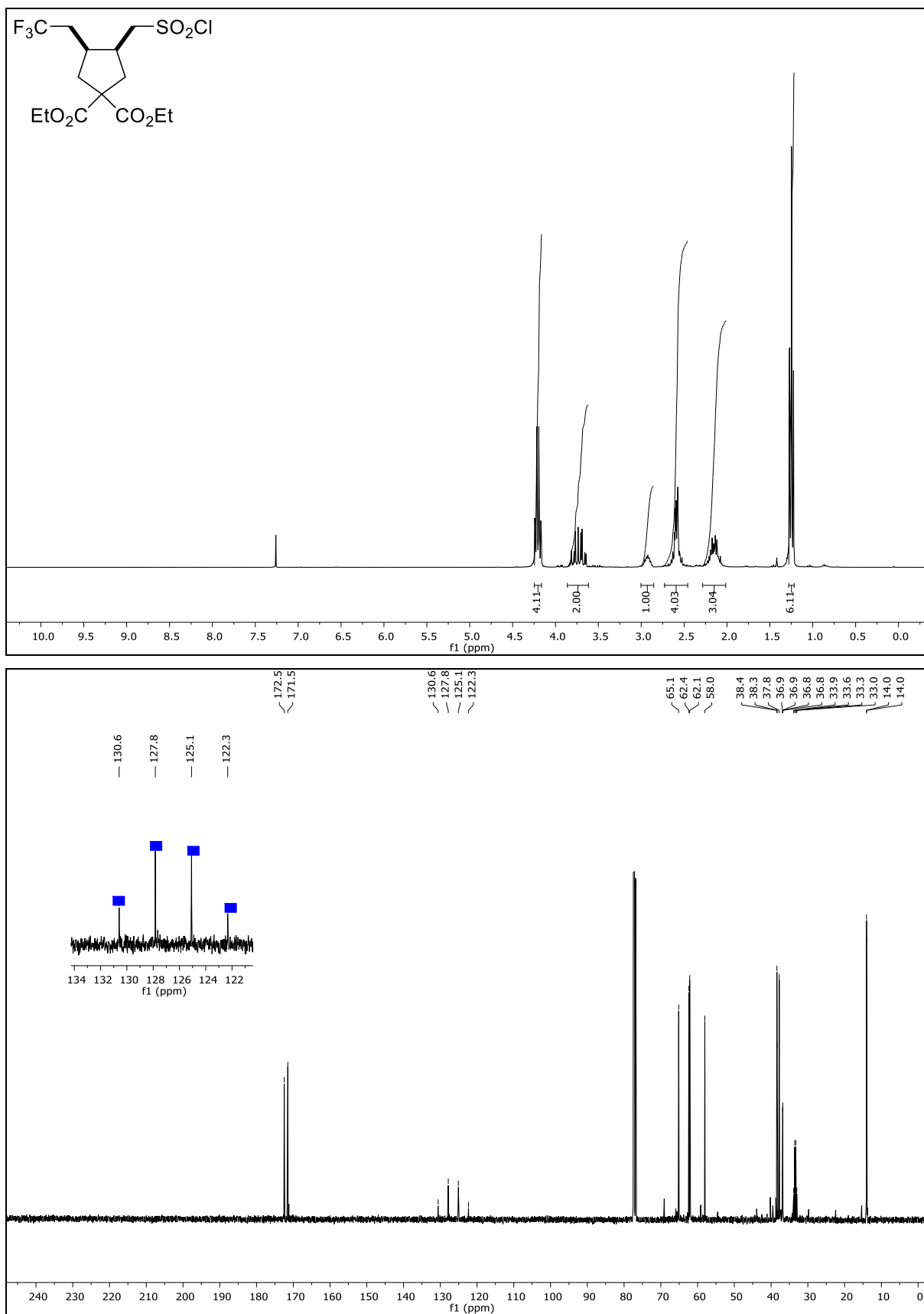
R_f (pentane-Et₂O, 5:1) = 0.45. **Staining:** KMnO₄ (UV inactive). **¹H-NMR** (300 MHz, CDCl₃) δ = 3.93 (dtd, *J* = 8.7, 5.8, 2.7 Hz, 1H), 3.44 (td, *J* = 5.9, 2.2 Hz, 2H), 3.33 (s, 3H), 3.07 (dq, *J* = 15.5, 10.5, 2.7 Hz, 1H), 2.67 – 2.48 (m, 1H), 2.31 (dq, *J* = 14.4, 7.2 Hz, 1H), 2.12 (dtd, *J* = 15.1, 7.2, 6.7, 5.1 Hz, 1H), 1.91 – 1.81 (m, 2H). **¹⁹F-NMR** (282 MHz, CDCl₃) δ = -64.22 (s, 3F). **¹³C-NMR** (75 MHz, CDCl₃) δ = 125.0 (q, *J* = 277.2 Hz), 71.7, 69.7 (q,

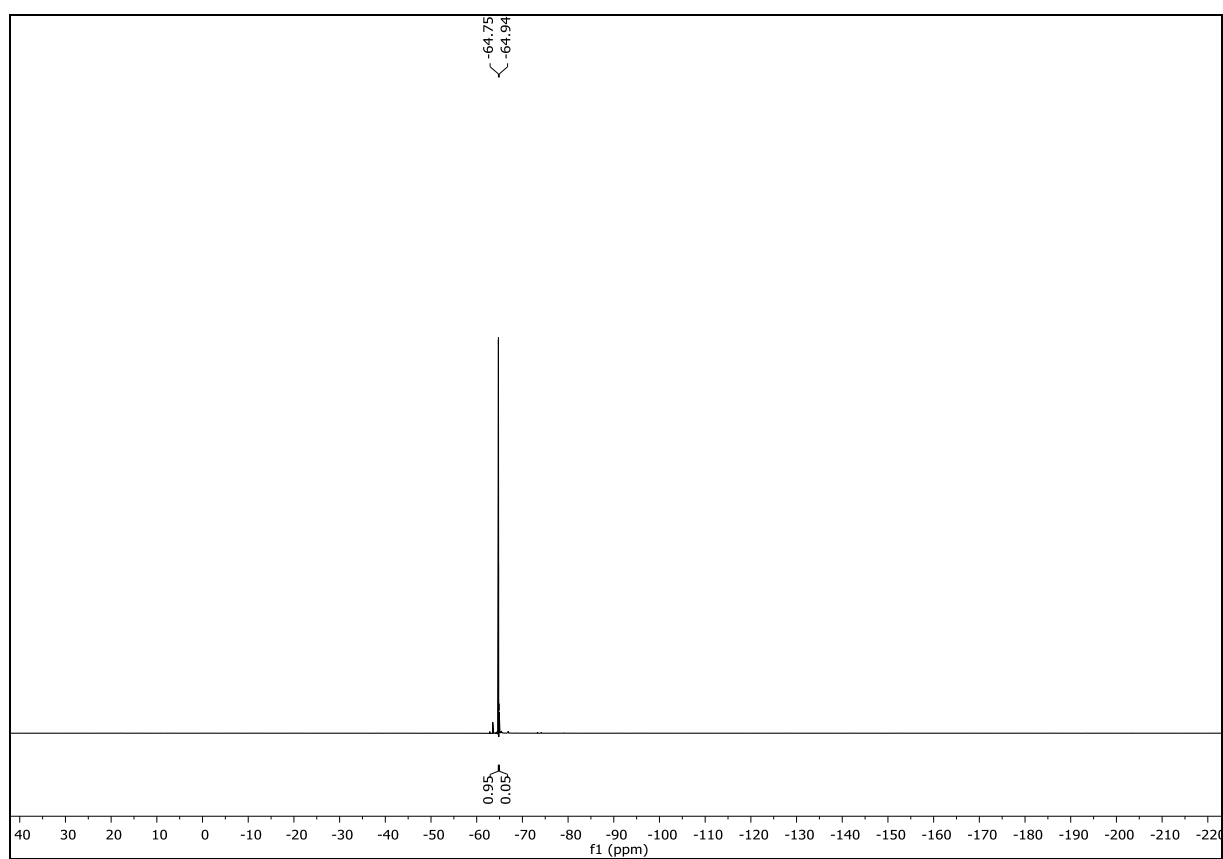
$J = 2.3$ Hz), 58.8, 35.0 (q, $J = 30.9$ Hz), 28.1, 26.2. **IR** (neat, cm^{-1}): 2933, 2881, 2837, 1439, 1372, 1320, 1260, 1156, 1118, 1070, 1029, 902, 842, 772. **HRMS** (CI) exact mass calc. for $\text{C}_7\text{H}_{13}\text{ClF}_3\text{O}_3\text{S}$: m/z 269.0221, found: m/z 269.0220 $[\text{M}+\text{H}]^+$.

4.6. NMR Spectra

^1H -NMR		first image
^{13}C -NMR		second image
^{19}F -NMR		third image

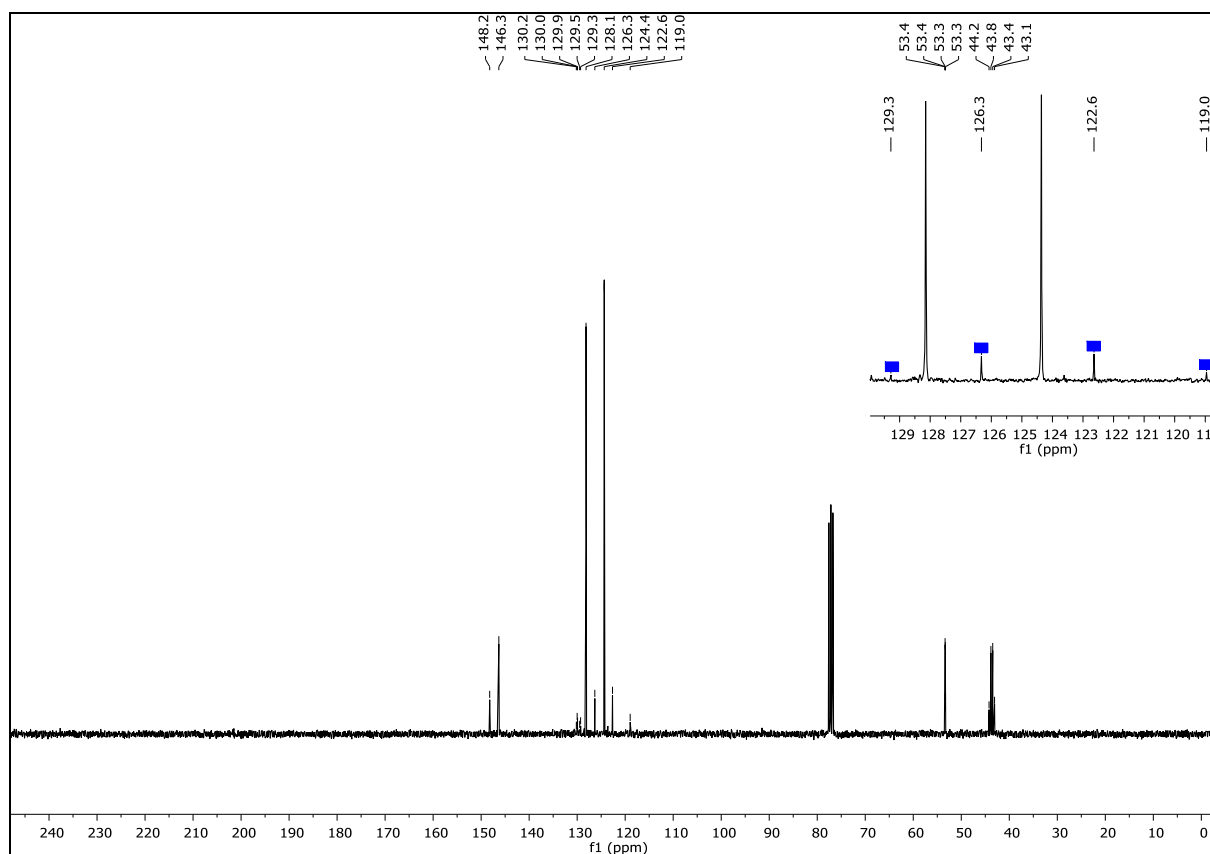
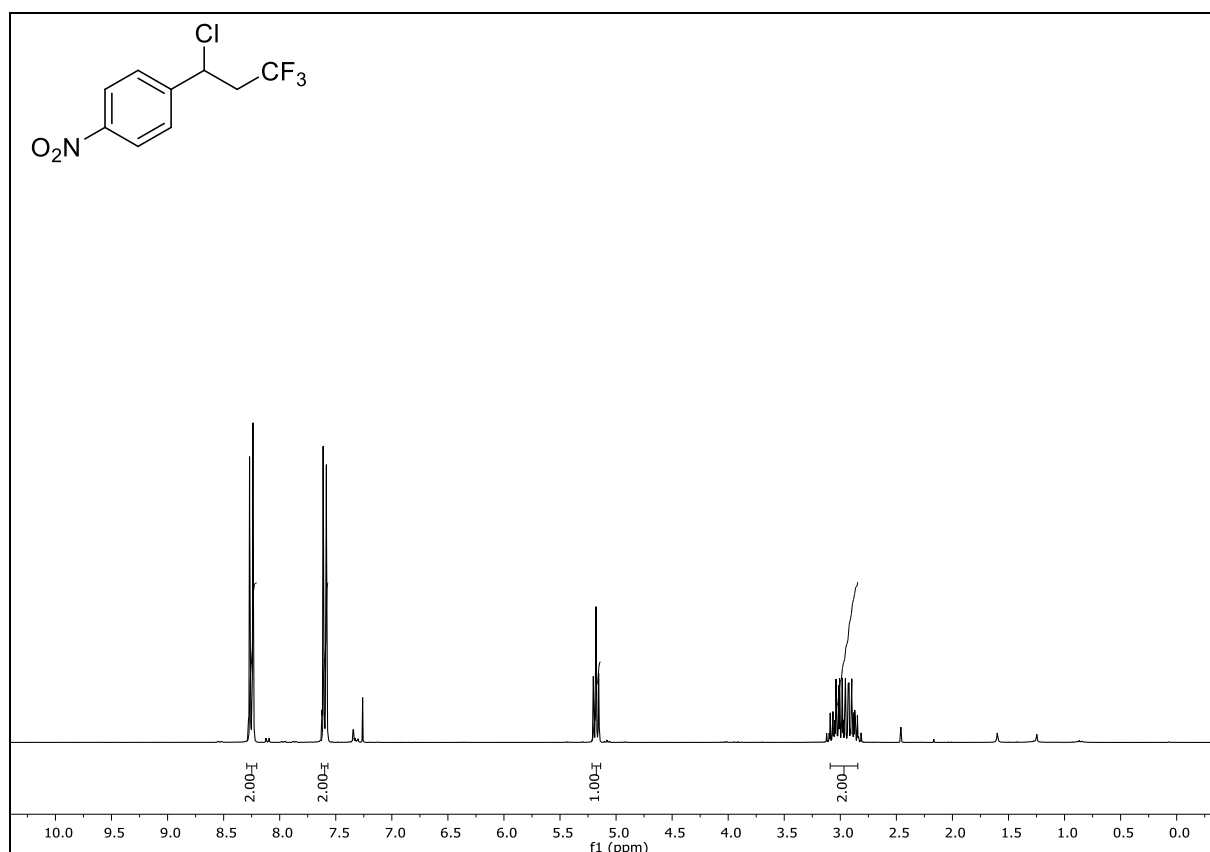
Diethyl (3S,4S)-3-((chlorosulfonyl)methyl)-4-(2,2,2-trifluoroethyl)cyclopentane-1,1-dicarboxylate (12g)

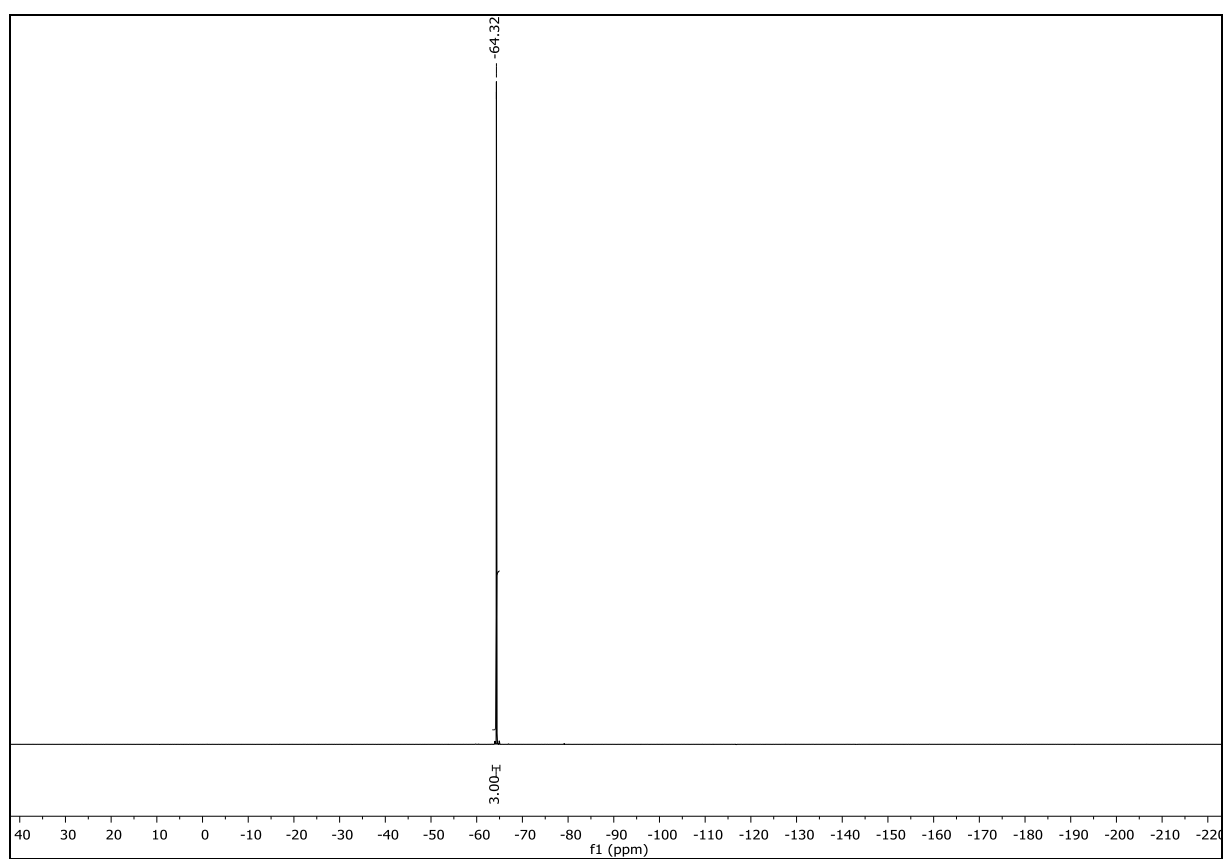




NMR-Solvent: CDCl_3

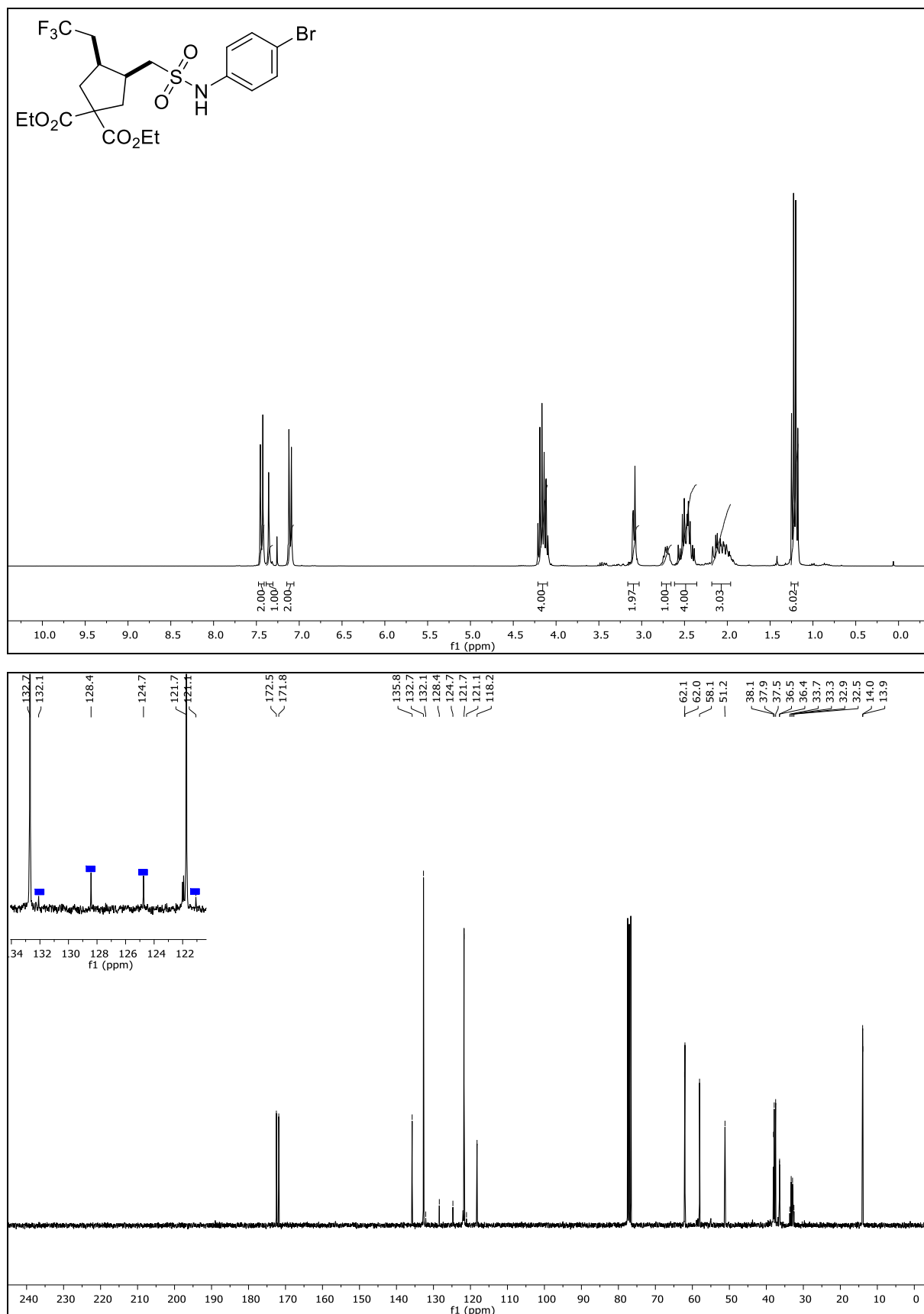
1-(1-Chloro-3,3,3-trifluoropropyl)-4-nitrobenzene (13b)

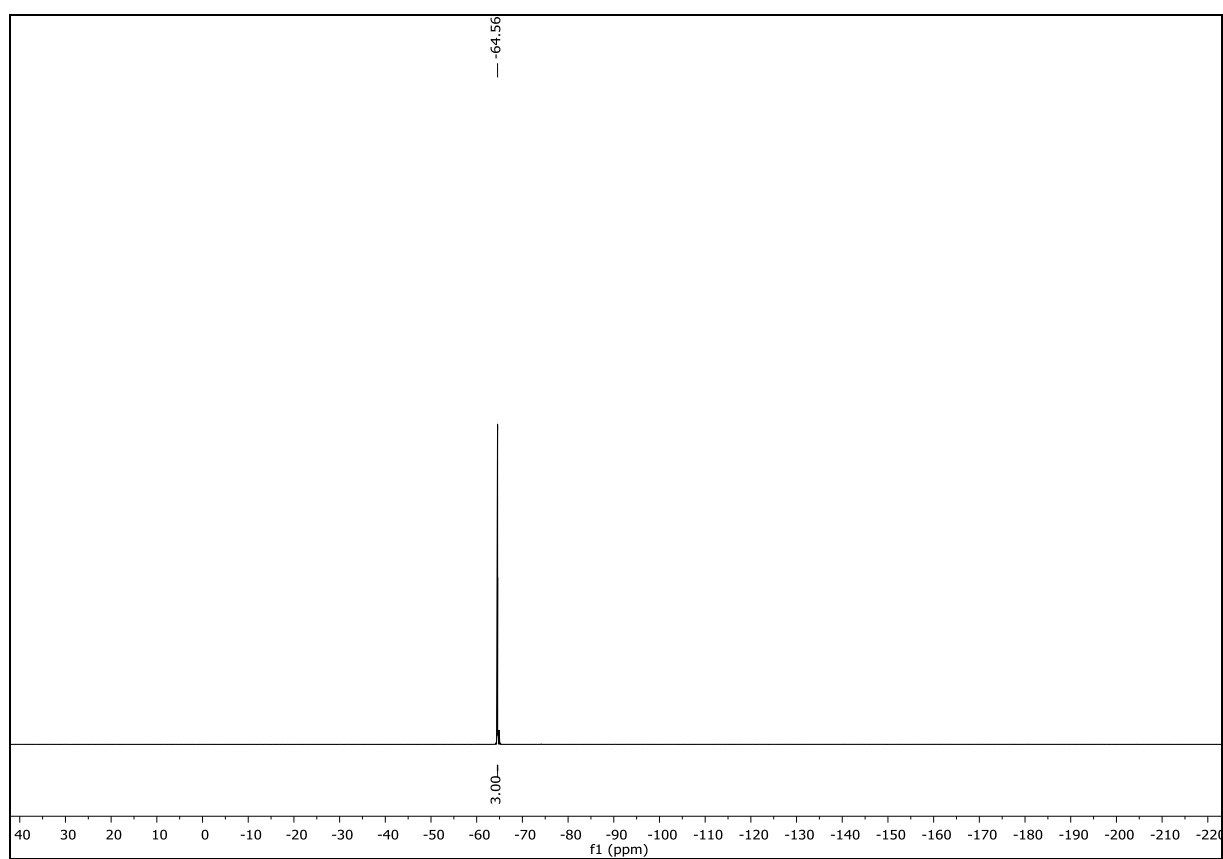




NMR-Solvent: CDCl_3

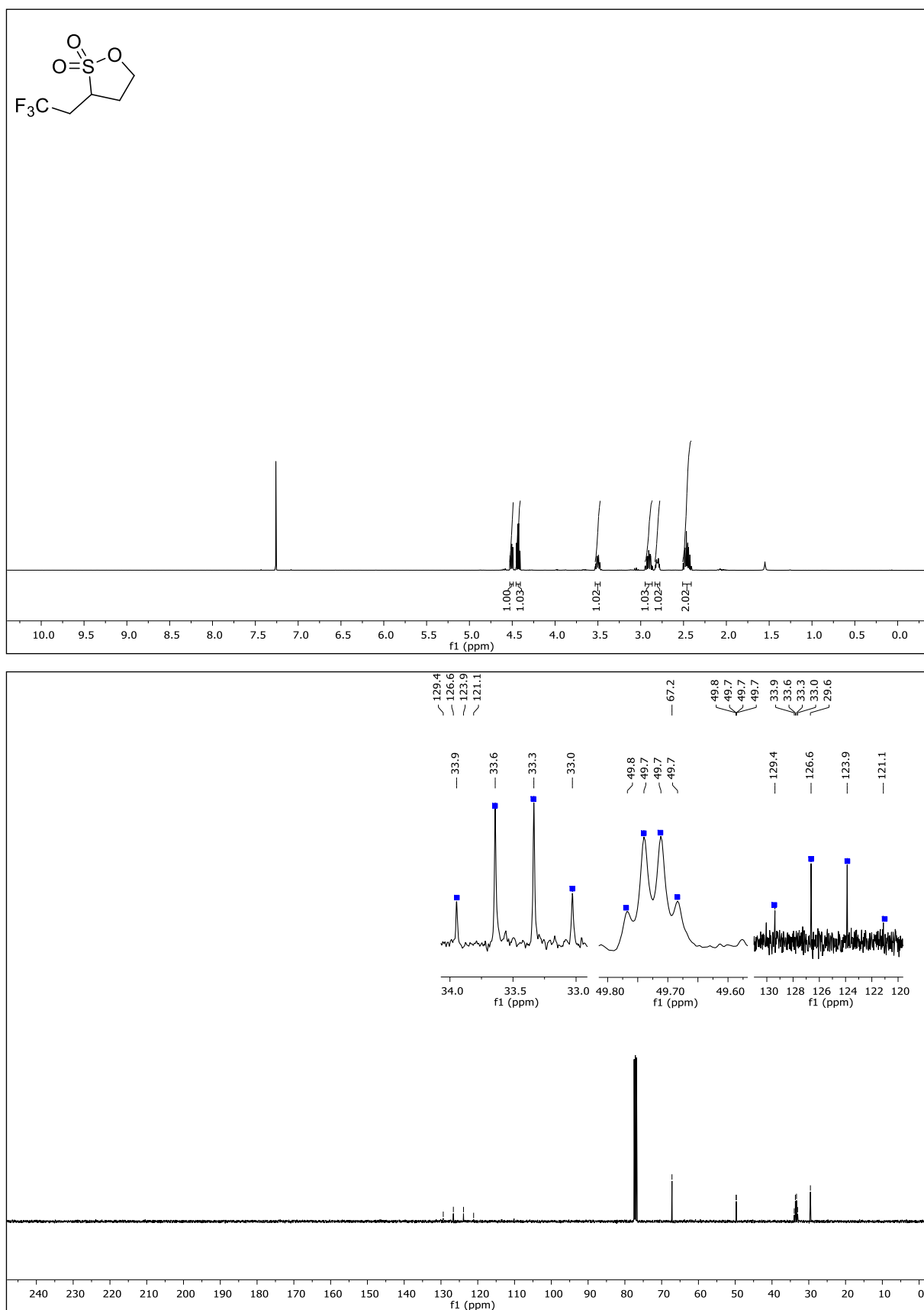
Diethyl-(3*S*,4*S*)-3-((*N*-(4-bromophenyl)sulfamoyl)methyl)-4(2,2,2-trifluoroethyl)cyclopentane-1,1-dicarboxylate (15)

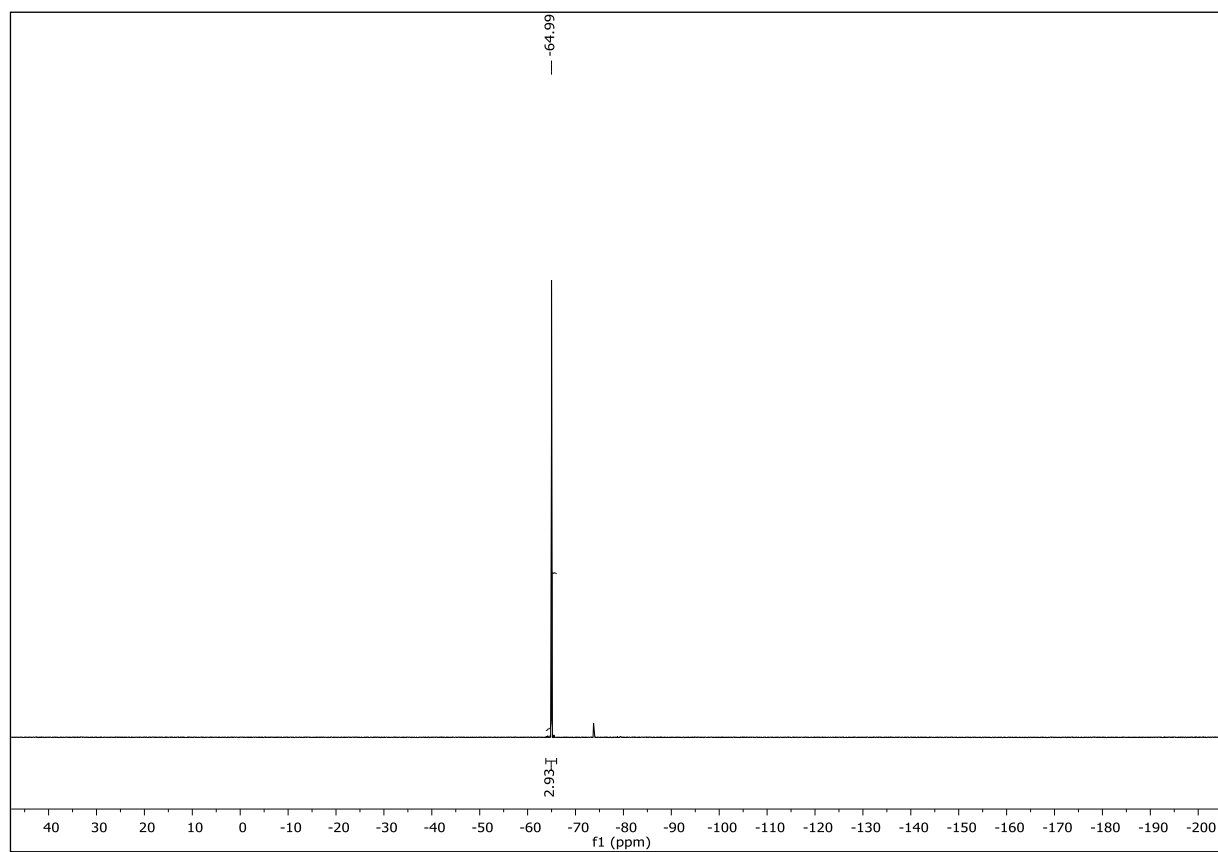




NMR-Solvent: CDCl_3

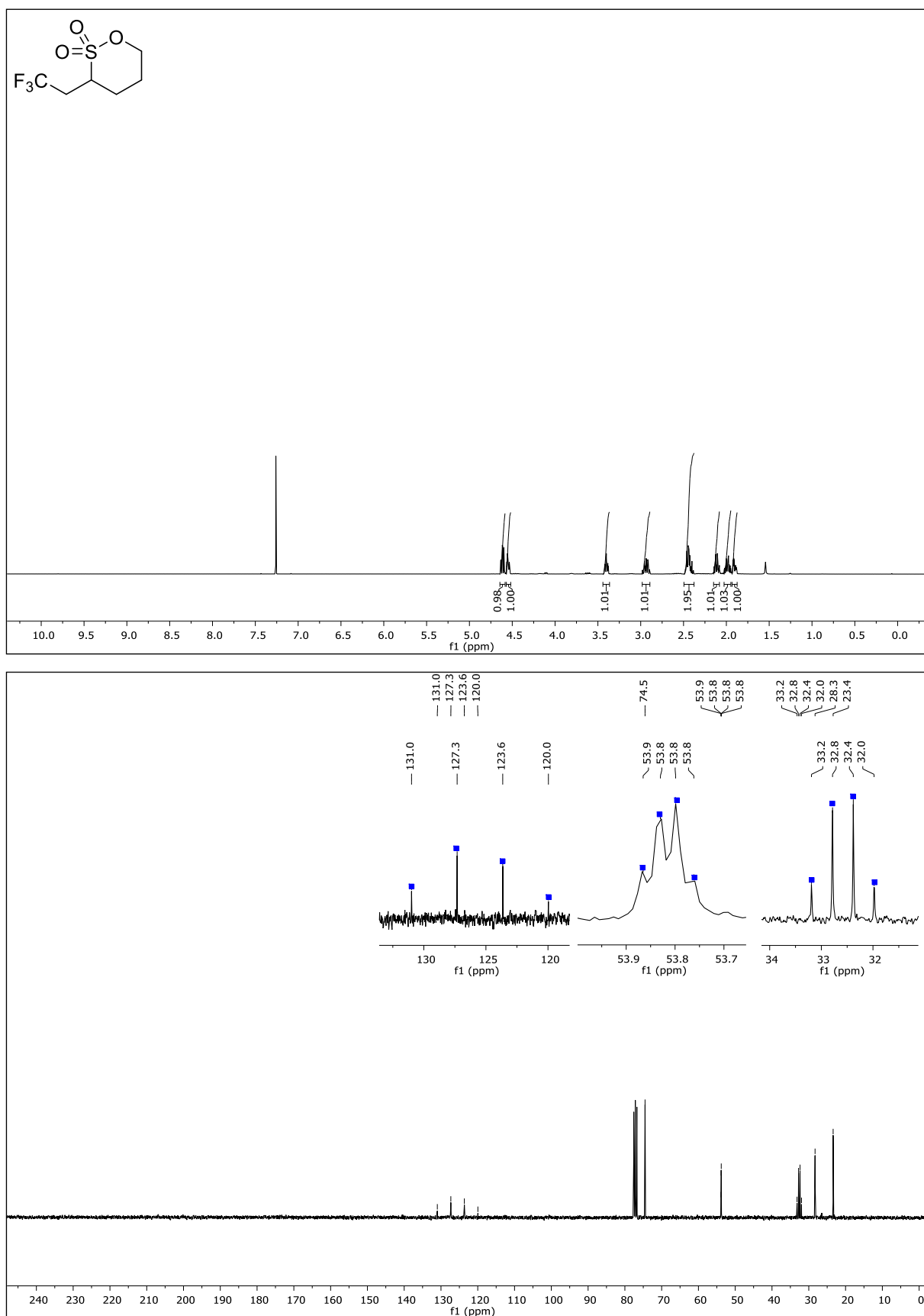
3-(2,2,2-Trifluoroethyl)-1,2-oxathiolane 2,2-dioxide (26a)

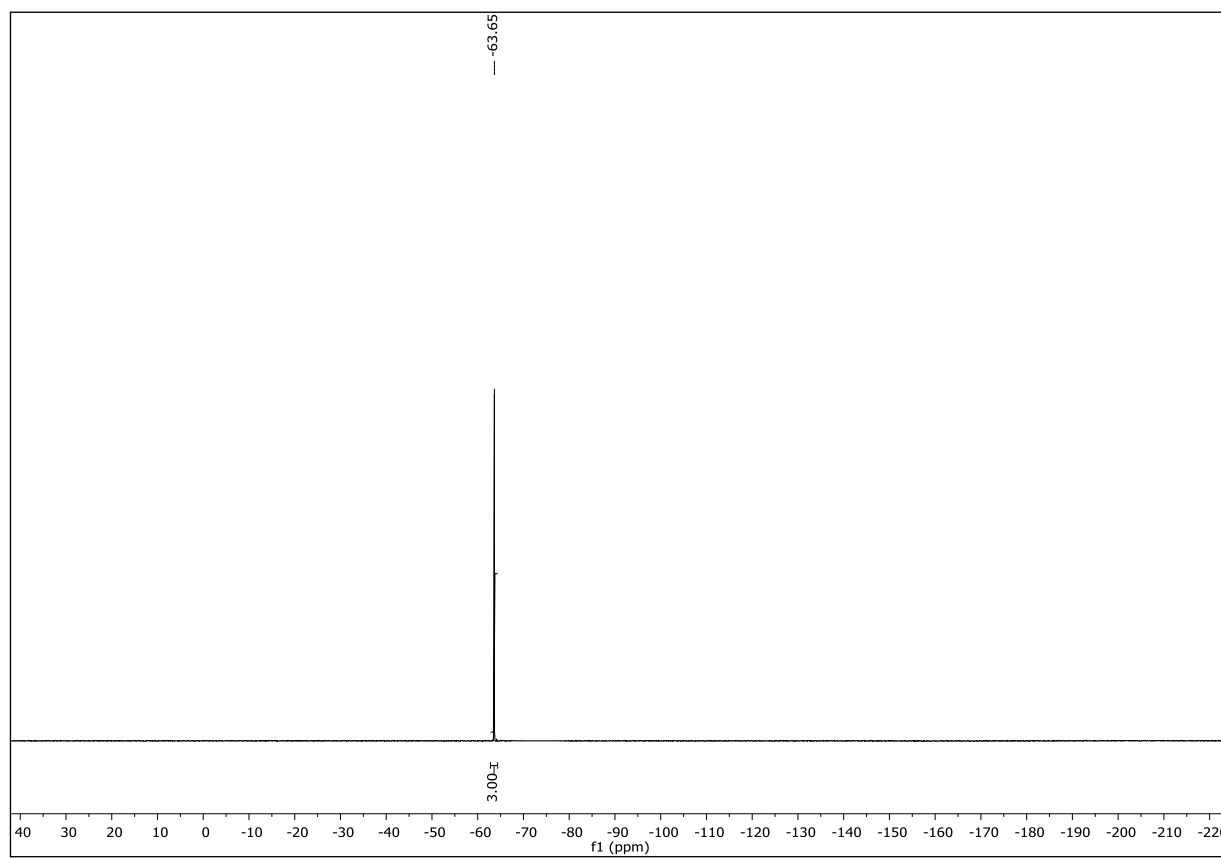




NMR-Solvent: CDCl_3

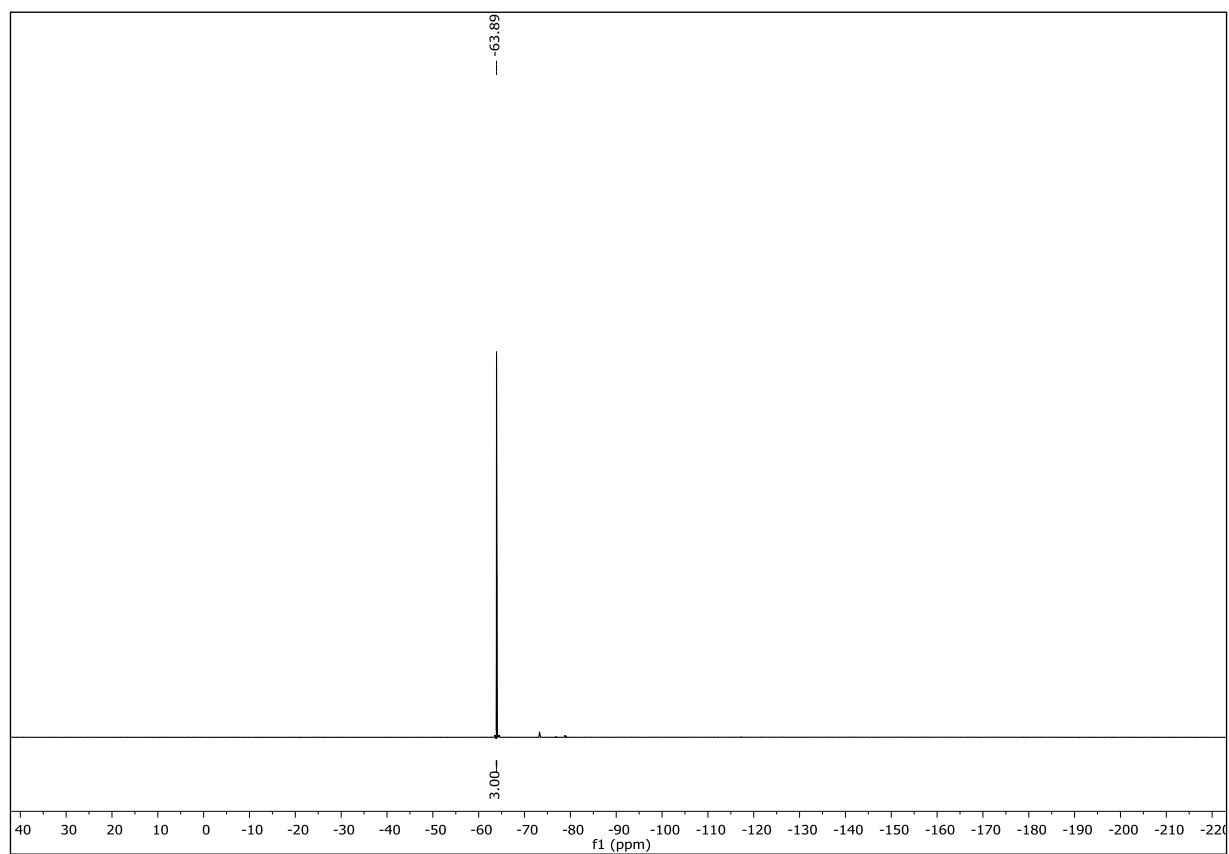
3-(2,2,2-Trifluoroethyl)-1,2-oxathiane 2,2-dioxide (26b)





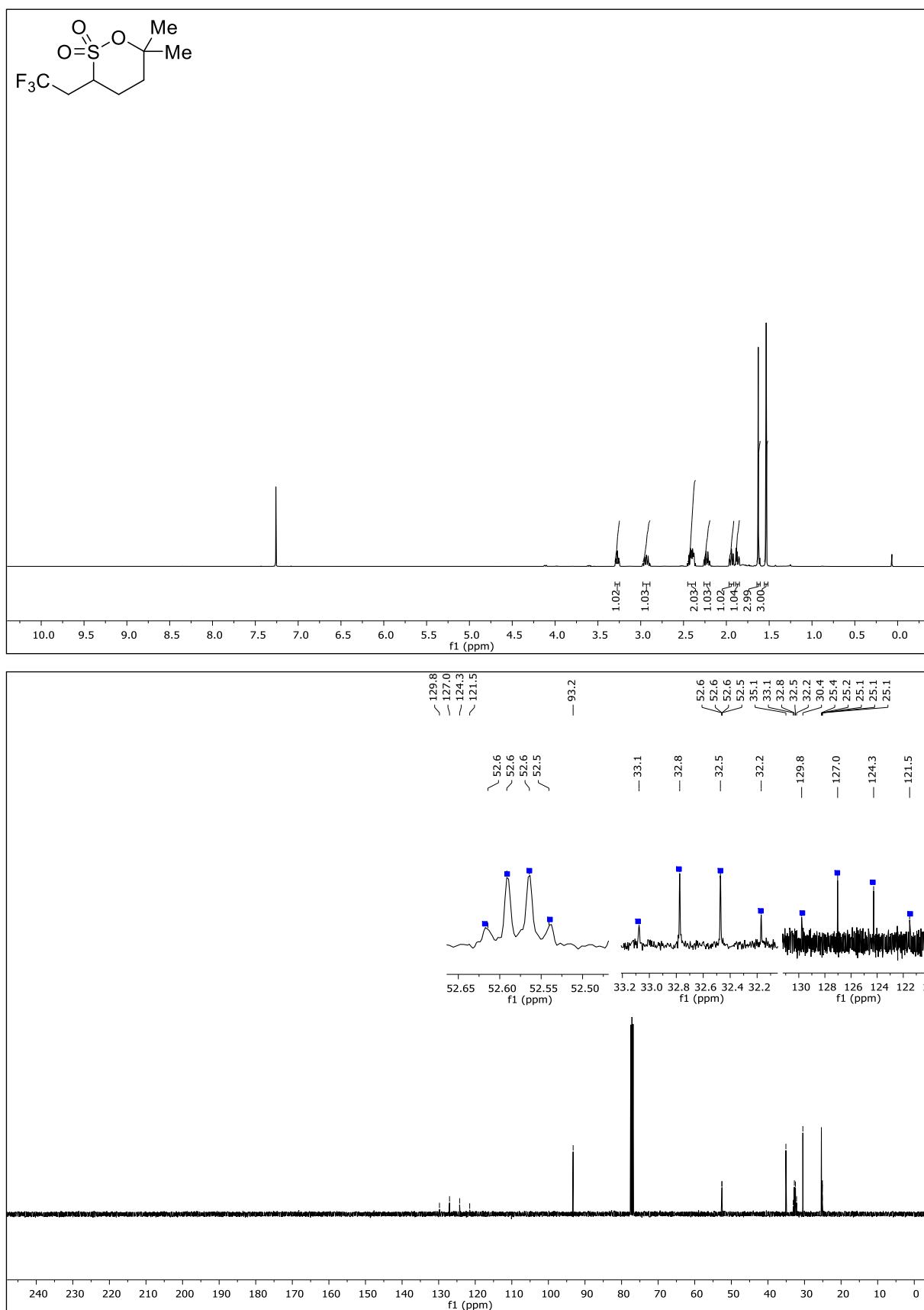
NMR-Solvent: CDCl_3

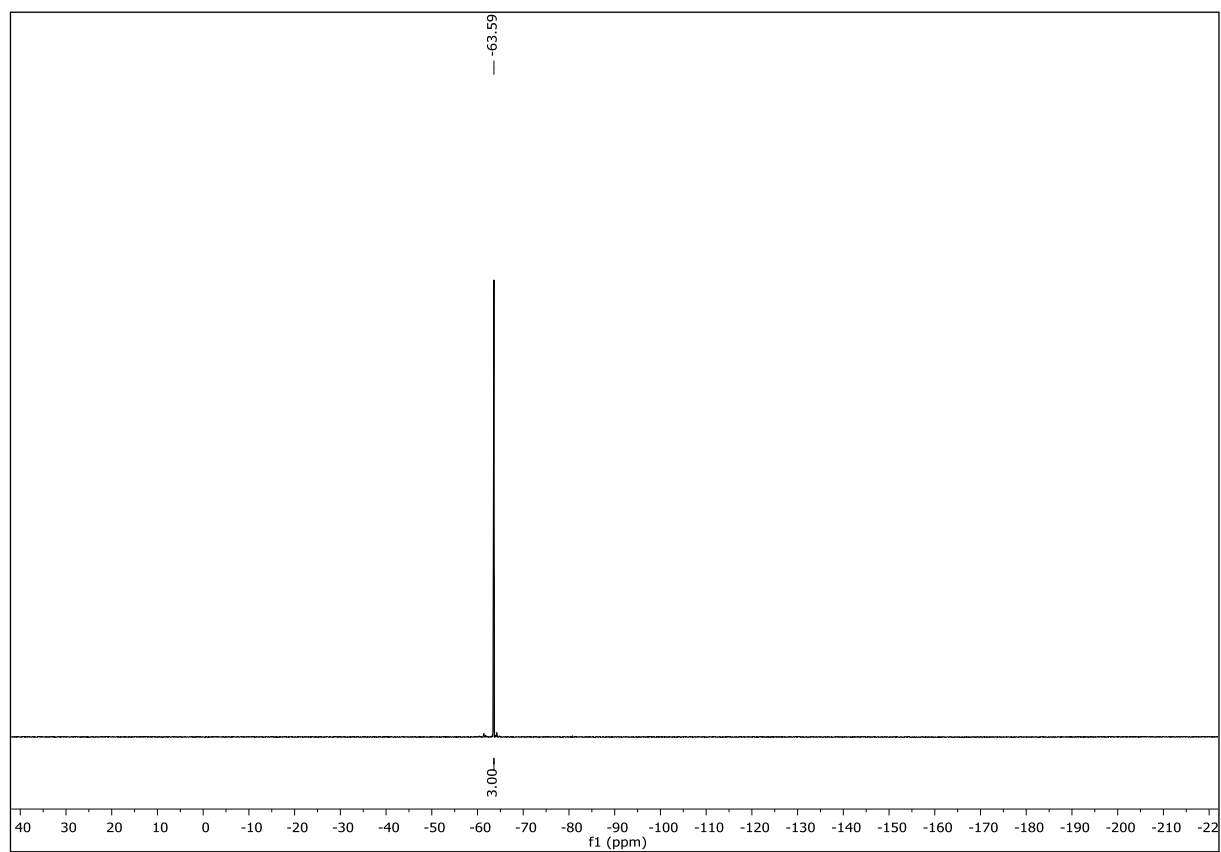




NMR-Solvent: CDCl_3

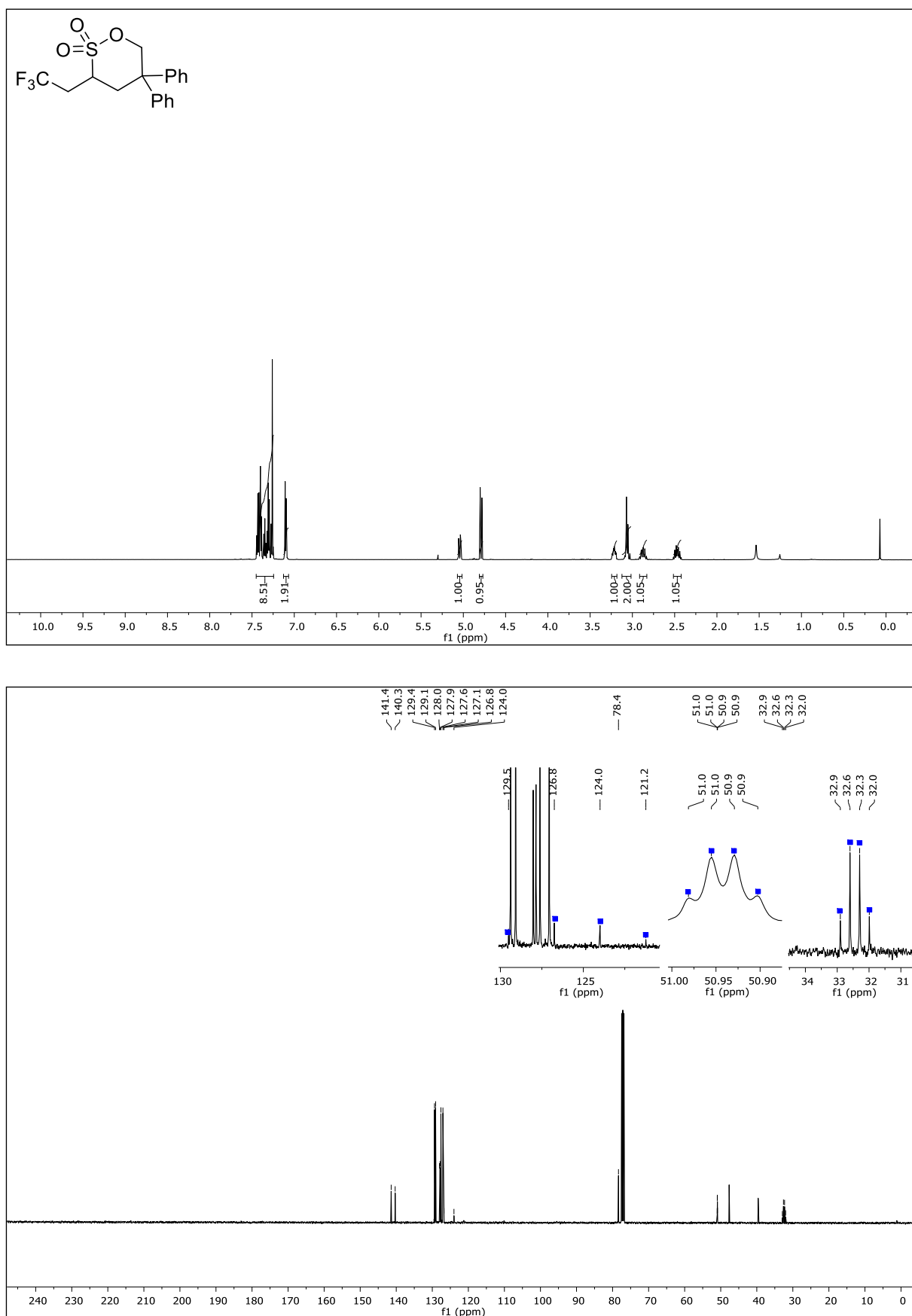
6,6-Dimethyl-3-(2,2,2-trifluoroethyl)-1,2-oxathiane 2,2-dioxide (26e)

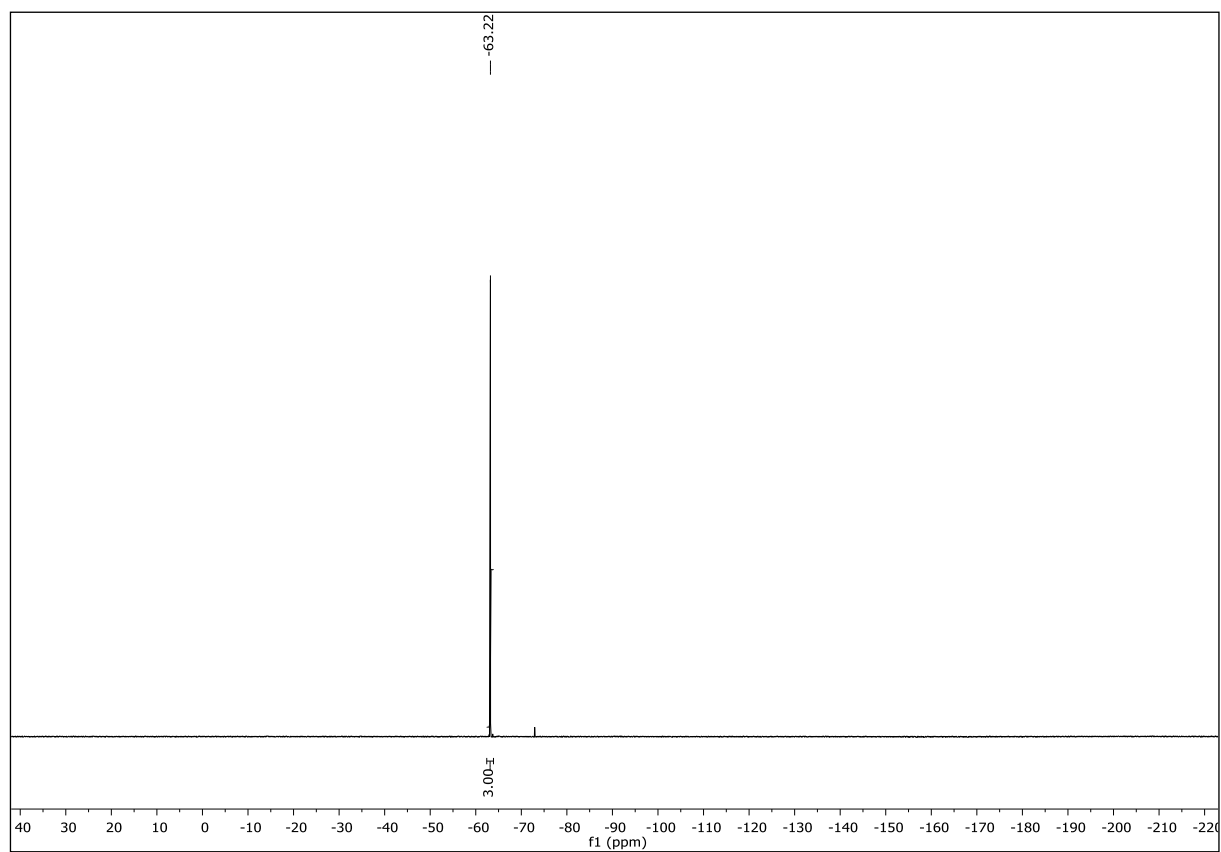




NMR-Solvent: CDCl_3

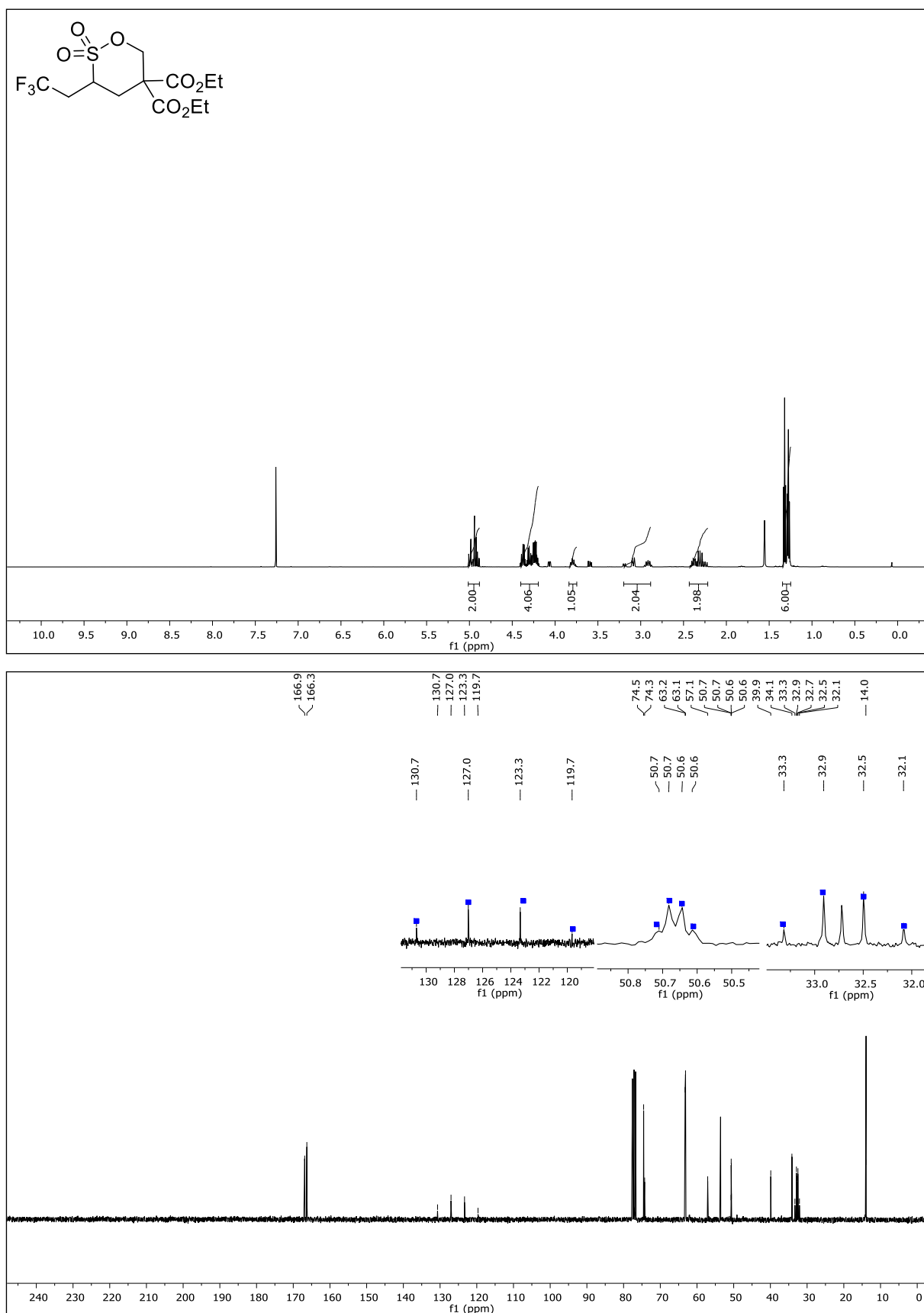
5,5-Diphenyl-3-(2,2,2-trifluoroethyl)-1,2-oxathiane 2,2-dioxide (26f)

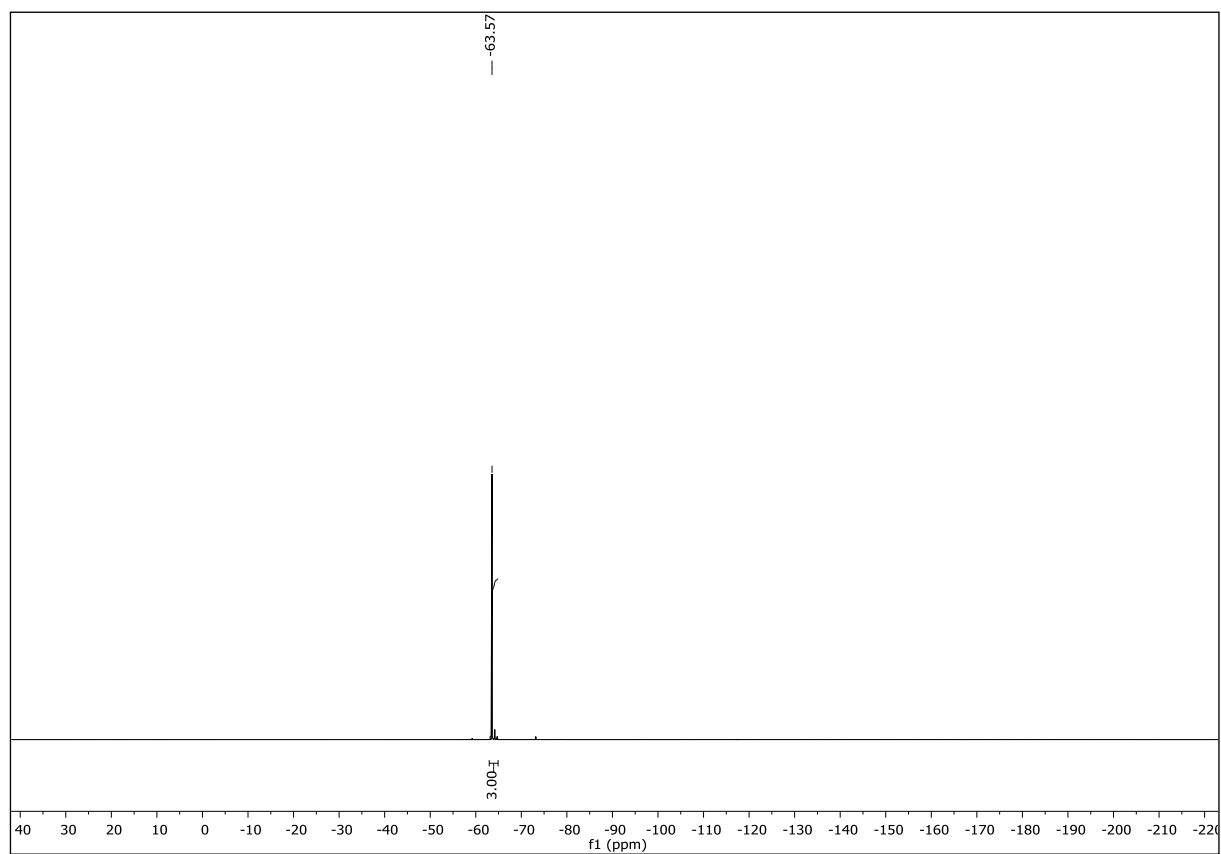




NMR-Solvent: CDCl_3

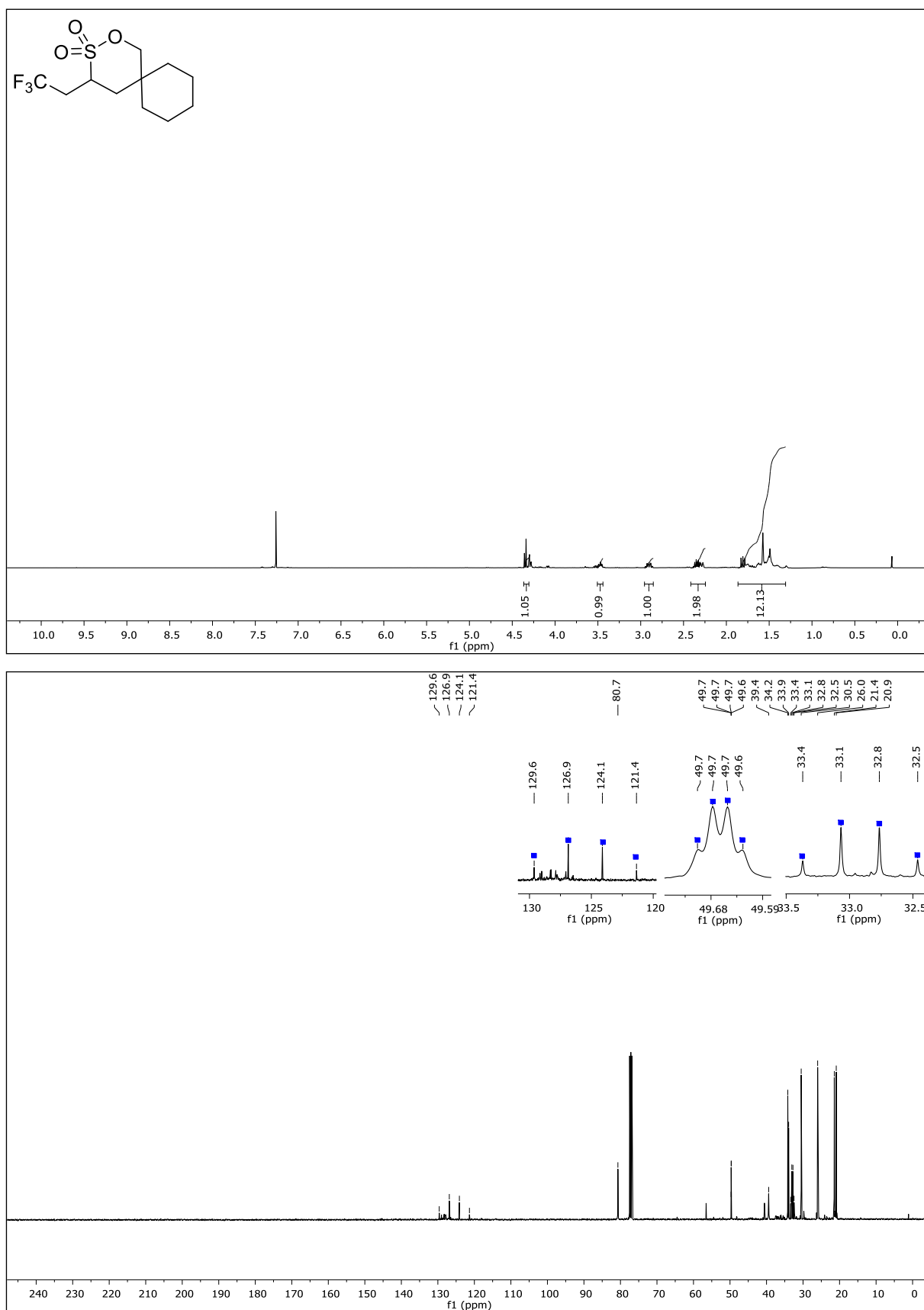
Diethyl 3-(2,2,2-trifluoroethyl)-1,2-oxathiane-5,5-dicarboxylate 2,2-dioxide (26g)

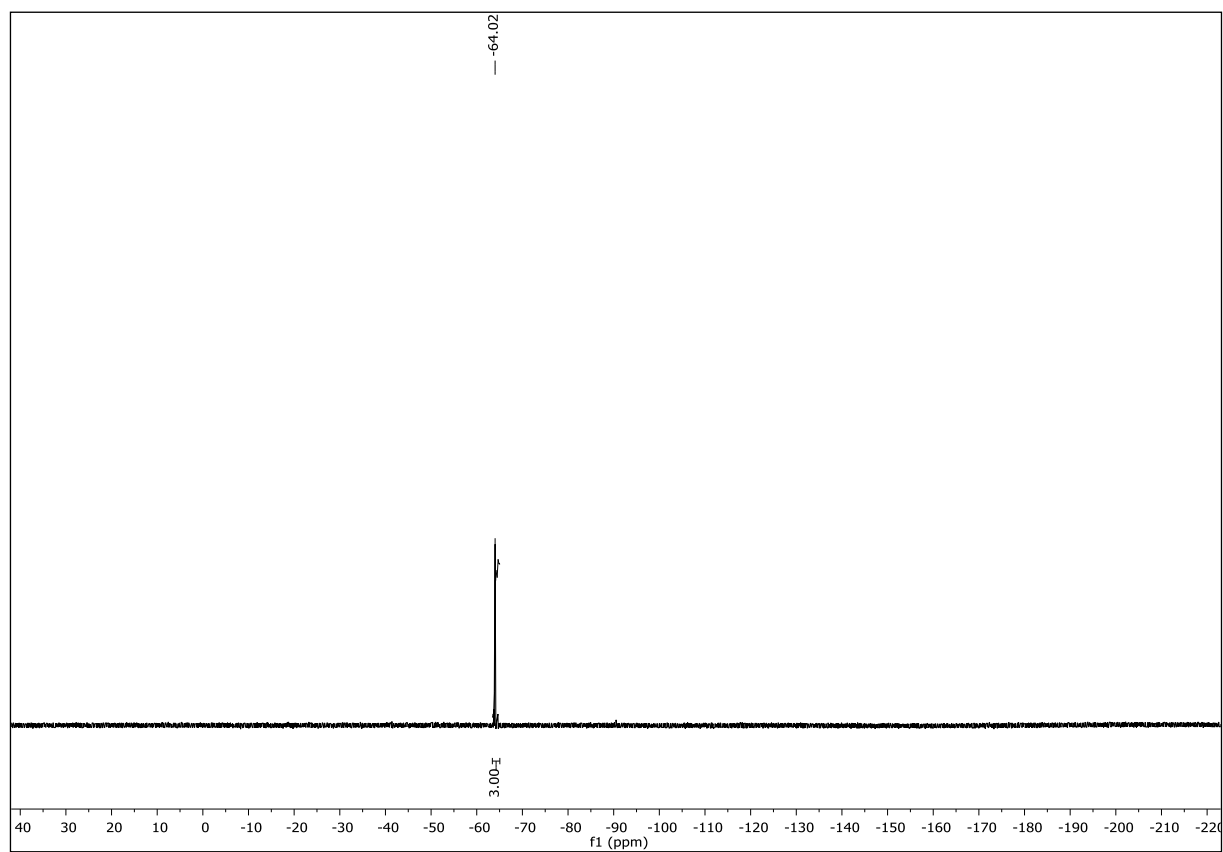




NMR-Solvent: CDCl_3

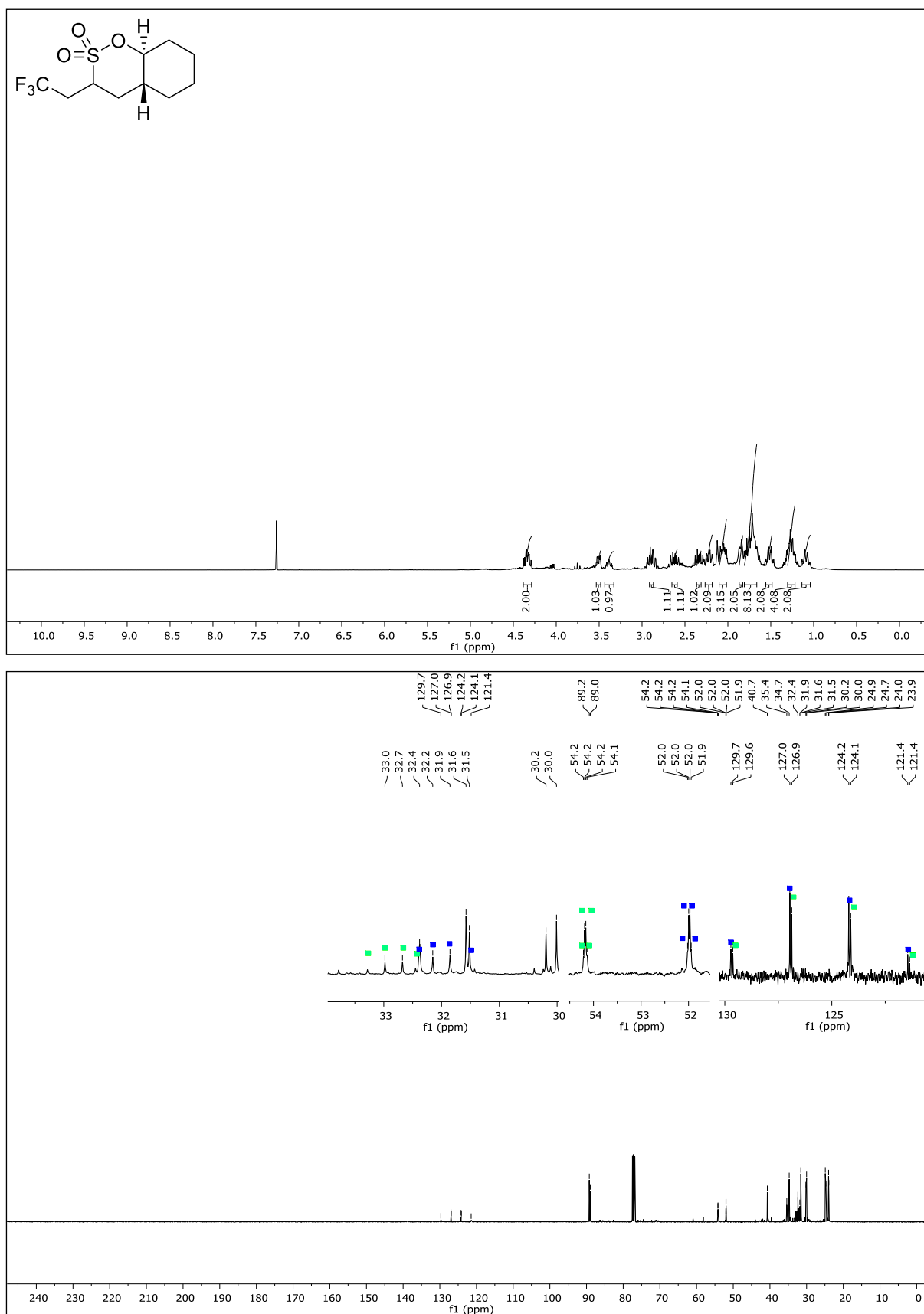
4-(2,2,2-Trifluoroethyl)-2-oxa-3-thiaspiro[5.5]undecane 3,3-dioxide (26h)

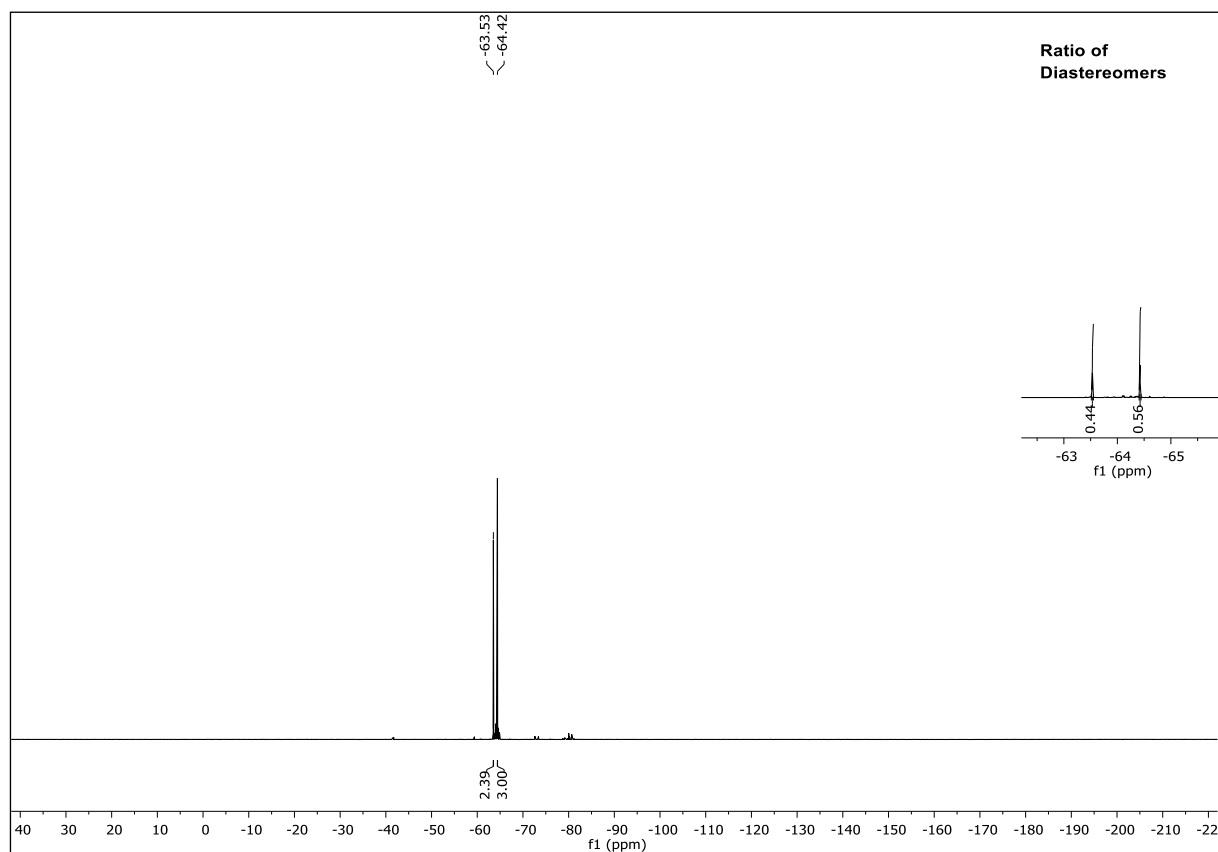




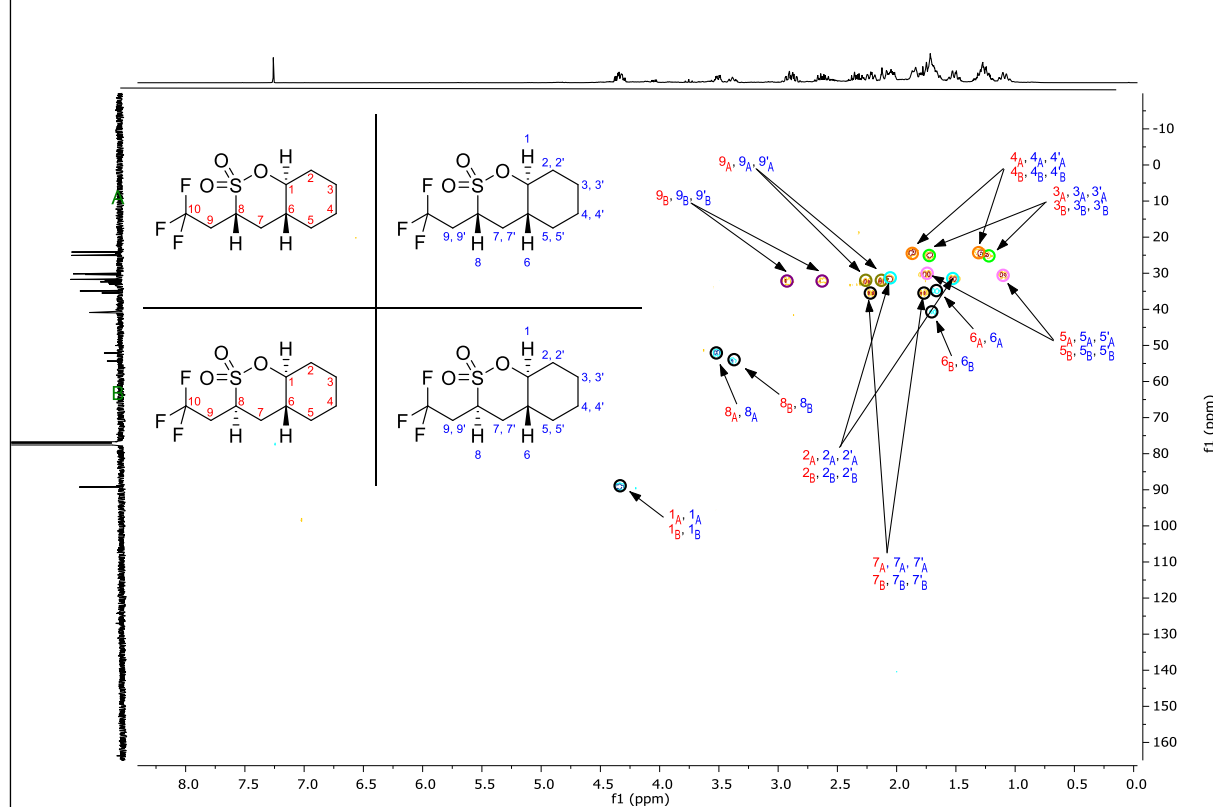
NMR-Solvent: CDCl_3

***rel*-(4*aR*,8*aS*)-3-(2,2,2-Trifluoroethyl)octahydrobenzo[*e*][1,2]oxathiine 2,2-dioxide (26i)**



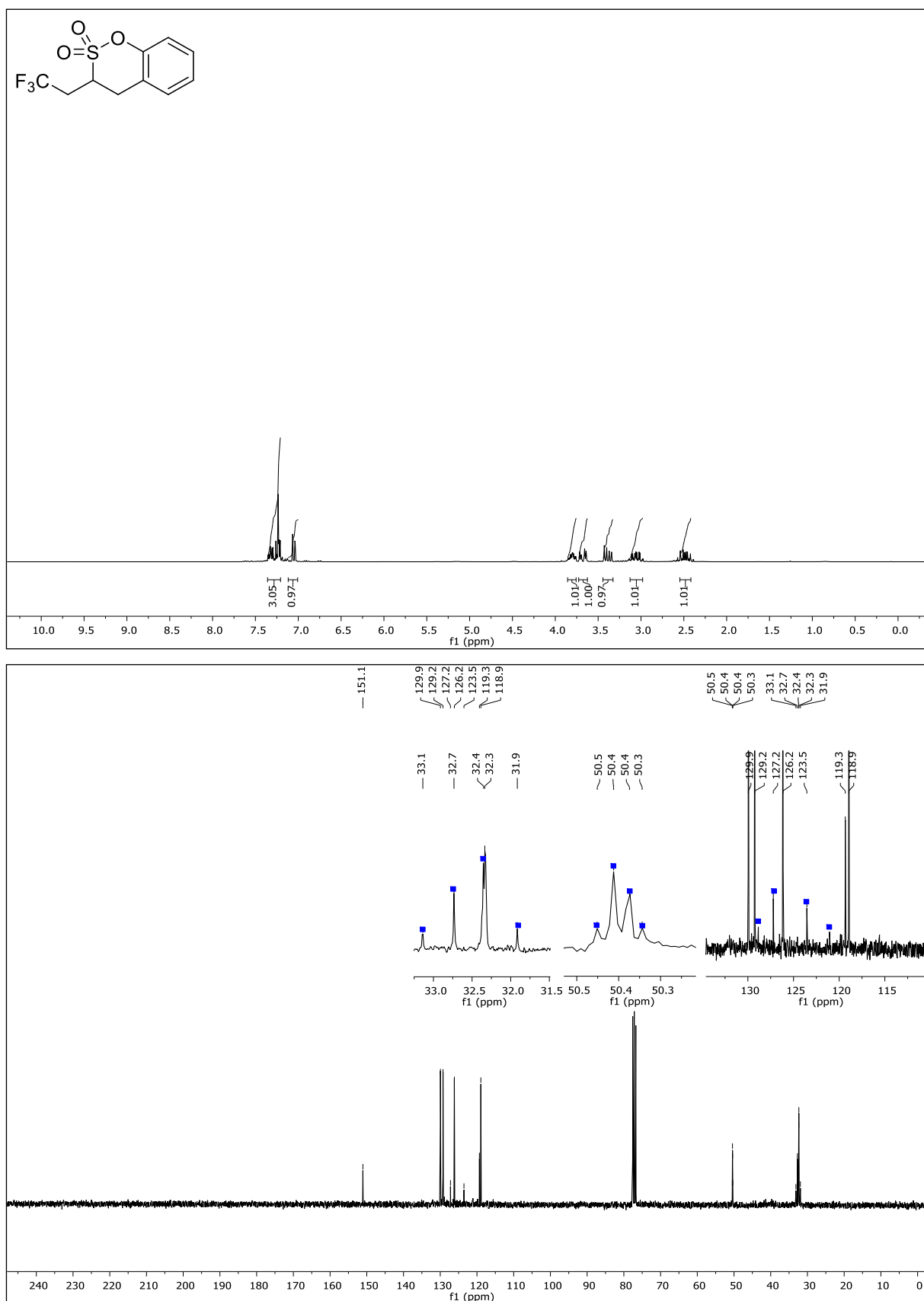


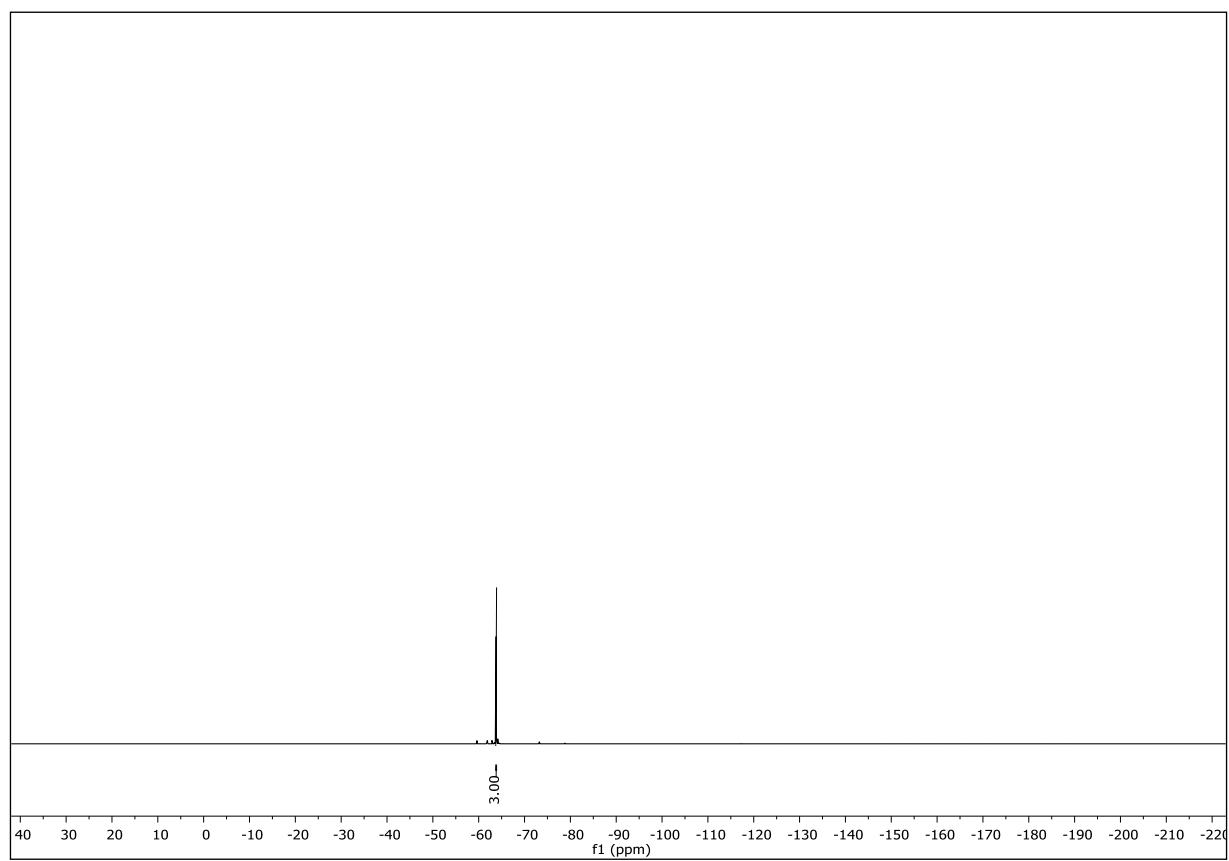
HSQC with DEPT



NMR-Solvent: CDCl_3

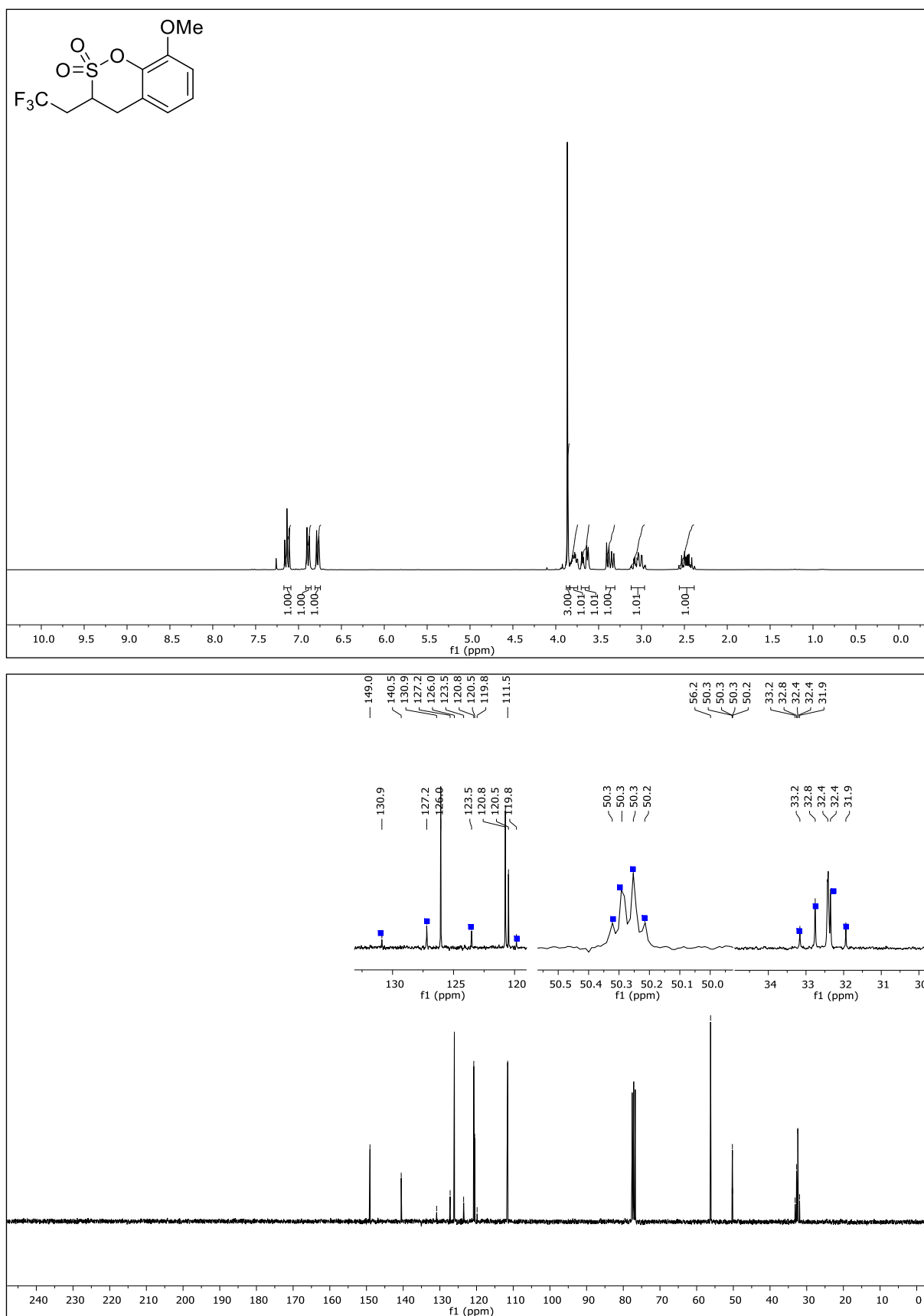
3-(2,2,2-Trifluoroethyl)-3,4-dihydrobenzo[e][1,2]oxathiine 2,2-dioxide (26j)

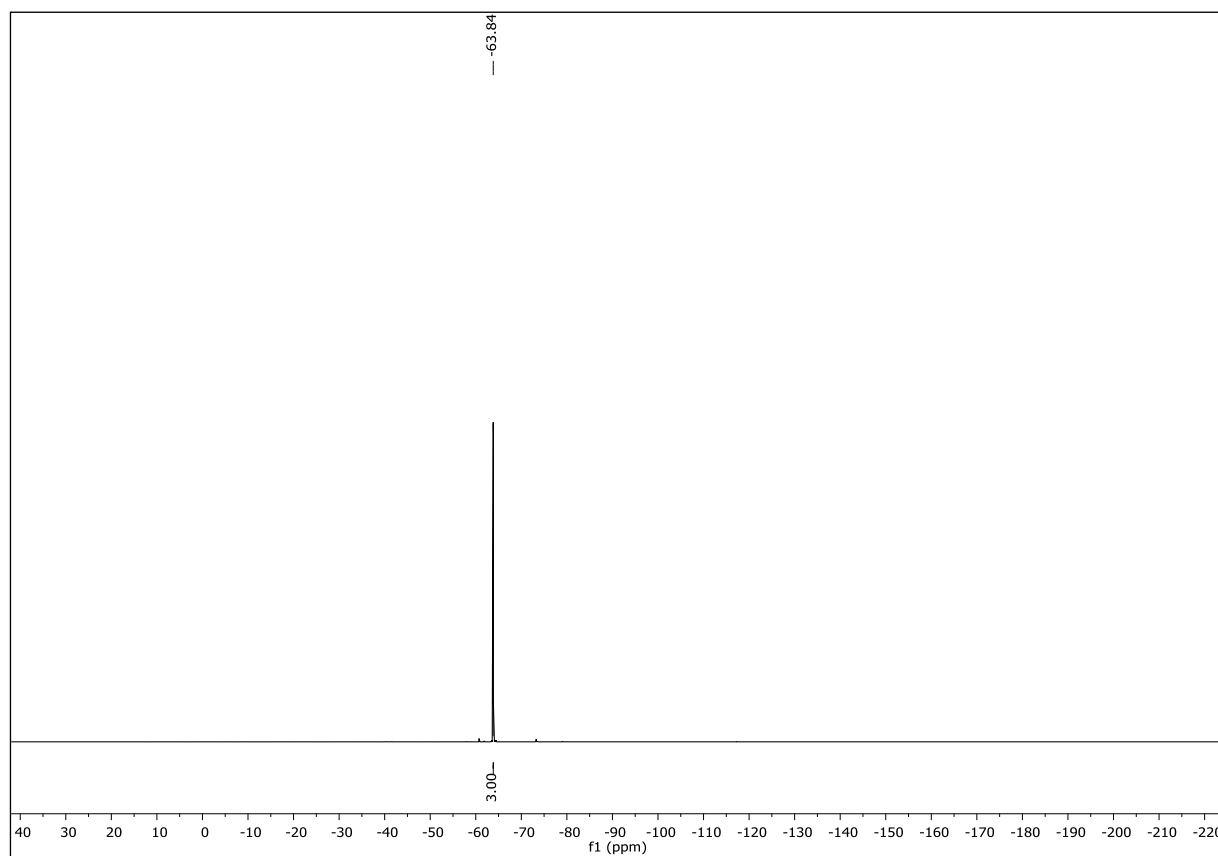




NMR-Solvent: CDCl_3

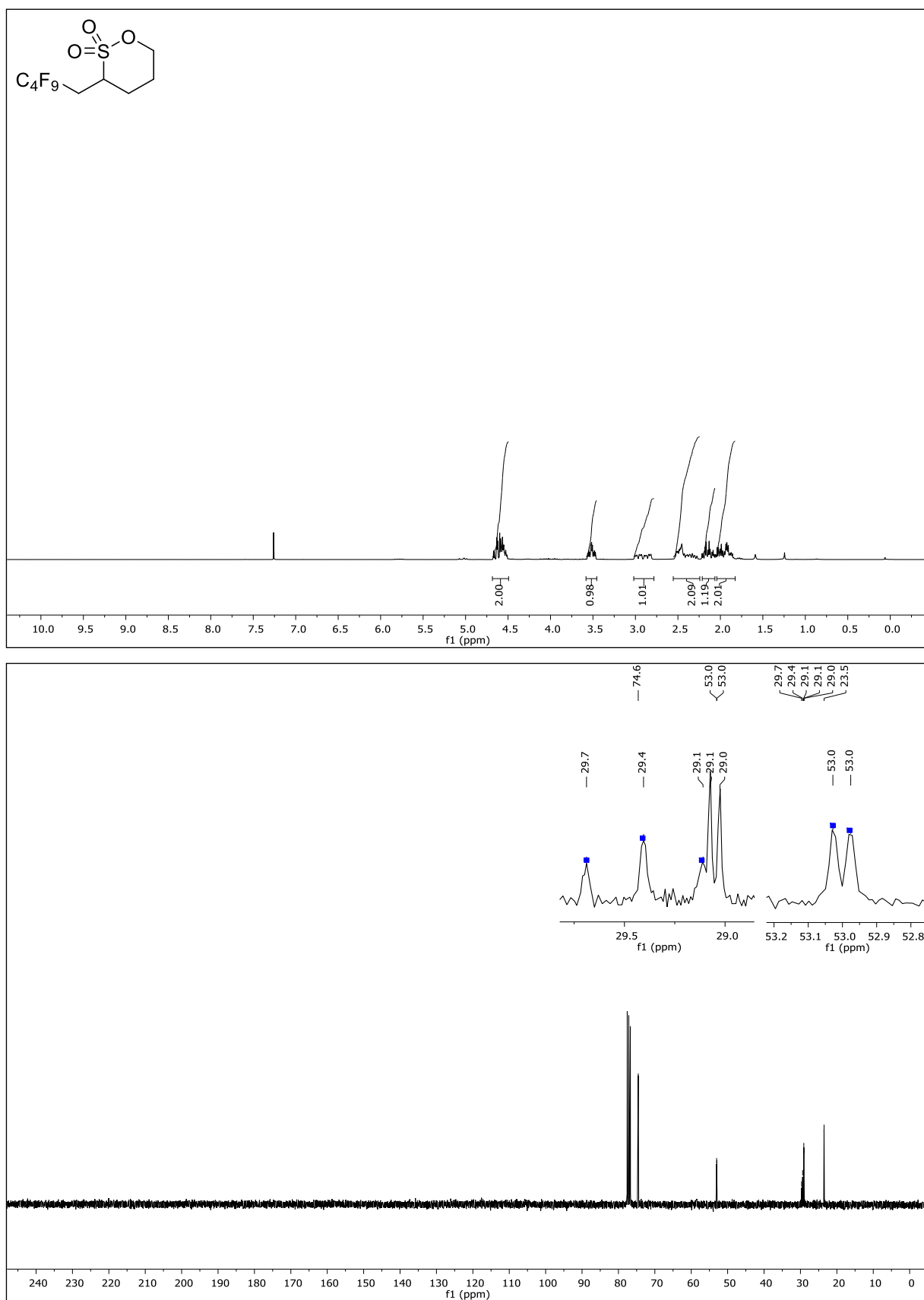
8-Methoxy-3-(2,2,2-trifluoroethyl)-3,4-dihydrobenzo[e][1,2]oxathiane 2,2-dioxide (26n)

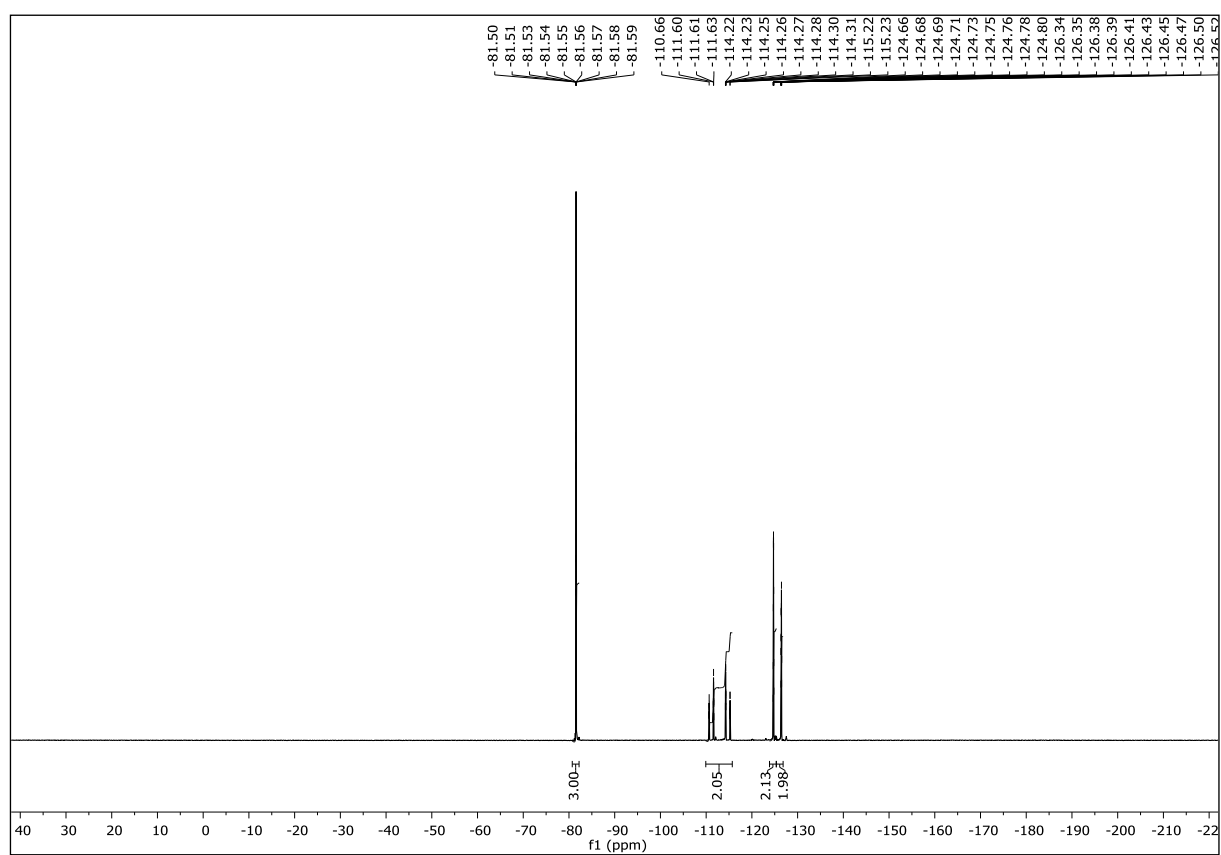




NMR-Solvent: CDCl_3

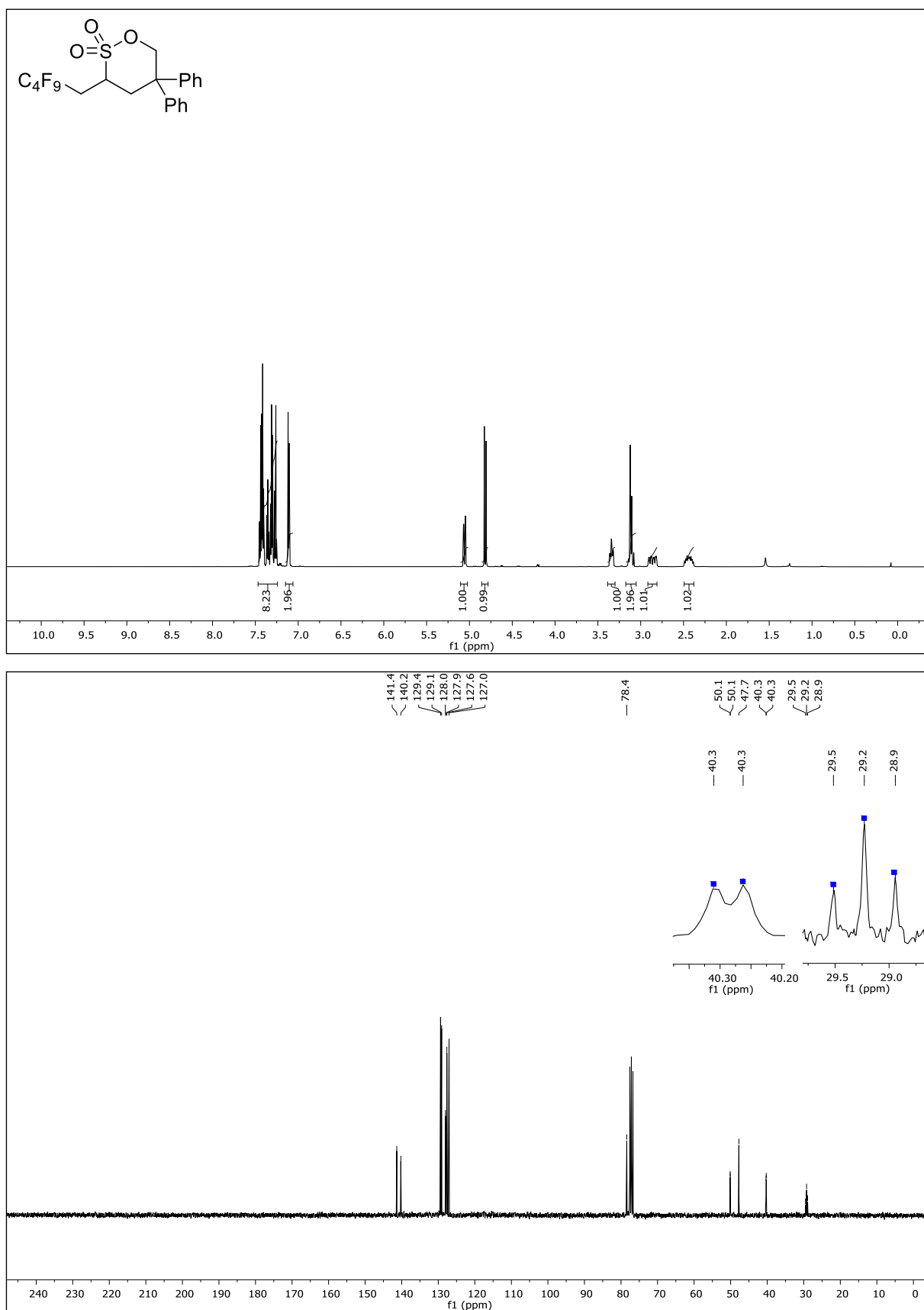
3-(2,2,3,3,4,4,5,5,5-Nonafluoropentyl)-1,2-oxathiane 2,2-dioxide (33a)

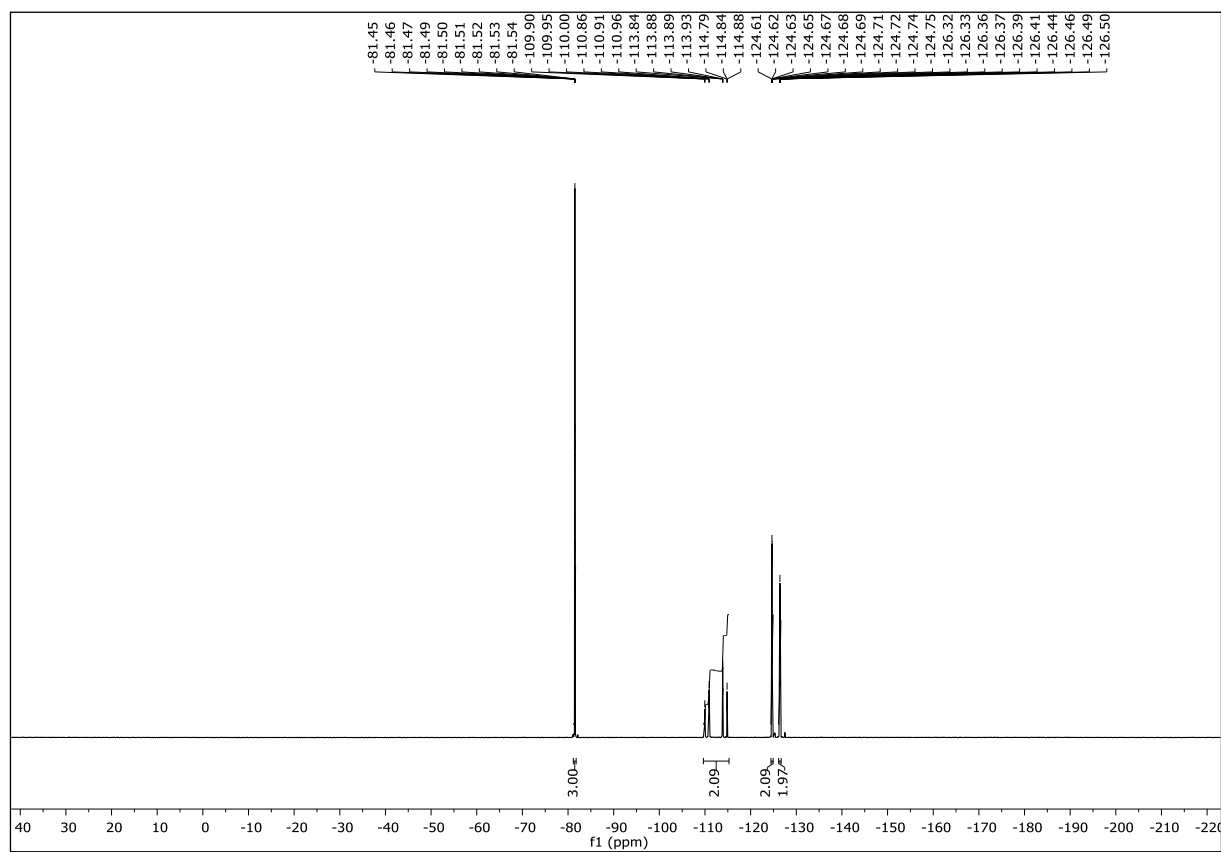




NMR-Solvent: CDCl_3

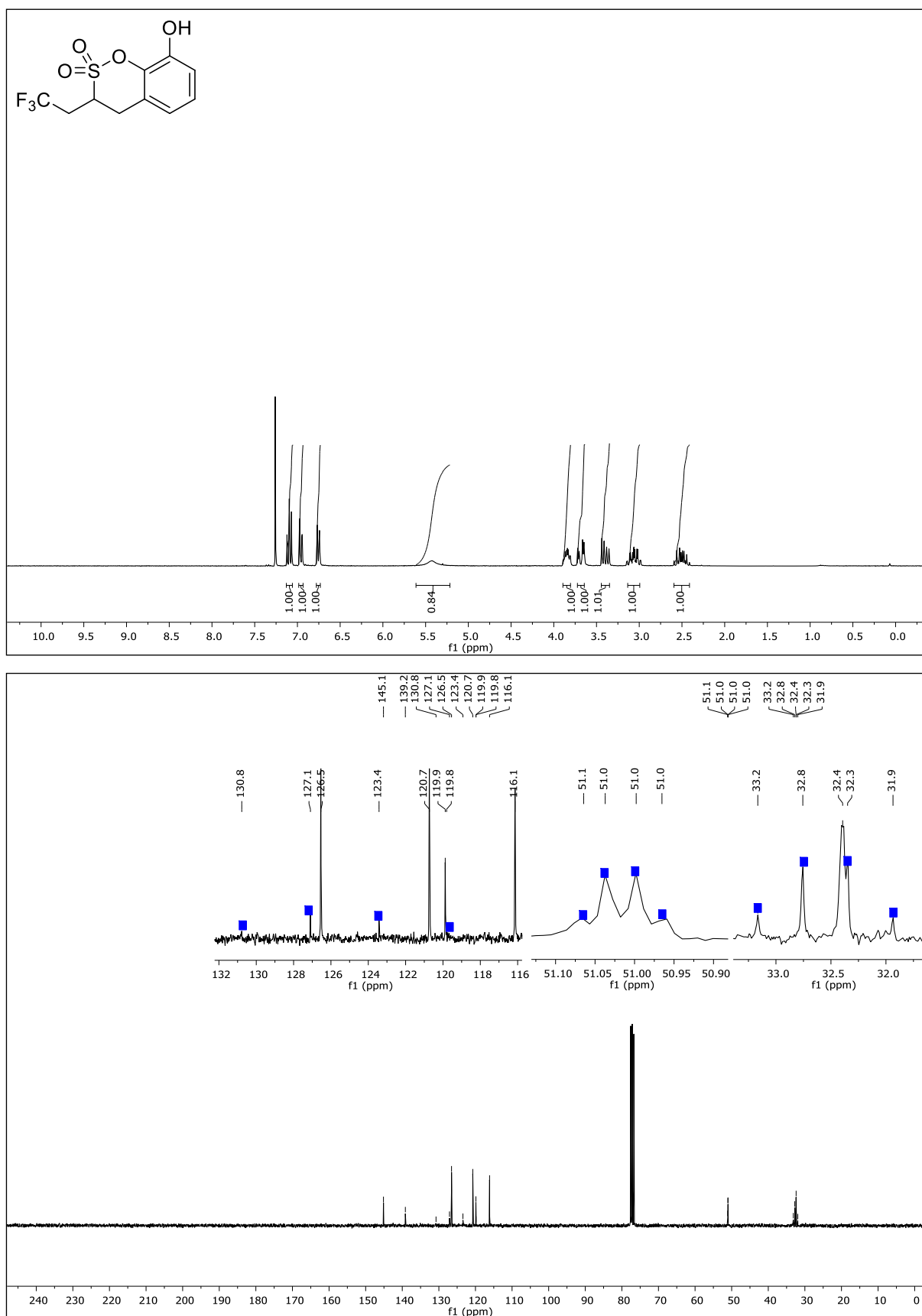
3-(2,2,3,3,4,4,5,5,5-Nonafluoropentyl)-5,5-diphenyl-1,2-oxathiane 2,2-dioxide (33b)

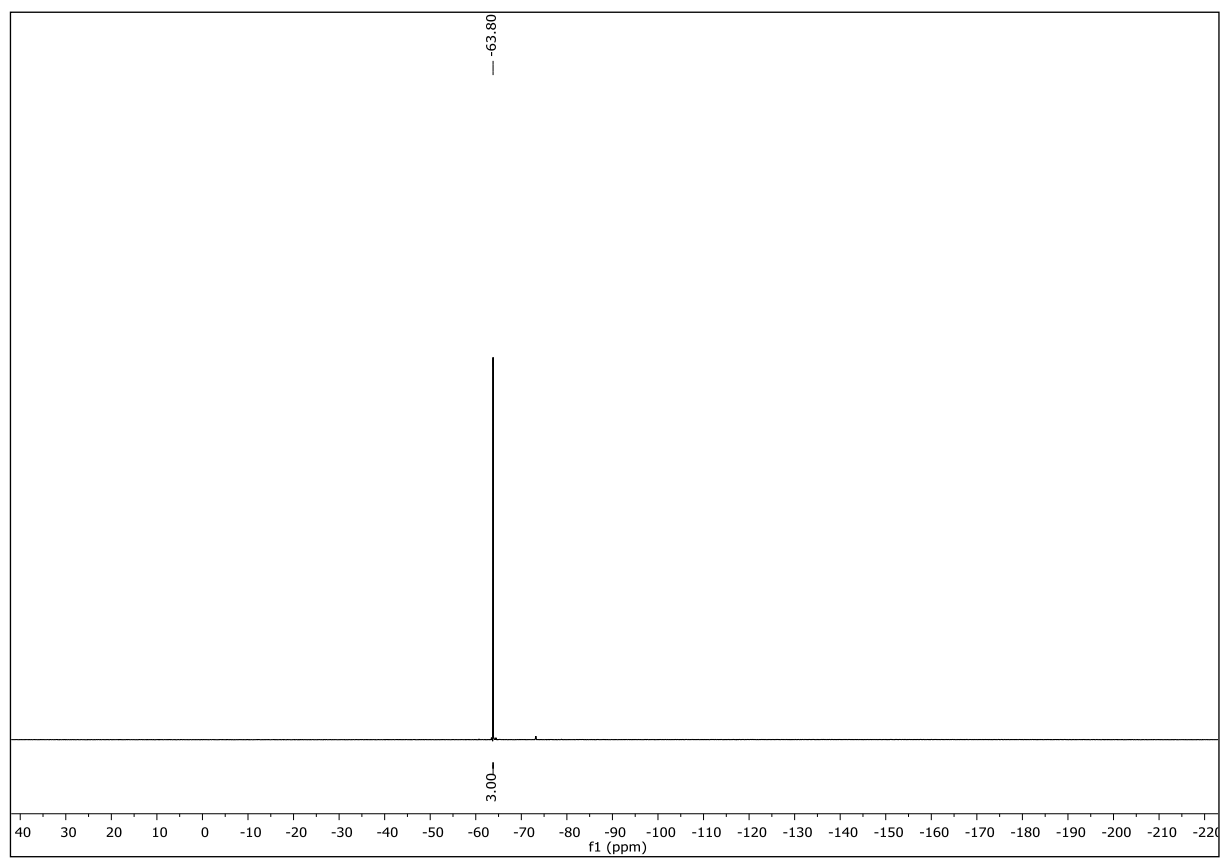




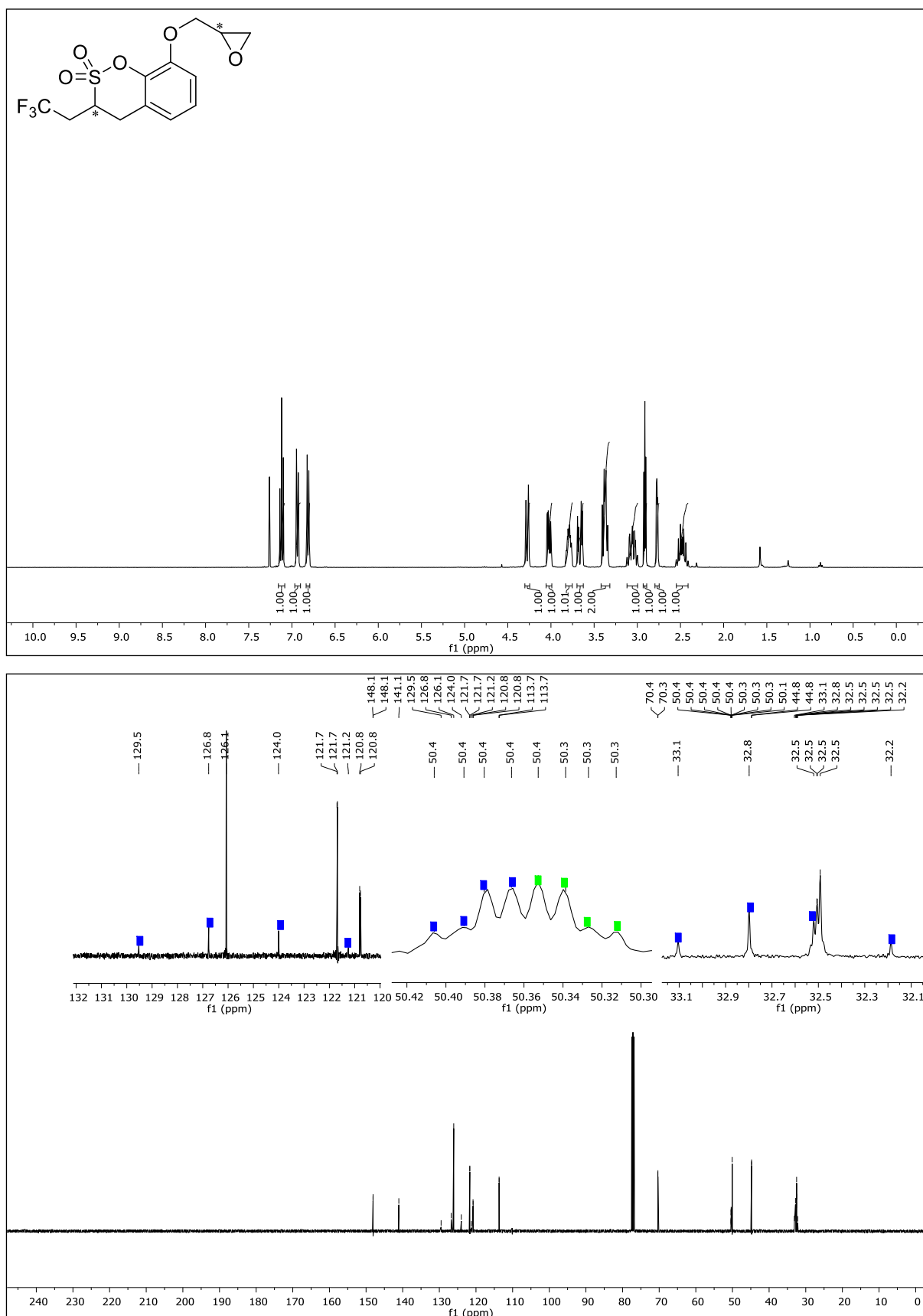
NMR-Solvent: CDCl_3

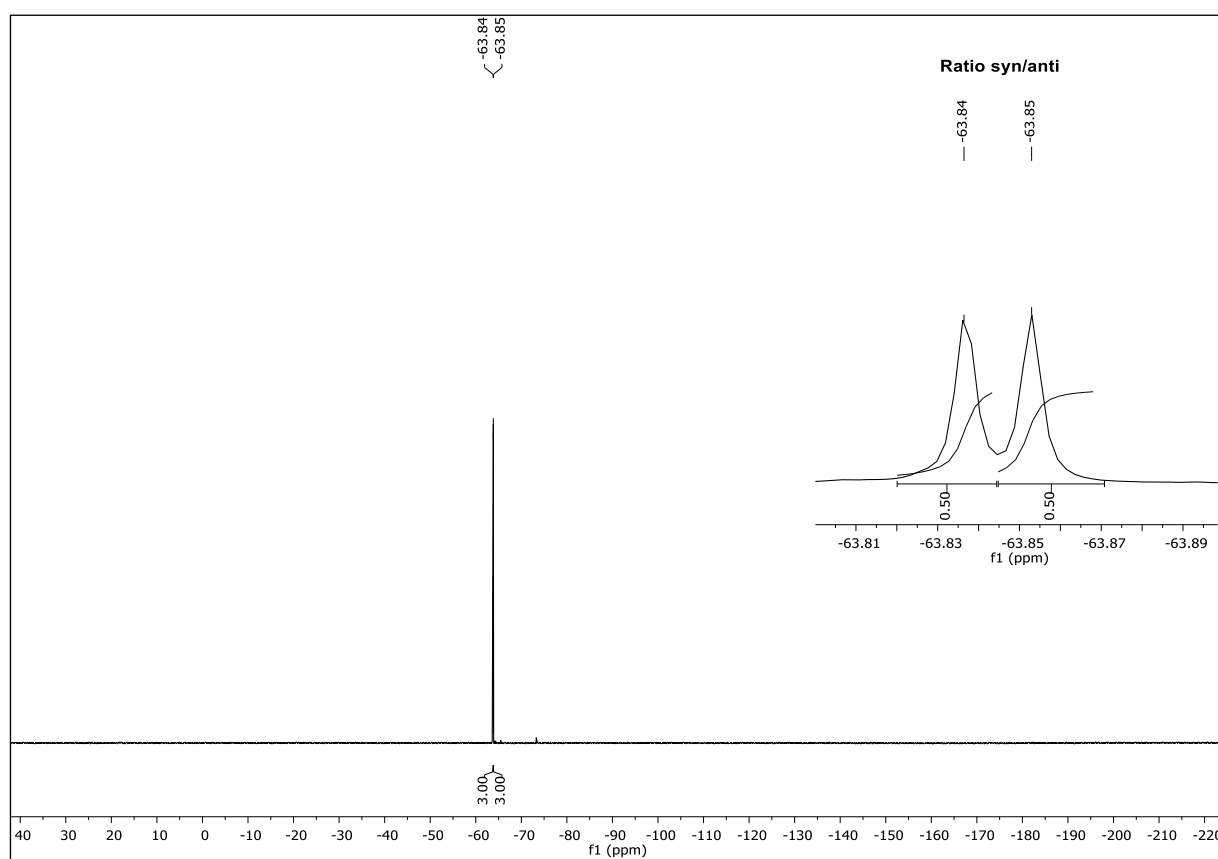
8-Hydroxy-3-(2,2,2-trifluoroethyl)-3,4-dihydrobenzo[e][1,2]oxathiine 2,2-dioxide (37)





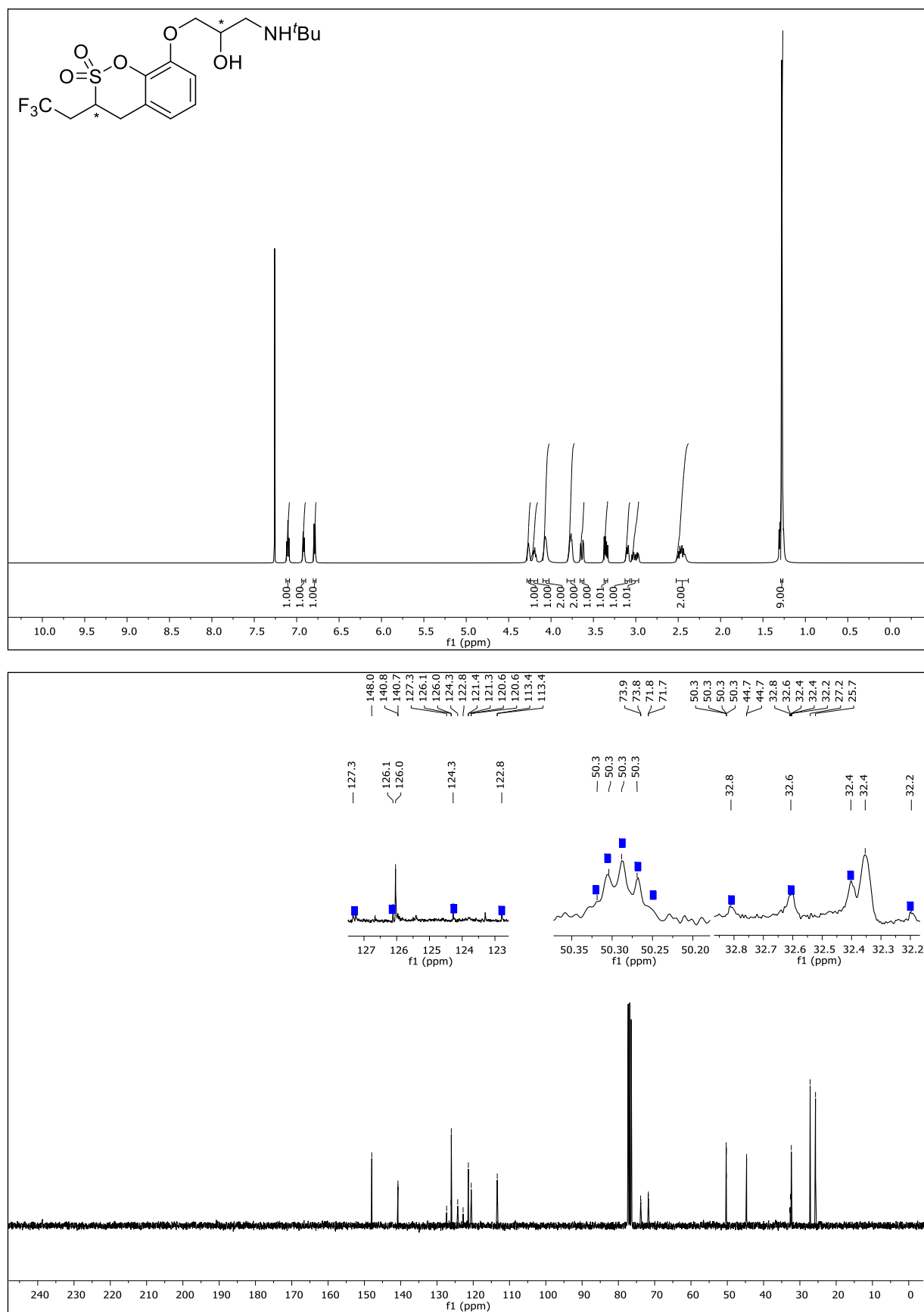
NMR-Solvent: CDCl_3

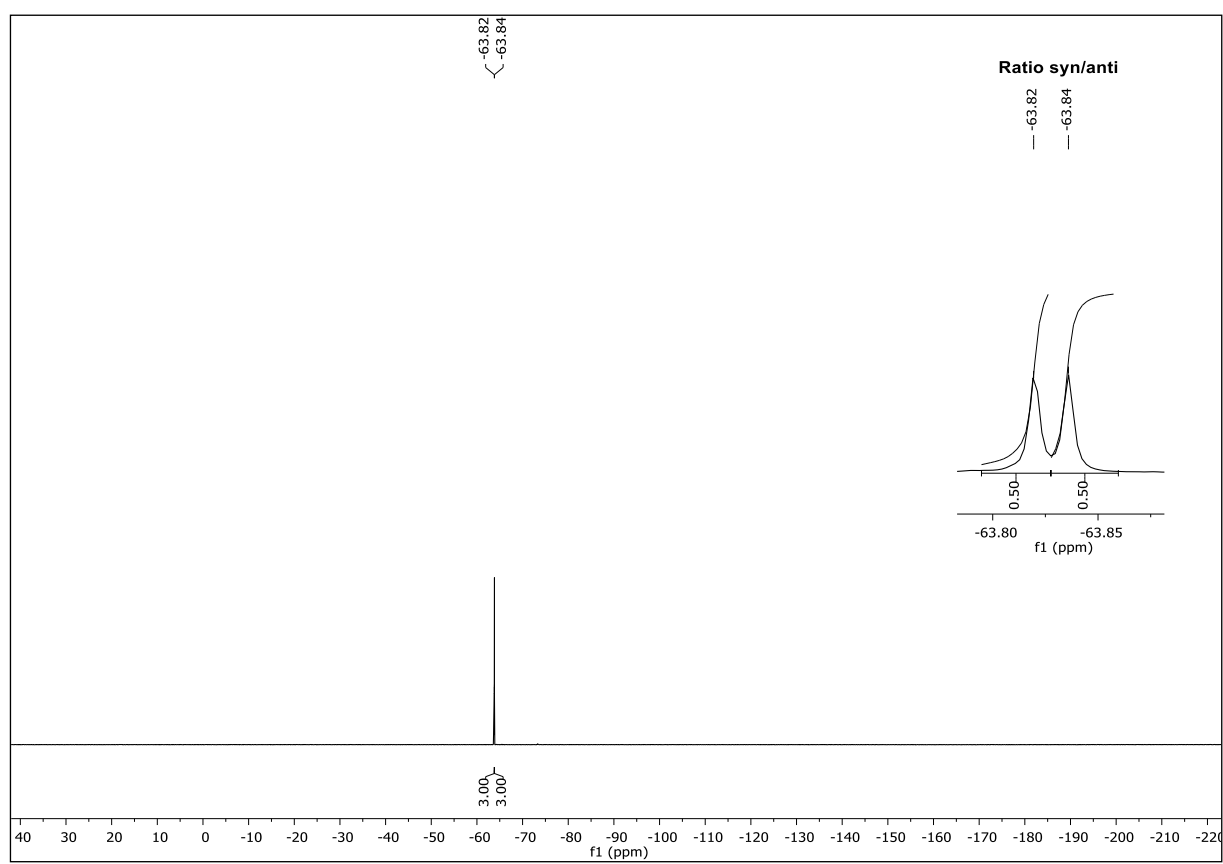
8-(Oxiran-2-ylmethoxy)-3-(2,2,2-trifluoroethyl)-3,4-dihydrobenzo[e][1,2]oxathiine 2,2-dioxide (38)



NMR-Solvent: CDCl_3

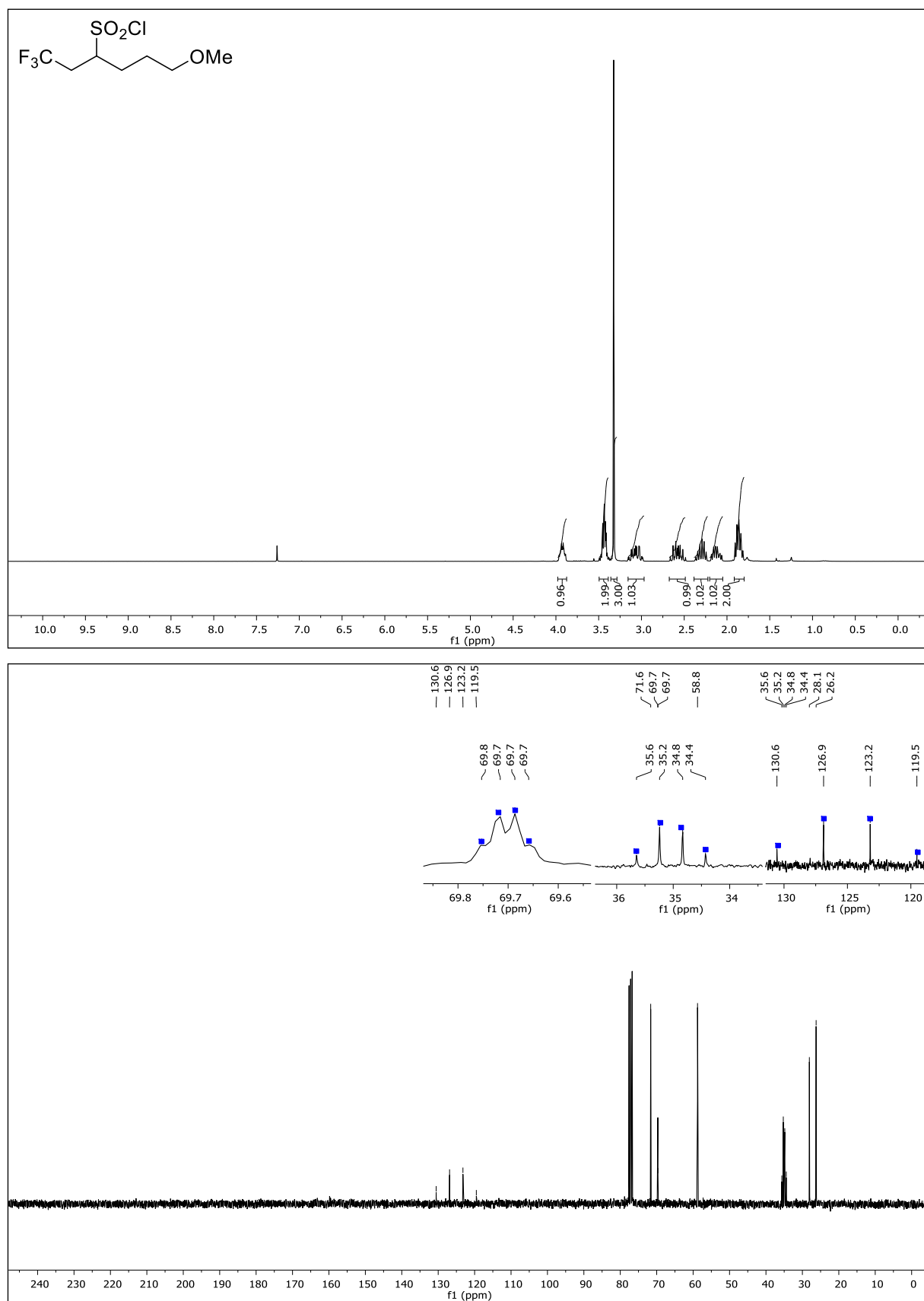
8-(3-(*tert*-Butylamino)-2-hydroxypropoxy)-3-(2,2,2-trifluoroethyl)-3,4-dihydrobenzo [e][1,2]oxathiine 2,2-dioxide (39)

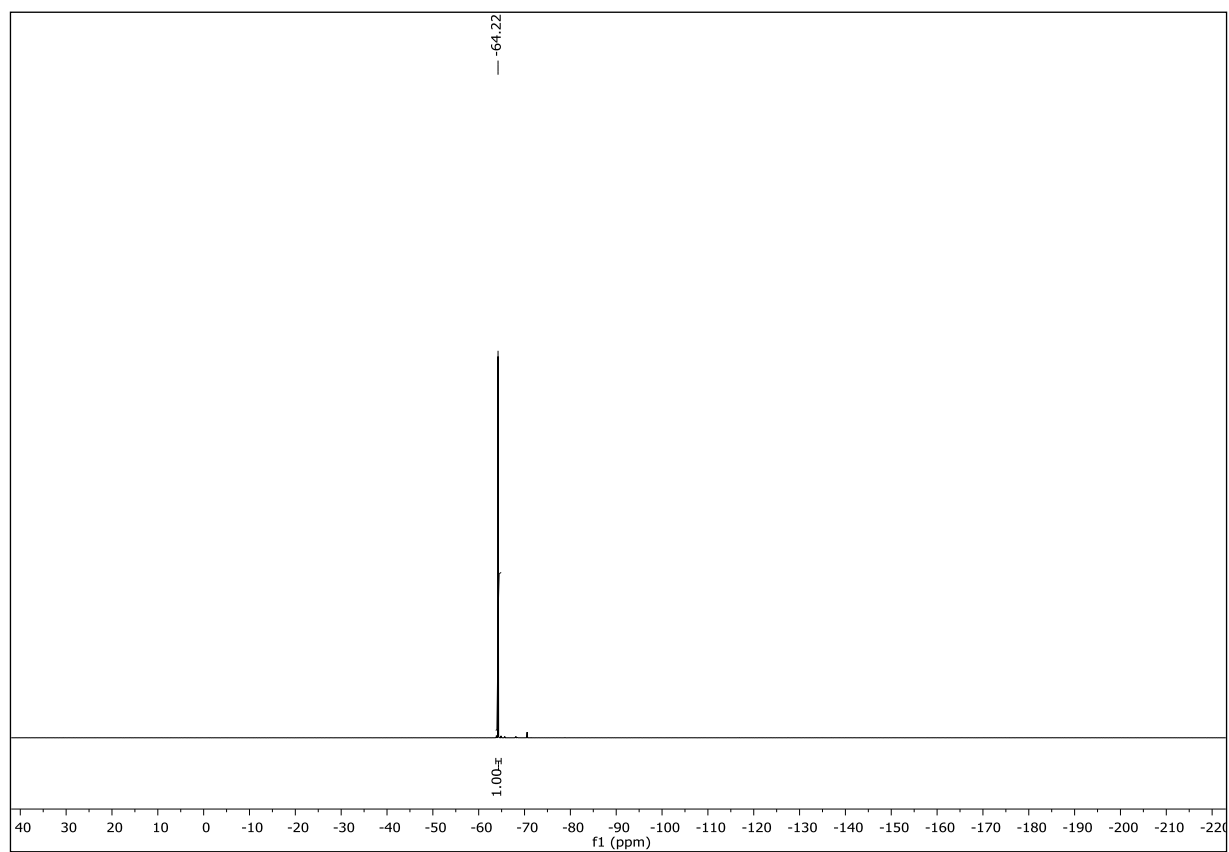




NMR-Solvent: CDCl₃

1,1,1-Trifluoro-6-methoxyhexane-3-sulfonyl chloride (45)





NMR-Solvent: CDCl₃

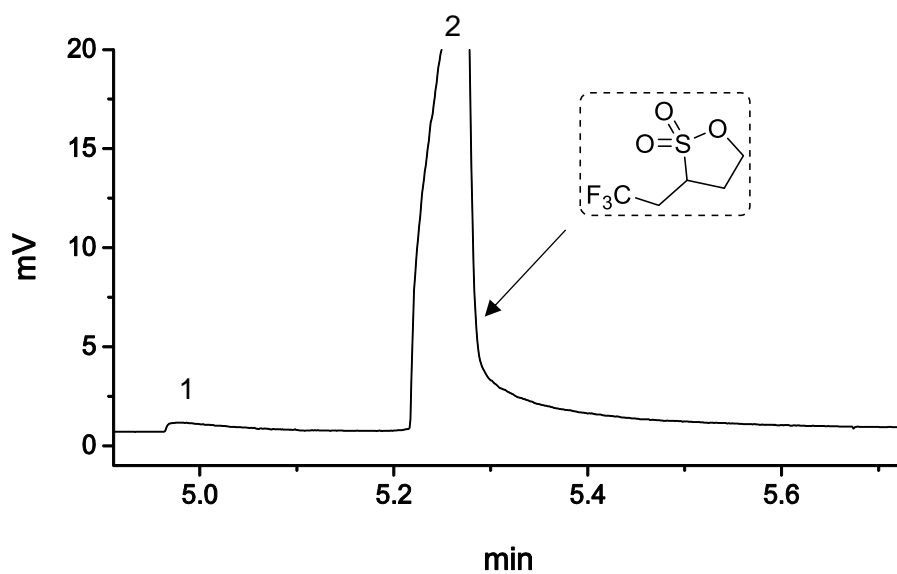
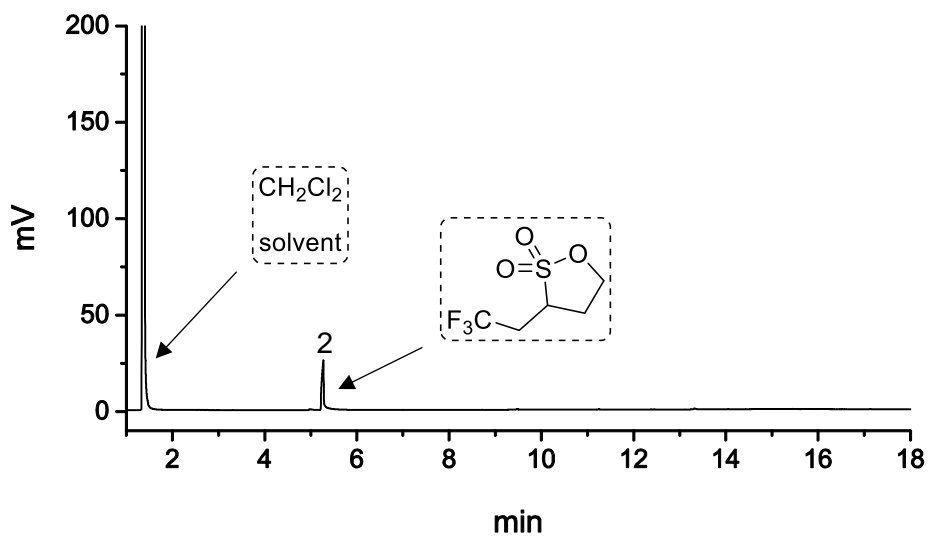
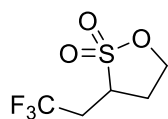
4.7. GC-MS Spectra

Gas chromatography was performed on a Fisons GC 8000 Series with a flame ionization detector (FID). DB1 (100% Dimethylpolysiloxan, 30 m, ID 0.25 mm, 0.25 μ m Film) was used as stationary phase. GC instrument conditions: Inlet temperature = 250 °C; detector temperature = 300 °C.

GC Method

50 °C for 5 min, then temperature ramp (10 °C/min) for 25 min to 300 °C followed by an isothermal period at 300 °C for 5 min.

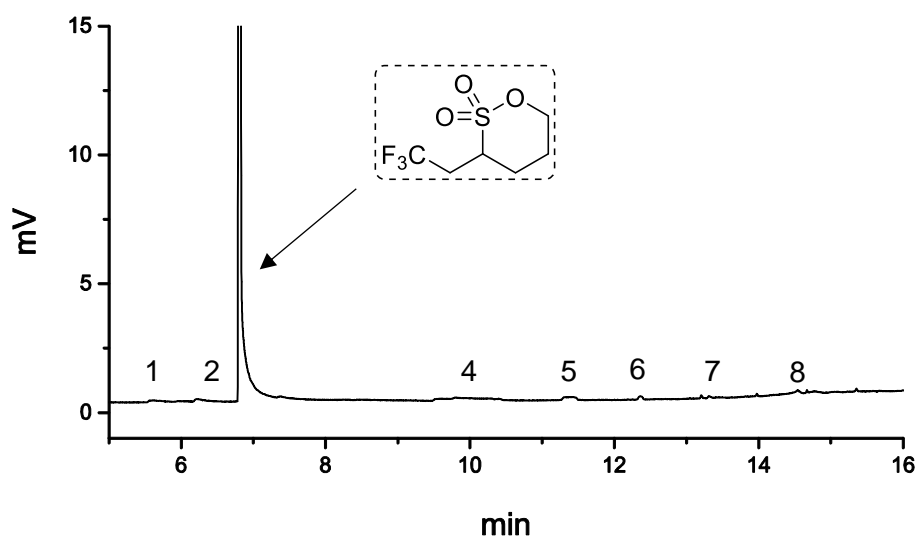
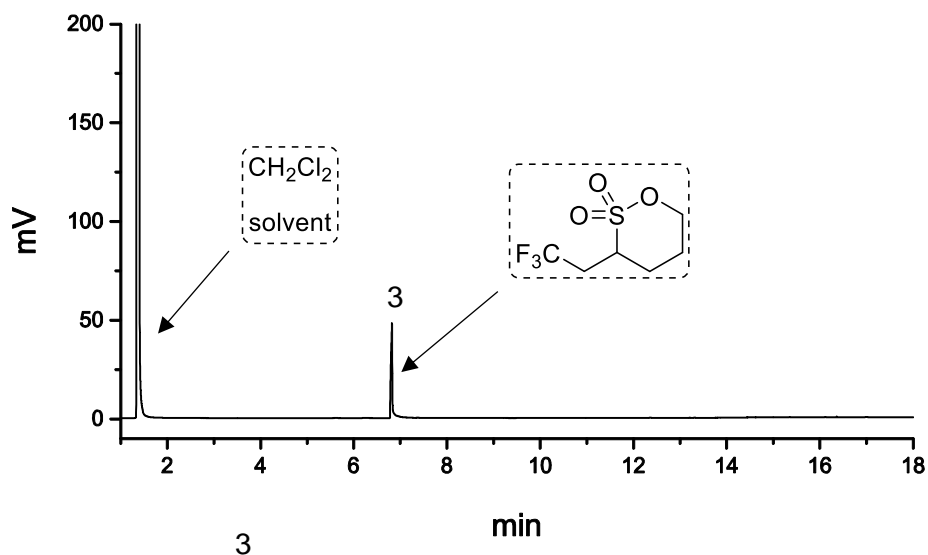
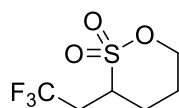
3-(2,2,2-Trifluoroethyl)-1,2-oxathiolane 2,2-dioxide (26a)



Peak	Retention Time t_R	Area	%Ar	Height
1	4.980	2.132	2.23	0.445
2	5.276	89.908	94.00	25.815

GC-Analysis: purity 94%, t_R = 5.276 min

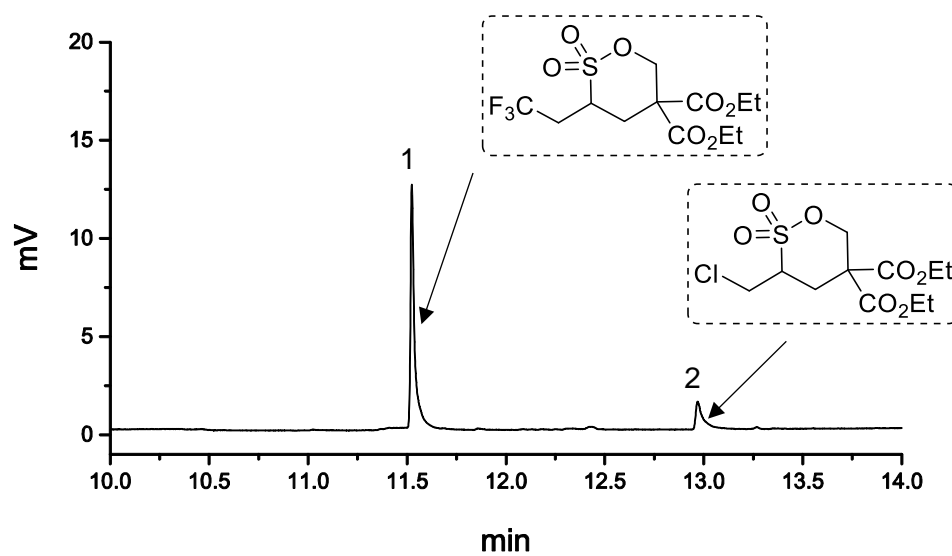
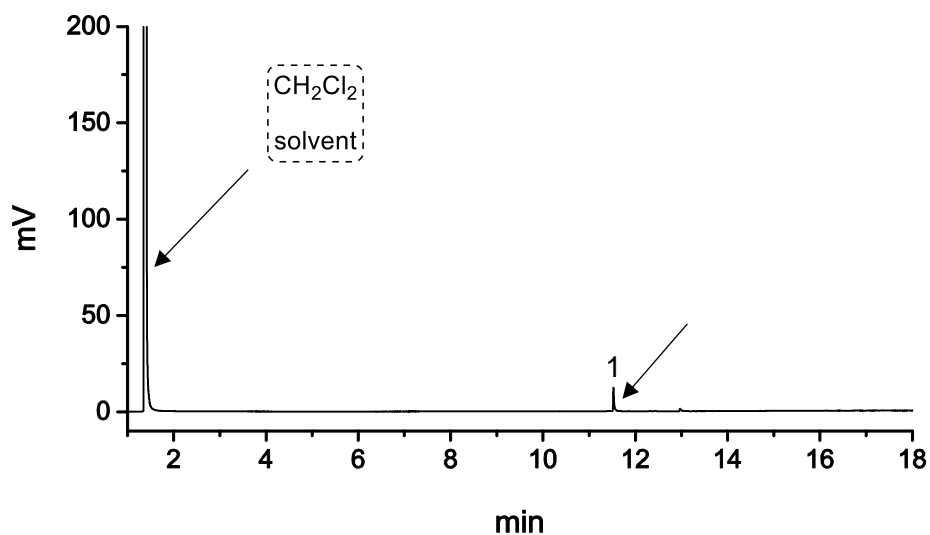
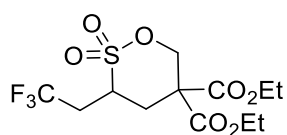
3-(2,2,2-Trifluoroethyl)-1,2-oxathiane 2,2-dioxide (26b)



Peak	Retention Time t_R	Area	%Ar	Height
1	5.669	0.868	0.80	0.075
2	6.247	0.575	0.53	0.089
3	6.821	103.295	95.12	47.628
4	9.663	0.739	0.68	0.066
5	11.370	1.400	1.29	0.124
6	12.370	0.516	0.48	0.135
7	13.263	0.346	0.32	0.114
8	14.464	0.853	0.79	0.119

GC-Analysis: purity 95%, t_R = 6.821 min

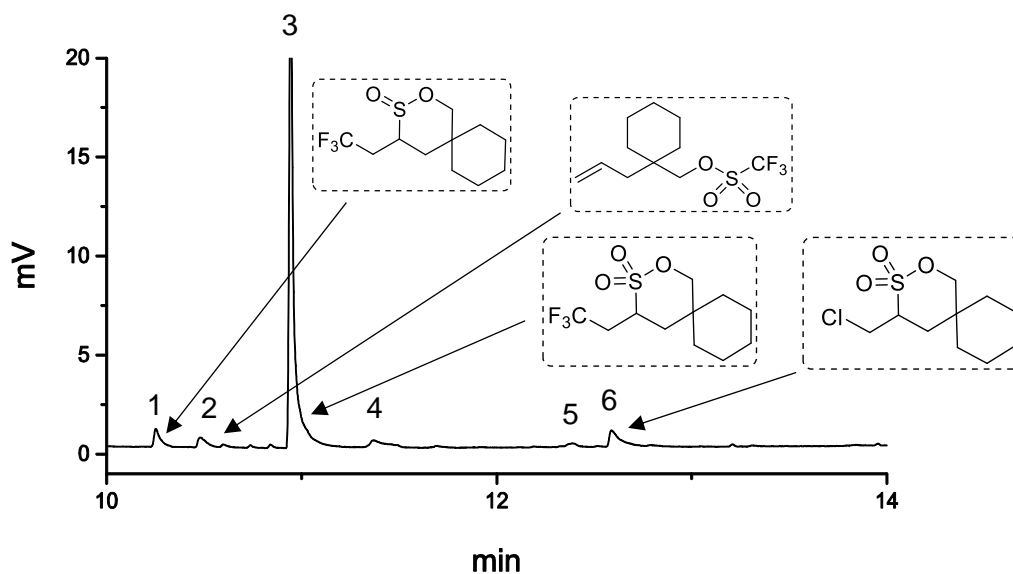
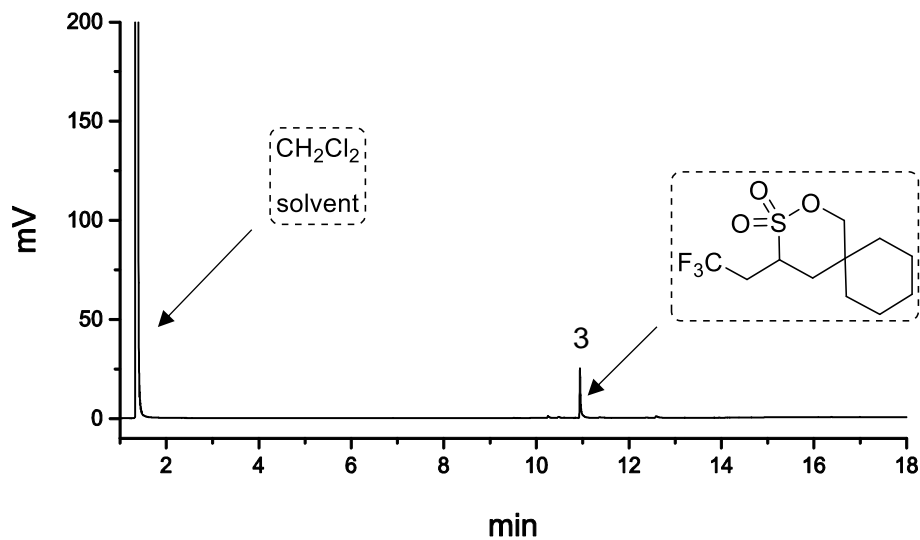
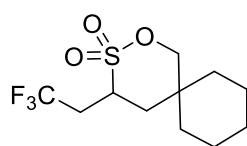
Diethyl 3-(2,2,2-trifluoroethyl)-1,2-oxathiane-5,5-dicarboxylate 2,2-dioxide (26g)



Peak	Retention Time t_R	Area	%Ar	Height
1	11.526	32.880	87.76	24.781
2	12.973	4.585	12.24	2.238

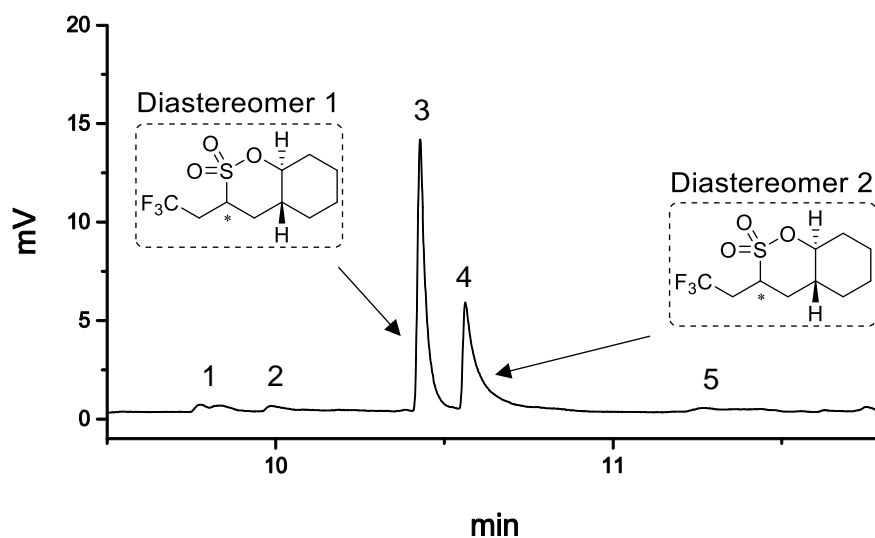
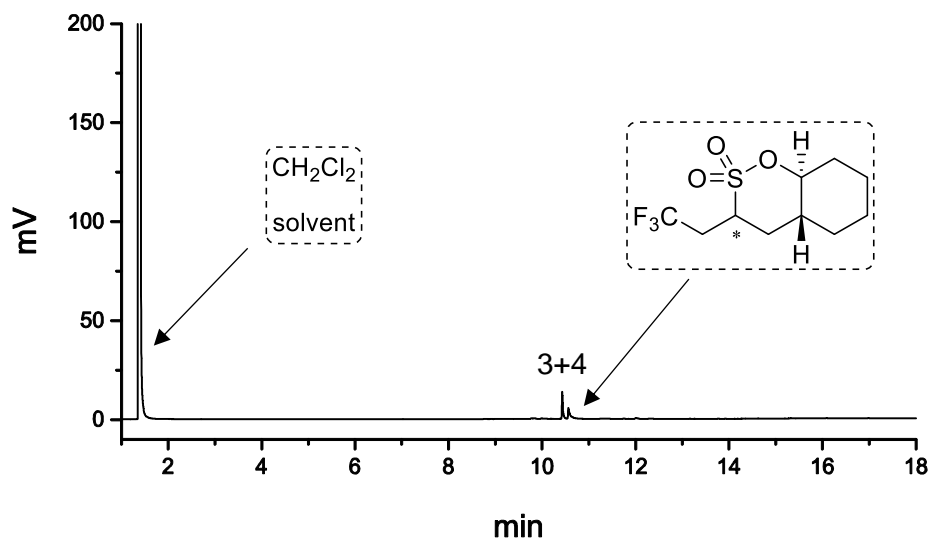
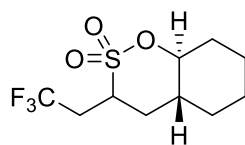
GC-Analysis: purity 88%, t_R = 11.526 min

4-(2,2,2-Trifluoroethyl)-2-oxa-3-thiaspiro[5.5]undecane 3,3-dioxide (26h)



Peak	Retention Time t_R	Area	%Ar	Height
1	10.254	0.906	3.06	0.461
2	10.484	0.689	2.33	0.268
3	10.945	26.111	88.17	11.360
4	11.371	0.961	3.24	0.208
5	12.394	0.178	0.60	0.093
6	12.591	0.771	2.60	0.327

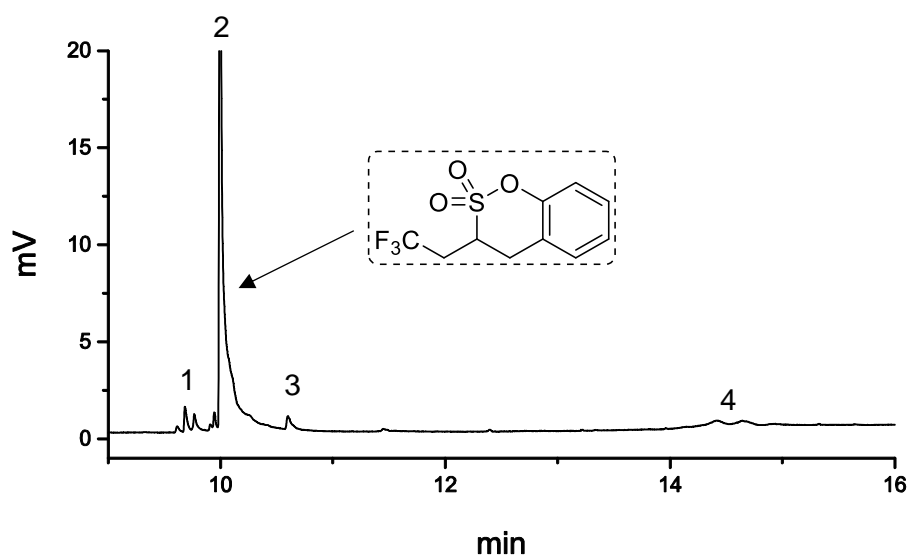
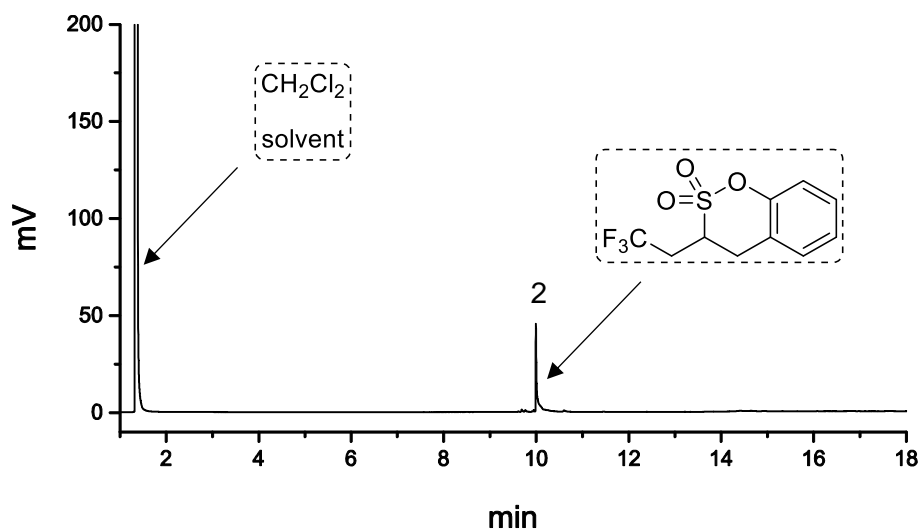
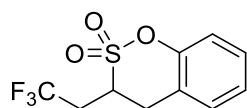
GC-Analysis: purity 88%, t_R = 10.945 min

***rel*-(4a*R*,8a*S*)-3-(2,2,2-Trifluoroethyl)octahydrobenzo[*e*][1,2]oxathiine 2,2-dioxide (26i)**

Peak	Retention Time t_R	Area	%Ar	Height
1	9.805	0.915	3.77	0.168
2	9.985	0.225	0.93	0.079
3	10.427	12.280	50.60	2.487
4	10.564	9.649	39.75	1.954
5	11.270	1.201	4.95	0.106

GC-Analysis: purity 90%, t_R = 10.496 min (two diastereomers)

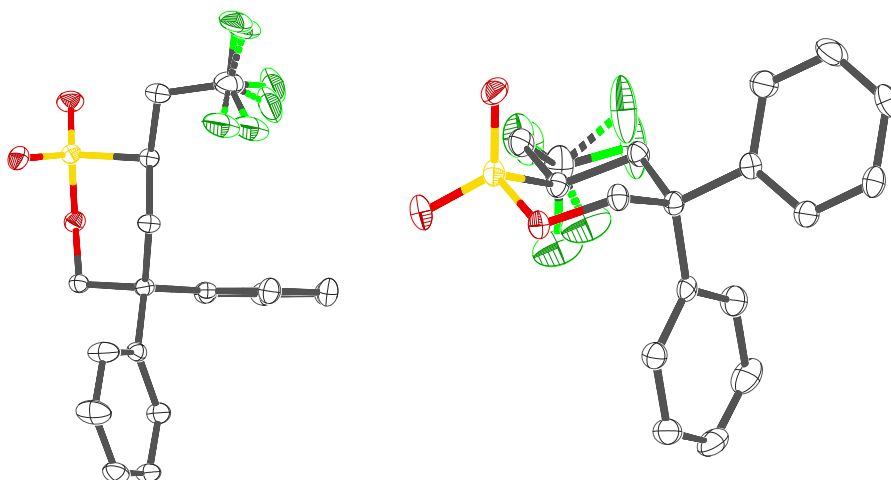
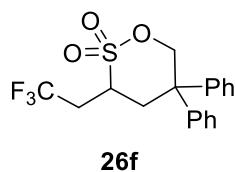
3-(2,2,2-Trifluoroethyl)-3,4-dihydrobenzo[e][1,2]oxathiine 2,2-dioxide (26j)



Peak	Retention Time t_R	Area	%Ar	Height
1	9.676	5.804	5.02	1.331
2	10.004	102.782	88.85	45.489
3	10.606	3.03	2.86	0.781
4	14.435	3.791	3.28	0.266

GC-Analysis: purity 89%, t_R = 10.004 min

4.8. X-ray



formula	C ₁₈ H ₁₇ F ₃ O ₃ S
$D_{\text{calc.}}/\text{g cm}^{-3}$	1.467
μ/mm^{-1}	2.148
formula weight	370.38
colour	clear colourless
shape	prism
max size/mm	0.22
mid size/mm	0.12
min size/mm	0.08
T/K	293(2)
crystal system	monoclinic
space group	P2 ₁ /c
$a/\text{\AA}$	9.15161(18)
$b/\text{\AA}$	9.9023(2)
$c/\text{\AA}$	18.6303(4)
$\alpha/^\circ$	90
$\beta/^\circ$	96.675(2)
$\gamma/^\circ$	90
$V/\text{\AA}^3$	1676.87(6)
Z	4
Z'	1
$\Theta_{\text{min}}/^\circ$	4.780
$\Theta_{\text{max}}/^\circ$	73.493
measured refl.	8691
independent refl.	3251
reflections used	2955
R_{int}	0.0233
parameters	236
restraints	6
largest peak	0.297
deepest hole	-0.424
GooF	1.039
wR_2 (all data)	0.0864
wR_2	0.0837
R_1 (all data)	0.0351
R_1	0.0318

5. References

- [1] a) Armarego, W. L. F.; Chai, C. L. L. *Purification of Laboratory Chemicals*; 6 ed.; Elsevier: Oxford, 2009; b) Hünig, S.; Felderhoff, M.; Kemmerer, M.; Kreitmeier, P.; Märkl, G.; Sauer, J.; Seifert, M.; Sustmann, R.; Troll *Integriertes Organisch-Chemisches Praktikum (I.O.C.-Praktikum)*; 1. ed.; Lehmanns, 2007.
- [2] a) Pavlishchuk, V. V.; Addison, A. W. *Inorg. Chim. Acta* **2000**, 298, 97-102; b) Smith, T. J.; Stevenson, K. J. Chapter 4: Reference Electrodes In *Handbook of Electrochemistry*; 1 ed.; Zoski, C. G., Ed.; Elsevier: Amsterdam, 2007, p 73-110.
- [3] Dennis, E. G.; Jeffery, D. W.; Perkins, M. V.; Smith, P. A. *Tetrahedron* **2011**, 67, 2125-2131.
- [4] Rashkin, M. J.; Hughes, R. M.; Calloway, N. T.; Waters, M. L. *J. Am. Chem. Soc.* **2004**, 126, 13320-13325.
- [5] Tang, S.; Liu, M.; Gu, C.; Zhao, Y.; Lu, P.; Lu, D.; Liu, L.; Shen, F.; Yang, B.; Ma, Y. *J. Org. Chem.* **2008**, 73, 4212-4218.
- [6] a) Banwell, M. G.; Cameron, J. M.; Collis, M. P.; Crisp, G. T.; Gable, R. W.; Hamel, E.; Lambert, J. N.; Mackay, M. F.; Reum, M. E.; Scoble, J. A. *Aust. J. Chem.* **1991**, 44, 705-728; b) Zysman-Colman, E.; Arias, K.; Siegel, J. S. *Can. J. Chem* **2009**, 87, 440-447.
- [7] a) Nishimura, N.; Yoza, K.; Kobayashi, K. *J. Am. Chem. Soc.* **2010**, 132, 777-790; b) Mirrington, R. N.; Feutrill, G. I. *Organic Syntheses* **1973**, 53, 90.
- [8] Pavlyuk, O.; Teller, H.; McMills, M. C. *Tetrahedron Lett.* **2009**, 50, 2716-2718.
- [9] Han, P.; Wang, R.; Wang, D. Z. *Tetrahedron* **2011**, 67, 8873-8878.
- [10] Coleman, G. H.; Honeywell, G. E. *Organic Syntheses* **1936**, 16, 54.
- [11] Hosomi, A.; Iguchi, H.; Sakurai, H. *Chem. Lett.* **1982**, 223-226.
- [12] Li, L. H.; Wang, D.; Chan, T. H. *Tetrahedron Lett.* **1991**, 32, 2879-2882.
- [13] Lipshutz, B. H.; Hackmann, C. *J. Org. Chem.* **1994**, 59, 7437-7444.
- [14] Frey, J.; Kraus, T.; Heitz, V.; Sauvage, J.-P. *Chem. Eur. J.* **2007**, 13, 7584-7594.
- [15] Pirtsch, M.; Paria, S.; Matsuno, T.; Isobe, H.; Reiser, O. *Chem. Eur. J.* **2012**, 18, 7336-7340.
- [16] Knorn, M.; Rawner, T.; Czerwieniec, R.; Reiser, O. *ACS Catalysis* **2015**, 5, 5186-5193.
- [17] Asano, K.; Uesugi, Y.; Yoshida, J. *Org. Lett.* **2013**, 15, 2398-2401.
- [18] Bagal, D. B.; Kachkovskyi, G.; Knorn, M.; Rawner, T.; Bhanage, B. M.; Reiser, O. *Angew. Chem. Int. Ed.* **2015**, 54, 6999-7002.
- [19] Necas, D.; Katora, M. *Org. Lett.* **2008**, 10, 5261-5263.
- [20] Vasil'ev, A. A.; Lyubimov, S. E.; Serebryakov, E. P.; Davankov, V. A.; Struchkova, M. I.; Zlotin, S. G. *Russ. Chem. Bull.* **2010**, 59, 605-610.
- [21] Tayama, E.; Sugai, S. *Tetrahedron Lett.* **2007**, 48, 6163-6166.

- [22] Lin, Z.-M.; Zheng, C.; Xiao, J.-J.; Chen, R.-F.; Zhao, P.; Song, J.; An, Z.-F.; Tian, H.; Huang, W. *New J. Chem.* **2012**, 36, 1512-1518.
- [23] Nishio, R.; Sugiura, M.; Kobayashi, S. *Org. Lett.* **2005**, 7, 4831-4834.
- [24] Schmidt, V. A.; Alexanian, E. J. *J. Am. Chem. Soc.* **2011**, 133, 11402-11405.
- [25] Stuart, D. R.; Bertrand-Laperle, M.; Burgess, K. M.; Fagnou, K. *J. Am. Chem. Soc.* **2008**, 130, 16474-16475.
- [26] Kitazume, T.; Ikeya, T. *J. Org. Chem.* **1988**, 53, 2350-2352.
- [27] a) Schomaker, J. M.; Travis, B. R.; Borhan, B. *Org. Lett.* **2003**, 5, 3089-3092; b) Šmit, B. M.; Pavlović, R. Z. *Tetrahedron* **2015**, 71, 1101-1108.
- [28] Canney, D.; Gao, R.; Fan, R. *Synlett* **2015**, 26, 661-665.
- [29] a) Ozoe, Y.; Eto, M. *Agric. Biol. Chem.* **1982**, 46, 411-418; b) Boyd, S.; Davies, C. D. *Tetrahedron Lett.* **2014**, 55, 4117-4119.
- [30] Fujita, S.; Abe, M.; Shibuya, M.; Yamamoto, Y. *Org. Lett.* **2015**, 17, 3822-3825.
- [31] Constantino, M. G.; Lacerda, V.; Aragão, V. *Molecules* **2001**, 6, 770-776.
- [32] Garcia, A.; Otte, D. A.; Salamant, W. A.; Sanzone, J. R.; Woerpel, K. A. *Angew. Chem. Int. Ed.* **2015**, 54, 3061-3064.
- [33] Fernandez-Mateos, A.; Madrazo, S. E.; Teijon, P. H.; Gonzalez, R. R. *J. Org. Chem.* **2015**, 80, 4378-4391.
- [34] Wenkert, E.; Michelotti, E. L.; Swindell, C. S.; Tingoli, M. *J. Org. Chem.* **1984**, 49, 4894-4899.
- [35] Hemelaere, R.; Carreaux, F.; Carboni, B. *Eur. J. Org. Chem.* **2015**, 2015, 2470-2481.
- [36] Kanazawa, A.; Muniz, M. N.; Greene, A. E. *Synlett* **2005**, 1328-1330.
- [37] Zhdanko, A.; Maier, M. E. *Eur. J. Org. Chem.* **2014**, 2014, 3411-3422.
- [38] a) Barbry, D.; Hasiak, B. *Collect. Czech. Chem. Commun.* **1983**, 48, 1734-1744; b) Brooks, L. A.; Snyder, H. R. *Organic Syntheses* **1945**, 25, 84.
- [39] Megerle, U.; Lechner, R.; König, B.; Riedle, E. *Photochem. Photobiol. Sci.* **2010**, 9, 1400-1406.

G. Appendix

1. Curriculum Vitae

Personal Data

Name : Thomas Martin Rawner

Date and place of birth : 20.09.1986 in Schwientochlowitz, Poland

Nationality : German

Email : thomas.rawner@gmail.com

Education

10/2013 - 06/2016	PhD Thesis at the University of Regensburg under supervision of Prof. Dr. Oliver Reiser <i>"Copper(I) Phenanthrolines in Photocatalysis"</i>
11/2014 - 01/2015	Research Project at the UAB in Barcelona (Spain) under the supervision of Prof. Dr. Rosa M. Ortuño <i>"1,4-Diaminoalcohols Containing Cyclobutane for Asymmetric Catalysis"</i>
09/2013	Graduation: Master of Science
01/2013 - 09/2013	Master Thesis at the University of Regensburg under supervision of Prof. Dr. Oliver Reiser <i>„Iron-catalyzed Deoxygenation of Allylic Alcohols“</i>
10/2010 - 09/2012	Studies in Chemistry (M. Sc.), University of Regensburg, Germany
10/2009 - 10/2010	Studies in Education (Staatsexamen), University of Regensburg, Germany
09/2009	Graduation: Bachelor of Science
10/2006 - 09/2009	Studies in Chemistry (B. Sc.), University of Regensburg, Germany
09/1997 - 06/2006	Abitur (A-levels), Werner von Siemens Gymnasium, Regensburg, Germany (High school certificate equivalent)
09/1993 - 09/1997	Primary School, Grundschule am Sallerner Berg, Regensburg, Germany

Languages

German (native)

English (fluently)

Polish (basics)

Professional References

Prof. Dr. Oliver Reiser

Institut für Organische Chemie

Universität Regensburg, Universitätsstr. 31

93053 Regensburg, Germany

Phone: +49 941 9434631

E-mail: oliver.reiser@chemie.uni-regensburg.de

Prof. Dr. Rosa M. Ortuno

Departament de Química

Universitat Autònoma de Barcelona

08193 Bellaterra (Barcelona), Spain

Phone: +34 93 581 1602

Email: rosa.ortuno@uab.es

2. Congresses and Scientific Meetings

- [1] GRK 1626, Regensburg, Germany, **2014**
A6: The different faces of transition metal complexes in photoredox catalyzed processes
T. Rawner, D. B. Bagal, C. Faderl, G. Kachkovskyi, V. Kais, P. Kohls, S. Paria, M. Pirtsch, D. Rackl, , O. Reiser
- [2] Tag der Chemie, Regensburg, Germany, **2014**
The photocatalyst [Cu(dap)₂]Cl and its application
T. Rawner, M. Pirtsch, D. B. Bagal, S. Paria, O. Reiser
- [3] 5th EUCHEMS Chemistry Congress, Istanbul, Turkey, **2014**
Cu(phenanthroline)(bisisonitrile)⁺-complexes for visible-light photoredox atom transfer radical additions (ATRA)
M. Knorn, T. Rawner, O. Reiser
- [4] 24. Lecture Conference on Photochemistry, Köln, Germany, **2014**
Visible light mediated copper-catalyzed ATRA reactions for the synthesis of perfluoroalkyl tagged molecules
T. Rawner, O. Reiser
- [5] 24. Lecture Conference on Photochemistry, Köln, Germany, **2014**
Extending the scope of the [Cu(dap)₂]Cl catalyst for visible light mediated photoredox reactions by modifications in the ligand structure
C. Lankes, T. Rawner, O. Reiser
- [6] Cicle de Conferències de Química, Barcelona, Spain, **2014**
1,4-Diaminoalcohols Containing Cyclobutane for Asymmetric Catalysis
T. Rawner und O. Reiser
- [7] GDCh-Wissenschaftsforum Chemie, Dresden, Germany, **2015**
Trifluoromethylchlorosulfonylation of Alkenes: Evidence for an Inner-Sphere Mechanism by a Copper Phenanthroline Photoredox Catalyst
T. Rawner, D. B. Bagal, G. Kachkovskyi, M. Knorn, O. Reiser
- [8] 17. Weihnachtskolloqium, Regensburg, Germany, **2015**
Light Wars – The Force of Copper Awakens
T. Rawner und O. Reiser

3. List of Publications

- [1] D. B. Bagal, G. Kachkovski, M. Knorn, T. Rawner, B. M. Bhanage and O. Reiser
“Trifluoromethylchlorosulfonylation of alkenes - evidence for an inner sphere mechanism by a copperphenanthroline photoredox catalyst”
Angew. Chem. Int. Ed. **2015**, 54, 6999 - 7002; *Angew. Chem.* **2015**, 127, 7105 – 7108;
DOI: 10.1002/anie.201501880
- [2] M. Knorn, T. Rawner, R. Czerwieniec and O. Reiser
“New [Copper(phenanthroline)(bisisonitrile)]⁺-Complexes for the Visible Light-Mediated Atom Transfer Radical Addition and Allylation Reactions”
ACS Catal., **2015**, 5, 5186 – 5193;
DOI: 10.1021/acscatal.5b01071
- [3] T. Rawner, M. Knorn, Eugen Lutsker, Asik Hossain and O. Reiser
“Synthesis of Trifluoromethylated Sultones from Alkenols Using a Copper Photoredox Catalyst”
JOC **2016** accepted (Special Issue: Photochemistry)
DOI: 10.1021/acs.joc.6b01001

H. Acknowledgement

I would like to thank my research supervisor *Prof. Dr. Oliver Reiser* for giving me the opportunity to work in his research group and for this challenging and interesting topic. I am very grateful for his helpful suggestions on chemical problems and the freedom to materialize own ideas. Moreover, I would like to express my sincere gratitude for the opportunity to go abroad and all his support during my work.

Furthermore, I would like to thank *Prof. Dr. Rosa M. Ortuño* for offering me the chance to work in her labs at the UAB Barcelona. Warm thank goes to all former and present co-workers, especially my new friends *Oriol Porcar*, *Bernat Pi*, *Jimena Ospina*, *Carme Robledillo* and *Dr. Ona Illa* of the Ortuño group for their continuous support and help in all catalan “problems” during my stay in Barcelona.

I would like to thank *Dr. Peter Kreitmeier*, *Brigitte Eichenseher*, *Georg Adolin*, *Klaus Döring*, *Roxane Harteis* and *Helena Konkel* for their technical help and support during the daily lab work. Thanks to our secretaries *Antje Weigert* and *Hedwig Ohli*.

A special thank goes to all co-workers in the central analytical department, especially the NMR department (*Fritz Kastner*, *Annette Schramm* und *Georgine Stuhler*) for carrying out spectroscopic measurements and their helpful suggestions on analyzing the obtained spectra. Moreover, a big thank goes to the mass spectroscopy (*Josef Kiermaier* und *Wolfgang Söllner*) for the continuous search of my molecule peaks i.e. in the perfluoroalkylation project.

In addition, I would like to thank the team of the “Glasbläserei” (*Markus Lindner*, *Carl-Heinz Hierl*, *Noah Schürmann* and *Helena Ackermann*) for repairing all my broken glasware and for the manufacturing of new equipment.

I would like to thank *Regina Hoheisel* for the kind introduction to cyclic voltammetry and the quick CV measurements of all of my compounds.

Thanks to *Dr. Rafał Czerwieniec* for your patience in explaining me the world of physical chemistry and the discussions about copper(I) phenanthroline complexes. Furthermore, thank you for the physical measurements of the copper complexes.

A special thank also goes to my lab colleagues *Vinh Ngoc Huynh*, *Eugen Lutsker*, *Thomas Weinbender* and *Christian Lankes* for the great lab atmosphere, the help and discussions on chemical and practical problems and the talks about non-chemical stuff! Thereby, I especially would like to thank *Vinh* and his wife *Thanh Thao* as well as *Eugen* and *Cori* for the activities outside the university.

A big thank goes to all former and present co-workers of the Reiser group. For the activities in- and outside the university, the fun during the work and the friendly atmosphere. Just to mention a few: *Eugen Lutsker, Christian Kaiser, Verena Lehner, Benjamin Kastl, Daniel Dobler, Dr. Nanaji Arisetti, Dr. Andreas Bergmann, Dr. Michael Pirtsch, Dr. Georgiy Kachkoskyi, and Dr. Matthias Knorn.*

Moreover, I want to thank *Dr. Andreas Okun, Dr. Viktor Kais, Dr. Daniel Rackl and Dr. Manuel Achatz* for our daily lunch and the discussions about anything and everything.

A special credit deserves *Dr. Matthias Knorn*. We did so many projects together which resulted in three very good publications. Also, without you we could not sell them so efficiently! In addition, I would like to thank you for your honesty, patience, the discussions about everything, and being a great friend.

I would like to thank all my Bachelor students (*Andreas Schmidberger, Lukas Traub and Barbara Kaiser*) and research students (*Eugen Lutsker, Lisa Schindler, Aritra Sil, Tobias Brandhofer, Robert Winkler and Alexander Zimmermann*) for their work in the lab and their fruitful input.

For proof reading of the present PhD thesis I have to thank *Eugen Lutsker, Christian Kaiser and Dr. Michael Pirtsch* for their spent time and very helpful remarks.

Besides, a special thanks deserve my study colleagues *Thomas Broja, Helmut Weikl, Constantin Pompe and Tanja Fieber*. We had so much fun during our learn sessions, practical courses and lectures.

Finally, it is time to thank my family and all my friends. I am very grateful to all of you! First of all, I pay my due respect and sincere regards to my parents *Alexander und Lucie*, whose love, blessings and believe are always with me for all the support, I had so far and that I am going to have in the future. Also a warm thank to my grandparents *Paul, Johanna, Alicja and Bernard*. I would like to thank my wife *Angelika* for all of her support, love and encouragement. You are the one who always keeps me grounded and without your support and love, it would not have been possible for me to overcome every trial or tribulations that have been thrown at me. I am also thankful to my parents-in-law *Helmut and Martha* who have treated me like their own son.

I. Declaration

Herewith I declare that this present PhD thesis is a presentation of my original work prepared single-handed. Wherever contributions from others are involved, all of them are marked clearly, with reference to the literature, license and acknowledgement of collaborative research.

Regensburg, 04.05.2016

Thomas Rawner